Synthesis and structural elucidation of novel synthetic coumarin scaffolds for their potential pharmacological properties

Submitted in fulfillment of the requirements for the degree of

Doctor of Philosophy
In
Biotechnology

Department of Biotechnology and Food Science, Faculty of Applied Science, Durban University of Technology, Durban, South Africa

KABANGE KASUMBWE LAUREL

Supervisor: Prof. Viresh Mohanlall

Co-Supervisor: Dr. Katharigatta Narayanaswamy Venugopala

REFERENCE DECLARATION

I, **Mr Kabange Kasumbwe Laurel – (Student number: 2010321)**, **Prof Viresh Mohanlall** and **Dr Katharigatta Narayanaswamy Venugopala** do hereby declare that in respect of the following dissertation:

Title: **Synthesis and structural elucidation of novel synthetic coumarin scaffolds for their potential pharmacological properties**

1. As far as we ascertain:
   (a) No other similar dissertation exists.

2. All references as detailed in the dissertation are complete in terms of all personal communications engaged in and published works consulted.

	03/03/2022
Signature of student	**Date**
	03/03/2022
Signature of supervisor	**Date**
	03/03/2022
Signature of co-supervisor	**Date**

AUTHORS DECLARATION

This study presents original work by the author. It has not been submitted in any form to another academic institution. Where use was made of the work of others, it has been duly acknowledged in the text. The research described in this dissertation was carried out in the Department of Biotechnology and Food Science, Faculty of Applied Sciences, Durban University of Technology, South Africa, under the supervision of **Prof Viresh Mohanlall** and **Dr Katharigatta Narayanaswamy Venugopala.**

Student's signature

DEDICATION

This work is dedicated to my father, Mwilambwe Ngoy Celestin, my mother, Muyombi Kasumbwe Marie Jeanne, my daughter Happiness Angel Kabange and my wife Kakudji Kisimba Claudine for their love and support.

ACKNOWLEDGEMENTS

First of all, I would like to thank God for giving me the strength to be determined while pursuing my studies. His grace and blessings enable me to overcome all the obstacles in completing my study.

I wish to offer my sincere gratitude to my supervisor, Prof Viresh Mohanlall and co-supervisor, Dr K.N Venugopala, for their support and guidance throughout my research work.

I am grateful to Prof. John Jason Mellem for his support and laboratory facilities to conduct anticancer assays.

I'd like to convey my sincere appreciation to Dr Sabiu Saheed for his technical assistance.

I am also thankful to Dr Sandeep Chandrashekharappa for assistance in compounds characterization, Mr Melendhran Pillay's support, laboratory facilities to conduct the anti-mycobacterial assays and Prof Bharti Odhav for her advice and support.

I am grateful to Dr Rene Myburg from the School of Medical Biochemistry, UKZN for providing guidance and laboratory facilities to conduct my assays.

I would also like to acknowledge Dr Talent Makhanya and Dr Depika Dwarka for their support. I would also like to thank Prof Maharaj and Mr Vishan Lakan from the Medical Research Council for the laboratory facility to conduct the antimalaria tests.

I am thankful to the National Research Foundation and the Durban University of Technology for their financial support.

Finally, I would like to express my sincere gratitude to my parents, father-in-law, mother-in-law and daughter for their love, encouragement, and support. In addition, I wish to extend my most profound appreciation to my wife, who encouraged me to pursue this study and helped me resolve various research problems.

ABBREVIATIONS

15-LO	:	15-Lipoxygenase inhibitor
FTIR	:	Fourier-transform infrared spectroscopy
CO_2	:	Carbon dioxide
COX	:	Cyclo-oxygenase
DEET	:	*N,N*- Diethyl-meta-toluamide
DMEM	:	Dulbecco`s Modified Eagle`s Medium
DMSO	:	Dimethyl sulphoxide
DPPH	:	2,2-Diphenyl-1-picrylhydrazyl
ELISA	:	Enzyme-linked Immunosorbent Assay
FCS	:	Foetal Calf Serum
FITC	:	Fluorescein isothiocyanate
IC_{50}	:	Concentration of inhibitor necessary for 50% inhibition
LOX	:	Lipoxygenase
MIC	:	Minimum inhibition concentration
MRC	:	Medical Research Council
MTT	:	3-(4, 5-Dimethylthiazol-2-yl)-2, 5-diphenyltetrazolium bromide
ROS	:	Reactive oxygen species
TLC	:	Thin layer chromatography
WHO	:	World Health Organization
UV	:	Ultraviolet
SVM 1	:	(*E*)-3-(2-(benzylidene amino) thiazol-4-yl)-6,8-dichloro-2*H*-chromen-2-one
SVM 2	:	(*E*)-6,8-dichloro-3-(2-((4-methoxybenzylidene) amino) thiazol-4-yl)-2*H*-chromen-2-one
SVM 3	:	(*E*)-6,8-Dichloro-3-(2-((4-chlorobenzylidene) amino) thiazol-4-yl)-2*H*-chromen-2-one
SVM 4	:	(*E*)-6,8-dichloro-3-(2-((4-fluorobenzylidene) amino) thiazol-4-yl)-2*H*-chromen-2-one
SVM 5	:	(*E*)-6,8-dichloro-3-(2-((thiophen-2-ylmethylene) amino) thiazol-4-yl)-2*H*-chromen-2-one
SVM 6	:	(*E*)-6,8-dichloro-3-(2-((pyridin-4-ylmethylene) amino) thiazol-4-yl)-2*H*-chromen-2-one

SVM 7 : (*E*)-6,8-dichloro-3-(2-((2-hydroxybenzylidene) amino) thiazol-4-yl)-2*H*-chromen-2-one

SVM 8 : (*E*)-6,8-dichloro-3-(2-((3,4-dihydroxybenzylidene) amino) thiazol-4-yl)-2*H*-chromen-2-one

SVM 9 : (*E*)-6,8-dichloro-3-(2-((2-methoxybenzylidene) amino) thiazol-4-yl)-2*H*-chromen-2-one

SVM 10 : (*E*)-6,8-dichloro-3-(2-((2-hydroxy-5 nitro benzylidene) amino) thiazol-4-yl)-2*H*-chromen-2-one

SVM 11 : (*E*)-6,8-dichloro-3-(2-((3,5-dichloro 2hydroxybenzylidene) amino) thiazol-4-yl)-2*H*-chromen-2-one

SVN 1 : (*E*)-3-(2-(benzylidene amino) thiazol-4-yl)-6-nitro-2*H*-chromen-2-one

SVN 2 : (*E*)-3-(2-((4-methoxybenzylidene) amino) thiazol-4-yl)-6-nitro-2*H*-chromen-2-one

SVN 3 : (*E*)-3-(2-((4-chlorobenzylidene) amino) thiazol-4-yl)-6-nitro-2*H*-chromen-2-one

SVN 4 : (*E*)-3-(2-((4-Fluorobenzylidene) amino) thiazol-4-yl)-6-nitro-2*H*-chromen-2-one

SVN 5 : (*E*)-6-nitro-3-(2-((thiophen-2-ylmethylene) amino) thiazol-4-yl)-2*H*-chromen-2-one

SVN 6 : (*E*)-6-nitro-3-(2-((pyridin-4-ylmethylene) amino) thiazol-4-yl)-2*H*-chromen-2-one

SVN 7 : (*E*)-3-(2-((2-hydroxybenzylidene) amino) thiazol-4-yl)-6-nitro-2*H*-chromen-2-one

SVN 8 : (*E*)-3-(2-((3,4-dihydroxybenzylidene) amino) thiazol-4-yl)-6-nitro-2*H*-chromen-2-one

SVN 9 : (*E*)-3-(2-((2-methoxybenzylidene) amino) thiazol-4-yl)-6-nitro-2*H*-chromen-2-one

SVN10 : (*E*)-3-(2-((2-hydroxy-5-nitrobenzylidene) amino) thiazol-4-yl)-6-nitro-2*H*-chromen-2-one

SVN 11 : (*E*)-3-(2-((3,5-dichloro-2-hydroxybenzylidene) amino) thiazol-4-yl)-6-nitro-2*H*-chromen-2-one

PATENT

KASUMBWE, Kabange, VENUGOPALA, Katharigatta Narayanaswamy, CHANDRASHEKHARAPPA, Sandeep, PILLAY, Melendhran, ODHAV, Bharti, MOHANLALL, Viresh. TREATMENT OF TUBERCULOSIS, 2019/05328 dated 13/08/2019, 2020/03088 dated 5/27/2020. Patent Journal June 2021; 54(06):199.

ACCEPTED PUBLICATION

KASUMBWE, K., SAHEED, S., MAKHANYA, T. R., VENUGOPALA, K. N. & MOHANLALL, V. 2021. Coumarin containing hybrids and their pharmacological activities. *PhytoChem & BioSub Journal; Vol. 15, Issue 3.*

MANUSCRIPTS IN PROGRESS FOR SUBMISSION

Kabange Kasumbwe, Sandeep Chandrashekarappa, Melendhran Pillay, Bharti Odhav, Viresh Mohanlall and Katharigatta N.Venugopala. 2022. Synthesis and structural elucidation of novel Schiff bases of 3-(2-aminothiazol-4-yl)-6, 8-dichloro-2*H*-chromen-2-ones (**SVM 1-11**) as potential anti-TB agents against *Mycobacterium tuberculosis.* Nature Communication. 2022

Kabange Kasumbwe, Melendhran Pillay, Sandeep Chandrashekarappa, Viresh Mohanlall and Katharigatta N.Venugopala. 2022. Synthesis and structural elucidation of novel Schiff bases of 3-(2-aminothiazol-4-yl)-6-nitro-2H-chromen-2-one (**SVN1-11**) as potential anti-TB agents against *Mycobacterium tuberculosis.* Nature Communications 2022.

CONFERENCE PRESENTATIONS/WORKSHOP

Kasumbwe, K*., Katharigatta N. Venugopala and Mohanlall, V. (2019). Properties of Thiazolyl nitro coumarin against *Anopheles arabiensis*, Durban University of Technology South Africa, Research Day, November 2019.

Kasumbwe, K*., Katharigatta N. Venugopala and Mohanlall, V. (2020). Novel Schiff bases of amino thiazolyl dichlorocoumarins and amino thiazolyl nitro coumarins as anti-TB agents against multidrug-resistant tuberculosis, Moses Kotane innovation awards South Africa, November 2020.

TABLE OF CONTENTS

LIST OF FIGURES

LIST OF TABLES

ABSTRACT

Two novel series of Schiff bases of 3-(2-aminothiazol-4-yl)-6,8-dichloro-2*H*-chromen-2-one (**SVM 1-11**) and 3-(2-aminothiazol-4-yl)-6-nitro-2*H*-chromen-2-one (**SVN 1-11**) were synthesized and confirmed by FT-IR, NMR, LC-MS and elemental analysis. The resulting compounds were evaluated for anti-tuberculosis activity using the micro Alamar blue assay (MABA) against susceptible strain H37Rv (ATCC25177) and multidrug-resistant (MDR) strains of *Mycobacterium tuberculosis* (MTB). A computational method was also used to identify the molecular targets for these compounds. Larvicidal and insecticidal activity were evaluated against *Anopheles arabiensis* using the standard WHO larvicidal assay and cone bioassay methods. Anticancer activity was assessed using the MTT assay against human breast adenocarcinoma cells (MCF-7) and human epithelial lung adenocarcinoma cells (A549). The antioxidant and lipoxygenase inhibitory capacity was measured using the DPPH assay and Lipoxygenase inhibitory kit, respectively.

The antimycobacterial efficacy of the synthesized **SVM 1-11** showed that **SVM 8** and **SVM 10** were the most active compounds, with MIC values of 0.5 µg/mL against H37Rv-MTB and 8 µg/mL against MDR-MTB. Among the synthesized **SVN 1-11**, the most active compounds were **SVN 3** and **SVN 4**, having MICs of 0.5 and 1 µg/mL against H37Rv-MTB, respectively, and 8 and 4 µg/mL against MDR-MTB. The docking study performed with the target enzymes DprE1and Pks13 indicated that the compounds had a high affinity for the druggable targets DprE1 and Pks13 enzymes of *Mycobacterium tuberculosis* compared to the reference standards rifampicin and isoniazid. The larvicidal and adulticidal tests revealed that compounds **SVM 6** and **SVM 9** were the most effective, with larvicidal mortality (100%) equal to the reference drug' Themephos; additionally, the above compounds exhibited significant adulticidal activity of 73.5±1.5 and 77.3±2.3%, respectively. Compounds **SVN 6**, **7**, **8**, and **9**, on the other hand, were the most potent larvicidal and adulticidal, exhibiting 100% larvae mortality after 24 hours, and significant adulticidal activity. The anticancer activity study indicates that these compounds had a significant effect on MCF-7 cells. **SVM 2**, **4**, **8** and **11** were the most effective with IC_{50} values ranging from 5.7 to 9.2 µg/mL. Compounds **SVN 1**, **2**, **4**, **9**, **10**, and **11**, on the other hand, had a remarkable cytotoxicity effect on MCF-7, with IC_{50} range from 6.2-16.38 µg/mL. The

caspase-Glo® kit test (Caspase 3/7, 8 and 9) was used to assess the mechanism involved in the anticancer activity of the selected active compounds against MCF-7. The results showed that the apoptosis generated by these compounds was triggered in part by the activation of caspase-3/7 and caspase-9, which may be the primary mechanism of apoptosis.

The antioxidant results revealed that compounds **SVM 3** and **SVM 8** were the most potent, with a percentage scavenging capacity of 92.7±1.1 and 89.7±1.7%, respectively. Compounds **SVN 5** and **9**, on the other hand, were the most active, with a percentage scavenging capacity of 80.5±0.6 and 85.4±1.3%, respectively. The lipoxygenase inhibitory assay revealed that compounds **SVM 3**, **8**, and **11** were the most potent LO inhibitors, with inhibitory capacity ranging from 60 to 67%. Compound **SVN 11**, on the other hand, was the most effective, with a percentage inhibitory capacity of 61.3±0.3%.

Our results suggest that integrating different functional groups on the phenyl ring at the fourth position of the thiazole moiety, connected to the primary coumarin nucleus at the third position, contributed significantly to the biological activity of the compounds. These active compounds could be used as a scaffold for structural optimization to develop highly effective and selective antimycobacterial, anticancer, antioxidant, larvicidal, and adulticidal agents and promote further development of more efficient lipoxygenase inhibitors of novel structurally similar analogues.

CHAPTER I. INTRODUCTION

Infectious diseases such as tuberculosis and malaria continue to be among the world's most significant public health concerns, contributing considerably to worldwide mortality (Noji, 2001). Tuberculosis is considered one of the threatening diseases caused by *Mycobacterium tuberculosis* after the human immunodeficiency virus (HIV) (Keri *et al*., 2015). Among the challenges in TB treatment is the appearance of resistance pathogen *Mycobacterium tuberculosis* to the current existing drug, resulting in multidrug-resistant tuberculosis (MDR-TB) and extensively drug-resistant tuberculosis (XDR-TB) (Muthukrishnan *et al*., 2011, Reddy *et al*., 2018, Makam *et al*., 2013). MDR-TB and XDR-TB have been a domain of increasing concern; it is considered a threat to the general effort to control tuberculosis due to mismanagement of MDR-TB with irregular use of second-line drugs, resulting in the development of XDR-TB (Prasad and Srivastava, 2013). Globally in 2020, there were an estimated 1.3 million deaths among HIV-negative individuals, up from 1.2 million in 2019 and an additional 214000 deaths among HIV-positive individuals (WHO, 2021a). One of the most significant barriers to malaria control has been the emergence of drug-resistant strains of the malaria parasite *Plasmodium falciparum*. Drugs previously used to treat malaria, such as chloroquine, are now practically worthless in many parts of the world (Tanser and Le Sueur, 2002).

Cancer, a class of diseases characterized by uncontrolled cell growth, is still regarded as a life-threatening disease in many parts of the world (Parikh *et al*., 2022, Correia *et al*., 2014). Numerous cancer therapy reports reveal that no anticancer agent shows 100% efficacy without side effects (Vaarla *et al*., 2015). According to World Health Organization (WHO), cancer is the second leading cause of death after cardiovascular disease worldwide, with about 10 million deaths in 2020; breast cancer and prostate cancer are among the most notorious cancer types in women and men (WHO, 2020b). The statistical analysis of cancer mortality worldwide in the year 2020 was as follows, lung (1.80 million), colon and rectum (935 000), liver (830 000), stomach (769 000) and breast (685 000 deaths) (WHO, 2020b). Given the abovementioned, there is a growing need to discover and develop innovative therapies with a different structural framework and perhaps a different mode of action than currently available drugs. In this context, it is beneficial to develop and synthesize various new compounds with increased

biological activity, improved safety profiles and promising applications as anti-tuberculosis, anti-malarial, anti-cancer, antioxidant and anti-inflammatory agents.

Numerous compounds with biological activities, either synthetic or natural, have been explored; however, many are not suitable for therapeutic application due to their toxicity (Kostova, 2005). Nowadays, it is possible to modify the active chemical structures to synthesize compounds with improved therapeutic activity and reduced toxicity (Koppula and Purohit, 2013). Coumarins are the simplest naturally occurring phenolic compounds with fused benzene and α-pyrone rings classified as the fundamental molecules of various derivatives (Grazul and Budzisz, 2009). Coumarins are extensively used as additives in food, perfumes, agrochemicals, cosmetics, and pharmaceuticals (Maheswara *et al*., 2006). Coumarin derivatives are generally simple to synthesize and have good solubility, low cytotoxicity, and good permeability to the cells (Sun *et al*., 2014). The synthesis of coumarins and their derivatives have attracted the interest of organic and medicinal chemists as significant numbers of natural products possess this heterocyclic nucleus (Barot *et al*., 2015, Keri *et al*., 2015). The synthesis of substituted coumarins is accomplished by various chemical reactions based on the different substitutions on the coumarin nucleus. Coumarin and its derivatives may be synthesized by Pechmann, Perkin, Reformastky and Knoevenagel reaction in the laboratory (Singh and Pathak, 2016). Several essential compounds originated from coumarin include warfarin, acenocoumarol, novobiocin, clorobiocin and hymecromone (Ostrowska, 2020). Coumarins are reported to exhibit various biological activities such as antibacterial (Feng et al., 2020), anticancer (Song *et al*., 2020), anticoagulant (Tang *et al*., 2015), antifungal (Prusty and Kumar, 2019), anti-tubercular (Hu *et al*., 2017), antiviral (Hu *et al*., 2019a), antioxidant (Tataringa *et al*., 2016), antileishmanial (Mandlik *et al*., 2016), antidiabetic (Gupta *et al*., 2020), anti-inflammatory (Dawood *et al*., 2015) (Shaik *et al*., 2016), anti-Alzheimer (Shaik *et al*., 2016) and anti-parkinsonian activities (Olaya *et al*., 2020).

Another promising group, thiazole, has emerged among the most significant heterocycles in medicinal chemistry and has demonstrated remarkable biological effects (Mishra *et al*., 2017). Thiazoles are key members of the heterocyclic compound and exhibit various biological activities (Gümüş *et al*., 2019). Thiazole compounds have been shown to possess antioxidant (Dincel *et al*., 2020), antibacterial (Althagafi *et al*., 2019), anticancer (de Santana *et al*., 2018), antiviral (Singh *et al*., 2019b), anti-inflammatory (Kamat *et al*., 2020), antimalarial (Sahu *et al*., 2019), antifungal effects (Yang *et al*., 2021) and many more. Additionally, thiazole moiety

is a key pharmacophore for synthesizing different chemotherapeutic agents (Reddy et al., 2016). Coumarin derivatives with various substitutions of thiazole rings at carbon three have shown various pharmacological activities, including analgesic (Salar *et al*., 2016), anti-inflammatory (Kashyap *et al*., 2012), antibacterial and antitumor (Sonmez *et al*., 2017) properties. Due to the differences in coumarin structure complexity, identifying key structural features within the coumarin molecule is vital for designing and developing novel coumarin analogues with improved pharmacological properties (He *et al*., 2014, Sandhu *et al*., 2014).

A new approach to developing hybrid molecules by incorporating bioactive moieties into a single molecule through a hybrid pharmacophore is rational in drug development (Osman *et al*., 2018b). The molecular hybridization approach has been used to design novel coumarin hybrids with various bioactive groups to produce molecules with increased pharmacological properties and pharmacokinetic profiles (Sahoo *et al*., 2021, Fotopoulos and Hadjipavlou-Litina, 2020). Considering the significance of coumarins and thiazoles in medicinal chemistry and exploring the scope of these motifs, this study focused on developing a novel structural entity that incorporates these two structural moieties, including a potential functional group, into a single molecular framework to develop drugs that attribute new targets and mechanisms of action for better treatment. Thus, this study aimed to synthesize two novel Schiff bases of 3-(2-aminothiazol-4-yl)-6,8-dichloro-2*H*-chromen-2-one (**SVM 1-11**) and 3-(2-aminothiazol-4-yl)-6-nitro-2*H*-chromen-2-one (**SVN 1-11**) and assess their antimycobacterial, anti-mosquito, anticancer, antioxidant and anti-inflammatory activities.

CHAPTER II. LITERATURE REVIEW

2.1 Introduction

Benzopyrones are heterocyclic compounds formed by fusing the pyrone ring with the benzene nucleus. Coumarin is one of the benzopyrones, an important class of oxygen-containing heterocycles occurring in plants (El-Sawy *et al*., 2021). The synthesis of coumarins and their derivatives has caught the interest of organic and medicinal chemists because this heterocyclic nucleus comprises numerous natural compounds (Venugopala *et al*., 2013c, Keri *et al*., 2015). Numerous heterocyclic compounds of coumarin rings are linked with different biological properties (Morsy *et al*., 2017). The pharmacological properties of coumarin derivatives are highly affected by their substitution. Integrating bioactive molecules into a single molecule by a hybrid pharmacophore is a reasonable approach to drug development (Osman *et al*., 2018b). A variety of coumarins have shown anticancer and antimicrobial activities that have been the reason for their insertion in the hybrid's scaffold. The hybridization of the coumarin nucleus with other molecules results in different molecules of more significant biological activity (Kraljević *et al*., 2016). This chapter highlights the various research findings of coumarin derivatives as potential therapeutic agents, which can be explored for future design and development.

2.2 Coumarins classifications

Coumarins consist of a combination of benzene and α-pyrone rings; based on a variety of substituents on the coumarin nucleus. Coumarins are divided into four main groups, including the simple coumarins, furanocoumarins, pyranocoumarins and the pyrone-substituted coumarins, as shown in Table 1 (Rohini and Srikumar, 2014). Simple coumarins and analogues are a class of compounds that have been demonstrated to possess various pharmacological activities. There has been increased interest in their synthesis due to their various biological activities displayed (Salem *et al*., 2016). Ammoresinol, ostruthin, novobiocin and coumermycin are simple coumarins possessing antibacterial activity, while osthole possesses anticancer activity (Table 1) (Venugopala *et al*., 2013b). The furanocoumarin is composed of imperatorin, psoralen, bergapten marmalade, and other compounds possessing anti-inflammatory, anti-mycobacterial and antifungal properties. There are two types of pyranocoumarins, linear type including grandivittin, agasyllin, and aegelinol benzoate

possessing an antibacterial activity (Basile *et al*., 2009) and angular type including inophyllum (A, B, C, E, P, G), calanolide (A, B, F) possessing antiviral activity (Table 1). Besides the types mentioned above, the coumarin structure also has other forms, such as biscoumarins, which possess anticoagulant activity (Xu *et al*., 2015).

Table1: Types of coumarins and their pharmacological activities (Venugopala *et al*., 2013c, Küpeli Akkol *et al*., 2020).

Type of coumarin	**General chemical structure**	**Examples**	**Pharmacological activity**
Simple coumarins	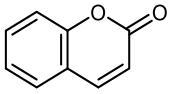	Coumarin Ammoresinol Ostruthin Novobiocin Coumermycin Chartreusin	Anti-inflammatory Anti-bacterial Antifungal Anticancer
Furano coumarins	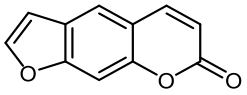	Imperatorin Psoralen Bergapten Marmalde	Anti-inflammatory Anti-TB Antifungal
Pyrano coumarins	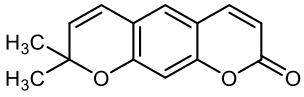 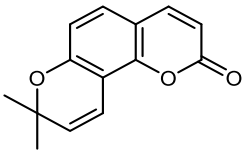	Gradivittin Agasyllin Xanthyletin Inophyllum (A, B, C, E, P, G) Calanolide (A, B, F)	Antibacterial Anti-TB Antiviral
Other coumarins	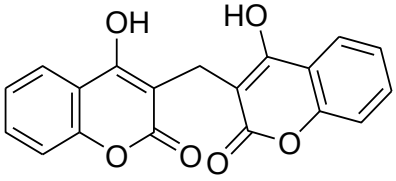	Dicoumarol	Anticoagulant

2.3 Synthesis of coumarin derivatives

Coumarins were first synthesized using Perkin's reaction; several simple coumarins are still being prepared using this technique. Knoevenagel reaction appeared as a primary synthetic method to fuse coumarin derivatives with a carboxylic acid at the C3-position. Numerous other synthetic methods for substituted coumarin derivatives have been reported, including the Pechmann, Reformatsky and Wittig reactions (Shaabani *et al*., 2009, Dighe *et al*., 2010). Pechmann and the Knoevenagel reactions are extremely useful for coumarin synthesis with simple reaction conditions and good product yield. In particular, Knoevenagel condensation is widely used to synthesize different coumarin backbones, suitable for preparing various compounds of medicinal and industrial significance (Vekariya and Patel, 2014). In recent years, attempts have been made to prepare coumarin derivatives using alternative methods such as solid-phase synthesis, microwave irradiation, and ultrasonication. Furthermore, coumarin hybrid synthesis with resveratrol and estrogen was one of the strategies used to reach potential therapeutic agents (Jayashree *et al*., 2014). Literature results suggest that pyrrole, pyrazole, thiadiazole and triazoles are desirable targets due to their biological properties (Tataringa and Zbancioc, 2019).

2.3.1 Pechmann reaction

Pechmann reaction is a long-standing reaction that is one of the simplest and most basic techniques for synthesizing coumarins. The method is based primarily on the condensation of phenols with ketoesters in the presence of a range of reagents and produces a good yield of 4- substituted coumarins (Khaligh, 2012). Several acid catalysts have been used in the von Pechmann reaction, which necessitates their usage in excess and the disposal of excess acid waste pollutes the environment. As a result, there is room for improvement in friendlier reaction conditions, more significant substituent variability in both components and improved yields. The synthesis of coumarins through the indium (III) chloride catalyzed condensation of phenol and ketoesters is an efficient and vastly improved modification of the von Pechmann procedure (Figure 1). In addition to its simplicity and moderate reaction conditions, this technique can tolerate many substitutions in both components (Bose *et al*., 2002).

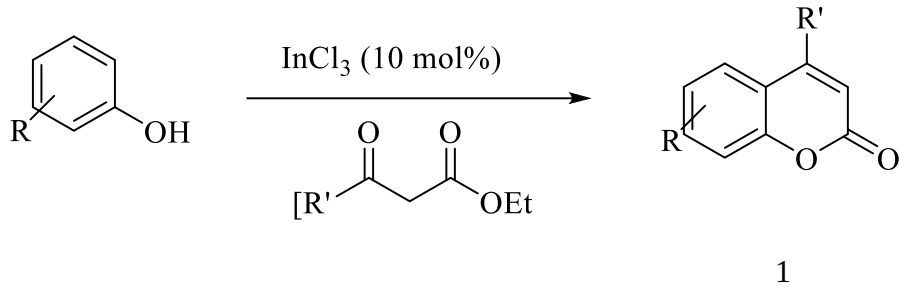

1

Figure 1: Catalytic activity of indium (III) chloride in the formation of coumarins (Bose *et al*., 2002).

2.3.2 Knoevenagel reaction

One of the most critical C=C bond formation processes in organic synthesis is the Knoevenagel condensation that produces excellent chemical intermediates and products (Valizadeh and Vaghefi, 2009). The resulting α and β unsaturated products have been used as intermediates to synthesize therapeutic drugs, natural products, functional polymers, fine chemicals, herbicides and insecticides. It is usually carried out in organic solvents and catalyzed by organic bases like piperidine or pyridine (Verdía *et al*., 2011). Figure 2 depicts the synthesis of substituted coumarin-3-carboxylic acid derivatives at room temperature utilizing the Knoevenagel condensation reaction between ethyl malonate coupled to the Wang resin and ortho-hydroxybenzaldehyde in the presence of pyridine and piperidine.

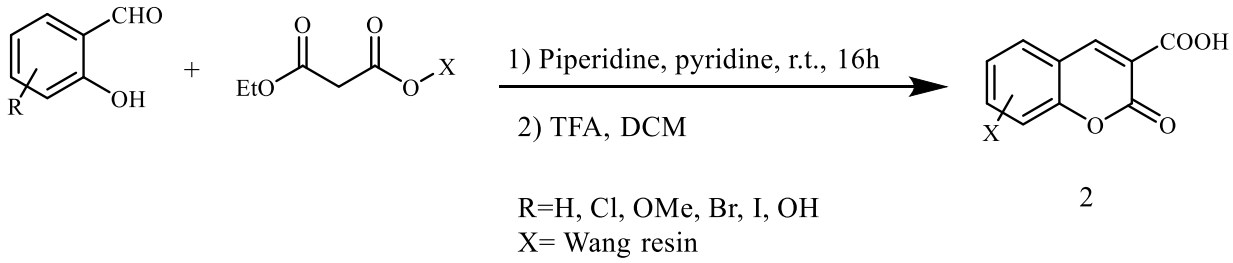

2

Figure 2: Synthesis of coumarin-3-carboxylic acid (Vekariya and Patel, 2014).

2.3.3 Wittig reaction

Shockravi *et al*. (2003) studied a one-pot and convenient synthesis of coumarins in a solventless system. They reported the Wittig reaction of in situ prepared carbethoxymethylene triphenylphosphorane and salicylaldehydes in the presence of MgO for efficient and solvent-free synthesis of simple coumarins. It was found that simple coumarins may be synthesized in a single step with high yields. The combination of salicylaldehydes (or its derivatives), triphenylphosphine and chloroethyl acetate in the presence of MgO produced coumarins 3 (Figure 3). It should be noted that the addition of sodium methoxide increases the reaction rate, and no unwanted products (such as trans-cinnamates) other than coumarins have been found in either case (Shockravi *et al*., 2003).

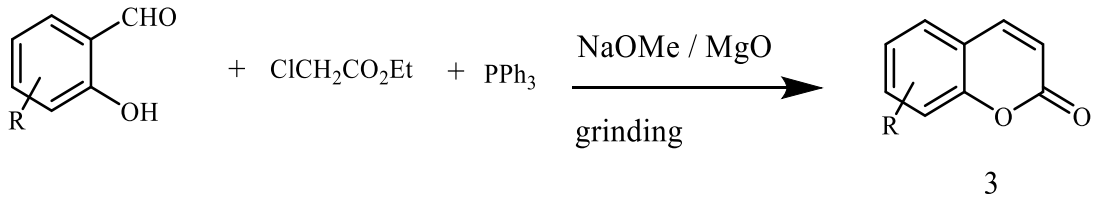

Figure 3: Synthesis of coumarin via Wittig reaction (Shockravi et al., 2003).

2.4 Coumarin-containing hybrids

2.4.1 Coumarin- thiazole hybrids

Thiazoles are an important heterocyclic class of compounds present in numerous active pharmacological drugs such as sulfathiazole, abafungin, tiazofurin (antimicrobial) and ritonavir (antiviral) (Hussein and Zitouni, 2018, Zablotskaya *et al*., 2013). Due to its low toxicity, the thiazole nucleus is an essential pharmacophore for synthesizing different molecules with various biological properties (Reddy *et al*., 2016). The molecular hybridization of thiazole and coumarin pharmacophores has been regarded as a strategy for extracting more active compounds that function through multiple targets (Osman *et al*., 2018b). Coumarin derivatives with various substitution of thiazole rings at C3 have shown pharmacological activities including analgesic (Salar *et al*., 2016), anti-inflammatory (Kashyap *et al*., 2012), antioxidant (Secci *et al*., 2016), antibacterial and antitumor activity (Sonmez *et al*., 2017, Arshad *et al*., 2011, El-Gaby *et al*., 2009).

The synthesis of coumarin-thiazole analogues through an effective synthetic way for their biological potential against aldose/aldehyde reductase is shown in Figure 4. The desired compounds 4(a-o) from the coumarinyl thiazole series were synthesized using a multi-component reaction technique. The 3-(2-bromoacetyl)-*2H*-chromen-2-one was synthesized via condensation of salicylaldehyde, and ethyl acetoacetate catalyzed by base (piperidine) after bromination. Therefore, the intermediate was treated in one pot with different substituted acetophenones and thiosemicarbazide in the presence of glacial acetic acid as a catalyst to yield the title compounds 4(a-o)(Ibrar *et al*., 2016).

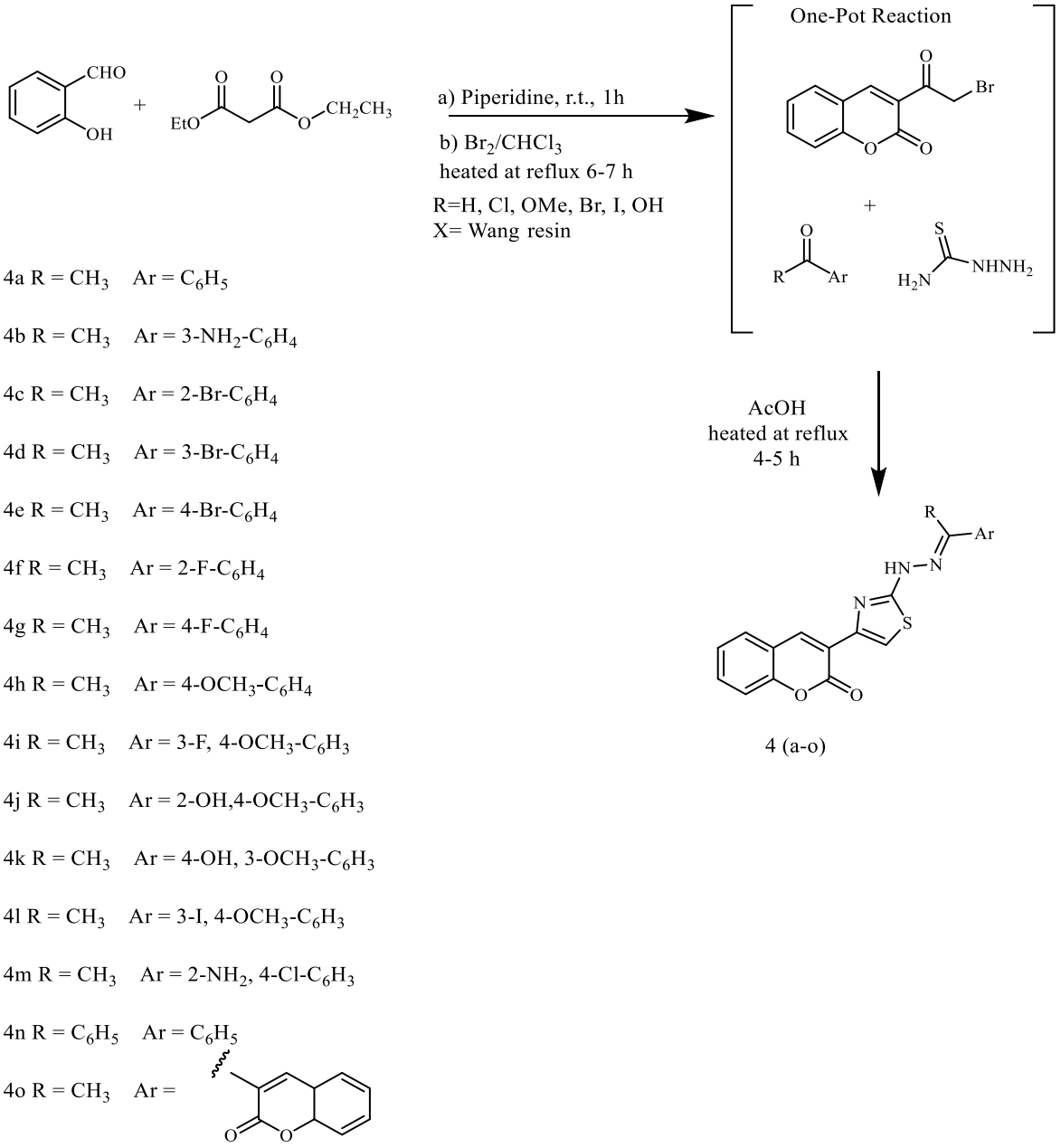

4a R = CH_3 Ar = C_6H_5

4b R = CH_3 Ar = 3-NH_2-C_6H_4

4c R = CH_3 Ar = 2-Br-C_6H_4

4d R = CH_3 Ar = 3-Br-C_6H_4

4e R = CH_3 Ar = 4-Br-C_6H_4

4f R = CH_3 Ar = 2-F-C_6H_4

4g R = CH_3 Ar = 4-F-C_6H_4

4h R = CH_3 Ar = 4-OCH_3-C_6H_4

4i R = CH_3 Ar = 3-F, 4-OCH_3-C_6H_3

4j R = CH_3 Ar = 2-OH,4-OCH_3-C_6H_3

4k R = CH_3 Ar = 4-OH, 3-OCH_3-C_6H_3

4l R = CH_3 Ar = 3-I, 4-OCH_3-C_6H_3

4m R = CH_3 Ar = 2-NH_2, 4-Cl-C_6H_3

4n R = C_6H_5 Ar = C_6H_5

4o R = CH_3 Ar =

Figure 4: Synthesis of coumarinyl thiazole analogues via a one-pot condensation reaction (Ibrar *et al*., 2016).

2.4.2 Combination of triazole ring and coumarin

For the development of new bioactive molecules, the triazole ring is an essential five-membered heterocycle structure. This electron-rich heterocycle effectively binds to different enzymes and receptors (Kulabaş *et al*., 2016). Triazoles, including 1,2,3-triazole and 1,2,4-triazole and coumarins, have been reported to possess various biological and pharmacological properties, including antituberculosis, antimalarial, antibacterial, anti-inflammatory, antiviral, anti-Alzheimer and antifungal (Fan *et al*., 2018). The 1,2,4-Triazoles are flexible scaffolds in molecular hybrid synthesis; 1, 2, 4-triazole clubbed heterocycles demonstrate improved biological activities similar to those of the parent group and are thus more commonly used in medicinal chemistry (Basappa *et al*., 2020). Recently, a library of 1,2,3-triazole-conjugated coumarin derivatives has been synthesized and shown to possess anticancer and antimicrobial activities (Kraljević *et al*., 2016, Xu *et al*., 2019). The synthesis process of coumarin-triazole hybrids is indicated in Figure 5.

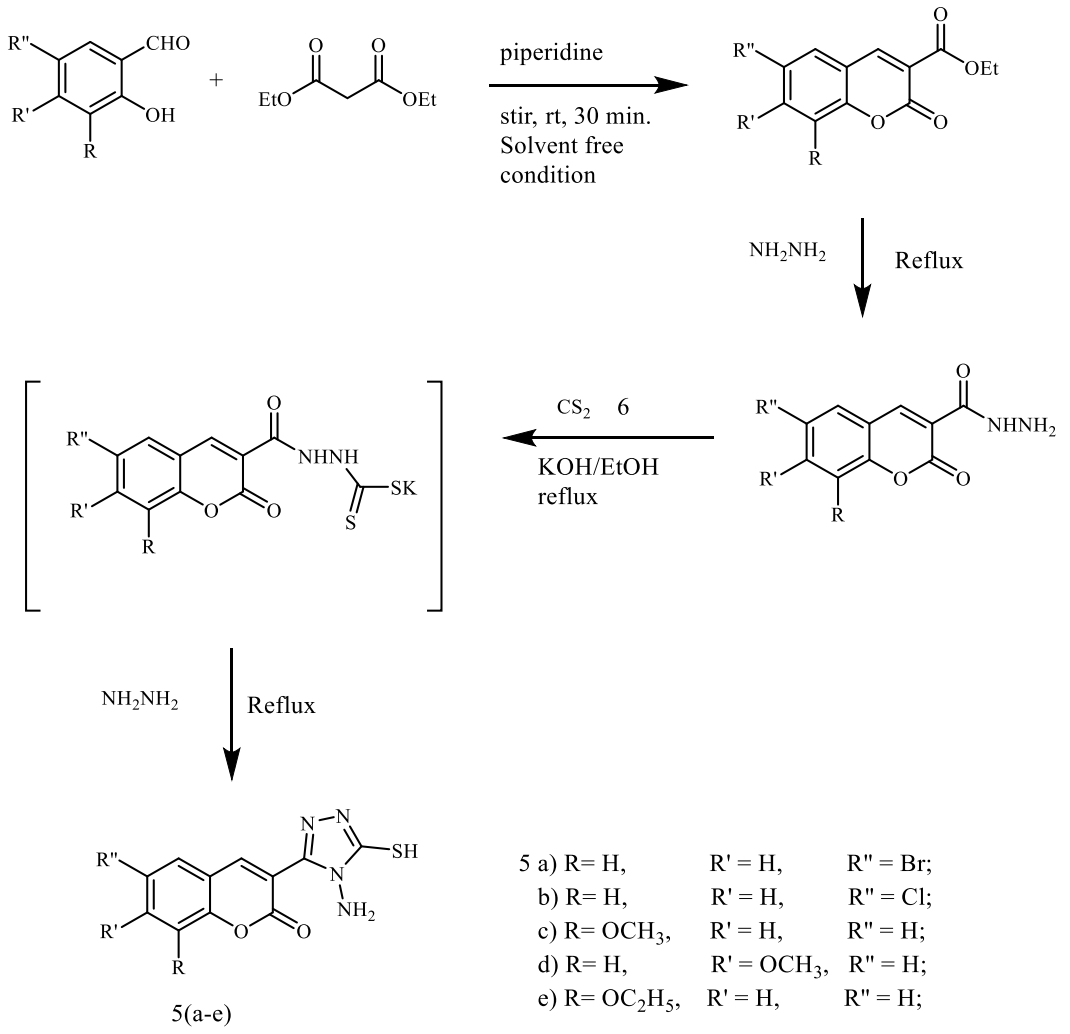

Figure 5: Coumarin-triazole hybrids synthesis (Basappa et al., 2020).

2.4.3 Coumarinyl chalcone hybrids

Chalcones are unsaturated ketones that serve as the basic building block for several important bioactive compounds. They are present in plants and serve as biogenetic precursors to flavonoids and isoflavonoids. Many organic chemists have fused chalcones with bio-active pharmacophores to generate a novel class of molecules due to their distinctive open-chain shape (Reddy *et al*., 2021). Various substituted natural and synthetic chalcones have shown important pharmacological activities such as anti-inflammatory, antibacterial, antioxidant, antimalarial and anticancer. This class of compounds has created considerable interest in potential therapeutic applications due to their abundance in plants and ease of synthesis (Kang *et al.*, 2018, Yadav *et al*., 2011, Sharma *et al*., 2013, K Sahu *et al*., 2012). The coumarinyl chalcones can be produced in two phases, as indicated in Figure 6. The first step is to synthesize the precursor 4-hydroxy-3-acetyl coumarin by combining 4-hydroxy coumarin with phosphorous oxychloride and glacial acetic acid. The second stage was the Knoevenagel condensation of the same amount of 4-hydroxy-3-acetyl coumarin and substituted benzaldehydes with chloroform in the presence of piperidine (Patel *et al*., 2011).

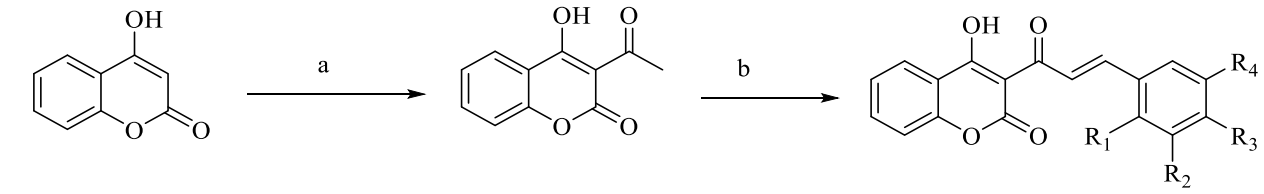

4-hydroxy-2H-chromen-2-one 3-acetyl-4-hydroxyl-2H-chromen-2-one

6a-j

a) denotes Glacial acetic acid, POCL3

b) is substituted benzaldehydes, CHCL3, piperidine (Catalytic)

Code	R^1	R^2	R^3	R^4
6a	H	H	H	H
6b	Cl	H	H	H
6c	H	H	Cl	H
6d	Cl	H	Cl	H
6e	H	NO_2	H	H
6f	H	H	NO_2	H
6g	H	H	$N(CH_3)_2$	H
6h	H	OCH_3	OCH_3	H
6i	OCH_3	OCH_3	OCH_3	H
6j	H	OCH_3	OCH_3	OCH_3

Figure 6: Synthesis of the 3-cinnamony-4hydroxy-2*H*-chromen-2-ones (Patel *et al*., 2011).

2.4.4 Combination of pyrazoline ring and coumarin

Pyrazolone and pyrazoline derivatives are commonly well-known five-membered heterocyclic compounds containing nitrogen. Pyrazolone derivatives play a significant role as substructures for many pharmaceuticals, agrochemicals, colourants, and pigments, as well as chelating and extraction agents (Sun and Cui, 2009). Similarly, Coumarins are benzopyrone derivatives occurring naturally in plants and are characterized by substantial chemo-diversity and various pharmacological activities (Ajani *et al*., 2018). Several analogues of pyrazolidin-3, 5-diones, pyrazolin-3-ones, and pyrazolin-5-ones have found therapeutic use as NSAIDs; Felcobuzone and Mefobutazone are examples of this. Pyrazolinyl coumarins were also synthesized and recorded for their bioactivity (Khode *et al*., 2009). Several pyrazolines have been synthesized via microwaves. An Equimolar amount of various chalcones and substituted hydrazine (Acetyl hydrazine or Phenyl hydrazine) were added to the microwave tube then microwaved for the specified amount of time (Figure 7). After the reaction was completed, the mixture was immersed in ice-cold water. The solid isolated was filtered and purified using a column to get pure pyrazoline derivatives (Akhtar *et al*., 2017b).

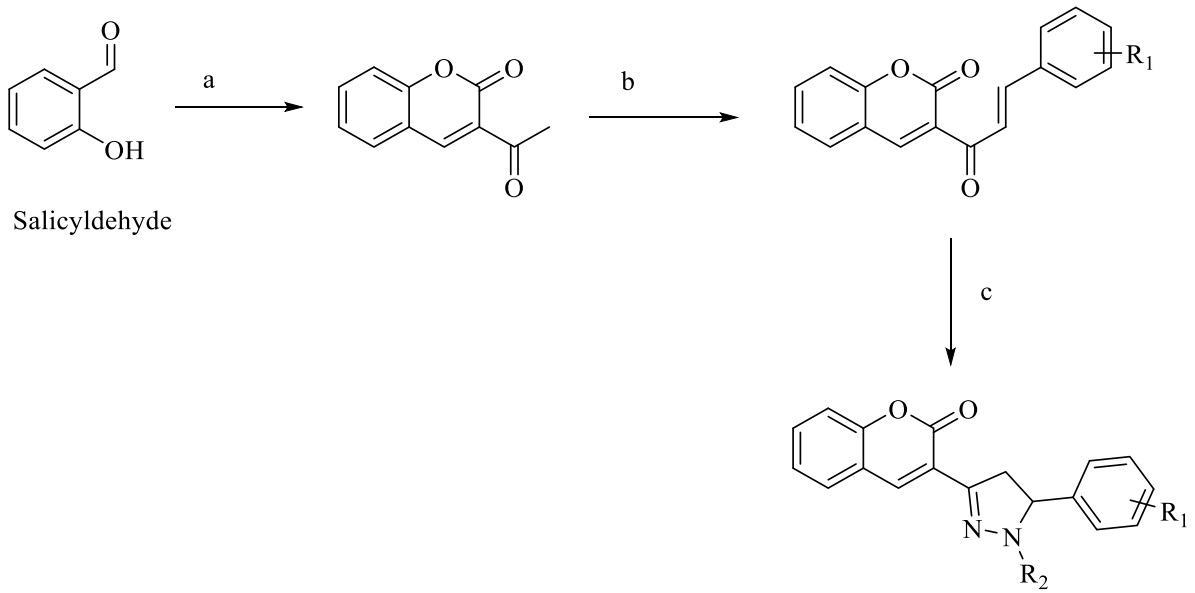

Salicyldehyde

7a-7i

(a) Ethylacetoacetate, ethanol, piperidine, reflux
(b) Aldehyde, n-BuOH, reflux;
(c) Hydrazines, ethanol: acetic acid(1:1), Microwave(2-4min)

Code	R1	R2
7a	3,4-$(OCH_3)_2$	$COCH_3$
7b	3,4,5-$(OCH_3)_3$	$COCH_3$
7c	4- CH_3	$COCH_3$
7d	4-Cl	$COCH_3$
7e	3- OCH_3	C_6H_5
7f	3,4-$(OCH_3)_2$	C_6H_5
7g	3,4,5-$(OCH_3)_3$	C_6H_5
7h	4- CH_3	C_6H_5
7i	4-Cl	C_6H_5

Figure 7: Synthesised pyrazoline-coumarin derivatives (Akhtar et al., 2017b).

2.4.5 Combination of pyridine ring and quinolone with coumarin nucleus

In several biological processes and cancer pathogenesis, pyridine and pyrimidine structures have been recognized for their activities, rendering these attractive scaffolds to discover novel anticancer drugs (Prachayasittikul *et al*., 2017, Akhtar *et al*., 2017a). Coumarins fused with pyridine were synthesized and tested for biological activities such as antimicrobial and anti-cholinesterase (Alipour *et al*., 2012). Coumarins and quinolones are essential precursors to organic synthesis and are present in many natural compounds with a wide range of biological activities (Ansary *et al*., 2019). A series of 3-acetyl coumarins were synthesized by condensing salicylaldehyde and ethyl acetoacetate, which was brominated to yield 3-bromo acetyl coumarins. 3-bromo acetyl coumarins on treatment with methyl and ethyl esters of nicotinic acid, isonicotinic acid yielded 3-coumarinoyl pyridinium bromides (a-l) and with quinoline yielded 3-coumarinoyl quinolinium bromides (m-o) (Porwal *et al*., 2010). The synthesized pyridine/quinolone coumarin derivatives are shown in Figure 8.

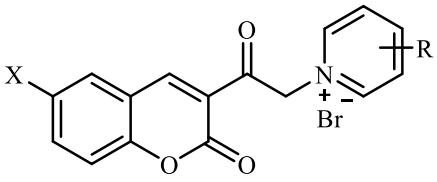

9A-L

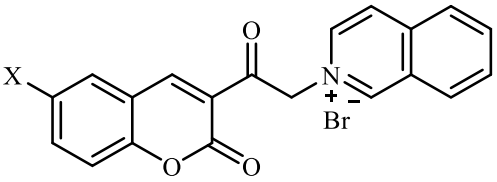

10M-O

Code	X	R
9A	H	p-$COOC_2H_5$
9B	Br	p-$COOC_2H_5$
9C	Cl	p-$COOC_2H_5$
9D	H	m-$COOC_2H_5$
9E	Br	m-$COOC_2H_5$
9F	Cl	m-$COOC_2H_5$
9G	H	p-$COOCH_3$
9H	Br	p-$COOCH_3$
9I	Cl	p-$COOCH_3$
9J	H	m-$COOCH_3$
9K	Br	m-$COOCH_3$
9L	Cl	m-$COOCH_3$
10M	H	
10N	Br	
10O	Cl	

Figure 8: Synthesised pyridine/quinoline-coumarin derivatives (Porwal *et al*., 2010).

2.5 Pharmacological activities of coumarins analogues

2.5.1 Coumarin in cancer therapy

Anticancer drugs have the potential to inhibit the division of cancer cells utilizing various mechanisms, including DNA cross-linking agents, topoisomerase inhibitors, cytoskeleton disrupting agents and anti-metabolites (Klenkar and Molnar, 2015). Coumarins inhibit kinase activity, induced apoptosis, angiogenesis inhibition, heat shock protein inhibition, telomerase inhibition, antiproliferative activity, carbonic anhydrase inhibition, monocarboxylate transporters inhibition, aromatase inhibition, and sulfatase inhibition in cancer (Thakur *et al*., 2015). An integrated approach using scientific knowledge is needed to treat and manage cancer. One such approach for improving existing therapeutic strategies to treat cancer is mainly inducing the cell death process, known as apoptosis. Apoptosis programs are significant for the therapeutic effectiveness of many anticancer remedies (Fulda, 2015).

2.5.1.1 Overview of apoptosis

Apoptosis is defined as programmed cell death consisting of different genetic and biochemical pathways that participate significantly in the development and homeostasis in normal tissues (Wlodkowic *et al*., 2011). It plays a role in removing unnecessary cells to maintain a healthy balance between cell survival and cell death in metazoan (Hassan *et al*., 2014). Cell death plays a critical function in various biological processes, starting from embryogenesis to immunity (Tait *et al*., 2014).

2.5.1.1.1 Morphological characteristic of apoptosis and necrotic cells

2.5.1.1.1.1 Apoptotic cells

Apoptosis is an essential strategy for maintaining the dynamic balance in living systems. Apoptotic cell death plays a crucial role in various biological processes; it is a regulated physiological process that involves the programmed death of cells to allow the degradation of dysfunctional or damaged cells (Vermeulen *et al*., 2005). Figure 8 shows how apoptotic cells have a different shape during the apoptotic process. When a cell receives a signal to die, it begins to express proteins that aid in the death process, eventually improving the activity of a set of enzymes that break other proteins. These enzymes break down cytoskeleton components, causing the cell to round up and shrink (Kroemer *et al*., 2005, Baig *et al*., 2017). Chromatin condensation begins at the nuclear membrane's perimeter, generating a crescent or ring-like shape; the chromatin then condenses farther into the cell until it breaks apart (Wong, 2011). The plasma membrane is undamaged during the entire process; some morphological features were observed at the later stage of apoptosis and consisted of membrane blebbing, ultrastructural modification of cytoplasmic organelles, and a loss of membrane integrity (Kroemer *et al*., 2005). The apoptotic blebs are eventually engulfed and destroyed by scavenger cells called macrophages.

2.5.1.1.1.2 Necrotic cells

The substitute for apoptotic cell death is necrosis, considered a toxic procedure (Elmore, 2007). Necrosis results in the disruption and progressive breakdown of cell structures in response to environmental agitation, such as mechanical trauma, extreme temperatures, and severe hypoxia (Krysko *et al*., 2008). In contrast, necrosis is characterized by rapid cytoplasmic swelling; it

culminates in rupture of the plasma membrane and organelle breakdown. The physicochemical stressors that cause necrosis, like heat, osmotic shock, and mechanical stress, have long been known. Because of the direct effect of stress on the cell, cell death happens quickly in these circumstances. As a result, cell death has been characterized as uncontrollable (Krysko *et al.*, 2008).

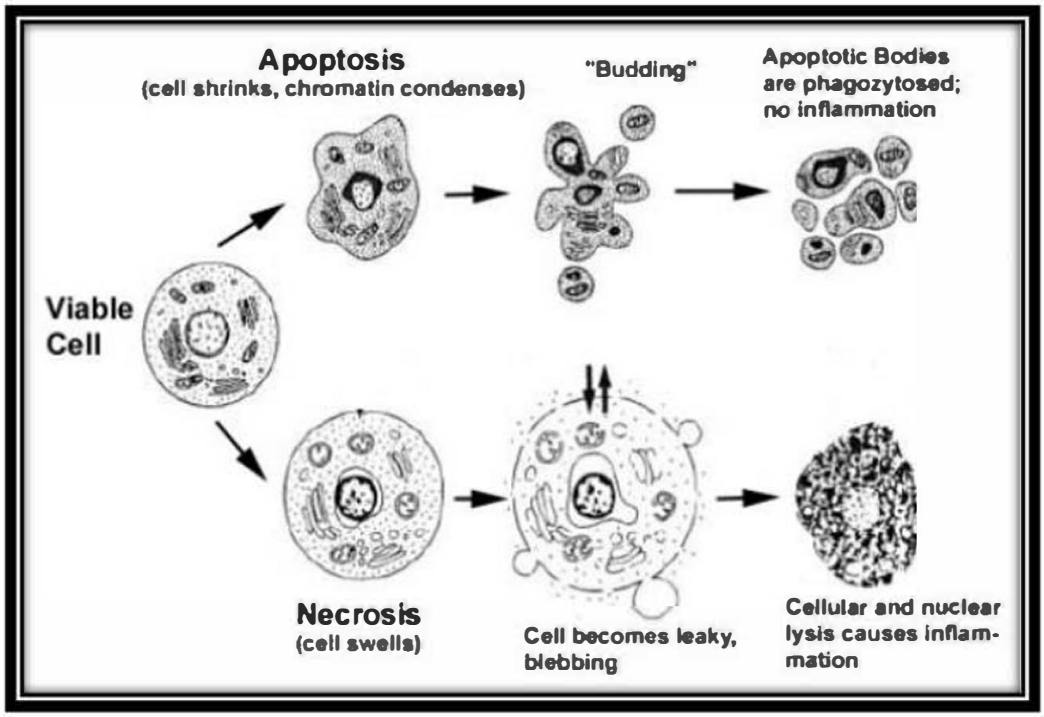

Figure 8: Morphological characteristics of a cell undergoing apoptosis or necrosis (Van Cruchten and Van Den Broeck, 2002).

2.5.1.2 Apoptosis signaling pathways

Caspases are essential to the apoptosis mechanism because they are both initiators and executors. For apoptosis to occur and be detected, it is necessary to understand how this highly complex process operates. Apoptosis is executed by two distinct signaling pathways that converge on the activation of executioner caspase-3 and Caspase-7, called intrinsic (or mitochondrial) and extrinsic (or death receptor) pathways of apoptosis (Kaiser *et al.*, 2013). Both mechanisms converge at activating intracellular caspases, which belong to a family of cysteine-dependent aspartate-directed proteases (Vermeulen *et al.*, 2005). These proteases are essential for the execution and signaling of events of apoptosis.

2.5.1.2.1 Intrinsic apoptotic pathway

The characteristic apoptotic pathway is initiated by various intracellular stimuli, oxidative stress, DNA damage, hypoxia, and growth factor deficiency, which cause permeabilization of the external mitochondrial membrane (Galluzzi *et al*., 2012). Furthermore, the intrinsic route, regulated by mitochondrial proenzymes, contributes to apoptosis. External or intracellular signals activate a cell in both cases; external mitochondrial membranes become permeable inside cytochrome c (Wong and Puthalakath, 2008, Su *et al*., 2015). During apoptosis, pro-apoptotic Bax dimerization and insertion into the external mitochondrial membrane cause the intrinsic apoptotic pathway. Cytochrome c is released into the cytosol after mitochondrial permeabilization. It binds to apoptotic protein and results in the activation of factor-1 (Apaf-1), which initiates the production of apoptosome (Ouyang *et al*., 2012). The apoptosome is a multi-protein platform with a seven-spoke wheel-shaped complex and is essential for enlistment after caspase-9 is initiated (Yuan and Akey, 2013). Caspase-9 activates caspase-3 once initiated, which converges in apoptosis (Galluzzi *et al*., 2012, Altieri, 2010).

2.5.1.2.2 Extrinsic apoptotic pathway

Death receptors activate the extrinsic apoptotic pathway, cell-surface receptors that bind specific ligands and convey apoptotic signals. Such ligands include tumour necrosis factor family soluble molecules that bind TNF-receptor family members along with TNFR-1, Fas/ CD95, and DR-4 and DR-5 TRAIL receptors. Ligand binding induces trimerization and eventual activation of the receptors (Mathew *et al*., 2009, Ouyang *et al*., 2012). TNF-receptor contains a death domain that attracts other protein-containing death domains, such as TNF-receptor type 1-connect death domain protein and Fas-associated protein with death domain. Such proteins bind to the initiator caspases-8 and 10, thereby allowing homodimerization and the eventual initiation of death-inducing complex signaling (Lee *et al*., 2012, Pennarun *et al*., 2010). The DISC initiates the assembly and activates procaspase-8 and then processes downstream caspases, cleaving specific substrates leading to cell death (Chowdhury *et al*., 2008). The activation of the execution effectors caspases, together with caspase 3/6/7, is the last step of apoptosis, whether extrinsic or intrinsic. These caspases trigger the activation of cytoplasmic endonucleases, which break down nuclear material and proteases, which degrade nuclear and cytoskeletal proteins (Zahedifard *et al*., 2015).

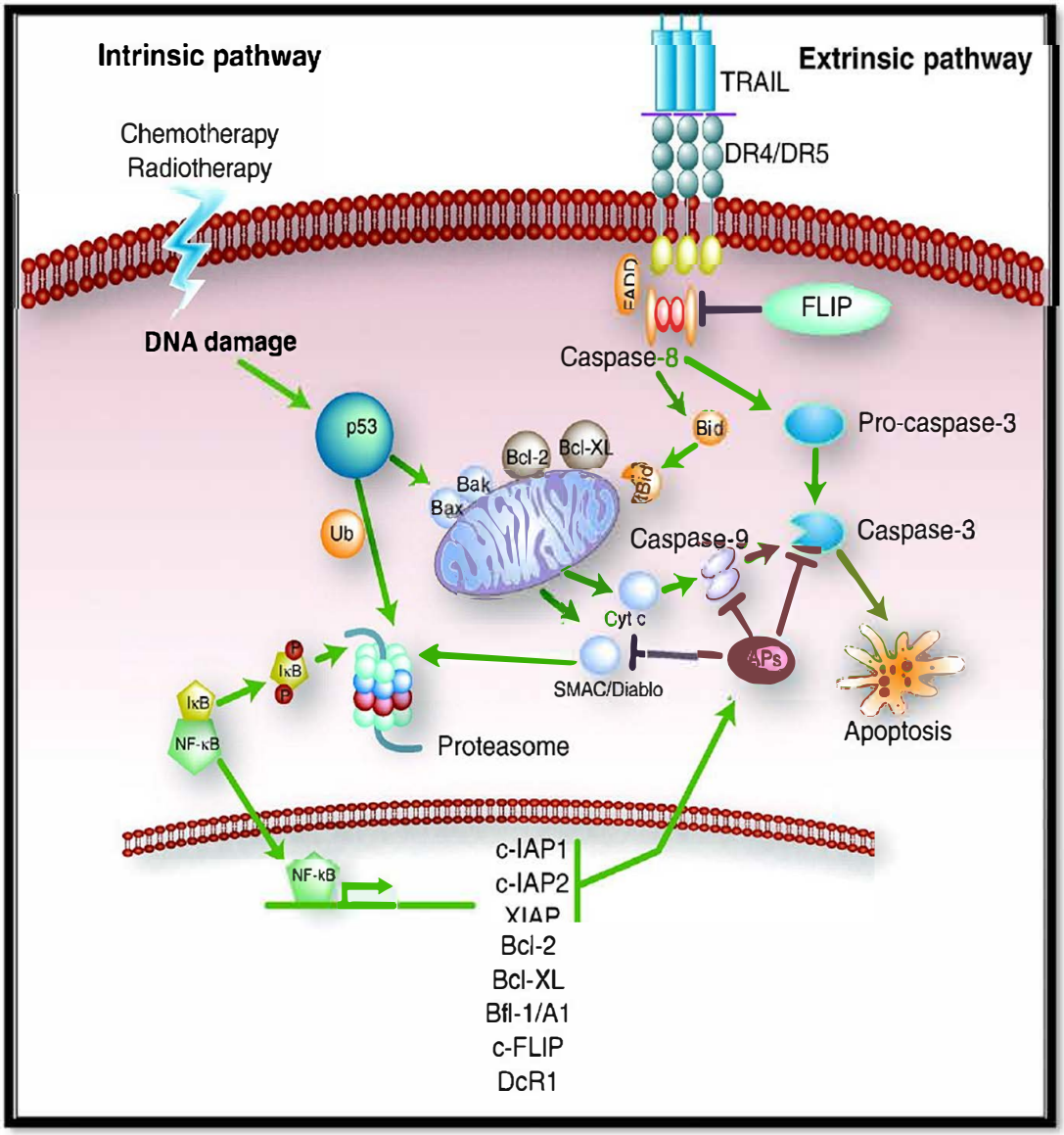

Figure 9: Intrinsic and extrinsic apoptotic pathways (de Vries *et al.*, 2006).

2.5.1.3 Anticancer activity of coumarin analogues

Thota *et al.* (2015) synthesized a series of coumarin thiazole derivatives as anticancer agents against molt 4/C_8, CEM, L1210, BEL7402 and HL60 cells. The results showed that these compounds demonstrated cytotoxicity ranging from 6.2 to 18µg/mL against CEM, 8.2 to 21 µg/mL against L1210, 09 to 19µg/mL against molt 4/C_8, 8.6 to12 µg/mL against HL60 and 8 to 16 µg/mL against BEL7402 cells, respectively. Compounds **11** and **12** were the most reported active agents against the tested cells (Thota *et al.*, 2015).

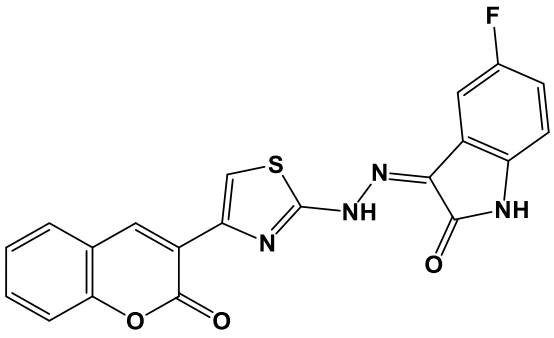

11

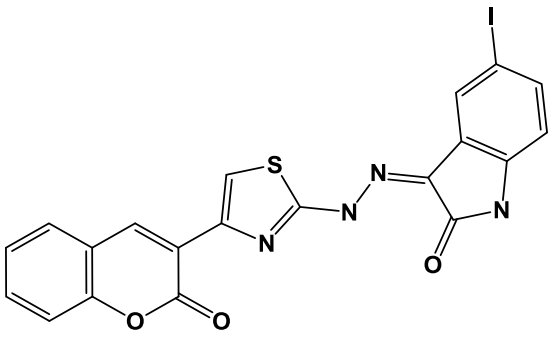

12

Similarly, Zhang *et al*. (2014) synthesized and assessed a series of 4-(1, 2, 3-triazol-1-yl) coumarin for its potential anticancer activity against three cancer cell lines, including MCF-7, SW480 and A549. These compounds exhibited remarkable antitumor activity, with compound **13** being the most potent with IC_{50} of 5.89, 1.99 and 0.52 μM against MCF-7, SW480, and A549, respectively, comparable to doxorubicin control (Zhang *et al*., 2014).

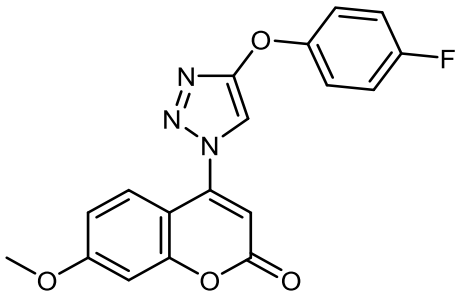

13

Ayati *et al*. (2018) synthesized 3-(4-aminothiazole-5-carbonyl)-2H-chromen-2-ones containing cyclic amine, cyclic amine substitute, aniline or aniline or aniline substitute and assessed their anticancer potentials. The findings showed that most compounds displayed good cytotoxicity activity against MCF-7, HepG2 and SW400 cells. Compound **14** was the most active, with IC_{50} values ranging from 7.5 to 16.9 μg/mL (Ayati *et al*., 2018).

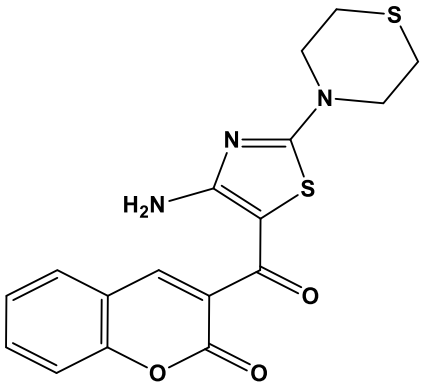

14

Another study by Kamath *et al*. (2015) involved the synthesis and evaluation of new indole coumarin hybrids for their anticancer properties against the MCF-7 cancer cell and normal cell line (Vero). The results revealed that compounds 1**5, 16** and 1**7** were the most active against MCF-7 cells with IC_{50} values of 7.4, 5.5, 13.5 µM, respectively (Kamath *et al.,* 2015).

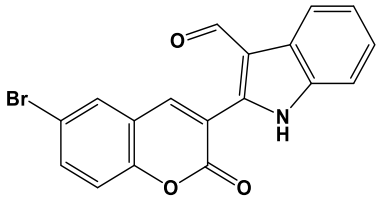

15

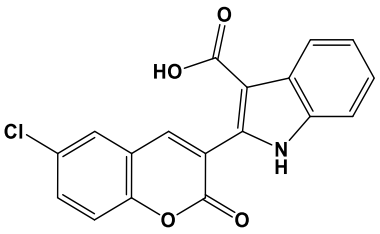

16

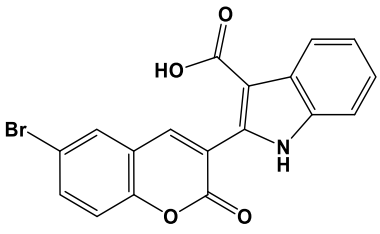

17

Also, Goud *et al*. (2019) synthesized several novel coumarin triazole hybrid morpholines and evaluated their anti-proliferative potential against bone (MG-63), lung (A549), breast (MDA-MB-231), colon (HCT-15), and liver (HepG2) cancer cells. Compound 1**8** was the most active with an IC_{50} value of 0.80 ± 0.22 µM against MG-63 cells (Goud *et al*., 2019).

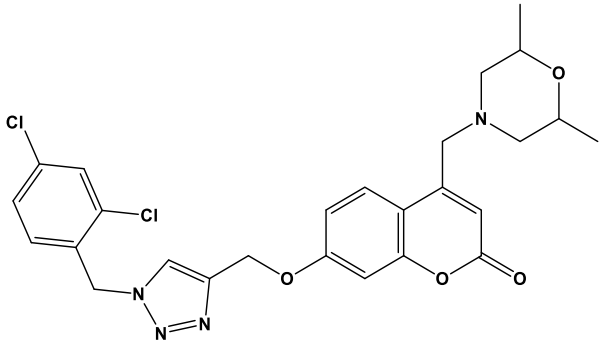

18

In 2019, Durgapal and Soma designed and synthesized coumarin-proline sulphonamide derivatives and evaluated their anticancer activity against cancer cell A549 and MCF-7, as well as their antidiabetic potential. Of the compounds evaluated, compound 1**9** was the most promising with an IC_{50} value of 1.07 µM against MCF-7 cells, while others displayed moderate activity (Durgapal and Soman, 2019).

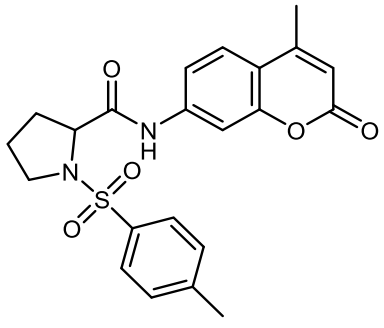

19

Just recently, Kurt *et al*. (2020) designed, synthesized and tested a series of coumarin chalcone derivatives containing urea moiety against H4IIE and HepG2 cells for their anticancer capacity. The results revealed that most compounds showed excellent antitumor activity against the tested cells. Compounds **20** and **21** elicited the most significant effect against H4IIE and HepG2 cells with IC_{50} values of 1.62 and 2.326 µM, respectively (Kurt *et al*., 2020).

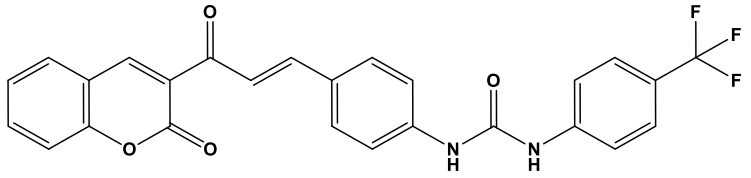

20

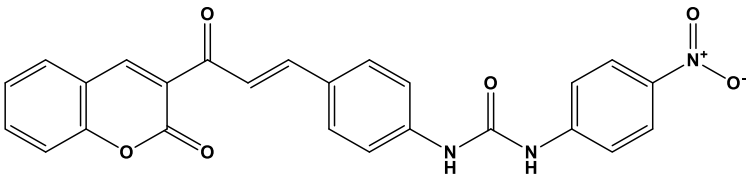

21

A series of coumarin pyridine/fused pyridine hybrids were designed, synthesized and accessed by Fayed *et al*. (2019) for their anticancer activities against MCF-7, HCT-116, HepG and A549 cells. The results demonstrated that compounds **22**, **23** and **24** were the most active, with IC_{50} values ranging from 1.1 to 2.4 µM against MCF-7 cells (Fayed *et al*., 2019).

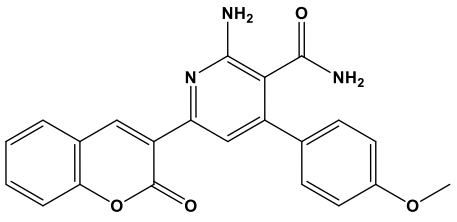

22

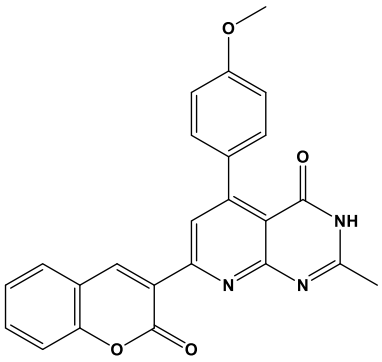

23

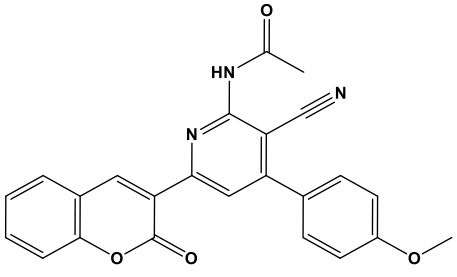

24

Chougala *et al*. (2015) synthesized a series of 3-(3-benzofuranyl)-coumarin derivatives for their anticancer potential against the HeLa cell. The results showed that compounds **25**, **26** and **27** demonstrated anticancer activity against HeLa cells with IC_{50} values of 20 and 25 μg/mL, respectively (Chougala *et al*., 2015).

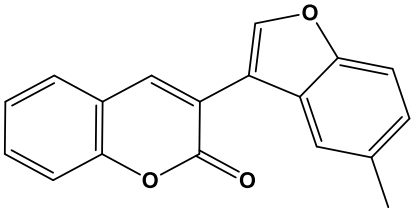

25

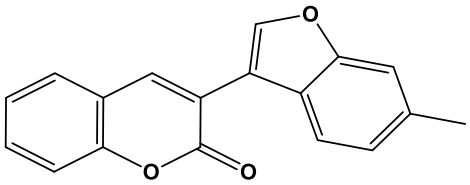

26

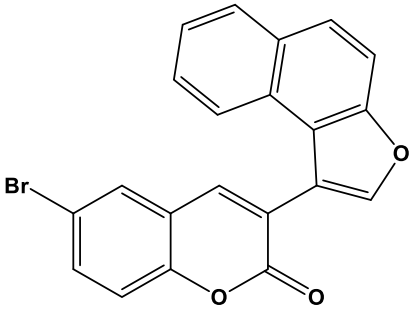

27

Kasumbwe *et al*. (2017) synthesized a series of mono/di- halogenated coumarins derivatives as anticancer agents against MCF-7(Human breast cancer cell) and UACC-62 (Human melanoma cell lines) cells. The results revealed that compounds **28**, **29**, **30** and **31** strongly suppressed cell proliferation of MCF-7 and UACC-62 cells. Compounds **29** and **30** were the most active against UACC-62 cancer cells with IC_{50} values of 7.28±0.03 and 1.77±0.01, respectively (Kasumbwe *et al*., 2017).

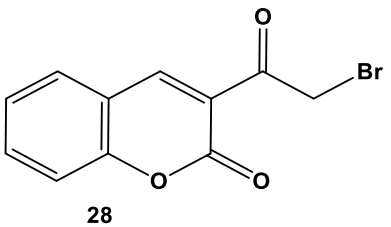

28

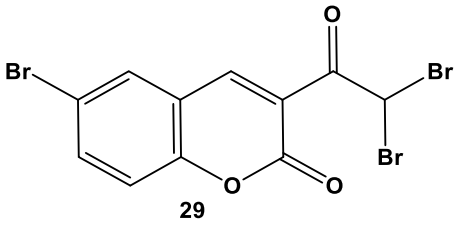

29

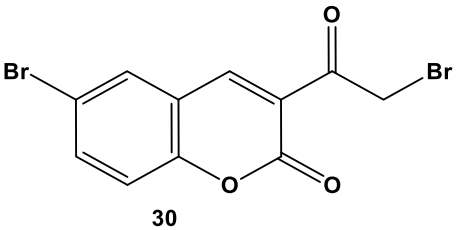

30

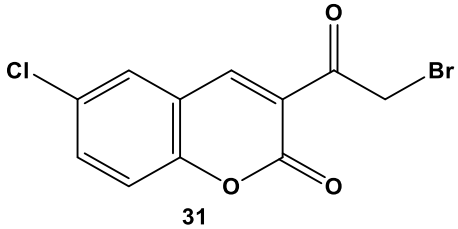

31

2.5.2 Coumarin as antimicrobial agent

Today, the number of multidrug-resistant bacteria is increasing. Several Gram-positive bacteria such as *Staphylococcus aureus* and fungi such as Candida species resist the chemotherapeutic agents currently available (Klein *et al*., 2007, Okuma *et al*., 2002). The resistance process continuously develops in pathogenic bacteria to the available antimicrobial agents (V Patel *et al*., 2012). Lack of successful treatments is the cause of this problem; despite the accessibility of various antibiotics, the growing clinical importance of drug-resistant microbial pathogens has lent to supplementary need in microbiological and antifungal research (Sahoo and Paidesetty, 2017). The growing population of antibiotic resistance of bacterial strains due to enzymatic drug inactivation, modification of target sites, and efflux extrusion has become a significant task in drug design and discovery research (Renuka and Kumar, 2015).

A potential solution to antibiotic resistance is designing and investigating new heterocyclic compounds with a novel mode of action (Desai *et al*., 2013). The coumarin skeleton has been identified as part of the structure of a few antibiotics. Novobiocin is derived from *Streptomyces niveus* and is most potent against Gram-positive bacteria (Smyth *et al*., 2009). Coumarin derivatives have a broad range of structural changes and may act as molecular models for new drugs. Coumarin derivatives are also known as possible antimicrobial agents (Shi and Zhou, 2011, Al-Majedy *et al*., 2017).

A series of thiazole-containing coumarin derivatives were synthesized and screened by Osman *et al*. (2018b) as antibacterial agents against two Gram-positive (*S. pneumonia and S. aureus*) and three Gram-negative bacteria (*E. coli, E. aerogenes and S. typhi*). The results revealed compounds 32 and 33 were the most promising among the synthesized compounds, with a MIC value of 73 μM against all tested bacteria (Osman *et al*., 2018b).

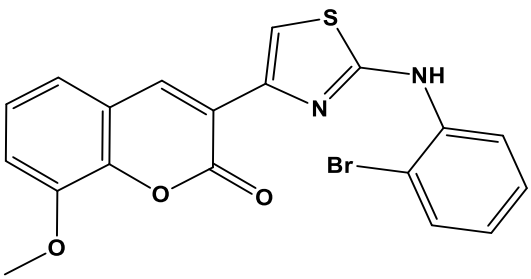

32

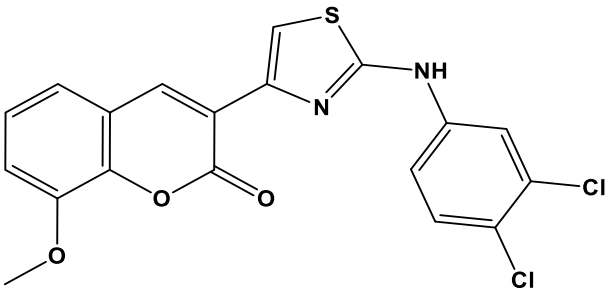

33

Aggarwal *et al*. (2013) synthesized and screened new series of 2-(5-hydroxy-5-trifluoromethyl-4-5 dihydropyrazol-1-yl)-4-(coumarin-3-yl) thiazoles for their antibacterial activity against *S. aureus, B. subtilis, S. Epidermidis, K. aerogenes, E. coli, P. mirabilis,* and *P. aeroginosa*. The results demonstrated that all tested compounds showed moderate to good antibacterial activity. Compounds **34** and **35** were the most effective against *E. coli* and *P. mirabilis* with MIC values of 2 and 4 µg/mL, respectively (Aggarwal *et al*., 2013).

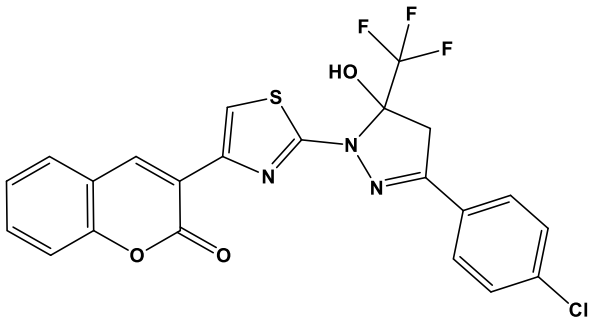

34

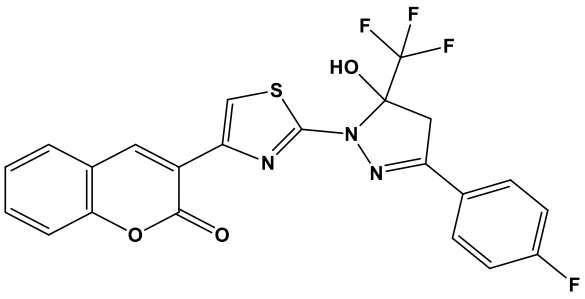

35

A new series of coumarin-tagged β- lactam triazole hybrid was synthesized and tested by Dhawan *et al*. (2020) for their antimicrobial activity against *Pseudomonas aeruginosa*, *Klebsiella pneumonia*, *Escherichia coli, Acinetobacter baumannii,* and two fungal including *Candida albicans* and *Cryptococcus neoformans*. The results showed that compounds **36** and **37** had shown moderate antimicrobial activity against *Pseudomonas aeruginosa* and *Candida albicans* strains (Dhawan *et al*., 2020).

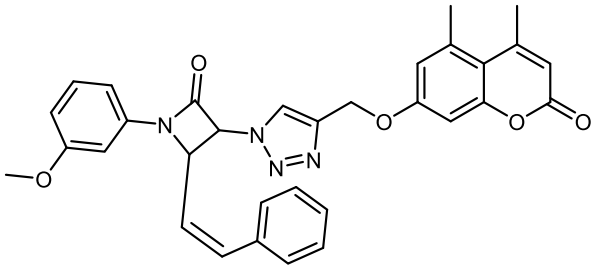

36

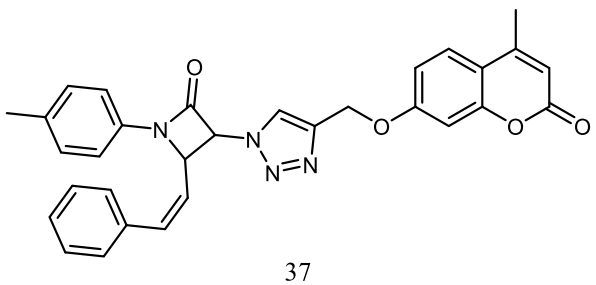

37

Laxmi *et al*. (2013) synthesized a series of coumarin pyrazole pyrimidine 2, 4, 6(*1H, 3H, 5H*) triones and thioxopyrimidine 4, 6(*1H, 5H*) diones for their antibacterial and antifungal activity against *bacillus subtilis, Staphylococcus aureus, Staphylococcus epidermidis, Escherichia coli, Pseudomonas aeruginosa, Klebsiella pneumonia, and* fungi, *Aspergillus niger*. The results showed that these compounds were moderately active against the microorganisms used. Compounds **38** and **39** demonstrated good antifungal activity with 14 and 7 mm inhibition zone, respectively, against *Aspergillus niger* (Laxmi *et al*., 2013).

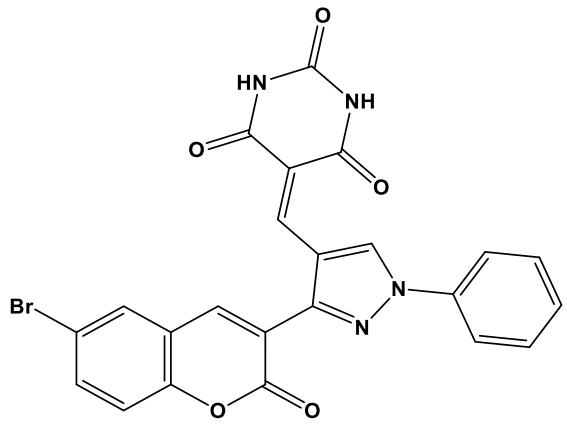

38

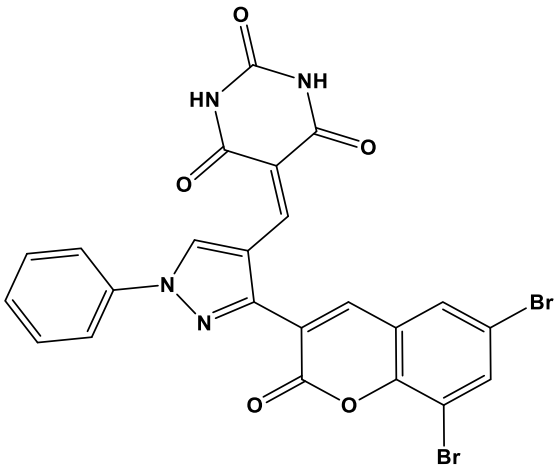

39

In another study, a series of oxadiazole and pyrazole derivatives were designed and synthesized by Mahesh *et al*. (2016) as possible antimicrobial agents against *Staphylococcus aureus, Escherichia coli,* and *Aspergillus niger*. Among all tested derivatives, compounds **40** and **41** were more active against all microorganisms with a MIC value of 75 µg / mL (Mahesh *et al*., 2016).

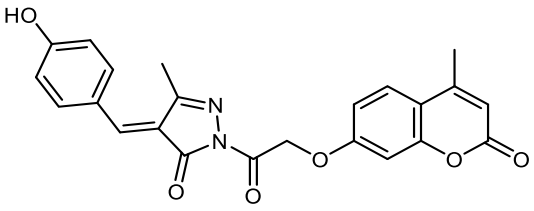

40

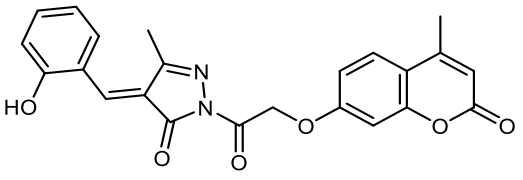

41

Sanad and Mekky, (2020) synthesized and evaluated a series of nicotinonitrile coumarin hybrids for their antibacterial activity against *Escherichia coli, Klebsiella pneumonia, Pseudomonas aeruginosa, Staphylococcus aureus,* and *Streptococcus mutans*. The results showed that compounds **42** and **43** were the most promising among synthesized compounds, with MIC values ranging from 1.9 to 7.8 and 3.9 to 15.6 µg/mL, respectively, against the tested bacterial strain (Sanad and Mekky, 2020).

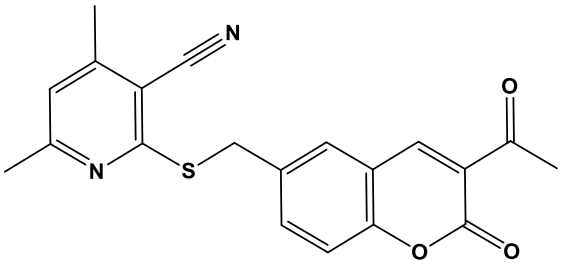

42

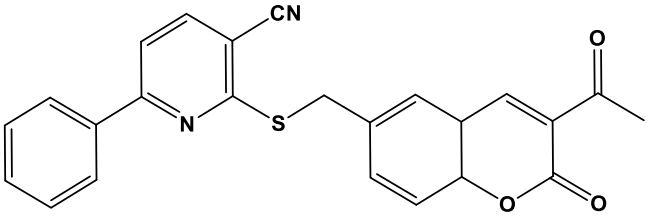

43

Mangasuli *et al*. (2018b) designed, synthesized and assessed the antifungal efficacy of carbonodithioate derivatives of coumarin against *Aspergillus flavus, Trichoderma harzianum, Penicillium chrysogenum,* and *Candida albicans*. The results demonstrated that compound **44** was the most potent against *Aspergillus flavus* and *Trichoderma harzianum,* with a MIC value of 0.25µg/mL. In contrast, compound **45** exhibited excellent antifungal activity against *Aspergillus flavusand Trichoderma harzianum* with a MIC of 0.5 µg/mL (Mangasuli *et al*., 2018b).

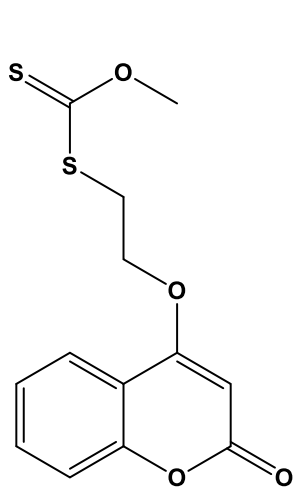

44

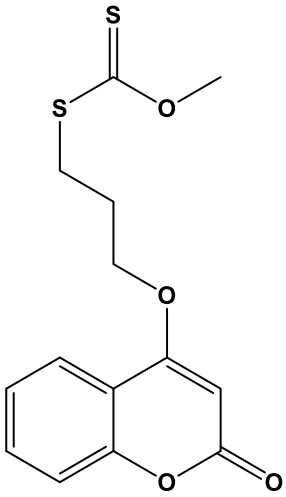

45

In another development, Bhagat *et al*. (2019) synthesized novel indolinedione coumarin hybrids as antimicrobial agents against *Escherichia coli, Salmonella enteric, Staphylococcus aureus* and fungi, *Candida albicans, Alternaria mali, Penicillium sp*., and *Fusarium oxysporum*. The results revealed that compounds **46** and **47** showed the best growth inhibitory activity with 30 and 312 µg/mL MIC values against *Penicillium sp.* and *S. aureus,* respectively (Bhagat *et al*., 2019).

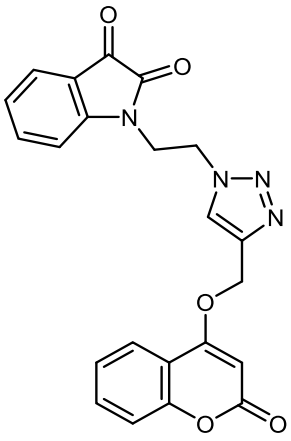

46

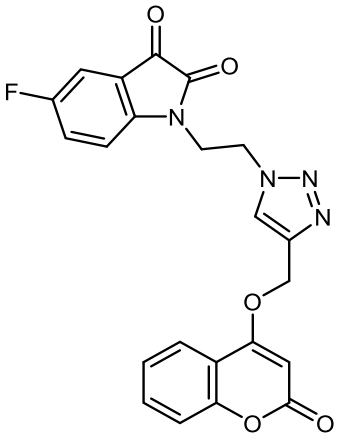

47

Liu *et al*. (2020) synthesized and evaluated a series of thiazolyl esters of coumarin derivatives as an antibacterial agent against *Staphylococcus aureus, Listeria monocytogenes* and *Escherichia coli*. Compound **48** was the most active among all synthesized analogues with MICs values of 0.05, 0.05 and 8 µg / mL, respectively (Liu *et al*., 2020).

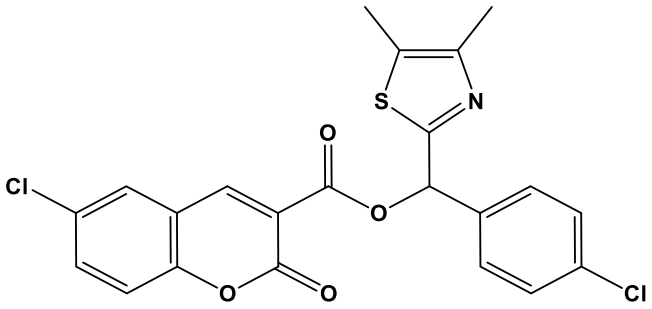

48

Ajani *et al*. (2019) synthesised a series 3-(5-(substituted-phenyl)-4, 5-dihydro-1*H*-pyrazol-3-yl)-2*H*-chromen-2-one and assessed their antibacterial activity. The results revealed that compound **49** emerged as the most potent antibacterial activity with MICs values of 3.91±0.22 µg/mL against *Staphylococcus aureus* and *Enterococcus faecalis* and 15.63±0.94 µg/mL against *K. pneumonia* and *P. vulgaris* (Ajani *et al*., 2019).

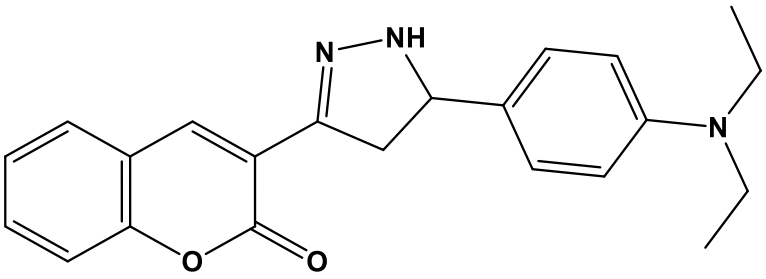

49

Jayashree *et al*. (2005b) synthesized novel triazole thiadiazinyl bromo coumarin derivatives and assessed the antibacterial efficacy against *Bacillus subtilis, Staphylococcus aureus, Escherichia coli, Klebsiella pneumoniae,* and *Pseudomonas aeruginosa*. The results showed that compounds **50** and **51** were the most potent with a zone of inhibition ranging between 27 to 34 mm and 36 to 40 mm, respectively, against *Bacillus subtilis, Staphylococcus aureus, Escherichia coli, Klebsiella pneumonia* and *Pseudomonas aeruginosa* (Jayashree *et al*., 2005b).

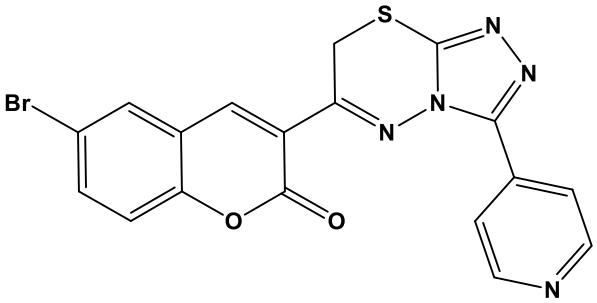

50

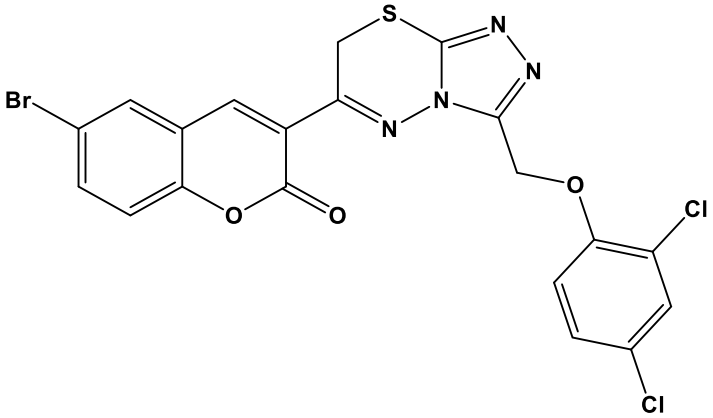

51

Jayashree *et al*. (2006) synthesized and assessed a series of triazolo thiadiazinyl chlorocoumarin derivatives for their antibacterial activity against *Bacillus subtilis, Staphylococcus aureus, Escherichia coli, Klebsiella pneumonia* and *Pseudomonas aeruginosa*. Among the synthesized analogues, compound **52** was the most active against the tested bacteria, with a zone of inhibition ranging from 38 to 42 mm compared to the standard drug amoxicillin (36 to 39 mm)(Jayashree *et al*., 2006).

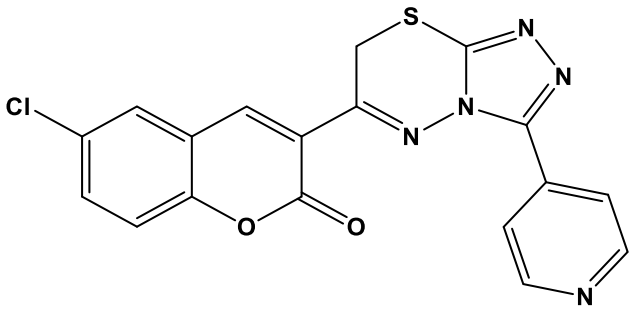

52

A series of triazole derivatives of coumarins was designed, synthesized by Jayashree *et al*. (2007) and assessed their antibacterial activity against *Bacillus subtilis, Staphylococcus aureus, E. coli, K. pneumonia* and *P. aeruginosa.* Compounds **53**, **54** and **55** have shown good

antibacterial activity with a zone of inhibition ranging between 31 to 38 mm, 40 to 43 mm and 18 to 36 mm, respectively, against the tested bacterial strain (Jayashree *et al*., 2007).

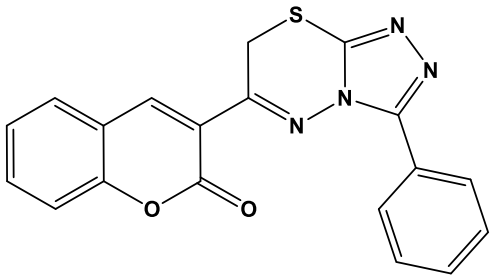

53

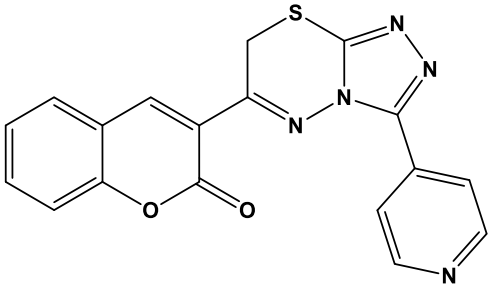

54

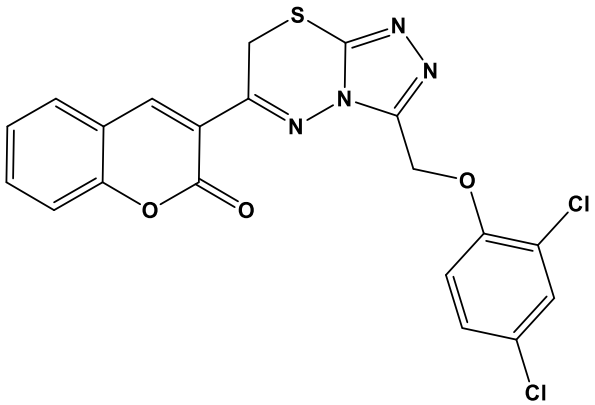

55

2.5.3 Coumarin as anti-mycobacterial agent

Mycobacterium tuberculosis, a human pathogen causing tuberculosis, claims more lives than other bacterial pathogens (Manvar *et al*., 2008). Despite the availability of a wide range of drugs, tuberculosis continues to be a significant threat to humans. The main obstacle to tuberculosis eradication is the emergence of *Mycobacterium tuberculosis* resistance to existing drugs. This resulted in multidrug-resistant tuberculosis (MDR-TB), extensively resistant tuberculosis (XDR-TB) and totally drug-resistant tuberculosis (TDR-TB) (Basanagouda *et al*., 2014, Reddy *et al*., 2021). Another problem is the co-morbidity of TB with HIVAIDS, and in some cases, almost two-thirds of people infected with TB are still seropositive to HIV-1. The rationale for developing new structural groups of antituberculosis drugs comes from the appearance of multi-drug resistant strains (MDR) to widely used medications, considerably longer therapy durations needed due to resistance, and disease resurgence in immune-compromised patients (Nayyar and Jain, 2005).

Among the oxygen heterocycles, coumarin moiety is well-regarded as a 'privileged' structural motif due to its extensive range of pharmacological, biological such as anticancer and antituberculosis. Moreover, coumarin's unique structure allows its derivatives to interact readily with a diversity of biomacromolecules through weak interactions and thus exhibit broad potential in medicines (Peng *et al*., 2013). Coumarin-derived compounds were explored as promising lead targets in medicinal chemistry and were also recently considered potential candidates for tuberculosis treatment (Liu *et al*., 2018).

Patel *et al*. (2013) designed and synthesized a series of coumarin-based 1, 3, 4-oxadiazol-2ylthio-*N*-phenyl/benzothiazolyl acetamides and assessed their *in-vitro* anti-mycobacterial activity against *Mycobacterium tuberculosis* H37Rv. The results showed that compounds **56** and **57** were the most promising anti-mycobacterial with a MIC value of 12.51 µg/mL, comparable to the reference drug pyrazinamide (6.25 l µg /mL) (Patel *et al*., 2013).

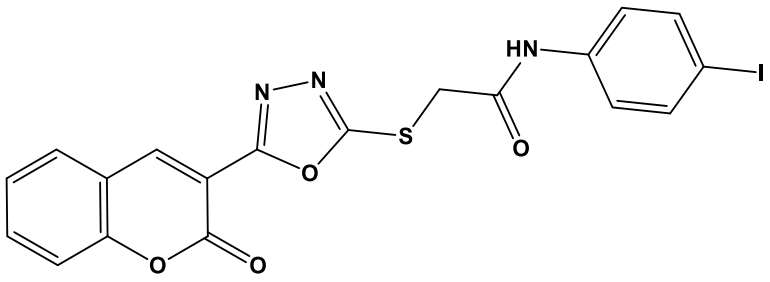

56

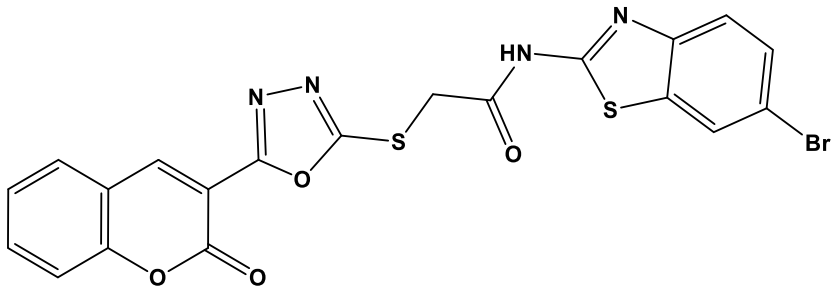

57

In another study, Yusufzai *et al*. (2017) synthesized a series of hydrazinyl thiazolyl coumarin derivatives for their *in-vitro* anti-mycobacterial activity against *Mycobacterium tuberculosis* H37Rv (ATCC 25618). The results revealed that compounds **58, 59, 60, 61** and **62** were the most potent antitubercular agents with a MIC value of 50 µg / mL (KhanYusufzai *et al*., 2017).

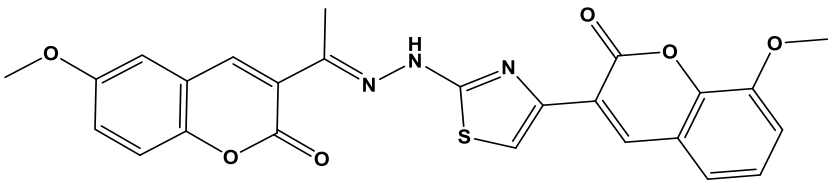

58

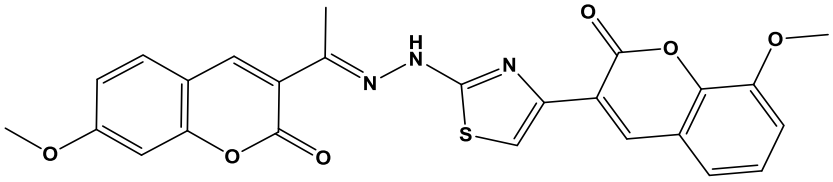

59

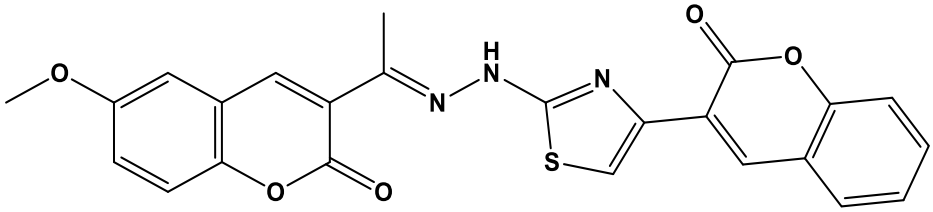

60

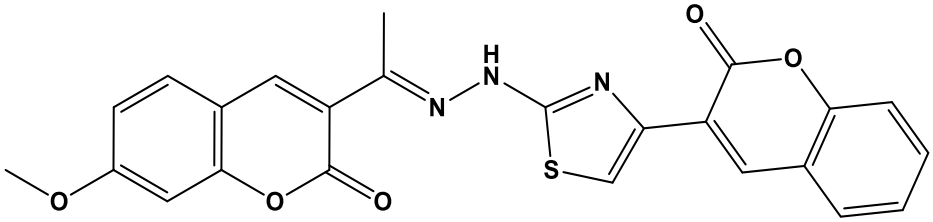

61

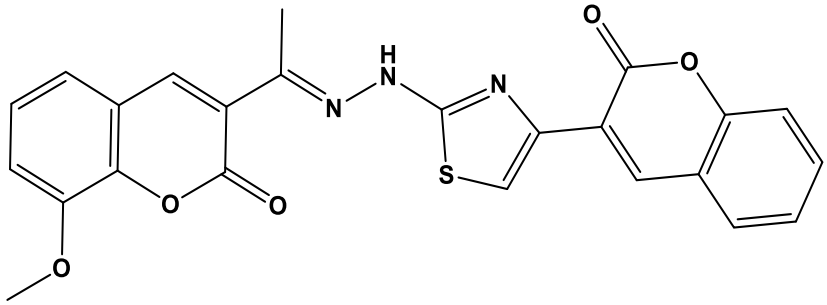

62

Furthermore, a series of novel hydrazide hydrazone derivatives with 2*H*-chromene and coumarin scaffold was synthesized by Angelova *et al*. (2016) for their anti-mycobacterial activity against H37Rv strains of *Mycobacterium tuberculosis*. Isoniazid and ethambutol were used as reference drugs. Compounds **63, 64** and **65** were the most active with MIC values of 0.13, 0.15 and 0.17 μM, respectively, against H37Rv strains of *Mycobacterium tuberculosis* (Angelova *et al*., 2017).

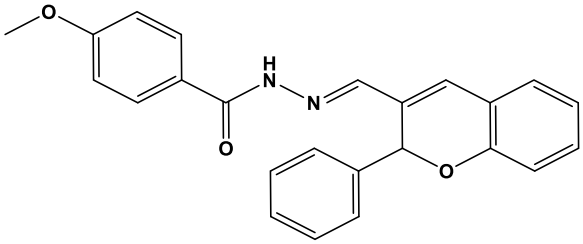

63

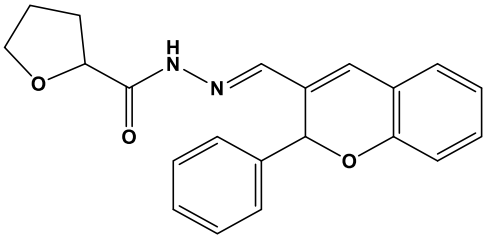

64

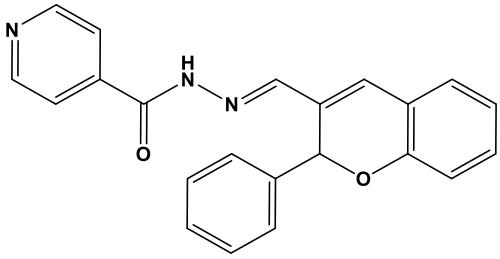

65

Reddy *et al*. (2018) synthesized and evaluated a series of novel coumarin- oxime ethers anti-mycobacterial activity against H37Rv strains of *Mycobacterium tuberculosis*. The results demonstrated that compound **66** was the most active with a MIC value of 0.04 μg/mL, compared to the positive control, Isoniazid (0.02 μg/mL) (Reddy *et al*., 2018).

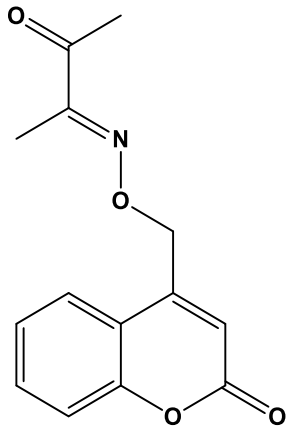

66

A series of hybrid coumarin analogues were synthesized and assessed by Hassan *et al*. (20219)for their anti-mycobacterial activity against the H37Rv TB strain. Among the newly synthesized compounds, the results showed that compounds **67** and **68** exhibited excellent anti-mycobacterial activity against H37Rv TB (Hassan *et al*., 2019).

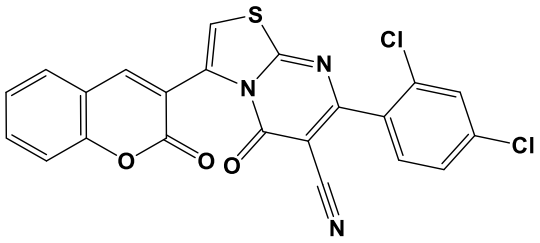

67

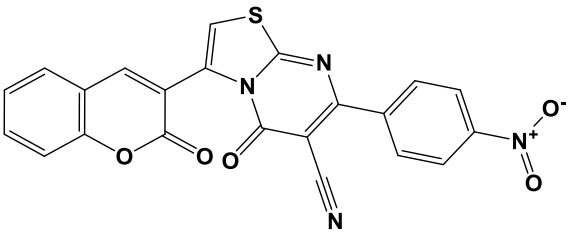

68

Danne *et al*., 2018 synthesized and evaluated a series of triazole-biscoumarin conjugates as a possible anti-mycobacterial agent against active and dormant Mtb H37Rv. The results demonstrated that compound **69** displayed excellent antitubercular activity against latent Mtb H37Rv, with a MIC value of 1.44 µg/mL (Danne *et al*., 2018).

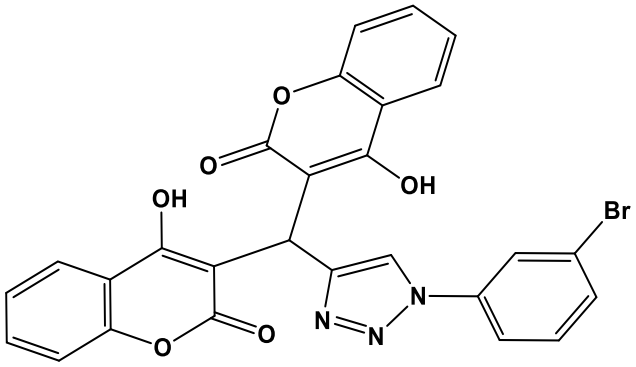

69

A series of polycyclic acridin-(9-yl-amino) thiazol-5-yl)-2*H*-chromen-2-one derivatives was synthesized by Mane *et al*. (2020) for their anti-mycobacterial efficacy against H37Rv MTB. Among the synthesized derivatives, compounds **70** and **71** showed excellent anti-mycobacterial activity with MICs values of 0.78 and 1.56 µg/mL, respectively (Mane *et al*., 2020).

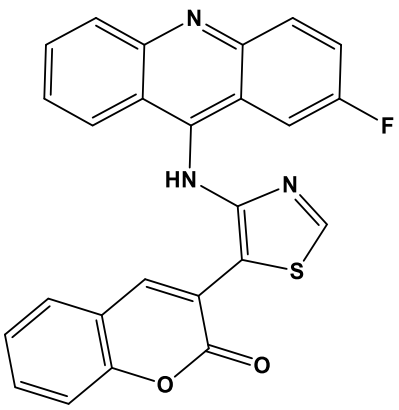

70

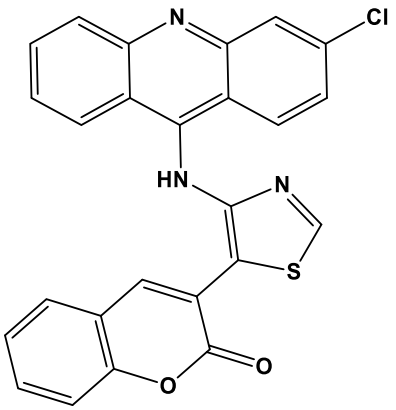

71

2.5.4 Coumarin as anti-antioxidant agents

Free radicals are independent molecular species that possess an unpaired electron in an atomic orbital; they are typically unstable and highly reactive. Critical metabolic processes usually produce these substances in the human body. Still, they may also come from environmental causes such as X-rays, pollution, tobacco smoke, air contaminants, and synthetic chemicals (Tataringa *et al*., 2016). Antioxidants play an important role in the body's protective system by controlling the production and removal of reactive oxygen species (ROS) induced by prolonged oxidative stress and regular metabolic activity, such as hydroxyl radicals, superoxide radicals, singlet oxygen, and hydrogen peroxide radicals. The body's protective mechanism involves superoxide dismutase (SOD), catalase and glutathione peroxidase, and antioxidants often control the ROS concentration by interfering with them and avoiding their effect on other molecules (Shaikh *et al*., 2016a). As a result, the discovery and development of innovative synthetic radical scavengers in organic chemistry have become extremely important. Several coumarin derivatives have a unique potential to scavenge free radicals or reactive oxygen species such as hydroxyl, superoxide, or hypochlorous acid and affect free radical damage processes (Patel Rajesh and Patel Natvar, 2011).

In a study conducted by Thota *et al*. (2015), a series of coumarin thiazole derivatives were synthesized and assessed for their antioxidant activity using the DPPH scavenging method. The results showed that these compounds showed moderate to high scavenging capacity compared to the standard drug. Compounds **72**, **73** and **74** were the most active with IC_{50} values of 11.04±0.18, 11.28±0.06 and 12.16±0.28 μg/mL, respectively (Thota *et al*., 2015).

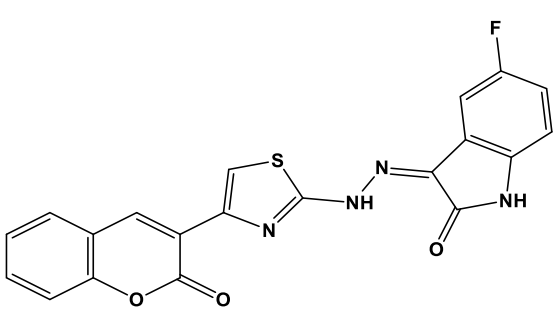

72

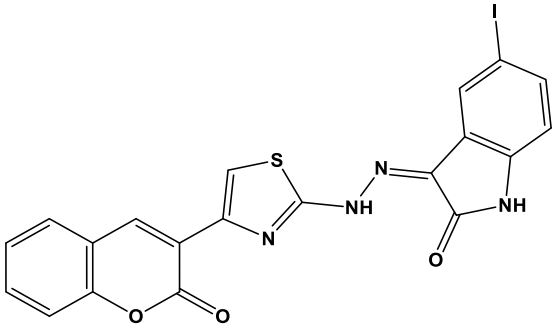

73

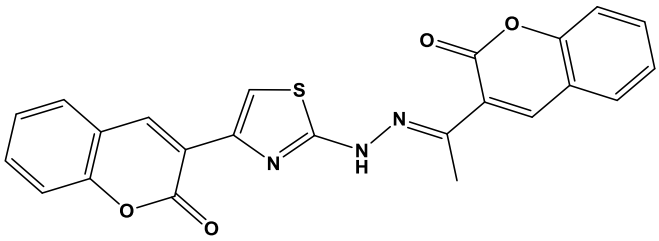

74

Kurt *et al*. (2015) designed and synthesized a series of urea/thiourea substituted coumarinyl thiazole derivatives as antioxidant agents. The results indicated that the most active compounds, **75**, **76**, **77**, **78** and **79**, exhibited high scavenging capacity with IC_{50} values of 1.64, 1.82, 2.69, 3.31 and 5.49 μM, respectively (Kurt *et al*., 2015).

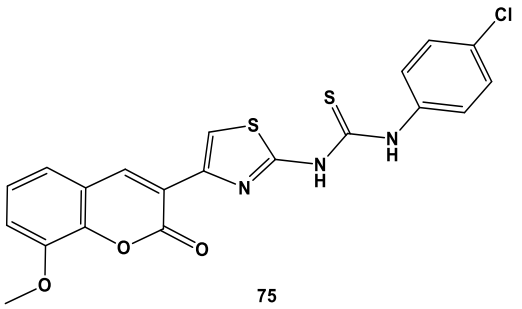

75

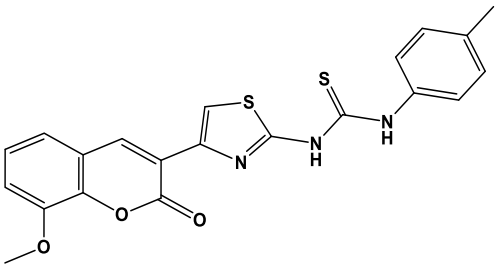

76

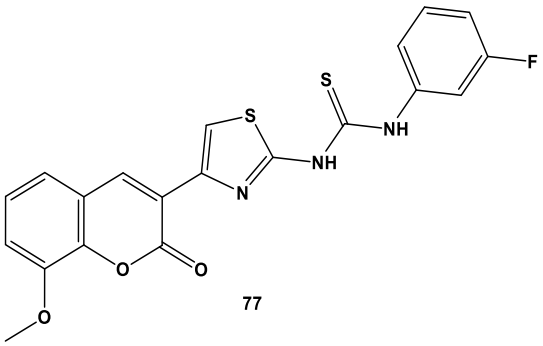

77

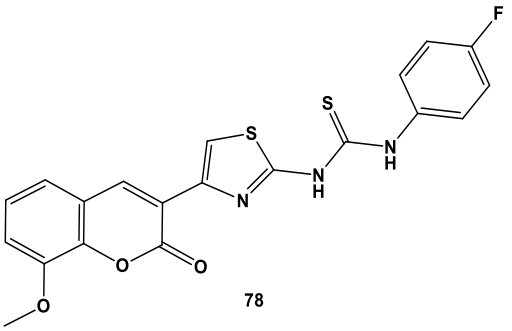

78

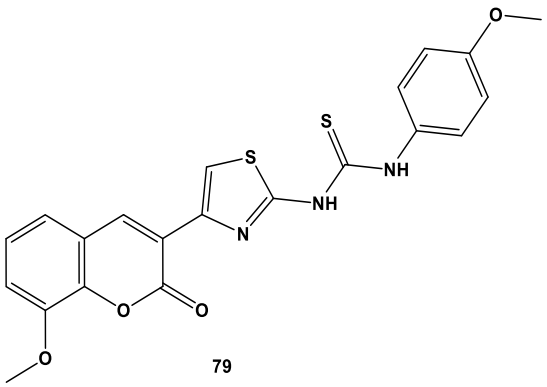

79

Chauhan et al. (2018) designed and synthesized a series of coumarin nuclei clubbed with thiazine scaffolds was and evaluated the antioxidant capacity using DPPH and ABTS bioassay. The results revealed that compounds **80** and **81** were the most active IC_{50} values of 33.9±0.3 and 35.3±0.47 µg/mL in DPPH and ABTS bioassay, respectively (Chauhan *et al*., 2018).

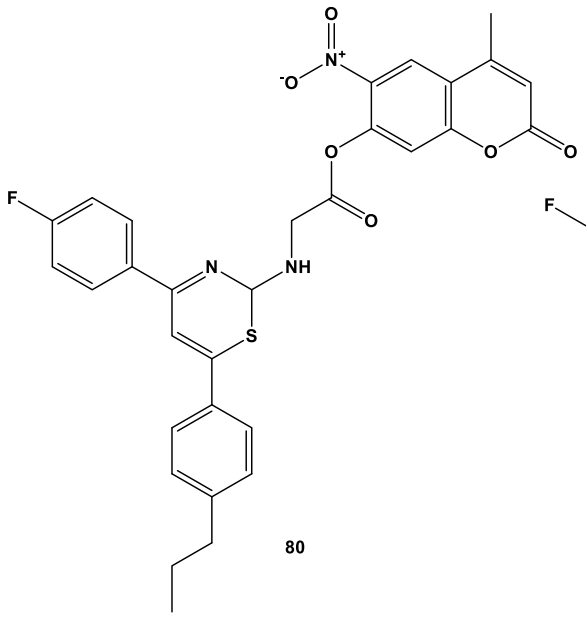

80

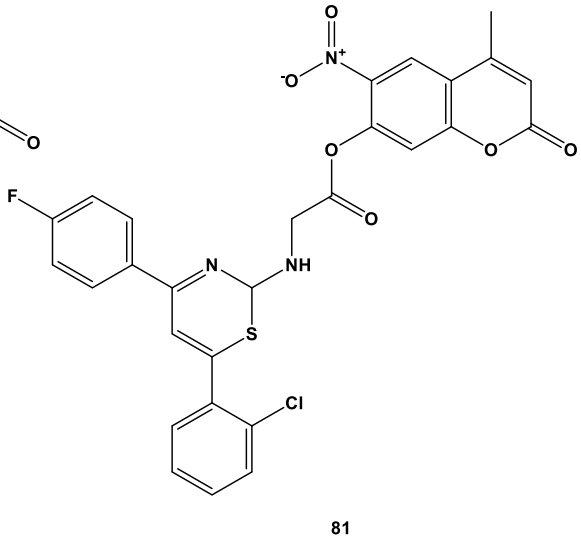

81

Shaikh *et al*. (2016) synthesized a series of coumarin-based 1, 2, 3 triazoles and evaluated their antioxidant activity. The results showed that compounds **82** and **83** having chloro-substituent on phenyl ring demonstrated potent antioxidant capacity with IC_{50} values of 12.48 and 16.30 µg/mL, respectively (Shaikh *et al*., 2016b).

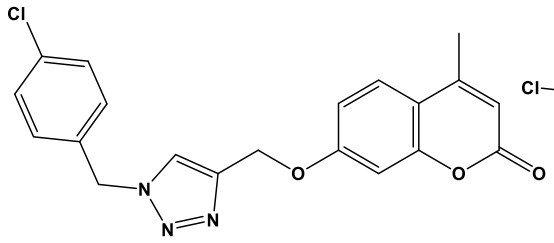

82

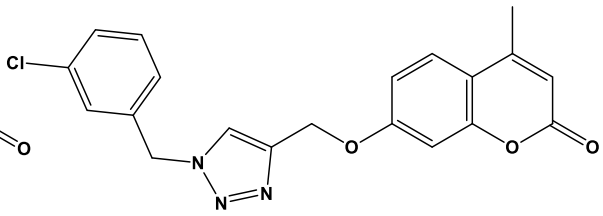

83

In another study, Matos *et al*. (2015) synthesized a series of hydroxylated 3-phenylcoumarins and assessed their antioxidant efficacy. The results showed that compound **84** was the most active in the four assays performed (ORAC-FL=11.8, the capacity of scavenging hydroxyl radicals=54%, TROLOX index=2.33, and AI_{30} index=0.18)(Matos *et al*., 2015).

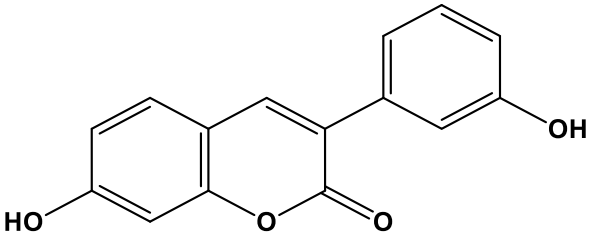

84

Shaikh *et al*. (2016) synthesized a series of 1, 2, 3 triazole incorporated coumarin derivatives as possible antioxidant agents. The results showed that all synthesized compounds exhibited high to moderate antioxidant capacity compared to the standard drug butylated hydroxytoluene (BHT). Compounds **85, 86, 87** and **88** were the most potent with IC_{50} values of 15.20, 16, 15.99 and 15.29 µg/mL, respectively (Shaikh *et al*., 2016a).

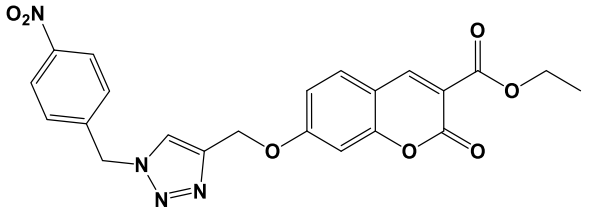

85

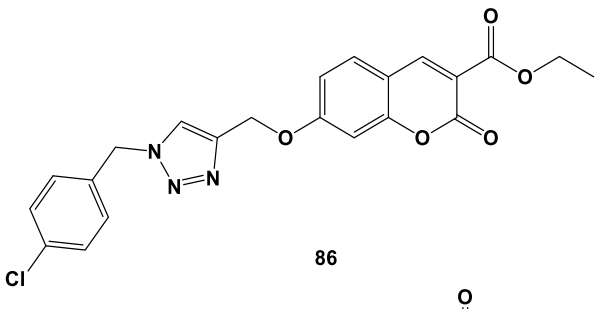

86

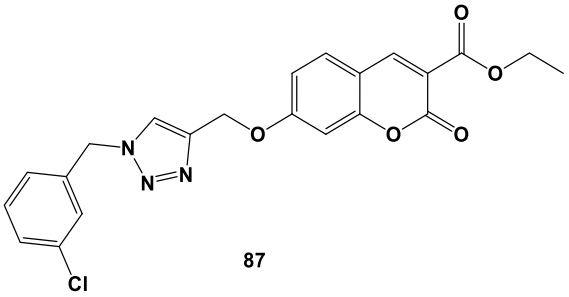

87

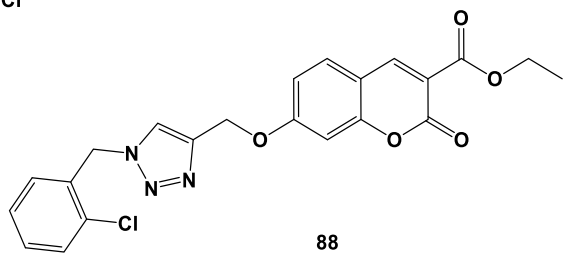

88

Jayashree *et al*. (2008b) synthesized a series of 5 ((substituted and unsubstituted phenyl)-1-phenyl-2pyrazoline-3-yl)-6-chloro and evaluated their antioxidant activity. The results showed that compound **89** was a potential candidate for scavenging radical oxygen (Jayashree *et al*., 2008).

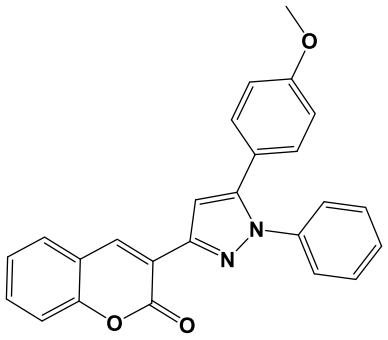

89

Kasumbwe *et al*., 2014 synthesized a series of mono/di halogenated coumarins for their antioxidant activity. The results showed that compound **90** was the most promising, with a percentage scavenging capacity of 85% (Kasumbwe *et al*., 2014).

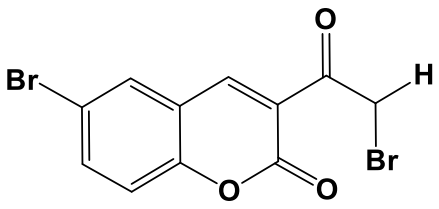

90

2.5.5 Coumarin as an antiviral agent

Viral infections are responsible for multiple diseases, and the latest outbreaks have increased questions regarding public health. Despite the availability of specific antiviral drugs, they are often ineffective and less selective against their target virus due to the production of viral mutations. Thus the need to discover novel antiviral drugs is critical (Mishra *et al*., 2020). Coumarins are a privileged structure for developing new antiviral agents with high affinity and specificity to various molecular targets (Penta, 2015).

Srivastav *et al*. (2018) designed and synthesized a series of 6-acetylcoumarin derivatives and evaluated their antiretroviral activity in the C8166 T-cell line infected with HxBru-Gluc strain of human immunodeficiency virus-1. The results revealed that compounds **91**, **92** and **93** showed potent inhibitory efficacy against human immunodeficiency virus infection with IC_{50} values of 4.7, 4.5, and 0.35 µM, respectively (Srivastav *et al*., 2018).

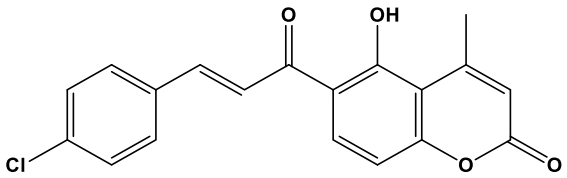

91

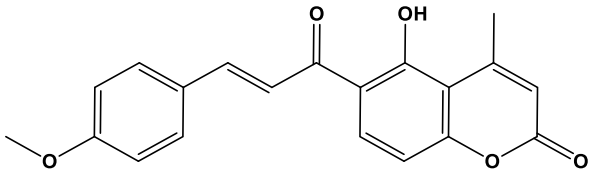

92

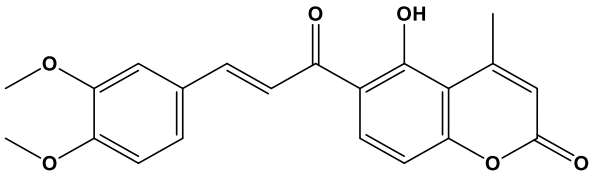

93

Hu *et al*. (2019b) synthesized and evaluated a series of coumarin derivatives for their antiviral activity by comparing the half-maximum inhibitory concentrations (IC_{50}) of the synthesized compounds tested in Epithelioma Papulosum Cyprini (EPC) cells infected with IHNV. Compound **94** was selected for further validation studies with an IC_{50} of 2.53 μM at 72 h against IHNV glycoprotein. Additional experiments revealed that compound **94** could inhibit apoptosis and morphological damage induced by IHNNV (Hu *et al*., 2019b).

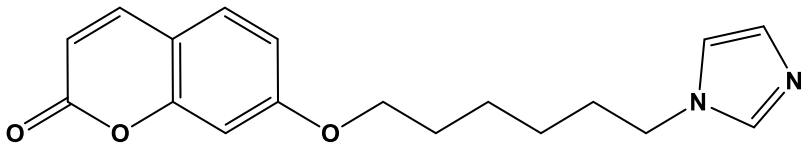

94

2.5.6 Coumarin as anti-mosquito agent

Mosquitoes are among the most common insect pests that affect human and domestic animal health worldwide. The yellow fever mosquito, *Aedes aegypti*, attacks predominantly day and night (Soonwera and Phasomkusolsil, 2017). The emergence and spread of increasing resistance to the first-line antimalarial is a troubling cause of severe malaria control management, causing the need for new drugs to be more potent than before with better absorption, delivery, metabolism, and excretion profiles (Sashidhara *et al*., 2012). Coumarins, which exhibited various biological properties, showed possible *in vitro* anti-plasmodial and *in vivo* antimalarial activity. Several coumarin derivatives have also been used to diagnose many diseases in clinical practice. As a result, coumarin derivatives play a crucial role in medicinal chemistry, thus making them attractive candidates for treatment (Hu *et al*., 2018).

Venugopala *et al*. (2014) synthesized a series of 3-mono acetyl, 6- halogenated coumarins analogues and evaluated their larvicidal activity against an *Anopheles arabiensis*. The results showed that compounds **95, 96, 97** and **98** exhibited close to 100% larvae mortality within 24 hours of exposure (Venugopala *et al*., 2014).

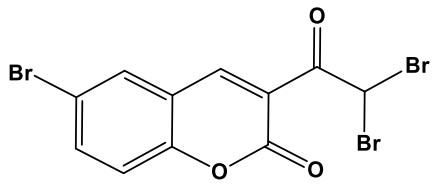

95

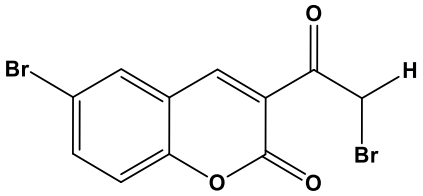

96

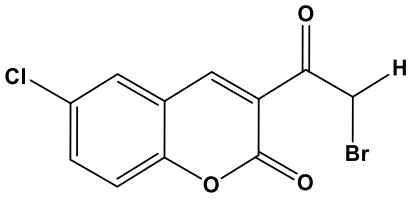

97

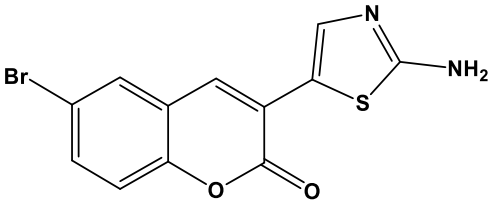

98

Another study by Shao *et al*. (2018) designed and synthesized a series of coumarin-dibenzothiophene or -carbazole derivatives as a larvicidal agent against fourth instars larvae of *Aedes aegypti*. These compounds demonstrated moderate to high larvicidal mortality Tow coumarin-linked dibenzothiophene hybrids **99, 100** and six coumarin linked carbazole hybrids **101**, **102**, **103**, **104**, **105** and **106** showed potent toxicity (88.53 to 100%) (Shao *et al*., 2018).

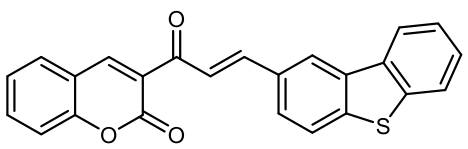

99

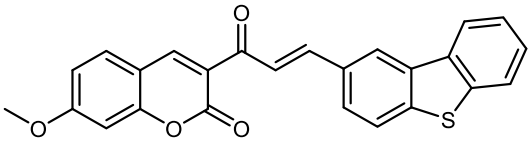

100

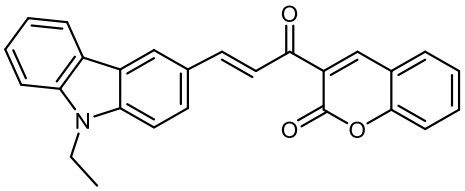

101

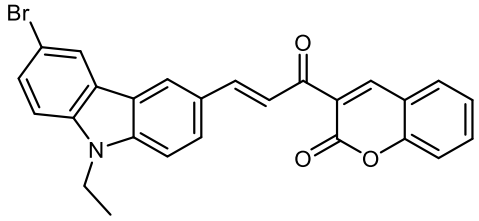

102

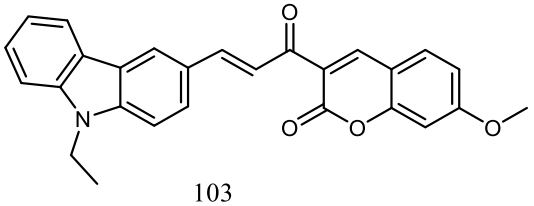

103

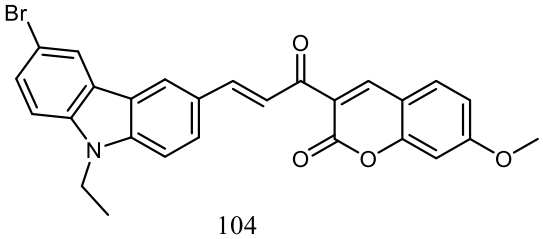

104

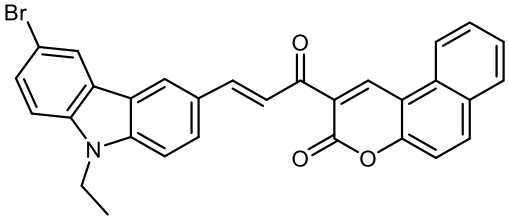

105

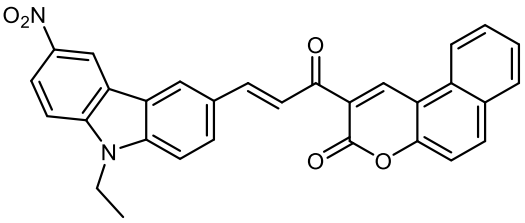

106

2.5.7 Coumarin as an analgesic and anti-inflammatory agent

Inflammation is caused by the reaction of living tissues to injury and includes systemic and local responses (Said Fatahala *et al*., 2017). The main action of anti-inflammatory agents is the overproduction of leukotrienes and prostanoids (prostaglandins and thromboxane) in the arachidonic acid pathway and inhibition of cyclooxygenase enzymes responsible for converting arachidonic acid to prostaglandins (Chougala *et al*., 2018). Non-steroidal anti-inflammatory drugs (NSAIDs) have been widely used to treat various inflammatory diseases such as arthritis and rheumatisms to relieve everyday life's aches and pain (Day and Graham, 2013). A significant number of non-steroidal anti-inflammatory medications block both COX-1 and COX-2 at clinical doses. Compelling data shows that suppression of prostanoids produced by COX-2 can be attributed to NSAIDs' anti-inflammatory, analgesic, and anti-

pyretic activity (El-Haggar and Al-Wabli, 2015). Coumarins possess anti-inflammatory properties and have been used to treat oedema, helping wound healing. Its removes protein and oedema fluid from injured tissue by stimulating phagocytosis and proteolytic enzyme production (Tomasz Kubrak *et al*., 2017). Coumarin and related derivatives intercept arachidonic acid metabolism by inhibiting lipoxygenase (LOX) or cyclooxygenase (COX). These also possess good antioxidant activity (Sandhu *et al*., 2014).

A series of Schiff bases of 2-amino-4-(6-chloro-3-coumarinyl) thiazole as potent NSAIDs were designed and synthesized by Jayashree *et al*. (2005) and tested the anti-inflammatory efficacy. The results revealed that compounds **107**, **108**, **109**, **110**, **111**, **112** and **113** were the most active; their analgesic activity was more significant than the reference drug (aspirin). The anti-inflammatory results have shown that compounds **109** and **114** were almost as potent as the reference drug (ibuprofen) (Jayashree *et al*., 2005a).

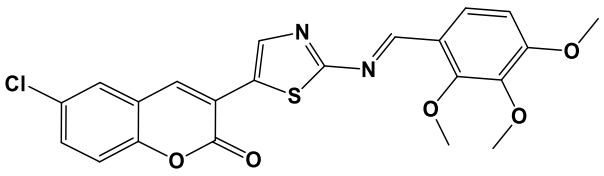

107

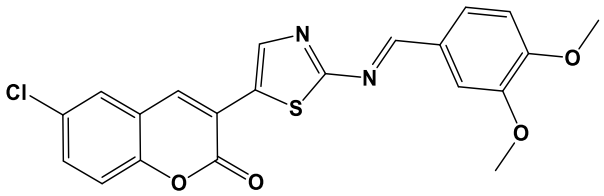

108

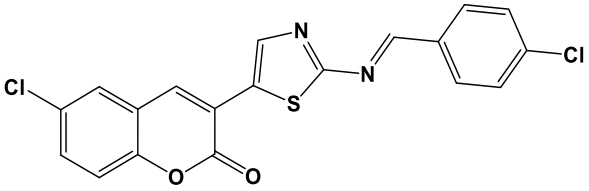

109

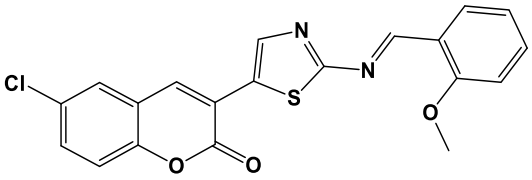

110

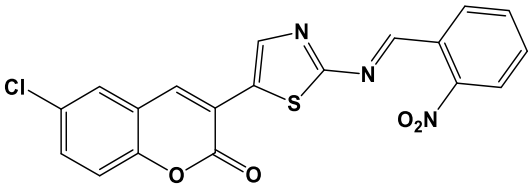

111

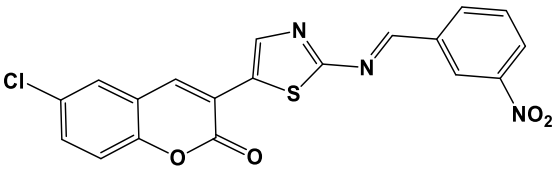

112

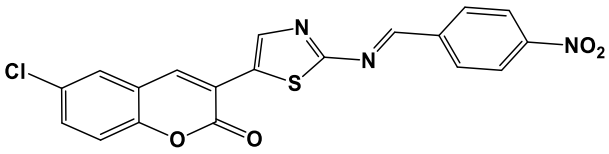

113

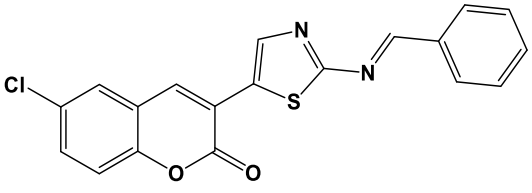

114

Madar *et al*. (2018) synthesized a series of coumarins with pyrido (1, 2-a) pyrimidinone as anti-inflammatory agents against matrix metalloproteinase's (MMPs) family such as MMP-2 and MMP-9. The results revealed that compounds **115** and **116** were highly active against MMP-2, showing 90% inhibition and 95% inhibition of tetracycline, compounds **117**, **118**, **119** and **120** display inhibitions of 85, 88, 89 and 87%, respectively. Compounds **121** and **122** demonstrate 82% and 75% inhibition against MMP-2, respectively (Madar *et al*., 2018).

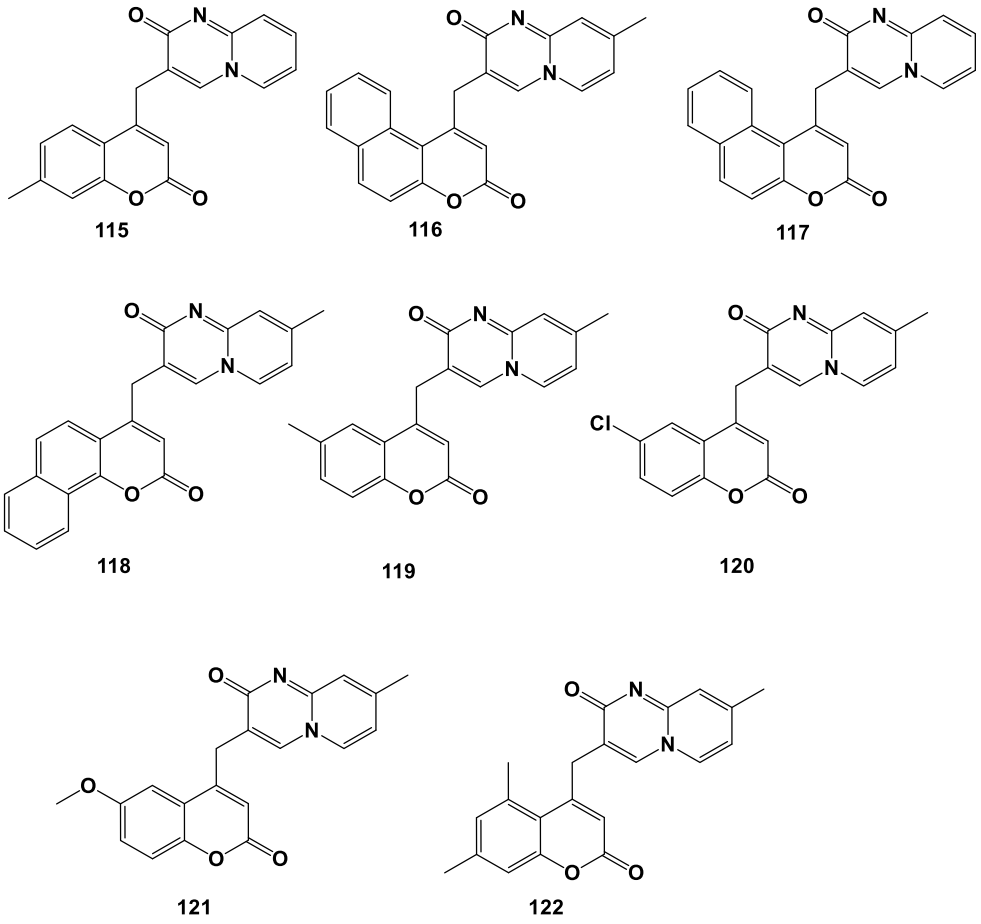

Kulkarni *et al*. (2018) developed a series of coumarin-pyrazolone derivatives and assessed their anti-inflammatory activity using the protein denaturation method. The results showed that these compounds were excellent anti-inflammatory agents; among them, compounds **123** and **124** displayed good anti-inflammatory activity (Kulkarni *et al*., 2018).

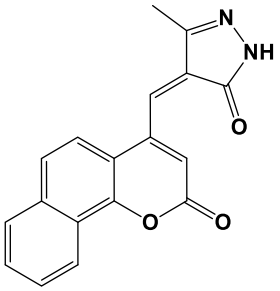

123

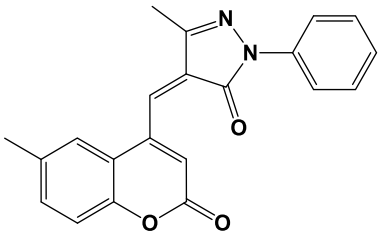

124

Venugopala and Jayashree (2004) synthesized a series of Schiff bases of amino thiazolyl bromo coumarin for their analgesic and anti-inflammatory activity by acetic acid-induced abdominal constriction method in mice using acetylsalicylic acid as standard and carrageenan-induced rat hind paw oedema method respectively using phenylbutazone as standard. The results revealed that compounds **125, 126, 127, 128, 129, 130, 131** and **132** showed excellent anti-inflammatory activity compared to standard phenylbutazone. The analgesic results demonstrated that compounds **125, 128, 129** and **132** possess higher activity than aspirin (Venugopala and Jayashree, 2004b).

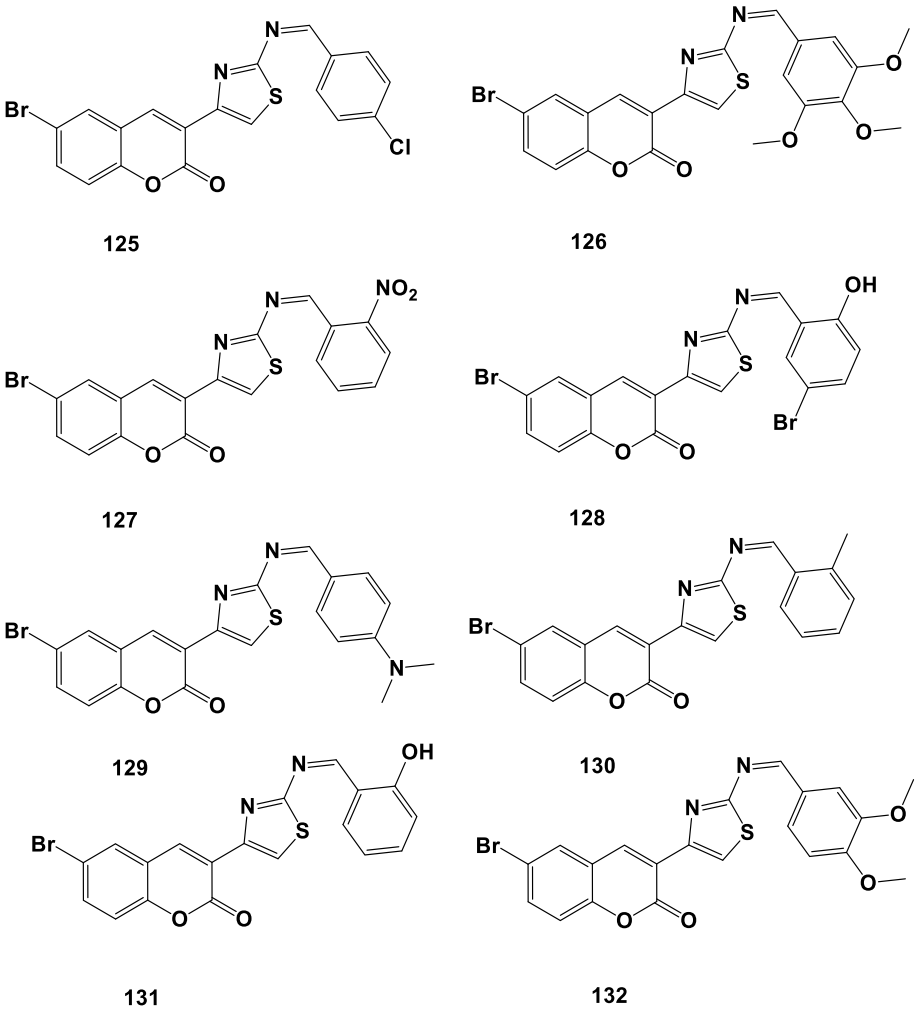

In another study, Venugopala *et al*. (2004) designed and synthesized a series of substituted 2-arylamino coumarinyl thiazoles as potent NSAIDs by acetic acid-induced abdominal constriction method acetylsalicylic acid as standard and carrageenan-induced rat hind paw oedema method respectively using ibuprofen as standard. The results showed that compounds **133, 134, 135, 136** and **137** demonstrated good analgesic activity (68.56, 60.37, 71.69, 66367, and 64.15%, respectively) compared with the standard diclofenac sodium (72.98%). Compounds **138**, **139**, **140** and **141** showed an anti-inflammatory activity of 56.80, 52.06, 59.86, and 52.14 %, respectively, compared to ibuprofen as standard (74%) (Venugopala *et al*., 2004).

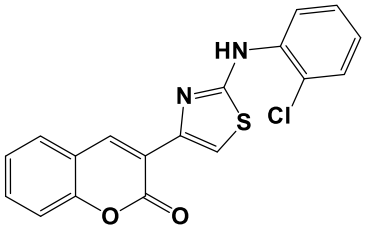

133

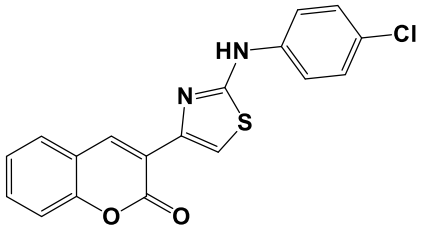

134

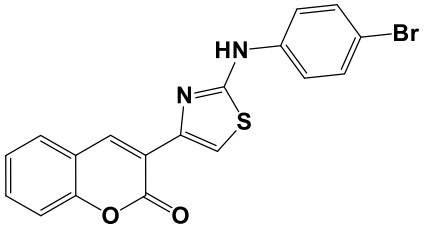

135

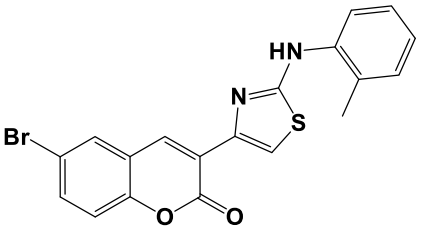

136

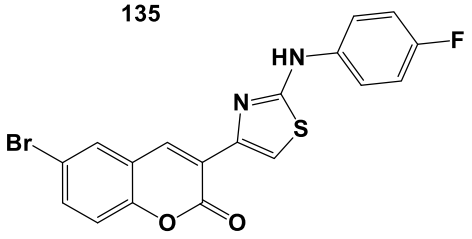

137

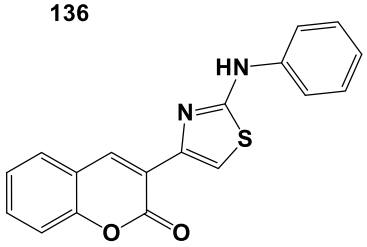

138

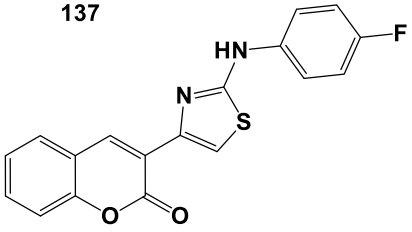

139

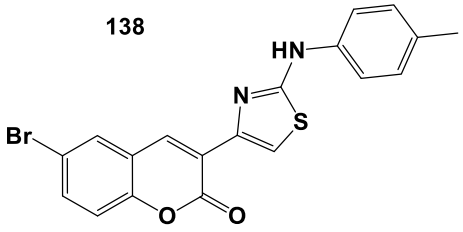

140

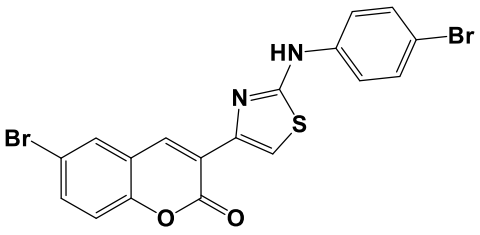

141

Venugopala and Jayashree (2003) synthesized a series of carboxamides of 2-amino-4-(6-bromo-3-coumarinyl) thiazole as an analgesic and anti-inflammatory agent. The results obtained revealed that **142**, **143**, **144**, **145** and **146** had shown significant analgesic activity at 41.66, 41.66, 40.29, 41.66 and 40.29%, respectively, compared to that of standard drug acetylsalicylic acid (37.45%). Compounds **147** and **148** have shown significant anti-inflammatory activity at 46.96 and 53.59%, respectively, compared to the standard drug phenylbutazone(45.30%) (Venugopala and Jayashree, 2003).

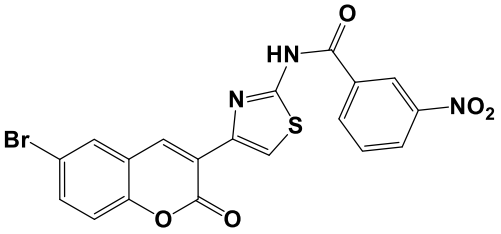

142

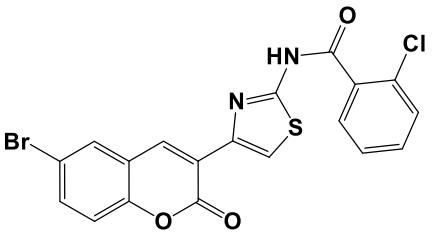

143

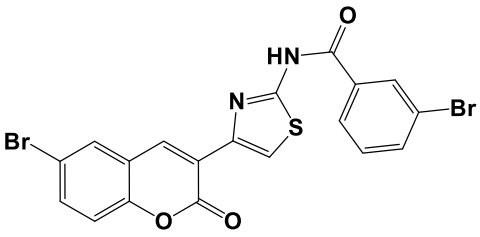

144

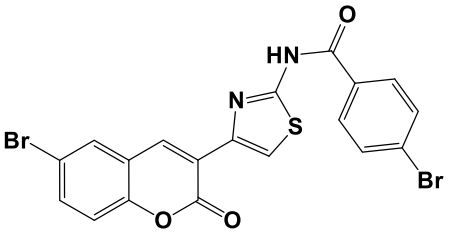

145

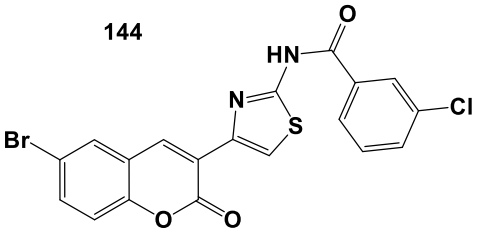

146

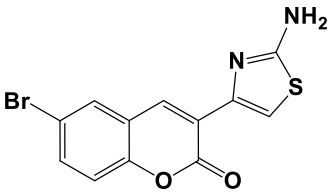

147

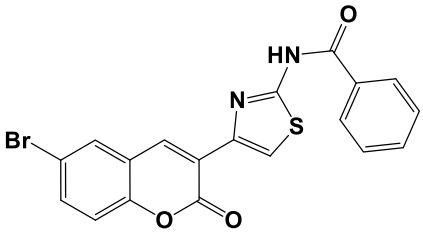

148

Jayashree *et al*. (2004) synthesized and evaluated a series of Schiff bases of 2- amino-4-(3-coumarinyl) thiazole as potential NSAIDs using acetylsalicylic acid as standard and carrageenan-induced rat hind paw oedema method using diclofenac sodium as standard. The results showed that compounds **149, 150** and **151** showed anti-inflammatory activity at 38.00%, while compounds **152**, **153** and **154** displayed moderate activity at 37% compared to standard (44%) (Jayashree *et al*., 2004).

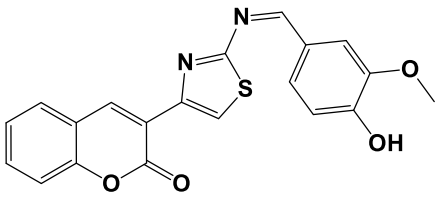

149

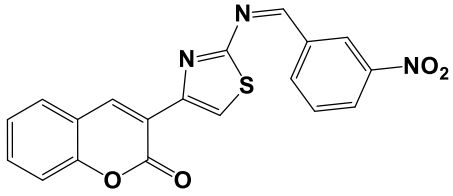

150

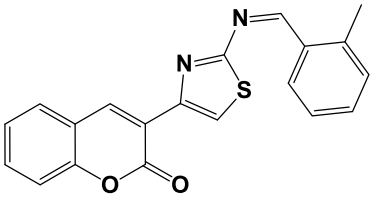

151

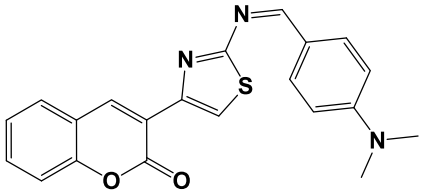

152

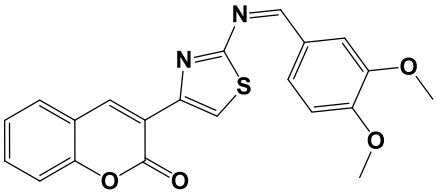

153

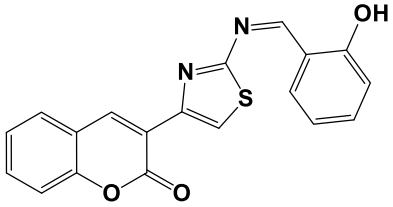

154

2.6 Conclusion

This literature review shows that coumarin derivatives are flexible scaffolds with considerable therapeutic potential for discovering, designing and developing novel therapeutic agents such as anticancer, antimicrobial, antiviral, anti-mycobacterium, antioxidant, acetylcholinesterase inhibitors, antidiabetic and anticonvulsant.

2.7 Research Hypotheses, Aim and Objectives.

2.7.1 Research Hypotheses

The synthesized compounds will demonstrate significant anti-mycobacterial, larvicidal, adulticidal, antioxidant, anti-inflammatory and anticancer properties.

2.7.2 Research Aim

The current study aimed to synthesize novel Schiff bases of 3-(2-aminothiazol-4-yl)-6,8-dichloro-*2H*-chromen-2-one (**SVM 1-11**) and 3-(2-aminothiazol-4-yl)-6-nitro-*2H*-chromen-2-one (**SVN 1-11**) for their biological properties.

2.7.3 Research Objectives

1. Synthesis, purification and structural elucidation of novel Schiff bases of 3-(2-aminothiazol-4-yl)-6,8-dichloro-*2H*-chromen-2-one (**SVM 1-11**) and 3-(2-aminothiazol-4-yl)-6-nitro-*2H*-chromen-2-one (**SVN 1-11**)
2. Evaluate the synthesized compounds' anti-mycobacterial, larvicidal, adulticidal, antioxidant, and lipoxygenase inhibitory capacity.
3. Determine the binding affinities of the most promising compounds against *Mycobacterium tuberculosis* targets, polyketide synthase (PKs13) and decaphrenylphosphoryl-β-D-ribose-2- epimerase (DprE1) *in silico*.
4. Evaluate the growth inhibitory potential of the synthesized compounds against human lung cancer **(**A549) and breast cancer (MCF-7) cells.
5. Evaluate the apoptotic-inducing effects of the active compounds using the caspase Glo® kit assay.

CHAPTER III. SYNTHESIS AND CHARACTERIZATION OF NOVEL SCHIFF BASES OF 3-(2-AMINOTHIAZOL-4-YL)-6,8-DICHLORO-2*H*-CHROMEN-2-ONE (SVM1-11) AND (*E*) 3-(2-AMINOTHIAZOL-4-YL)-6-NITRO-2*H*-CHROMEN-2-ONE (SVN1-11)

The synthesis of novel Schiff bases of 3-(2-aminothiazol-4-yl)-6,8-dichloro-2*H*-chromen-2-one (**SVM1-11**) and 3-(2-aminothiazol-4-yl)-6-nitro-2*H*-chromen-2-one (**SVN1-11**) were conducted according to the protocol described by (Venugopala and Jayashree, 2004a). All chemicals were obtained from Merck chemical company. The progress of the reaction completion was monitored using Thin Layer Chromatography (TLC). TLC was performed on Merck 60 F-254 silica gel plates and visualized on UV light. The melting points of all synthesized compounds were measured using a Büchi B-545 melting point apparatus, Fourier-transform infrared (FT-IR) spectra of the synthesized compounds were measured using a Shimadzu FT-IR spectrophotometer, ^{1}H- and ^{13}C-NMR spectra were measured using DMSO as a solvent on a Bruker AVANCE III 400 MHz instrument, mass spectra were measured alongside the MSD using liquid chromatography-mass spectrometry (LC-MS; Agilent 1100 series), as well as 0.1% aqueous trifluoroacetic acid in an acetonitrile system on the C18-BDS column, and elemental analysis was recorded using a LECO-183 CHNS analyzer.

3.1 Synthesis, purification and characterization of novel Schiff bases of 3-(2-aminothiazol-4-yl)-6,8-dichloro-2*H*-chromen-2-one (SVM 1-11)

Scheme 1 shows the synthesis technique used to produce **SVM 1-11**.

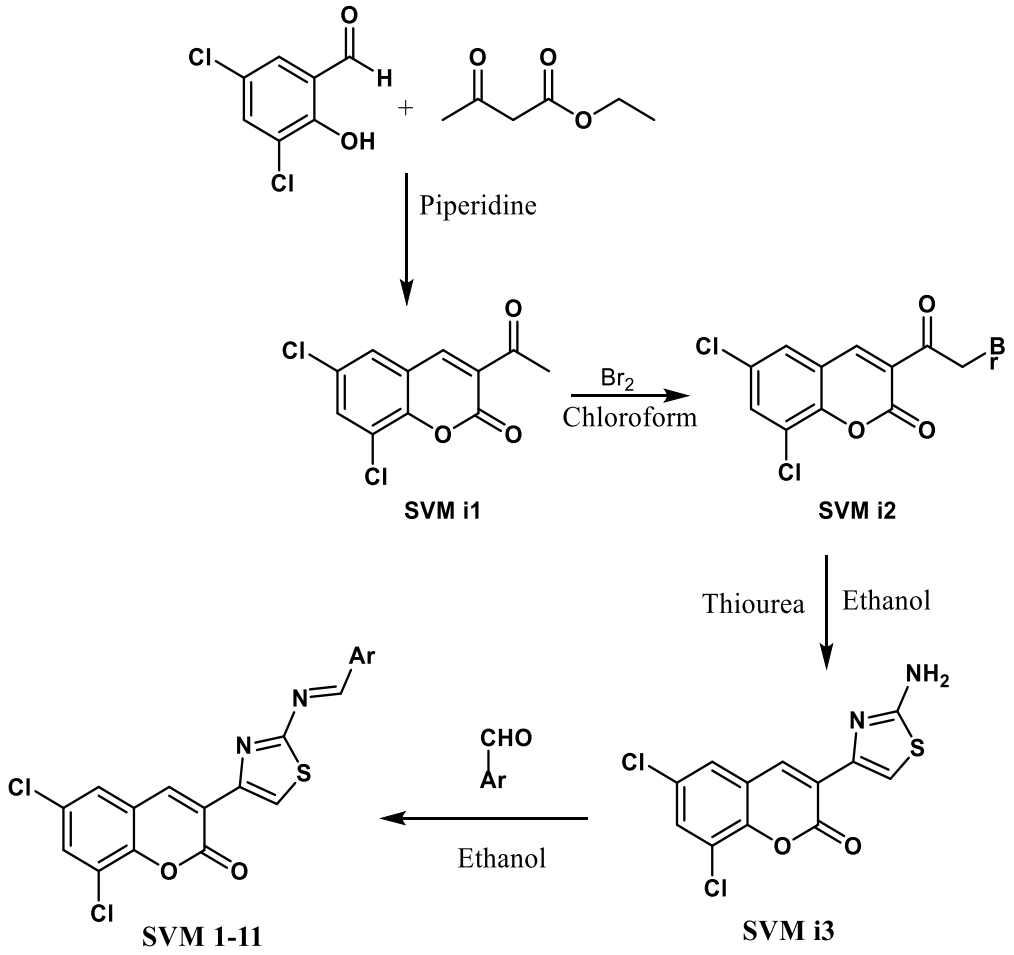

SVM1 = Ar = phenyl
SVM2 = Ar = 4-OCH_3
SVM3 = Ar = 4-Cl phenyl
SVM4 = Ar = 4-F phenyl
SVM5 = Ar = thiophene
SVM6 = Ar = pyridyl
SVM7 = Ar = 2-OH phenyl
SVM8 = Ar = 3,4-OH phenyl
SVM9 = Ar = 2-OCH_3 phenyl
SVM10 = Ar = 2-OH, 5-NO_2 phenyl
SVM11 = Ar = 2-HO, 3,6-dichloro phenyl

Scheme 1: Synthetic scheme for developing novel Schiff bases of 3-(2-aminothiazol-4-yl)-6,8-dichloro-2*H*-chromen-2-one (**SVM 1-11**).

3.1.1 Synthesis of 3-acetyl-6, 8-dichloro-2*H*-chromen-2-one (SVM i1)

To a stirred solution of 3,5-dichloro-2-hydroxybenzaldehyde **1** (3 g, 15.79 mmol) and ethyl acetoacetate **2** (2.05 g, 15.79 mmol) in a 100 mL RB flask, The reaction mixture was allowed to stir overnight at room temperature after a few drops of piperidine were added dropwise with continual stirring. TLC was used to monitor the reaction's completion. After the reaction was finished, the reaction medium was diluted with ethyl acetate (200 mL), the ethyl acetate layer was washed with water (50 mL X1), brine (50 mL X1) and dried over anhydrous sodium sulphate, the solvent was evaporated afterwards under reduced pressure to get the crude chemical. The crude product was refined using 60-120 mesh column chromatography with ethyl acetate as the eluent and hexane as the eluent to get 3.2 g of pure 3-acetyl-6,8-dichloro-2H-chromen-2-one (**SVM i1**).

3.1.2 Synthesis of 3-(2-bromoacetyl)-6,8-dichloro-2*H*-chromen-2-one (SVM i2)

Bromine (1.22 g, 7.81 mmol) in chloroform was added dropwise to a stirred solution of 3-acetyl-6,8-dichloro-4-hydroxy-*2H*-chromen-2-one (**SVM i1**) (2 g, 7.81 mmol) in 50 mL chloroform at 4°C and the reaction mixture was heated at 50°C for 5 hours. The reaction completion was monitored on TLC; the mixture was allowed to attain room temperature and the solid product precipitated after reaction completion. The solid was again dissolved in hot chloroform and allowed to room temperature. The solid was filtered out and dried under vacuum to get 2.1 g of 3-(2-bromoacetyl)-6,8-dichloro-2*H*-chromen-2-one **(SVM i2)**(81% yield).

3.1.3 Synthesis of 3-(2-aminothiazol-4-yl)-6,8-dichloro-2*H*-chromen-2-one (SVM i3)

To a 50 mL of ethanol, a mixture of 3-(2-bromoacetyl)-6,8-dichloro-4-hydroxy-2*H*-chromen-2-one **(SVM i2)** (2 g, 5.99 mmol), and thiourea (0.46 g, 5.99 mmol) was added, and the reaction mixture was refluxed overnight. The reaction completion was monitored on TLC. After the reaction completion, the solvent was evaporated under reduced pressure. The residue obtained was diluted with ethyl acetate (200 mL), washed the ethyl acetate layer with water (50 mL X1), brine (50 mL X1), and dried over anhydrous sodium sulphate. The ethyl acetate solvent was evaporated under reduced pressure to obtain the crude compound. The crude compound was purified by column chromatography using 60-120 mesh using chloroform and methanol as an

eluent to get pure 1.5 g of 3-(2-aminothiazol-4-yl)-6,8-dichloro-2*H*-chromen-2-one **(SVM i3)** (81% yield).

3.1.4 General procedure for the synthesis of Schiff bases of 3-(2-aminothiazol-4-yl)-6,8-dichloro-2*H*-chromen-2-one (SVM 1-11)

The final Schiff bases (**SVM1-11**) were prepared by condensation of parent compound 3-(2-aminothiazol-4-yl)-6-nitro-2*H*-chromen-2-one **(SVM i3)** with substituted aromatic aldehydes in the presence of ethanol by the conventional reflux method. The final Schiff bases (**SVM 1-11**) were characterized by Fourier-transform infrared spectroscopy (FT-IR), Nuclear Magnetic resonance (NMR), LC-MS, and elemental analysis. The physicochemical constants of the title compounds are tabulated in Table 2.

Table 2: Physicochemical constants (*E*)-3-(2-(substituted benzylideneamino)thiazol-4-yl)-6,8-dichloro-2*H*-chromen-2-one (**SVM 1-11**).

Code	Mol formulae (Mass)	Ar	Physical appearance	Yield (%)	m.p (°C)
SVM i1	$C_{11}H_6Cl_2O3$ (255)	-	White crystalline	79	169
SVM i2	$C_{11}H_5BrCl_2O_3$ (333)	-	Yellow crystalline	81	158
SVM i3	$C_{12}H_6Cl_2N_2O_2S$ (311)	-	Yellow amorphous	81	246
SVM 1	$C_{19}H_{10}Cl_2N_2O_2S$ (399)	phenyl	Brown crystalline	67	118
SVM 2	$C_{20}H_{12}Cl_2N_2O_3S$ (429)	4-OCH_3 phenyl	Yellow amorphous	69	175
SVM 3	$C_{19}H_9Cl_3N_2O_2S$ (433)	4-Cl phenyl	Dark brown crystalline	62	248
SVM 4	$C_{19}H_9Cl_2FN_2O_2S$ (417)	4-F phenyl	Yellow amorphous	73	159
SVM 5	$C_{17}H_8Cl_2N_2O_2S_2$ (405)	thiophene	Yellow amorphous	66	244
SVM 6	$C_{18}H_9Cl_2N_3O_2S$ (400)	pyridyl	Yellow amorphous	70	223
SVM 7	$C_{19}H_{10}Cl_2N_2O_3S$ (415)	2-OH phenyl	Yellow amorphous	64	237

SVM 8	$C_{19}H_{10}Cl_2N_2O_4S$ (431)	3,4-OH phenyl	Brown crsystalline	69	223
SVM 9	$C_{20}H_{12}Cl_2N_2O_3S$ (429)	2-OCH_3 phenyl	Yellow amorphous	74	211
SVM 10	$C_{19}H_9Cl_2N_3O_5S$ (460)	2-OH, 5-NO_2 phenyl	Yellow amorphous	68	249
SVM 11	$C_{19}H_8Cl_4N_2O_3S$ (483)	2-HO, 3,6-dichloro phenyl	Yellow amorphous	66	244

3.1.4.1 3-acetyl-6, 8-dichloro-2*H*-chromen-2-one (SVM i1)

FT-IR (neat cm^{-1}): 2950, 1753, 1677, 1541. ^{1}H-NMR (400 MHz, $CDCl_3$) δ: 8.62 (1H, s), 8.61 (1H, s), 8.08 (1H, s), 2.51 (3H, s). ^{13}C-NMR (100 MHz, $CDCl_3$) δ 194.67, 157.14, 148.91, 145.30, 133.04, 128.60, 128.41, 126.05, 120.73, 120.58, 29.91. LC-MS (ESI, Positive): *m/z* $(M)^+$; 256. Anal calculated for: $C_{11}H_6Cl_2O_3$: C, 51.40, H, 2.35: Found: C, 51.44, H, 2.39.

3.1.4.2 3-(2-bromoacetyl)-6,8-dichloro-2*H*-chromen-2-one (SVM i2)

FT-IR (neat cm^{-1}): 1743, 1687, 1535. ^{1}H-NMR (400 MHz, $CDCl_3$) δ 8.98 (1H, s), 8.70 (1H, s), 8.64 (1H, s), 4.45 (2H, s). ^{13}C-NMR (100 MHz, $CDCl_3$) δ 196.58, 194.82,157.02, 156.25, 148.80, 148.68, 145.52, 133.16, 132.96, 128.82, 128.65, 128.51, 128.49, 128.32, 125.29, 124.58, 120.85, 120.77, 120.55, 120.41, 25.44. LC-MS (ESI, Positive): *m/z* $(M)^+$; 334. Anal calculated for: $C_{11}H_5BrCl_2O_3$: C, 39.33, H, 1.50: Found: C, 39.34, H, 1.49.

3.1.4.3 3-(2-aminothiazol-4-yl)-6,8-dichloro-2*H*-chromen-2-one (SVM i3)

FT-IR (neat cm^{-1}): 3377, 3201. 2923, 1691, 1622, 1537. ^{1}H-NMR (400 MHz, $CDCl_3$) δ 8.44 (1H, s), 8.26 (1H, s), 8.00-7.93 (3H, m), 7.57 (1H, s). ^{13}C-NMR (100 MHz, $CDCl_3$) δ 168.16, 167.60, 157.34, 156.31, 147.69, 146.63, 142.75, 141.31, 136.87, 131.48, 130.62, 128.46, 128.43, 126.98, 126.76, 122.45, 121.57, 120.91, 120.80, 120.73, 120.51, 110.23. LC-MS (ESI, Positive): *m/z* $(M)^+$; 312. Anal calculated for: $C_{12}H_6Cl_2N_2O_2S$: C, 46.03, H, 1.93, N, 8.95: Found: C, 46.04, H, 1.95, N, 8.90.

3.1.4.4 (*E*)-3-(2-(benzylidene amino) thiazol-4-yl)-6,8-dichloro-2*H*-chromen-2-one (SVM 1)

FT-IR (neat cm^{-1}): 2941, 1735, 1566, 1454. ^{1}H-NMR (400 MHz, $CDCl_3$) δ 8.56 (1H, s), 8.44 (1H, s), 8.02 (1H, s), 7.93-7.91 (2H, m), 7.63-7.61 (2H, m), 7.57-7.51 (3H, m). ^{13}C-NMR (100 MHz, $CDCl_3$) δ 193.22, 167.53, 167.35, 157.55, 146.50, 139.52, 136.64, 136.27, 134.55,

130.20, 130.10, 129.45, 129.13, 128.29, 128.20, 128.12, 127.39, 127.12, 126.85, 126.72, 121.99, 121.87, 120.37, 120.29. LC-MS (ESI, Positive): *m/z* $(M)^+$; 400. Anal calculated for: $C_{19}H_{10}Cl_2N_2O_2S$: C, 56.87, H, 2.51, N, 6.98: Found: C, 56.88, H, 5.59, N, 6.92.

3.1.4.5 (*E*)-6,8-dichloro-3-(2-((4-methoxybenzylidene) amino) thiazol-4-yl)-2*H*-chromen-2-one (SVM 2)

FT-IR (neat cm^{-1}): 3166, 1747, 1670, 1600, 1566. ^{1}H-NMR (400 MHz, $CDCl_3$) δ 9.87 (1H, s), 8.44 (1H, s), 8.00 (1H, s), 7.90-7.87 (2H, m), 7.57 (1H, s), 7.22 (1H, s), 7.14-7.12 (2H, m) 3.87 (3H, s). ^{13}C-NMR (100 MHz, $CDCl_3$) δ 191.30, 167.53, 164.18, 157.52, 146.47, 142.74, 136.27, 131.98, 131.78, 130.20, 129.60, 128.29, 126.72, 122.00, 121.87, 120.37, 114.74, 55.66. LC-MS (ESI, Positive): *m/z* $(M)^+$; 430. Anal calculated for: $C_{20}H_{12}Cl_2N_2O_3S$: C, 55.70, H, 2.80, N, 6.50: Found: C, 55.74, H, 2.79, N, 6.52.

3.1.4.6 (*E*)-6,8-Dichloro-3-(2-((4-chlorobenzylidene) amino) thiazol-4-yl)-2*H*-chromen-2-one (SVM 3)

FT-IR (neat cm^{-1}): 1737, 1608, 1475. ^{1}H-NMR (400 MHz, $CDCl_3$) δ 10.01 (1H, s), 8.44 (1H, s), 8.07 (1H, s), 7.99-7.95 (2H, m), 7.82 (1H, s), 7.70 (1H, s), 7.68-7.65 (2H, m). ^{13}C-NMR (100 MHz, $CDCl_3$) δ 171.99, 167.54, 157.52, 146.47, 142.73, 136.27, 131.16, 130.19, 129.34, 128.96, 128.61, 128.45, 128.29, 128.25, 128.15, 127.94, 126.72, 122.00, 121.87, 120.37. LC-MS (ESI, Positive): *m/z* $(M)^+$; 434. Anal calculated for: $C_{19}H_9Cl_3N_2O_2S$: C, 52.38, H, 2.08, N, 6.43: Found: C, 52.40, H, 2.09, N, 6.50.

3.1.4.7 (*E*)-6,8-dichloro-3-(2-((4-fluorobenzylidene) amino) thiazol-4-yl)-2*H*-chromen-2-one (SVM 4)

FT-IR (neat cm^{-1}): 1737, 1573, 1385, 1542. ^{1}H-NMR (400 MHz, $CDCl_3$) δ 8.40 (1H, s), 8.16-8.14 (1H, m), 8.08 (1H, s), 8.00 (1H, s), 7.90-7.87 (2H, m), 7.57 (1H, s), 7.37-7.27 (2H, m). ^{13}C-NMR (100 MHz, $CDCl_3$) δ 172.90, 167.54, 166.78, 157.52, 146.47, 142.73, 136.27, 130.19, 128.29, 126.72, 122.00, 121.87, 120.36, 115.30, 110.27. LC-MS (ESI, Positive): *m/z*$(M)^+$; 418. Anal calculated for: $C_{19}H_9Cl_2FN_2O_2S$: C, 54.43, H, 2.16, N, 6.68: Found: C, 54.44, H, 2.19, N, 6.71.

3.1.4.8 (*E*)-6,8-dichloro-3-(2-((thiophen-2-ylmethylene) amino) thiazol-4-yl)-2*H*-chromen-2-one (SVM 5)

FT-IR (neat cm^{-1}): 1735, 1649, 1573, 1542. ^{1}H-NMR (400 MHz, $CDCl_3$) δ 8.75 (1H, s), 8.44 (1H, s), 7.99 (1H, s), 7.89 (1H, s), 7.65-7.63 (2H, m), 7.56 (1H, s), 7.27-7.24 (1H, m). ^{13}C-NMR (100 MHz, $CDCl_3$) δ 173.29, 167.55, 157,51, 146.46, 142.27, 136.26, 130.18, 138.29,

128.29, 126.72, 121.99, 121.86, 120.36, 110.27. LC-MS (ESI, Positive): *m/z* $(M)^+$; 406. Anal calculated for: $C_{17}H_8Cl_2N_2O_2S_2$: C, 50.13, H, 1.98, N, 6.88: Found: C, 50.15, H, 1. 97, N, 6.91.

3.1.4.9 (*E*)-6,8-dichloro-3-(2-((pyridin-4-ylmethylene) amino) thiazol-4-yl)-2*H*-chromen-2-one (SVM 6)

FT-IR (neat cm^{-1}): 1737, 1541, 1457. ^{1}H-NMR (400 MHz, $CDCl_3$) δ 10.10 (1H, s), 8.89-8.87 (2H, m), 8.60 (1H, s), 8.44 (1H, s), 7.86-7.82 (2H, m), 7.57 (1H, s), 7.48 (1H, s). ^{13}C-NMR (100 MHz, $CDCl_3$) δ 193.39, 167.53, 158.21, 157.52, 151.08, 149.54, 146.47, 142.73, 136.28, 130.20, 128.29, 126.73, 122.12, 122.00, 121.88, 121.46, 120.37, 110.29. LC-MS (ESI, Positive): *m/z* $(M)^+$; 401. Anal calculated for: $C_{18}H_9Cl_2N_3O_2S$: C, 53.75, H, 2.26, N, 10.45: Found: C, 53.80, H, 2. 28, N, 10.49.

3.1.4.10 (*E*)-6,8-dichloro-3-(2-((2-hydroxybenzylidene) amino) thiazol-4-yl)-2*H*-chromen-2-one (SVM 7)

FT-IR (neat cm^{-1}): 1737, 1575, 1541.^{1}H-NMR (400 MHz, $CDCl_3$) δ 10.29 (1H, s), 9.45 (1H, s), 8.85 (1H, s), 8.25 (1H, s), 7.57-7,54 (2H, m), 7.52 (1H, s), 7.08-7,02 (2H, m). ^{13}C-NMR (100 MHz, $CDCl_3$) δ 190.94, 172.96, 157,52, 146.47, 142.73, 136.27, 135.94, 130.19, 128.29, 127.80, 126.72, 122.00, 121.87, 120.36, 118.73, 116.88, 110.28. LC-MS (ESI, Positive): *m/z* $(M)^+$; 416. Anal calculated for: $C_{19}H_{10}Cl_2N_2O_3S$: C, 54.69, H, 2.42, N, 6.71: Found: C, 54.65, H, 2. 47, N, 6.69.

3.1.4.11 (*E*)-6,8-dichloro-3-(2-((3,4-dihydroxybenzylidene) amino) thiazol-4-yl)-2*H*-chromen-2-one (SVM 8)

FT-IR (neat cm^{-1}): 1735, 1589, 1527, 1452. ^{1}H-NMR (400 MHz, $CDCl_3$) δ 9.60 (1H, s), 8.72 (1H, s), 8.43 (1H, s), 8.21 (1H, s), 8.06 (1H, s), 7.92-7.88 (1H, m), 7.56 (1H, s), 7.37 (1H, s), 7.28-7.26 (2H, m), 6.77-6.74 (1H, m). ^{13}C-NMR (100 MHz, $CDCl_3$) δ 190.22, 173.43, 169.65, 167.73, 163.56, 159.94, 158.11, 146.43, 144.34, 143.67, 142.38, 138.44, 132.87, 129.54, 128.89, 128.54, 127.66, 127.11, 124.32, 122.19, 121.54, 120.39, 117.98, 116.56, 114.12. LC-MS (ESI, Positive): *m/z* $(M)^+$; 432. Anal calculated for: $C_{19}H_{10}Cl_2N_2O_2S$: C, 52.67, H, 2.33, N, 6.47: Found: C, 52.65, H, 2. 36, N, 6.49.

3.1.4.12 (*E*)-6,8-dichloro-3-(2-((2-methoxybenzylidene) amino) thiazol-4-yl)-2*H*-chromen-2-one (SVM 9)

FT-IR (neat cm^{-1}): 1730, 1622, 1537, 1454. ^{1}H-NMR (400 MHz, $CDCl_3$) δ 8.80 (1H, s), 8.43 (1H, s), 8.10-8.07 (1H, m), 7.98 (1H, s), 7.93 (1H, s), 7.70-7.64 (2H, m), 7. 56 (1H, s), 7.11-7.10 (1H, m), 3.96 (3H, s). ^{13}C-NMR (100 MHz, $CDCl_3$) δ 167.50, 160.38, 160.04, 157.50,

146.88, 145.05, 142.72, 138.04, 136.45, 135.36, 130.78, 130.18, 128.38, 128.28, 127.20, 126.71, 122.26, 121.98, 121.85, 120.97, 120.36, 55.89. LC-MS (ESI, Positive): *m/z* $(M)^+$; 430. Anal calculated for: $C_{20}H_{12}Cl_2N_2O_3S$: C, 55.70, H, 2.80, N, 6.50: Found: C, 55.69, H, 2. 88, N, 6.55.

3.1.4.13 (*E*)-6,8-dichloro-3-(2-((2-hydroxy-5 nitro benzylidene) amino) thiazol-4-yl)-2*H*-chromen-2-one (SVM 10)

FT-IR (neat cm^{-1}): 1741, 1604, 1537, 1481. ^{1}H-NMR (400 MHz, $CDCl_3$) δ 10.30 (1H, s), 8.45-8.43 (1H, m), 8.35-8.33 (1H, m), 8.00 (1H, s), 7.91 (1H, s), 7.57 (1H, s), 7.21 (1H, s), 7.16-7.14 (2H, m). ^{13}C-NMR (100 MHz, $CDCl_3$) δ 189.11, 167.53, 157.52, 146.48, 142,74, 136.28, 130.65, 130.21, 128.29, 126.72, 124.46, 122.19, 121.88, 120.37, 118.74, 110.29. LC-MS (ESI, Positive): *m/z* $(M)^+$; 461. Anal calculated for: $C_{19}H_9Cl_2N_3O_5S$: C, 49.37, H, 1.96, N, 9.09: Found: C, 49.35, H, 2.0, N, 9.10.

3.1.4.14 (*E*)-6,8-dichloro-3-(2-((3,5-dichloro 2hydroxybenzylidene) amino) thiazol-4-yl)-2*H*-chromen-2-one (SVM 11)

FT-IR (neat cm^{-1}): 1739, 1442, 1596. ^{1}H-NMR (400 MHz, $CDCl_3$) δ 10.14 (1H, s), 8.84 (1H, s), 8.45 (1H, s), 8.00 (1H, s), 7.92 (1H, s), 7.72 (1H, s), 7.57 (1H, s), 7.40 (1H, s). ^{13}C-NMR (100 MHz, $CDCl_3$) δ 192.08, 168.53, 158.52, 147.48, 143,54, 137.58, 131.15, 130.01, 129.11, 127.72, 125.46, 123.19, 122.88, 121.37, 119.74, 110.29. LC-MS (ESI, Positive): *m/z* $(M)^+$; 484. Anal calculated for: $C_{17}H_8Cl_2N_2O_2S_2$: C, 50.13, H, 1.98, N, 6.88: Found: C, 50.15, H, 1. 97, N, 6.91.

3.2 Synthesis, purification and characterization of novel Schiff bases (*E*) 3-(2-aminothiazol-4-yl)-6-nitro-2*H*-chromen-2-one (SVN 1-11)

The synthesis of **SVN 1-11** was achieved following a similar procedure the synthetic route is illustrated in scheme 2.

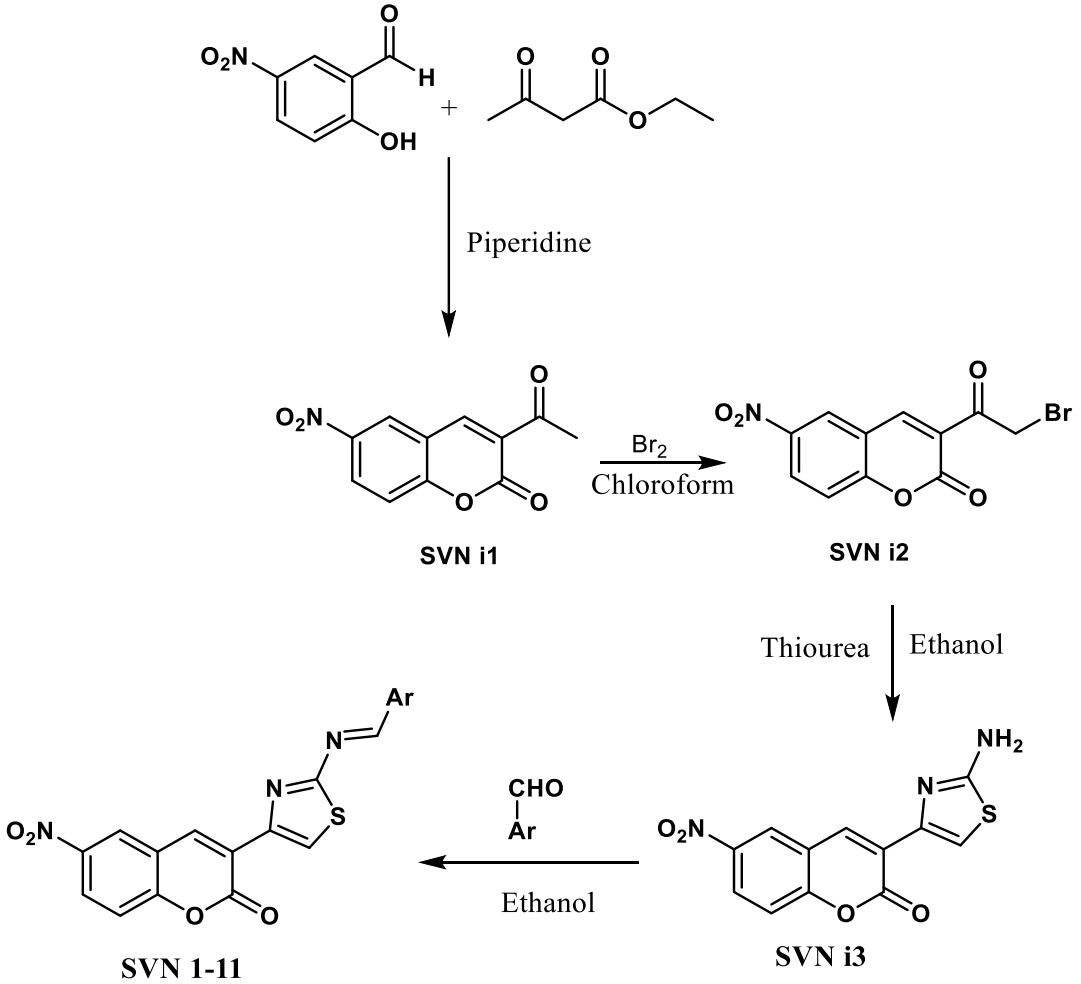

SVN1 = Ar = phenyl
SVN2 = Ar = 4-OCH_3 phenyl
SVN3 = Ar = 4-Cl phenyl
SVN4 = Ar = 4-F phenyl
SVN5 = Ar = thiophene
SVN6 = Ar = pyridyl
SVN7 = Ar = 2-OH phenyl
SVN8 = Ar = 3,4-OH phenyl
SVN9 = Ar = 2-OCH_3 phenyl
SVN10 = Ar = 2-OH, 5-NO_2 phenyl
SVN11 = Ar = 2-HO, 3,6-dichloro phenyl

Scheme 2. Synthetic scheme for the development of novel Schiff bases of 3-(2-aminothiazol-4-yl)-6-nitro-2*H*-chromen-2-one (**SVN 1-11**).

3.2.1 Synthesis of 3-acetyl-6-nitro-2*H*-chromen-2-one (SVN i1)

To a stirred solution of 2-hydroxy-5-nitrobenzaldehyde, **1** (3 g, 17.96 mmol), and ethyl acetoacetate **2** (2.33 g, 17.96 mmol) in a 100 mL round bottom flask, a few drops of piperidine was added dropwise with continued stirring. The reaction mixture was allowed to stir overnight, and the completion of the reaction was monitored using TLC. After the reaction completion, the reaction medium was diluted with ethyl acetate (200 mL), washed the ethyl acetate layer with water (50 mL X1), brine (50 mL X1) and dried over anhydrous sodium sulphate, evaporated the solvent under reduced pressure to get the crude compound. The crude mixture was purified using ethyl acetate and hexane with column chromatography using 60-120 mesh to obtain the pure 2.5g of 3-acetyl-6-nitro-2*H*-chromen-2-one **(SVN i1)** (60% yield).

3.2.2 Synthesis of 3-(2-bromoacetyl)-6-nitro-2*H*-chromen-2-one (SVN i2)

An amount of 1.34 g of bromine (8.58 mmol) was added to a stirred solution of 3-acetyl-6-nitro-2H-chromen-2-one (SVN i1) (2 g, 8.58 mmol) in 50 mL chloroform at 4°C. TLC was used to monitor the reaction's completion after it was heated for 5 hours at 50°C. When the reaction was completed, the liquid was allowed to cool to room temperature. The precipitated solid product was filtered out and dried under vacuum to obtain 3-(2-bromoacetyl)-6-nitro-2*H*-chromen-2-one **(SVN i2)** (2 g, 75% yield)**.**

3.2.3 Synthesis of 3-(2-aminothiazol-4-yl)-6-nitro-2*H*-chromen-2-one (SVN i3)

A mixture of 3-(2-bromoacetyl)-6-nitro-2*H*-chromen-2-one **(SVN i2)** (2 g, 6.43 mmol), thiourea (0.49 g, 6.43 mmol), in 50 mL of ethanol was refluxed overnight. The completion of the reaction was monitored on TLC. After reaction completion, the reaction medium was evaporated under reduced pressure and the residue obtained was diluted with ethyl acetate (200 mL). The ethyl acetate layer was washed with water (50 mL X1), brine (50 mL X1) and dried over anhydrous sodium sulphate. The solvent was evaporated under reduced pressure to yield a crude compound. The crude compound was purified by column chromatography using 60-120 mesh employing chloroform and methanol as an eluent to obtain pure 1.5 g of 3-(2-aminothiazol-4-yl)-6-nitro-2*H*-chromen-2-one **(SVN i3)** (80% yield).

3.2.4 General procedure for the synthesis of Schiff bases of 3-(2-aminothiazol-4-yl)-6-nitro-2*H*-chromen-2-one (SVN 1-11)

The final Schiff bases (**SVN 1-11**) were prepared by condensation of parent compound 3-(2-aminothiazol-4-yl)-6-nitro-2*H*-chromen-2-one **(SVN i3)** with substituted aromatic aldehydes in the presence of ethanol by the conventional reflux method. The final Schiff bases (**SVN 1-11**) were characterized by Fourier-transform infrared spectroscopy (FT-IR), Nuclear Magnetic resonance (NMR), LC-MS, and elemental analysis. The physicochemical constants of the title compounds are tabulated in the table below.

Table 3: Physicochemical constant (*E*) 3-(2-aminothiazol-4-yl)-6-nitro-2*H*-chromen-2-one (SVN 1-11).

Code	Mol formulae (Mass)	Ar	Physical appearance	Yield (%)	m.p (°C)
SVN i1	$C_{11}H_7NO_5$ (233)	-	Yellow crystalline	60	164
SVN i2	$C_{11}H_6BrNO_5$ (310)	-	Yellow crystalline	75	151
SVN i3	$C_{12}H_7N_3O_4S$ (289)	-	Yellow amorphous	80	241
SVN 1	$C_{19}H_{11}N_3O_4S$ (377)	phenyl	Yellow amorphous	62	112
SVN 2	$C_{20}H_{13}N_3O_5S$ (407)	4-OCH_3 phenyl	Yellow amorphous	65	169
SVN 3	$C_{19}H_{10}ClN_3O_4S$ (411)	4-Cl phenyl	Yellow crystalline	71	241
SVN 4	$C_{19}H_{10}FN_3O_4S$ (395)	4-F phenyl	Yellow amorphous	69	152
SVN 5	$C_{17}H_9N_3O_4S_2$ (383)	thiophene	Yellow amorphous	74	218
SVN 6	$C_{18}H_{10}N_4O_4S$ (378)	pyridyl	Brown crystalline	70	205
SVN 7	$C_{19}H_{11}N_3O_5S$ (393)	2-OH phenyl	Brown amorphous	66	243
SVN 8	$C_{19}H_{11}N_3O_6S$ (409)	3,4-OH phenyl	Brown amorphous	68	237
SVN 9	$C_{20}H_{13}N_3O_5S$ (407)	2-OCH_3 phenyl	Brown amorphous	66	205
SVN 10	$C_{19}H_{10}N_4O_7S$ (438)	2-OH, 5-NO_2 phenyl	Brown amorphous	65	234

SVN 11	$C_{19}H_9Cl_2N_3O_5S$ (460)	2-HO, 3,6-dichloro phenyl	Brown amorphous	64	239

3.2.4.1 3-acetyl-6-nitro-2*H*-chromen-2-one (SVN i1)

FT-IR (neat cm^{-1}): 1745, 1687, 1652, 1548. ^{1}H-NMR (400 MHz, $CDCl_3$) δ: 8.95 (1H, s), 8.81 (1H, s), 8.52-8.50 (1H, m), 7.70-7.67 (1H, m), 2.60 (3H, s); ^{13}C-NMR (100 MHz, $CDCl_3$) δ 194.68, 158.00, 157.44, 145.77, 143.70, 128.45, 126.41, 126.08, 118.51, 117.66, 29.88. LC-MS (ESI, Positive): *m/z* $(M)^+$; 234. Anal calculated for: $C_{11}H_7NO_5$: C, 56.66, H, 3.03, N, 6.01: Found: C, 56.64, H, 3.08, N, 6.05.

3.2.4.2 3-(2-bromoacetyl)-6-nitro-2*H*-chromen-2-one (SVN i2)

FT-IR (neat cm^{-1}): 1753, 1728, 1679, 1606, 1554. ^{1}H-NMR (400 MHz, $CDCl_3$) δ 8.98 (1H, s), 8.72 (1H, s), 8.65 (1H, s), 4.41 (2H, s). ^{13}C-NMR (100 MHz, $CDCl_3$) δ 194.92,157.74, 156.70, 149.33, 145.91, 143.78, 129.39, 128.37, 126.68, 125.43, 118.56, 117.97, 117.80, 117.51, 103.47, 43.77. LC-MS (ESI, Positive): *m/z* $(M)^+$; 311. Anal calculated for: $C_{11}H_6BrNO_5$: C, 42.34, H, 1.93, N, 4.49: Found: C, 42.35, H, 1.98, N, 4.52.

3.2.4.3 3-(2-aminothiazol-4-yl)-6-nitro-2*H*-chromen-2-one (SVN i3)

FT-IR (neat cm^{-1}): 1712, 1641, 1612, 1529, 1479. ^{1}H-NMR (400 MHz, $CDCl_3$) δ : 8.82 (1H, s), 8.61 (1H, s), 8.39-8.36 (1H, m), 7.65-7.62 (1H, m), 7.24 (1H, s); ^{13}C-NMR (100 MHz, $CDCl_3$) δ 167.59, 157.81, 155.65, 143.77, 142.27, 136.81, 125.71, 124.41, 121.75, 119.72, 117.27, 110.14. LC-MS (ESI, Positive): *m/z* $(M)^+$; 290. Anal calculated for: $C_{12}H_7N_3O_4S$: C, 49.83, H, 2.44, N, 14.53: Found: C, 49.84, H, 2.49, N, 14.50.

3.2.4.4 (*E*)-3-(2-(benzylidene amino) thiazol-4-yl)-6-nitro-2*H*-chromen-2-one (SVN 1)

FT-IR (neat cm^{-1}): 1712, 1647, 1571, 1411. ^{1}H-NMR (400 MHz, $CDCl_3$) δ: 8.91 (1H, s), 8.65 (1H, s), 8.44-8.42 (1H, m), 7.99-7.97 (1H, m), 7.66-7.57 (2H, m), 7.26 (1H, m), 7.12-7.07 (2H, m) 6.25-6.19 (2H, m); ^{13}C-NMR (100 MHz, $CDCl_3$) δ 173.49, 167.55, 160.40, 157.45, 155.24, 143.39, 142.37, 136.33, 131.2, 129.22, 128.74, 125.40, 124.22, 121.79, 119.50, 117.08, 110.01. LC-MS (ESI, Positive): *m/z* $(M)^+$; 378. Anal calculated for: $C_{19}H_{11}N_3O_4S$: C, 60.47, H, 2.94, N, 11.14: Found: C, 60.48, H, 2.90, N, 11.15.

3.2.4.5 (*E*)-3-(2-((4-methoxybenzylidene) amino) thiazol-4-yl)-6-nitro-2*H*-chromen-2-one (SVN 2)

FT-IR (neat cm^{-1}): 1731, 1622, 1589, 1558, 1537. ^{1}H-NMR (400 MHz, $CDCl_3$) δ : 8.91 (1H, s), 8.45 (1H, s), 8.39-8.37 (2H, m), 8.00 (1H, s), 7.66-7.64 (2H, m), 7.90-7.87 (2H, m), 7.57 (1H, s), 7.26 (1H, s), 3.87 (3H, s); ^{13}C-NMR (100 MHz, $CDCl_3$) δ 173.51, 167.55, 162.19, 160.30, 157.66, 155.44, 143.39, 142.37, 136.33, 129.12, 128.57, 125.40, 124.22, 121.79, 119.40, 117.28, 110.21. LC-MS (ESI, Positive): *m/z* $(M)^+$; 408. Anal calculated for: $C_{20}H_{13}N_3O_5S$: C, 58.97, H, 3.23, N, 10.31: Found: C, 58.94, H, 3.28, N, 10.35.

3.2.4.6 (*E*)-3-(2-((4-chlorobenzylidene) amino) thiazol-4-yl)-6-nitro-2*H*-chromen-2-one (SVN 3)

FT-IR (neat cm^{-1}): 2945, 1735, 1556, 1456. ^{1}H-NMR (400 MHz, $CDCl_3$) δ: 8.84 (1H, s), 8.63 (1H, s), 8.39-8.37 (3H, m), 7.66-7.57 (3H, m), 7.21 (2H, s); ^{13}C-NMR (100 MHz, $CDCl_3$) δ 172.94, 167.51, 157.86, 155.65, 143.79, 142.78, 136.73, 130.2, 129.88, 128.82, 125.70, 124.42, 121.98, 119.80, 117.28, 110.16. LC-MS (ESI, Positive): *m/z* $(M)^+$; 412. Anal calculated for: $C_{19}H_{10}ClN_3O_4S$: C, 55.42, H, 2.45, N, 10.20: Found: C, 55.45, H, 2.44, N, 10.15.

3.2.4.7 (*E*)-3-(2-((4-Fluorobenzylidene) amino) thiazol-4-yl)-6-nitro-2*H*-chromen-2-one (SVN 4)

FT-IR (neat cm^{-1}): 1739, 1652, 1608, 1475. ^{1}H-NMR (400 MHz, $CDCl_3$) δ: 8.85 (1H, s), 8.63 (1H, s), 8.40-8.38 (1H, m), 8.08 (1H, s), 8.00 (1H, s), 7.66-7.64 (2H, m), 7.58 (1H, s), 7.22-7.21 (2H, m). ^{13}C-NMR (100 MHz, $CDCl_3$) δ 172.92, 167.51, 166.81, 157.86, 155.56, 143.79, 142.78, 136.74, 125.71, 124.43, 121.99, 119.80, 117.20, 110.17; LC-MS (ESI, Positive): *m/z* $(M)^+$; 396. Anal calculated for: $C_{19}H_{10}FN_3O_4S$: C, 57.72, H, 2.55, N, 10.63: Found: C, 57.73, H, 2.58, N, 10.65.

3.2.4.8 (*E*)-6-nitro-3-(2-((thiophen-2-ylmethylene) amino) thiazol-4-yl)-2*H*-chromen-2-one (SVN 5)

FT-IR (neat cm^{-1}): 1739, 1608, 1479, 1342. ^{1}H-NMR (400 MHz, $CDCl_3$) δ: 9.95 (1H, s), 8.84 (1H, s), 8.63 (1H, s), 8.40-8.37 (1H, m), 7.66-7.58 (2H, m), 7.35-7.34 (2H, m) 7,23-7,14 (1H, m); ^{13}C-NMR (100 MHz, $CDCl_3$) δ 184.30,167.51, 157.85, 155.66, 143.79, 142.65, 141.55, 137.96, 136.09, 128.95, 128.52, 125.72, 127.22, 124.42, 121.93, 119.78, 117.29, 110.17. LC-MS (ESI, Positive): *m/z* $(M)^+$; 384. Anal calculated for: $C_{17}H_9N_3O_4S_2$: C, 53.26, H, 2.37, N, 10.96: Found: C, 53.24, H, 2.40, N, 10.97.

3.2.4.9 (*E*)-6-nitro-3-(2-((pyridin-4-ylmethylene) amino) thiazol-4-yl)-2*H*-chromen-2-one (SVN 6)

FT-IR (neat cm^{-1}): 1733, 1652, 1583, 1537. ^{1}H-NMR (400 MHz, $CDCl_3$) δ: 10.09 (1H, s), 8.89 (1H, s), 8.84 (1H, s), 8.74-8.71 (2H, m), 8.39-8.37 (1H, m), 8.07 (1H, s), 7.82-7.73 (2H, m), 7.65-7.63 (1H, m); ^{13}C-NMR (100 MHz, $CDCl_3$) δ 172.00, 167.51, 166.12, 157.85, 155.64, 151.02, 150.50, 143.78, 142.73, 138.10, 136,74, 125.70, 124.41, 123.84, 122.75, 122.13, 121.96, 119.78, 110.17. LC-MS (ESI, Positive): *m/z* $(M)^+$; 379. Anal calculated for: $C_{18}H_{10}N_4O_4S$: C, 57.14, H, 2.66, N, 14.81: Found: C, 57.15, H, 2.68, N, 14.83.

3.2.4.10 (*E*)-3-(2-((2-hydroxybenzylidene) amino) thiazol-4-yl)-6-nitro-2*H*-chromen-2-one (SVN 7)

FT-IR (neat cm^{-1}): 1728, 1535, 1477. ^{1}H-NMR (400 MHz, $CDCl_3$) δ: 8.56 (1H, s), 8.34 (1H, s), 8.25-8.23 (2H, m), 8.15-8.14 (1H, m), 8.09 (1H, s), 7.65-7.62 (2H, m), 7.57-7.55 (1H, m) 7.48-7.46 (1H, m), 6.98-6.87 (1H, m); ^{13}C-NMR (100 MHz, $CDCl_3$) δ 172.01, 161.92, 161.12, 160.00, 151.12, 149.42, 146.14, 144.62, 132.22, 132.11, 129.44, 124.51, 124.42, 123.12, 121.42, 121.22, 120.23, 118.42, 117.54. LC-MS (ESI, Positive): *m/z* $(M)^+$; 394. Anal calculated for: $C_{19}H_{11}N_3O_5S$: C, 58.01, H, 2.82, N, 10.68: Found: C, 58.04, H, 2.80, N, 10.70.

3.2.4.11 (*E*)-3-(2-((3,4-dihydroxybenzylidene) amino) thiazol-4-yl)-6-nitro-2*H*-chromen-2-one (SVN 8)

FT-IR (neat cm^{-1}): 1735, 1647, 1573. ^{1}H-NMR (400 MHz, $CDCl_3$) δ: 10.72 (1H, s), 10.26 (1H, s), 8.85 (1H, s), 8.63 (1H, s), 8.40-8.38 (2H, m), 7.66-7.50 (3H, m), 7.09-6.98 (2H, m), 7.57-7.55 (1H, m) 7.48-7.46 (1H, m), 6.98-6.87 (1H, m); ^{13}C-NMR (100 MHz, $CDCl_3$) δ 191.70, 167.51, 160.67, 157.86, 155.56, 143.79, 142.75, 136.76, 136.39, 129.17, 125.72, 124.43, 121.98, 119.80, 119.45, 117.29, 110.17. LC-MS (ESI, Positive): *m/z* $(M)^+$; 410. Anal calculated for: $C_{19}H_{11}N_3O_6S$: C, 55.75, H, 2.71, N, 10.26: Found: C, 55.74, H, 2.75, N, 10.28.

3.2.4.12 (*E*)-3-(2-((2-methoxybenzylidene) amino) thiazol-4-yl)-6-nitro-2*H*-chromen-2-one (SVN 9)

FT-IR (neat cm^{-1}): 1747, 1670, 1650, 1600, 1512. ^{1}H-NMR (400 MHz, $CDCl_3$) δ: 10.11 (1H, s), 9.55 (1H, s), 8.85 (1H, s), 8.63 (1H, s), 8.40-8.38 (2H, m), 7.66-7.64 (1H, m), 7.58 (1H, s), 7.28-7.26 (2H, m), 3.87 (3H, s); ^{13}C-NMR (100 MHz, $CDCl_3$) δ 191.05, 167.52, 157.86, 155.66, 152.09, 145.84, 143.80, 142.68, 136.77, 128.81, 125.72, 124.44, 121.95, 119.80,

119.45, 117.29, 115.48, 110.17. LC-MS (ESI, Positive): *m/z* $(M)^+$; 408. Anal calculated for: $C_{20}H_{13}N_3O_5S$: C, 58.96, H, 3.22, N, 10.31: Found: C, 58.98, H, 3.20, N, 10.36.

3.2.4.13 (*E*)-3-(2-((2-hydroxy-5-nitrobenzylidene) amino) thiazol-4-yl)-6-nitro-2*H*-chromen-2-one (SVN 10)

FT-IR (neat cm^{-1}): 1735, 1676, 1589, 1527. ^{1}H-NMR (400 MHz, $CDCl_3$) δ: 10.30 (1H, s), 8.86 (1H, s), 8.64 (1H, s), 8.42-8.32 (2H, m), 7.66-7.58 (1H, m), 7.21-7.13 (2H, m), 6.87 (1H, s) 6.66 (1H, s); ^{13}C-NMR (100 MHz, $CDCl_3$) δ 171.82, 167.22, 161.90, 160,05, 159.23, 149.44, 146.62, 144.54, 140.39, 129,72, 128.62, 128.33, 124.51, 124.11, 123.59, 123.54, 119.97, 118.56, 118.23, 110.21. LC-MS (ESI, Positive): *m/z* $(M)^+$; 439. Anal calculated for: $C_{19}H_{10}N_4O_7S$: C, 52.06, H, 2.30, N, 12.78: Found: C, 52.05, H, 2.35, N, 12.80.

3.2.4.14 (*E*)-3-(2-((3,5-dichloro-2-hydroxybenzylidene) amino) thiazol-4-yl)-6-nitro-2*H*-chromen-2-one (SVN 11)

FT-IR (neat cm^{-1}): 1733, 1552, 1452. ^{1}H-NMR (400 MHz, $CDCl_3$) δ: 10.26 (1H, s), 8.86 (1H, s), 8.64 (1H, s), 8.40-8.38 (1H, m), 7.72-7.58 (1H, m), 7.21-7.13 (1H, m), 7.09 (1H, s), 7.03 (1H, s); ^{13}C-NMR (100 MHz, $CDCl_3$) δ 167.51, 159.87, 157.86, 155.66, 143.80, 142.76, 136.75, 134.34, 128.55, 128.14, 126.93, 125.72, 124.44, 119.81, 117.29, 110.17. LC-MS (ESI, Positive): *m/z* $(M)^+$; 461. Anal calculated for: $C_{19}H_9Cl_2N_3O_5S$: C, 49.37, H, 1.96, N, 9.09: Found: C, 49.34, H, 1.93, N, 9.13.

3.3 RESULTS AND DISCUSSION

The synthetic strategy used to produce **SVM 1-11** and **SVN 1-11** is illustrated in schemes 1 and 2, respectively. Synthesis of the title compounds **SVM 1-11** and **SVN 1-11** from schemes 1 and 2 was achieved through Knoevenagel condensation of substituted salicylaldehyde (0.01 mol) and ethyl acetoacetate (0.012 mol) in the presence of the catalytic amount of piperidine at low temperature to obtain the intermediates 3-acetyl 6-substituted coumarin (**SVM i1** and **SVN i1**). The intermediate was purified by the recrystallization method using ethanol as solvent. The intermediates **SVM i1** and **SVN i1** were characterized by Fourier-transform infrared spectroscopy (FT-IR), Nuclear magnetic resonance (NMR), LC-MS, and elemental analysis. The carbonyl functional group on the benzopyrone nucleus is observed at 1753 and 1745 cm^{-1} for **SVM i1** and **SVN i1**, respectively. Singlet peak for three protons on ^{1}H-NMR for methyl group at δ 2.51 and 2.6 for **SVM i1** and **SVN i1**, respectively. The carbonyl group on ^{13}C-NMR is observed at δ 194.67 and 194.68 for **SVM i1** and **SVN i1**, respectively, confirming the formation of products. In LC-MS, the molecular ion peak for intermediates **SVM i1** and **SVN i1** is observed at 256$(M)^{+}$ and 234$(M)^{+}$, respectively. The molecular ion peaks of the intermediates were in good agreement with the proposed molecular weight, and elemental analysis results were within $\pm$0.4% of the calculated values. The intermediates 3-acetyl 6-substituted coumarin (**SVM i1** and **SVN i1**) (0.01 mol) were subjected to bromination (0.01 mol) in a chloroform medium to obtain the intermediates 3-bromoacetyl 6-substituted coumarins (**SVM i2** and **SVN i2**). The resulting 3-bromoacetyl 6-substituted coumarins (**SVM i2** and **SVN i2**) were purified by washing with chloroform. The intermediates **SVM i2** and **SVN i2** were characterized by Fourier-transform infrared spectroscopy (FT-IR), Nuclear magnetic resonance (NMR), LC-MS, and elemental analysis. The carbonyl functional group on the benzopyrone nucleus is observed at 1743 and 1753 cm^{-1} for **SVM i2** and **SVN i2**, respectively. Singlet peak for two protons on ^{1}H-NMR for methyl group at δ 4.45 and 4.41for **SVM i2** and **SVN i2**, respectively. The carbonyl group on ^{13}C-NMR is observed at δ 196.58 and 194.92 for **SVM i2** and **SVN i2**, respectively, confirming the formation of products. In LC-MS, the molecular ion peak for intermediates **SVM i2** and **SVN i2** is observed at 334 $(M)^{+}$ and 311 $(M)^{+}$, respectively. The molecular ion peaks of the intermediates were in good agreement with the proposed molecular weight, and elemental analysis results were within $\pm$0.4% of the calculated values. The 3-bromoacetyl 6-substituted coumarins (**SVM i2** and **SVN i2**) were cyclized with thiourea in an ethanol medium to yield the parent compounds 3-(2-aminothiazol-4-yl)-6,8-dichloro-2*H*-chromen-2-one (**SVM i3**) and 3-(2-aminothiazol-4-yl)-6-nitro-2*H*-

chromen-2-one (**SVN i3**). The final Schiff bases (**SVM1-11** and **SVN1-11**) were prepared by condensation of parent compounds 3-(2-aminothiazol-4-yl)-6,8-dichloro-2*H*-chromen-2-one (**SVM i3**) and 3-(2-aminothiazol-4-yl)-6-nitro-2*H*-chromen-2-one (**SVN i3**) with substituted aromatic aldehydes in the presence of ethanol by the conventional reflux method. The parent compounds **SVM i3,** and **SVN i3** were characterized by Fourier-transform infrared spectroscopy (FT-IR), Nuclear magnetic resonance (NMR), LC-MS, and elemental analysis. The cyclized parent products **SVM i3** and **SVN i3** are confirmed by the appearance of primary amine (doublet peak on FT-IR at 3377, 3201 for **SVM i3** and **SVN i3**, respectively. The carbonyl functional group on the benzopyrone nucleus is observed at 1691 and 1712 cm^{-1} for **SVM i3** and **SVN i3**, respectively. The disappearance of aliphatic protons on ^{1}H-NMR and the disappearance of the highly deshielded carbonyl group on ^{13}C-NMR confirmed the formation of parent compounds **SVM i3** and **SVN i3.** In LC-MS, the molecular ion peak for parent compounds **SVM i3,** and **SVN i3** is observed at 312 $(M)^{+}$ and 290 $(M)^{+}$, respectively. The molecular ion peaks of the parent compounds were in good agreement with the proposed molecular weight, and elemental analysis results were within $\pm$0.4% of the calculated values. The final Schiff bases **SVM1-11** and **SVN1-11** were characterized by Fourier-transform infrared spectroscopy (FT-IR), Nuclear magnetic resonance (NMR), LC-MS, and elemental analysis. The yield of the final compounds **SVM 1-11** and **SVN 1-11** were in the range of 62 to 74%, as shown in Tables 2 and 3. The formation of Schiff bases **SVM1-11** and **SVN1-11** were confirmed by the appearance of methine (singlet) peak on FT-IR at 2941 and 2945 for **SVM1-11** and **SVN1-11**, respectively. The carbonyl functional group on the benzopyrone nucleus is observed in the range of 1735-1747 and 1712-1747 cm^{-1} for **SVM1-11** and **SVN1-11**, respectively. The appearance of an aliphatic proton on ^{1}H-NMR in the range of δ 7.22-8.02 and 7.26-8.63 for **SVM i2** and **SVNi2**, respectively. The aliphatic carbon in Schiff bases of methine group on ^{13}C-NMR is observed at δ 110.27-114.74 and 110.01-110.17 for **SVM1-11** and **SVN1-11**, respectively, confirming the formation of products. The molecular ion peaks of the Schiff bases were in good agreement with the proposed molecular weight, and elemental analysis results were within $\pm$0.4% of the calculated values.

CHAPTER IV. ANTI-TB ACTIVITY OF SCHIFF BASES OF 3-(2-AMINOTHIAZOL-4-YL)-6,8-DICHLORO-2*H*-CHROMEN-2-ONE (SVM1-11) AND (*E*) 3-(2-AMINOTHIAZOL-4-YL)-6-NITRO-2*H*-CHROMEN-2-ONE (SVN 1-11) AGAINST H37RV-MTB AND MULTIDRUG-RESISTANT TB (MDR-TB)

4.1 Anti-TB activity of Schiff bases of 3-(2-aminothiazol-4-yl)-6,8-dichloro-2*H*-chromen-2-one (SVM1-11) against H37Rv-MTB and multidrug-resistant TB (MDR-TB)

Abstract

Tuberculosis is one of the most diagnosed diseases among HIV-infected and diabetic individuals and its prevalence has been substantially increasing over the years. Mycobacterium-resistant strains have been a source of concern due to the inefficacy of conventional anti-mycobacterial therapy. Hybridization of two molecules has emerged as a potential method for discovering new candidates with a more extensive range of activity, greater efficacy, reduced toxicity and various modes of action. This chapter presents the report of the *in vitro* and *in-silico* anti-mycobacterial activity of the synthesized Schiff bases of 3-(2-aminothiazol-4-yl)-6,8-dichloro-2*H*-chromen-2-one (**SVM 1-11**) against H37Rv MTB and multidrug-resistant MDR-MTB strains. For the *in vitro* evaluation, the tested compounds exhibited anti-tuberculosis (TB) activity in the range of 0.5-4 µg/mL against H37Rv MTB and 8- 64 µg/mL against MDR-MTB. The test compounds **SVM 3, 4, 8** and **10** emerged as the most promising against both strains H37Rv MTB and MDR-MTB with a MIC value ranging from 0.5 to 8 µg/mL.

Moreover, compounds **SVM 7** and **11** displayed a remarkable anti- TB activity with a MIC value of 1 µg/mL against H37Rv MTB. Similarly, compounds **SVM 5** was potent against MDR-MTB, exhibiting a MIC value of 8 µg/mL. Molecular docking against druggable targets DprE1 and Pks13 enzymes of *M. tuberculosis* revealed high affinity of the synthesized compounds relative to the reference standards, which could be attributed to the differences in their interactions with the active site amino acid residues of the respective protein. These results could be considered remarkable and suggest that the novel Schiff bases 3-(2-aminothiazol-4-yl)-6,8-dichloro-2*H*-chromen-2-one (**SVM1-11**) may be regarded as a new series with improved anti-mycobacterial activity, which could be further optimized and developed as potential leads for TB treatment.

4.1.1 Introduction

Tuberculosis is a significant public health problem; in 2020, the number of fatalities officially classified as TB-related (1.3 million) was nearly double that of HIV/AIDS (0.68 million), the COVID-19 pandemic in 2020 has had a more significant impact on TB death than HIV/AIDS (WHO, 2021a). Although the availability of standard anti-TB drugs such as isoniazid and rifampicin, pyrazinamide and ethambutol, the TB mortality rate continues to rise. The inability of patients to adhere and comply with the approximately six months treatment period of the current conventional first or second-line anti-TB drugs has raised the risk of drug resistance (Angelova *et al*., 2017). The standard therapy's efficacy is frequently interrupted due to drug side effects, prolonged treatment, and drug resistance development, such as multidrug resistance (MDR) and extensively drug-resistant (XDR) TB. (Khara *et al*., 2014, Manvar *et al*., 2008, Xu *et al*., 2017). Hence, there is the need to develop new active anti-TB drugs against numerous virulent forms of *Mycobacterium tuberculosis* with low toxicity, a shorter treatment period and that can act against the targets involved in resistance (Bhatt *et al*., 2015, Hoagland *et al*., 2016, Singh and Mizrahi, 2017).

Coumarin's unique structure has a remarkable capacity that helps its derivatives interact efficiently with various enzymes and receptors in species by weak bond interactions that potentiate broad medicinal importance (Reddy *et al*., 2015). The synthesis of several substituted coumarin derivatives with a heterocyclic ring, such as thiazole, pyrazole/pyrazoline moiety, has been reported to possess various pharmacological activities such as antimicrobial, anti-inflammatory and analgesic activities (Aggarwal *et al.*, 2013). Integrating two or more pharmacophores into a single molecular structure, known as molecular hybridization, can increase affinity and activity, minimize side effects and reduce drug resistance (Mishra and Singh, 2016). Due to multiple activities displayed by coumarin derivatives and thiazole, this chapter aimed to synthesize novel Schiff bases of 3-(2-aminothiazol-4-yl)-6,8-dichloro-2*H*-chromen-2-one (**SVM 1-11**) and subsequently assess their anti-mycobacterial effect against H37Rv-MTB and MDR-MTB strains using both *in vitro* (the micro alamar blue assay) and *in silico* (molecular docking) methods.

4.1.2 Materials and Methods

4.1.2.1 Antimycobacterial activity

SVM 1-11 was tested for its antimycobacterial activity against M. tuberculosis H37Rv (ATCC 25177) and clinical isolate MDR-TB using Micro Alamar Blue Test (MABA) plate assay. A volume of 200 µL of sterile deionized water was added to all outer-perimeter wells of sterile 96 well plates. 100 µL of Middlebrook 7H9 broth was poured into each of the 96 well plates to decrease the evaporation of the medium in the test wells during incubation. A volume of 100 µL of Middlebrook 7H9 broth was added into each of the 96 well plates and the compounds **SVM 1-11** were serially diluted on the plate. The final drug concentrations tested ranged from 128 to 0.125 µg/mL. Plates were wrapped in parafilm and incubated at 37°C for five days. The plate was then incubated for 24 hours with a freshly prepared 1:1 solution of Alamar Blue (Accumed International, Westlake, Ohio) reagent and 10% tween 80. A blue tint showed no bacterial growth, but a pink colour suggested growth. The MIC (minimal inhibitory concentration) was the lowest treatment concentration, which prevented a blue-to-pink colour shift (Vergara et al., 2009).

4.1.2.2 Computational study

4.1.2.2.1 The Protein

The crystal structures of the two druggable targets, Pks13 thioesterase and DprE1 (decaprenylphosphoryl-Beta-d-ribose 2`epimerase1), were obtained from the RCSB Protein Databank (https://www.rcsb.org). For the *M. tuberculosis* DprE1, the crystal structure in complex with the non-covalent inhibitor Ty38c (PDB ID: 4P8K) was used. In contrast, for the MTB Pks13 thioesterase domain, the crystal structure in complex with inhibitor TAM16 (PDB ID: 5v3y) was employed. Only normal residues of chain A were included in the calculations. The protonation states of all the residues were identified by examining the hydrogen-bond pattern around the His residues, the solvent accessibility, and the possibility of ionic pair formation. All Arg, Lys, Asp, Cys, and Glu residues were supposed to be charged. His-132, 136, 160, and 315 were considered protonated on the ND1 atom in DprE1, whereas His-216 was considered protonated on both the ND1 and NE2 atoms (and therefore positively charged). The remaining five His residues (81, 137, 145, 359, and 428) were modelled with a proton on the NE2 atom. TRP-230 has two different conformations with identical occupation numbers.

We used alternative A in the computations and left out the other. His-1632 was supposed to be protonated on the ND1 atom for the thioesterase, whereas His-1475, 1654, and 1699 were assumed to be protonated on both the ND1 and NE2 atoms (and therefore positively charged). The remaining five His residues (1664 and 1714), on the other hand, were modelled with a proton on the NE2 atom (Kumar *et al*., 2020b).

4.1.2.2.2 Molecular Docking

The anti-tubercular target compounds were chosen for further theoretical study using docking calculations. The GaussView and Gaussian09 software packages were used to create the first structures of probable compounds (Frisch et al., 2009). The molecular mechanics' technique was used to optimize each structure, and the AM1 semi-empirical method was implemented in the Gaussian09 code to get the structures to their energy ground state. Water and other co-crystallized molecules were removed from the protein structure. The Autodock4 software (Molinspiration database) was utilized to construct the structures of the ligand compounds (SVM 1-11) and the protein macromolecule and execute docking calculations. Polar hydrogens and Kollman unified atom-type charges were used to neutralize the protein structure. The force field parameters were generated using Autogrid4 with a grid box size of 60 x 60 x 60 and point separation of 0.375Å. The Lamarckian genetic algorithm, regarded as one of the most acceptable docking methods, was utilized to perform the docking with the active site prediction by FTSite server (Ngan et al., 2011). The docked conformations were grouped and ranked based on the binding or docking free energy (ΔG), wherein complexes with higher negative binding energy values were considered to have higher affinity for the target. The intermolecular interactions of protein inhibitors in the active site were visualized using the Discovery studio 5.0 visualizer (Venugopala *et al*., 2020).

4.1.3 Results and Discussion

4.1.3.1 Antimycobacterial activity of SVM 1-11

The anti-mycobacterial activity of the compounds **SVM1-11** was assessed against H37Rv (ATCC25177) of *Mycobacterium tuberculosis* and the clinical isolate MDR-MTB strain. The MIC values of compounds were determined along with the standard drug (rifampicin and isoniazid); the results are tabulated in Table 4. The results showed that the synthesized compounds emerged as active compounds against mycobacterium strain H37Rv-MTB and MDR-MTB. The Schiff bases of 3-(2-aminothiazol-4-yl)-6,8-dichloro-2*H*-chromen-2-one (**SVM 1-11**) showed inhibitory activity against H37Rv-MTB with a MIC ranging from 0.5 to 4 µg/mL (Table 4). **SVM 8** and **SVM 10** were the most active among these compounds, having MIC values of 0.5 µg/mL against H37Rv-MTB higher than the reference drug rifampicin (1 µg/mL) and isoniazid (3 µg/mL), followed by compounds **SVM 3**, **4, 7** and **11** with a MIC of 1 µg/mL against H37Rv MTB same as the standard drug rifampicin (1 µg/mL). Furthermore, compounds **SVM 2, 5** and **6** showed a MIC of 2 µg/mL, whereas compounds **SVM 1** and **9** displayed a MIC value of 4 µg/mL against H37Rv TB (Table 4).

The above results are comparable to Kumar *et al*. (2020), who synthesized a series of acrylic pyrazole coumarin derivatives and acrylic pyrazole – quinoline derivatives for their anti-tubercular activity against *Mtb* H37Rv. These compounds displayed MIC values ranging from 3.125 to 12.5 µg/mL against *M. Tuberculosis* strain H37Rv (Kumar *et al*., 2020a). In another study, Angelova *et al*. (2016) synthesized a series of coumarins with various substituted hydrazide-hydrazone pharmacophores linked to the chromene ring's third position, which were tested *in vitro* against Mycobacterium TB H37Rv and compared to the first-line anti-tuberculosis drugs isoniazid (INH) and ethambutol (EMB). The antimycobacterial activity was shown at submicromolar concentrations for the most active compounds (12*E*)-4-methoxy-*N*-((2-phenyl-2*H*-chromen-3-yl)methylene)benzohydrazide (**7m)** (MIC 0.13µM), (*E*)-*N*-(3-phenoxy-3-phenylpropylidene)furan-2-carbohydrazide (**7o)** (MIC 0.15µM) and (*E*)-*N*-(3-phenoxy-3-phenylpropylidene) isonicotinohydrazide (**7k)** (MIC 0.17 µM) (Angelova *et al*., 2017). Similarly, Hassan *et al*. (2019) synthesized new hybrid coumarin analogues and tested them for anti-mycobacterial activity against Mtb H37Rv. Amongst these synthesized compounds, 7-(2,4-dichlorophenyl)-5- oxo-3-(2-oxo-2*H*-chromen-3-yl)-5*H*-thiazolo[3,2-a]pyrimidine-6-carbonitrile and 7-(4-nitrophenyl)- 5-oxo-3-(2-oxo-2*H*-chromen-3-yl)-5H-

thiazolo[3,2-a]pyrimidine-6-carbonitrile emerged as the most effective anti-tubercular agents, with MICs of 12.5 µM greater than the cycloserine (Hassan *et al*., 2019).

Compounds **SVM 1-11** were also screened against MDR-MTB; the anti-mycobacterial activity of these compounds was greater than that of the reference drugs. The title compounds, **SVM 3, 4, 5, 8** and **10,** appeared to be the most promising against MDR-MTB, exhibiting a MIC value of 8 µg/mL (Table 4). Moreover, compounds **SVM 2, 6, 9** and **11** showed a MIC value of 16 µg/mL, while compounds **SVM 1** and **7** displayed 64 and 32 µg/mL, respectively (Table 4). The Test compounds were potent against clinical isolates of multi-drug-resistant mycobacterial strains resistant to rifampicin and isoniazid.

These results are comparable to Xu *et al*. (2018), who synthesized a series of isatin (thio)semi carbazide/oxime-1H-1,2,3-triazole-coumarin hybrids and investigated their anti-mycobacterial activity against *M. tuberculosis* (MTB) H37Rv and MDR-TB *in-vitro.* The fundings revealed that the synthesized hybrids showed weak to moderate inhibitory efficacy against MTB H37Rv and MDR-TB (MIC: 50–>200 µg/mL). Compound 2-(5-Fluoro-1-(2-(4-(((4-methyl-2-oxo-2H-chromen-7-yl)oxy)methyl) -1H-1,2,3-triazol-1-yl)ethyl) -2-oxoindolin-3-ylidene)hydrazine carboxamide (**8h**) was the most potent displaying a MIC value of 50 µg/mL against MDR-TB (Xu *et al*., 2018).

Table 4: Anti-TB results of Schiff bases of 3-(2-aminothiazol-4-yl)-6,8-dichloro-2*H*-chromen-2-one (**SVM 1-11**) with the docking free energy (kcal/mol).

Name of Drug	Level of activity (µg/mL)		Docking scores (kcal/mol)	
	H37RV	**MDR**	**Pks13**	**DprE1**
SVM 1	4	64	-8.98	-8.51
SVM 2	2	16	-9.74	-9.01
SVM 3	1	8	-9.79	-9.42
SVM 4	1	8	-8.85	-8.40
SVM 5	2	8	-8.50	-8.21
SVM 6	2	16	-8.42	-8.09
SVM 7	1	32	-9.29	-8.36
SVM 8	0.5	8	-9.41	-8.63
SVM 9	4	16	-9.81	-9.42
SVM 10	0.5	8	-10.30	-9.21
SVM 11	1	16	-9.00	-7.82
Rifampicin	1	na	-7.9	-7.9
Isoniazid	3	na	-6.1	-5.4
DMSO	na	na	-	-

4.1.3.2 Molecular Docking

Docking is now regarded as an important routine calculation in drug development research (Deb *et al*., 2018). It provides more qualitative and quantitative information on the inhibitor's binding affinity at the target enzyme's active site (Deb *et al.*, 2014). The estimated binding free energy and intramolecular interactions are the most important aspects to consider when comparing inhibitor lists, which might be difficult to obtain experimentally. The 11 synthesized compounds (**SVM 1-11**) were docked into the active sites of the two target proteins in this work, Pks13 and DprE1, and their docking scores are presented in Table 4. The results revealed that all the novel coumarin derivatives generally had stronger binding energy towards Pks13 than DprE1. The binding energy ranged from -8.42 to -10.30 kcal/mol for Pks13 relative to -7.82 to -9.42 kcal/mol for DprE1 (Table 4). Except for **SVM 11**, with a marginally lower binding affinity than rifampicin towards DprE1, all the newly synthesized compounds had a better affinity towards the two targets than the two reference standards used in this study (Table

4). Specifically, **SVM 3, 4, 8** and **10** demonstrated excellent binding affinity against both proteins, consistent with the results of the *in vitro* evaluation.

The type of interaction formed, such as H-bonds, pi-pi and van der Waals interactions, has influenced the binding affinity of compounds. The differences in binding affinity and the observed high affinity of the synthesized compounds relative to the reference standards in this study could be attributed to the differences in their interactions with the active site amino acid residues of the respective protein (Figures 10 and 11). For instance, except for isoniazid that formed 11 interactions (4 hydrogens and Van der Waal bonds each, 2 **π**-alkyl and one unfavorable bond) against DPrE1 (Figure 10 F), **SVM 3, 4, 8**, and **10** had either 14 or 15 interactions with DPrE1 (Figures 10 A – D). The 14 interactions observed with rifampicin (Figure 10E) may also account for its relatively higher binding energy than isoniazid. Both **SVM 3** and **4** established hydrogen bond interactions with Ser59 and Gly133 alongside Van der Waals interactions with Gly117 (Figures 10A and B). Compound **SVM 4** also formed additional Van der Waals interactions with Pro316 and Ala417 (Figure 10 B). Compound **SVM 8** similarly had hydrogen bond interactions with Ser59, Gly117, Pro316 and Van der Waals interactions with Arg58, Pro116, Val365 (Figure 10 C), while **SVM 10** exhibited hydrogen bond interactions with Arg58, Thr118, Tyr60, Lys418, Asn385 and Van der Waals interactions with Pro116, Gln336, Gly117, Ser228 (Figure 10 D). More notably, **SVM 3, 4, 8** and **10** had 8 (Trp230, Lys134, Tyr314, Val365, Pro116, Ile131, Arg58 and Val121), 7 (Trp230, Lys134, Tyr314, Val365, Pro116, Arg58 and Val121), 6 (Trp230, Lys134, Ile131, Tyr314, Ala417 and Val121), 5 (Trp16, Val365, Lys314, Phe369, and Lys367) pi-pi interactions with the active site amino acid residues, respectively (Figures 10 A - D). These interactions also contributed to the overall binding affinity of the respective resulting complexes relative to rifampicin (no pi-pi interaction) and isoniazid (2 pi-pi bonds) (Figures 10E and F). Overall, the newly synthesized compounds **SVM 3, 4, 8** and **10** interacted with the distinct catalytically important amino acid residues Ser59, Arg58, Gly117, Gly133, and Thr118 of DprE1 when compared to the reference standards, which might be responsible for their reported activity in this study.

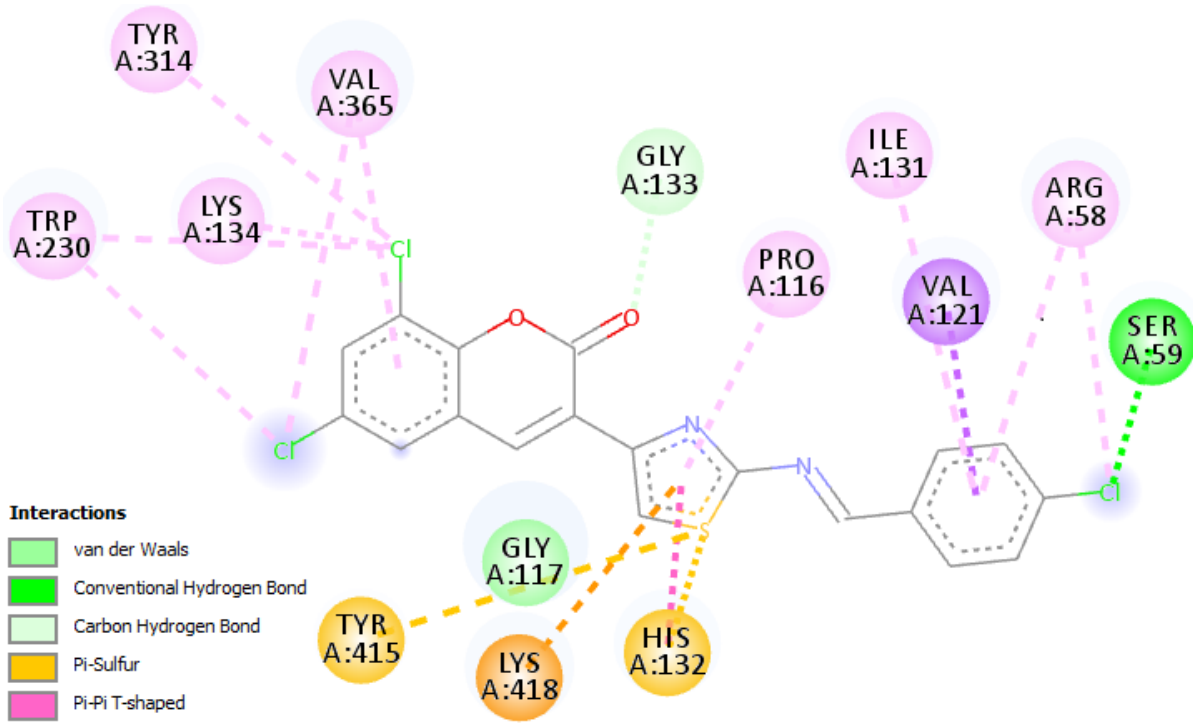
TYR A:314
VAL A:365
LYS A:134
TRP A:230
GLY A:133
ILE A:131
ARG A:58
PRO A:116
VAL A:121
SER A:59
Cl
O
O
N
N
S
Cl
Cl
GLY A:117
TYR A:415
LYS A:418
HIS A:132
Interactions
van der Waals
Conventional Hydrogen Bond
Carbon Hydrogen Bond
Pi-Sulfur
Pi-Pi T-shaped

(A) SVM 3

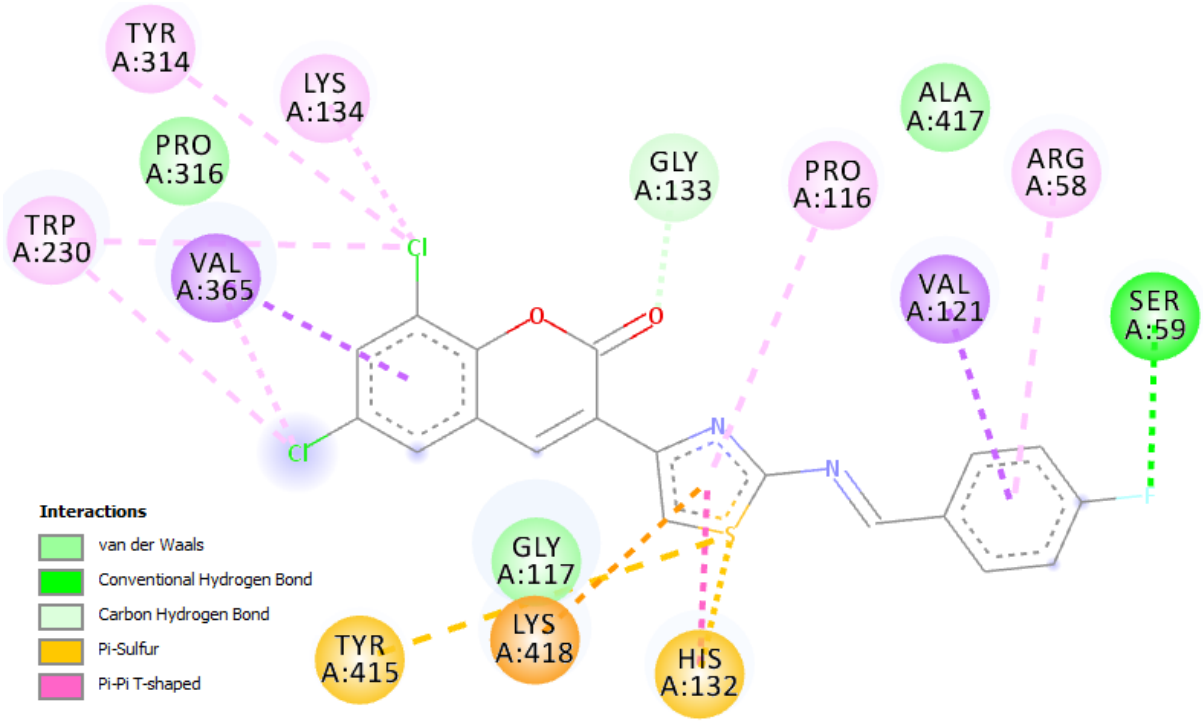
TYR A:314
LYS A:134
PRO A:316
ALA A:417
GLY A:133
PRO A:116
ARG A:58
TRP A:230
VAL A:365
VAL A:121
SER A:59
Cl
O
O
N
N
S
F
Cl
GLY A:117
TYR A:415
LYS A:418
HIS A:132
Interactions
van der Waals
Conventional Hydrogen Bond
Carbon Hydrogen Bond
Pi-Sulfur
Pi-Pi T-shaped

(B) SVM 4

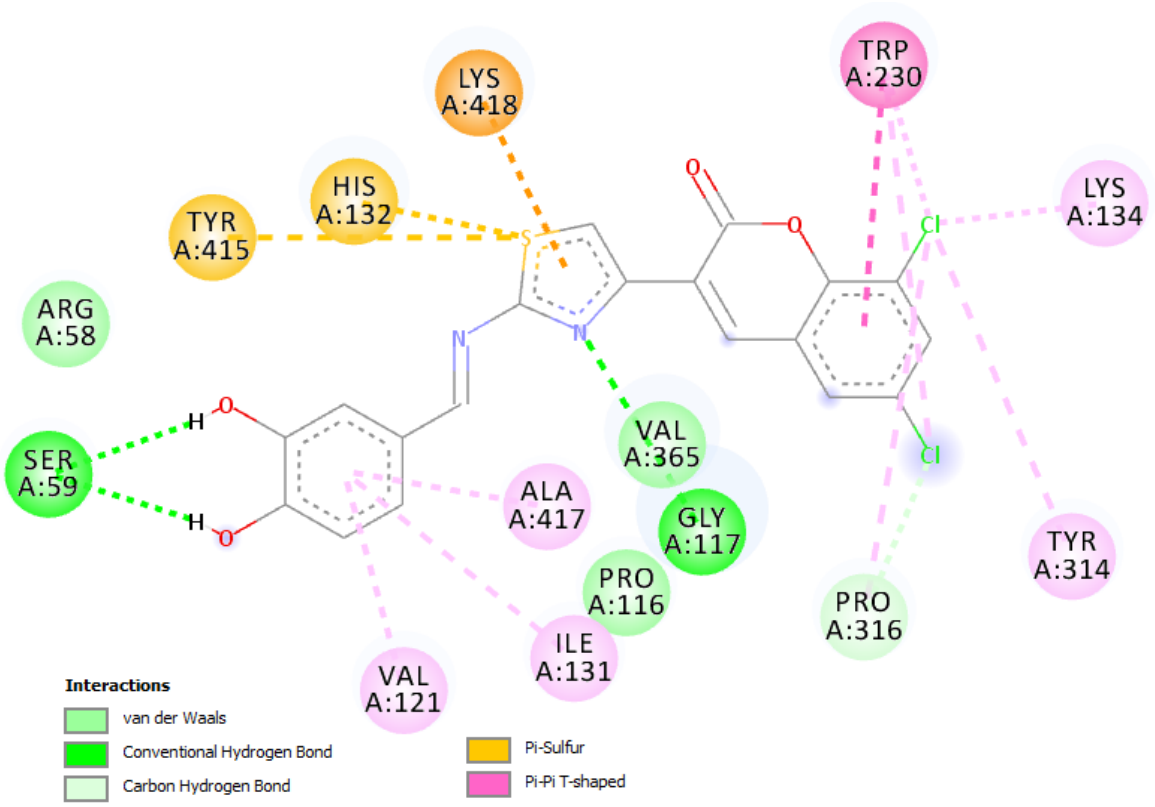

(C) SVM 8

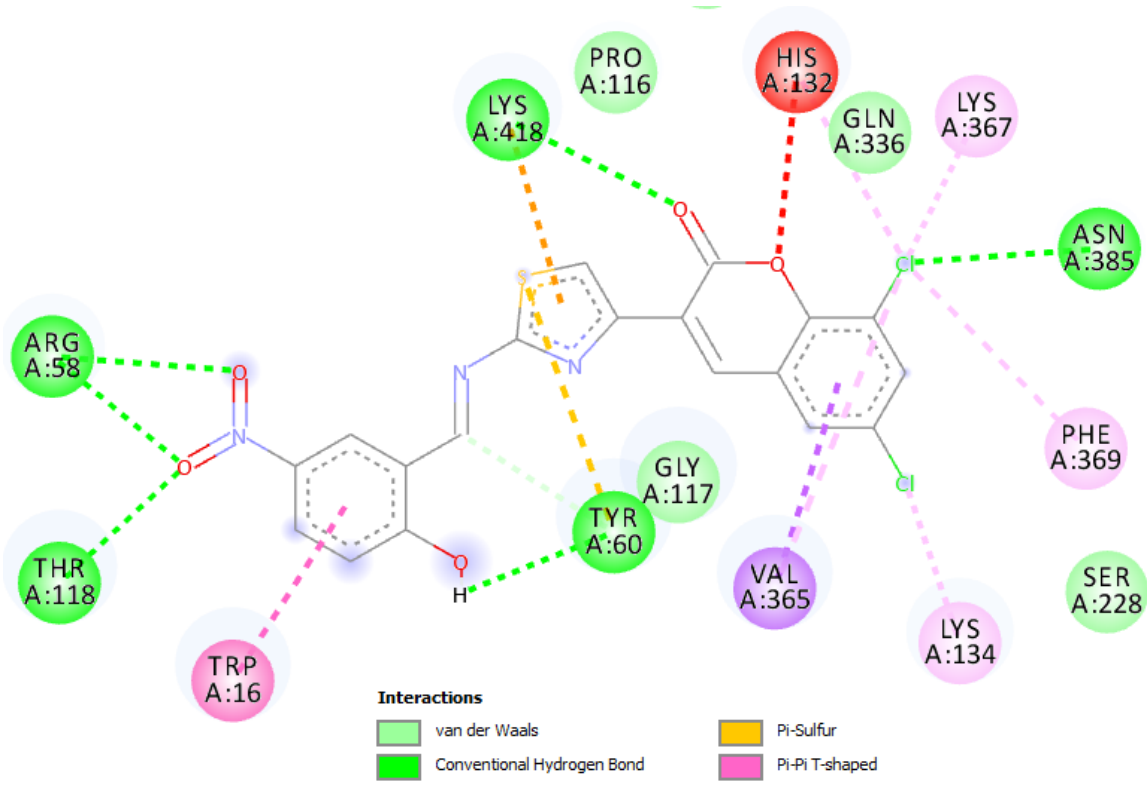

(D) SVM 10

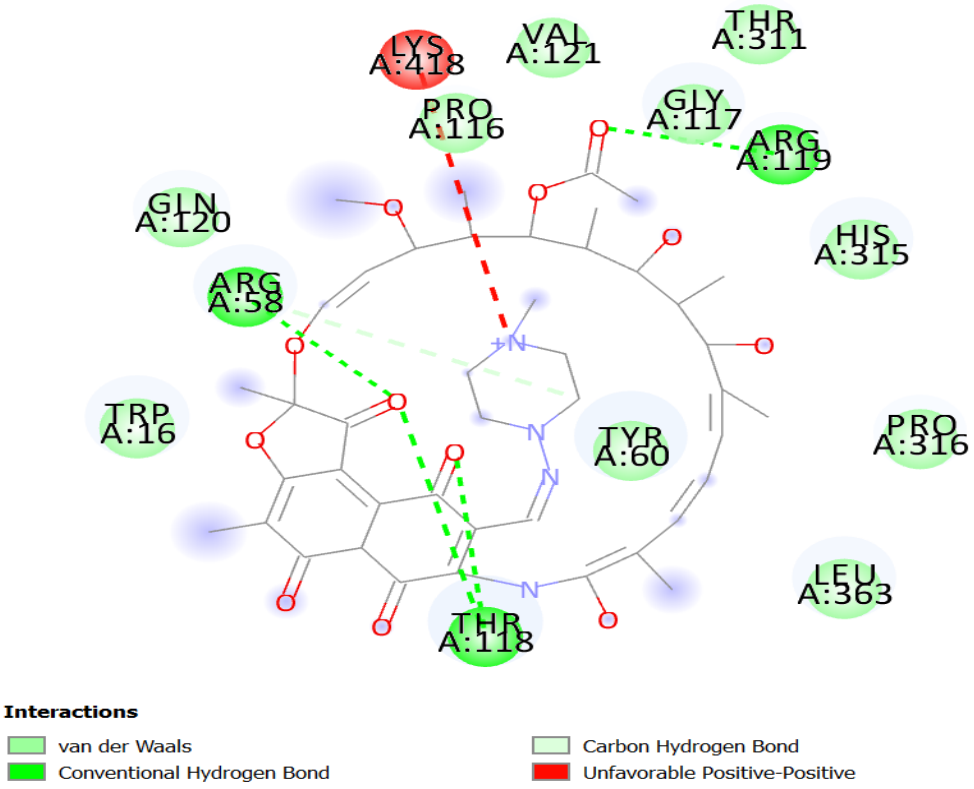

(E) Rifampicin

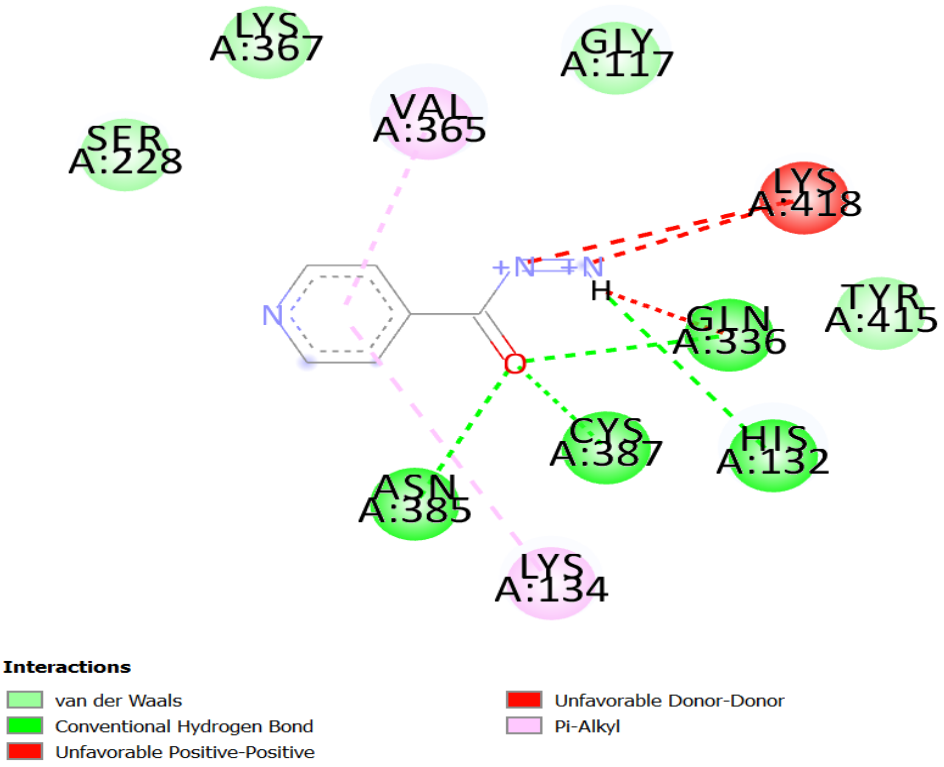

(F) Isoniazid

Figure 10: Interaction plots of (**A**) (**SVM 3**), (**B**) (**SVM 4**), (**C**) (**SVM 8**), (**D**) (**SVM 10**), (**E**) Rifampicin and (**F**) Isoniazid with the active site amino acid residues of DprE1.

The ligand interaction plots of SVM **3, 4, 8**, and **10** against PKs13 are shown in Figure 11. **SVM 3** did not form any interaction with the hydrogen bond; it exhibited Van der Waals interactions with Gln1633, Tyr1637, and Asn1640 (Figure 11A). Similarly, **SVM 4** displayed Van der Waals interactions with Tyr1637 (Figure 11B), while **SVM 8** had hydrogen bond interactions with Gln1633, Asp1644, Arg1641 amino acid residue, and Van der Waals interactions with Tyr1637 and Tyr1582. With Gln1633, Tyr1637, and Ala1667 (Figure 11C). Compound **SVM 10** forms hydrogen bonds with Gln1633, Tyr1637, Ala1667, and Van der Waals interactions with Ser1636, Asn1640, Glu1671, Tyr1674 (Figure 11D). on the other hand, rifampicin showed hydrogen bond interactions with Ala1477 and Gln1633 alongside Van der Waals interactions with His1632, Ser1636, Ile1700, Leu1534, Pro1476, Ile1643, Val1562, Tyr1674, Arg1641, Asp1644, Glu1671, Asp1666 (Figure 11E). Isoniazid displayed hydrogen bond interaction with Asn1640, Asp1644 and Van der Waals interactions with Arg164, Phe1670, Glu1671 (Figure 11F). While **SVM 8** and **10** showed interactions with the same amino acid residues such as hydrogen bond with Gln1633 as rifampicin against PKs13, **SVM 10** also had Van der Waals interactions with Glu1671 and Tyr1674 as rifampicin. Generally, some of the amino acid residues established by the synthesized compounds with PKs13 are different from those of the reference drugs; this could be identified as crucial interactions responsible for their prominent inhibitory effect as elicited in the *in vitro* evaluation.

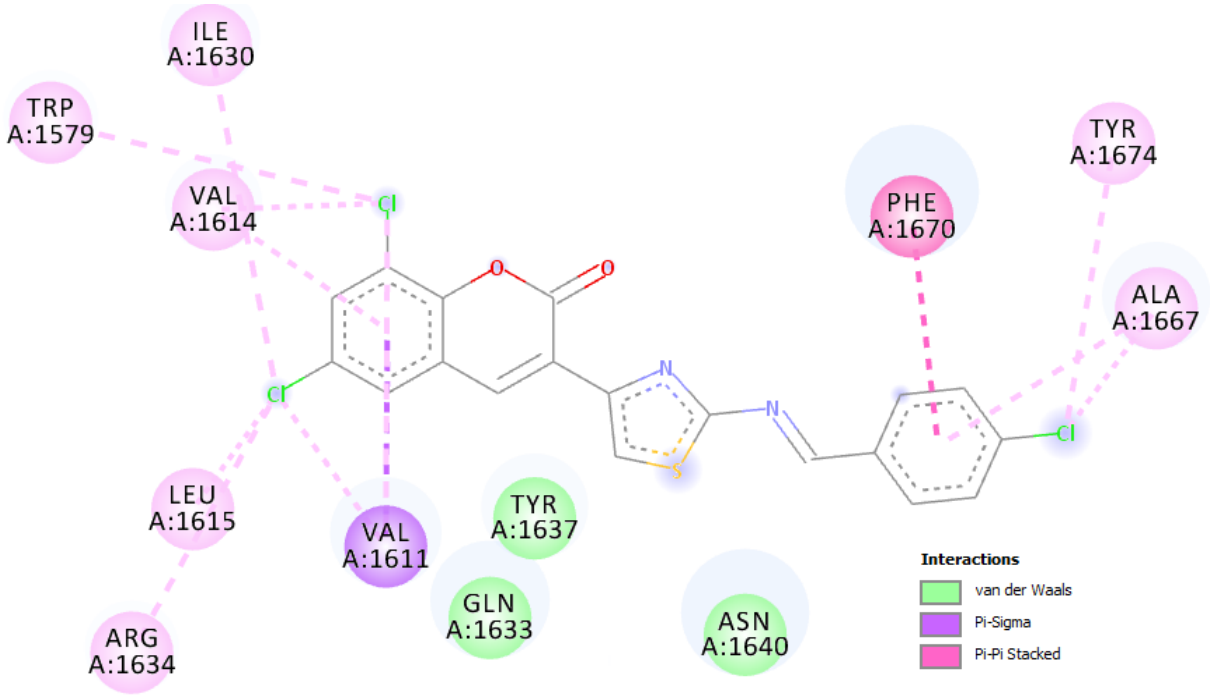
ILE
A:1630
TRP
A:1579
VAL
A:1614
TYR
A:1674
PHE
A:1670
ALA
A:1667
LEU
A:1615
VAL
A:1611
TYR
A:1637
GLN
A:1633
ASN
A:1640
ARG
A:1634
Interactions
van der Waals
Pi-Sigma
Pi-Pi Stacked

(A) SVM 3

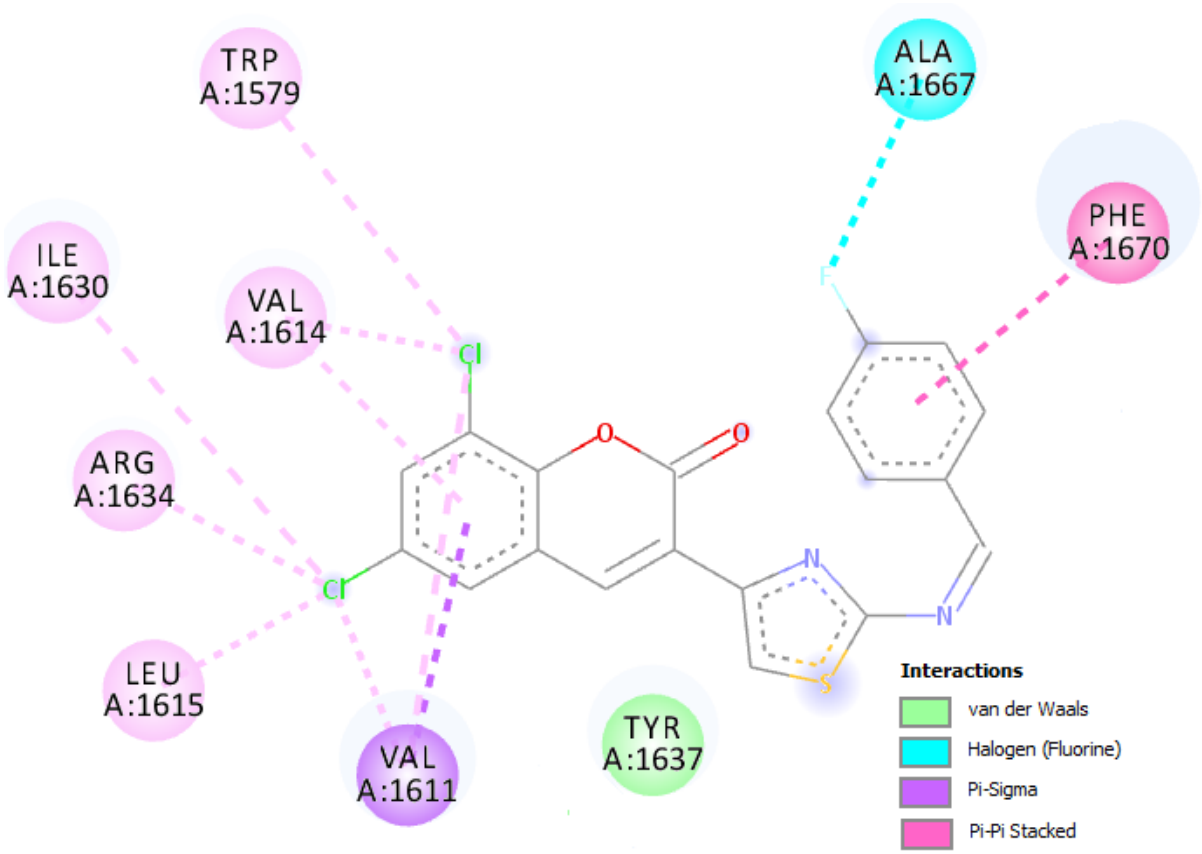
TRP
A:1579
ALA
A:1667
ILE
A:1630
PHE
A:1670
VAL
A:1614
ARG
A:1634
LEU
A:1615
VAL
A:1611
TYR
A:1637
Interactions
van der Waals
Halogen (Fluorine)
Pi-Sigma
Pi-Pi Stacked

(B) SVM 4

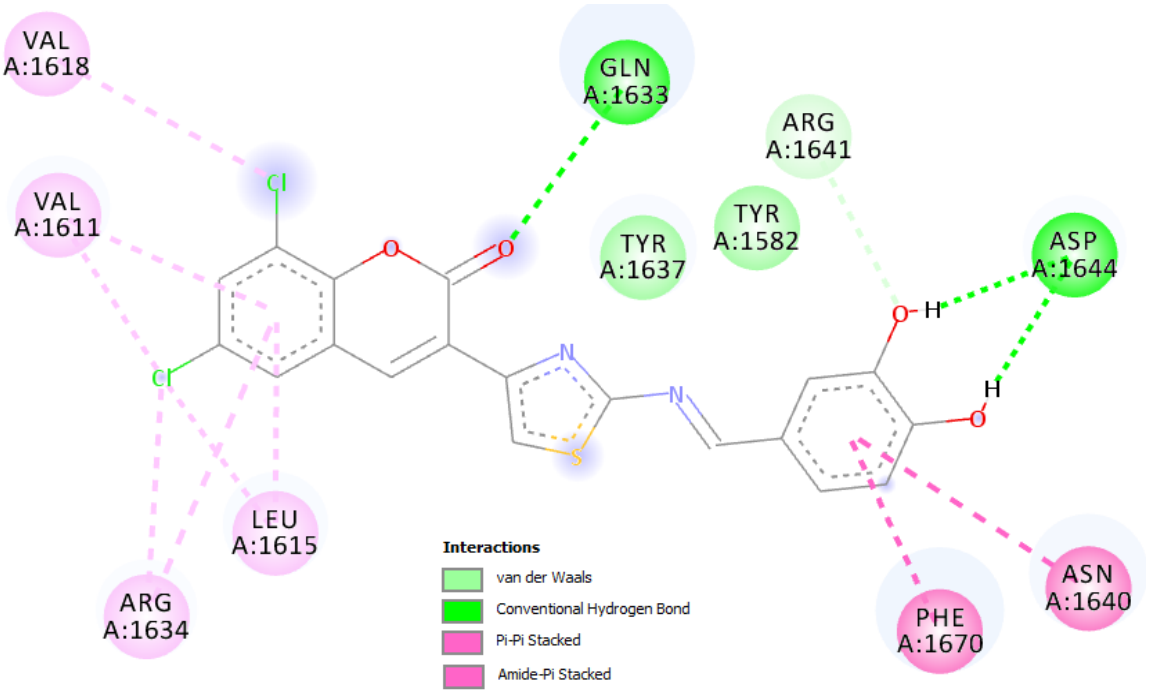

(C) SVM 8

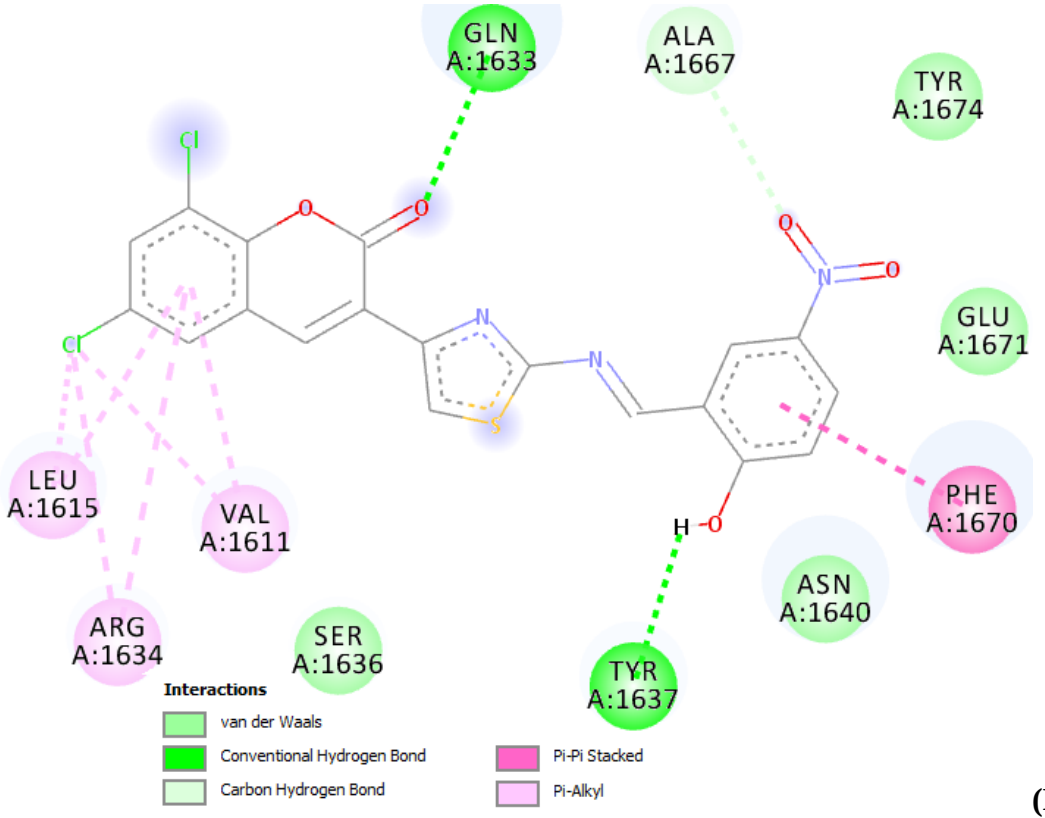

(D)

SVM 10

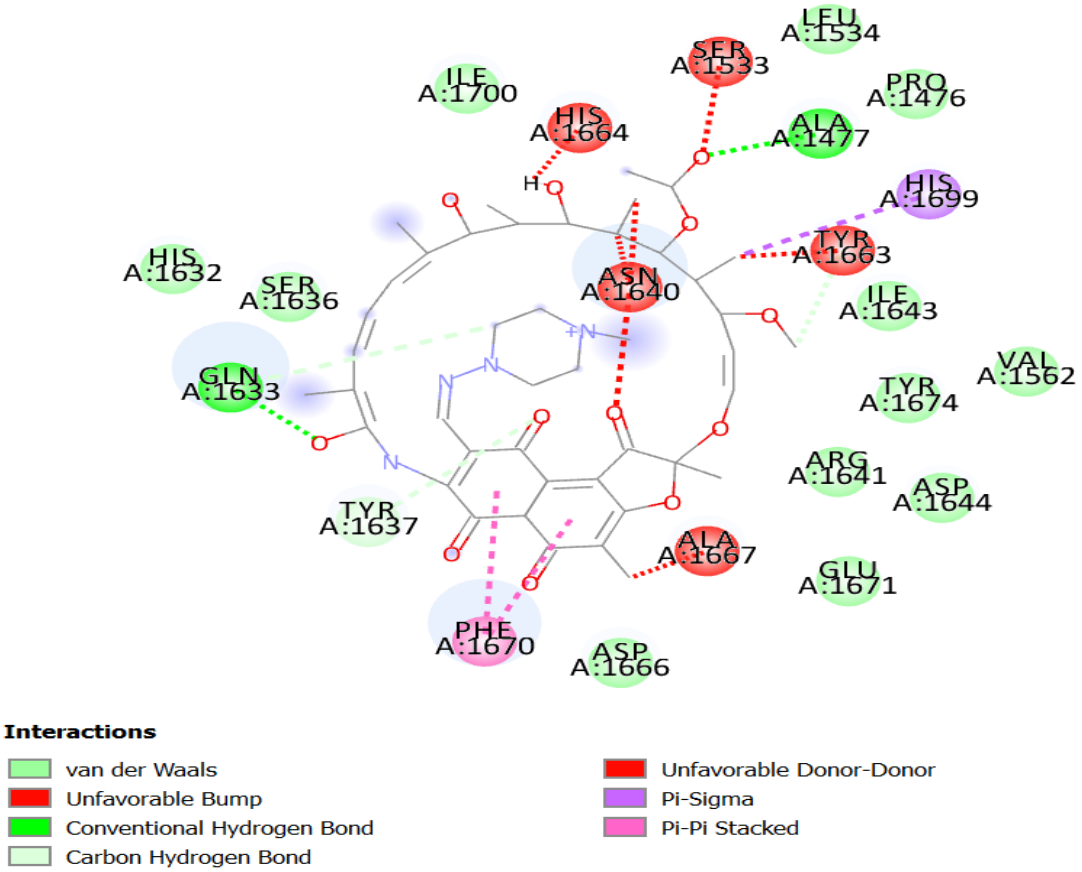

(E) Rifampicin

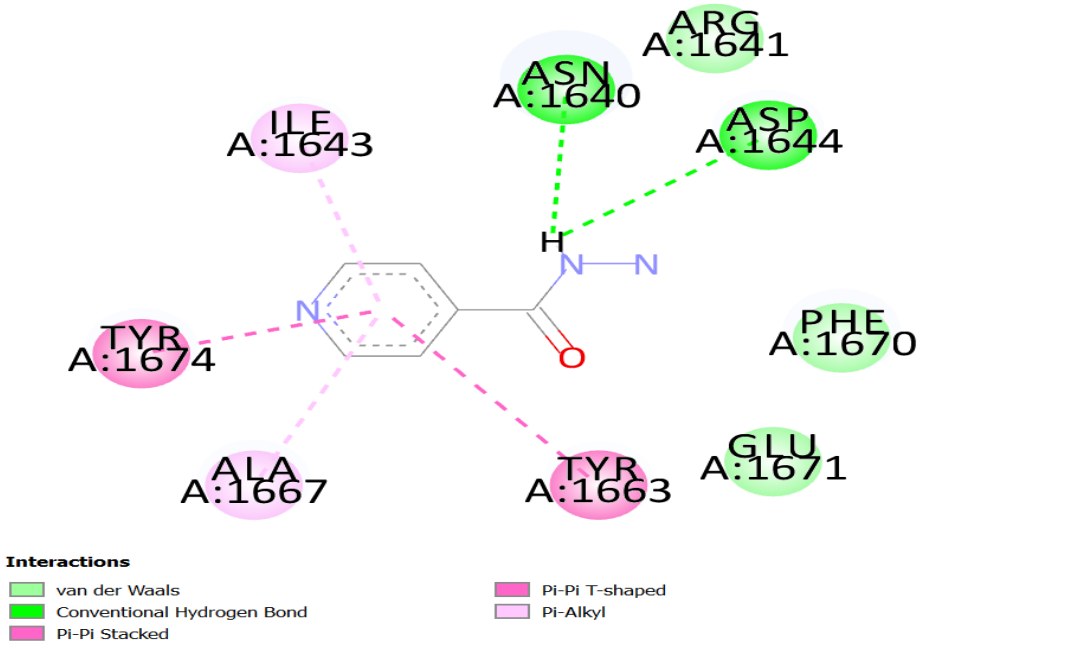

(F) Isoniazid

Figure 11: 2D interaction plots of (**A**) (**SVM 3**), (**B**) (**SVM 4**), (**C**) (**SVM 8**), (**D**) (**SVM 10**), (**E**) Rifampicin and (**F**) Isoniazid with the active amino acid residues of Pks13.

4.1.4 Conclusions

The novel Schiff bases of (*E*) 3-(2-aminothiazol-4-yl)-6,8-dichloro-2*H*-chromen-2-one (**SVM 1-11**) were successfully synthesized, characterized and purified. The results of the *in vitro* evaluation against H37Rv MTB and MDR-TB revealed that the compounds had remarkable inhibitory potential against both *Mycobacterium* strains. Compounds **SVM 8** and **10** were the most active against H37Rv MTB, while compounds **SVM 3, 4, 5, 8** and **10** were the most potent against MDR-TB. These compounds had better MICs comparable to those of the commonly used antimycobacterial drugs rifampicin and isoniazid. Interestingly, the *in-vitro* analysis results were consistent with the computational evaluations. The synthesized compounds established remarkable interactions responsible for the observed activities against the DprE1 and Pks13 enzymes of *M. tuberculosis.* Overall, these results are significant and indicate that the synthesized compounds could be considered a new series with enhanced anti-mycobacterial activity and a potentially promising new class of anti-tuberculosis agents.

4.2 Anti-TB activity of Schiff bases of (*E*) 3-(2-aminothiazol-4-yl)-6-nitro-2*H*-chromen-2-one (SVN 1-11) against H37Rv MTB and multidrug-resistant MTB (MDR-TB)

Abstract

Mycobacterium tuberculosis is an obligated aerobe capable of long-term persistence under the condition of low oxygen tension. Hybridization has emerged as an effective method in developing novel drugs, particularly those with complementary activities and numerous pharmacological targets that could be used to prevent disease resistance to drugs. This chapter presents the results of *in-vitro* and *in silico* anti-tuberculosis (TB) activity of the newly synthesized compounds **SVN 1-11** against H37Rv-MTB and multidrug-resistant TB (MDR-MTB, resistant to isoniazid and Rifampicin). Among the compounds synthesized, **SVN 3, 4, 7, 8, 10** and **11** were shown to have significant anti-TB activity against H37Rv-MTB and MDR-MTB, with minimum inhibitory concentrations ranging from 0.25 to 1 µg/mL and 4 to 16 µg/mL, respectively. Compounds **SVN 3** and **4** were shown to be the most promising, with MICs ranging from 0.5 to 1 µg/mL and 4 to 8 µg/mL against H37Rv-MTB and MDR-MTB, respectively. These observations were further confirmed using molecular docking against DprE1 and PKs13 enzymes of *M. tuberculosis*. The *in-vitro* analysis confirmed the interactions formed between synthesized compounds and amino acid residues at the active site of the targets and their affinities towards enzymes compared to the reference standards. Both **SVN 3** and **4** demonstrated significant binding affinity towards both proteins. Thus, these compounds could be further optimized and developed as potential lead compounds for the management and treatment of TB.

4.2.1 Introduction

Tuberculosis (TB), caused by *Mycobacterium tuberculosis*, is a highly infectious, airborne disease. Due to its frequent prevalence in cohorts of HIV/AIDS patients, the incidence of TB has now been regarded to be alarming (KhanYusufzai *et al*., 2017). Drug-susceptible diseases are often treated with a two-month intensive phase, including isoniazid, rifampicin, ethambutol, and pyrazinamide, followed by a four-month recovery phase using isoniazid and rifampicin alone. Tuberculosis therapy is further challenged by the rapid spread of multidrug-resistant (MDR) and extensively drug-resistant (XDR) *M. tuberculosis* strains, as well as the medications used to treat them (Joshi, 2011). Thus, there is an increasing need to produce more affordable new medicines, less toxic in treating TB to reduce its global societal and economic burden.

Numerous heterocyclic compounds of coumarin rings are linked with different biological properties (Morsy *et al*., 2017). Some coumarin compounds with nitrogen-containing heterocyclic moieties, such as pyridine, thiazolyl, Pyrazolo, and pyrazole pyrimidine, showed antibacterial and antitubercular properties (Mangasuli *et al.*, 2018a). Thiazoles were found in a wide range of biologically active molecules, including Sulfathiazol (antimicrobial drug), Ritonavir (an antiretroviral drug), Abafungin (an antifungal drug), and Tiazofurin (antineoplastic drug) (Siddiqui *et al*., 2009). Molecular hybridization is now being studied to generate a single biological structure with high affinity and activity by combining two or more heterocyclic pharmacophores. As a result, novel compounds with increased biological activity have been produced by combining the coumarin nucleus with other moieties (Kerru *et al.*, 2017). This chapter presents the results of the *in vitro* and *in-silico* anti-TB activity of the synthesized series of Schiff bases of (*E*) 3-(2-aminothiazol-4-yl)-6-nitro-2*H*-chromen-2-one (**SVN 1-11**) against H37Rv-MTB and multidrug-resistant MTB (MDR-MTB).

4.2.2 Materials and Methods

4.2.2.1 Antimycobacterial activity of SN 1-11

The anti-mycobacterial activity was evaluated using the procedure outlined in section 4.1.2.1.

4.2.2.2 Computational studies

The computational investigation was carried out according to the protocols outlined in section 4.1.2.2.

4.2.3 Results and Discussion

4.2.3.1 Antimycobacterial activity of SVN 1-11

The H37Rv of *Mycobacterium tuberculosis* and MDR-TB strain were used to determine the anti-tuberculosis potential of the Schiff bases of (*E*) 3-(2-aminothiazol-4-yl)-6-nitro-2*H*-chromen-2-one (**SVN 1-11**). The MIC values were determined alongside the standard drug rifampicin; the results are tabulated in Table 5. The results obtained revealed that compound **SVN 8** was the most potent against H37Rv MTB with a MIC value of 0.25 µg/mL; furthermore, compounds **SVN 3** and **9** also showed high efficiency with a MIC value of 0.5 µg/mL; these compounds had a MIC at higher concentrations compared to the commonly used antimycobacterial drug rifampicin and isoniazid (Table 5). Compounds **SVN 4**, **1**0 and **11,** produced a MIC of 1 µg/mL, the same as the reference drug whereas, compounds **SVN 1** and **SVN 2** displayed MIC values of 2 µg/mL. Lastly, **SVN 5** and **6** showed a MIC value of 4 µg/mL against H37Rv MTB (Table 5).

These results are comparable to Patel et *al*. (2013), who synthesized a series of coumarin-based 1, 3, 4-oxadiazol-2-ylthio-*N*-phenyl/benzo thiazolyl acetamides. In this series, all synthesized compounds were assessed for their *in vitro* anti-mycobacterial activity against *Mycobacterium tuberculosis* H37Rv. The results showed that the most promising anti-mycobacterial displayed a MIC value of 12.51 µg/mL, close to the reference drug pyrazinamide (6.25 µg/mL) (Patel et al., 2013). In another study, Yusufzai *et al*., 2017 synthesized a series of hydrazonyl thiazolyl coumarin derivatives for their *in-vitro* anti-mycobacterial activity against *Mycobacterium tuberculosis* H37Rv (ATCC 25618). The results revealed that the synthesized compounds were

found to be a potent anti-tubercular agent with a MIC value of 50 µg/mL (KhanYusufzai et al., 2017).

The Schiff bases of (*E*) 3-(2-aminothiazol-4-yl)-6-nitro-2*H*-chromen-2-one (**SVN 1-11**) were also screened against MDR-TB. The test compounds were effective against clinical isolates of multi-drug-resistant mycobacterial strains resistant to rifampicin and isoniazid. Compounds **SVN 3, 4, 5** and **8** exhibited high anti-tuberculosis (TB) activity with a MIC value of 8 µg/mL against MDR-TB. The most potent synthetic compound against MDR-TB was **SVN 4**, with a MIC value of 4 µg/mL (Table 9). Compounds **SVN 3** and **5** exhibited a MIC value of 8 µg/mL, whereas compounds **SVN 2, 6, 7, 10,** and **11** showed a MIC value of 16 µg/mL against MDR-TB (Table 9). **SVN 1** and **9** were less active than the other compounds with a MIC value of 32 µg/mL (Table 5). Furthermore, molecular docking analysis has been conducted against DprE1 and Pks13 enzymes of *M. tuberculosis,* which revealed excellent binging interactions (Figure 12 and 13).

These results are comparable to those of Jin *et al*. (2017), who synthesized a new class of ethylene/propylene-1H-1, 2, 3-triazole-4-methylene-tethered isatin coumarin integrating three anti-tuberculosis pharmacophore coumarin, isatin, and 1, 2, 3-triazole compounds. These hybrids were evaluated for their *in vitro* anti-TB activity against MTB H37Rv and MDR-TB. The results showed that the most active hybrid showed a MIC value of 50 µg/mL against H37Rv and MDR- MTB (Jin *et al*., 2017).

Table 5: Anti-TB results of Schiff bases of (*E*) 3-(2-aminothiazol-4-yl)-6-nitro-2*H*-chromen-2-one (**SVN 1-11**) with the docking free energy (kcal/mol)

Name of Drug	Level of activity (µg/mL)		Docking scores (kcal/mol)	
	H37RV	**MDR**	**Pks13**	**DprE1**
SVN 1	2	32	-9.0	-8.2
SVN 2	2	16	-8.8	-8.0
SVN 3	0.5	8	-8.5	-7.9
SVN 4	1	4	-8.8	-8.2
SVN 5	4	8	-7.7	-8.0
SVN 6	4	16	-8.1	-7.9
SVN 7	1	16	-8.9	-8.5
SVN 8	0.25	16	-8.8	-8.1
SVN 9	0.5	32	-8.9	-8.4
SVN 10	1	16	-8.8	-8.5
SVN 11	1	16	-8.7	-7.9
Rifampicin	1	na	-7.9	-7.9
Isoniazid	3	na	-6.1	-5.4
DMSO	na	na	-	-

4.2.3.2 Molecular Docking

Molecular docking provides an effective method for different interactions that control a molecule's binding to the biological receptor (Meng *et al.*, 2011). Indeed, the binding free energy and intramolecular interactions represent the critical parameters for studying a database of inhibitors (Meng *et al.*, 2011). Therefore, molecular docking analysis was carried out to rationalize the observed *in vitro* anti-tubercular effects and explore potential interactions of the compounds studied. The results of molecular docking against M. tuberculosis DprE1 and Pks13 enzymes revealed that all synthesized compounds had higher affinity for the two targets than the two reference standards used in this study (Table 5), which are in the range of -7.7 to -9.0 kcal/mol for Pks13 and -7.9 to -8.5 kcal/mol for DprE1 (Table 5). Except for **SVN 3, 6** and **11** with similar binding affinities as rifampicin towards DprE1 and SVN5 with a slightly lower affinity for Pks13 than rifampicin, all the newly synthesized compounds had a better affinity

towards the two targets than the two reference standards used in this study (Table 5). The interaction plots of compounds **SVN 3, 4, 7, 8, 10** and **11,** adjudged as active and having good interactions with the proteins' active site, are depicted in Figures 12 and 13.

Similarly with the *in vitro* results, both **SVN 3** and **4** displayed considerable binding affinity towards both proteins (Table 5); their intramolecular interactions are depicted in Figures 12 A and B, as well as Figures 13 A and B. Regarding DprE1, **SVN 3** had hydrogen bonding interactions with Asn385, Gln336, His315 and van der Waals interactions with Gly117, Lys418, Cys387, His132, Ser228, Lys134, Trp230 (Figure 12A), whereas **SVN 4** had hydrogen bonding interactions with Asn385, Arg58, His132, Gly117, and Van der Waals interactions with Gln120, Tyr60, Leu363, Cys387, Gln336, Lys367, Phe369, Gly133, Ser228, Trp230, His315, Pro316, Tyr314, Thr118. Interestingly, these compounds interacted via hydrogen bonding since they shared the same DprE1 amino acid residue between **SVN 3** and isoniazid (Asn385, Gln336). **SVN 4** formed hydrogen bonds with Asn385 and Arg58 in the same way that rifampicin and isoniazid did. Furthermore, **SVN 3** showed Van der Waals interactions with an amino acid residue identical to those seen in isoniazid (Ser228). Van der Waals interactions with amino acids similar to those found in rifampicin were detected in **SVN 4** (Gln120, Pro316 and Leu363). More notably, **SVN 3, 4, 7, 8, 10 and 11** had 2 (Pro316, and Val365), 3 (Val365, Lys134 and Trp16), (Trp16, Val365 and Lys367), 3 (Lys134, Trp16 and Val365), 3 (Val365, Lys134 and Pro316), and 4 (Val365, Lys134, Pro316 and His315) pi-pi interactions with the active site amino acid residues, respectively (Figures 12 A - F). These interactions also contributed to the overall binding affinity of the respective resulting complexes relative to rifampicin (no pi-pi interaction) and isoniazid (2 pi-pi bonds) (Figures 12 G and H). Nevertheless, different catalytically essential amino acid residues of DprE1 were identified to establish crucial interactions with **SVN 3** and SVN **4** than with rifampicin and isoniazid, which might explain the higher in vitro activity seen with these drugs compared to others.

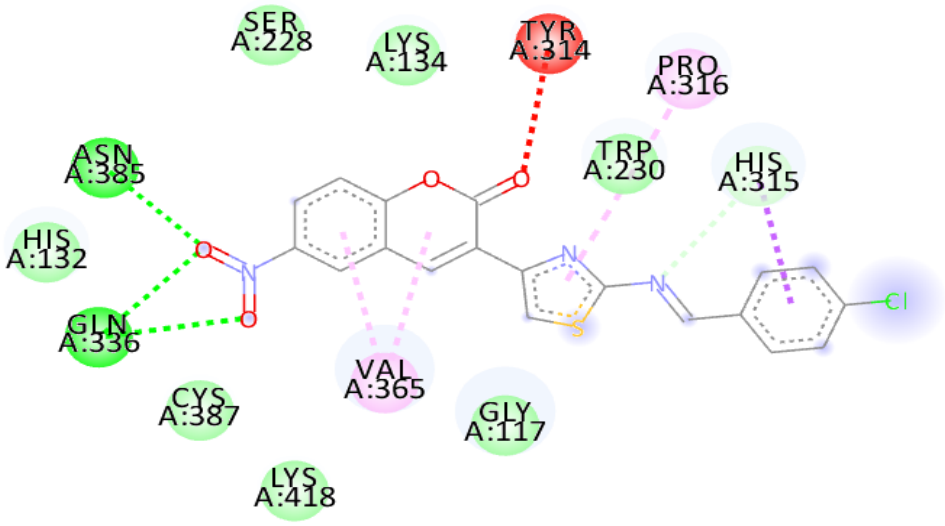
SER A:228
LYS A:134
TYR A:314
PRO A:316
ASN A:385
TRP A:230
HIS A:315
HIS A:132
GLN A:336
VAL A:365
CYS A:387
GLY A:117
LYS A:418
Cl
Interactions
van der Waals
Conventional Hydrogen Bond
Carbon Hydrogen Bond
Unfavorable Acceptor-Acceptor
Pi-Sigma
Pi-Alkyl

(A) **SVN3**

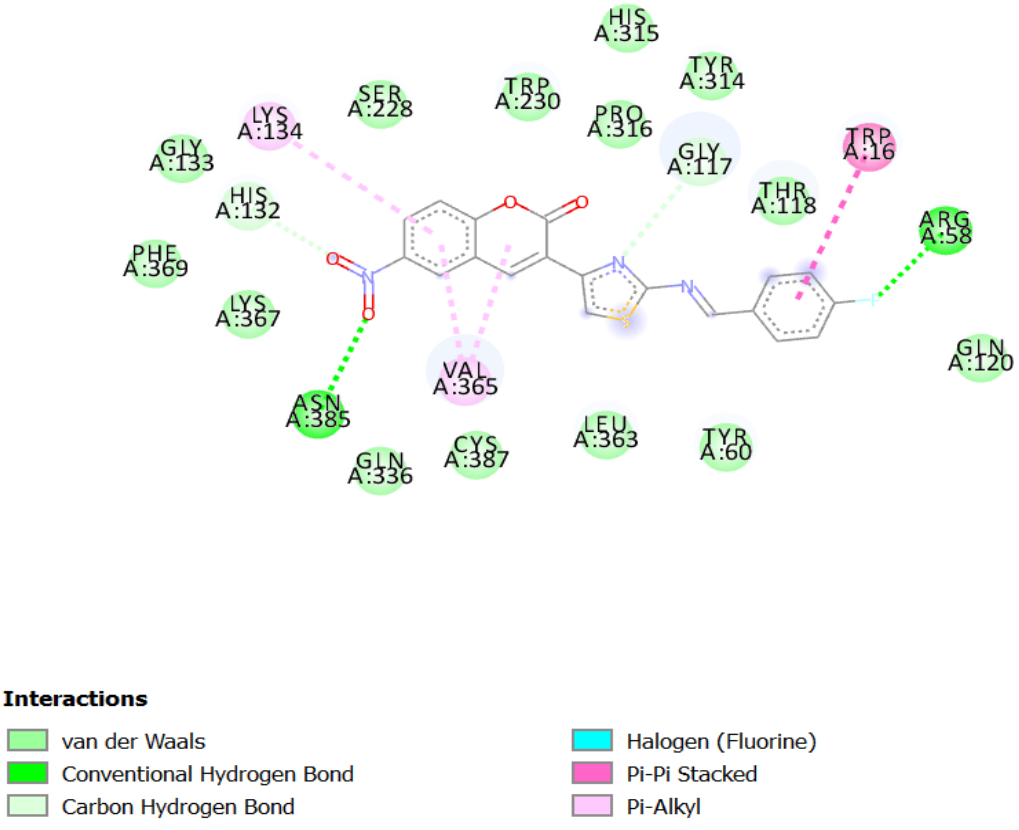
HIS A:315
TYR A:314
SER A:228
TRP A:230
LYS A:134
PRO A:316
GLY A:133
GLY A:117
TRP A:16
HIS A:132
THR A:118
ARG A:58
PHE A:369
LYS A:367
GLN A:120
VAL A:365
ASN A:385
LEU A:363
TYR A:60
CYS A:387
GLN A:336
F
Interactions
van der Waals
Conventional Hydrogen Bond
Carbon Hydrogen Bond
Halogen (Fluorine)
Pi-Pi Stacked
Pi-Alkyl

(B) SVN 4

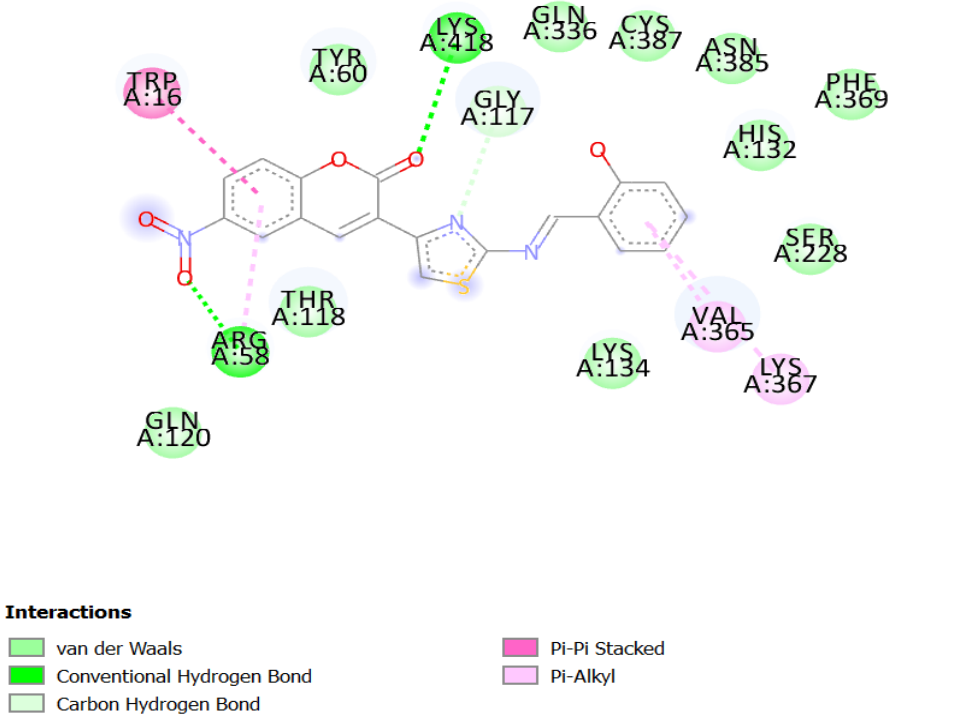
LYS A:418
GLN A:336
CYS A:387
ASN A:385
PHE A:369
TYR A:60
TRP A:16
GLY A:117
HIS A:132
SER A:228
THR A:118
VAL A:365
ARG A:58
LYS A:134
LYS A:367
GLN A:120
Interactions
van der Waals
Conventional Hydrogen Bond
Carbon Hydrogen Bond
Pi-Pi Stacked
Pi-Alkyl

(C) SVN 7

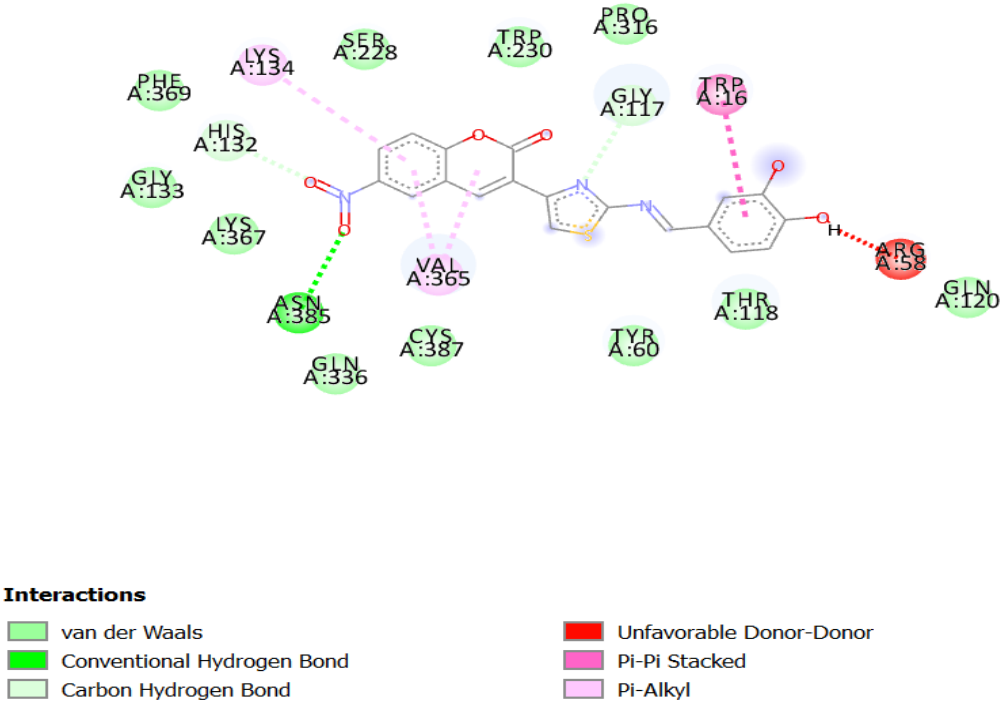
PRO A:316
SER A:228
TRP A:230
LYS A:134
PHE A:369
GLY A:117
TRP A:16
HIS A:132
GLY A:133
LYS A:367
VAL A:365
ARG A:58
ASN A:385
THR A:118
GLN A:120
CYS A:387
TYR A:60
GLN A:336
Interactions
van der Waals
Conventional Hydrogen Bond
Carbon Hydrogen Bond
Unfavorable Donor-Donor
Pi-Pi Stacked
Pi-Alkyl

(D) SVN 8

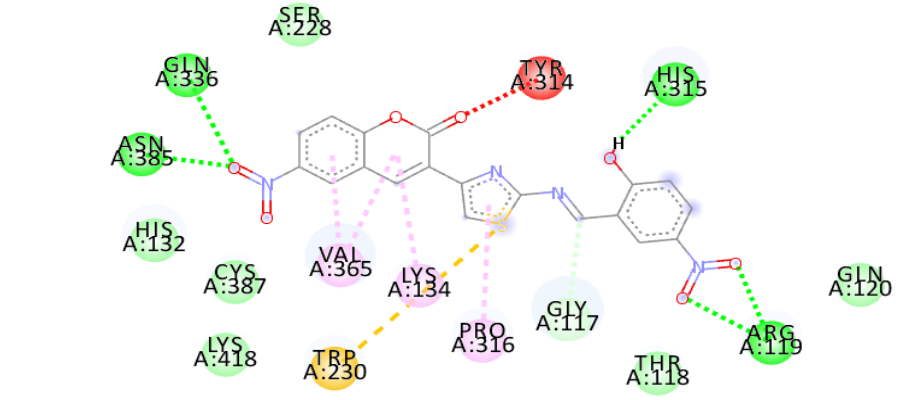

(E) SVN 10

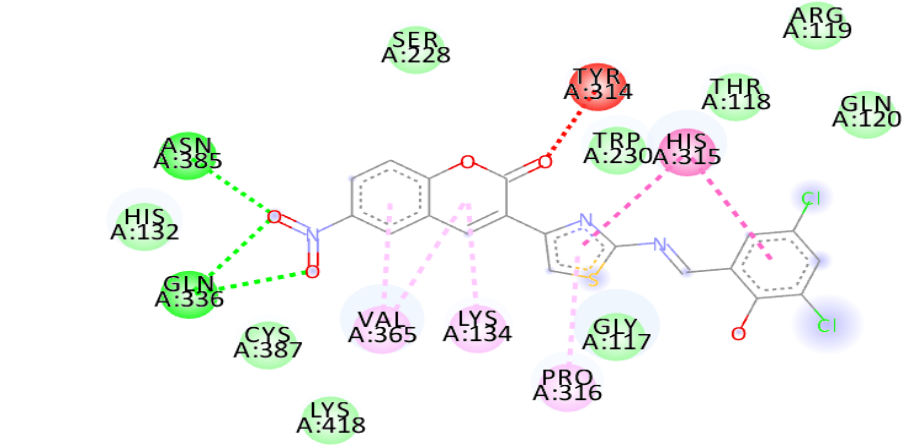

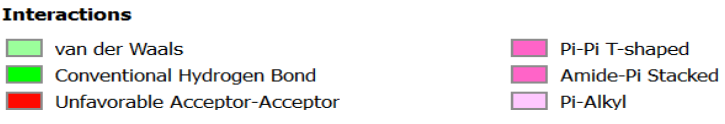

(F) SVN 11

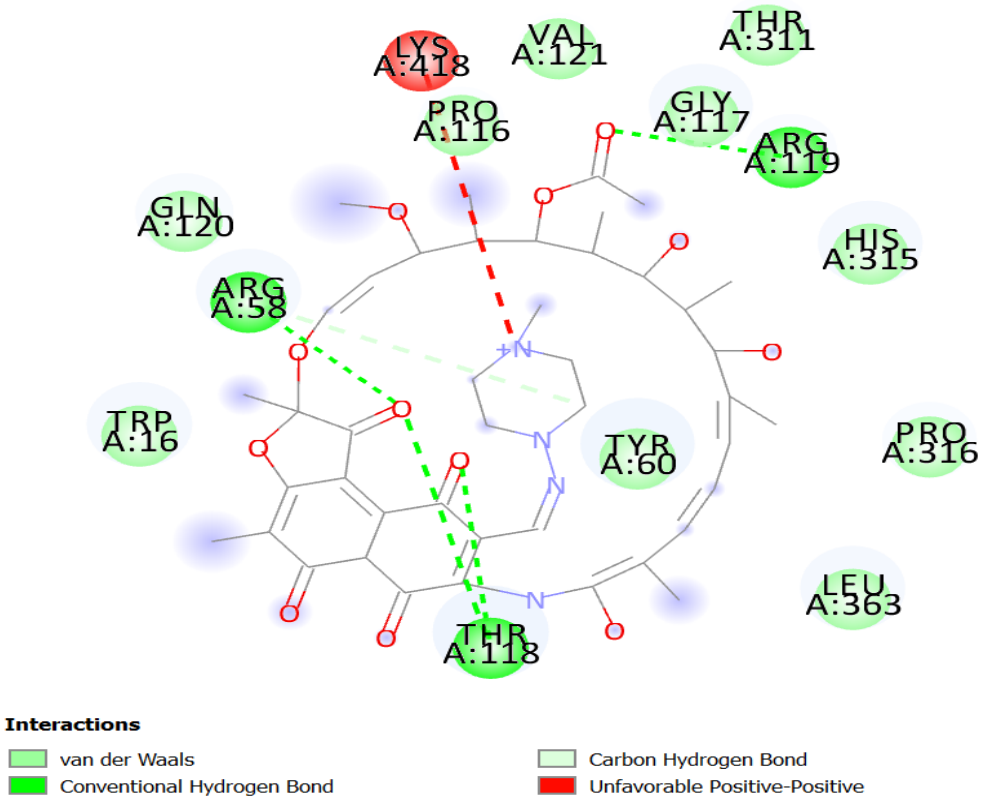

(G) Rifampicin

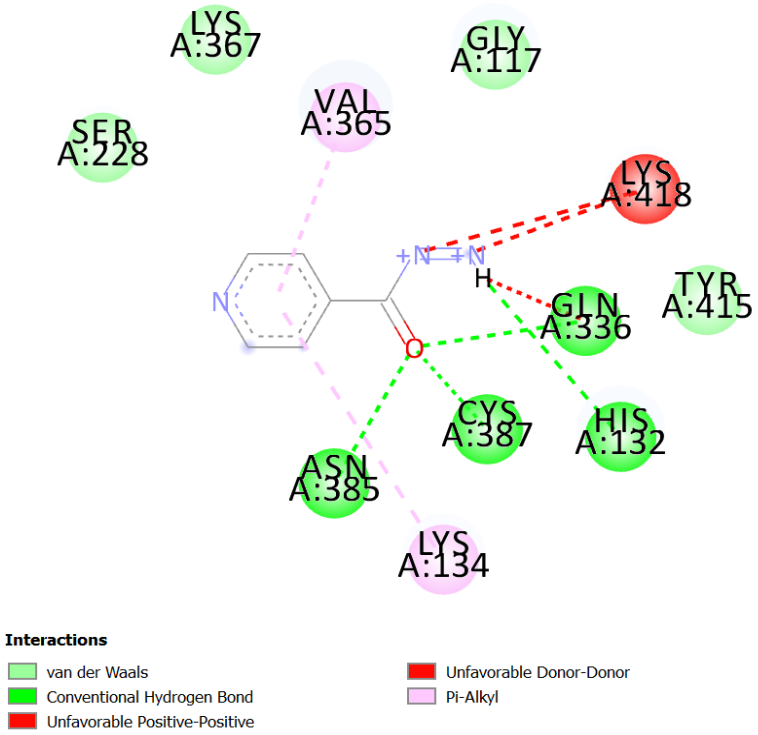

(H) Isoniazid

Figure 12: 2D interaction plots of (A) SVN 3, (B) SVM 4, (C) SVM 7, (D) SVM 8, (E) SVN 10, (F) SVN 11, (G) Isoniazid, and (H) Rifampicin with the active site amino acid residues of DprE1.

Similarly, against PKs13, **SVN 3** forms hydrogen binding interactions with Gln1633 and Arg1634 residues, as well as Van der Waals interactions with Ile1630, Tyr1637, Val1611, Leu1615, Val1614, Arg1641, Asp1644, Asn1640, Tyr1674, Glu1671 (Figure 13A), meanwhile **SVN 4** forms Van der Waals interactions with Tyr1674, Glu1671, Asn1640, Tyr167. **SVN 3** demonstrated comparable Van der Waals interactions with Arg1641, Asp1644, and Glu1671 as isoniazid (Figure 13G) and rifampicin (Figure132H). **SVN 4** also displayed Van der Waals interactions with PKs13 via a similar amino acid residue as rifampicin (Tyr1674). The per-residue interaction analysis revealed that several strong van der Waals interactions were critical in **SVN 1-11** binding to the active site of PKs13 (Figure 13). These could have aided the *in vitro* activity as observed mainly for **SVN 3** and **4**.

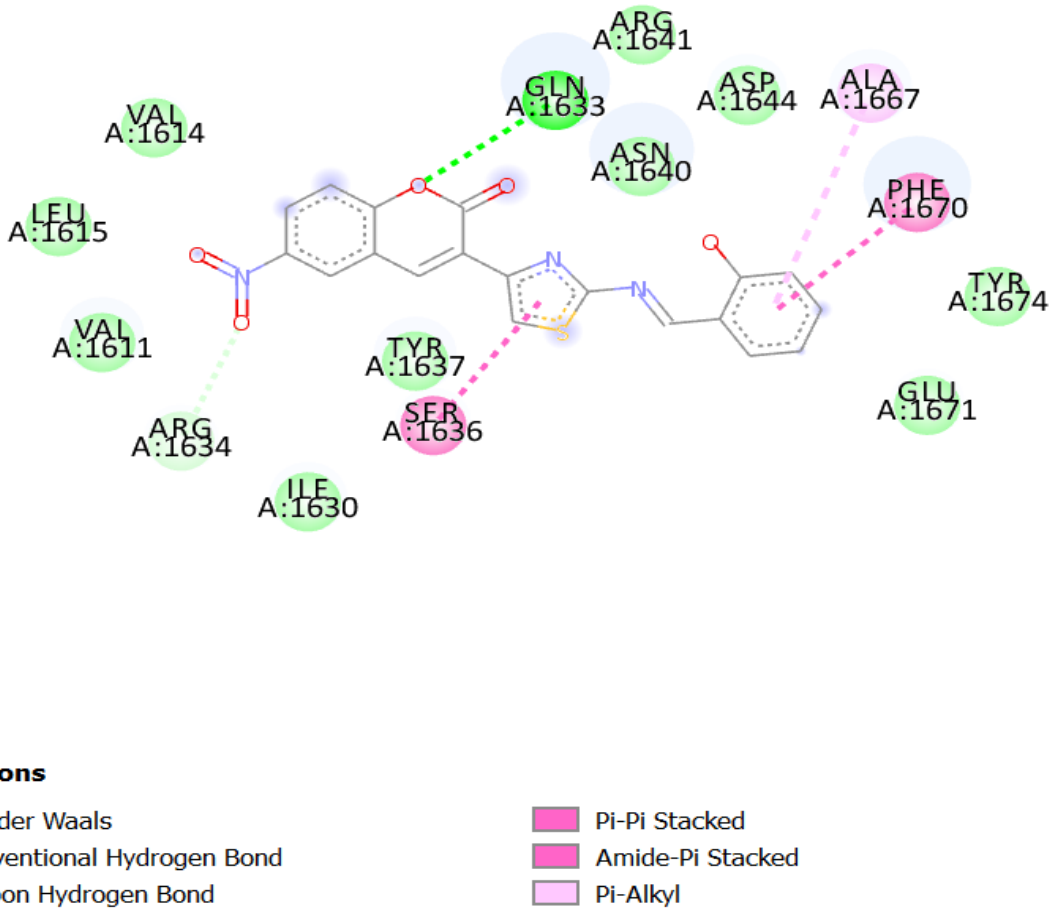

(A) SVN 3

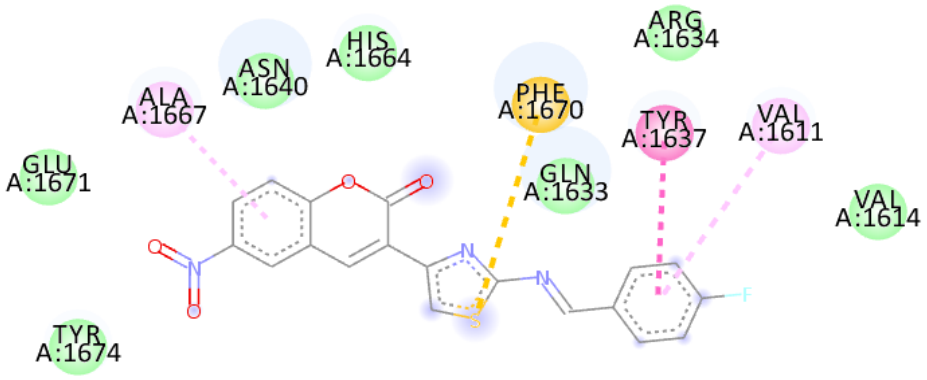
ARG
A:1634
HIS
A:1664
ASN
A:1640
ALA
A:1667
PHE
A:1670
TYR
A:1637
VAL
A:1611
GLU
A:1671
GLN
A:1633
VAL
A:1614
TYR
A:1674
Interactions
van der Waals
Pi-Sulfur
Pi-Pi Stacked
Pi-Alkyl

(B) SVN 4

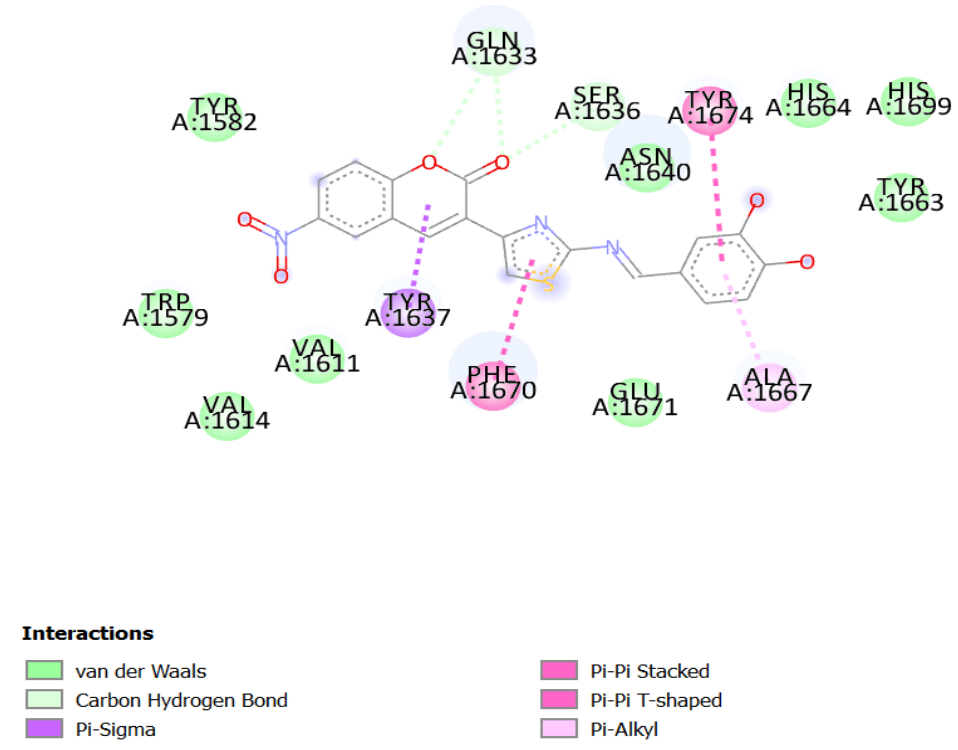
GLN
A:1633
TYR
A:1582
SER
A:1636
TYR
A:1674
HIS
A:1664
HIS
A:1699
ASN
A:1640
TYR
A:1663
TRP
A:1579
TYR
A:1637
VAL
A:1611
PHE
A:1670
GLU
A:1671
ALA
A:1667
VAL
A:1614
Interactions
van der Waals
Carbon Hydrogen Bond
Pi-Sigma
Pi-Pi Stacked
Pi-Pi T-shaped
Pi-Alkyl

(C) SVN 7

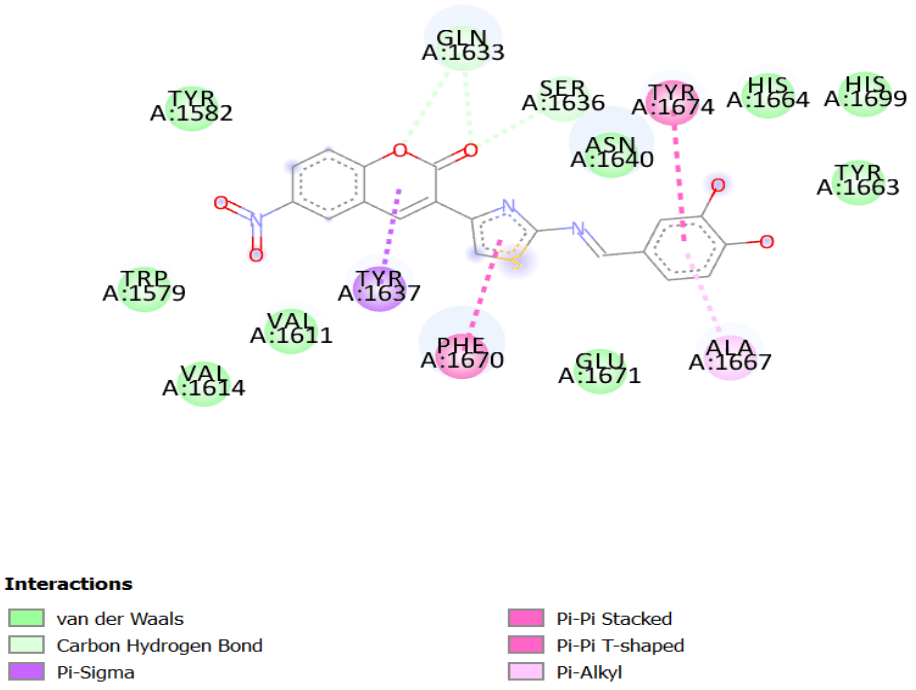

(D) SVN 8

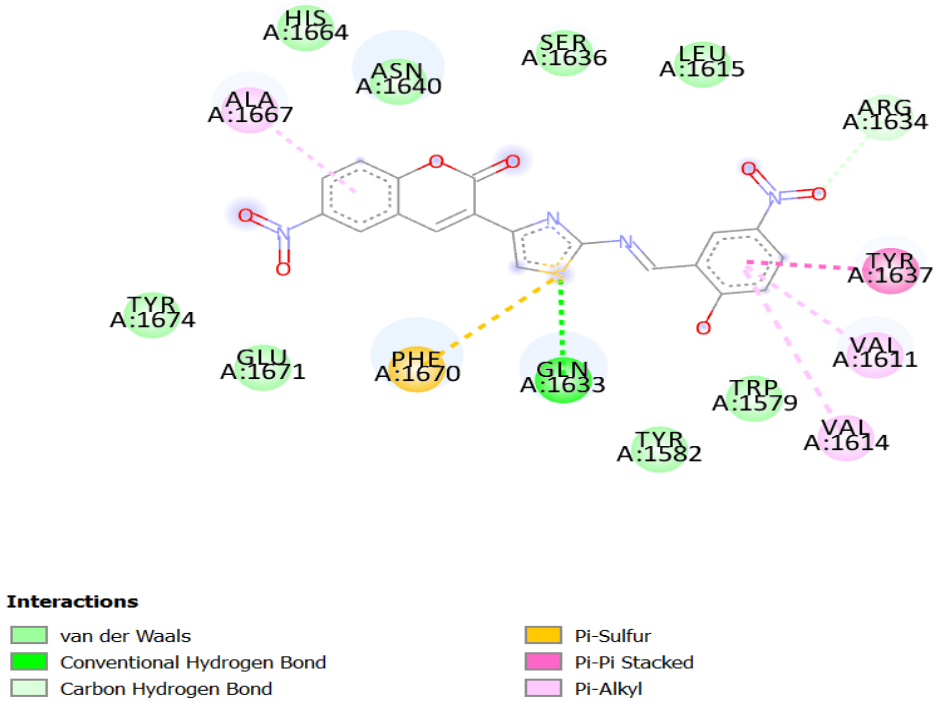

(E) SVN 10

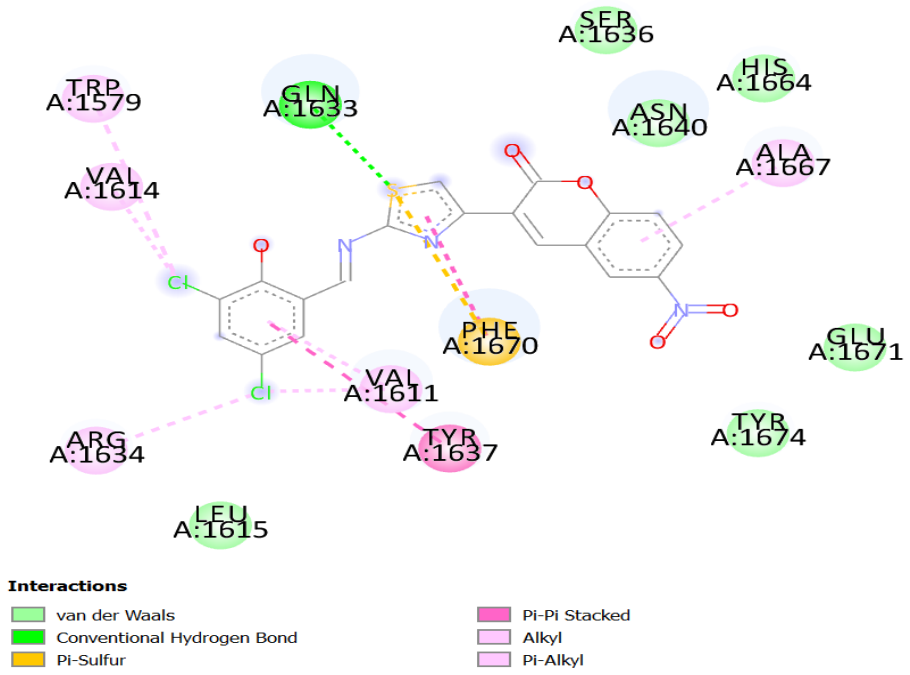

(F) SVN 11

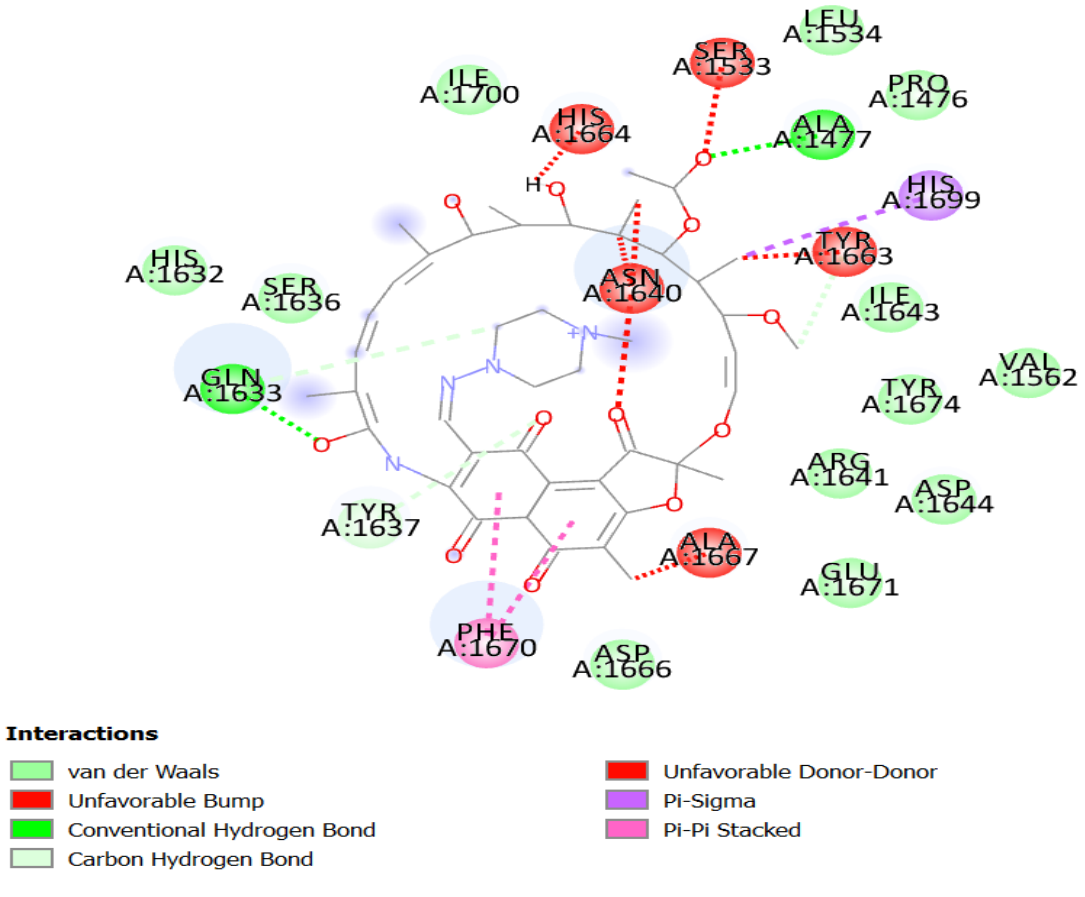

(G) Rifampicin

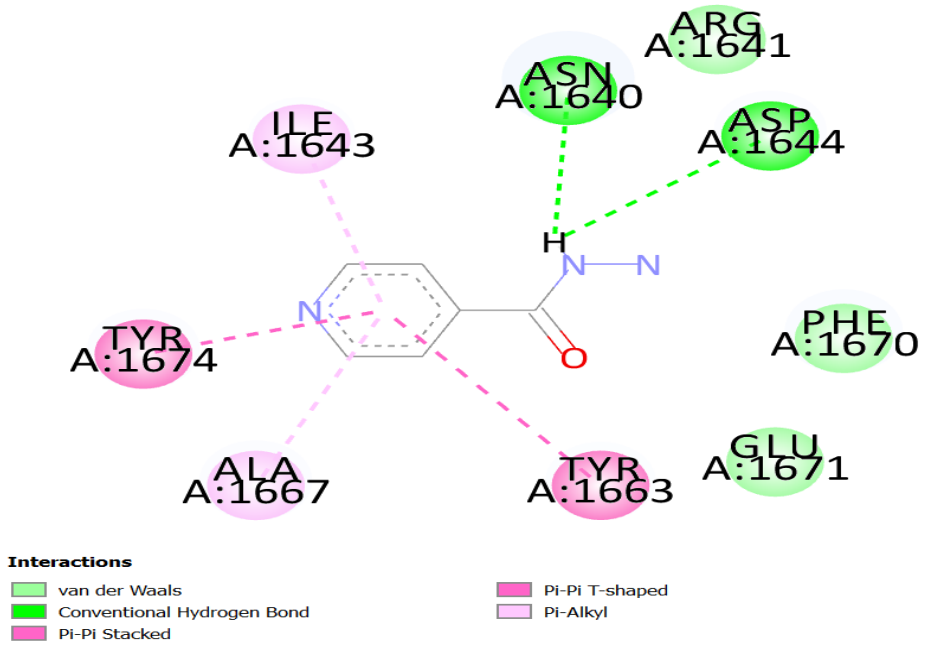

(H) Isoniazid

Figure 13: 2D interaction plots of (A) SVN 3, (B) SVN 4, (C) SVN 7, (D) SVN 8, (E) SVN 10, (F) SVN 11, (G) Isoniazid, and (H) Rifampicin with the active site amino acid residues of Pks13.

4.2.4 Conclusions

In this study, we reported our medicinal chemistry efforts, which included screening novel Schiff bases of (*E*) 3-(2-aminothiazol-4-yl)-6-nitro-2*H*-chromen-2-one (**SVN 1-11**) to assess their anti-TB potency in vitro and the active molecules were docked computationally. Both H37Rv MTB and MDR-TB mycobacterium strains were tested, and the title compounds **SVN 3, 4, 7, 8, 10** and **11** showed considerable inhibitory activity. **SVN 3** and **4** have been identified as the most promising anti-TB drugs against H37Rv MTB and MDR-TB mycobacterium strains. According to the docking results, both **SVN 3** and **4** displayed a high affinity for both proteins, which appeared to represent the observed biological activity. Because of their potent bioactivity, these compounds might be used in further in-vitro or in-vivo studies to develop more effective inhibitors and novel anti-mycobacterial drugs or prodrugs that could be used in antibiotic therapy.

CHAPTER V. LARVICIDAL AND ADULTICIDAL ACTIVITY OF SCHIFF BASES OF 3-(2-AMINOTHIAZOL-4-YL)-6,8-DICHLORO-2*H*-CHROMEN-2-ONE (SVM1-11) AND (*E*) 3-(2-AMINOTHIAZOL-4-YL)-6-NITRO-2*H*-CHROMEN-2-ONE(SVN 1-11) AGAINST *ANOPHELES ARABIENSIS*

5.1 Larvicidal and adulticidal activity of Schiff bases of 3-(2-aminothiazol-4-yl)-6,8-dichloro-2*H*-chromen-2-ones (SVM1-11) against *Anopheles arabiensis*

Abstract

Mosquitoes are the leading vectors of diseases and parasites, such as those that cause malaria, the vector-borne illness. The negative environmental impacts of commercial pesticides and pesticide resistance promote research and development of new, less harmful, and ecologically acceptable compounds to manage vector control successfully. In this study, a series of novel Schiff bases of 3-(2-aminothiazol-4-yl)-6,8-dichloro-2*H*-chromen-2-ones (**SVM 1-11**) were synthesized and tested for their larvicidal and adulticidal activity against *A. arabiensis* to find new potential larvicide and adulticidal drugs. The results showed that title compounds **SVM 6** and **9** were the most promising larvicidal, with the same mortality rate as the positive control Themephos (100%), these compounds also displayed significant adulticidal activity of 73.5±1.5 and 77.3±2.3%, respectively, but lower than the reference drug K-Othrine (100%). Moreover, **SVM 3** displayed high larvicidal activity (90%) and moderate adulticidal potency (64%). **SVM 8** and **10** showed a high adulticidal activity of 70.5±2.3 and 76.2±2.3%, respectively, but lower larvicidal efficiency. Based on these findings, the title compounds were identified as promising larvicidal or adulticidal agents for further investigation and development. The larvicidal mortality was between 90 to 100%, and the adulticidal mortality was around 70 to 77%.

5.1.1 Introduction

In many tropical nations, vector-borne illnesses are still the leading causes of mortality. Malaria, lymphatic filariasis, dengue fever, and yellow fever are the most common vector-borne illnesses; the pathogens responsible for these diseases are transmitted by arthropod vectors, particularly mosquitoes, the primary agents (WHO, 2020c). Mosquitoes are the primary vectors of parasites and diseases that affect humans and domestic pets. The extensive development of pesticides resulted in significant demand for developing new, less harmful and ecologically acceptable compounds to manage vector control successfully (Venugopala *et al*., 2014).

A wide range of biological activity may be found in several heterocyclic compounds with a five-membered ring in their structure. Thiazoles are a type of heterocyclic molecule with five members. The heterocyclic nucleus of this molecule can be found in a variety of pharmacologically active compounds (Kumawat, 2018). Coumarin (benzopyran-2-one) is an important structural component in developing and identifying new therapeutic compounds with high affinity and specificity for various molecular targets (Ibrar *et al*., 2018). Natural and synthetic coumarin derivatives have demonstrated various pharmacological activities, including insecticidal activity (Jin *et al*., 2020). Molecular hybridization methods are generally used to design and synthesize hybrids by finding pharmacophoric sub-units in the molecular skeleton of two or more recognized biologically active derivatives (Singh *et al*., 2019a). The synthesis of hybrid multifunctional molecules is still a major topic in research; hybrid compounds add additional aspects to drug development by reducing the risk of drug-drug interactions and decreasing drug resistance (Singh *et al*., 2019a). Thus, this chapter aimed to synthesize novel Schiff bases of (*E*) 3-(2-aminothiazol-4-yl)-6,8-dichloro-2*H*-chromen-2-one (**SVM 1-11**) and investigate their larvicidal and adulticidal activities.

5.1.2 Materials and Methods

5.1.2.1 Larvicidal activity

The *A. arabiensis* tested in this investigation was a colonized strain from Zimbabwe that was maintained following WHO (1975) recommendations. The insectary's temperature (27.5°C), humidity (70%) and lighting (12/12) characteristics matched those of a malaria-endemic habitat. One milliliter of the test sample (1 mg/mL in acetone) was added to 249 mL of distilled water. Negative controls included acetone and water, while positive controls included tempos (Mostop, Agrivo), a potent emulsifiable organophosphate larvicide employed by the malaria control program. The experiment was conducted in triplicate; each container was checked for larval mortality at 24-hour intervals for two days and the percentage mortality was determined relative to the original number of exposed larvae. Larvae were fed specially prepared cat food with low oil/fat content at regular intervals throughout the experiment. When larvae were moribund or unable to move, they were termed dead. The number of dead larvae was counted, and the average percentage mortality in proportion to the number of exposed larvae at the start was calculated.

5.1.2.2 Adulticidal activity

The insecticidal activity was determined by exposing susceptible adult mosquitos to a treated surface, as recommended by the World Health Organization (WHO) in 1975. One mL of test compound solution (1 mg/mL) was sprayed onto a clean, dry, nonporous ceramic tile using a Potter's Tower apparatus that had been precalibrated. Within 24 hours of spraying, the assay began by putting a cone over the sprayed tile and injecting thirty non-blood-fed adult *A. arabiensis* mosquitoes inside the cone. To evaluate the effect of the test drugs, researchers employed the knockdown rate based on transitory paralysis of mosquitos during a 60-minute exposure period and death 24 hours later. Deltamethrin (15 g/L; K-Othrine) was used as the standard medication and acetone as the negative control.

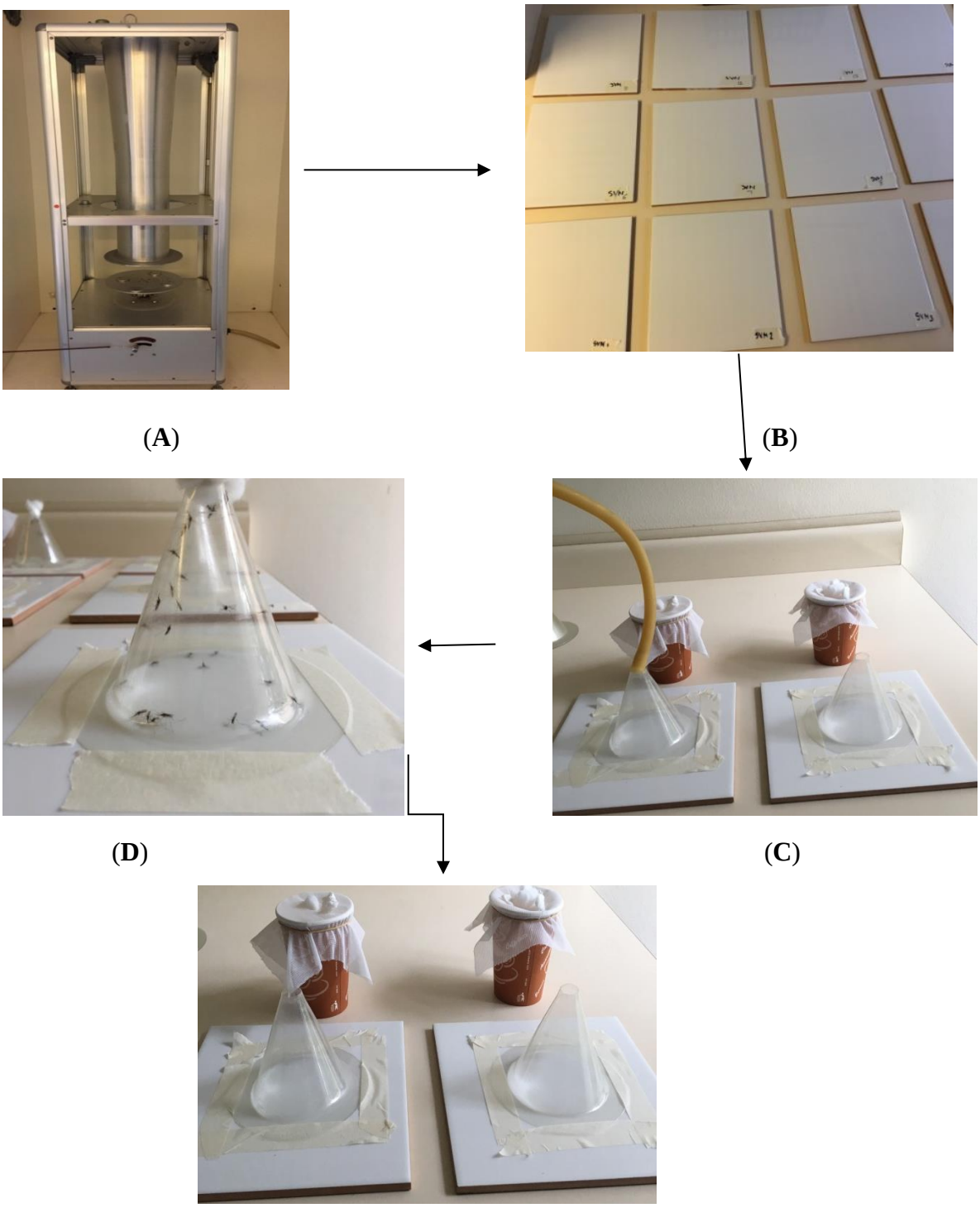

Figure 14: Methodology and Workplan of protocol for insecticidal assay (**A**) Potters tower, (**B**) Coumarins sprayed on ceramic non–porous tiles left for 24 h to dry, (**C**) *A. arabiensis* (30) females introduced in bioassay cone, (**D**) Observation for a knockdown, (**E**) Transferred to holding cage containing nutrient solution overnight to check for mortality

5.1.2.3 Statistical analysis

Each experiment was done three times, and the results are reported as means with standard deviations (SD). A one-way ANOVA test was used to determine the statistical significance of differences between the groups, followed by a post hoc Bonferroni's test. Mean values with $p<0.05$ probability values were considered statistically significant.

5.1.3 Results and Discussion

5.1.3.1 Larvicidal activity of Schiff bases of 3-(2-aminothiazol-4-yl)-6,8-dichloro-2*H*-chromen-2-one (SVM 1-11)

The larvicidal results showed a significant impact of the treatment exposure time on larvae mortality. The mortality of larvae exposed to any of the compounds tested was higher than the negative control acetone, indicating toxicity against *A. arabiensis* larvae. Adulticides may temporarily decrease the adult population; thus, mosquito control programs currently focus on eliminating mosquitoes in the larval stage at their breeding sites with larvicides. As a result, focusing on the larvae would be a more efficient way to lower the mosquito population (Chung *et al*., 2009, Conti *et al*., 2010). This study showed the highest larvicidal activity with compounds **SVM 6** and **9**, displaying 100% mortality, comparable to the positive control Termephos. This well-known commercial insecticide showed excellent larvae mortality (100%) at 24 hours exposure time (Table 6). Compounds **SVM 2**, **3** and **5** also showed a high larvae mortality rate after 24 hours exposure time of 73.8±2.5, 90.3±1.2 and 70.2±1.2%, respectively, lower than the reference drug, Termephos (100%).

Furthermore, moderate larvicidal activity was observed with compounds **SVM 4** and **7** displaying 60.5±2.5 and 63.9±3.5%, respectively (Table 6). The remaining compounds, **SVM 1, 8, 10** and **11,** showed low larvae mortality rate below 50%. The ANOVA test indicated that certain compounds had substantially varied larvicidal mortality rates after 24 hours of exposure, as shown in Table 6. Still, others did not exhibit significant variability in larvae mortality. These results are comparable to Shao *et al*. (2018), who synthesized a series of coumarin-dibenzothiophene or -carbazole derivatives as a larvicidal agent against fourth instars larvae *Aedes aegypti*. The bioassay results suggested that most coumarin-linked derivatives of dibenzothiophene and carbazole had moderate to high activity. Toxicity was seen in two

coumarin-linked dibenzothiophene hybrids and six coumarin-linked carbazole hybrids (88.53 to 100.00%)(Shao *et al*., 2018). In another study, Vargas-Soto *et al*. (2017) investigated the toxicity of coumarins produced using Pechmann-Duisberg condensation to Drosophila melanogaster larvae. Their findings revealed that compounds 7-hydroxy-4-propyl-coumarin, 7-methoxy-4-propyl-coumarin, 7-hydroxy-4-phenyl-coumarin, and 7-hydroxy-4-chloromethyl- coumarin have the most potent insecticidal efficacy. Compound 6-hydroxy-4-propyl-coumarin has a decreased activity, which can be attributed to the shift in the position of the hydroxyl group between positions 6 and 7. A similar scenario was seen with compounds with the lowest activity (Vargas-Soto *et al*., 2017).

Table 6: Mortality of *A. arabiensis* larvae exposed to **SVM 1-11**

Compounds Code	Larvicidal activity (hours)	
	24 hours	**48 hours**
SVM 1	20.2 ± 2.1^{c}	47.4 ± 1.7^{g}
SVM 2	33.7 ± 2.5^{de}	73.8 ± 2.5^{ij}
SVM 3	43.1 ± 2.5^{fg}	90.3 ± 1.2^{l}
SVM 4	40.6 ± 2.5^{f}	60.5 ± 2.5^{h}
SVM 5	$43.4\pm2.5f^{g}$	70.2 ± 1.2^{i}
SVM 6	57.2 ± 1.5^{h}	100.0 ± 0.0^{l}
SVM 7	37.7 ± 2.1^{ef}	63.9 ± 3.5^{h}
SVM 8	30.2 ± 2.1^{d}	33.3 ± 2.3^{de}
SVM 9	43.8 ± 2.6^{fg}	100.0 ± 0.0^{l}
SVM 10	13.6 ± 1.5^{b}	27.1 ± 0.6^{d}
SVM 11	27.5 ± 1.5^{d}	40.5 ± 2.5^{f}
Water	00.0 ± 0.0^{a}	00.0 ± 0.0^{a}
Acetone	00.0 ± 0.0^{a}	00.0 ± 0.0^{a}
Temephos	100.0 ± 0.0^{l}	100.0 ± 0.0^{l}

Values are represented mean ±SD, means of treatment mortality without a common letter differ significantly ($p<0.05$).

5.1.3.2 Adulticidal activity of Schiff bases of 3-(2-aminothiazol-4-yl)-6,8-dichloro-2*H*-chromen-2-one (SVM 1-11)

Table 7 summarizes the findings of the adulticidal experiment utilizing the several synthetic compounds SVM1-11. From the first 30 minutes of exposure, the positive control K-Othrine demonstrated 100% knockdown/mortality. For the first 30 minutes, the produced compounds SVM1-11 did not kill mosquitos, but after 24 hours, they killed them substantially more. Mosquitoes exposed to compounds **SVM 1-11** showed significant adulticidal activity, among the active compounds, **SVM 6, 8, 9** and **10** were the most potent with the percentage mortality of 73.5±1.5, 70.5±2.3, 77.3±2.3 and 76.2±2.3%, respectively, lower than the reference drug K-Othrine (100%) (Table 7). It was also observed that compounds **SVM 3, 5** and **11** showed considerable adulticidal activity of 63.3±2.1, 60.5±2.0, and 67.8±1.7%, respectively, lower than the reference drug, K-Othrine. Compounds **SVM 1, 2, 4** and **7** displayed low to weak adulticidal activity ranging from 40 to 57% against *A. arabiensis* as shown in Table 7. The ANOVA test showed that certain compounds had noticeably different adulticidal mortality rates against *A. arabiensis* mosquitoes after 24 hours of exposure time, as shown in Table 7, but others did not.

These results are comparable to Venugopala *et al*. (2014), who synthesized a series of 3-mono acetyl, 6- halogenated coumarins analogues and evaluated their larvicidal activity against an *A. arabiensis*. The results showed that the synthesized compounds exhibited close to 100% larvae mortality within 24 hours of exposure. In another study, Pingaew *et al*. (2014) developed a series of chalcone–coumarin derivatives linked by a 1,2,3-triazole ring generated via an azide-alkyne dipolar cycloaddition synthesis as anticancer and antimalarial agents. They subsequently tested these hybrid compounds for cytotoxicity against MOLT-3 cell line and antimalarial efficacy against *Plasmodium falciparum*. Based on this biological study, it was discovered that most of these hybrids had anticancer potential against the MOLT-3 cell line.

Moreover, coumarin tri-azole chalcone was discovered to be particularly effective against *P. falciparum* and may be considered a lead molecule for developing antimalarial agents (Pingaew *et al*., 2014). Similarly, Tok *et al*. (2018) investigated the adulticidal efficacy of various novel oxadiazole derivatives, including a 1,3,4-oxadiazole group having an imidazolidine moiety. The structure-activity relationship of these compounds revealed that among the phenyl substituents studied, chloro, nitro, methyl and bromo substituents were

efficient in enhancing adulticidal capacity suggesting that structural variation may result in the development of more efficient insecticides (Tok *et al*., 2018).

Table 7: Mortality of *A. arabiensis* adult exposed to **SVM 1-11**

Compounds Code	Adulticidal activity (h)	
	Knockdown (**60 min)**	Mortality (**24 h)**
SVM 1	23.5 ± 1.5^{bc}	40.9 ± 2.3^{e}
SVM 2	37.6 ± 2.0^{e}	53.8 ± 2.1^{gh}
SVM 3	20.1 ± 1.2^{b}	63.3 ± 2.2^{ij}
SVM 4	47.3 ± 2.0^{fg}	57.4 ± 2.1^{hi}
SVM 5	43.7 ± 3.0^{ef}	60.5 ± 2.0^{i}
SVM 6	40.1 ± 1.2^{e}	73.5 ± 1.5^{klm}
SVM 7	27.6 ± 2.3^{cd}	43.1 ± 2.9^{ef}
SVM 8	47.1 ± 3.1^{fg}	70.5 ± 2.3^{kl}
SVM 9	37.2 ± 1.2^{e}	77.3 ± 2.3^{mn}
SVM 10	43.7 ± 4.0^{ef}	76.2 ± 2.3^{mn}
SVM 11	43.5 ± 2.5^{ef}	67.8 ± 1.7^{jk}
Water	00.0 ± 0.0^{a}	00.0 ± 0.0^{a}
Acetone	00.0 ± 0.0^{a}	00.0 ± 0.0^{a}
K-Othrine	100.0 ± 0.0^{o}	100.0 ± 0.0^{o}

Values are represented mean ±SD; means of treatment mortality without a common letter differ significantly ($p<0.05$).

5.1.3.3 Structure-activity relationship (SAR)

Based on the above observations, the introduction of different functional groups on phenyl ring at the fourth position of thiazole moiety, which is connected to the primary coumarin nucleus at the third position, appeared to be significant contributors to the larvicidal and adulticidal activity. The following structure-activity relationships (SARs) were proposed based on the larvicidal and adulticidal activity of the studied Schiff bases of 3-(2-aminothiazol-4-yl)-6,8-dichloro-2*H*-chromen-2-ones (**SVM 1-11**). The title compounds **SVM 6** and **9** have pyridyl ring in place of the phenyl ring and methoxy group at the second position of the phenyl ring, respectively, on coumarinyl thiazole emerged as the most effective larvicidal, also exhibited high adulticidal efficacy. Compound **SVM 2** has 4-methoxy on the phenyl ring, compound **SVM 3** has 4-chloro on phenyl ring and compound **SVM 5** has thiophene nucleus in place of

phenyl ring on coumarinyl thiazole nucleus, exhibited substantial larvicidal activity higher than that of **SVM 1,** which has unsubstituted phenyl ring, **SVM 4,** has fluorine atom at the fourth position of the phenyl ring, **SVM 7** has hydroxy at the second position of the phenyl ring, **SVM 8** has dihydroxy at third and fourth positions of the phenyl ring, **SVM 10** has 2-hydroxy, 5-nitro on phenyl ring and **SVM 11** has 2-hydroxy and 3,6-dichloro substitutions on phenyl ring which is on coumarinyl thiazole nucleus. Compounds **SVM 8** and **10** exhibited high adulticidal activity whereas, compounds **SVM 3, 5** and **11** showed moderate adulticidal activity. However, these activities were less effective than compound **SVM 6** and **9**. Electron-withdrawing (groups on phenyl ring such as chlorine, fluorine, methoxy, nitro, pyridine) and releasing groups on phenyl ring (such as hydroxy) and thiophene itself varied the larvicidal and adulticidal activity against *A. arabiensis.*

5.1.4 Conclusions

The title compound **SVM 1-11** was synthesized in good yields. FT-IR, NMR (^{1}H & ^{13}C) and elemental analyses were used to characterize the named compounds. The compounds **SVM 2, 3, 5, 6** and **9** were shown to be the most efficient larvicidal and have greater adulticidal efficacy. Furthermore, **SVM 6**, **8, 9** and **10** were the most effective adulticidal. The results obtained suggest that incorporating various functional groups on the phenyl ring at the fourth position of the thiazole moiety, which is linked to the central coumarin nucleus at the third position, proved to be significant contributors to the larvicidal and adulticidal activities. The above active compounds may be produced as an insecticide against mosquitoes *A. arabiensis*, but further research needs to be completed to determine the toxicity and impact on non-target species and the environment.

5.2 Larvicidal and Adulticidal activity of Schiff bases of 3-(2-Aminothiazol-4-yl)-6-nitro-2*H*-chromen-2-ones (SVN 1-11) as Anti-mosquito Agents against *Anopheles arabiensis*

Abstract

Malaria is a parasitic illness spread to people by infected *Anopheles* mosquitoes. It is one of the deadliest infections. Pesticides are currently used to reduce malaria transmission; however, there are growing concerns regarding their safety for living systems and the environment. As a result, there is a significant demand for developing new, less harmful and ecologically acceptable compounds to manage vector control successfully. In this study, a series of novel Schiff bases of 3-(2-aminothiazol-4-yl)-6,8-dichloro-2*H*-chromen-2-ones (**SVN 1-11**) were synthesized and screened for larvicidal and insecticidal activity against *A. arabiensis* by standard WHO larvicidal assay and cone bioassay methods. The results showed that compounds **SVN 6**, **7**, **8** and **9** were the most potent, showing 100% larvae mortality after 24 hours of exposure, the same as the positive control Termephos (100%).

Furthermore, compounds **SVN 5, 7** and **9** were the most active adulticidal with percentage mortality of 86.3±2.1, 80.2±1.2 and 90.4±2.0%, respectively, compared to the reference drug K-Othrine® (100%). The larvicidal activity was much more significant than adulticidal activity. Thus, these compounds were shown to constitute a novel class of *A. arabiensis* insecticides that can be utilized as lead compounds to synthesize more effective and safer larvicidal and adulticidal agents.

5.2.1 Introduction

Mosquito-borne diseases such as dengue and malaria are significant public health concerns in tropical and subtropical nations due to their climate conditions. Climate change is predicted to extend the geographical range of vector and vector-borne illnesses, with substantial social and economic impact (Kannathasan *et al*., 2011). The main reason for the dramatic increase in malaria deaths is the spread of *Plasmodium falciparum* strains resistant to the mainstay anti-malarial chloroquine (Sashidhara *et al*., 2012). Human malaria is mainly caused by Plasmodium species (*P. falciparum*, *P. vivax*, *P. ovale* and *P. malariae*). The female mosquito of the *Anopheles* genus is the vector of *Plasmodium* (Da Silva *et al*., 2011). Due to mosquitos developing resistance to currently marketed insecticides, there is an urgent need to find and develop compounds with alternative mechanisms of action than those currently in use (Ramírez-Lepe and Ramírez-Suero, 2012).

Coumarin and its related analogues are heterocycles that occur naturally as secondary metabolites. Compounds from this chemical class are used as a base to generate several biological and chemical agents. Furthermore, coumarin derivatives with thiazole, azetidinone, and oxazole rings have been shown to have potent antifungal and antibacterial properties (Ujan *et al*., 2021). On the other hand, Thiazoles are widely employed in several chemical processes as parent nuclei, intermediates and substituents (Turner *et al*., 2007). These heterocycles have also been used to synthesize several thiazolyl coumarin derivatives (Holla *et al*., 2003). Thiazole has been found to have a variety of pharmacological actions, including insecticidal and larvicidal activity (Venugopala *et al*., 2013a). Molecular hybridization is a drug design method frequently used by medicinal chemists to discover and develop novel lead molecules. This method produces new molecules capable of interacting with multiple sites via novel molecular interactions. Moreover, the molecular hybrids developed are rigid scaffolds that interact effectively with the target (Konidala *et al*., 2021). Thus, this chapter aimed to synthesize and screen the novel Schiff bases of 3-(2-aminothiazol-4-yl)-6,8-dichloro-2*H*-chromen-2-ones (**SVN 1-11**) for larvicidal and adulticidal activity against *A. arabiensis* mosquito.

5.2.2 Materials and Methods

5.2.2.1 Larvicidal activity

The larvicidal activity was assessed according to the protocol described in section 5.1.2.1

5.2.2.2 Adulticidal activity

The adulticidal activity was assessed according to the protocol described in section 5.1.2.2

5.2.2.3 Statistical analysis

The statistical analysis was conducted according to the procedure described in section 5.1.2.3

5.2.3 Results and Discussion

5.2.3.1 Larvicidal activity of Schiff bases of 3-(2-aminothiazol-4-yl)-6-nitro-2*H*-chromen-2-one (SVN 1-11)

The larvicidal results obtained using the various compounds **SVN 1-11** are summarized in Table 8. The results indicated that the compounds' toxicity levels on the larvae depend on the duration of exposure. There were progressive increases in the lethal effect on the *Anopheles* larvae after 24 hours of exposure to the compounds. Mortality of larvae exposed to either of the assessed compounds was more significant than negative control acetone, demonstrating toxicity to the Larvae. The highest larvae mortality rate was shown with compounds **SVN 6, 7, 8** and **9**, displaying 100% larvae mortality after 24 hours of exposure, the same as the reference drug Termephos (100%) (Table 8).

Furthermore, high larvicidal mortality was also seen with compound **SVN 11** (77.2±1.2%). Compounds **SVN 5** and **10** showed moderate larvicidal activity of 64.3±1.2, 63.6±1.2 respectively, whereas compounds **SVN1, 2, 3** and **4** showed low to weak larvicidal activity ranging from 27 to 50% (Table 8). The ANOVA test revealed that several compounds had significantly different larvicidal mortality rates against *A. arabiensis* after 24 hours of exposure time, as shown in Table 8, whereas others did not.

These findings are comparable to earlier evidence of larvicidal activity reported by Venugopala *et al*. (2013), who synthesized a series of 2,6- and 2,4-substituted benzo[d]thiazole analogues against *A. arabiensis*. The study results showed that many benzothiazole analogues caused mild to moderate mortality in larvae and adults of *Aedes arabiensis* (Venugopala *et al*., 2013a).

Other related investigations include synthesizing Osthole compounds (derivatives of coumarin) with Grignard reagents, and their larvicidal activity against mosquitoes was reported by Liu *et al*. (2015). The Osthole design was modified to improve larvicidal efficiency against mosquitoes. With Grignard reagents, a new successful synthesis of Osthole derivatives was obtained. Bio-activity testing found that these compounds have higher capacities than Osthole (Liu *et al.*, 2015).

Table 8: Mortality of *A. arabiensis* larvae exposed to **SVN 1-11**

Compounds Code	Larvicidal activity (hours)	
	24 h	**48 h**
SVN1	7.3 ± 2.1^{b}	50.7 ± 2.0^{i}
SVN 2	17.2 ± 2.0^{c}	40.5 ± 1.5^{fg}
SVN 3	3.1 ± 0.6^{ab}	23.5 ± 2.5^{d}
SVN 4	13.6 ± 3.5^{c}	50.1 ± 2.5^{i}
SVN 5	37.7 ± 2.0^{ef}	64.3 ± 1.2^{j}
SVN 6	47.4 ± 2.5^{hi}	100.0 ± 0.0^{l}
SVN 7	43.8 ± 1.5^{gh}	100.0 ± 0.0^{l}
SVN 8	50.0 ± 2.5^{i}	100.0 ± 0.0^{l}
SVN 9	47.3 ± 3.2^{hi}	100.0 ± 0.0^{l}
SVN 10	43.1 ± 1.7^{gh}	63.6 ± 1.2^{j}
SVN 11	37.7 ± 1.5^{ef}	77.2 ± 1.2^{k}
Water	0.0 ± 0.0^{a}	0.0 ± 0.0^{a}
Acetone	0.0 ± 0.0^{a}	0.0 ± 0.0^{a}
Termephos	100.0 ± 0.0^{l}	100.0 ± 0.0^{l}

Values are represented mean ±SD, means of treatment mortality without a common letter differ significantly ($p<0.05$).

5.2.3.2 Adulticidal activity of Schiff bases of 3-(2-aminothiazol-4-yl)-6-nitro-2*H*-chromen-2-one (SVN 1-11)

The results of the adulticidal assay using the various synthetic **SVN 1-11** compounds are summarized in Table 9. The positive control K-Othrine demonstrated 100% knockdown/mortality from the first 60 minutes of treatment, while the synthetic compounds **SVN 1-11** showed higher knockdown after 24 hours (Table 9). The highest mean mortality rate was observed in mosquitoes exposed to compounds **SVN 5, 6, 7, 8** and **9,** showing percentage

mortality rates of 86.3±2.1, 73.1±2.0, 80.2±1.2, 71.5±1.5 and 90.4±2.0%, respectively, lower than the reference drug K-Othrine (100%) (Table 9). A moderate adulticidal activity was displayed by compound **SVN 4** (67.4±2.0%), whereas compounds **SVN 1, 2, 3, 10** and **11** showed low to weak insecticidal mortality ranging from 50 to 31% (Table 9). the ANOVA test demonstrated that many compounds had substantially different larvicidal mortality rates against *A. arabiensis* after 24 hours of exposure, but others did not, as indicated in Table 9.

These findings are comparable to Narayanaswamy *et al*. (2014), who reported on the adulticidal activity of some halogenated coumarins derivatives against *A. arabiensis.* The results showed that the heterocyclic coumarins knocked adult mosquitoes down reversibly yet did not kill them after 24 hours of treatment. In contrast, the compounds' adulticidal activity was only mild to moderate (Narayanaswamy *et al*., 2014). Another study by Moreira *et al*. (2007) showed that short exposure to freshly applied coumarin analogues knocked down mosquitoes, but they recovered in the next 24 h. Coumarins have been shown to immobilize insects in previous studies. Insect poisoning by coumarins such as surangin B has been associated with a slowly increasing paralysis that finally leads to death (Moreira *et al*., 2007, Nicholson and Zhang, 1995). Muscle bioenergetic disturbance has been identified as a key mechanism behind surangin B's insecticidal effect (Zheng *et al*., 1998).

Table 9: Mortality of *A. arabiensis* adult exposed to **SVN 1-11**

Compounds Code	Adulticidal activity (h)	
	Knockdown (60 min)	Mortality (24 h)
SVN1	18.2 ± 1.2^{b}	37.6 ± 1.7^{efg}
SVN 2	44.8 ± 2.1^{hi}	50.0 ± 2.0^{j}
SVN 3	29.6 ± 2.5^{c}	42.2 ± 2.3^{gh}
SVN 4	41.4 ± 2.1^{fgh}	67.4 ± 2.0^{l}
SVN 5	53.1 ± 1.7^{j}	86.3 ± 2.1^{o}
SVN 6	59.5 ± 2.5^{k}	73.1 ± 2.0^{m}
SVN 7	43.2 ± 2.0^{hi}	80.2 ± 1.2^{n}
SVN 8	41.1 ± 0.6^{fgh}	71.5 ± 1.5^{lm}
SVN 9	42.5 ± 1.2^{gh}	90.4 ± 2.0^{o}
SVN 10	41.2 ± 2.5^{fgh}	48.3 ± 2.5^{ij}
SVN 11	34.1 ± 1.6^{cde}	42.3 ± 2.5^{gh}
Water	00.0 ± 0.0^{a}	00.0 ± 0.0^{a}
Acetone	00.0 ± 0.0^{a}	00.0 ± 0.0^{a}
K-Othrine	100.0 ± 0.0^{p}	100.0 ± 0.0^{p}

Values are represented mean ±SD, means of treatment mortality without a common letter differ significantly ($p<0.05$).

5.2.3.3 Structure-Activity relationships (SAR)

The following structure-activity relationships (SARs) were established by comparing the data obtained from the larvicidal and adulticidal activity of the studied Schiff bases of 3-(2-aminothiazol-4-yl)-6-nitro-2*H*-chromen-2-ones (**SVN 1-11)**. The title compounds **SVN 6** has pyridyl ring in place of the phenyl ring, **SVN 7** has hydroxy at the second position of the phenyl ring, **SVN 8** has hydroxy at the third and fourth positions of the phenyl ring and **SVN 9** has methoxy group at the second position of the phenyl ring, were the most effective. Additionally, compounds **SVN 5** has a thiophene nucleus in place of phenyl ring on coumarinyl thiazole nucleus exhibited remarkable adulticidal activity higher than **SVN 6**, **7** and **8**. **SVN 1, 2, 3** and **4** having unsubstituted phenyl ring, 4-methoxy on the phenyl ring, 4-chloro on phenyl ring and fluorine atom at the fourth position of the phenyl ring, respectively, displayed lower larvicidal and adulticidal effect. However, **SVN 10** has 2-hydroxy and 5-nitro on the phenyl ring. **SVN 11** has 2-hydroxy and 3,6-dichloro substitutions on the phenyl ring, which is on coumarinyl

thiazole nucleus, displayed considerable larvicidal activity but lower than **SVN 6, 7, 8** and **9.** These findings suggested that the relative substituent on the phenyl ring at the fourth position of the thiazole moiety, connected to the primary coumarin nucleus at the third position, influences the larvicidal and adulticidal activity of the tested compounds.

5.2.4 Conclusions

In conclusion, novel Schiff bases of thiazolyl nitro-coumarins were synthesized in this study, the characterization of the title compounds was performed by FT-IR, NMR (^{1}H &^{13}C), LC-MS and elemental analysis. The synthesized compounds **SVN 1-11** were screened for larvicidal and insecticidal activity against *Anopheles arabiensis* by standard WHO larvicidal assay and cone bioassay assay. The highest larvae mortality was observed in compounds **SVN 6**, **7**, **8** and **9**, displaying 100% larvae mortality after 24 hours, the same as the positive control, Termephos (100%). Moreover, compounds **SVN 5, 7** and **9** were the most potent adulticidal. This study shows that integrating different functional groups on the phenyl ring at the fourth position of the thiazole moiety, connected to the primary coumarin nucleus at the third position, contributed significantly to the larvicidal and adulticidal effects. These findings suggest that the synthesized compounds might be used against *A. arabiensis* mosquitos. However, further research is needed to determine its toxicity and impacts on non-target species and the environment. The current study's findings could also promote research to develop new mosquito control agents.

CHAPTER VI. ANTICANCER ACTIVITY OF NOVEL SCHIFF BASES OF 3-(2-AMINOTHIAZOL-4-YL)-6,8-DICHLORO-2*H*-CHROMEN-2-ONE (SVM1-11) AND (*E*) 3-(2-AMINOTHIAZOL-4-YL)-6-NITRO-2*H*-CHROMEN-2-ONE (SVN1-11).

6.1 Anticancer activity of novel Schiff bases of 3-(2-aminothiazol-4-yl)-6, 8-dichloro-2*H*-chromen-2-ones (SVM1-11)

Abstract

The anticancer activity of the novel Schiff bases of 3-(2-aminothiazol-4-yl)-6, 8-dichloro-2*H*-chromen-2-ones (**SVM 1-11**) was evaluated against MCF-7 (human breast adenocarcinoma cells) and A549 (Human epithelial lung cancer cells) cell lines. The results revealed an overall higher cytotoxicity effect of the compounds **SVM 1-11** against MCF-7 compared to A549 cancer cells, suggesting that these compounds significantly reduce the viability of MCF-7 cells. A dose-dependent increase in cytotoxicity activity was observed for each synthesized compound as the concentration increased. Compound **SVM 2, 4,** 8 and **11** were the most potent, with an IC_{50} ranging from 5.7 to 9.2 µg/mL against MCF-7 cells. The best IC_{50} value was obtained with compounds **SVM 2** and **8** showing 5.7 and 6.8 µg/mL, respectively.

Furthermore, to establish the mechanism involved in the antitumor activity against MCF-7 of the selected active compounds, **SVM 2, 4, 8** and **11**, Caspase-Glo® kit assay was used to determine the apoptosis (caspase-3/7, -8 and -9). The results indicated that apoptosis caused by these compounds is partly due to activation of caspase-3/7 and caspase-9, which may be the critical mechanism of action for apoptosis. In addition, the apoptosis induced on the MCF-7 cell line by these compounds was more significant than its effect on Caspase 8. This study shows that **SVM 2, 4, 8** and **11** compounds induced apoptosis through the mitochondrial-dependent intrinsic pathway. Whereas **SVM 2** induced apoptosis in MCF-7 through intrinsic and extrinsic pathways. These results highlight the relevance of **SVM 2, 4, 8** and **11** as lead scaffolds for designing and developing novel coumarin pharmacophore-based anticancer agents.

6.1.1 Introduction

Cancer is a critical health problem characterized by unregulated mechanisms that guide cell proliferation and differentiation (Abd El-Karim *et al*., 2019). Anticancer agents are necessary for cancer therapy; more than a hundred drugs have been developed for this reason (Islam *et al*., 2019). However, most of them have developed multidrug resistance and lethal side effects due to non-selectivity and poor efficacy (Qing *et al*., 2018, Wang *et al*., 2017). Coumarin and other heterocyclic compounds are essential in developing modern drugs, natural resources, agricultural products, analytical reagents and dyes. As a result of growing resistance to anticancer medicines, developing new structural heterocyclic moieties is critical to generate potential anticancer agents with remarkable therapeutic uses (Gorle *et al*., 2017). Coumarin and its derivatives are known to have a range of biological activities, including anticancer activity (Song *et al*., 2020).

On the other hand, the thiazole motif is a fascinating building block for developing and synthesizing various bioactive drugs. Several investigations found that numerous thiazole compounds had potent anticancer activity by inhibiting specific molecular targets such as receptor tyrosine kinases, the Bcl-2 family and histone deacetylases (Ankali *et al*., 2021). Thus, molecular hybridization, a fusion of two or even more pharmacophores into a single molecular structure, can enhance affinity and activity, decrease side effects, and overcome drug resistance. Hybridization of the coumarin moiety with another anticancer pharmacophore can provide low toxicity, high specificity and excellent efficacy for novel anticancer candidates against drug-susceptible and drug-resistant cancers (Zhang and Xu, 2019). Hence, this chapter aimed to synthesize and screen the novel Schiff bases of 3-(2-aminothiazol-4-yl)-6,8-dichloro-2*H*-chromen-2-ones (**SVM1-11**) for their anticancer activity against MCF-7 (Breast cancer) and A549 (Lung cancer) cancer cell line.

6.1.2 Materials And Methods

6.1.2.1. Cell lines

The MCF-7 (human breast adenocarcinoma cells) and A549 (Human epithelial lung cancer cells) cell lines were donated by the Department of Human Physiology, University of Kwazulu Natal (Westville Campus), South Africa. These cells were stored in 25 cm^2 tissue culture flasks and incubated at 37^{o}C in a humidified incubator (SnjidersHepa, United Scientific, Cape Town, South Africa) that contains 5% CO_2 atmosphere. Upon arrival, the cells were transferred into

two different 75 cm^2 flasks (Greiner, Germany) until cells reached 80% confluence in each flask.

6.1.2.2 Maintenance of Cells

All cell culture maintenance experiments were conducted in the laminar flow cabinet (Scientific Engineering, INC) to preserve a sterile environment. Before cell culture experiments, the UV light was used to sterilize the laminar flow cabinet and swab regularly with 70% ethanol (Merck, South Africa). The MCF-7 and A549cell lines were grown separately in Dulbecco`s Modified Eagle Medium (DMEM) (glucose ($4.5gl^{-1}$), 1 mM L-glutamine, and 1 mM sodium pyruvate) (Sigma-Aldrich, Inc). The DMEM was supplemented with 1% heat-inactivated fetal calf serum (FCS) and 1% penicillin/streptomycin (antibiotic) solution (Sigma-Aldrich, Inc). These cells were sub-cultured once the flasks happened to 80% confluency every 2-3 days to ensure that the cells were in the exponential growth phase. Supplemented-DMEM was drowned out of the flasks, and the monolayer of cells was washed twice with 5 mL Phosphate Saline Buffer (PBS) during sub-culturing. Afterwards, an aliquot of 1 mL trypsin was added to the flasks. The monolayer of cells was then incubated at 37^oC in a humidified incubator with a 5% CO_2 atmosphere for three minutes. The flasks were tapped on the side for 20 seconds to detach the monolayer. Ten mL of supplemented DMEM was added to each flask, and 1 mL of cell culture was subsequently transferred to each separate flask. A final aliquot of 20 mL DMEM was added to each flask, and this was followed by incubation at 37^oC in a humidified incubator containing a 5% CO_2 atmosphere. The cells were monitored for contamination daily by noting medium colour and turbidity changes during the incubation period. Cell growth was examined with an inverted microscope (Nikon, Japan).

6.1.2.3 Cell line storage

Cell culture flasks that reached 80% confluent were washed twice with 5 mL PBS and treated with trypsin, as described during the sub-culturing process. An aliquot of 10 mL DMEM was then added to each flask, and the cells were later transferred to 50 ml tubes. The 50 mL tubes were then centrifuged at 1500 rpm for 10 minutes to collect cell pellets. A volume of 2 mL of cryo-protective medium (10% DMSO, 20% FBS, and 70% DMEM) was added to re-constitute the pellet. An aliquot of 1 mL cryo-protective/cell-containing solution was added to the cryotubes (Corning, South Africa). These tubes were placed on ice before adding the cryo-

protective solution to allow for slow cooling. The tubes were transferred to thermos flasks and stored overnight at – 20°C. The cells were then stored in a – 80°C freezer.

6.1.2.4 Cell regeneration

Cells were removed from storage at – 80°C and rapidly thawed for use. After that, cells were transferred into 20 mL pre-warmed supplemented-DMEM in 75 cm^2 tissue culture flasks. These cells were then incubated at 37°C in a humidified incubator containing a 5% CO_2 atmosphere.

6.1.2.5 Enumeration of cells

Cells were enumerated using trypan blue; a dye used to count viable cells. This staining technique is based on the principle that viable cells would not use the trypan blue dye, while non-viable cells would. In this study, 200 µL trypan blue (Bio Whittaker, Walkersville, USA) was mixed with 200 µL cell suspension cultures in a tube. This tube was then incubated at room temperature for about a minute. After that, an aliquot of 10 µL trypan-suspended cell cultures was loaded into both chambers of the Neubauer hemocytometer. The cells within the middle square and in the four 1 mm corner squares of the two chambers were counted. The following equation shown below was used to determine the number of cells in suspension:

Cells/mL = Average number of cells from 5 primary squares X 2 X10 000

Total cell count = 16 squares x 4

= Cell counts in 4 sets of 16 squares

16 squares = 2 x 10^4/mL

Therefore, cells per mL = $\frac{\text{total cell count}}{4}$ x 2 x 10^4 per mL

= cells per mL

6.1.2.6 Seeding of cells

Cells grown to 75-80% confluency were washed twice with 5 mL of PBS, trypsinized, centrifuged and re-suspended as described above. Subsequently, aliquots of 90 µL ($3x10^3$ cells/well) of the cell suspension were seeded into 96 well microtiter plates (Costar, Sigma-Aldrich, Inc). After 200 µL of distilled water was pipette into the outer well of the plates to prevent evaporation of the medium. The plates were then incubated for 24 hours at 37°C in a humidified incubator with 5% CO_2.

6.1.2.7 Microscopic examination of the cells

The morphological features of MCF-7 cells treated and untreated were observed under an inverted microscope (Nikon) at 100 x magnification.

6.1.2.8 Growth inhibition measurement using MTT assay

6.1.2.8.1 Description

The MTT [3-(4, 5-dimethylthiazol-2-yl)-2, 5-diphenyltetrazolium bromide] assay is based on the cellular reductase activity (NADH and NADPH) present in viable cells. These enzymes cleave the tetrazolium ring of MTT substrate, thereby reducing this yellow dye to violet formazan crystals that can be dissolved in DMSO. The resulting purple solution is spectrophotometrically measurable.

6.1.2.8.2 Cytotoxicity assay

The MTT assay was carried out according to Sonmezet al. (2017) procedure with slight adjustments. A549 and MCF-7 cells were plated into a 96-well microtiter plate (90 µL of cell culture: 3×10^3 cells/mL) and treated with 10 µL of 50 and 100 µg/mL of SVM1-11 compounds. The positive control was camptothecin (6 µg/mL), while the negative control was DMSO (0.2%). After 48 hours of treatment with the produced compounds, ten microliters of a 5 mg/mL MTT solution were applied to the cells. The microtiter plates were incubated for 4 hours at 37°C in a humidified incubator with 5% CO_2. Following that, 100 µL of DMSO was added to the cells to dissolve the formazan crystals, and the plates were incubated for another hour. A 570 nm ELISA plate reader was used to measure the absorbance of the formazan solutions (Sonmez *et al*., 2017). The following calculation was used to determine the percentage growth inhibition (percent GI) observed by the investigated compounds.

$$\%GI = \frac{\text{(Abs of negative control-Abs of drug)}}{\text{Abs of negative control}} \times 100$$

Abs negative control: Absorbance of cells treated with DMSO

Abs drug: Absorbance of cells treated with the test drug

%GI: Percentage growth inhibition

6.1.2.8.3 Minimum inhibitory concentration (IC_{50}) of the active compounds

All compounds that inhibited the proliferation of the two cell lines (MCF –7 and A549 cells) by 70% were further tested to determine their IC_{50} using the MTT assay described by Sonmez et al. (2017). The IC_{50} values of the active compounds were determined by analyzing them at eleven different concentrations, as described in section 6.1.2.8.2. In addition, the percentage growth inhibition data were imported to GraphPad Prism 4 to create the logarithmic form of the dose-response curves for calculating IC_{50} values.

6.1.2.9 Statistical analysis

The statistical significance of differences between the groups was analyzed using the procedure described in section 5.1.2.3

6.1.2.10 Caspase activity

Caspase-Glo^{TM}-3/7, -8 and -9 activities were determined using commercial kits purchased from Promega Company (USA) according to the manufacturer's recommendations. The assays use a luminogenic caspase-3/caspase-7, caspase-8 or caspase-9 substrate in a buffer solution to measure caspase activity in cell lysates. The degree of caspase activity present is proportional to the luciferase signal produced. In brief, MCF-7 cells (20,000 cells/well) in DMEM with 10% FBS were seeded on a white 96-well plate (SPL, Korea) and incubated overnight at 37˚C with 5% CO_2. The medium was then replaced, and the cells were treated with the IC_{50} concentration of **SVM 2**, **4**, **8** and **11** compounds. Cells treated with DMSO served as a control. After treatment, the Caspase-Glo^{TM}-3/7, -8 and -9 reagents were prepared and added directly to the cells in 96-well plates and incubated for 60 minutes. Luminescence was determined using a plate reader. All tests were carried out in triplicate; data are expressed as the number of relative light units (RLU).

6.1.3 Results and Discussion

6.1.3.1 Assessment of the growth inhibitory potential of 3-(2-aminothiazol-4-yl)-6, 8-dichloro-2*H*-chromen-2-ones (SVM1-11) on A549 and MCF-7 cells.

The assessment of the cytotoxicity of these compounds to a cancer cell line was necessary to examine how the compounds affected the viability and proliferation of the cells. The cytotoxicity activity displayed by compounds **SVM 1-11** against A549 and MCF-7 is summarized in Table 10. The percentage growth inhibition of these compounds was investigated at 50 and 100 µg/mL. All experiments were conducted in triplicate. The average absorbance readings were calculated according to the negative solvent control DMSO (at 0.2%), noting that DMSO could be toxic to the cells at high concentrations. The results revealed a dose-dependent increase in cytotoxicity activity observed for each synthesized compound as the concentration increases. Camptothecin, a cancer chemotherapy drug, was used as a positive control, showed a percentage growth inhibition of 94.65±1.2 and 91.52±1.5% against MCF-7 and A549 cells, respectively (Table 10). Compounds **SVM 2, 4, 8** and **11** were the most potent with a cytotoxicity percentage ranging from 80 to 86% against MCF-7 (IC_{50} ranging between 5.7 to 9.2 µg/mL) lower than the reference drug Camptothecin 94.6% (IC_{50} of 0.06 µg/mL) (Table 10 and 11). Moderate cell growth inhibition was shown with **SVM 3, 9** and **10** against MCF-7 cells of 53.8±0.17, 53.4±0.1 and 55.5±0.07%, respectively (Table 10).

On the other hand, low cytotoxicity activity was apparent at 50 µg/mL with **SVM 1, 4, 5, 6, 7, 9, 10** and **11** against A549, showing a cytotoxicity capacity ranging from 22 to 46% (Table 10). Compounds **SVM 2, 3, 8** and **11** demonstrated moderate cell growth inhibitory effect of 54.1±1.4, 56.2±0.8 and 58.7±0.8 and 50.9 ±1.0% respectively (Table 10). Camptothecin showed a growth inhibitory activity of 91.52±1.5% against A549 cells (Table 10). These results revealed that **SVM 1-11** compounds had a low overall cytotoxicity impact on A549 cells.

The ANOVA test was conducted on the growth inhibitory data to determine significant differences between the A549 and the MCF-7 cell line. Some compounds displayed significantly different growth inhibition values between cell lines, as seen in Table 10, whereas others did not show considerable variability in growth inhibition values between cell lines.

Table 10: *In vitro* cytotoxicity of **SVM 1-11** against A549 and MCF-7 cell lines

Compounds	Cell Growth inhibition (%)			
	A549 Cells		MCF-7 Cells	
	50 µg/mL	100 µg/mL	50 µg/mL	100 µg/mL
SVM1	38.8 ± 0.7^{cx}	51.6 ± 1.6^{bx}	37.8 ± 0.1^{bx}	57.8 ± 0.40^{by}
SVM 2	54.1 ± 1.4^{ghx}	67.4 ± 0.6^{dx}	86.8 ± 0.5^{iy}	91.2 ± 0.21^{fy}
SVM 3	56.2 ± 0.8^{hiy}	68.2 ± 1.1^{dy}	53.8 ± 0.17^{ex}	61.1 ± 0.30^{cdx}
SVM 4	49.3 ± 1.3^{efx}	57.5 ± 0.6^{cx}	80.6 ± 0.14^{gy}	89.1 ± 0.10^{efy}
SVM 5	46.8 ± 0.9^{ex}	55.3 ± 0.7^{cx}	48.8 ± 0.25^{dy}	59.3 ± 0.12^{bcy}
SVM 6	22.2 ± 0.8^{ax}	37.5 ± 1.4^{ax}	35.6 ± 0.34^{ay}	45.1 ± 0.99^{ay}
SVM 7	28.4 ± 1.8^{bx}	50.7 ± 1.3^{by}	41.8 ± 0.02^{cy}	47.7 ± 1.07^{ax}
SVM 8	58.7 ± 0.8^{ix}	69.4 ± 1.0^{dx}	81.8 ± 0.13^{gy}	86.1 ± 0.47^{ey}
SVM 9	42.9 ± 1.5^{dx}	49.9 ± 1.3^{bx}	53.4 ± 0.1^{ey}	64.0 ± 0.32^{dy}
SVM0	46.4±1.1dex	50.4 ± 1.2^{bx}	55.5 ± 0.07^{fy}	63.8 ± 0.25^{dy}
SVM 11	50.9 ± 1.0^{fgx}	58.1 ± 0.9^{cx}	84.5 ± 1.2^{hy}	88.7 ± 0.65^{efy}
Camptothecin	91.52 ± 1.5^{jx}	93.6 ± 1.6^{ex}	94.65 ± 1.2^{jy}	95.29 ± 2.8^{gy}

Values are represented as mean ±SD; means of growth inhibition without a common letter differ significantly ($p<0.05$).

6.1.3.2 Determination of the minimum inhibitory concentration (IC_{50}) of active compounds against MCF-7

Minimum inhibitory concentration (IC_{50}) values were determined for compounds that inhibited cell growth by 70% or more against MCF-7 or A549 cells at 50 µg/mL. Thus, compounds **SVM 2, 4, 8** and **11** significantly inhibited the MCF-7 cells (Table 11) and were selected for future study. The logarithmic form of the dose-response curves was generated to determine the concentration of compounds that inhibits 50% of cells. The IC_{50} values of the compounds were compared to the standards Camptothecin, as shown in Table 11. The data obtained revealed that compound **SVM 2** showed a high IC_{50} of 5.7 µg/mL followed by compounds **SVM 8** and **SVM 11**, which displayed an IC_{50} of 6.8 and 7.8 µg/mL respectively, lastly compounds **SVM 4** showed an IC_{50} of 9.2 µg/mL (Table 11).

These results are comparable to those of Vaarla *et al*. (2019), who synthesized new series 3-(2-(5 amino-3-aryl-1*H*-pyrol-1-yl) thiazol-4-yl)2*H*-chromen-2-ones and evaluated their anticancer activity against L1210, CEM, DU145, HeLa, and MCF-7. The 6-diethylamino substituted compounds showed excellent activity against the test cancer cell lines among the studied compounds. In contrast, 6,8-ditert-butyl substituted compounds showed good activity

against DU-145 and MCF-7 cancer cell lines with IC_{50} values of 7±1 and 9±6 μM, respectively (Vaarla *et al*., 2019). In another study, Thota *et al*. (2015) synthesized a series of coumarin thiazole derivatives as anticancer agents against molt 4/C_8, CEM, L1210, BEL7402 HL60 cells. The results showed that these compounds demonstrated cytotoxicity ranging from 6.2-18 μg/mL against CEM, 8.2-21 μg/mL against L1210, 09-19 μg/mL against molt 4/$C_{8,}$ 8.6-12 μg/mL against HL60, and 8-16 μg/mL against BEL7402, respectively (Thota *et al*., 2015). Similarly, Zhang *et al*. (2014) synthesized and reported a series of 4-(1, 2, 3-triazol-1-yl) coumarin for its potential anticancer activity against three cancer cell lines MCF-7, SW480, and A549. Most of the compounds exhibited remarkable antitumor activity; the most potent compound demonstrated an IC_{50} of 5.89, 1.99 and 0.52 μM against MCF-7, SW480, and A549, respectively. These activities were compared favourably with those of the positive control, doxorubicin (IC_{50}: 3.51, 2.43, 1.65 μM), used in the study (Zhang *et al*., 2014).

Table 11: The minimum inhibitory concentration (IC_{50}) of the active compounds against MCF-7 cancer cells.

Compounds	IC_{50} (μg/mL)
	MCF-7
SVM 2	5.7
SVM 4	9.2
SVM 8	6.8
SVM 11	7.8
Camptothecin	0.06

6.1.3.3 Morphology of cells treated with the active compounds

Cells treated with active compounds **SVM 2, 4, 8** and **11** were also studied for morphological changes microscopically. The findings revealed that untreated cells had a normal shape and an intact structure (Figure 15A and 15B, respectively). Figures 15 (15C, 15D, 15E and 15F) showed that cells treated with the active compounds caused rounding of cells; furthermore, cells treated with **SVM 11** (Figure 15F) allowed apoptotic bodies to form.

Thus, these results showed that the active compounds induced the MCF-7 cells to undergo apoptosis. Apoptotic cells have a different shape during the apoptotic process; when a cell

receives a death signal, it begins to express proteins that aid in the death process, eventually leading to increased activity of a set of enzymes that break other proteins. These enzymes dig the cell's cytoskeleton, causing the cell to round up and shrink (Kroemer *et al*., 2005; Baig *et al*., 2017). The results above are comparable to Archana *et al*., who stated that rounding and budding of cells are signs of apoptosis (Archana *et al*., 2013).

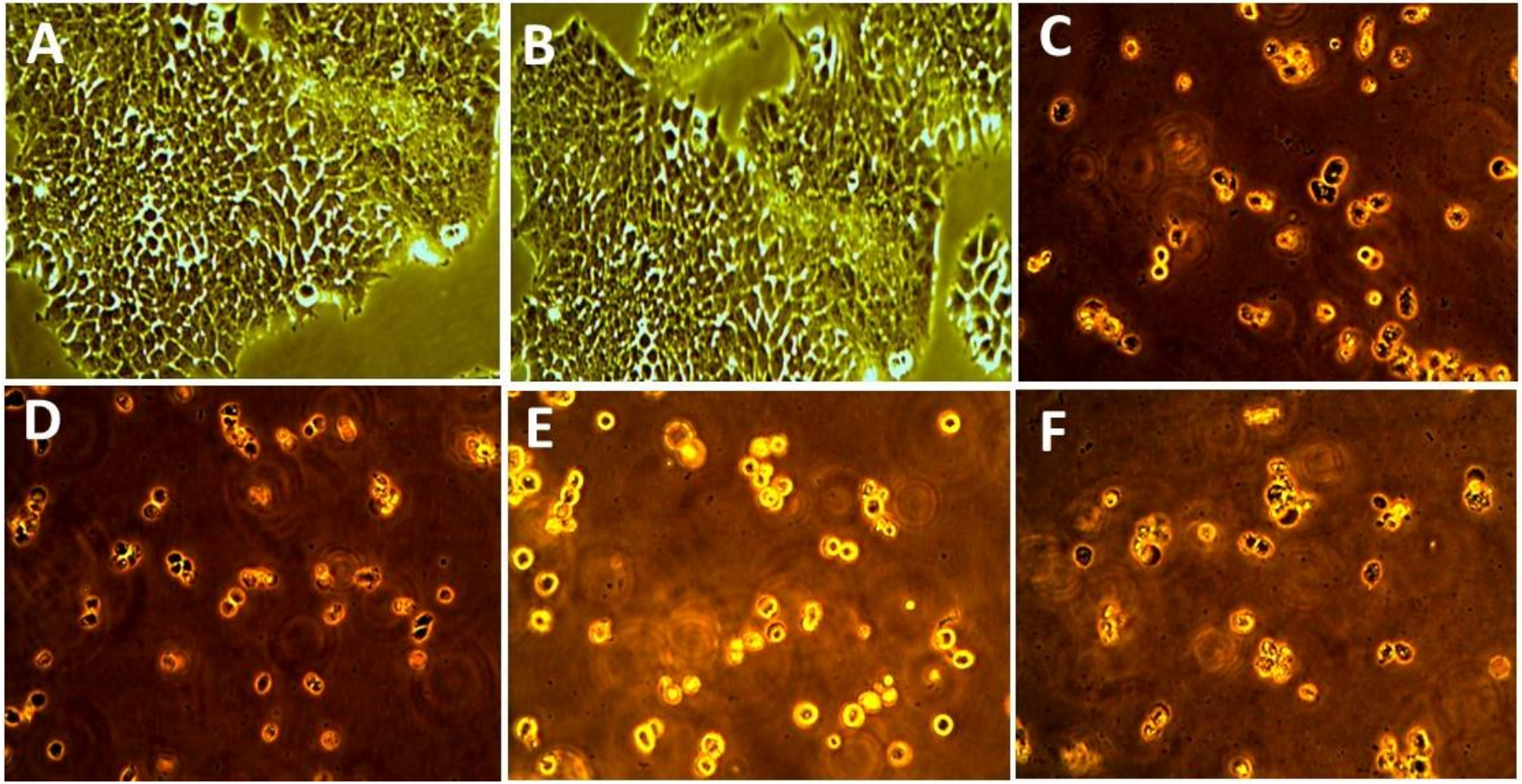

Figure 15: Cells morphology of MCF-7 (100X magnification) (A) untreated, (B) treated with DMSO (0.2%), (C) treated with SVM 2, (D) treated with SVM 4, (E) treated with SVM 8,(F) treated with SVM11.

6.1.3.4 Caspases-3/7, Caspases-8 and Caspases-9 activity.

Apoptosis induction is regulated explicitly by the cascade of caspases via both intrinsic and extrinsic pathways. Caspases play an essential role in apoptosis, which involves two major classes of initiators and executioners (Faraj *et al.*, 2014). Caspases are a cysteine protease family classified into executioner caspases, such as caspase-3 or -7 and initiator caspases, such as caspase-8 and -9. Kumar (1999) reported that the initiator caspase-8 is activated by extrinsic pathways, while caspase-9 is activated by mitochondrial cytochrome C leakage (Kumar, 1999). Caspase-3 or -7 can be activated by all initiator caspases, which commit cells to apoptosis (Woo et al., 2011). Caspase-3/7, 8 and 9 activity were enhanced in MCF-7 cells following treatment with the selected active compounds (**SVM 2, 4, 8** and **11)** compared to control.

The results showed that compounds **SVM 2, 4, 8** and **11** could induce apoptosis by activating caspase 3/7 in MCF-7 treated with the number of relative light units ranging between 80.000 to 170.000 RLU (Figure 16A). These compounds were also shown to induce caspase-9 activity in MCF-7 treated with relative light units ranging between 30.000 to 80.000 RLU, which was significantly higher when compared to control cells (Figure 16C). The results suggested that the activation of caspase-9 is triggered by incubation with compounds **SVM 2, 4, 8** and **11**, whereas caspase-8 activities of the selected compounds remain at the baseline level except for compound **SVM 2** (Figure 16B). Compounds **SVM 2** induced apoptosis via death receptors by activating caspase-8 with the relative light units of 110.000 RLU higher than the control cells (Figure 16B). The rise in activity of caspase-9 was concurrent with the increase in activity of caspase-3/7. These findings indicate that apoptosis caused by these compounds is, in part, due to activation of caspses3/7 and caspase 9, which may be the mechanism of action for apoptosis. In addition, the apoptosis induced on the MCF-7 cell line by the tested target compounds was more prominent than its effect on Caspase 8. This study shows that **SVM 4, 8** and **11** compounds induced apoptosis through the mitochondrial-dependent intrinsic pathway. On the other hand, **SVM 2** induced apoptosis in MCF-7 through intrinsic and extrinsic pathways.

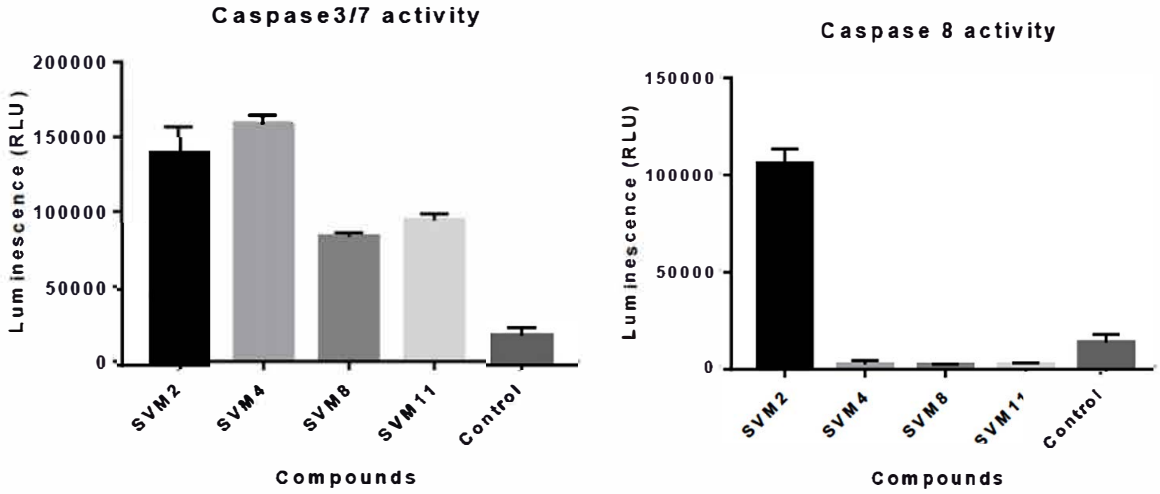

(A)

(B)

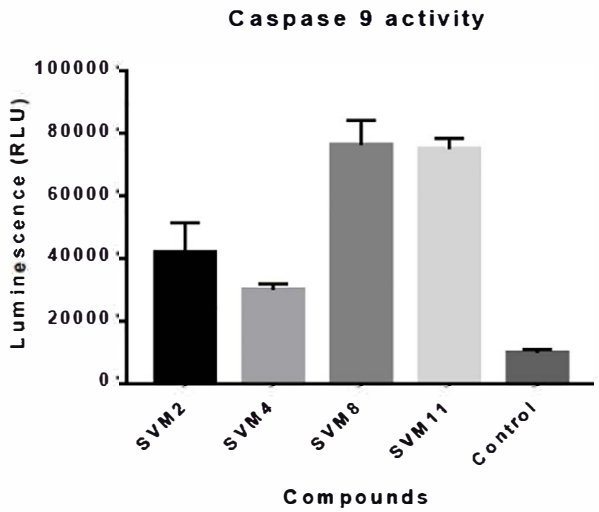

(C)

Figure 16: Relative luminescence expression (RUL) of Caspase: (A) Caspase3/7, (B) Caspase 8 and (C) Caspase 9 in MCF-7 cells treated with SVM2, SVM4, SVM 8 and SVM 11.

6.1.4 Conclusions

The Schiff bases of 3-(2-aminothiazol-4-yl)-6,8-dichloro-2*H*-chromen-2-one (**SVM 1-11**) showed that the compounds significantly reduced the viability of MCF-7 cells. **SVM 2, 4, 8** and **11** were the most promising against MCF-7 cells. This study indicates that **SVM 4, 8** and **11** compounds induced apoptosis through the mitochondrial-dependent intrinsic pathway. On the other hand, **SVM 2** induced apoptosis in MCF-7 through intrinsic and extrinsic pathways. This study showed that the activity of these compounds might be attributed to the introduction

substituent on the phenyl ring at the fourth position of the thiazole moiety, which is coupled to the main coumarin nucleus at the third position, is responsible for the test compounds' activity. Thus, the current studies explicitly illustrate the significance of selected compounds as anticancer agents and highlight the importance of **SVM 2, 4, 8** and **11** as lead scaffolds for designing and developing new coumarin pharmacophore-based anticancer agents.

6.2 Anticancer activity of novel Schiff bases of 3-(2-aminothiazol-4-yl)-6-nitro-2*H*-chromen-2-one (SVN 1-11)

Abstract

Cancer is a disease caused by uncontrolled cell proliferation that remains one of the fatal diseases globally. Despite the availability of a range of anticancer medications, no available treatments can kill cancer cells without causing harm to normal tissues. As a result, medicinal chemists are increasingly focused on developing novel anticancer drugs and more selective cancer therapy techniques. In this study, novel Schiff bases of 3-(2-aminothiazol-4-yl)-6-nitro-2*H*-chromen-2-one (**SVN 1-11**) were synthesized and assessed for their anticancer activity against MCF-7 and A549 cancer cell lines using the MTT assay. The results obtained showed that compounds **SVN 1-11** had a low cytotoxicity effect on A549 compared to MCF-7 cancer cells, implying that the **SVN 1-11** significantly decreased the viability of MCF-7 cells. The cytotoxicity activity increased dose-dependent as the concentration of each of the compounds increased. Compounds **SVN 1, 2, 4, 9, 10** and **11** exhibited high cytotoxicity activity against MCF-7, with percentage inhibition ranging from 73-83% (IC_{50} ranging from 9.38-16.04 µg/mL). Compounds **SVN 7** and **10** were the most potent, displaying percentage cytotoxicity of 82.6 and 83.4%, respectively. Cells treated with the most active compounds were observed to exhibit the characteristic features of apoptosis. These compounds caused rounding of some cells and allowed the rest of the cells to remain attached, which are signs of apoptosis. Moreover, Caspase 3/7, 8 and 9 assays were performed to determine the mechanism involved in the anticancer activity of the selected active compounds. The results showed that **SVN 2** could induce caspase activation in both the extrinsic and the intrinsic apoptotic pathways, whereas **SVN 1, 4, 9, 10** and **11** induced caspase activation through an intrinsic mechanism.

6.2.1 Introduction

Cancer is an illness that has a significant impact on the world today. It is the world's second-biggest cause of mortality after cardiovascular illnesses, and it is expected to become the primary cause of death in the future years (Roleira *et al*., 2018). The discovery of novel structures that may be beneficial in developing new, effective, selective, and less toxic anticancer drugs remains a crucial problem for medicinal chemistry researchers (Gorle *et al*., 2017). Despite significant advancements in the research and development of numerous cancerostatic medicines in recent years, existing antitumor chemotherapy still suffers from two fundamental limitations. The first is that current chemotherapy medications do not distinguish between diseased and non-cancerous cells; the second is cancer cells developing multidrug resistance (Bhaskar and Mohite, 2010). As a result, there is a need to discover and develop new lead compounds with simple structures that demonstrate optimum *in vitro* anticancer efficacy and novel modes of action.

Coumarin and its derivatives are essential pharmacophores with multiple medicinal chemistry and pharmaceutical applications. They have attracted a lot of attention due to their pharmacological properties and because their synthetic derivatives have a significant cytotoxicity effect against various cancer cells (Kurt *et al*., 2020). On the other hand, the thiazole moiety is one of the most widely used scaffolds in synthesizing novel lead compounds, mainly anticancer drugs. Antitumor activity has been discovered in several thiazole-containing drugs (Farghaly *et al*., 2020). A hybrid drug consisting of two pharmacophores' integration in one molecule is designed to interact with multiple targets or intensify their impact by acting on another bio target as a single molecule (Nepali *et al*., 2014). This chapter aimed to synthesize and test a series of **SVN 1-11** for anticancer efficacy against MCF-7 and A549 cancer cells.

6.2.2 Materials and Methods

6.2.2.1 Assessment of the growth inhibitory potential of SVN 1-11 compounds

The cytotoxicity activity of the synthesis of the novel Schiff bases of (*E*) 3-(2-aminothiazol-4-yl)-6-nitro-2*H*-chromen-2-one (**SVN 1-11**) against MCF-7 and A549 was achieved following the protocols described in section 6.1.2.8

6.2.2.2 Determination of the minimum inhibitory concentration (IC_{50}) of active compounds

The minimum inhibitory was determined according to the protocol described in section 6.1.2.8.3

6.2.2.3 Determination of cell morphology treated with the active compounds

The morphological changes of the cells were observed and photographed on an inverted microscope (Nikon, Japan).

6.2.2.4 Caspases-3/7, -8, and -9 activation analysis of (*E*) 3-(2-aminothiazol-4-yl)-6-nitro-2*H*-chromen-2-one (SVN 1-11)

The caspase-3/7, caspase-8 and caspase-9 activation was achieved according to the protocol is described in section 6.1.2.10

6.2.3 Results and Discussion

6.2.3.1 Cytotoxicity activity of SVN 1-11

The growth inhibition activity of compounds **SVN 1-11** was investigated against A549 and MCF-7 cells at 50 and 100 µg/mL. All experiments were conducted in triplicate; the average absorbance readings were calculated according to the negative solvent control (0.2 % DMSO). The percentage cytotoxicity results are summarized in Table 12. The results revealed a decreased growth of the tested cancer cells as concentration increased.

The synthesized compounds **SVN 1-11** exhibited a significant cytotoxicity effect against MCF-7 than A549 cancer cells, inducing significant morphological changes and a dose-dependent decrease in the number of cells. The results obtained in Table 12 indicated that the overall growth inhibitory potential against MCF-7 at 50 µg/mL was exceptional with compounds **SVN 1, 2, 4, 9, 10** and **11**, which exhibited a high cytotoxicity effect of 76.5±0.3, 75.9±0.5, 82.6±0.10, 73.7±0.14, 83.4±0.2 and 78.3±0.31%, respectively. These compounds were the most potent, still lower than the reference drug Camptothecin 94.65±1.2% (Table 12). Moderate cytotoxicity effect ranging from 56 to 57% was shown with compounds **SVN 2, 3, 4** and **9** against A549, whereas compounds **SVN 3, 5** and **7** showed moderate activity against MCF-7 (Table 12).

These findings are similar to those of Ayati et *al*. (2018) synthesized novel coumarins bearing a 2,4-diaminothiazole-5-carbonyl moiety and assessed for anticancer potential. The findings showed that The 2-thiomorpholinothiazole derivative 3k exhibited excellent cytotoxicity against the investigated cell lines MCF-7, HepG2, and SW480, with IC_{50} values ranging from 7.5 to 16.9 µg/ml. Flow cytometric research revealed that this molecule induces apoptotic cell death in MCF-7 cells and G1-phase arrest in the cell cycle (Ayati et al., 2018). In another study, Zhu *et al*. (2015) synthesized a series of triphenylethylene coumarin hybrids and evaluated their anticancer activity against MCF-7, A549, K562, and Hela cells. The results demonstrated that some compounds, such as N^1, N^3-bis(4-(7-(2-(diethylamino)ethoxy)-4-(4-(2-(diethylamino)ethoxy)phenyl)-2-oxo-2*H*-chromen-3-yl)phenyl)malonamide(**7a**), N^1,N^{10}-bis(4-(7-(2-(diethylamino)ethoxy)-4-(4-(2-(diethylamino)ethoxy)phenyl)-2-oxo-2*H*-chromen-3-yl)phenyl)decanediamide(**9a**) and N^1 ,N^6-bis(4-(2-oxo-7-(2-(piperidin-1-yl)ethoxy)-4-(4-(2-(piperidin-1-yl)ethoxy) phenyl)-2*H*-chromen-3-yl)phenyl)adipamide (**8b**) most active compounds demonstrated MIC values ranging from 1.5 to 8.7 µM (Zhu *et al*., 2015).

To determine whether there were significant differences between the A549 and MCF-7 cell line, the ANOVA test was conducted on growth inhibitory potential results. Some compounds displayed significantly different growth inhibition values between cell lines, as seen in Table 12, whereas others did not show considerable variability in growth inhibition values between cell lines.

s

Table 12: *In vitro* cytotoxicity of **SVN 1-11** against MCF-7 and A549 cell lines.

Compounds	**Cell Growth inhibition (%)**			
	A549 Cells		**MCF-7 Cells**	
	50 µg/mL	**100 µg/mL**	**50 µg/mL**	**100µg/mL**
SVN1	41.0 ± 1.1^{cx}	55.0 ± 0.8^{bx}	76.5 ± 0.3^{ey}	79.2 ± 0.15^{ey}
SVN 2	56.3 ± 0.8^{fgx}	67.2 ± 0.6^{ix}	75.9 ± 0.5^{ey}	84.4 ± 0.20^{fy}
SVN 3	58.4 ± 0.3^{gx}	64.1 ± 0.2^{ghx}	56.1 ± 0.1^{cy}	62.4 ± 0.16^{cy}
SVN 4	53.5 ± 0.7^{fx}	60.2 ± 0.5^{ex}	82.6 ± 0.10^{gy}	89.5 ± 0.21^{hy}
SVN 5	40.0 ± 0.7^{cx}	57.7 ± 0.2^{cdx}	56.9 ± 0.7^{cy}	64.3 ± 0.1^{cdy}
SVN 6	26.6 ± 1.5^{ax}	51.0 ± 0.2^{ax}	49.2 ± 0.23^{by}	58.5 ± 0.1^{by}
SVN 7	30.8 ± 0.4^{by}	58.4 ± 3.6^{defy}	26.0 ± 0.18^{ax}	47.6 ± 0.32^{ax}
SVN 8	48.7 ± 1.0^{ex}	55.9 ± 1.0^{bcx}	57.09 ± 0.17^{cy}	65.4 ± 0.7^{dy}
SVN 9	57.2 ± 0.6^{gx}	62.1 ± 0.7^{fgx}	73.7 ± 0.14^{dy}	85.6 ± 0.63^{fgy}
SVN 10	47.4 ± 1.5^{dex}	65.2 ± 0.6^{hix}	83.4 ± 0.2^{gy}	87.3 ± 0.15^{ghy}
SVN 11	45.0 ± 0.0^{dx}	62.3 ± 1.0^{fgx}	78.3 ± 0.31^{fy}	84.0 ± 0.2^{fy}
Camptothecin	91.52 ± 1.5^{hx}	93.6 ± 1.6^{jx}	94.65 ± 1.2^{hy}	95.29 ± 2.8^{ix}

Values are represented as mean ±SD, means of growth inhibition without a common letter differ significantly ($p<0.05$).

6.2.3.2 Determination of the minimum inhibitory concentration (IC_{50}) of active compounds

Minimum inhibitory concentration (IC_{50}) values were determined using compounds that inhibited cell growth by 70% or more against MCF-7 or A549 cells at 50 g/mL. Thus, compounds **SVN 1, 2, 4, 9, 10** and **11** significantly inhibited MCF-7 cells and were selected for further study (Table 13). The results showed that most tested active compounds exhibited significant activity but were lower than the reference drug Camptothecin (0.06 µg/mL). From the results in Table 13, it was found that compounds **SVN 10** displayed the best IC_{50} of 6.24 µg/mL, followed by **SVN 4** and **SVN 11** with an IC_{50} of 9.38 and 9.8 µg/mL, respectively. Lastly, compounds **SVN 1** and **SVN 2** displayed an IC_{50} of 13.4 and 16.04 µg/mL, respectively.

Table 13: The minimum inhibitory concentration (IC_{50}) of the active SVN compounds against MCF-7 cancer cells.

Compounds code	MCF-7 (IC_{50} µg/mL)
SVN 1	13.4
SVN 2	16.04
SVN 4	9.38
SVN 9	14.5
SVN 10	6.24
SVN 11	9.8
Camptothecin	0.06

6.2.3.3 Morphological features of MCF-7 cells treated with the active compounds

Cells treated with compounds **SVN 1, 2, 4, 9, 10** and **11** were also examined microscopically for morphological alterations. The untreated cells or treated with DMSO remained attached and healthy (Fig17A, 17B). Figures 17C, 17D, 17E, 17F, 17G and 17F demonstrated that these compounds caused rounding of cells. In addition, compounds **SVN 1**, **2**, **4** and **10** permitted clustering of the cells (Figure 17C, D, E and G). These results indicated that cells treated with the active compounds induced MCF-7 to undergo apoptosis. Apoptotic cells were first distinguished from healthy and necrotic cells by certain morphological characteristics. These characteristics are still valuable for apoptosis studies; some of these characteristics are cell rounding and shrinkage. Cell shrinkage is one of the most common features of cell death,

occurring in almost all apoptosis cases regardless of the stimulus. Cells lose touch with and detach from neighbouring cells and the extracellular matrix as they shrink (ECM) (Doonan and Cptter, 2008). In another study, Archana *et al*. also stated that rounding and budding of cells are signs of apoptosis (Archana *et al.*, 2013).

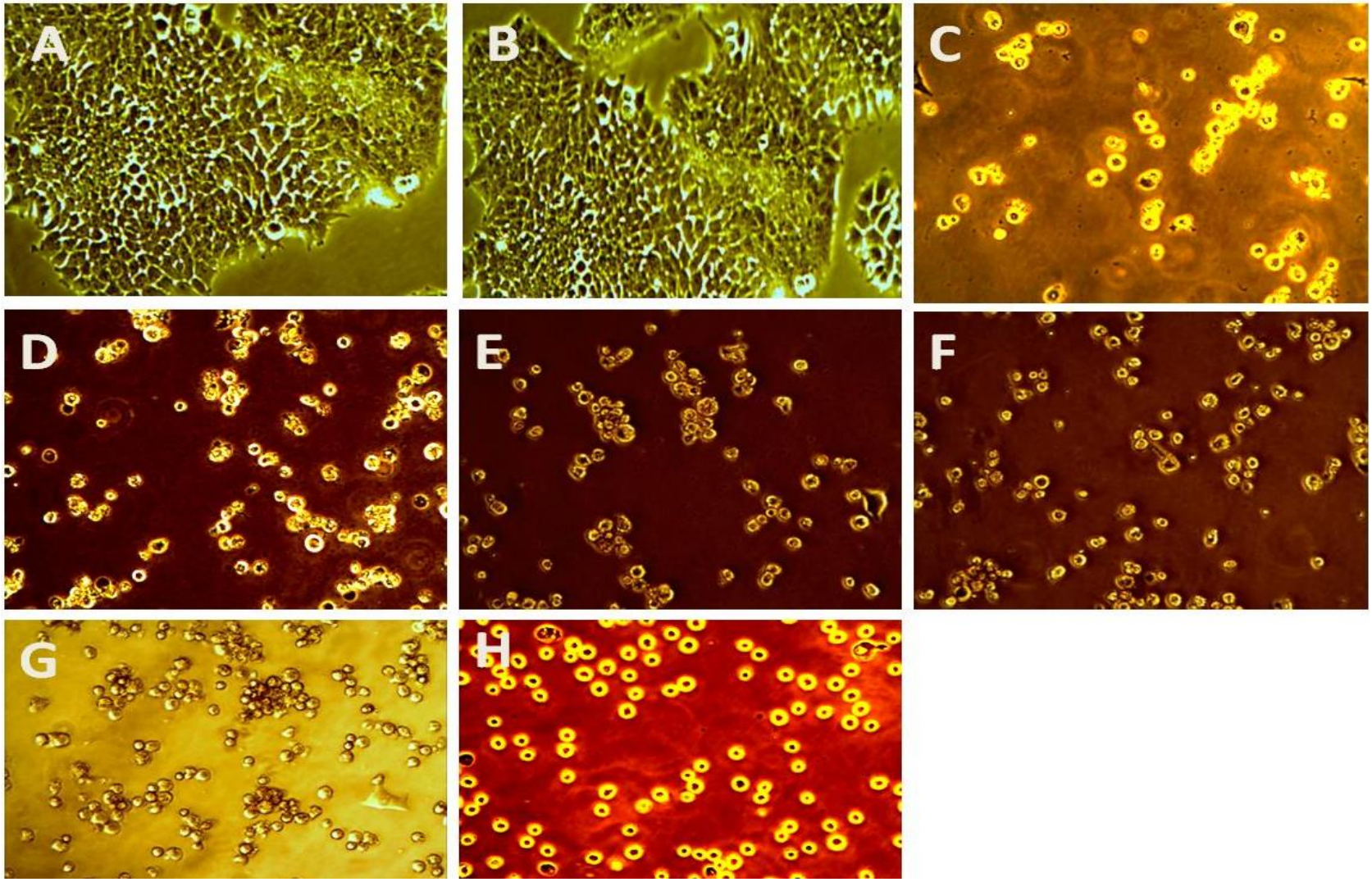

Figure 17: Cells morphology of MCF-7 (100X magnification) untreated (A), treated with DMSO (0.2%) (B), (C) treated with SVN 1, (D) treated with SVN 2, (E) treated with SVN 4, (F) treated with SVN 9, (G) treated with SVN 10 and (H) treated with SVN 11 against MCF-7.

6.2.3.4 Caspases-3/7, -8 and -9 activity

Among the dead proteases are caspases, a type of cysteine-dependent aspartate-directed protease (He et al., 2006). Upstream (initiator) caspases and downstream (effector) caspases are the two basic types of caspases (Carter et al., 2005). Caspases like caspase-8 and caspase-9 work upstream, cleaving inactive pro-forms of downstream caspases like caspase-3 and caspase-7, which then cleave proteins implicated in cell death (Riedl and Shi, 2004). In this study, caspase-3/7 activity in treated cells was significantly higher than in the control cells. When the initiator caspases are activated, the executioner caspases are activated; Caspases-3 and -7 activate apoptosis in cells. The results showed that **SVN 1, 2**, **4, 9, 10** and **11** could induce apoptosis by activating caspase-3/7 in MCF-7 treated with relative lights units ranging between 40000 to 140000 RLU (Figure 18A), which was higher compared to the DMSO treated cells.

Caspases that initiate apoptosis (caspase-8 and caspase-9) are implicated in the cell's response to specific stimuli that trigger cell death. Caspase-9 activity was also increased in MCF-7 cells treated with the selected active compounds. The title compounds **SVN 1, 2, 4, 9, 10** and **11** induced caspase-9 activation with a relative unit ranging between 30.000 to 90.000 RLU (Figure 18C). Overall, all six compounds, **SVN 1, 2, 4, 9, 10** and **11**, displayed increased caspase-3/7 and caspase-9 activity, implying an increase in activating the intrinsic pathway. At the same time, **SVN 2** also showed an increase in caspase-8 activity with relative units' number of 120.000 RLU, which was significantly higher than in the control cell. All compounds excluding compound **SVN 2** showed low caspase-8 activity (Figure 18B). Thus, **SVN 2** induces apoptosis through Intrinsic and extrinsic apoptotic pathways. Activated caspase-8 and caspase-9 may cause the caspase cascade to be serially initiated and activated, leading to the activation of caspase-3, cleaving cytoskeletal proteins, activating DNAse and causing cell death by apoptosis (Hajiaghaalipour *et al*., 2015).

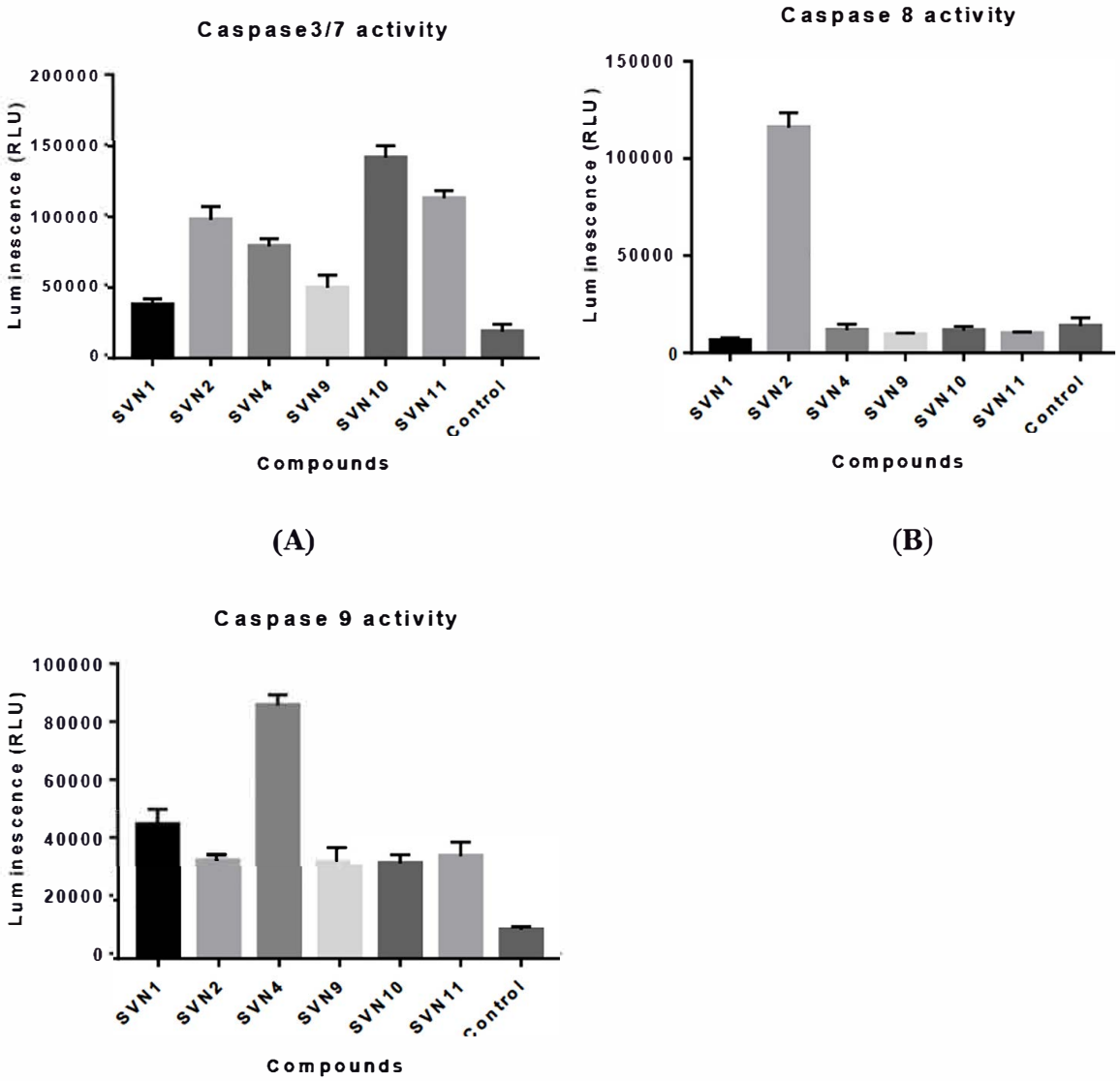

Figure 18: Relative luminescence expression (RUL) of (A) Caspase3/7, (B) Caspase 8 and (C) Caspase 9 in MCF-7 cells treated with SVN 1, SVN 2, SVN 4, SVN 9, SVN 10 and SVN 11.

6.2.4 Conclusions

Novel Schiff bases of 3-(2-aminothiazol-4-yl)-6-nitro-2*H*-chromen-2-one (SVNl-11) have been well synthesized and assessed for their cytotoxicity activity against two different human cancer cell lines (MCF-7 and A549 cells). Compounds **SVN 1, 2, 4, 9, 10** and **11** were the most potent, displaying a wide variety of anti-proliferative activities against MCF-7 cancer cell lines among the tested compounds. Further, the apoptotic assay showed that the **SVN 2** compound could induce caspase activation in extrinsic and intrinsic apoptotic pathways. In contrast, the remaining compounds cause caspase activation through an intrinsic mechanism. The

interpretation of the data indicates that the compounds **SVN 1, 2, 4, 9, 10** and **11** may be regarded as good antitumor agents, which might be considered the starting point for further development to obtain more potent anticancer drugs.

CHAPTER VII. ANTIOXIDANT AND LIPOXYGENASE INHIBITORY ACTIVITIES OF NOVEL SCHIFF BASES OF 3-(2-AMINOTHIAZOL-4-YL)-6, 8-DICHLORO-2*H*-CHROMEN-2-ONE (SVM1-11) AND (*E*) 3-(2-AMINOTHIAZOL-4-YL)-6-NITRO-2*H*-CHROMEN-2-ONE (SVN1-11)

7.1 Antioxidant and lipoxygenase inhibitory activities of novel Schiff bases of 3-(2-aminothiazol-4-yl)-6, 8-dichloro-2*H*-chromen-2-one (SVM 1-11)

Abstract

Coumarin derivatives are a class of biologically active compounds with several applications in pharmacy and medicine. Many studies have shown that coumarin and its derivatives have various biological effects. Several enzymes, including lipoxygenases, have been demonstrated to be inhibited by coumarins. Lipoxygenases are iron-containing enzymes that convert polyunsaturated fatty acids into physiologically active compounds that play a role in immune and inflammatory responses. In this study, a novel series of 3-(2-aminothiazol-4-yl)-6, 8-dichloro-2*H*-chromen-2-one (**SVM 1-11**) were synthesized and evaluated for their antioxidant and lipoxygenases inhibitory capacity as an indication of their potential anti-inflammatory activity. The results showed that compounds **SVM 3** and **8** were the most potent antioxidant, with a radical scavenging capacity of 92.7±1.1 and 89.7±1.7%, comparable to the reference drug Rutin 97.3±1.5%. They were followed by compounds **SVM 2, 4** and **6** with a radical scavenging capacity of 68.1±1.4, 70.1±1.4 and 68.4±0.7%. Regarding the lipoxygenase inhibitory assay, compounds **SVM 3, 8** and **11** were the most active lipoxygenase inhibitors, with a percentage inhibitory capacity of 64.1±0.2, 60.3±0.3 and 67.3±0.2%, respectively. The information presented enables medicinal chemists to design and develop novel molecular analogues antioxidant and lipoxygenase inhibitors and broaden the scope of next-generation effective and safer coumarin-based antioxidant and lipoxygenase inhibitors.

7.1.1 Introduction

Antioxidants are important components of the body's protective system because they regulate the production and removal of reactive oxygen species (ROS) such as hydroxyl radicals, superoxide radicals, singlet oxygen, and hydrogen peroxide radicals, which are produced as a result of oxidative stress and normal metabolic activity (Shaikh *et al*., 2016a). Free radicals are linked to various illnesses and disorders, including carcinogenesis, inflammation, mutagenesis, arthritis, cancer, and genotoxicity. These conditions develop due to oxidative stress caused by an imbalance between free radical formation and quenching. Lipoxygenases (LOXs) are nonsulfur iron dioxygenase that converts arachidonic, linoleic, and other polyunsaturated fatty acids into physiologically active metabolites. They play a role in inflammatory and immunological responses. Mammalian lipoxygenases have recently become a source of worry due to their presence in various biological organs and tissues (Lončarić *et al*., 2020).

Several organic compounds have been identified as LOX inhibitors, including coumarins (Melagraki *et al.*, 2009), thiazolidinediones (Bozdağ-Dündar *et al*., 2009) and quinazolinone-1,2,3-triazoles (Farjadmand *et al.*, 2016). Coumarin continues to be the scaffold of choice despite repeated efforts to find more potent antioxidant agents. It has proven efficacy in free radical quenching and has enormous potential for research as a candidate molecule for therapeutic development against diseases caused by oxidative damage (Nagamallu *et al*., 2016). The importance of thiazole compounds is well known, as thiazole is an essential constituent of many currently available drugs. Despite this, thiazole compounds have various biological characteristics, including antioxidant and anti-inflammatory properties (Sharma *et al*., 2019).

In this respect, molecular hybridization has emerged as one of the best synthetic techniques to synthesize active compounds with different mechanisms of action and structural modification to maximize their binding affinity and efficiency (Lal *et al*., 2018). This study aimed to synthesize and structurally characterize a series of 3-(2-aminothiazol-4-yl)-6, 8-dichloro-2*H*-chromen-2-ones (**SVM 1-11**) and assess the *in-vitro* antioxidant and LOX inhibitor capacity.

7.1.2 Materials and Methods

7.1.2.1 Antioxidant activity of novel Schiff bases of 3-(2-aminothiazol-4-yl)-6,8-dichloro-2*H*-chromen-2-one (SVM 1-11)

The antioxidant activity of the synthesized coumarin compounds will be determined according to the protocol described by Choi *et al*. (2002) using 1,1-diphenyl-2-picrylhydrazyl (DPPH) radical photometric assay. Compounds were prepared in methanol to the final concentration 1000, 500, 250, 100, 80, 40, 40, 20 and 10 µg/mL. The results were compared with rutin (Sigma-Aldrich), a potent antioxidant. For the test, 400 µL of 0.3 mM DPPH in methanol was added to 1 mL of coumarin compounds and incubated in the dark for 30 min. The negative control was 1 mL of methanol and 400 µL of DPPH, and the positive control will be DPPH and 610 µg/mL rutin solution (Choi *et al*., 2002). The absorbance values were measured against the blank using a spectrophotometer at 518 nm. The percentage inhibition of free radical production from DPPH was calculated using the following formula:

$$\text{Scavenging capacity } \% = \frac{(\text{Abs of Sample} - \text{Abs of blank})}{\text{Abs of negative control}} \times 100$$

7.1.2.2 Statistical analysis

Each experiment was performed in triplicate, and the data are presented as means ± standard deviation (SD). The statistical significance of differences between the groups was analyzed using a one-way ANOVA test followed by a post hoc Bonferroni's test. Mean values with probability values of $p<0.05$ were taken as statistically significant.

7.1.2.3 Lipoxygenase inhibitory activity of novel Schiff bases of 3-(2-aminothiazol-4-yl)-6,8-dichloro-2*H*-chromen-2-one (SVM 1-11)

The anti-inflammatory activity was assessed using the lipoxygenase inhibitory screening kit assay (Cayman Chemicals, Ann Arbor, MI, USA) following the manufacturer's protocol. The inhibitory activity of novel Schiff bases of 3-(2-aminothiazol-4-yl)-6,8-dichloro-2*H*-chromen-2-one (**SVM 1-11**) were tested at the concentration of 1000, 500, 250 and 100 µg/mL using the 15-lipoxygenase as a positive control. The analysis included blank wells with assay buffer added, 100% initial activity wells (90 µL lipoxygenase enzyme, 10 µL DMSO) and inhibitor wells (90 µL 15-LO-standard and 10 µL assay buffer). The reaction started with adding 10 µL

of Arachidonic Acid to the wells. The plates were shaken for 5 minutes with a plate shaker. A volume of 100 µL of chromogen was added to each well to inhibit enzyme catalysis and develop the reaction. After shaking for 5 minutes and covering the plate with a cover sheet, the result of the enzymatic reaction was measured spectrophotometrically at 490 nm. The following equation was used to calculate the percentage inhibition:

$$\%\ \text{inhibition} = \frac{\text{Initial activity} - \text{Inhibitor}}{\text{Initial activity}} \text{X } 100$$

7.1.2.4 Statistical analysis

The statistical significance of differences between the groups was analyzed using a one-way ANOVA test followed by a post hoc Bonferroni's test as described in section 7.1.2.2

7.1.3 Results and Discussions

7.1.3.1 Antioxidant activity of SVM 1-11

The antioxidant activity of novel Schiff bases of 3-(2-aminothiazol-4-yl)-6,8-dichloro-2*H*-chromen-2-one (**SVM 1-11**) was carried out using DPPH radical scavenging assay. This method evaluates the capacity of synthesized compounds to donate hydrogen and converts the purple DPPH radical to yellow hydrazine. Rutin, a flavonoid, was used as the positive control in the experiment. The experiment was carried out at nine concentrations in triplicates; the results are expressed as mean ± standard deviation (SD) and are summarized in Table 14. The results reveal that the gradual increase in the activity in all the cases was observed with an increase in compounds concentrations. Compounds **SVM 3** and **8** exhibited the highest radical scavenging capacity of 92.7±1.1% and 89.7±1.7%, respectively, comparable to the positive control Rutin 97.3±1.5% (Table 14). They were followed by compounds **SVM 2, 4** and **6** displaying radical scavenging capacity of 68.1±1.4, 70.1±1.4 and 68.4±0.7%. The remaining compounds, **SVM 1, 5, 7, 9, 10** and **11**, exhibited low to weak radical scavenging capacity ranging from 45-14.7±0.4% at 1 mg/mL. These compounds had lower activity than **SVM 3**, **8** and the standard antioxidant Rutin (Table 14). The ANOVA test was conducted to determine significant differences between the tested compounds and the concentration. Some compounds displayed significantly different radical scavenging capacity values between the compounds as the concentration increases, as shown in Table 14, whereas other compounds did not display a significant difference.

These results are comparable to Thota *et al*. (2015), who synthesized a series of coumarin thiazole derivatives for their antioxidant activity using the DPPH scavenging method. The results showed that the synthesized compounds displayed moderate to high scavenging capacity compared to the standard drug. The most active compounds displayed IC_{50} values of 11.04 ± 0.18, 11.28 ± 0.06, and 12.16 ± 0.28 μg/mL, respectively (Thota *et al*., 2015). In another study, Kurt *et al*. (2015) designed and synthesized a series of urea/thiourea substituted coumarinyl thiazole derivatives as antioxidant agents. The results indicated that these compounds exhibited good radical scavenging capacity with IC_{50} values of 1.64, 1.82, 2.69, 3.31, and 5.49 μM, respectively (Kurt *et al*., 2015).

Table 14: Free-radical scavenging percentage activity of **SVM 1-11**

Compounds code	% Free-radical Scavenging capacity								
	1000	**500**	**250 µg/mL**	**100 µg/mL**	**80 µg/mL**	**60 µg/mL**	**40 µg/mL**	**20 µg/mL**	**10 µg/mL**
SVM1	45.2±0.2^{deH}	32.3±0.1^{cG}	29.2±1.2^{cF}	20.9±0.5^{bE}	16.2±1.1^{bD}	12.6±0.6^{bC}	10.1±0.3^{bB}	8.3±0.5^{cAB}	5.8±0.1^{bA}
SVM 2	68.1±1.4^{fI}	65.4±0.6^{gH}	59.1±1.6^{fG}	53.6±1.7^{eF}	45.2±0.2^{eE}	39.1±1.2^{dD}	23.2±1.1^{dC}	17.6±0.8^{eB}	8.5±0.5^{cA}
SVM 3	92.7±1.1^{gH}	90.9±0.5^{iH}	78.4±1.9^{ghG}	66.2±0.4^{fF}	60.1±0.3^{gE}	56.5±1.6^{efD}	50.1±0.1^{gC}	39.4±0.2^{hB}	15.2±0.5^{eA}
SVM 4	70.1±1.4^{fI}	64.3±0.7^{gH}	61.1±1.8^{fG}	55.6±1.5^{eF}	48.2±0.5^{fE}	40.1±0.2^{dD}	36.2±0.6^{eC}	25.8±0.1^{fB}	10.2±0.1^{dA}
SVM 5	35.3±0.3^{bH}	26.2±0.6^{bG}	16.5±1.1^{abF}	14.6±0.2^{aE}	10.4±0.8^{aD}	6.5±0.5^{aC}	5.6±0.6^{aB}	3.2±0.1^{aA}	2.2±0.2^{aA}
SVM 6	68.4±0.7^{fH}	55.7±0.5^{fG}	52.1±1.5^{eF}	43.8±1.9d^{E}	35.1±0.6^{dD}	26.9±1.2^{cC}	19.6±0.5^{cB}	11.2±0.5^{dA}	8.5±0.1^{cA}
SVM 7	27.1±1.5^{aG}	23.5±0.6^{ab} F	20.1±1.2^{bE}	13.3±1.1^{aD}	9.1±0.1^{aC}	8.9±0.1^{aC}	4.1±0.1^{aB}	3.2±0.2^{aAB}	1.5±0.5^{aA}
SVM 8	89.7±1.7^{gH}	87.1±0.5^{hH}	75.6±0.2^{gG}	64.2±1.3^{fF}	60.4±0.6^{gE}	53.6±1.5^{eD}	42.1±1.1^{fC}	33.1±0.4^{gB}	11.7±0.1^{dA}
SVM 9	41.5±0.1^{cG}	38.5±1.8^{dF}	36.8±1.2^{dF}	30.1±0.5^{cE}	25.7±1.1^{cD}	13.2±0.8^{bC}	6.4±0.2^{aB}	5.4±0.1^{bB}	2.6±0.2^{aA}
SVM 10	24.7±0.4^{aI}	21.8±0.1^{aH}	15.6±0.2^{aG}	11.6±0.1^{aF}	9.8±0.6^{aE}	6.2±0.3^{aD}	4.0±0.1^{aC}	2.8±0.4^{aB}	1.9±0.3^{aA}
SVM 11	45.8±1.2^{eF}	43.4±1.5^{eF}	32.5±0.5^{cE}	21.6±1.6^{bD}	17.1±1.7^{bC}	12.1±0.3^{bB}	9.9±1.1^{bAB}	8.3±0.5^{cA}	6.5±0.6^{bA}
Rutin	97.3±1.5^{hI}	90.1±1.2^{iH}	80.5±0.5^{hG}	73.6±0.9^{gF}	65.2±0.2^{hE}	56.8±1.6^{fD}	51.2±1.5^{gC}	41.5±0.5^{iB}	18.3±1.2^{fA}

Values are represented as mean ±SD, means of treatment without a common letter differ significantly ($p<0.05$).

7.1.3.2 *In-vitro* lipoxygenase inhibitory activity of SVM 1-11

The capacity of the novel Schiff bases of 3-(2-aminothiazol-4-yl)-6,8-dichloro-2*H*-chromen-2-one (**SVM1-11**) to suppress lipoxygenase was determined as a sign of possible anti-inflammatory activity using the UV absorbance-based enzyme assay. All the tested compounds were dose-dependent inhibitors of lipoxygenase activity; the results are summarized in Table 15. The results showed that **SVM 2, 3, 4, 6, 8, 9, 10** and **11** were effective lipoxygenase inhibitors with percentage inhibitions in the range of 50-67%. DMSO was used as a negative control and did not alter enzyme activity. The most active lipoxygenase inhibitor among the tested compounds was **SVM 3, 8** and **11** with a percentage inhibitory of 64.1±0.2, 60.3±0.3, and 67.3±0.2%, respectively, below the positive control 15-LO (98.5±0.7%) at 1 mg/mL (Table 15). Compounds **SVM 2** (57.3±0.3%), **SVM 4** (56.0±0.3%), **SVM 6** (51±0.3%), **SVM 9** (50.9±0.4%) and **SVM 10** (53.3±0.2%) showed moderate lipoxygenase inhibitory capacity. The remaining compounds, including **SVM 1, 5** and **7**, showed weak lipoxygenase inhibitory capacity, lower than 50% (Table 15). The ANOVA test was conducted to determine significant differences between the tested compounds and the concentrations. Some compounds displayed significantly different lipoxygenase inhibitory capacity as the concentration increased, whereas others did not display a considerable difference (Table 15).

These results are comparable to Roussaki *et al*. (2010), who synthesized a series of 3-aryl coumarin analogues and assessed the antioxidant and LOX inhibitory activities. The results revealed that most active compounds showed 86% LOX inhibition (Roussaki et al., 2010). Coumarin derivatives have been reported to display significant lipoxygenase Inhibition efficacy (Hadjipavlou-Litina *et al*., 2007, Srivastava *et al*., 2016). Reactive oxygen species (ROS) have been documented as involved in the cyclooxygenase and lipoxygenase mediated transformation of arachidonic acid into pro-inflammatory intermediates (Melagraki *et al*., 2009). Several forms of coumarin have been documented to possess the unique capacity to scavenge reactive oxygen species and affect free radical-injury processes. Coumarin derivatives were also observed inhibiting lipid peroxidation and having anti-inflammatory activity. In addition, coumarin and related derivatives have been used as regulators of lipoxygenase and cyclooxygenase pathways of arachidonic acid metabolism (Hadjipavlou-Litina et al., 2007, Kontogiorgis *et al*., 2006).

Table 15: Lipoxygenase inhibitory capacity of **SVM 1-11**

Compounds code	% Anti-inflammatory activity			
	1000 µg/mL	**500 µg/mL**	**250 µg/mL**	**100 µg/mL**
SVM1	45.3 ± 0.09^{cz}	13.8 ± 0.15^{by}	9.2 ± 0.1^{bx}	1.4 ± 0.10^{aw}
SVM 2	57.3 ± 0.32^{gz}	26.5 ± 0.25^{ey}	13.8 ± 0.4^{ex}	12.0 ± 0.2^{fw}
SVM 3	64.1 ± 0.2^{iz}	46.9 ± 0.12^{iy}	27.0 ± 0.21^{hx}	23.5 ± 0.15^{hw}
SVM 4	56.0 ± 0.34^{fz}	23.3 ± 0.14^{dy}	12.4 ± 0.16^{dx}	7.8 ± 0.09^{ew}
SVM 5	35.2 ± 0.15^{az}	17.7 ± 0.11^{cy}	11.4 ± 0.17^{cx}	6.5 ± 0.13^{dw}
SVM 6	51.03 ± 0.34^{dz}	25.6 ± 0.2^{ey}	18.0 ± 0.13^{fw}	7.6 ± 0.12^{ew}
SVM 7	38.5 ± 0.10^{bz}	9.8 ± 0.16^{ay}	6.9 ± 0.1^{ax}	5.4 ± 0.11^{cw}
SVM 8	60.3 ± 0.3^{hz}	37.4 ± 0.25^{hy}	25.5 ± 0.2^{gx}	14.3 ± 0.1^{gw}
SVM 9	50.9 ± 0.42^{dz}	33.9 ± 0.12^{gy}	14.4 ± 0.15^{ex}	6.3 ± 0.1^{dw}
SVM 10	53.3 ± 0.26^{ez}	10.2 ± 0.18^{ay}	6.7 ± 0.1^{ax}	3.3 ± 0.1^{bw}
SVM 11	67.3 ± 0.2^{jz}	28.8 ± 0.21^{fy}	6.8 ± 0.2^{ax}	4.1 ± 0.2^{bw}
15-LO	98.5 ± 0.7^{kz}	80.2 ± 0.9^{jy}	65.1 ± 1.2^{xi}	60.5 ± 0.8^{iw}

Values are represented as mean ±SD of three replicate from three independent experiments. Means of treatment inhibition without a common letter differ significantly ($p<0.05$).

7.1.3.4 Structure-activity relationship (SAR)

The following structure-activity relationships (SARs) were suggested for the studied compounds **(SVM 1 - 11**) based on antioxidant and lipoxygenase inhibitory capacity. The title compounds **SVM 3** and **8** having 4-chloro on phenyl ring and dihydroxy at third and fourth positions of the phenyl ring, respectively, emerged as the most effective, displaying high radical scavenging efficacy and lipoxygenase inhibitory capacity. Whereas Compound **SVM 2** has 4-methoxy on the phenyl ring, **SVM 4** has fluorine atom at the fourth position of the phenyl ring, **SVM 6** have pyridyl ring in place of the phenyl ring showed considerable radical scavenging capacity and moderate lipoxygenase inhibitory activity**;** however, these activities were less effective compared to **SVM 3** and **8.** Furthermore, compound **SVM 11** has 2-hydroxy and 3,6-dichloro substitutions on phenyl ring on coumarinyl thiazole nucleus were the most effective lipoxygenase inhibitor. Still, it displayed lower radical scavenging capacity than **SVM 2, 3**, **4**, **6** and **8**. The insertion of various functional groups on phenyl ring at the fourth position of thiazole moiety, which is connected to the primary coumarin nucleus at the third position, appears to be an essential contributor to the radical scavenging capacity lipoxygenase inhibitory activity based on the findings.

7.1.4 Conclusions

To conclude, we have synthesized novel Schiff bases of 3-(2-aminothiazol-4-yl)-6,8-dichloro-2*H*-chromen-2-one (**SVM 1-11**) and evaluated their antioxidant and lipoxygenase inhibitory capacity. The synthesized compounds demonstrated promising antioxidant capacity compared to the standard drug Rutin. The title compounds, **SVM 3** and **8,** were the most promising radical scavenging capacity among all the compounds, followed by **SVM 2**, **4** and **6**. Regarding the lipoxygenase inhibitory activity, **SVM 3, 8** and **11** Showed considerable lipoxygenase inhibitory capacity, among which **SVM 11**, having 2-hydroxy and 3,6-dichloro substitutions on the phenyl ring on the coumarinyl thiazole nucleus, was the most potent lipoxygenase inhibitor. These findings suggest that these active compounds might be considered a starting point for designing and developing new coumarin pharmacophore-based antioxidant and lipoxygenase inhibitory agents.

7.2 Antioxidant and Lipoxygenase inhibitory activity of Novel Schiff bases of 3-(2-aminothiazol-4-yl)-6-nitro-2*H*-chromen-2-ones (SVN1-11)

Abstract

Coumarin and thiazole are two significant pharmacophores with various pharmacological properties and their synthesis is becoming increasingly relevant in medicinal chemistry. The study aimed to develop new Schiff bases of 3-(2-aminothiazol-4-yl)-6-nitro-2H-chromen-2-ones (SVN1-11). The antioxidant capacity of all of these compounds was tested in vitro using the DPPH assay. The radical scavenging capacity data revealed that compounds SVN 5 and SVN 9 are the most effective, with percentage scavenging capacities of .80.5±0.6% and 85.4±1.3%, respectively. Furthermore, compounds **SVN 4, 6, 8, 10** and **11** demonstrated substantial radical scavenging capacities of 71.5±1.5, 74.9±0.7, 76.8±1.3, and 73.8±0.7%, respectively. The lipoxygenase inhibitory kit assay was used to assess the lipoxygenase inhibitory capability of all produced **SVN 1-11**. The results showed that all test compounds studied inhibited lipoxygenase enzyme to varying degrees, with **SVN 11** being the most active (61.3±0.3%). Compounds **SVN 4, 5, 8, 9** and **10** displayed moderate lipoxygenase inhibitory activity capacity of 52.3±0.15, 55.8±0.2, 55.4±0.2, 55.3±0.1 and 53.8±0.15%, respectively. These compounds might be considered lead candidates for designing new coumarin pharmacophore-based antioxidant and lipoxygenase inhibitor drugs.

7.2.1 Introduction

Free radicals of various types are continually produced for metabolic requirements and are quenched by the body's effective antioxidant network. When these species' production surpasses the antioxidant system levels, oxidative damage to tissues and biomolecules occurs, resulting in disease states, particularly degenerative conditions (Patel Rajesh and Patel Natvar, 2011). Many synthetic and natural coumarin derivatives have a unique capacity to scavenge free radicals and affect processes involving free radical damage (Khoobi *et al*., 2011). Lipoxygenases are essential enzymes in lipid metabolism because they convert polyunsaturated fatty acids, such as arachidonic acid and linoleic acid, to their metabolites (Orafaie *et al*., 2018). The use of lipoxygenase inhibitors for medicinal purposes is gaining popularity. 15-LOX inhibitors have been synthesized and classified according to their chemical composition, including heterocyclic, phenolic, allyl and allyloxy benzene derivatives. Coumarin is one of the most well-known heterocyclic structures that have been identified as lipoxygenase inhibitors (Zerangnasrabad *et al*., 2021).

Coumarins are predicted to alter the production and scavenging of reactive oxygen species (ROS) and processes involved in free radical-mediated injury (Fylaktakidou *et al*., 2004). Many synthetic coumarin derivatives have significant pharmacological potential since they are effective inhibitors of many enzymes, including human 5-lipoxygenase, aromatase, horseradish peroxidase, and hAChE/BACE1 (Roussaki *et al*., 2010). Thiazole is a key scaffold for a wide range of synthesized chemicals. Its broad pharmacological potency is shown in several clinically authorized thiazole-containing compounds, with a wide range of biological properties. (Borcea *et al*., 2021). A hybrid pharmacophore is a rational approach to drug development since it combines two bioactive components into a single molecule (Osman *et al*., 2018a). To generate more active molecules reacting on numerous targets, molecular hybridization of thiazole and coumarin pharmacophores was chosen as an approach. This study aimed to synthesize novel Schiff bases of 3-(2-aminothiazol-4-yl)-6-nitro-2*H*-chromen-2-ones (**SVN1-11**) as antioxidant and lipoxygenase inhibitory agents.

7.2.2 Materials and methods

7.2.2.1 Antioxidant activity of novel Schiff bases of 3-(2-aminothiazol-4-yl)-6-nitro-2*H*-chromen-2-ones (SVN 1-11)

The antioxidant activity was determined according to the protocol described in section 7.1.2.1

7.2.2.2 Lipoxygenase inhibitory activity of novel Schiff bases of 3-(2-aminothiazol-4-yl)-6-nitro-2*H*-chromen-2-ones (SVN 1-11)

The lipoxygenase inhibitory capacity was determined according to the protocol described in section 7.1.2.3

7.2.2.3 Statistical analysis

The statistical analysis was conducted as described in section 7.1.2.2

7.2.3 Results and Discussions

7.2.3.1 Antioxidant activity of SVN 1-11

The antioxidant activity of the synthesized coumarin compounds **SVN1-11** was evaluated *in vitro* using the DPPH assay. This method is based on measuring the decrease in absorption of the methanolic solution of DPPH in the presence of antioxidant compounds at 517 nm. To accept an electron or hydrogen-free radical, the DPPH requires an odd electron. Due to hydrogen transfer from antioxidants, this odd electron is combined in the presence of antioxidants, and hence the absorption of DPPH decreases (Thota et al., 2015). The effect on radical scavenging of the various synthetic compounds was compared to Rutin, which was used as a positive control; the results are summarized in Table 16. The DPPH test shows that an increase in compound concentration resulted in increased free radical scavenging capacity. We observed that some synthesized compounds among **SVN 1-11** show high radical scavenging capacity comparable to the control (Rutin). The radical scavenging capacity results indicated that **SVN 5** and **9** were the most potent, with a percentage scavenging capacity of 80.5±0.6% and 85.4±1.3%, respectively, compared to that of standard drug Rutin 97.3±1.5% (Table 16). In addition, compounds **SVN 4, 6, 8, 10** and **11** also showed significant radical scavenging capacity of 71.5±1.5, 74.9±0.7, 76.8±1.3 and 73.8±0.7%, respectively (Table 16); whereas compound **SVN 10** displayed a moderate scavenging capacity of 67.2±1.8%. The remaining compounds, including **SVN 1, 2, 3** and **7**, exhibited low to weak radical scavenging activity, as shown in Table 16.

These results are comparable to Shaikh *et al*. (2016), who synthesized a series of coumarin-based 1, 2, 3 triazoles and evaluated their antioxidant activity. The results showed that compounds having chloro-substituent on phenyl ring demonstrated potent antioxidant capacity with IC_{50} values of 12.48 and 16.30 µg/mL, respectively (Shaikh *et al.*, 2016b). In another study, Kasumbwe *et al*. (2014) synthesized a series of mono/di halogenated coumarins for their antioxidant activity. The results showed that compounds 6-bromo-3-(2-bromoacetyl)-2*H*-chromen-2-one was the most promising, with a percentage scavenging capacity of 86% (Kasumbwe *et al*., 2014). Similarly, Kaushik and Chahal (2021) synthesized a series of coumarin appended 1,4- disubstituted 1,2,3-triazoles for their antioxidant activities. They were found to be potent antioxidants compared with the standard drug (Kaushik and Chahal, 2021).

Table 16: Free-radical scavenging percentage activity of novel Schiff bases of 3-(2-aminothiazol-4-yl)-6-nitro-2*H*-chromen-2-ones (SVN1-11).

Compounds code	% Free-radical Scavenging capacity								
	1000	**500**	**250 µg/mL**	**100 µg/mL**	**80 µg/mL**	**60 µg/mL**	**40 µg/mL**	**20 µg/mL**	**10 µg/mL**
SVN1	33.5 ± 1.5^{bG}	28.6 ± 1.6^{bF}	19.5 ± 1.5^{bE}	13.6 ± 0.3^{aD}	9.1 ± 1.2^{abC}	7.6 ± 0.7^{abBC}	7.3 ± 0.2^{bBC}	4.5 ± 0.1^{abAB}	2.8 ± 0.6^{abA}
SVN 2	43.2 ± 0.5^{cH}	37.1 ± 0.5^{cG}	30.5 ± 0.4^{cF}	23.7 ± 1.2^{bE}	18.0 ± 1.5^{cD}	14.9 ± 0.6^{cC}	10.7 ± 0.1^{cB}	5.0 ± 0.1^{bA}	4.1 ± 0.2^{bA}
SVN 3	22.4 ± 1.4^{aF}	18.6 ± 0.6^{aE}	15.3 ± 0.9^{aD}	10.8 ± 1.1^{aC}	8.9 ± 1.2^{aC}	5.7 ± 0.6^{aB}	4.4 ± 0.2^{aB}	3.3 ± 0.1^{aAB}	1.1 ± 0.1^{aA}
SVN 4	71.5 ± 1.5^{eI}	67.8 ± 1.2^{eH}	60.1 ± 0.5^{eG}	56.9 ± 0.9^{dF}	49.5 ± 0.2^{efE}	32.4 ± 0.2^{eD}	28.3 ± 0.3^{eC}	23.9 ± 0.6^{eB}	13.6 ± 0.2^{deA}
SVN 5	80.5 ± 0.6^{gI}	73.1 ± 0.4^{gH}	70.9 ± 0.6^{gG}	66.3 ± 0.8^{fF}	58.5 ± 0.2^{gE}	50.6 ± 0.1^{gD}	43.1 ± 0.2^{hC}	32.7 ± 0.2^{hB}	16.4 ± 0.4^{fA}
SVN 6	74.9 ± 0.7^{efI}	71.3 ± 0.2^{fgH}	63.1 ± 0.6^{fG}	56.6 ± 0.3^{dF}	50.7 ± 0.6^{fE}	41.2 ± 0.9^{fD}	35.6 ± 0.5^{gC}	26.9 ± 0.5^{gB}	14.5 ± 0.1^{eA}
SVN 7	24.2 ± 1.2^{aE}	30.3 ± 0.5^{bF}	14.9 ± 1.5^{aD}	12.8 ± 0.1^{aCD}	11.5 ± 0.1^{bC}	8.2 ± 0.5^{bB}	5.1 ± 0.1^{abA}	3.1 ± 1.1^{aA}	2.6 ± 1.2^{abA}
SVN 8	76.8 ± 1.3^{fgI}	72.7 ± 1.1^{gH}	69.1 ± 0.5^{gG}	61.8 ± 1.6^{eF}	57.3 ± 0.2^{gE}	49.1 ± 0.2^{gD}	31.1 ± 1.2^{fC}	25.2 ± 0.5^{fB}	12.1 ± 0.2^{dA}
SVN 9	85.4 ± 1.3^{hI}	80.3 ± 1.1^{hH}	70.9 ± 0.6^{gG}	66.1 ± 1.5^{fF}	57.9 ± 0.8^{gE}	48.2 ± 0.3^{gD}	34.3 ± 1.6^{gC}	28.1 ± 0.2^{gB}	15.2 ± 0.5^{efA}
SVN 10	67.2 ± 1.8^{dI}	55.3 ± 1.3^{dH}	48.0 ± 0.6^{dG}	41.9 ± 1.2^{cF}	33.9 ± 0.1^{dE}	25.0 ± 0.5^{dD}	22.1 ± 0.1^{dC}	16.5 ± 0.4^{cB}	10.2 ± 0.1^{cA}
SVN 11	73.8 ± 0.7^{efH}	68.6 ± 0.4^{efG}	61.1 ± 1.2^{eF}	58.5 ± 0.9^{dF}	47.5 ± 1.1^{eE}	40.1 ± 1.5^{fD}	30.4 ± 0.5^{efC}	20.8 ± 0.3^{dB}	11.9 ± 0.3^{cdA}
Rutin	97.3 ± 1.5^{iI}	90.1 ± 1.2^{iH}	80.5 ± 0.5^{hG}	73.6 ± 0.9^{gF}	65.2 ± 0.2^{hE}	56.8 ± 1.6^{hD}	51.2 ± 1.5^{iC}	41.5 ± 0.5^{iB}	28.3 ± 1.2^{gA}

Values are represented as mean ±SD; means of treatment without a common letter differ significantly ($p<0.05$).

7.2.3.2 *In vitro* lipoxygenase inhibitory capacity of SVN 1-11

The synthesized novel Schiff bases of 3-(2-aminothiazol-4-yl)-6-nitro-2*H*-chromen-2-ones (**SVN1-11**) were tested at the concentrations of 1000, 500, 250, 100 µg/mL for lipoxygenase inhibitory capacity using a 15-lipoxygenase enzyme as a positive control, the results are presented in percentage inhibition as shown in Table 17. All the test compounds studied inhibited lipoxygenase enzyme at different degrees, with **SVN 11** showing the highest lipoxygenase inhibitory capacity of 61.3±0.3% at 1 mg/mL. Compounds **SVN 4, 5, 8, 9** and **10** displayed moderate lipoxygenase inhibitory activity of 52.3±0.15, 55.8±0.2, 55.4±0.2, 55.3±0.1 and 53.8±0.15%, respectively (Table 17). On the contrary, compounds **SVN 1, 2, 3, 6, 7** showed lower potency when compared to other compounds ranging from 13 to 47%. There were significant differences in each treated group compared to the standard drug 15- LO (Table 17). These results are comparable to those of Srivastava *et al.* (2016), who synthesized a series of 7 substituted coumarins derivatives for their lipoxygenase inhibitory activity. The *in vitro* study of lipoxygenase enzyme inhibition showed that these compounds were found in all screening methods to be the most active compounds (Srivastava *et al.*, 2016). In another study, Roussaki *et al*. (2010) synthesized and assessed new 3-aryl coumarins for lipoxygenase inhibitory activities. The results indicated that the pyrazole coumarin inhibited lipoxygenase much more than the reference drug Trolox.

The coumarin nucleus has been suggested in various research as a possible candidate for anti-inflammatory drug production (Grover and Jachak, 2015). Several other coumarin-derived compounds have potent anti-inflammatory and antioxidant properties. A significant number of coumarin derivatives have also been developed, tested through various mechanisms, and possessed mild to high anti-inflammatory activity (Bansal *et al*., 2013). Studies also included oxygen-free radicals in inflammation by inhibiting lipoxygenase activity, blocking the cascade phase of arachidonic acid metabolism. It can serve as a scavenger of reactive free radicals formed during arachidonic acid metabolism. The potent inhibitory effects on arachidonic acid metabolism through the lipoxygenase pathway may be an indication of the anti-inflammatory activities of the synthesized compounds (Akula and Odhav, 2013).

Table 17: Lipoxygenase inhibitory rate of novel Schiff bases of 3-(2-aminothiazol-4-yl)-6-nitro-2*H*-chromen-2-ones **SVN 1-11**.

Compounds code	Anti-inflammatory activity (%)			
	1000 µg/mL	500 µg/mL	250 µg/mL	100 µg/mL
SVN1	13.2 ± 0.12^{az}	9.4 ± 0.15^{ay}	3.5 ± 0.16^{ax}	2.3 ± 0.18^{aw}
SVN 2	41.5 ± 0.2^{cz}	35.3 ± 0.17^{fy}	28.3 ± 0.22^{gx}	9.5 ± 0.16^{cw}
SVN 3	17.3 ± 0.18^{bz}	16.8 ± 0.15^{by}	6.8 ± 0.17^{bx}	3.5 ± 0.1^{bw}
SVN 4	52.3 ± 0.15^{fz}	38.2 ± 0.16^{gy}	29.6 ± 0.21^{hx}	17.4 ± 0.1^{e4w}
SVN 5	55.8 ± 0.23^{hz}	49.1 ± 0.21^{jy}	41.9 ± 0.28^{jx}	26.7 ± 0.21^{iw}
SVN 6	44.9 ± 0.2^{dz}	33.8 ± 0.12^{ey}	21.3 ± 0.11^{dx}	19.5 ± 0.15^{fw}
SVN 7	47.2 ± 0.35^{ez}	40.58 ± 0.27^{hy}	14.36 ± 0.15^{cx}	9.24 ± 0.19^{cw}
SVN 8	55.4 ± 0.2^{hz}	45.7 ± 0.25^{iy}	34.4 ± 0.15^{ix}	23.3 ± 0.19^{hw}
SVN 9	55.3 ± 0.1^{hz}	31.09 ± 0.01^{cy}	26.9 ± 0.11^{fx}	13.4 ± 0.2^{dw}
SVN 10	53.8 ± 0.15^{gz}	32.5 ± 0.23^{dy}	24.3 ± 0.13^{ex}	13.6 ± 0.12^{dw}
SVN 11	61.3 ± 0.3^{iz}	38.2 ± 0.11^{gy}	31.26 ± 0.17^{ix}	20.4 ± 0.15^{gw}
15-LO	98.5 ± 0.7^{jzS}	80.2 ± 0.9^{ky}	65.1 ± 1.2^{kx}	60.5 ± 0.8^{jw}

Values are represented as mean ±SD; means of treatment inhibition without a common letter differ significantly ($p\leq0.05$).

7.2.3.3 Structure-activity relationship (SAR)

The structure-activity relationships (SARs) proposed for the antioxidant and lipoxygenase inhibitory capabilities of the investigated compounds **SVN 1-11** based on their structures are as the following: compounds **SVN 5** and **9** have thiophene nucleus in place of phenyl ring on coumarinyl thiazole nucleus and methoxy group at the second position of the phenyl ring, appears to be a key contributing factor to the remarkable radical scavenging efficacy and lipoxygenase inhibitory capacity. Compound **SVN 11** has 2-hydroxy and 3,6-dichloro substitutions on phenyl ring on coumarinyl thiazole nucleus were the most potent lipoxygenase inhibitor, higher than **SVN 5** and **9**. Compounds **SVN 4** has fluorine atom at the fourth position of the phenyl ring, **SVN 6, 8, 10** and **11** have pyridyl ring in place of the phenyl ring, dihydroxy at third and fourth positions of the phenyl ring, 2-hydroxy and 5-nitro on phenyl ring on coumarinyl thiazole nucleus, respectively, exhibited good radical scavenging capacity; however, this activity was lower than **SVN 5** and **9.** Electron-withdrawing, electron-releasing groups varied the larvicidal and adulticidal potency of the tested compounds on the phenyl ring and thiophene itself.

7.2.4 Conclusion

The synthesized compounds **SVN 1-11** were screened for antioxidant and lipoxygenase inhibitory capacity in the present study. The structural components most likely contributing to free radical scavenging capacity and lipoxygenase inhibitory capacity include introducing different functional groups on phenyl ring at the fourth position of thiazole moiety, connected to the primary coumarin nucleus at third position, appeared to be significant contributors. Electron-withdrawing (groups on phenyl ring such as chlorine, fluorine, methoxy, nitro, pyridine) and releasing groups on phenyl ring (such as hydroxy) and thiophene itself varied the antioxidant and lipoxygenase inhibitory capacity. **SVN 4, 5, 6, 8, 9** and **11** displayed high antioxidant activity. However, the flexibility with which the coumarin pattern can be incorporated allows further optimization of radical scavenging activity. The vast antioxidant capacity revealed in most studied coumarins enables us to suggest them as templates in developing molecules that effectively treat human illnesses involving reactive oxygen species (ROS). Compound **SVN 11** had the highest lipoxygenase inhibitory capability, while **SVN 4, 5, 8, 9** and **10** had moderate lipoxygenase inhibitory capacity. Our results suggest that these compounds appear to be suitable candidates for further chemical modification and may be biologically active and useful as ligands in coordination chemistry due to the presence of pharmacologically active moieties like coumarin and thiazole, as well as a potential functional group in their structures.

CHAPTER VIII. General Discussion

Coumarin moiety is widely recognized as a "privileged" structural motif because of its vast range of pharmacological capacity (Brahmachari, 2015). Furthermore, the distinctive structure of coumarin enables its derivatives to easily interact with a wide range of biomacromolecules via weak interactions, indicating a broad potential in medicine. As a result, coumarin-derived compounds have been investigated as potentially viable lead compounds (Reddy *et al.*, 2018).

In this study, two series of novel Schiff bases of 3-(2-aminothiazol-4-yl)-6,8-dichloro-2*H*-chromen-2-one (**SVM1-11**) and 3-(2-aminothiazol-4-yl)-6-nitro-2*H*-chromen-2-one (**SVN 1-11**) were prepared by Knoevenagel condensation of substituted salicylaldehyde and ethyl acetoacetate in the presence of the catalytic amount of piperidine at low temperature to obtain the intermediates 3-acetyl 6-substituted coumarin (SVM i1 and SVN i1) as a starting material. The intermediates 3-acetyl 6-substituted coumarin (SVM i1 and SVN i1) were subjected to bromination in chloroform medium to obtain the intermediates 3-bromoacetyl 6-substituted coumarins (SVM i2 and SVN i2). The resulting 3-bromoacetyl 6-substituted coumarins (SVM i2 and SVN i2) were purified by washing with chloroform. The 3-bromoacetyl 6-substituted coumarins (SVM i2 and SVN i2) were cyclized with thiourea in ethanol medium to yield the parent compounds 3-(2-aminothiazol-4-yl)-6,8-dichloro-2*H*-chromen-2-one (SVM i3) and 3-(2-aminothiazol-4-yl)-6-nitro-2*H*-chromen-2-one (SVN i3). The final Schiff bases (**SVM 1-11** and **SVN 1-11**) were prepared by condensation of parent compounds 3-(2-aminothiazol-4-yl)-6,8-dichloro-2*H*-chromen-2-one (SVM i3) and 3-(2-aminothiazol-4-yl)-6-nitro-2*H*-chromen-2-one (SVNi3) with substituted aromatic aldehydes in the presence of ethanol by the conventional reflux method. The final Schiff bases **SVM 1-11** and **SVN 1-11** were confirmed by FT-IR, NMR, LC-MS, and elemental analysis. The yield of the final compounds **SVM 1-11** and **SVN 1-11** were in the range of 62 to 74%. The synthesized compounds (**SVM 1-11**) and (**SVN11**) were screened for their *in-vitro* anti-tuberculosis activity, larvicidal and adulticidal properties against *A. arabiensis,* anticancer activity, antioxidant activity and lipoxygenase inhibitory efficacy.

The increasing resistance of microorganisms to conventional antibiotics has necessitated developing novel, efficient and cost-effective infectious disease management methods (Khan *et al.*, 2016). Cell wall biosynthesis is a significant target for anti-mycobacterial treatment due to the basic nature of cell wall production and assembly. Therefore, the mycobacterial cell wall has become the most frequently exploited target of anti-TB drugs (Abrahams and Besra, 2018). In

this study, the synthesized compounds **SVM 1-11** and **SVN 1-11** were evaluated for their anti-TB activity against H37Rv MTB and multidrug-resistant MDR-TB strains. These compounds demonstrated various degrees of anti-mycobacterial potency against *M. tuberculosis* H37Rv (ATCC 25177) and well-characterized clinical isolates of MDR TB as shown in Table 4 and Table 5, respectively.

The novel Schiff bases of 3-(2-aminothiazol-4-yl)-6,8-dichloro-2*H*-chromen-2-one (**SVM1-11**) displayed remarkable growth inhibitory activity against H37Rv MTB with a MIC value ranging from 0.5 to 4µg/mL (Table 4). Compounds **SVM 8** and **10** were the most potent, with a MIC value of 0.5 µg/mL against H37Rv MTB; these compounds had a better MIC value than the commonly used antimycobacterial drug Rifampicin and isoniazid. Furthermore, **SVM 3, 4, 7** and **11** exhibited a MIC of 1 µg/mL against H37Rv MTB, same as the standard Rifampicin, but lower than **SVM 8** and **10** (Table 4). These results can be compared to those of Yusufzai *et al.* (2018) who, synthesized coumarin-thiazolidinone hybrids and tested their anti-TB activity against *Mycobacterium tuberculosis* H37Rv. The results revealed that the unsubstituted coumarin conjugated with thiazolidinone displayed higher anti-TB activity with MIC of 83 µg/ml than other conjugates (Yusufzai *et al*., 2018). In another study by Mane *et al.* (2020), a series of polycyclic acridin-(9-yl-amino) thiazol-5-yl)-2*H*-chromen-2-one derivatives were synthesized for their anti-mycobacterial capacity against H37Rv MTB. The results showed that compounds 3-(4-(Fluoroacridin-9-yl-amino) thiazol-5yl)-2H-chromen-2-one and 3-(4-(3-chloroacridin-9-yl-amino) thiazol-5yl)-2*H*-chromen-2-one were the most potent with MICs values of 0.78 and 1.56 µg/mL, respectively (Mane *et al*., 2020).

The synthesized compounds (**SVM 1-11**) proved promising against MDR-TB, resistant to first and second-line TB drugs displaying MICs values ranging from 8 to 64 µg/mL. Compounds **SVM 3, 4, 5, 8** and **10** were the most active against MDR-TB with a MIC value of 8 µg/mL higher than the commonly used antimycobacterial drug (Table 4). Compounds **SVM 2, 6, 9** and **11** had MIC values of 16 µg/mL, whereas **SVM 1** and **7** had MIC values of 64 and 32 µg/mL against MDR-TB, respectively (Table 4). Molecular docking studies of the synthesized compounds **SVM 1-11** showed a high affinity for the active domain of the DprE1 and Pks13 enzymes, providing a solid foundation for future structure-based design efforts (Figure 10 and 11). These results are comparable to the study conducted by Gao *et al*. (2018), who synthesized a series of ethylene tethered Isatin-coumarin hybrids for their antimycobacterial effect against H37Rv- MTB and MDR-MTB. All hybrids showed anti-mycobacterial activity against MTB H37Rv and MDR-TB, with MICs ranging from 32 to 256 µg/mL. In particular, MTB H37Rv and MDR-TB strains were particularly susceptible to the hybrid 3-(ethoxyimino)-5-fluoro-1-(2-

((4-methyl-2-oxo-2*H*-chromen-7-yl)oxy)ethyl)indolin-2-one (MIC: 50 and 32 µg/mL) (Gao *et al*., 2018).

On the other hand, the Schiff bases of 3-(2-aminothiazol-4-yl)-6-nitro-2*H*-chromen-2-one (**SVN1-11**) showed excellent anti-mycobacterial activity against H37Rv strain of MTB with a MIC ranging from 0.25 to 4 µg/mL (Table 5). **SVN 3, 8** and **9** were the most potent among the synthesized compounds, showing MICs values ranging from 0.25-0.5 µg/mL against H37Rv MTB, greater than the commonly used antimycobacterial drug Rifampicin and isoniazid (Table 5). Furthermore, **SVN 4, 7, 10** and **11** displayed significant anti-mycobacterial activity, same as the reference drug rifampicin. Whereas **SVN 1, 2, 5** and **6** displayed anti-mycobacterial activity ranging between 2 to 4 µg/mL (Table 5). These results are comparable to the study of Danne *et al*. (2018), who synthesized and evaluated a series of triazole-biscoumarin conjugates as a possible anti-mycobacterial agent against H37Rv MTB. The results showed that compound 3,3 ((1-(3-bromophenyl)-1*H*-1,2,3-triazol-4-yl)methylene)bis(4-hydroxy-2*H*-chromen-2-one) (**6h**) was the most active against the latent H37Rv MTB, with MIC value of 1.44 µg/mL (Danne *et al.*, 2018). The Schiff bases of (*E*) 3-(2-aminothiazol-4-yl)-6-nitro-2*H*-chromen-2-one (**SVN 1-11**) were also tested against MDR-TB, compounds **SVN 4** was the most potent against MDR-TB, showing a MIC value of 4 µg/mL higher than the reference drug Rifampicin (Table 5). **SVN 3** and **SVN 5** also displayed remarkable anti-mycobacterial efficacy against MDR-TB, with MIC values of 8 µg/mL. However, compounds **SVN 2, 6, 7, 10** and **11** showed a MIC value of 16 µg/mL against MDR-TB (Table 5). **SVN 1** and **SVN 9** were less active than the other compounds, showing a MIC value of 32 µg/mL (Table 5).

A docking study was performed with the target enzymes DprE1 and Pks13; the results indicated that high affinity produced by the synthesized compounds might be attributed to their strong interactions with the active site amino acid residues of the protein. These interactions include hydrogen bonds and van der Waals forces (Figures 10, 11, 12 and 13). In general, some of the amino acid residues produced by the synthesized compounds differ from those of the reference drugs, which might be recognized as critical interactions responsible for their substantial inhibitory activity as revealed *in in-vitro* assays.

These findings showed that coumarin derivatives are effective against multidrug-resistant clinical isolates, making them prospective candidates for treating tuberculosis. The results obtained can be compared to Pires *et al*. (2020) study, which assessed various coumarin derivatives for anti-mycobacterial activity against *M. tuberculosis* H37Rv and MDRTB. The results revealed that compounds 6-((3,3-dimethyloxiran-2-yl)-5,7-dihydroxy-8-(2-

methylbutanolyl)-4-phenyl-2*H*-chromen-2-one (**1g**) 4-hydroxy-7-methoxy-2*H*-chromen-2-one, 7-ethoxy-4-hydroxy-2*H*-chromen-2-one (**5**), 7-ethoxy-4-hydroxy-2h- chromen-2-one (**6**), 4-ethyl-2-hydroxy-4,4a-dihydropyrano (3,2 c)chromen-5(10b*H*)-one (**12**) and 8-ethyl-4-ethyl-2-hydroxy-3,4-dihydropyrano(3,2-c)chromen-5(2*H*)-one (**14**) were the most potent against *M. tuberculosis* H37Rv and multidrug-resistant clinical isolates, with MIC values ranging from 15.6 to 62.5 µg/ml (Pires *et al*., 2020).

The larvicidal and adulticidal properties of the Schiff bases of 3-(2-aminothiazol-4-yl)-6,8-dichloro-2*H*-chromen-2-one **SVM 1-11** were evaluated against *A. arabiensis.* The results showed that introducing different functional groups on phenyl ring at the fourth position of thiazole moiety, connected to the primary coumarin nucleus at the third position, appeared to be significant contributors to the larvicidal and adulticidal activity. Compounds **SVM 6** and **SVM 9** have pyridyl ring in place of the phenyl ring and methoxy group at the second position of the phenyl ring, respectively on coumarinyl thiazole emerged as the most effective larvicidal displaying 100% larvae mortality same as the reference dug Themephos (100%), their adulticidal efficacy was 73 and 77%, respectively, compared the reference drug K-Othrine was 100% (Table 6 and 7). **SVM 2** has 4-methoxy on the phenyl ring, **SVM 3** has 4-chloro on phenyl ring and **SVM 5** has thiophene nucleus in place of phenyl ring on coumarinyl thiazole nucleus exhibited significant larvicidal mortality of 73.8±2.5, 90.3±1.2 and 70.2±1.2%, respectively (Table 6). **SVM 3** and **5** had a lower adulticidal activity with a percentage morality of 63.3±2.2 and 60.5±2.0%, respectively, lower than the reference drug. **SVM 4** and **7** showed larvicidal mortality of 60.5±2.5 and 63.9±3.5%, respectively, but moderate adulticidal potency (Table 6 and 7). **SVM 8** and **10** have dihydroxy at the third and fourth places of the phenyl ring and 2-hydroxy and 5-nitro on the phenyl ring, respectively, both showed higher adulticidal activity (70.5±2.3 and 76.2±2.3%, respectively) (Table 7). Except for **SVM 11**, which exhibited a 67.8±1.7% adulticidal activity, the remaining compounds displayed low larvicidal and adulticidal activity.

On the other hand, significant larvae mortality was seen among the Schiff bases of 3-(2-aminothiazol-4-yl)-6-nitro-2*H*-chromen-2-one **SVN 1-11**, compounds **SVN 6, 7, 8, 9** have pyridyl ring in place of the phenyl ring, hydroxy at the second position of the phenyl ring, dihydroxy at third and fourth positions of the phenyl ring and methoxy group at the second position of the phenyl ring on coumarinyl thiazole nucleus, respectively, were the most effective, showing 100% larvae mortality after 24 hours, similar to the reference drug Temephos (100%) (Table 8). These compounds also demonstrated high adulticidal activity ranging from 71 to 90%, lower than the reference drug K-Othrine (100%) (Table 9). Furthermore, compounds **SVN 5** has

thiophene nucleus in place of phenyl ring on coumarinyl thiazole nucleus exhibited substantial adulticidal activity (86.3±2.1%) higher than **SVN 6**, **7** and **8** (Table 9); however, its larvicidal activity was considered moderate (64.3±1.2%) (Table 8). Additionally, **SVN 10** and 11 have 2-hydroxy and 5-nitro on phenyl ring and 2-hydroxy and 3,6-dichloro substitutions on phenyl ring which is on coumarinyl thiazole nucleus, respectively, displayed the considerable larvicidal activity of 63.6±1.2 and 77.2±1.2%, lower than **SVN 6**, **7**, **8** and **9** (Table 8). The remaining compound substitutions displayed lower larvicidal and adulticidal efficacy (Table 8 and 9). Moreira *et al*. (2017) reported that short exposure to freshly applied coumarin analogues knocked down mosquitoes, but they recovered in the next 24 h. It is apparent from the obtained biological data those structural variations in the substitution pattern linked to the parent scaffold led to a detectable variation in the larvicidal and adulticidal potency. These findings emphasize the importance of these compounds as lead scaffolds in designing and developing new coumarin pharmacophore-based larvicidal and adulticidal agents. These results are comparable to Shao *et al*. (2018), who synthesized a series of coumarin-dibenzothiophene or carbazole derivatives as a larvicidal agent against fourth instars larvae *Aedesaegypti*. The bioassay results suggested that most coumarin-linked derivatives of dibenzothiophene and carbazole had moderate to high activity. The results revealed that two coumarin-linked dibenzothiophene hybrids and six coumarin carbazole hybrids showed toxicity (88.53 to 100.00%) (Shao *et al*., 2018).

The effect of compounds **SVM 1-11** and **SVN 1-11** was assessed *in-vitro* against MCF-7 (breast cancer) and A549 (lung cancer) cancer cell lines using the MTT assay compared to Camptothecin as a reference drug. Compounds with a high percentage of cells growth inhibition were tested for apoptosis using the Promega caspase-Glo^{TM} assay kit (Caspase 3/7, Caspase 8 and Caspase-9). The results summarized in Table 10 revealed that the compounds exhibited antiproliferative and growth-inhibiting properties in cultured human breast cancer MCF-7 cells. The dying cells in the most active compounds exhibit the ultrastructural and biochemical features that characterize apoptosis. The most exciting finding in this study was the pronounced and concentration-dependent reduction in cell growth of MCF-7 and A549 cells by the compounds. The results showed an overall low cytotoxicity effect of these compounds against A549 compared to MCF-7 cancer cells, indicating that these compounds significantly decrease the viability of MCF-7 cells. Compound **SVM 2**, **4, 8** and 11 were the most potent against MCF-7 cells displaying a cytotoxicity activity ranging between 80-86% against MCF-7 (IC_{50} ranging between 5.7-9.2 µg/mL). However, the efficacy of both derivatives was lower than that of the reference drug Camptothecin (Table 10). Compounds **SVM 2, 3, 8**, **9**, **10** and **11** showed

moderate cytotoxicity effect against MCF-7 and A549 cells, ranging between 50 and 58% (Table 10).

On the other hand, Compounds **SVN 1**, **2**, **4**, **9**, **10** and **11** were the most potent against MCF-7 cells showing a percentage inhibition ranging from 73-83% (IC_{50} ranging from 6.2-16.38 µg/mL) comparable to the reference drug Camptothecin (94.65%) (Table 12). **SVN 4** and **10** were the most potent among these compounds, displaying cell growth inhibition of 82.6 and 83.4%, respectively (Table 12). Furthermore, **SVN 2**, **3**, **4, 5**, **8** and **9** exhibited lower activity against A549 and MCF-7 with a percentage inhibition ranging from 53 to 578% (Table 12). These results confirmed the efficacy of the thiazolyl coumarin scaffold in achieving the expected anticancer activity. Structural differences in the substituents linked to the parent scaffold substantially impact the activity.

These results can be compared to Kamath *et al.* (2015), who synthesized and assessed novel indole coumarin hybrids for their anticancer activities against the MCF-7 cancer cell and the Vero (normal) cell line. The results revealed that compounds 2-(6-bromo-2oxo-2*H*-chromen-3-yl)-1*H*-indole-3-carbaldehyde,2-(6-chloro-2oxo-2*H*-chromen-3-yl)-1*H*-indole-3-carboxylic acid and 2-(6-bromo-2-oxo-2*H*-chromen-3-yl)-1*H*-indole-3-carboxylic acid were shown to be the most potent against MCF-7 cells (Kamath *et al*., 2015). In another study, Durgapal and Soman (2019) synthesized a series of coumarin-prolinesulphonamide derivatives and evaluated their anticancer activity against A549 and MCF-7 cancer cells. Among the compounds evaluated, compound *N*-(4-methyl-2-oxo-2*H*-chromen-7-yl)-1-tosylpyrrolidine-2-carboxamide was the most promising against MCF-7 cells, while others displayed moderate activity (Durgapal and Soman, 2019).

It's worth noting that caspase activation is the most well-known sign of apoptosis. The caspase cascade activities accurately mediate apoptosis activation via intrinsic or extrinsic mechanisms. Caspases have a role in cell shrinkage, chromatin condensation, and DNA fragmentation, all of which contribute to the triggering of apoptosis. Caspase 9 is active at the apoptosome during intrinsically induced apoptosis. As a result, detecting active caspase-3 and -9 is crucial for understanding cellular functions and processes (Abd El-Karim *et al.*, 2019). The mechanism involved in the antitumor activity was determined on selected active compounds. The bioluminescent intensities of caspases-3/7, 8 and 9 in MCF-7 cells treated with compounds **SVM 2, 4, 8, 11** and **SVN 1, 2, 4, 9, 10, 11,** respectively, for 24 hours were evaluated. Despite variances in cancer inhibition efficacy, all drugs could trigger apoptosis when the cell growth inhibition method was applied. The results obtained indicated that apoptosis caused by these

compounds is, in part, due to activation of caspses3/7 and caspase 9, which may be the key mechanism of action for apoptosis (Figure 16 and Figure 17). In addition, the apoptosis induced on the MCF-7 cell line by the tested compounds was more prominent than its effect on Caspase-8.

Compared to the control, the **SVM 2, 4, 8, 11** and **SVN 1, 2, 4, 9, 10, 11** treated cells showed a substantial rise in caspases-3/7 and -9 levels (Figure 16 and Figure 17). These compounds cause caspase activation through the mitochondrial-dependent intrinsic pathway. On the other hand, compounds **SVM 2** and **SVN 2** cause caspase activation in MCF-7 on both pathways, intrinsic and extrinsic pathways (Figure 16 and Figure 17).

These results can be compared to the study of Fayed *et al*. (2019), who synthesized a series of coumarin pyridine/fused pyridine hybrids and evaluated their anticancer activity against MCF-7, HCT-116, HepG, and A549 cancer cells. The results showed that compounds 2-amino-4-(4-methoxyphenyl)-6-(2-oxo-2*H*-chromen-3-yl) nicotinamide, 5-(4-methoxyphenyl)-2-methyl-7-(2-oxo-2*H*-chromen-3-yl) pyrido[2,3-d]pyrimidin-4(3*H*)-one and *N*-(3-cyano-4-(4-methoxyphenyl)-6-(2-oxo-2*H*-chromen-3- yl)pyridin-2-yl)acetamide were the most potent with IC_{50} values ranging from 1.1 to 2.4 µM against MCF-7 cells. These compounds caused cell cycle arrest in the G2/M phase, followed by apoptotic cell death. Caspase-3 activity in MCF-7 cells was evaluated, the results showed that these compounds significantly enhanced caspase-3 activity compared to the control group (Fayed *et al*., 2019).

The antioxidant activity of compounds **SVM 1-11** and **SVN 1-11** was performed using DPPH radical scavenging assay. The results indicated that the gradual increase in the activity in all cases was observed with an increase in the concentrations of the compounds. The results revealed that compounds **SVM 3** and **8** were the most effective, with percentage scavenging capacity of 92.7±1.1 and 89.7±1.7%, respectively, comparable to the positive control Rutin (97.31.5%) (Table 14). Furthermore, a remarkable radical scavenging capability was also observed with compounds **SVM 2, 4** and **6** at a percentage of 68.1±1.4, 70.1±1.4 and 68.4±0.7% (Table 14). Unfortunately, **SVM 1, 5**, **7**, **9,** 10 and **11** displayed lower radical scavenging capability (Table 14).

On the other hand, compounds **SVN 5** and **9** were the most potent with a percentage scavenging capacity of 80.5±0.6% and 85.4±1.3%, comparable to that of standard drug Rutin 97.3±1.5% (Table 16). Moreover, significant scavenging capacity in comparison to Rutin (97.31.5%) was also detected in compounds **SVN 4**, **6**, **8** and **11,** demonstrating a percentage scavenging capacity

of 71.5±1.5, 74.9±0.7, 76.8±1.3 and 73.8±0.7%, respectively (Table 16). Additionally, moderate scavenging capacity was shown by compound **SVN 10** (67.2±1.8%); the remaining compounds substitutions displayed weak scavenging capacity, as shown in Table 16.

These results are comparable to Bensalah *et al*. (2020), who synthesized and evaluated thiazolyl coumarin derivatives' antioxidant efficacy. Compounds (E)-3-(2-(benzylideneamino)thiazol-4-yl)-4-hyroxy-2H-chromen-2-one (2a), (E)-4-hydroxy-3-(2-((4-nitrobenzylidene)amino)thiazol-4-yl)-2H-chromen-2-one (2b), (E)-4-hydroxy-3-(2-((3-hydroxybenzylidene)amino)thiazol-4-yl)-2H-chromen-2-one (2c), 4-hydroxy-3-(2-((4-methylbenzylidene)amino)thiazol-4-yl)-2H-chromen-2-one (2e) displayed higher scavenging capacity with IC_{50} values ranging from 15–60 µM (Bensalah *et al*., 2020). In another investigation, Mohmoodi and Ghodsi (2017) synthesized and tested a series of thiazolyl-pyrazole-biscoumarins for their antioxidant activity. The findings revealed that the compound 1-(4-(8-methoxy-2-oxo-2*H*-chromen-3-yl)thiazol-2-yl)-5-(4-methoxyphenyl)-3-(2-oxo-2*H*-chromen-3-yl)-1*H*-pyrazol-1-ium(**4i**) was the most potent with an IC_{50} value of 0.25 mg/mL (Mahmoodi and Ghodsi, 2017).

The capacity of the newly synthesized compounds to suppress lipoxygenase was determined as a sign of possible anti-inflammatory activity using the UV absorbance-based enzyme assay. The results showed that **SVM 2, 3, 4, 6, 8, 9, 10** and 11 displayed moderate to high lipoxygenase inhibitory activity, with percentage inhibitions ranging from 50 to 67% (Table 15). **SVM 3, 8** and **11** were the most active lipoxygenase inhibitors among the investigated compounds, showing a percentage inhibitory value of 64.1±0.2, 60.3±0.3, and 67.3±0.2%, respectively, lower than that of the positive control **15-LO** (98.5±0.7%) (Table 15). **SVM 2**, **4**, **6**, **9** and **10** displayed moderate lipoxygenase inhibitory capacity ranging from 50 to 57%, lower than 15**-LO** and SVM **3, 8** and **11.** The remaining compounds, **SVM 1**, **5** and **7,** showed weak lipoxygenase inhibitory capacity (Table 15).

On the other hand, all examined compounds **SVN 1-11** inhibited the lipoxygenase enzyme to various degrees, with compound **SVN 11** having the most remarkable lipoxygenase inhibitory capacity of 61.3±0.3% (Table 17). Meanwhile, compounds **SVN 4, 5, 8, 9** and **10** exhibited moderate lipoxygenase inhibitory capacity ranging from 52 to 55.8%, lower than **SVN 11** (61.3±0.3%) and the reference drug **15-LO** (98.5±0.7%) (Table 17). The remaining compounds, **SVN 1, 3, 6** and **7,** demonstrated weak lipoxygenase inhibitory capacity than **SVN 11** (Table 17). These results are comparable to Lonari *et al.* (2020) who, synthesized coumarin derivatives and tested their lipoxygenase inhibitory activity against soybean lipoxygenase. These

compounds were shown to have a strong inhibitory effect on soybean lipoxygenase. The most potent compounds were 3-benzoyl-7-(benzyloxy)-2*H*-chromen-2-one (96.6%), followed by methyl 6-bromo-2-oxo-2*H*-chromen-3-carboxylate (85.1%) and 6-bromo-2-oxo-2*H*-chromen-3-carbonitrile (84.8%) (Lončarić *et al*., 2020).

CHAPTER IX. Conclusions and Recommendations

8.1 Conclusion

In summary, novel Schiff bases of 3-(2-aminothiazol-4-yl)-6,8-dichloro-2*H*-chromen-2-one (**SVM1-11**) and 3-(2-aminothiazol-4-yl)-6-nitro-2*H*-chromen-2-one (**SVN1-11**) were designed, synthesized and their structures were characterized by FT-IR, NMR, LC-MS and elemental analysis. The synthesized compounds were screened for their potential anti-tubercular activity against H37Rv and MDR-MTB, anti-mosquito properties against *A. arabiensis*, anticancer activity against MCF-7 and A549 cancer cells using the MTT assay, antioxidant capacity using DPPH assay and Lipoxygenase inhibitory capacity using the lipoxygenase Kit assay.

The anti-mycobacterial activity revealed that **SVM 8** and **10** were the most active against both H37Rv MTB and MDR-MTB strains within the **SVM 1–11** series. Compounds **SVN 3** and **4** from the **SVN 1-11** series were also the most efficient against H37Rv MTB and MDR-MTB. Molecular docking studies revealed that the compounds have strong binding affinities. These compounds might be considered as a novel series with better anti-mycobacterial activity and the potential for new anti-tubercular drugs. The larvicidal studies demonstrated that compounds **SVM 6** and **SVM 9** were the most effective within the **SVM1-11** series. Mosquitoes exposed to compounds **SVN 6, 7, 8,** and **9** exhibited the highest mean larvicidal activity. These compounds have the potential to be developed for malaria prevention and management by inhibiting the vector *A. arabiensis* at the larval stage. The anticancer activity indicates that compounds **SVM 2**, **4**, **8** and **11** were the most effective against MCF-7 cells. Compounds **SVN 1**, **2**, **4**, **9**, **10** and **11**, on the other hand, showed a remarkable cytotoxicity effect on MCF-7. The mechanism involved in the anticancer activity of the selected active compounds against MCF-7 showed that the apoptosis generated by these compounds was triggered in part by the activation of caspase-3/7 and caspase-9, which may be the primary mechanism of apoptosis. Thus, the studied compounds are potential cytotoxic that could be explored in more detail in the future to develop novel compounds against multifactorial drug-resistant cancers.

Thus, this study suggests that the above selected active compounds could be used as a scaffold for structural optimization to develop highly effective and selective anti-mycobacterial, anticancer and larvicidal agents.

8.2 Recommendations

The following recommendations for future work can be made based on the findings of this study:

- Future research can be conducted to investigate alternative structural changes for potential anti-tubercular activity and conduct synergistic experiments with first-line drugs already used in TB therapy and *in vivo* experiments. Future research on these molecules is also required to identify potential candidates for new anti-TB medicine, particularly MDR-MTB.
- Further research needs to see if these compounds may suppress cancer cell lines resistant to treatment. Moreover, safety experiments on normal cells are required to establish the toxicity of these compounds. Fibroblast cell lines (such as NIH-3T3 [normal mouse fibroblast] and MRC-5 [human lung fibroblast]), peripheral blood mononuclear cells and cardiomyocytes can be used. In addition, mouse models for testing these drugs' anticancer efficacy and toxicity in vivo should be determined.

REFERENCES

ABD EL-KARIM, S. S., SYAM, Y. M., EL KERDAWY, A. M. & ABDELGHANY, T. M. 2019. New thiazol-hydrazono-coumarin hybrids targeting human cervical cancer cells: Synthesis, CDK2 inhibition, QSAR and molecular docking studies. *Bioorganic Chemistry,* 86**,** 80-96.

ABRAHAMS, K. A. & BESRA, G. S. 2018. Mycobacterial cell wall biosynthesis: a multifaceted antibiotic target. *Parasitology,* 145**,** 116-133.

AGGARWAL, R., KUMAR, S., KAUSHIK, P., KAUSHIK, D. & GUPTA, G. K. 2013. Synthesis and pharmacological evaluation of some novel 2-(5-hydroxy-5-trifluoromethyl-4, 5-dihydropyrazol-1-yl)-4-(coumarin-3-yl) thiazoles. *European journal of medicinal chemistry,* 62**,** 508-514.

AJANI, O., ADEROHUNMU, D., OWOLABI, F., OLOMIEJA, A. & JOLAYEMI, E. 2018. Microwave assisted synthesis of pyrazoline-based coumarin derivatives: A comparative study. *Journal of Chemical Society of Nigeria,* 43.

AJANI, O. O., AKANDE, M. M., OCTOBER, N., SIYANBOLA, T. O., ADEROHUNMU, D. V., AKINSIKU, A. A. & OLORUNSHOLA, S. J. 2019. Microwave assisted synthesis, characterization and investigation of antibacterial activity of 3-(5-(substituted-phenyl)-4, 5-dihydro-1 H-pyrazol-3-yl)-2 H-chromen-2-one derivatives. *Arab Journal of Basic and Applied Sciences,* 26**,** 362-375.

AKHTAR, J., KHAN, A. A., ALI, Z., HAIDER, R. & YAR, M. S. 2017a. Structure-activity relationship (SAR) study and design strategies of nitrogen-containing heterocyclic moieties for their anticancer activities. *European journal of medicinal chemistry,* 125**,** 143-189.

AKHTAR, W., KHAN, M. F., VERMA, G., SHAQUIQUZZAMAN, M., AKHTER, M., MARELLA, A., PARMAR, S., KHATOON, R. & ALAM, M. M. 2017b. Coumarin-pyrazoline derivatives: Their one-pot microwave assisted synthesis and antimalarial activity. *Journal of Pharmaceutical and Medicinal Chemistry,* 3**,** 5-9.

AKULA, U. S. & ODHAV, B. 2013. In vitro 5-lipoxygenase inhibition of polyphenolic antioxidants from undomesticated plants of South Africa. *Journal of Medicinal Plants Research,* 2**,** 207-212.

AL-MAJEDY, Y., AL-AMIERY, A., KADHUM, A. A. & BAKARMOHAMAD, A. 2017. Antioxidant activity of coumarins. *Systematic Reviews in Pharmacy,* 8**,** 24.

ALIPOUR, M., KHOOBI, M., FOROUMADI, A., NADRI, H., MORADI, A., SAKHTEMAN, A., GHANDI, M. & SHAFIEE, A. 2012. Novel coumarin derivatives bearing N-benzyl pyridinium moiety: potent and dual binding site acetylcholinesterase inhibitors. *Bioorganic & medicinal chemistry,* 20**,** 7214-7222.

ALTHAGAFI, I., EL-METWALY, N. & FARGHALY, T. A. 2019. New series of thiazole derivatives: synthesis, structural elucidation, antimicrobial activity, molecular modeling and MOE docking. *Molecules,* 24**,** 1741.

ALTIERI, D. C. 2010. Survivin and IAP proteins in cell-death mechanisms. *Biochemical Journal,* 430**,** 199-205.

ANGELOVA, V. T., VALCHEVA, V., VASSILEV, N. G., BUYUKLIEV, R., MOMEKOV, G., DIMITROV, I., SASO, L., DJUKIC, M. & SHIVACHEV, B. 2017. Antimycobacterial activity of novel hydrazide-hydrazone derivatives with 2H-chromene and coumarin scaffold. *Bioorganic & medicinal chemistry letters,* 27**,** 223-227.

ANKALI, K. N., RANGASWAMY, J., SHALAVADI, M., NAIK, N. & NAIK KRISHNAMURTHY, G. 2021. Synthesis and Molecular Docking of novel 1, 3-Thiazole Derived 1, 2, 3-Triazoles and In vivo Biological Evaluation for their Anti anxiety and Anti inflammatory Activity. *Journal of Molecular Structure,* 1236**,** 130357.

ANSARY, I., ROY, H., DAS, A., MITRA, D. & BANDYOPADHYAY, A. K. 2019. Regioselective synthesis, molecular descriptors of (1, 5-disubstituted 1, 2, 3-triazolyl) coumarin/quinolone derivatives and their docking studies against cancer targets. *ChemistrySelect,* 4**,** 3486-3494.

ARCHANA, M., YOGESH, T. & KUMARASWAMY, K. 2013. Various methods available for detection of apoptotic cells-A review. *Indian journal of cancer,* 50**,** 274.

ARSHAD, A., OSMAN, H., BAGLEY, M. C., LAM, C. K., MOHAMAD, S. & ZAHARILUDDIN, A. S. M. 2011. Synthesis and antimicrobial properties of some new thiazolyl coumarin derivatives. *European journal of medicinal chemistry,* 46**,** 3788-3794.

AYATI, A., BAKHSHAIESH, T. O., MOGHIMI, S., ESMAEILI, R., MAJIDZADEH-A, K., SAFAVI, M., FIROOZPOUR, L., EMAMI, S. & FOROUMADI, A. 2018. Synthesis and biological evaluation of new coumarins bearing 2, 4-diaminothiazole-5-carbonyl moiety. *European journal of medicinal chemistry,* 155**,** 483-491.

BAIG, S., SEEVASANT, I., MOHAMAD, J., MUKHEEM, A., HURI, H. & KAMARUL, T. 2017. Potential of apoptotic pathway-targeted cancer therapeutic research: Where do we stand? *Cell death & disease,* 7**,** e2058.

BANSAL, Y., SETHI, P. & BANSAL, G. 2013. Coumarin: a potential nucleus for anti-inflammatory molecules. *Medicinal Chemistry Research,* 22**,** 3049-3060.

BAROT, K. P., JAIN, S. V., KREMER, L., SINGH, S. & GHATE, M. D. 2015. Recent advances and therapeutic journey of coumarins: current status and perspectives. *Medicinal Chemistry Research,* 24**,** 2771-2798.

BASANAGOUDA, M., JAMBAGI, V. B., BARIGIDAD, N. N., LAXMESHWAR, S. S. & DEVARU, V. 2014. Synthesis, structure–activity relationship of iodinated-4-

aryloxymethyl-coumarins as potential anti-cancer and anti-mycobacterial agents. *European journal of medicinal chemistry*, 74**,** 225-233.

BASAPPA, V. C., KAMESHWAR, V. H., KUMARA, K., ACHUTHA, D. K., KRISHNAPPAGOWDA, L. N. & KARIYAPPA, A. K. 2020. Design and synthesis of coumarin-triazole hybrids: biocompatible anti-diabetic agents, in silico molecular docking and ADME screening. *Heliyon,* 6**,** e05290.

BASILE, A., SORBO, S., SPADARO, V., BRUNO, M., MAGGIO, A., FARAONE, N. & ROSSELLI, S. 2009. Antimicrobial and antioxidant activities of coumarins from the roots of *Ferulago campestris* (Apiaceae). *Molecules,* 14**,** 939-952.

BENSALAH, D., MNASRI, A., CHAKCHOUK-MTIBAA, A., MANSOUR, L., MELLOULI, L. & HAMDI, N. 2020. Synthesis and antioxidant properties of some new thiazolyl coumarin derivatives. *Green Chemistry Letters and Reviews,* 13**,** 155-163.

BHAGAT, K., BHAGAT, J., GUPTA, M. K., SINGH, J. V., GULATI, H. K., SINGH, A., KAUR, K., KAUR, G., SHARMA, S. & RANA, A. 2019. Design, synthesis, antimicrobial evaluation, and molecular modeling studies of novel indolinedione–coumarin molecular hybrids. *ACS omega,* 4**,** 8720-8730.

BHASKAR, V. & MOHITE, P. 2010. Synthesis, characterization and evaluation of anticancer activity of some tetrazole derivatives. *J. Optoelectron. Biomed. Mater.,* 2**,** 249-259.

BHATT, J. D., CHUDASAMA, C. J. & PATEL, K. D. 2015. Pyrazole clubbed triazolo [1, 5-a] pyrimidine hybrids as an anti-tubercular agents: Synthesis, in vitro screening and molecular docking study. *Bioorganic & medicinal chemistry,* 23**,** 7711-7716.

BORCEA, A.-M., IONUȚ, I., CRIȘAN, O. & ONIGA, O. 2021. An overview of the synthesis and antimicrobial, antiprotozoal, and antitumor activity of thiazole and bisthiazole derivatives. *Molecules,* 26**,** 624.

BOSE, D. S., RUDRADAS, A. & BABU, M. H. 2002. The indium (III) chloride-catalyzed von Pechmann reaction: a simple and effective procedure for the synthesis of 4-substituted coumarins. *Tetrahedron Letters,* 43**,** 9195-9197.

BOZDAĞ-DÜNDAR, O., ÇOBAN, T., CEYLAN-ÜNLÜSOY, M. & ERTAN, R. 2009. Radical scavenging capacities of some thiazolylthiazolidine-2, 4-dione derivatives. *Medicinal chemistry research,* 18**,** 1-7.

BRAHMACHARI, G. 2015. Room temperature one-pot green synthesis of coumarin-3-carboxylic acids in water: a practical method for the large-scale synthesis. *ACS Sustainable Chemistry & Engineering,* 3**,** 2350-2358.

CARTER, B. Z., GRONDA, M., WANG, Z., WELSH, K., PINILLA, C., ANDREEFF, M., SCHOBER, W. D., NEFZI, A., POND, G. R. & MAWJI, I. A. 2005. Small-molecule

XIAP inhibitors derepress downstream effector caspases and induce apoptosis of acute myeloid leukemia cells. *Blood,* 105**,** 4043-4050.

CHAUHAN, N. B., PATEL, N. B., PATEL, V. M. & MISTRY, B. M. 2018. Synthesis and biological evaluation of coumarin clubbed thiazines scaffolds as antimicrobial and antioxidant. *Medicinal Chemistry Research,* 27**,** 2141-2149.

CHOI, C. W., KIM, S. C., HWANG, S. S., CHOI, B. K., AHN, H. J., LEE, M. Y., PARK, S. H. & KIM, S. K. 2002. Antioxidant activity and free radical scavenging capacity between Korean medicinal plants and flavonoids by assay-guided comparison. *Plant science,* 163**,** 1161-1168.

CHOUGALA, B. M., SHASTRI, S. L., HOLIYACHI, M., SHASTRI, L. A., MORE, S. S. & RAMESH, K. 2015. Synthesis, anti-microbial and anti-cancer evaluation study of 3-(3-benzofuranyl)-coumarin derivatives. *Medicinal Chemistry Research,* 24**,** 4128-4138.

CHOUGALA, B. M., SAMUNDEESWARI, S., HOLIYACHI, M., NAIK, N. S., SHASTRI, L. A., DODAMANI, S., JALALPURE, S., DIXIT, S. R., JOSHI, S. D. & SUNAGAR, V. A. 2018. Green, unexpected synthesis of bis-coumarin derivatives as potent anti-bacterial and anti-inflammatory agents. *European journal of medicinal chemistry,* 143**,** 1744-1756.

CHOWDHURY, I., THARAKAN, B. & BHAT, G. K. 2008. Caspases—an update. *Comparative Biochemistry and Physiology Part B: Biochemistry and Molecular Biology,* 151**,** 10-27.

CHUNG, I.-M., SEO, S.-H., KANG, E.-Y., PARK, S.-D., PARK, W.-H. & MOON, H.-I. 2009. Chemical composition and larvicidal effects of essential oil of Dendropanax morbifera against *Aedes aegypti* L. *Biochemical Systematics and Ecology,* 37**,** 470-473.

CONTI, B., CANALE, A., BERTOLI, A., GOZZINI, F. & PISTELLI, L. 2010. Essential oil composition and larvicidal activity of six Mediterranean aromatic plants against the mosquito Aedes albopictus (Diptera: Culicidae). *Parasitology research,* 107**,** 1455-1461.

CORREIA, I., ADAO, P., ROY, S., WAHBA, M., MATOS, C., MAURYA, M. R., MARQUES, F., PAVAN, F. R., LEITE, C. Q. & AVECILLA, F. 2014. Hydroxyquinoline derived vanadium (IV and V) and copper (II) complexes as potential anti-tuberculosis and anti-tumor agents. *Journal of inorganic biochemistry,* 141**,** 83-93.

DA SILVA, C. M., DA SILVA, D. L., MODOLO, L. V., ALVES, R. B., DE RESENDE, M. A., MARTINS, C. V. & DE FÁTIMA, Â. 2011. Schiff bases: A short review of their antimicrobial activities. *Journal of Advanced research,* 2**,** 1-8.

DANNE, A. B., CHOUDHARI, A. S., SARKAR, D., SANGSHETTI, J. N., KHEDKAR, V. M. & SHINGATE, B. B. 2018. Synthesis and biological evaluation of novel triazole-biscoumarin conjugates as potential antitubercular and anti-oxidant agents. *Research on Chemical Intermediates,* 44**,** 6283-6310.

DAWOOD, D. H., BATRAN, R. Z., FARGHALY, T. A., KHEDR, M. A. & ABDULLA, M. M. 2015. New coumarin derivatives as potent selective COX-2 inhibitors: Synthesis, anti-Inflammatory, QSAR, and molecular modeling studies. *Archiv der Pharmazie,* 348**,** 875-888.

DAY, R. O. & GRAHAM, G. G. 2013. Non-steroidal anti-inflammatory drugs (NSAIDs). *British Medical Journal,* 346**,** f3195.

DE SANTANA, T. I., DE OLIVEIRA BARBOSA, M., DE MORAES GOMES, P. A. T., DA CRUZ, A. C. N., DA SILVA, T. G. & LEITE, A. C. L. 2018. Synthesis, anticancer activity and mechanism of action of new thiazole derivatives. *European journal of medicinal chemistry,* 144**,** 874-886.

DE VRIES, E. G., GIETEMA, J. A. & DE JONG, S. 2006. Tumor Necrosis Factor–Related Apoptosis-Inducing Ligand Pathway and Its Therapeutic Implications. *Clinical cancer research,* 12**,** 2390-2393.

DEB, P. K., AHMAD, J., DINA, E., TAN, Y., NASR, E. M. & PICHIKA, M. R. 2014. Molecular docking studies and comparative binding mode analysis of FDA approved HIV protease inhibitors. *Asian J. Chem,* 26**,** 6227-6232.

DEB, P. K., MAILAVARAM, R., CHANDRASEKARAN, B., KAKI, V. R., KAUR, R., KACHLER, S., KLOTZ, K. N. & AKKINEPALLY, R. R. 2018. Synthesis, adenosine receptor binding and molecular modelling studies of novel thieno [2, 3-d] pyrimidine derivatives. *Chemical biology & drug design,* 91**,** 962-969.

DESAI, N., BHATT, N., SOMANI, H. & TRIVEDI, A. 2013. Synthesis, antimicrobial and cytotoxic activities of some novel thiazole clubbed 1, 3, 4-oxadiazoles. *European journal of medicinal chemistry,* 67**,** 54-59.

DHAWAN, S., AWOLADE, P., KISTEN, P., CELE, N., PILLAY, A. S., SAHA, S., KAUR, M., JONNALAGADDA, S. B. & SINGH, P. 2020. Synthesis, cytotoxicity and antimicrobial evaluation of new coumarin-tagged β-lactam triazole hybrid. *Chemistry & Biodiversity,* 17**,** e1900462.

DIGHE, N. S., PATTAN, S. R., DENGALE, S. S., MUSMADE, D. S., SHELAR, M., TAMBE, V. & HOLE, M. B. 2010. Synthetic and pharmacological profiles of coumarins: A review. *Scholard Research Library,* 2**,** 65-71.

DINCEL, E. D., GÜRSOY, E., YILMAZ-OZDEN, T. & ULUSOY-GÜZELDEMIRCI, N. 2020. Antioxidant activity of novel imidazo [2, 1-b] thiazole derivatives: Design, synthesis, biological evaluation, molecular docking study and in silico ADME prediction. *Bioorganic Chemistry,* 103**,** 104220.

DOONAN, F. & COTTER, T.G.2008. Morphological assessment of apoptosis. *Methods*, 44,200-204

DURGAPAL, S. D. & SOMAN, S. S. 2019. Evaluation of novel coumarin-proline sulfonamide hybrids as anticancer and antidiabetic agents. *Synthetic Communications,* 49**,** 2869-2883.

EL-GABY, M. S., ALI, G. A. E.-H., EL-MAGHRABY, A. A., EL-RAHMAN, M. T. A. & HELAL, M. H. 2009. Synthesis, characterization and in vitro antimicrobial activity of novel 2-thioxo-4-thiazolidinones and 4, 4′-bis (2-thioxo-4-thiazolidinone-3-yl) diphenylsulfones. *European journal of medicinal chemistry,* 44**,** 4148-4152.

EL-HAGGAR, R. & AL-WABLI, R. I. 2015. Anti-inflammatory screening and molecular modeling of some novel coumarin derivatives. *Molecules,* 20**,** 5374-5391.

EL-SAWY, E. R., ABDELWAHAB, A. B. & KIRSCH, G. 2021. Synthetic Routes to Coumarin (Benzopyrone)-Fused Five-Membered Aromatic Heterocycles Built on the α-Pyrone Moiety. Part II: Five-Membered Aromatic Rings with Multi Heteroatoms. *Molecules,* 26**,** 3409.

ELMORE, S. 2007. Apoptosis: a review of programmed cell death. *Toxicologic pathology,* 35**,** 495-516.

FAN, Y. L., KE, X. & LIU, M. 2018. Coumarin–triazole hybrids and their biological activities. *Journal of Heterocyclic Chemistry,* 55**,** 791-802.

FARAJ, F. L., ZAHEDIFARD, M., PAYDAR, M., LOOI, C. Y., ABDUL MAJID, N., ALI, H. M., AHMAD, N., GWARAM, N. S. & ABDULLA, M. A. 2014. Synthesis, characterization, and anticancer activity of new quinazoline derivatives against MCF-7 cells. *The Scientific World Journal,* 2014.

FARGHALY, T. A., MASARET, G. S., MUHAMMAD, Z. A. & HARRAS, M. F. 2020. Discovery of thiazole-based-chalcones and 4-hetarylthiazoles as potent anticancer agents: Synthesis, docking study and anticancer activity. *Bioorganic chemistry,* 98**,** 103761.

FARJADMAND, F., ARSHADI, H., MOGHIMI, S., NADRI, H., MORADI, A., EGHTEDARI, M., JAFARPOUR, F., MAHDAVI, M., SHAFIEE, A. & FOROUMADI, A. 2016. Synthesis and evaluation of novel quinazolinone-1, 2, 3-triazoles as inhibitors of lipoxygenase. *Journal of Chemical Research,* 40**,** 188-191.

FAYED, E. A., SABOUR, R., HARRAS, M. F. & MEHANY, A. B. 2019. Design, synthesis, biological evaluation and molecular modeling of new coumarin derivatives as potent anticancer agents. *Medicinal Chemistry Research,* 28**,** 1284-1297.

FENG, D., ZHANG, A., YANG, Y. & YANG, P. 2020. Coumarin-containing hybrids and their antibacterial activities. *Archiv der Pharmazie,* 353**,** 1900380.

FOTOPOULOS, I. & HADJIPAVLOU-LITINA, D. 2020. Hybrids of coumarin derivatives as potent and multifunctional bioactive agents: A review. *Medicinal Chemistry,* 16**,** 272-306.

FRISCH M.J., TRUCKS G.W., SCHLEGEL H.B., SCUSERIA G.E.2009. Gaussian 09, Revision B.1, Gaussian Inc, Wallinford, CT

FULDA, S. Targeting apoptosis for anticancer therapy. Seminars in cancer biology, 2015. Elsevier, 84-88.

FYLAKTAKIDOU, K. C., HADJIPAVLOU-LITINA, D. J., LITINAS, K. E. & NICOLAIDES, D. N. 2004. Natural and synthetic coumarin derivatives with anti-inflammatory/antioxidant activities. *Current pharmaceutical design,* 10**,** 3813-3833.

GALLUZZI, L., KEPP, O. & KROEMER, G. 2012. Mitochondria: master regulators of danger signalling. *Nature reviews Molecular cell biology,* 13**,** 780.

GAO, T., ZENG, Z., WANG, G., SUN, S. & LIU, Y. 2018. Synthesis of Ethylene Tethered Isatin-Coumarin Hybrids and Evaluation of Their in vitro Antimycobacterial Activities. *Journal of Heterocyclic Chemistry,* 55**,** 1484-1488.

GORLE, S., MADDILA, S., N MADDILA, S., NAICKER, K., SINGH, M., SINGH, P. & B JONNALAGADDA, S. 2017. Synthesis, molecular docking study and in vitro anticancer activity of tetrazole linked benzochromene derivatives. *Anti-Cancer Agents in Medicinal Chemistry (Formerly Current Medicinal Chemistry-Anti-Cancer Agents),* 17**,** 464-470.

GOUD, N. S., POOLADANDA, V., MAHAMMAD, G. S., JAKKULA, P., GATREDDI, S., QURESHI, I. A., ALVALA, R., GODUGU, C. & ALVALA, M. 2019. Synthesis and biological evaluation of morpholines linked coumarin–triazole hybrids as anticancer agents. *Chemical biology & drug design,* 94**,** 1919-1929.

GRAZUL, M. & BUDZISZ, E. 2009. Biological activity of metal ions complexes of chromones, coumarins and flavones. *Coordination chemistry reviews,* 253**,** 2588-2598.

GROVER, J. & JACHAK, S. M. 2015. Coumarins as privileged scaffold for anti-inflammatory drug development. *RSC Advances,* 5**,** 38892-38905.

GÜMÜŞ, M., YAKAN, M. & KOCA, İ. 2019. Recent advances of thiazole hybrids in biological applications. *Future medicinal chemistry,* 11**,** 1979-1998.

GUPTA, M. K., KUMAR, S. & CHAUDHARY, S. 2020. Synthesis and Investigation of Antidiabetic Response of New Coumarin Derivatives Against Streptozotocin Induced Diabetes in Experimental Rats. *Pharmaceutical Chemistry Journal***,** 1-6.

HADJIPAVLOU-LITINA, D., KONTOGIORGIS, C., PONTIKI, E., DAKANALI, M., AKOUMIANAKI, A. & KATERINOPOULOS, H. E. 2007. Anti-inflammatory and antioxidant activity of coumarins designed as potential fluorescent zinc sensors. *Journal of enzyme inhibition and medicinal chemistry,* 22**,** 287-292.

HAJIAGHAALIPOUR, F., KANTHIMATHI, M., SANUSI, J. & RAJARAJESWARAN, J. 2015. White tea (Camellia sinensis) inhibits proliferation of the colon cancer cell line,

HT-29, activates caspases and protects DNA of normal cells against oxidative damage. *Food Chemistry,* 169**,** 401-410.

HASSAN, M., WATARI, H., ABUALMAATY, A., OHBA, Y. & SAKURAGI, N. 2014. Apoptosis and molecular targeting therapy in cancer. *BioMed research international,* 2014.

HASSAN, M. Z., ALSAYARI, A., OSMAN, H., ALI, M. A., MUHSINAH, A. & AHSAN, M. J. 2019. Synthesis and evaluation of coumarin hybrids as antimycobacterial agents. *Acta Poloniae Pharmaceutica,* 76**,** 1029-1036.

HE, X., CHEN, Y.-Y., SHI, J.-B., TANG, W.-J., PAN, Z.-X., DONG, Z.-Q., SONG, B.-A., LI, J. & LIU, X.-H. 2014. New coumarin derivatives: Design, synthesis and use as inhibitors of hMAO. *Bioorganic & medicinal chemistry,* 22**,** 3732-3738.

HE, Y., HUANG, J. & CHIGNELL, C. 2006. Cleavage of epidermal growth factor receptor by caspase during apoptosis is independent of its internalization. *Oncogene,* 25**,** 1521-1531.

HOAGLAND, D. T., LIU, J., LEE, R. B. & LEE, R. E. 2016. New agents for the treatment of drug-resistant *Mycobacterium tuberculosis. Advanced drug delivery reviews,* 102**,** 55-72.

HOLLA, B. S., MALINI, K., RAO, B. S., SAROJINI, B. & KUMARI, N. S. 2003. Synthesis of some new 2, 4-disubstituted thiazoles as possible antibacterial and anti-inflammatory agents. *European journal of medicinal chemistry,* 38**,** 313-318.

HU, Y.-Q., XU, Z., ZHANG, S., WU, X., DING, J.-W., LV, Z.-S. & FENG, L.-S. 2017. Recent developments of coumarin-containing derivatives and their anti-tubercular activity. *European journal of medicinal chemistry,* 136**,** 122-130.

HU, X.-L., GAO, C., XU, Z., LIU, M.-L., FENG, L.-S. & ZHANG, G.-D. 2018. Recent development of coumarin derivatives as potential antiplasmodial and antimalarial agents. *Current topics in medicinal chemistry,* 18**,** 114-123.

HU, Y., CHEN, W., SHEN, Y., ZHU, B. & WANG, G.-X. 2019a. Synthesis and antiviral activity of coumarin derivatives against infectious hematopoietic necrosis virus. *Bioorganic & medicinal chemistry letters,* 29**,** 1749-1755.

HU, Y., LIU, L., LI, B., SHEN, Y., WANG, G.-X. & ZHU, B. 2019b. Synthesis of arctigenin derivatives against infectious hematopoietic necrosis virus. *European journal of medicinal chemistry,* 163**,** 183-194.

HUSSEIN, W. & ZITOUNI, T. 2018. Synthesis of new thiazole and thiazolyl derivatives of medicinal significant-a short review. *MOJ Biorg Org Chem,* 2**,** 53-56.

IBRAR, A., TEHSEEN, Y., KHAN, I., HAMEED, A., SAEED, A., FURTMANN, N., BAJORATH, J. & IQBAL, J. 2016. Coumarin-thiazole and-oxadiazole derivatives: synthesis, bioactivity and docking studies for aldose/aldehyde reductase inhibitors. *Bioorganic chemistry,* 68**,** 177-186.

IBRAR, A., SHEHZADI, S. A., SAEED, F. & KHAN, I. 2018. Developing hybrid molecule therapeutics for diverse enzyme inhibitory action: Active role of coumarin-based structural leads in drug discovery. *Bioorganic & medicinal chemistry,* 26**,** 3731-3762.

ISLAM, M. S., WANG, C., ZHENG, J., PAUDYAL, N., ZHU, Y. & SUN, H. 2019. The potential role of tubeimosides in cancer prevention and treatment. *European Journal of Medicinal Chemistry,* 162**,** 109-121.

JAYASHREE, B. S., JERALD, J. & VENUGOPALA, K. N. 2004. Synthesis and characterization of Schiff bases of 2-amino-4-(3-coumarinyl)thiazole as potential NSAIDs. *Oriental Journal of Chemistry,* 20**,** 123-126.

JAYASHREE, B. S., ANURADHA, D. & VENUGOPALA, K. N. 2005a. Synthesis and characterization of Schiff bases of 2'-amino-4'-(6-chloro-3-coumarinyl)thiazole as potential NSAIDs. *Asian Journal of Chemistry,* 17**,** 2093-2097.

JAYASHREE, B. S., SAHU, A. R., MURTHY, M. S. & VENUGOPALA, K. N. 2005b. Synthesis, determination of partition coefficient and antimicrobial activity of triazolo thiadiazinyl bromocoumarin derivatives. *Material Science Research India,* 3**,** 187-190.

JAYASHREE, B., NIGAM, S., PAI, A. & CHOWDARY, P. 2014. Overview on the recently developed coumarinyl heterocycles as useful therapeutic agents. *Arabian Journal of Chemistry,* 7**,** 885-899.

JAYASHREE, B. S., SAHU, A. R., MURTHY, M. S. & VENUGOPALA, K. N. 2006. Synthesis, characterization and determination of partition coefficient of some triazolothiadiazinyl chlorocoumarin derivatives for their antimicrobial activity. *Journal of Saudi Chemical Society,* 10 103-108.

JAYASHREE, B., SAHU, A., MURTHY, M. S. & VENUGOPALA, K. 2007. Synthesis, characterization and determination of partition coefficient of some triazole derivatives of coumarins for their antimicrobial activity. *Asian Journal of Chemistry,* 19**,** 73-78.

JAYASHREE, B. S., ARORA, S. & VENUGOPALA, K. N. 2008. Microwave assisted synthesis of substituted coumarinyl chalcones as reaction intermediates for biologically important coumarinyl heterocycles. *Asian Journal of Chemistry,* 20**,** 1-7.

JIN, X., XU, Y., YANG, X., CHEN, X., WU, M., GUAN, J. & FENG, L. 2017. Design, synthesis and in vitro anti-microbial evaluation of ethylene/propylene-1H-1, 2, 3-triazole-4-methylene-tethered isatin-coumarin hybrids. *Current topics in medicinal chemistry,* 17**,** 3213-3218.

JIN, Y., DING, Y.-H., DONG, J.-J., WEI, Y., HAO, S.-H. & FENG, B.-C. 2020. Design, synthesis and agricultural evaluation of derivatives of N-Acyl-N-(m-fluoro-benzyl)-6-amino-coumarin. *Natural Product Research***,** 1-7.

JOSHI, J. M. 2011. Tuberculosis chemotherapy in the 21st century: Back to the basics. *Lung India: official organ of Indian Chest Society,* 28**,** 193.

KAISER, W. J., UPTON, J. W. & MOCARSKI, E. S. 2013. Viral modulation of programmed necrosis. *Current opinion in virology,* 3**,** 296-306.

KAMAT, V., SANTOSH, R., POOJARY, B., NAYAK, S. P., KUMAR, B. K., SANKARANARAYANAN, M., FAHEEM, KHANAPURE, S., BARRETTO, D. A. & VOOTLA, S. K. 2020. Pyridine-and Thiazole-Based Hydrazides with Promising Anti-inflammatory and Antimicrobial Activities along with Their In Silico Studies. *ACS omega,* 5**,** 25228-25239.

KAMATH, P. R., SUNIL, D., AJEES, A. A., PAI, K. & DAS, S. 2015. Some new indole–coumarin hybrids; Synthesis, anticancer and Bcl-2 docking studies. *Bioorganic chemistry,* 63**,** 101-109.

KANG, L., GAO, X.-H., LIU, H.-R., MEN, X., WU, H.-N., CUI, P.-W., OLDFIELD, E. & YAN, J.-Y. 2018. Structure–activity relationship investigation of coumarin–chalcone hybrids with diverse side-chains as acetylcholinesterase and butyrylcholinesterase inhibitors. *Molecular diversity,* 22**,** 893-906.

KANNATHASAN, K., SENTHILKUMAR, A. & VENKATESALU, V. 2011. Mosquito larvicidal activity of methyl-p-hydroxybenzoate isolated from the leaves of Vitex trifolia Linn. *Acta Tropica,* 120**,** 115-118.

KASHYAP, S. J., GARG, V. K., SHARMA, P. K., KUMAR, N., DUDHE, R. & GUPTA, J. K. 2012. Thiazoles: having diverse biological activities. *Medicinal Chemistry Research,* 21**,** 2123-2132.

KASUMBWE, K., VENUGOPALA, K. N., MOHANLALL, V. & ODHAV, B. 2014. Antimicrobial and antioxidant activities of substituted halogenated coumarins. *Journal of Medicinal Plant Research,* 8**,** 274-281, 8 pp.

KASUMBWE, K., N VENUGOPALA, K., MOHANLALL, V. & ODHAV, B. 2017. Synthetic mono/di-halogenated coumarin derivatives and their anticancer properties. *Anti-Cancer Agents in Medicinal Chemistry (Formerly Current Medicinal Chemistry-Anti-Cancer Agents),* 17**,** 276-285.

KAUSHIK, C. & CHAHAL, M. 2021. Synthesis, antimalarial and antioxidant activity of coumarin appended 1, 4-disubstituted 1, 2, 3-triazoles. *Monatshefte für Chemie-Chemical Monthly***,** 1-12.

KERI, R. S., SASIDHAR, B., NAGARAJA, B. M. & SANTOS, M. A. 2015. Recent progress in the drug development of coumarin derivatives as potent antituberculosis agents. *European journal of medicinal chemistry,* 100**,** 257-269.

KERRU, N., SINGH, P., KOORBANALLY, N., RAJ, R. & KUMAR, V. 2017. Recent advances (2015–2016) in anticancer hybrids. *European journal of medicinal chemistry,* 142**,** 179-212.

KHALIGH, N. G. 2012. Synthesis of coumarins via Pechmann reaction catalyzed by 3-methyl-1-sulfonic acid imidazolium hydrogen sulfate as an efficient, halogen-free and reusable acidic ionic liquid. *Catalysis Science & Technology,* 2**,** 1633-1636.

KHAN, S. T., MUSARRAT, J. & AL-KHEDHAIRY, A. A. 2016. Countering drug resistance, infectious diseases, and sepsis using metal and metal oxides nanoparticles: current status. *Colloids and Surfaces B: Biointerfaces,* 146**,** 70-83.

KHANYUSUFZAI, S., OSMAN, H., KHAN, M. S., MOHAMAD, S., SULAIMAN, O., PARUMASIVAM, T., GANSAU, J. A. & JOHANSAH, N. 2017. Design, characterization, in vitro antibacterial, antitubercular evaluation and structure–activity relationships of new hydrazinyl thiazolyl coumarin derivatives. *Medicinal Chemistry Research,* 26**,** 1139-1148.

KHARA, J. S., WANG, Y., KE, X.-Y., LIU, S., NEWTON, S. M., LANGFORD, P. R., YANG, Y. Y. & EE, P. L. R. 2014. Anti-mycobacterial activities of synthetic cationic α-helical peptides and their synergism with rifampicin. *Biomaterials,* 35**,** 2032-2038.

KHODE, S., MADDI, V., ARAGADE, P., PALKAR, M., RONAD, P. K., MAMLEDESAI, S., THIPPESWAMY, A. & SATYANARAYANA, D. 2009. Synthesis and pharmacological evaluation of a novel series of 5-(substituted) aryl-3-(3-coumarinyl)-1-phenyl-2-pyrazolines as novel anti-inflammatory and analgesic agents. *European journal of medicinal chemistry,* 44**,** 1682-1688.

KHOOBI, M., EMAMI, S., DEHGHAN, G., FOROUMADI, A., RAMAZANI, A. & SHAFIEE, A. 2011. Synthesis and free radical scavenging activity of coumarin derivatives containing a 2-methylbenzothiazoline motif. *Archiv der Pharmazie,* 344**,** 588-594.

KLEIN, E., SMITH, D. L. & LAXMINARAYAN, R. 2007. Hospitalizations and deaths caused by methicillin-resistant *Staphylococcus aureus*, United States, 1999–2005. *Emerging infectious diseases,* 13**,** 1840.

KLENKAR, J. & MOLNAR, M. 2015. Natural and synthetic coumarins as potential anticancer agents. *J Chem Pharm Res,* 7**,** 1223-38.

KONIDALA, S. K., KOTRA, V., DANDUGA, R. C. S. R., KOLA, P. K., BHANDARE, R. R. & SHAIK, A. B. 2021. Design, multistep synthesis and in-vitro antimicrobial and antioxidant screening of coumarin clubbed chalcone hybrids through molecular hybridization approach. *Arabian Journal of Chemistry,* 14**,** 103154.

KONTOGIORGIS, C. A., SAVVOGLOU, K. & HADJIPAVLOU-LITINA, D. J. 2006. Antiinflammatory and antioxidant evaluation of novel coumarin derivatives. *Journal of enzyme inhibition and medicinal chemistry,* 21**,** 21-29.

KOPPULA, P. & PUROHIT, N. 2013. Synthesis of new biologically active triazolo, tetrazolo and coumarinoyl derivatives of isocoumarins. *Organic Communications,* 6**,** 148.

KOSTOVA, I. 2005. Synthetic and natural coumarins as cytotoxic agents. *Current Medicinal Chemistry-Anti-Cancer Agents,* 5**,** 29-46.

KRALJEVIĆ, T. G., HAREJ, A., SEDIĆ, M., PAVELIĆ, S. K., STEPANIĆ, V., DRENJANČEVIĆ, D., TALAPKO, J. & RAIĆ-MALIĆ, S. 2016. Synthesis, in vitro anticancer and antibacterial activities and in silico studies of new 4-substituted 1, 2, 3-triazole–coumarin hybrids. *European journal of medicinal chemistry,* 124**,** 794-808.

KROEMER, G., EL-DEIRY, W., GOLSTEIN, P., PETER, M., VAUX, D., VANDENABEELE, P., ZHIVOTOVSKY, B., BLAGOSKLONNY, M., MALORNI, W. & KNIGHT, R. 2005. Classification of cell death: recommendations of the Nomenclature Committee on Cell Death. *Cell death and differentiation,* 12**,** 1463-1467.

KRYSKO, D. V., BERGHE, T. V., D'HERDE, K. & VANDENABEELE, P. 2008. Apoptosis and necrosis: detection, discrimination and phagocytosis. *Methods,* 44**,** 205-221.

KULABAŞ, N., TATAR, E., ÖZAKPıNAR, Ö. B., ÖZSAVCı, D., PANNECOUQUE, C., DE CLERCQ, E. & KÜÇÜKGÜZEL, İ. 2016. Synthesis and antiproliferative evaluation of novel 2-(4H-1, 2, 4-triazole-3-ylthio) acetamide derivatives as inducers of apoptosis in cancer cells. *European Journal of Medicinal Chemistry,* 121**,** 58-70.

KULKARNI, R. C., MADAR, J. M., SHASTRI, S. L., SHAIKH, F., NAIK, N. S., CHOUGALE, R. B., SHASTRI, L. A., JOSHI, S. D., DIXIT, S. R. & SUNAGAR, V. A. 2018. Green synthesis of coumarin-pyrazolone hybrids: In vitro anticancer and anti-inflammatory activities and their computational study on COX-2 enzyme. *Chemical Data Collections,* 17**,** 497-506.

KUMAR, G., SIVA KRISHNA, V., SRIRAM, D. & JACHAK, S. M. 2020a. Pyrazole–coumarin and pyrazole–quinoline chalcones as potential antitubercular agents. *Archiv der Pharmazie***,** e2000077.

KUMAR, G., SIVA KRISHNA, V., SRIRAM, D. & JACHAK, S. M. 2020b. Pyrazole–coumarin and pyrazole–quinoline chalcones as potential antitubercular agents. *Archiv der Pharmazie,* 353**,** 2000077.

KUMAR, S. 1999. Regulation of caspase activation in apoptosis: implications in pathogenesis and treatment of disease. *Clinical and experimental pharmacology and physiology,* 26**,** 295-303.

KUMAWAT, M. K. 2018. Thiazole containing heterocycles with antimalarial activity. *Current drug discovery technologies,* 15**,** 196-200.

KÜPELI AKKOL, E., GENÇ, Y., KARPUZ, B., SOBARZO-SÁNCHEZ, E. & CAPASSO, R. 2020. Coumarins and coumarin-related compounds in pharmacotherapy of cancer. *Cancers,* 12**,** 1959.

KURT, B. Z., GAZIOGLU, I., SONMEZ, F. & KUCUKISLAMOGLU, M. 2015. Synthesis, antioxidant and anticholinesterase activities of novel coumarylthiazole derivatives. *Bioorganic chemistry,* 59**,** 80-90.

KURT, B. Z., KANDAS, N. O., DAG, A., SONMEZ, F. & KUCUKISLAMOGLU, M. 2020. Synthesis and biological evaluation of novel coumarin-chalcone derivatives containing urea moiety as potential anticancer agents. *Arabian Journal of Chemistry,* 13**,** 1120-1129.

LAL, K., YADAV, P., KUMAR, A., KUMAR, A. & PAUL, A. K. 2018. Design, synthesis, characterization, antimicrobial evaluation and molecular modeling studies of some dehydroacetic acid-chalcone-1, 2, 3-triazole hybrids. *Bioorganic chemistry,* 77**,** 236-244.

LAXMI, S. V., KUARM, B. S. & RAJITHA, B. 2013. Synthesis and antimicrobial activity of coumarin pyrazole pyrimidine 2, 4, 6 (1H, 3H, 5H) triones and thioxopyrimidine4, 6 (1H, 5H) diones. *Medicinal Chemistry Research,* 22**,** 768-774.

LEE, E.-W., SEO, J.-H., JEONG, M.-H., LEE, S.-S. & SONG, J.-W. 2012. The roles of FADD in extrinsic apoptosis and necroptosis. *BMB reports,* 45**,** 496-508.

LIU, B., HU, G., TANG, X., WANG, G. & XU, Z. 2018. 1H-1, 2, 3-Triazole-tethered Isatin–coumarin Hybrids: Design, Synthesis and In Vitro Anti-mycobacterial Evaluation. *Journal of Heterocyclic Chemistry,* 55**,** 775-780.

LIU, H., XIA, D.-G., CHU, Z.-W., HU, R., CHENG, X. & LV, X.-H. 2020. Novel Coumarin-Thiazolyl Ester derivatives as potential DNA Gyrase Inhibitors: Design, synthesis, and antibacterial activity. *Bioorganic Chemistry***,** 103907.

LIU, M., LIU, Y., HUA, X., WU, C., ZHOU, S., WANG, B. & LI, Z. 2015. Synthesis of osthole derivatives with grignard reagents and their larvicidal activities on mosquitoes. *Chinese Journal of Chemistry,* 33**,** 1353-1358.

LONČARIĆ, M., STRELEC, I., PAVIĆ, V., ŠUBARIĆ, D., RASTIJA, V. & MOLNAR, M. 2020. Lipoxygenase Inhibition Activity of Coumarin Derivatives—QSAR and Molecular Docking Study. *Pharmaceuticals,* 13**,** 154.

MADAR, J. M., SHASTRI, L. A., SHASTRI, S. L., HOLIYACHI, M., NAIK, N., KULKARNI, R., SHAIKH, F. & SUNGAR, V. 2018. Design, synthesis, characterization, and biological evaluation of pyrido [1, 2-a] pyrimidinone coumarins as promising anti-inflammatory agents. *Synthetic Communications,* 48**,** 375-386.

MAHESH, M., BHEEMARAJU, G., MANJUNATH, G. & VENKATA RAMANA, P. 2016. Synthesis and Characterization of Novel Oxadiazole and Pyrazole Hybrids as Potential Antimicrobial Agents. *Chem Sci Trans,* 5**,** 207-217.

MAHESWARA, M., SIDDAIAH, V., DAMU, G. L. V., RAO, Y. K. & RAO, C. V. 2006. A solvent-free synthesis of coumarins via Pechmann condensation using heterogeneous catalyst. *Journal of Molecular Catalysis A: Chemical,* 255**,** 49-52.

MAHMOODI, N. O. & GHODSI, S. 2017. Thiazolyl-pyrazole-biscoumarin synthesis and evaluation of their antibacterial and antioxidant activities. *Research on Chemical Intermediates,* 43**,** 661-678.

MAKAM, P., KANKANALA, R., PRAKASH, A. & KANNAN, T. 2013. 2-(2-Hydrazinyl) thiazole derivatives: Design, synthesis and in vitro antimycobacterial studies. *European journal of medicinal chemistry,* 69**,** 564-576.

MANDLIK, V., PATIL, S., BOPANNA, R., BASU, S. & SINGH, S. 2016. Biological activity of coumarin derivatives as anti-leishmanial agents. *PLoS One,* 11**,** e0164585.

MANE, S. G., KATAGI, K. S., KADAM, N. S., AKKI, M. C. & JOSHI, S. D. 2020. Design and Synthesis of Polycyclic Acridin-(9-yl-Amino) Thiazol-5-yl)-2H-Chromen-2-One Derivatives: As Antiproliferative and Anti-TB Pharmacophores. *Polycyclic Aromatic Compounds***,** 1-20.

MANGASULI, S. N., HOSAMANI, K. M., DEVARAJEGOWDA, H. C., KURJOGI, M. M. & JOSHI, S. D. 2018a. Synthesis of coumarin-theophylline hybrids as a new class of anti-tubercular and anti-microbial agents. *European journal of medicinal chemistry,* 146**,** 747-756.

MANGASULI, S. N., HOSAMANI, K. M., SATAPUTE, P. & JOSHI, S. D. 2018b. Synthesis, molecular docking studies and biological evaluation of potent coumarin–carbonodithioate hybrids via microwave irradiation. *Chemical Data Collections,* 15**,** 115-125.

MANVAR, A., MALDE, A., VERMA, J., VIRSODIA, V., MISHRA, A., UPADHYAY, K., ACHARYA, H., COUTINHO, E. & SHAH, A. 2008. Synthesis, anti-tubercular activity and 3D-QSAR study of coumarin-4-acetic acid benzylidene hydrazides. *European journal of medicinal chemistry,* 43**,** 2395-2403.

MATHEW, S. J., HAUBERT, D., KRÖNKE, M. & LEPTIN, M. 2009. Looking beyond death: a morphogenetic role for the TNF signalling pathway. *J Cell Sci,* 122**,** 1939-1946.

MATOS, M. J., MURA, F., VAZQUEZ-RODRIGUEZ, S., BORGES, F., SANTANA, L., URIARTE, E. & OLEA-AZAR, C. 2015. Study of coumarin-resveratrol hybrids as potent antioxidant compounds. *Molecules,* 20**,** 3290-3308.

MELAGRAKI, G., AFANTITIS, A., IGGLESSI-MARKOPOULOU, O., DETSI, A., KOUFAKI, M., KONTOGIORGIS, C. & HADJIPAVLOU-LITINA, D. J. 2009. Synthesis and evaluation of the antioxidant and anti-inflammatory activity of novel coumarin-3-aminoamides and their alpha-lipoic acid adducts. *European journal of medicinal chemistry,* 44**,** 3020-3026.

MENG, X.-Y., ZHANG, H.-X., MEZEI, M. & CUI, M. 2011. Molecular docking: a powerful approach for structure-based drug discovery. *Current computer-aided drug design,* 7**,** 146-157.

MISHRA, R., SHARMA, P. K., VERMA, P. K., TOMER, I., MATHUR, G. & DHAKAD, P. K. 2017. Biological potential of thiazole derivatives of synthetic origin. *Journal of Heterocyclic Chemistry,* 54**,** 2103-2116.

MISHRA, S., PANDEY, A. & MANVATI, S. 2020. Coumarin: An emerging antiviral agent. *Heliyon,* 6**,** e03217.

MISHRA, S. & SINGH, P. 2016. Hybrid molecules: The privileged scaffolds for various pharmaceuticals. *European journal of medicinal chemistry,* 124**,** 500-536.

MOREIRA, M. D., PICANÇO, M. C., BARBOSA, L. C. D. A., GUEDES, R. N. C., CAMPOS, M. R. D., SILVA, G. A. & MARTINS, J. C. 2007. Plant compounds insecticide activity against Coleoptera pests of stored products. *Pesquisa Agropecuária Brasileira*, 42**,** 909-915.

MORSY, S. A., FARAHAT, A. A., NASR, M. N. & TANTAWY, A. S. 2017. Synthesis, molecular modeling and anticancer activity of new coumarin containing compounds. *Saudi Pharmaceutical Journal*.

MUTHUKRISHNAN, M., MUJAHID, M., YOGEESWARI, P. & SRIRAM, D. 2011. Syntheses and biological evaluation of new triazole-spirochromone conjugates as inhibitors of Mycobacterium tuberculosis. *Tetrahedron Letters,* 52**,** 2387-2389.

NAGAMALLU, R., SRINIVASAN, B., NINGAPPA, M. B. & KARIYAPPA, A. K. 2016. Synthesis of novel coumarin appended bis (formylpyrazole) derivatives: Studies on their antimicrobial and antioxidant activities. *Bioorganic & medicinal chemistry letters,* 26**,** 690-694.

NARAYANASWAMY, V. K., GLEISER, R. M., KASUMBWE, K., ALDHUBIAB, B. E., ATTIMARAD, M. V. & ODHAV, B. 2014. Evaluation of halogenated coumarins for antimosquito properties. *The Scientific World Journal,* 2014.

NAYYAR, A. & JAIN, R. 2005. Recent advances in new structural classes of anti-tuberculosis agents. *Current medicinal chemistry,* 12**,** 1873-1886.

NEPALI, K., SHARMA, S., SHARMA, M., BEDI, P. & DHAR, K. 2014. Rational approaches, design strategies, structure activity relationship and mechanistic insights for anticancer hybrids. *European journal of medicinal chemistry*, 77**,** 422-487.

NICHOLSON, R. A. & ZHANG, A. 1995. Surangin B: insecticidal properties and mechanism underlying its transmitter-releasing action in nerve-terminal fractions isolated from mammalian brain. *Pesticide Biochemistry and Physiology,* 53**,** 152-163.

NOJI, E. K. 2001. The global resurgence of infectious diseases. *Journal of Contingencies and crisis Management,* 9**,** 223-232.

NGAN C-H, HALL DR, ZERBE B, GROVE LE, KOZAKOV D AND VAJDA S. 2011. New thiazol-hydrazono-coumarin hybrids targeting human cervical cancer cells: Synthesis, CDK2 inhibition, QSAR and molecular docking studies. *Bioorganic Chemistry,* 86**,** 80-96. FTSite: high accuracy detection of ligand binding sites on unbound protein structures. *Bioinformatics,* **28**, 286-287.

OKUMA, K., IWAKAWA, K., TURNIDGE, J. D., GRUBB, W. B., BELL, J. M., O'BRIEN, F. G., COOMBS, G. W., PEARMAN, J. W., TENOVER, F. C. & KAPI, M. 2002. Dissemination of new methicillin-resistant Staphylococcus aureus clones in the community. *Journal of Clinical Microbiology,* 40**,** 4289-4294.

OLAYA, M. D. P., VERGEL, N. E., LÓPEZ, J. L., VIÑA, D. & GUERRERO, M. F. 2020. 8-Propyl-6H-[1, 3] dioxolo [4, 5-g] chromen-6-one: A new coumarin with monoamine oxidase B inhibitory activity and possible anti-parkinsonian effects. *Brazilian Journal of Pharmaceutical Sciences,* 56.

ORAFAIE, A., MATIN, M. M. & SADEGHIAN, H. 2018. The importance of 15-lipoxygenase inhibitors in cancer treatment. *Cancer and Metastasis Reviews,* 37**,** 397-408.

OSMAN, H., YUSUFZAI, S. K., KHAN, M. S., ABD RAZIK, B. M., SULAIMAN, O., MOHAMAD, S., GANSAU, J. A., EZZAT, M. O., PARUMASIVAM, T. & HASSAN, M. Z. 2018. New thiazolyl-coumarin hybrids: Design, synthesis, characterization, X-ray crystal structure, antibacterial and antiviral evaluation. *Journal of Molecular Structure,* 1166**,** 147-154.

OSTROWSKA, K. 2020. Coumarin-piperazine derivatives as biologically active compounds. *Saudi Pharmaceutical Journal,* 28**,** 220-232.

OUYANG, L., SHI, Z., ZHAO, S., WANG, F. T., ZHOU, T. T., LIU, B. & BAO, J. K. 2012. Programmed cell death pathways in cancer: a review of apoptosis, autophagy and programmed necrosis. *Cell proliferation,* 45**,** 487-498.

PARIKH, P. H., TIMANIYA, J. B., PATEL, M. J. & PATEL, K. P. 2022. Microwave-assisted synthesis of pyrano [2, 3-c]-pyrazole derivatives and their anti-microbial, anti-malarial, anti-tubercular, and anti-cancer activities. *Journal of Molecular Structure,* 1249**,** 131605.

PATEL, K., KARTHIKEYAN, C., RAJA SOLOMON, V., S HARI NARAYANA MOORTHY, N., LEE, H., SAHU, K., SINGH DEORA, G. & TRIVEDI, P. 2011. Synthesis of some coumarinyl chalcones and their antiproliferative activity against breast cancer cell lines. *Letters in Drug Design & Discovery,* 8**,** 308-311.

PATEL R. M. & PATEL N.J. 2011. In vitro antioxidant activity of coumarin compounds by DPPH, Super oxide and nitric oxide free radical scavenging methods. *Journal of advanced pharmacy education & research,* 1**,** 52-68.

PATEL, V. R., PATEL, K. J., KUMARI, P. & CHIKHALIA, H. K. 2012. Synthesis of Novel Quinolone and Coumarin Based 1, 3, 4-Thiadiazolyl and 1, 3, 4-Oxadiazolyl N-Mannich Bases as Potential Antimicrobials. *Letters in Organic Chemistry,* 9**,** 478-486.

PATEL, R. V., KUMARI, P., RAJANI, D. P. & CHIKHALIA, K. H. 2013. Synthesis of coumarin-based 1, 3, 4-oxadiazol-2ylthio-N-phenyl/benzothiazolyl acetamides as antimicrobial and antituberculosis agents. *Medicinal Chemistry Research,* 22**,** 195-210.

PENG, X.-M., LV DAMU, G. & ZHOU, H. 2013. Current developments of coumarin compounds in medicinal chemistry. *Current pharmaceutical design,* 19**,** 3884-3930.

PENNARUN, B., MEIJER, A., DE VRIES, E. G., KLEIBEUKER, J. H., KRUYT, F. & DE JONG, S. 2010. Playing the DISC: turning on TRAIL death receptor-mediated apoptosis in cancer. *Biochimica et Biophysica Acta (BBA)-Reviews on Cancer,* 1805**,** 123-140.

PENTA, S. 2015. *Advances in Structure and Activity Relationship of Coumarin Derivatives*, Academic Press.

PINGAEW, R., SAEKEE, A., MANDI, P., NANTASENAMAT, C., PRACHAYASITTIKUL, S., RUCHIRAWAT, S. & PRACHAYASITTIKUL, V. 2014. Synthesis, biological evaluation and molecular docking of novel chalcone–coumarin hybrids as anticancer and antimalarial agents. *European Journal of Medicinal Chemistry,* 85**,** 65-76.

PIRES, C. T., SCODRO, R. B., CORTEZ, D. A., BRENZAN, M. A., SIQUEIRA, V. L., CALEFFI-FERRACIOLI, K. R., VIEIRA, L. C., MONTEIRO, J. L., CORRÊA, A. G. & CARDOSO, R. F. 2020. Structure–activity relationship of natural and synthetic coumarin derivatives against Mycobacterium tuberculosis. *Future Medicinal Chemistry,* 12**,** 1533-1546.

PORWAL, B., JAYASHREE, B. & ATTIMARAD, M. 2010. Synthesis of some new 3-coumarinoyl pyridinium and quinolinium bromides for their antimicrobial activity. *Journal of basic and clinical pharmacy,* 1.

PRACHAYASITTIKUL, S., PINGAEW, R., WORACHARTCHEEWAN, A., SINTHUPOOM, N., PRACHAYASITTIKUL, V., RUCHIRAWAT, S. & PRACHAYASITTIKUL, V. 2017. Roles of pyridine and pyrimidine derivatives as privileged scaffolds in anticancer agents. *Mini reviews in medicinal chemistry,* 17**,** 869-901.

PRASAD, R. & SRIVASTAVA, D. K. 2013. Multi drug and extensively drug-resistant TB (M/XDR-TB) management: Current issues. *Clinical epidemiology and global health,* 1**,** 124-128.

PRUSTY, J. S. & KUMAR, A. 2019. Coumarins: antifungal effectiveness and future therapeutic scope. *Molecular diversity***,** 1-17.

QING, Z.-X., HUANG, J.-L., YANG, X.-Y., LIU, J.-H., CAO, H.-L., XIANG, F., CHENG, P. & ZENG, J.-G. 2018. Anticancer and reversing multidrug resistance activities of natural isoquinoline alkaloids and their structure-activity relationship. *Current medicinal chemistry,* 25**,** 5088-5114.

RAMÍREZ-LEPE, M. & RAMÍREZ-SUERO, M. 2012. Biological control of mosquito larvae by Bacillus thuringiensis subsp. israelensis. *Insecticides—Pest Engineering*.

REDDY, D. S., HOSAMANI, K. M. & DEVARAJEGOWDA, H. C. 2015. Design, synthesis of benzocoumarin-pyrimidine hybrids as novel class of antitubercular agents, their DNA cleavage and X-ray studies. *European journal of medicinal chemistry,* 101**,** 705-715.

REDDY, G. M., GARCIA, J. R., REDDY, V. H., DE ANDRADE, A. M., CAMILO JR, A., RIBEIRO, R. A. P. & DE LAZARO, S. R. 2016. Synthesis, antimicrobial activity and advances in structure-activity relationships (SARs) of novel tri-substituted thiazole derivatives. *European journal of medicinal chemistry,* 123**,** 508-513.

REDDY, D. S., KONGOT, M., NETALKAR, S. P., KURJOGI, M. M., KUMAR, R., AVECILLA, F. & KUMAR, A. 2018. Synthesis and evaluation of novel coumarin-oxime ethers as potential anti-tubercular agents: Their DNA cleavage ability and BSA interaction study. *European journal of medicinal chemistry,* 150**,** 864-875.

REDDY, D. S., KONGOT, M. & KUMAR, A. 2021. Coumarin hybrid derivatives as promising leads to treat tuberculosis: Recent developments and critical aspects of structural design to exhibit anti-tubercular activity. *Tuberculosis***,** 102050.

RENUKA, N. & KUMAR, K. A. 2015. Synthesis and biological evaluation of fused pyrans bearing coumarin moiety as potent antimicrobial agents. *Philippine Journal of Science,* 144**,** 91-96.

RIEDL, S. J. & SHI, Y. 2004. Molecular mechanisms of caspase regulation during apoptosis. *Nature reviews Molecular cell biology,* 5**,** 897-907.

ROHINI, K. & SRIKUMAR, P. 2014. Therapeutic role of coumarins and coumarin-related compounds. *Journal of Thermodynamics & Catalysis,* 5**,** 1.

ROLEIRA, F. M., VARELA, C. L., COSTA, S. C. & TAVARES-DA-SILVA, E. J. 2018. Phenolic derivatives from medicinal herbs and plant extracts: anticancer effects and synthetic approaches to modulate biological activity. *Studies in Natural Products Chemistry,* 57**,** 115-156.

ROUSSAKI, M., KONTOGIORGIS, C. A., HADJIPAVLOU-LITINA, D., HAMILAKIS, S. & DETSI, A. 2010. A novel synthesis of 3-aryl coumarins and evaluation of their

antioxidant and lipoxygenase inhibitory activity. *Bioorganic & medicinal chemistry letters,* 20**,** 3889-3892.

SAHOO, C. R., SAHOO, J., MAHAPATRA, M., LENKA, D., SAHU, P. K., DEHURY, B., PADHY, R. N. & PAIDESETTY, S. K. 2021. Coumarin derivatives as promising antibacterial agent (s). *Arabian Journal of Chemistry,* 14**,** 102922.

SAHOO, J. & PAIDESETTY, S. K. 2017. Antimicrobial activity of novel synthesized coumarin based transitional metal complexes. *Journal of Taibah University Medical Sciences,* 12**,** 115-124.

K SAHU, N., S BALBHADRA, S., CHOUDHARY, J. & V KOHLI, D. 2012. Exploring pharmacological significance of chalcone scaffold: a review. *Current medicinal chemistry,* 19**,** 209-225.

SAHU, S., GHOSH, S. K., GAHTORI, P., SINGH, U. P., BHATTACHARYYA, D. R. & BHAT, H. R. 2019. In silico ADMET study, docking, synthesis and antimalarial evaluation of thiazole-1, 3, 5-triazine derivatives as Pf-DHFR inhibitor. *Pharmacological Reports,* 71**,** 762-767.

SAID FATAHALA, S., HASABELNABY, S., GOUDAH, A., MAHMOUD, G. I. & HELMY ABD-EL HAMEED, R. 2017. Pyrrole and fused pyrrole compounds with bioactivity against inflammatory mediators. *Molecules,* 22**,** 461.

SALAR, U., TAHA, M., KHAN, K. M., ISMAIL, N. H., IMRAN, S., PERVEEN, S., GUL, S. & WADOOD, A. 2016. Syntheses of new 3-thiazolyl coumarin derivatives, in vitro α-glucosidase inhibitory activity, and molecular modeling studies. *European journal of medicinal chemistry,* 122**,** 196-204.

SALEM, M., MARZOUK, M. & EL-KAZAK, A. 2016. Synthesis and characterization of some new coumarins with in vitro antitumor and antioxidant activity and high protective effects against DNA damage. *Molecules,* 21**,** 249.

SANAD, S. M. & MEKKY, A. E. 2020. Synthesis, in-vitro antibacterial and anticancer screening of novel nicotinonitrile-coumarin hybrids utilizing piperazine citrate. *Synthetic Communications***,** 1-18.

SANDHU, S., BANSAL, Y., SILAKARI, O. & BANSAL, G. 2014. Coumarin hybrids as novel therapeutic agents. *Bioorganic & medicinal chemistry,* 22**,** 3806-3814.

SASHIDHARA, K. V., KUMAR, A., DODDA, R. P., KRISHNA, N. N., AGARWAL, P., SRIVASTAVA, K. & PURI, S. 2012. Coumarin–trioxane hybrids: Synthesis and evaluation as a new class of antimalarial scaffolds. *Bioorganic & medicinal chemistry letters,* 22**,** 3926-3930.

SECCI, D., CARRADORI, S., BIZZARRI, B., CHIMENTI, P., DE MONTE, C., MOLLICA, A., RIVANERA, D., ZICARI, A., MARI, E. & ZENGIN, G. 2016. Novel 1, 3-

thiazolidin-4-one derivatives as promising anti-Candida agents endowed with anti-oxidant and chelating properties. *European journal of medicinal chemistry,* 117**,** 144-156.

SHAABANI, A., GHADARI, R., RAHMATI, A. & REZAYAN, A. 2009. Coumarin synthesis via Knoevenagel condensation reaction in 1, 1, 3, 3-N, N, N′, N′-tetramethylguanidinium trifluoroacetate ionic liquid. *Journal of the Iranian Chemical Society,* 6**,** 710-714.

SHAIK, J. B., PALAKA, B. K., PENUMALA, M., KOTAPATI, K. V., DEVINENI, S. R., EADLAPALLI, S., DARLA, M. M., AMPASALA, D. R., VADDE, R. & AMOORU, G. D. 2016. Synthesis, pharmacological assessment, molecular modeling and in silico studies of fused tricyclic coumarin derivatives as a new family of multifunctional anti-Alzheimer agents. *European journal of medicinal chemistry,* 107**,** 219-232.

SHAIKH, M. H., SUBHEDAR, D. D., KHAN, F. A. K., SANGSHETTI, J. N. & SHINGATE, B. B. 2016a. 1, 2, 3-Triazole incorporated coumarin derivatives as potential antifungal and antioxidant agents. *Chinese Chemical Letters,* 27**,** 295-301.

SHAIKH, M. H., SUBHEDAR, D. D., SHINGATE, B. B., KHAN, F. A. K., SANGSHETTI, J. N., KHEDKAR, V. M., NAWALE, L., SARKAR, D., NAVALE, G. R. & SHINDE, S. S. 2016b. Synthesis, biological evaluation and molecular docking of novel coumarin incorporated triazoles as antitubercular, antioxidant and antimicrobial agents. *Medicinal Chemistry Research,* 25**,** 790-804.

SHAO, G., XIA, Y., XIONG, H., HE, L., ZENG, Z., JIANG, D. & WANG, H. 2018. Synthesis and larvicidal activities of compounds based on coumarin and dibenzothiophene/carbazole. *Research on Chemical Intermediates,* 44**,** 1235-1245.

SHARMA, D., BANSAL, K. K., SHARMA, A., PATHAK, M. & SHARMA, P. C. 2019. A brief literature and review of patents on thiazole related derivatives. *Current Bioactive Compounds,* 15**,** 304-315.

SHARMA, V., KUMAR, V. & KUMAR, P. 2013. Heterocyclic chalcone analogues as potential anticancer agents. *Anti-Cancer Agents in Medicinal Chemistry (Formerly Current Medicinal Chemistry-Anti-Cancer Agents),* 13**,** 422-432.

SHI, Y. & ZHOU, C.-H. 2011. Synthesis and evaluation of a class of new coumarin triazole derivatives as potential antimicrobial agents. *Bioorganic & medicinal chemistry letters,* 21**,** 956-960.

SHOCKRAVI, A., VALIZADEH, H. & HERAVI, M. M. 2003. A one-pot and convenient synthesis of coumarins in solventless system. *Phosphorus, Sulfur, and Silicon and the Related Elements,* 178**,** 501-504.

SIDDIQUI, N., ARSHAD, M. F., AHSAN, W. & ALAM, M. S. 2009. Thiazoles: a valuable insight into the recent advances and biological activities. *Int J Pharm Sci Drug Res,* 1**,** 136-143.

SINGH, D. & PATHAK, D. P. 2016. Coumarins: an overview of medicinal chemistry. Potential for new drug molecules. *International Journal of Pharmaceutical Sciences and Research,* 7**,** 482.

SINGH, H., SINGH, J. V., BHAGAT, K., GULATI, H. K., SANDUJA, M., KUMAR, N., KINARIVALA, N. & SHARMA, S. 2019a. Rational approaches, design strategies, structure activity relationship and mechanistic insights for therapeutic coumarin hybrids. *Bioorganic & medicinal chemistry,* 27**,** 3477-3510.

SINGH, I. P., GUPTA, S. & KUMAR, S. 2019b. Thiazole Compounds as Antiviral Agents: An Update. *Med Chem,* 10.

SINGH, V. & MIZRAHI, V. 2017. Identification and validation of novel drug targets in *Mycobacterium tuberculosis*. *Drug discovery today,* 22**,** 503-509.

SMYTH, T., RAMACHANDRAN, V. & SMYTH, W. 2009. A study of the antimicrobial activity of selected naturally occurring and synthetic coumarins. *International journal of antimicrobial agents,* 33**,** 421-426.

SONG, X. F., FAN, J., LIU, L., LIU, X. F. & GAO, F. 2020. Coumarin derivatives with anticancer activities: An update. *Archiv der Pharmazie,* 353**,** 2000025.

SONMEZ, F., ZENGIN KURT, B., GAZIOGLU, I., BASILE, L., DAG, A., CAPPELLO, V., GINEX, T., KUCUKISLAMOGLU, M. & GUCCIONE, S. 2017. Design, synthesis and docking study of novel coumarin ligands as potential selective acetylcholinesterase inhibitors. *Journal of enzyme inhibition and medicinal chemistry,* 32**,** 285-297.

SOONWERA, M. & PHASOMKUSOLSIL, S. 2017. Adulticidal, larvicidal, pupicidal and oviposition deterrent activities of essential oil from Zanthoxylum limonella Alston (Rutaceae) against Aedes aegypti (L.) and Culex quinquefasciatus (Say). *Asian Pacific Journal of Tropical Biomedicine,* 7**,** 967-978.

SRIVASTAV, V., TIWARI, M., ZHANG, X. & YAO, X. 2018. Synthesis and Antiretroviral Activity of 6-Acetyl-coumarin Derivatives against HIV-1 Infection. *Indian Journal of Pharmaceutical Sciences,* 80**,** 108-117.

SRIVASTAVA, P., VYAS, V. K., VARIYA, B., PATEL, P., QURESHI, G. & GHATE, M. 2016. Synthesis, anti-inflammatory, analgesic, 5-lipoxygenase (5-LOX) inhibition activities, and molecular docking study of 7-substituted coumarin derivatives. *Bioorganic Chemistry,* 67**,** 130-138.

SUN, Y.-F. & CUI, Y.-P. 2009. The synthesis, structure and spectroscopic properties of novel oxazolone-, pyrazolone-and pyrazoline-containing heterocycle chromophores. *Dyes and Pigments,* 81**,** 27-34.

SUN, Q., PENG, D.-Y., YANG, S.-G., ZHU, X.-L., YANG, W.-C. & YANG, G.-F. 2014. Syntheses of coumarin–tacrine hybrids as dual-site acetylcholinesterase inhibitors and

their activity against butylcholinesterase, Aβ aggregation, and β-secretase. *Bioorganic & Medicinal Chemistry,* 22**,** 4784-4791.

SU, Z., YANG, Z., XU, Y., CHEN, Y. & YU, Q. 2015. Apoptosis, autophagy, necroptosis, and cancer metastasis. *Molecular cancer,* 14**,** 48.

TAIT, S. W., ICHIM, G. & GREEN, D. R. 2014. Die another way–non-apoptotic mechanisms of cell death. *J Cell Sci,* 127**,** 2135-2144.

TANG, T., LIU, J., ZUO, K., CHENG, J., CHEN, L., LU, C., HAN, S., XU, J., JIA, Z. & YE, M. 2015. Genotype-guided dosing of coumarin anticoagulants: a meta-analysis of randomized controlled trials. *Journal of cardiovascular pharmacology and therapeutics,* 20**,** 387-394.

TANSER, F. C. & LE SUEUR, D. 2002. The application of geographical information systems to important public health problems in Africa. *International journal of health geographics,* 1**,** 1-9.

TATARINGA, G., STAN, C., MIRCEA, C., JITAREANU, A. & ZBANCIOC, A.-M. 2016. Antioxidant evaluation of some coumarin derivatives. *Farmacia,* 64**,** 533-538.

TATARINGA, G. & ZBANCIOC, A. M. 2019. Coumarin Derivatives with Antimicrobial and Antioxidant Activities. *Phytochemicals in Human Health.* IntechOpen.

THAKUR, A., SINGLA, R. & JAITAK, V. 2015. Coumarins as anticancer agents: A review on synthetic strategies, mechanism of action and SAR studies. *European journal of medicinal chemistry,* 101**,** 476-495.

THOTA, S., NADIPELLY, K., SHENKESI, A. & YERRA, R. 2015. Design, synthesis, characterization, antioxidant and in vitro cytotoxic activities of novel coumarin thiazole derivatives. *Medicinal Chemistry Research,* 24**,** 1162-1169.

TOK, F., KOCYIGIT-KAYMAKCIOGLU, B., TABANCA, N., ESTEP, A. S., GROSS, A. D., GELDENHUYS, W. J., BECNEL, J. J. & BLOOMQUIST, J. R. 2018. Synthesis and structure–activity relationships of carbohydrazides and 1, 3, 4-oxadiazole derivatives bearing an imidazolidine moiety against the yellow fever and dengue vector, Aedes aegypti. *Pest management science,* 74**,** 413-421.

TOMASZ KUBRAK, T., RAFAŁ PODGÓRSKI, R. & MONIKA SOMPOR, M. 2017. Natural and Synthetic Coumarins and their Pharmacological Activity. *European Journal of Clinical and Experimental Medicine***,** 169-175.

TURNER, G. L., MORRIS, J. A. & GREANEY, M. F. 2007. Direct arylation of thiazoles on water. *Angewandte Chemie,* 119**,** 8142-8146.

UJAN, R., BAHADUR, A., SHABIR, G., IQBAL, S., SAEED, A., CHANNAR, P. A., MAHMOOD, Q., SHOAIB, M., ARSHAD, I. & SAIFULLAH, M. 2021. Facile synthesis of novel fluorescent thiazole coumarinyl compounds: Electrochemical, time

resolve fluorescence, and solvatochromic study. *Journal of Molecular Structure,* 1227**,** 129422.

VAARLA, K., KARNEWAR, S., PANUGANTI, D., PEDDI, S. R., VEDULA, R. R., MANGA, V. & KOTAMRAJU, S. 2019. 3-(2-(5-Amino-3-aryl-1H-pyrazol-1-yl) thiazol-4-yl)-2H-chromen-2-ones as Potential Anticancer Agents: Synthesis, Anticancer Activity Evaluation and Molecular Docking Studies. *ChemistrySelect,* 4**,** 4324-4330.

VAARLA, K., KESHARWANI, R. K., SANTOSH, K., VEDULA, R. R., KOTAMRAJU, S. & TOOPURANI, M. K. 2015. Synthesis, biological activity evaluation and molecular docking studies of novel coumarin substituted thiazolyl-3-aryl-pyrazole-4-carbaldehydes. *Bioorganic & medicinal chemistry letters,* 25**,** 5797-5803.

VALIZADEH, H. & VAGHEFI, S. 2009. One-pot Wittig and Knoevenagel reactions in ionic liquid as convenient methods for the synthesis of coumarin derivatives. *Synthetic Communications®,* 39**,** 1666-1678.

VAN CRUCHTEN, S. & VAN DEN BROECK, W. 2002. Morphological and biochemical aspects of apoptosis, oncosis and necrosis. *Anatomia, histologia, embryologia,* 31**,** 214-223.

VARGAS-SOTO, F. A., CÉSPEDES-ACUÑA, C. L., AQUEVEQUE-MUÑOZ, P. M. & ALARCÓN-ENOS, J. E. 2017. Toxicity of coumarins synthesized by Pechmann-Duisberg condensation against Drosophila melanogaster larvae and antibacterial effects. *Food and Chemical Toxicology,* 109**,** 1118-1124.

VEKARIYA, R. H. & PATEL, H. D. 2014. Recent advances in the synthesis of coumarin derivatives via knoevenagel condensation: A review. *Synthetic Communications,* 44**,** 2756-2788.

VENUGOPALA, K. N. & JAYASHREE, B. S. 2003. Synthesis of carboxamides of 2-amino-4-(6-bromo-3-coumarinyl thiazole as analgesic and antiinflammatory agents. *Indian Journal of Heterocyclic Chemistry,* 12**,** 307-310.

VENUGOPALA, K. & JAYASHREE, B. 2004a. Synthesis and characterization of Schiff bases of aminothiazolylbromo coumarin for their analgesic and anti-inflammatory activity. *Asian Journal of Chemistry,* 16**,** 407-411.

VENUGOPALA, K. N. & JAYASHREE, B. S. 2004b. Synthesis and characterization of Schiff bases of aminothiazolylbromocoumarin for their analgesic and anti-inflammatory activity. *Asian Journal of Chemistry,* 16**,** 407-411.

VENUGOPALA, K. N., JAYASHREE, B. S. & ATTIMARAD, M. 2004c. Synthesis and evaluation of some substituted 2-arylamino coumarinyl thiazoles as potential NSAIDs. *Asian Journal of Chemistry,* 16**,** 872-876.

VENUGOPALA, K. N., KRISHNAPPA, M., NAYAK, S. K., SUBRAHMANYA, B. K., VADERAPURA, J. P., CHALANNAVAR, R. K., GLEISER, R. M. & ODHAV, B. 2013a. Synthesis and antimosquito properties of 2, 6-substituted benzo [d] thiazole and 2, 4-substituted benzo [d] thiazole analogues against Anopheles arabiensis. *European journal of medicinal chemistry,* 65**,** 295-303.

VENUGOPALA, K. N., RASHMI, V. & ODHAV, B. 2013b. Review on natural coumarin lead compounds for their pharmacological activity. *BioMed research international,* 2013.

VENUGOPALA, K. N., RASHMI, V. & ODHAV, B. 2013c. Review on natural coumarin lead compounds for their pharmacological activity. *BioMed Research International,* 963248**,** 1-15.

VENUGOPALA, K. N., GLEISER, R. M., KASUMBWE, K., ALDHUBIAB, B. E., ATTIMARAD, M. V. & ODHAV, B. 2014. Evaluation of halogenated coumarins for antimosquito properties. *The Scientific World Journal,* 2014**,** 1-6.

VENUGOPALA, K. N., UPPAR, V., CHANDRASHEKHARAPPA, S., ABDALLAH, H. H., PILLAY, M., DEB, P. K., MORSY, M. A., ALDHUBIAB, B. E., ATTIMARAD, M. & NAIR, A. B. 2020. Cytotoxicity and antimycobacterial properties of pyrrolo [1, 2-a] quinoline derivatives: Molecular target identification and molecular docking studies. *Antibiotics,* 9**,** 233.

VERDÍA, P., SANTAMARTA, F. & TOJO, E. 2011. Knoevenagel reaction in [MMIm][MSO4]: Synthesis of coumarins. *Molecules,* 16**,** 4379-4388.

VERGARA, F. M., LIMA, C. H. D. S., MARIA DAS GRAÇAS, M. D. O., CANDÉA, A. L., LOURENÇO, M. C., FERREIRA, M. D. L., KAISER, C. R. & DE SOUZA, M. V. 2009. Synthesis and antimycobacterial activity of N′-[(E)-(monosubstituted-benzylidene)]-2-pyrazinecarbohydrazide derivatives. *European journal of medicinal chemistry,* 44**,** 4954-4959.

VERMEULEN, K., VAN BOCKSTAELE, D. R. & BERNEMAN, Z. N. 2005. Apoptosis: mechanisms and relevance in cancer. *Annals of hematology,* 84**,** 627-639.

WANG, L., DONG, C., LI, X., HAN, W. & SU, X. 2017. Anticancer potential of bioactive peptides from animal sources. *Oncology Reports,* 38**,** 637-651.

WHO.1975. Manual on practical entomology in Malaria. Part II—Methods and techniques. p189. https://apps.who.int/iris/handle/10665/42481(Accessed on 13th June 2021).

WHO.2020a. Global tuberculosis report 2021. https://www.who.int/news-room/fact-sheets/detail/tuberculosis (Accessed on 23th December 2021).

WHO.2020b. Global cancer report 2020. https://www.who.int/news-room/fact-sheets/detail/cancer (Accessed on 29th May 2021).

WHO.2020c. Vector-borne diseases. 2020. Available at https://www.who.int/news-room/fact-sheets/detail/vector-borne-diseases (Accessed on 28th June 2021).

WLODKOWIC, D., TELFORD, W., SKOMMER, J. & DARZYNKIEWICZ, Z. 2011. Apoptosis and beyond: cytometry in studies of programmed cell death. *Methods in cell biology.* Elsevier.

WONG, R. S. 2011. Apoptosis in cancer: from pathogenesis to treatment. *Journal of Experimental & Clinical Cancer Research,* 30**,** 87.

WONG, W. W. L. & PUTHALAKATH, H. 2008. Bcl-2 family proteins: The sentinels of the mitochondrial apoptosis pathway. *IUBMB life,* 60**,** 390-397.

WOO, H. J., LEE, J. Y., WOO, M. H., YANG, C. H. & KIM, Y. H. 2011. Apoptogenic activity of 2α, 3α-dihydroxyurs-12-ene-28-oic acid from Prunella vulgaris var. lilacina is mediated via mitochondria-dependent activation of caspase cascade regulated by Bcl-2 in human acute leukemia Jurkat T cells. *Journal of ethnopharmacology,* 135**,** 626-635.

XU, L., ZHAO, X.-Y., WU, Y.-L. & ZHANG, W. The study on biological and pharmacological activity of coumarins. 2015 Asia-Pacific Energy Equipment Engineering Research Conference, 2015. Atlantis Press.

XU, Y., DANG, R., GUAN, J., XU, Z., ZHAO, S. & HU, Y. 2018. Isatin-(thio) semicarbazide/oxime-1H-1, 2, 3-triazole-coumarin Hybrids: Design, Synthesis, and in vitro Anti-mycobacterial Evaluation. *Journal of Heterocyclic Chemistry,* 55**,** 1069-1073.

XU, Z., ZHANG, S., GAO, C., FAN, J., ZHAO, F., LV, Z.-S. & FENG, L.-S. 2017. Isatin hybrids and their anti-tuberculosis activity. *Chinese Chemical Letters,* 28**,** 159-167.

XU, Z., ZHAO, S. J., LV, Z. S., GAO, F., WANG, Y. L., ZHANG, F., BAI, L. Y., DENG, J. L., WANG, Q. & FAN, Y. L. 2019. Design, Synthesis, and Evaluation of Tetraethylene Glycol-Tethered Isatin–1, 2, 3-Triazole–Coumarin Hybrids as Novel Anticancer Agents. *Journal of Heterocyclic Chemistry,* 56**,** 1127-1132.

YADAV, V. R., PRASAD, S., SUNG, B. & AGGARWAL, B. B. 2011. The role of chalcones in suppression of NF-κB-mediated inflammation and cancer. *International immunopharmacology,* 11**,** 295-309.

YANG, G., SHI, L., PAN, Z., WU, L., FAN, L., WANG, C., XU, C. & LIANG, J. 2021. The synthesis of coumarin thiazoles containing a trifluoromethyl group and their antifungal activities. *Arabian Journal of Chemistry,* 14**,** 102880.

YUAN, S. & AKEY, C. W. 2013. Apoptosome structure, assembly, and procaspase activation. *Structure,* 21**,** 501-515.

YUSUFZAI, S. K., OSMAN, H., KHAN, M. S., ABD RAZIK, B. M., EZZAT, M. O., MOHAMAD, S., SULAIMAN, O., GANSAU, J. A. & PARUMASIVAM, T. 2018. 4-Thiazolidinone coumarin derivatives as two-component NS2B/NS3 DENV flavivirus serine protease inhibitors: synthesis, molecular docking, biological evaluation and structure–activity relationship studies. *Chemistry Central Journal,* 12**,** 1-16.

ZABLOTSKAYA, A., SEGAL, I., GERONIKAKI, A., EREMKINA, T., BELYAKOV, S., PETROVA, M., SHESTAKOVA, I., ZVEJNIECE, L. & NIKOLAJEVA, V. 2013. Synthesis, physicochemical characterization, cytotoxicity, antimicrobial, anti-inflammatory and psychotropic activity of new N-[1, 3-(benzo) thiazol-2-yl]-ω-[3, 4-dihydroisoquinolin-2 (1H)-yl] alkanamides. *European journal of medicinal chemistry,* 70**,** 846-856.

ZAHEDIFARD, M., FARAJ, F. L., PAYDAR, M., LOOI, C. Y., HAJREZAEI, M., HASANPOURGHADI, M., KAMALIDEHGHAN, B., MAJID, N. A., ALI, H. M. & ABDULLA, M. A. 2015. Synthesis, characterization and apoptotic activity of quinazolinone Schiff base derivatives toward MCF-7 cells via intrinsic and extrinsic apoptosis pathways. *Scientific reports,* 5**,** 11544.

ZERANGNASRABAD, S., JABBARI, A., KHAVARI MOGHADAM, E., SADEGHIAN, H. & SEYEDI, S. M. 2021. Design, synthesis, and structure–activity relationship study of O-prenylated 3-acetylcoumarins as potent inhibitors of soybean 15-lipoxygenase. *Drug Development Research*.

ZHANG, L. & XU, Z. 2019. Coumarin-containing hybrids and their anticancer activities. *European journal of medicinal chemistry,* 181**,** 111587.

ZHANG, W., LI, Z., ZHOU, M., WU, F., HOU, X., LUO, H., LIU, H., HAN, X., YAN, G. & DING, Z. 2014. Synthesis and biological evaluation of 4-(1, 2, 3-triazol-1-yl) coumarin derivatives as potential antitumor agents. *Bioorganic & medicinal chemistry letters,* 24**,** 799-807.

ZHENG, J., LEONG, D., LEES, G. & NICHOLSON, R. A. 1998. Studies on the interaction of surangin B with insect mitochondria, insect synaptosomes, and rat cortical neurones in primary culture. *Pesticide Biochemistry and Physiology,* 61**,** 1-13.

ZHU, M., ZHOU, L., YAO, Y., LI, S., LV, M., WANG, K., LI, X. & CHEN, H. 2015. Anticancer activity and DNA binding property of the dimers of triphenylethylene–coumarin hybrid with two amino side chains. *Medicinal Chemistry Research,* 24**,** 2314-2324.

APPENDIX 1

PATENT JOURNAL

INCLUDING TRADE MARKS, DESIGNS AND COPYRIGHT IN CINEMATOGRAPH FILMS

JUNE 2021 VOL 54 • No. 06

Companies and Intellectual Property Commission

a member of the dti group

Part II of II

ISSUED MONTHLY DATE OF ISSUE: 30 JUNE 2021

ISSN 2223-4837

PATENT JOURNAL

INCLUDING TRADE MARKS, DESIGNS AND COPYRIGHT IN CINEMATOGRAPH FILMS

VOL. 54 No. 06 Date of Issue: 30 JUNE 2021

PATENTS, TRADE MARKS, DESIGNS AND COPYRIGHT OFFICE

Official notices of proceedings under:

The Patents Act, 1978
The Designs Act, 1993
The Trade Marks Act, 1963
The Trade Marks Act, 1993
The Registration of Copyright in Cinematograph Films Act, 1977

Registrar of Patents, Trade Marks, Designs and Copyright

Note: CIPC acting on behalf of the Government of the Republic of South Africa, cannot guarantee the accuracy of its publications or undertake any responsibility for errors or omissions or their consequences.

the alkali lignin modifier in the polar solvent again to obtain an alkali lignin modifier solution, soaking a paper pulp in the solution, stirring and adding chitosan, and performing papermaking to obtain super-hydrophobic paper; the super-hydrophobic paper has strong hydrophobicity, reutilization property and seal-cleaning capacity, is simple in operation, adopts raw materials which are cheap and rich in source.

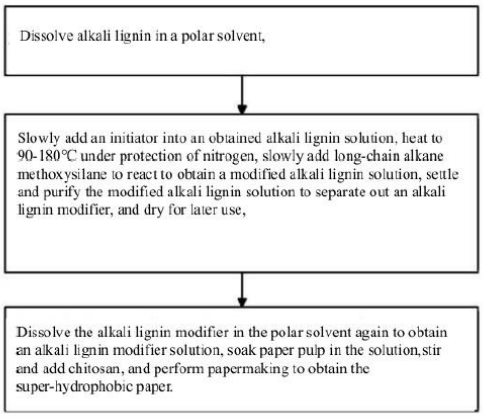

21: 2020/03045. 22: 22/05/2020. 43: 4/7/2021
51: A01N
71: EXA AG (PTY) LTD
72: VAN DYK, Johannes Jacobus, CROUS, Louis Rudolph
33: AU 31: 2018202204 32: 2018-03-28
54: SOIL TREATMENT COMPOSITION
00: -
A synergistic composition, method and kit for controlling, suppressing or preventing plant pathogens in soil is provided. The composition comprises (A) Tagetes (Marigold) essential oil, (B) Allium sativum (garlic) essential oil, (C) Brassica (mustard) essential oil, and (D) Capsicum (chilli) essential oil, in which the volume ratio of (A):(B):(C):(D) is from 1:1:60:1 to 10:10:80:20

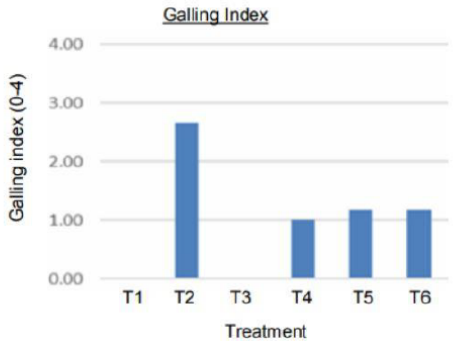

21: 2020/03088. 22: 5/27/2020. 43: 3/31/2021
51: A61K; C07C
71: DURBAN UNIVERSITY OF TECHNOLOGY
72: VENUGOPALA, Katharigatta Narayanaswamy, CHANDRASHEKHARAPPA, Sandeep, PILLAY, Melendhran, ODHAV, Bharti, MOHANLALL, Viresh, KASUMBWE, Kabange
33: ZA 31: 2019/05328 32: 2019-08-13
54: TREATMENT OF TUBERCULOSIS
00: -
The invention provides a compound of formula (1) or (2)

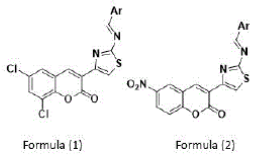

Formula (1) Formula (2)

and its usefulness in treatment of tuberculosis.

21: 2020/03089. 22: 5/27/2020. 43: 3/31/2021
51: E02D
71: SMART LOCKING LOGIC (PTY) LTD
72: SCOTT, Andrew Ernest, OLIVIER, Johan, DEARLING, Fabio
33: ZA 31: 2019/04867 32: 2019-07-25
54: AN ADAPTOR ASSEMBLY FOR A MANHOLE-TYPE ACCESS SYSTEM, AND SUCH AN ACCESS SYSTEM
00: -
An adaptor assembly is for a manhole-type access system having a manhole chamber, a coping above the manhole chamber, and manhole cover receivable by the coping. The adaptor assembly includes a base having an annular body with a radially outer edge and a radially inner edge, the base comprising attachment formations at its radially outer edge configured for connection to the manhole

APPENDIX 2

Table of contents

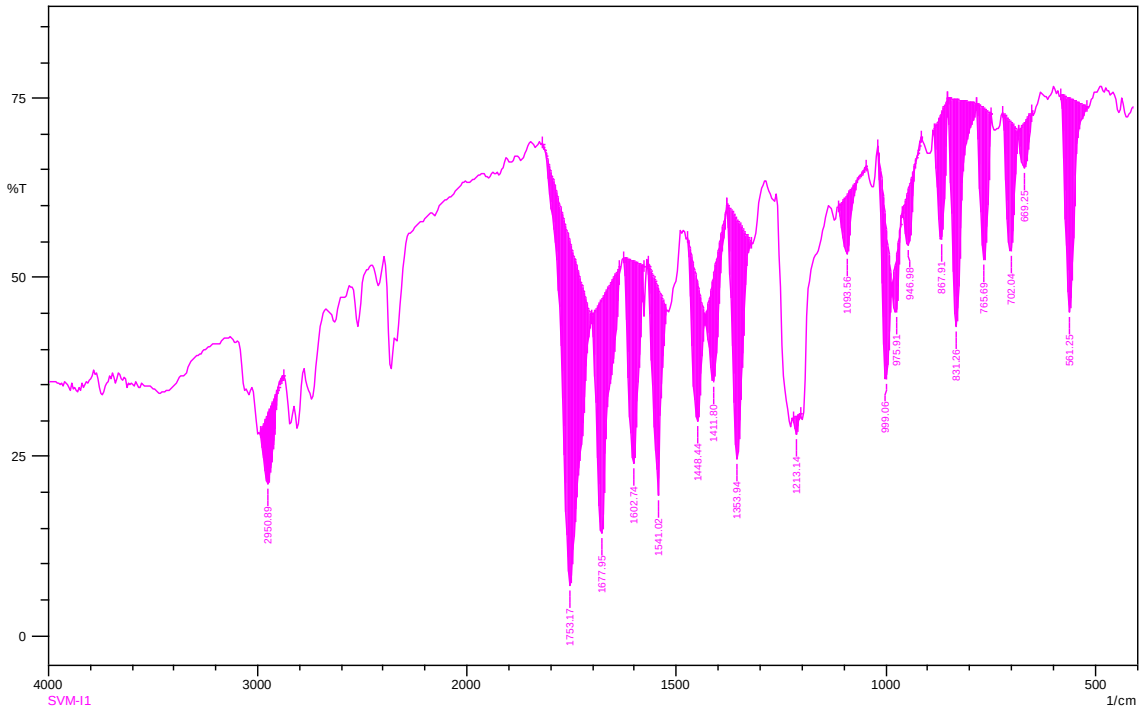

Figure S1: FT-IR of 3-acetyl-6, 8-dichloro-2*H*-chromen-2-one (SVM i1)

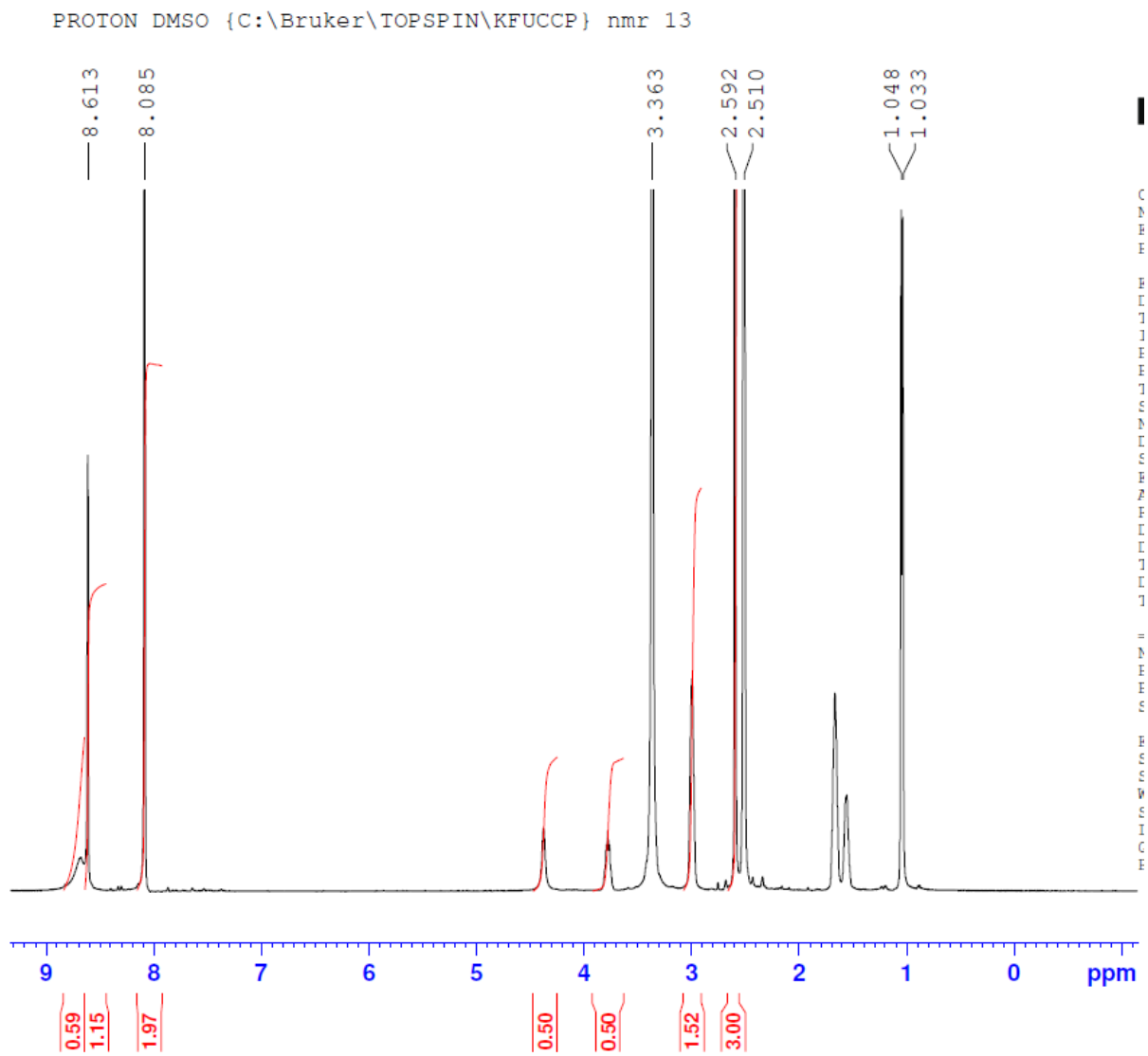

Figure S2: ^{1}H-NMR of 3-acetyl-6, 8-dichloro-2*H*-chromen-2-one (SVM i1)

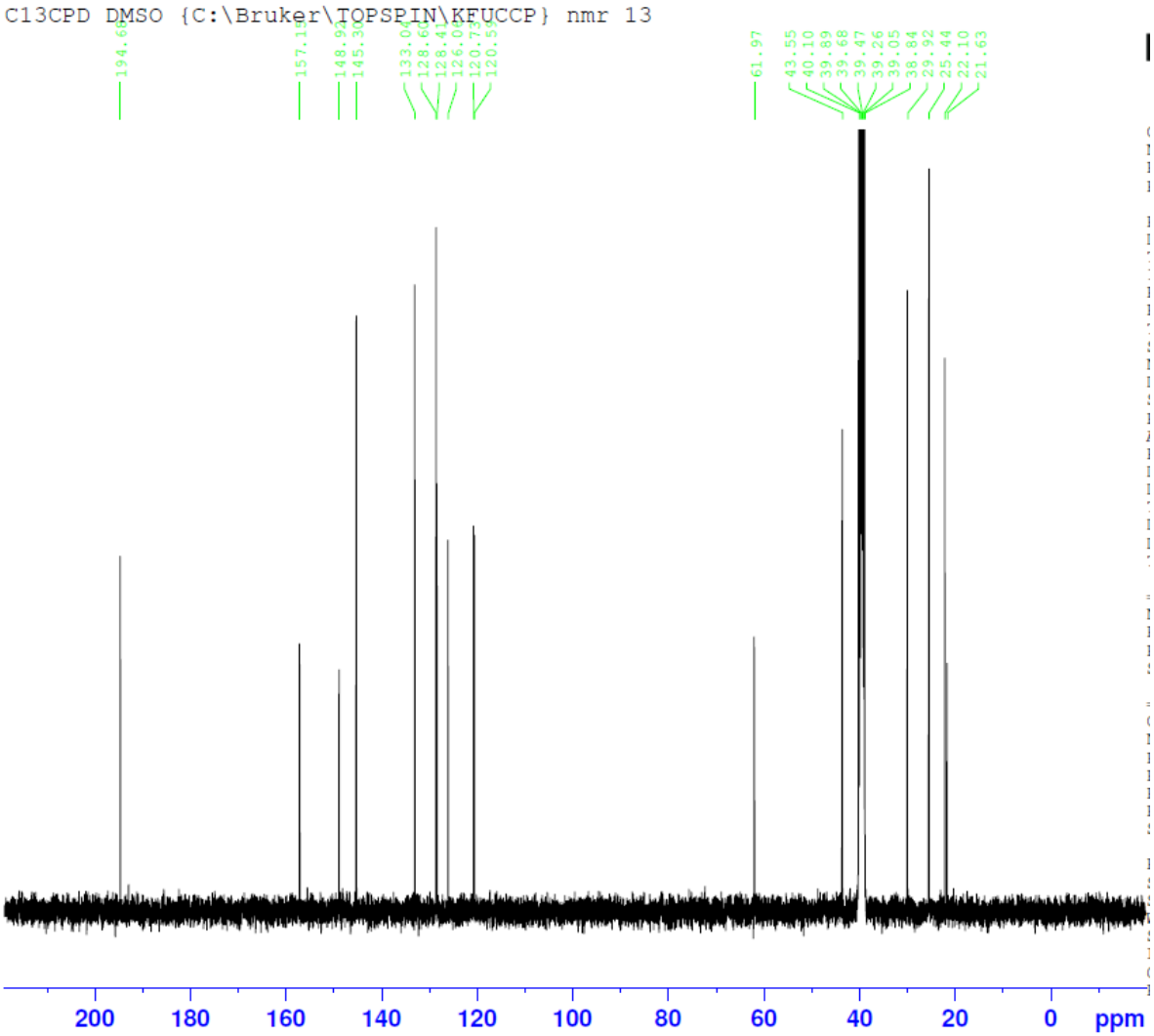

Figure S3: ^{13}C-NMR of 3-acetyl-6, 8-dichloro-2*H*-chromen-2-one (SVM i1)

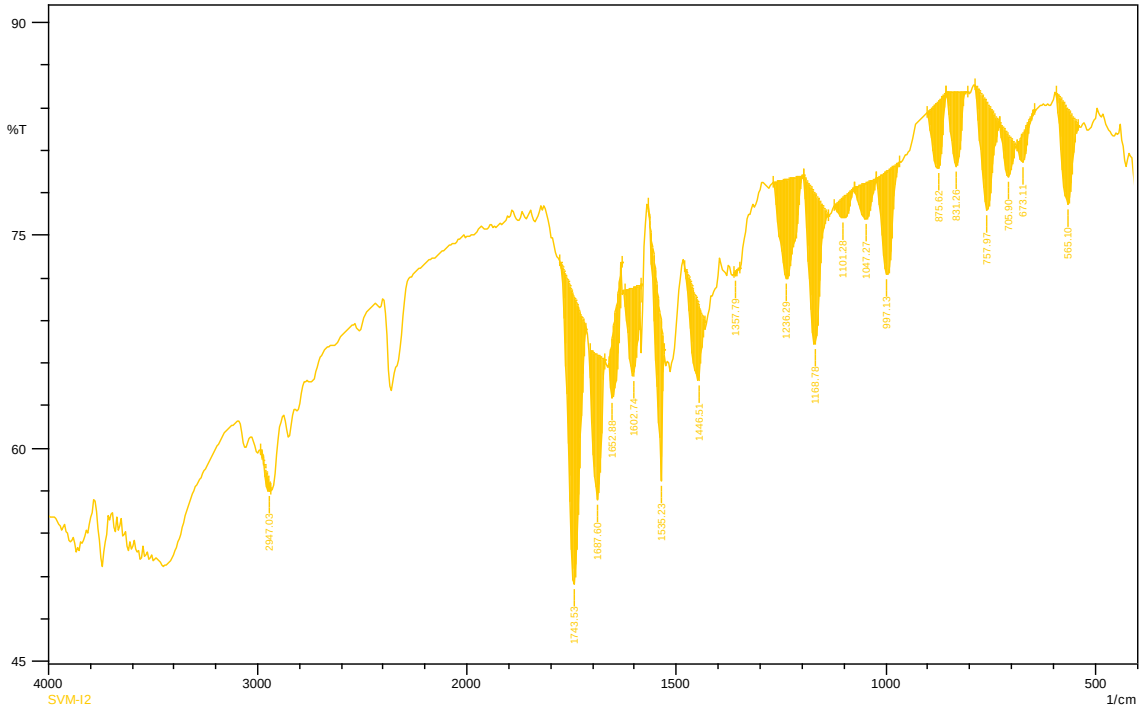

Figure S4: FT-IR of 3-(2-bromoacetyl)-6,8-dichloro-2*H*-chromen-2-one (SVM i2)

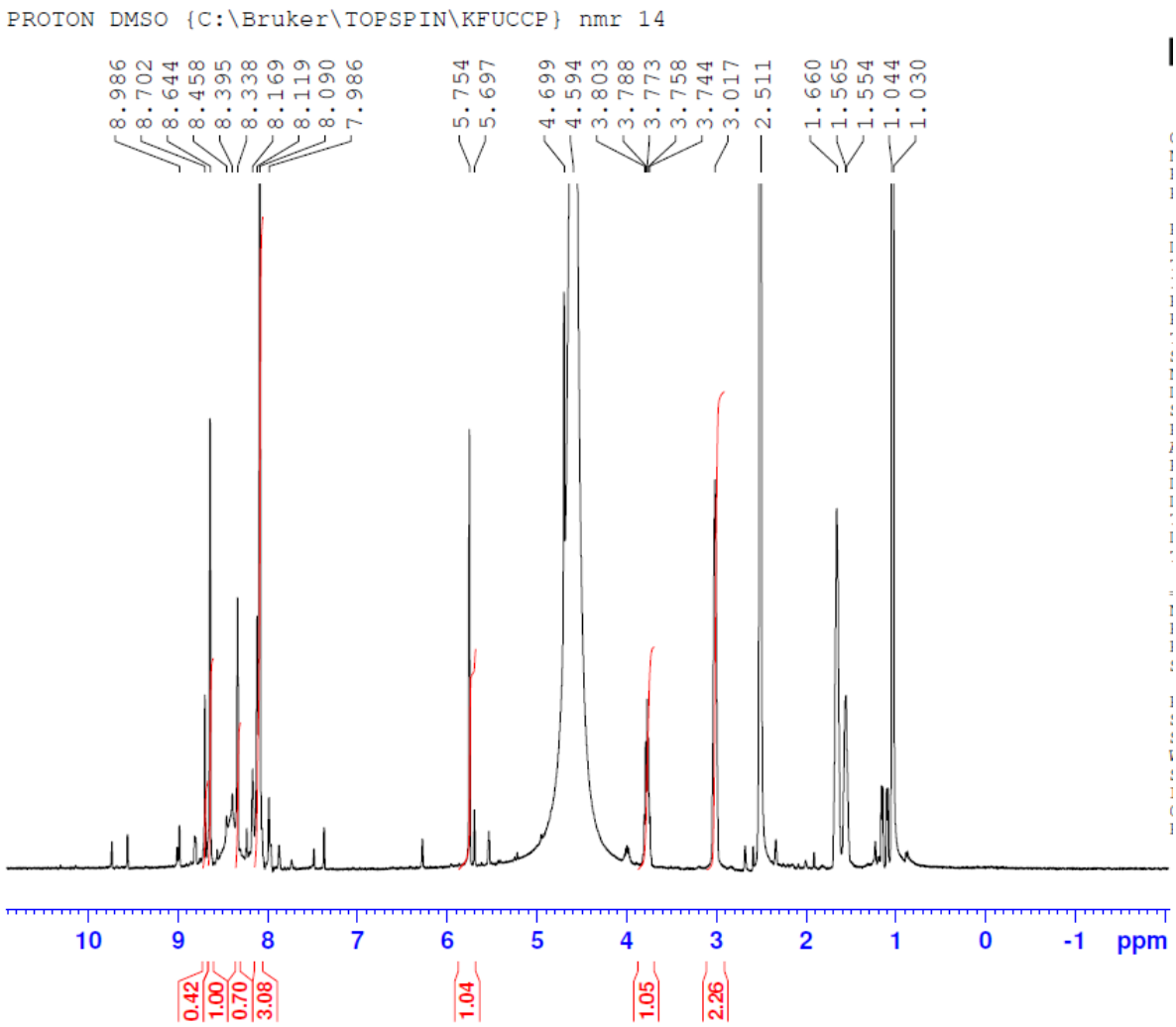

Figure S5: ^{1}H-NMR of 3-(2-bromoacetyl)-6,8-dichloro-2*H*-chromen-2-one (SVM i2)

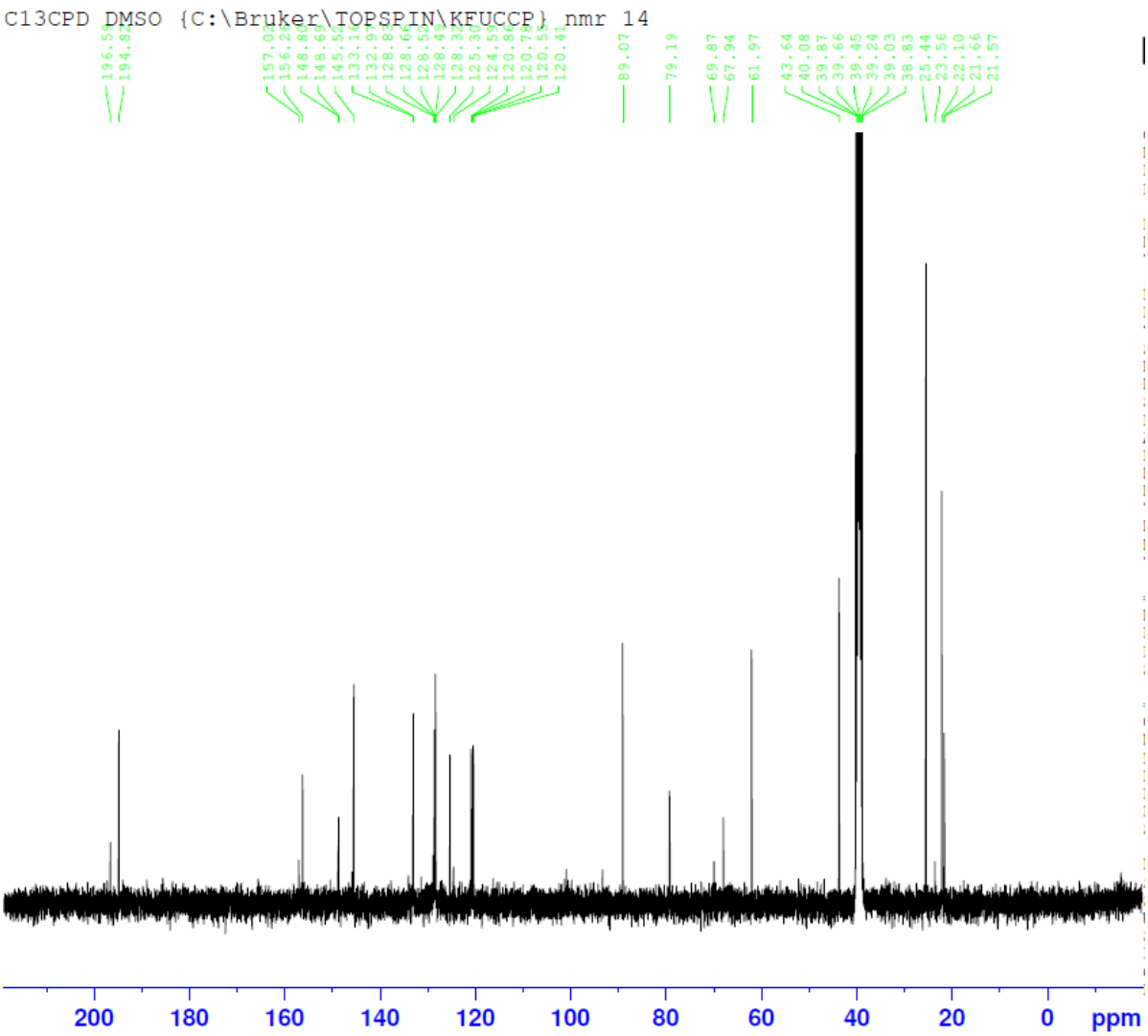

Figure S6: ^{13}C-NMR of 3-(2-bromoacetyl)-6,8-dichloro-2*H*-chromen-2-one (SVM i2)

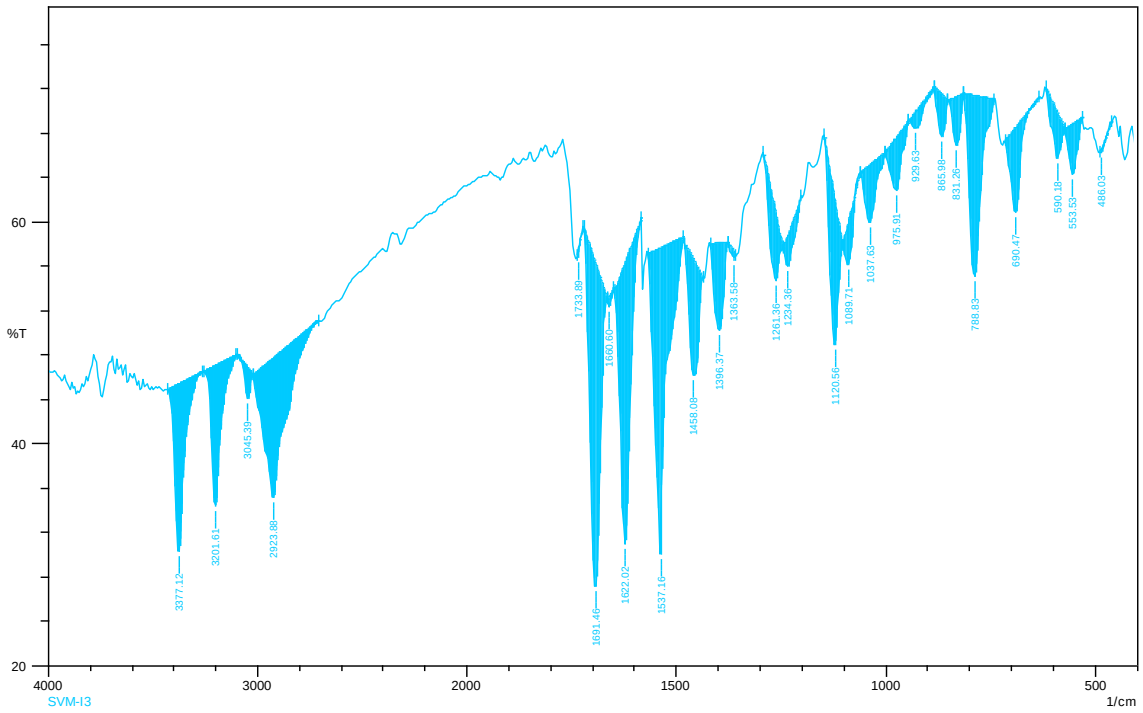

Figure S7: FT-IR of 3-(2-aminothiazol-4-yl)-6,8-dichloro-2*H*-chromen-2-one (SVM i3)

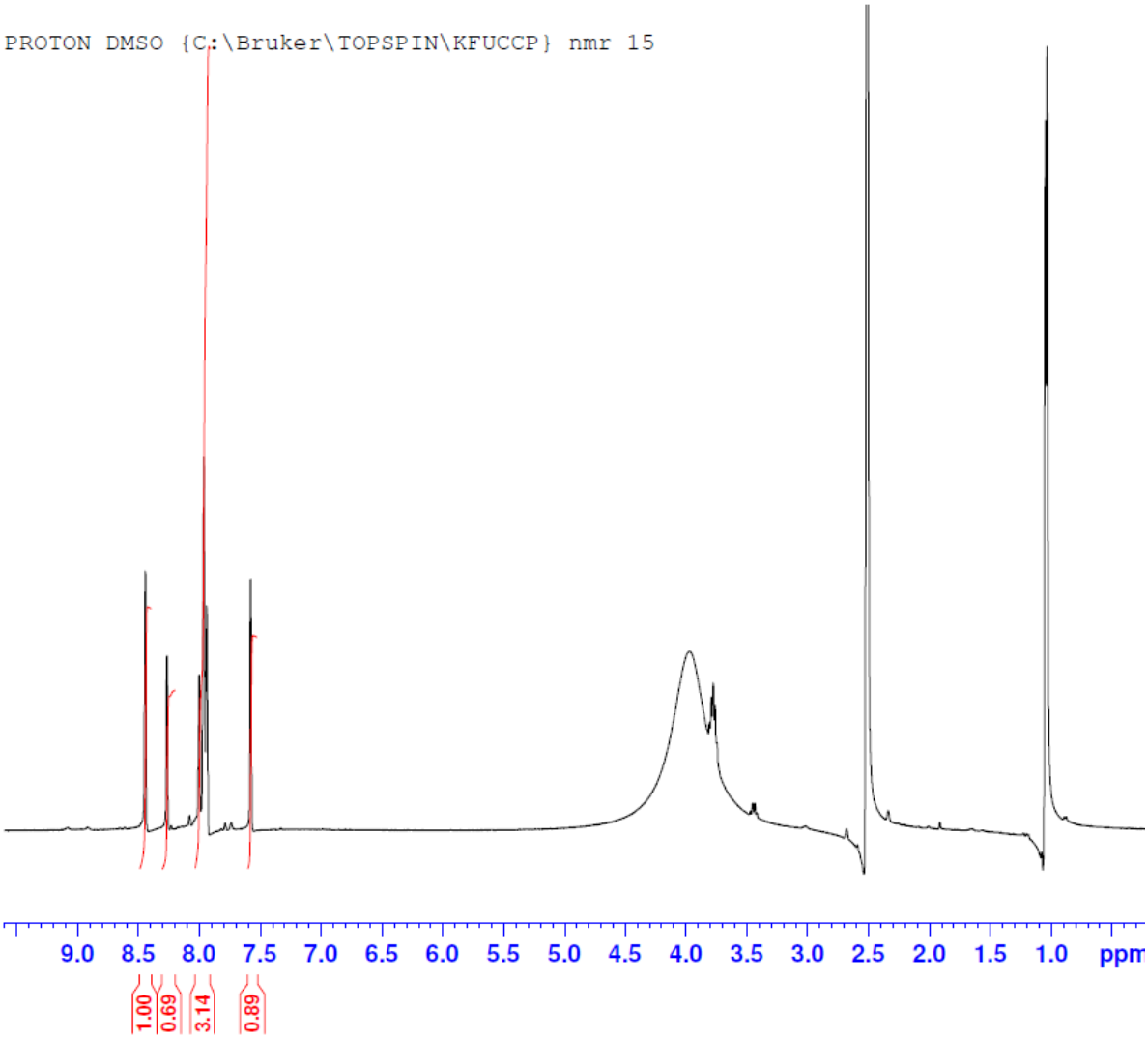

Figure S8: ^{1}H-NMR of 3-(2-aminothiazol-4-yl)-6,8-dichloro-2*H*-chromen-2-one (SVM i3)

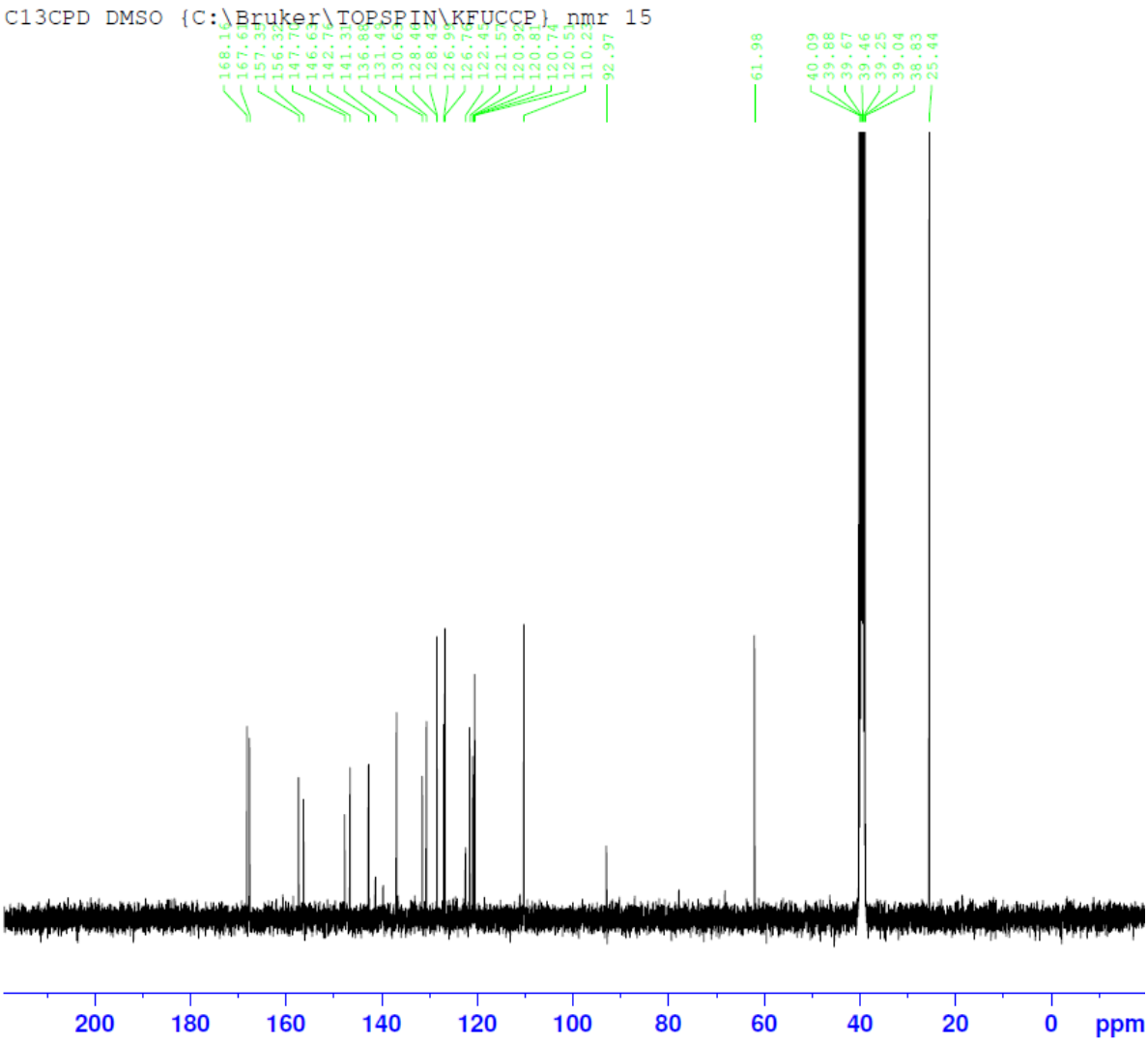

Figure S9: ^{13}C-NMR of 3-(2-aminothiazol-4-yl)-6,8-dichloro-2*H*-chromen-2-one (SVM i3)

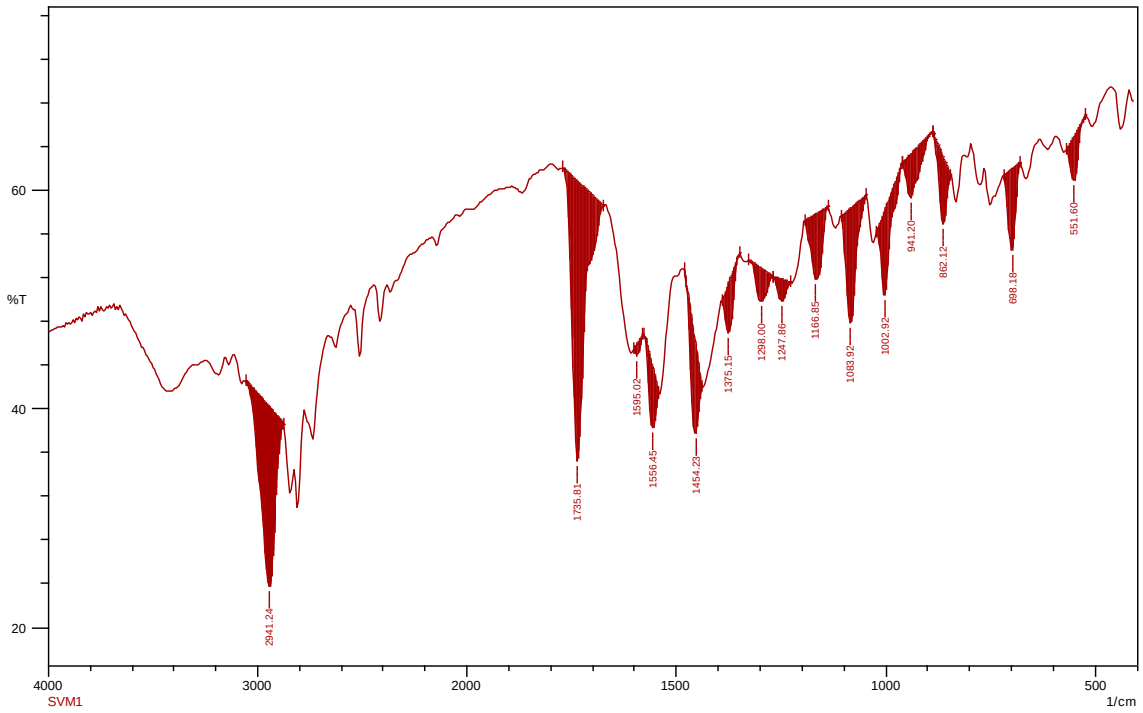

Figure S10: FT-IR of (*E*)-3-(2-(benzylidene amino) thiazol-4-yl)-6,8-dichloro-2*H*-chromen-2-one (SVM 1)

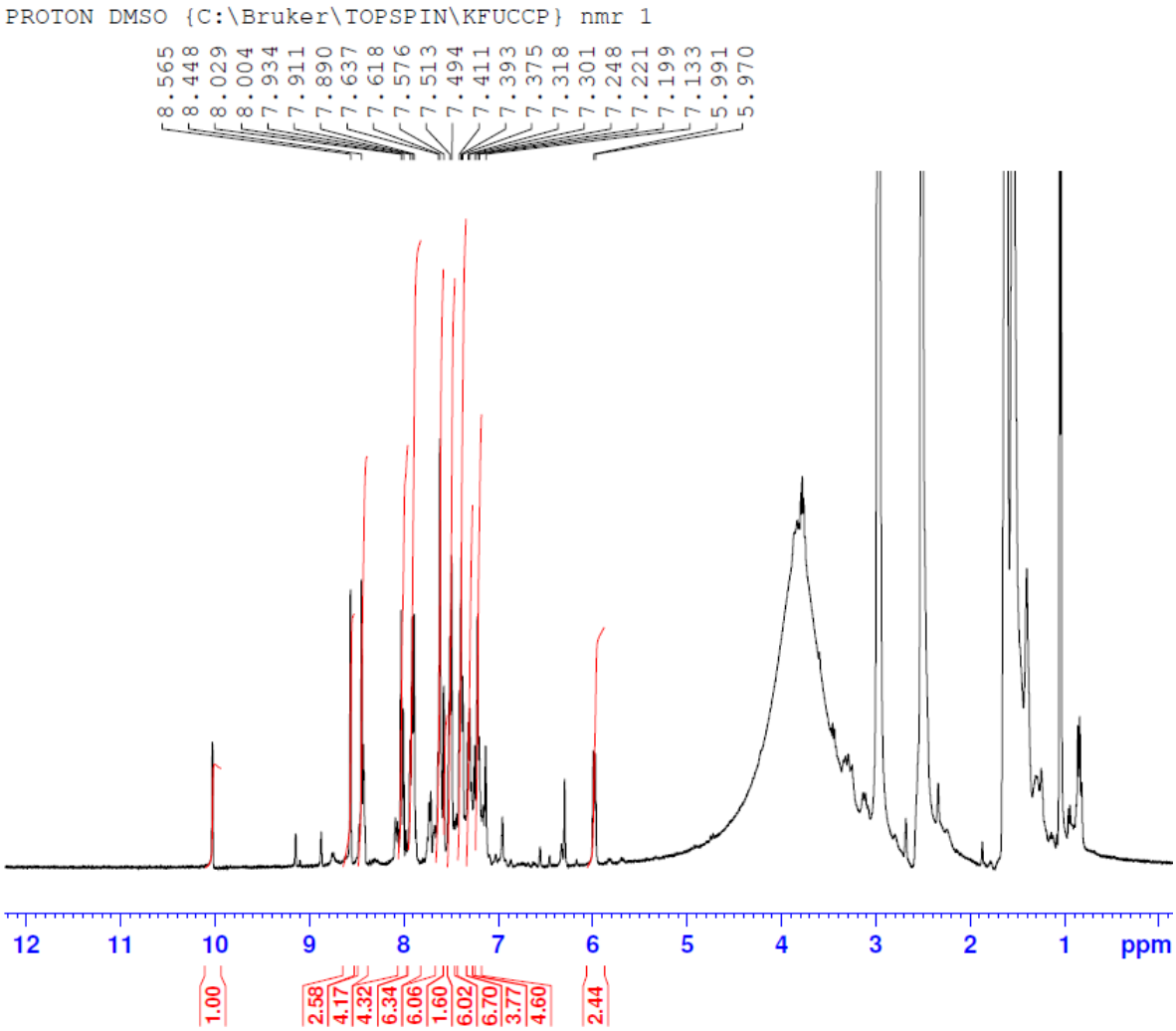

Figure S11: ^{1}H-NMR of (*E*)-3-(2-(benzylidene amino) thiazol-4-yl)-6,8-dichloro-2*H*-chromen-2-one (SVM 1)

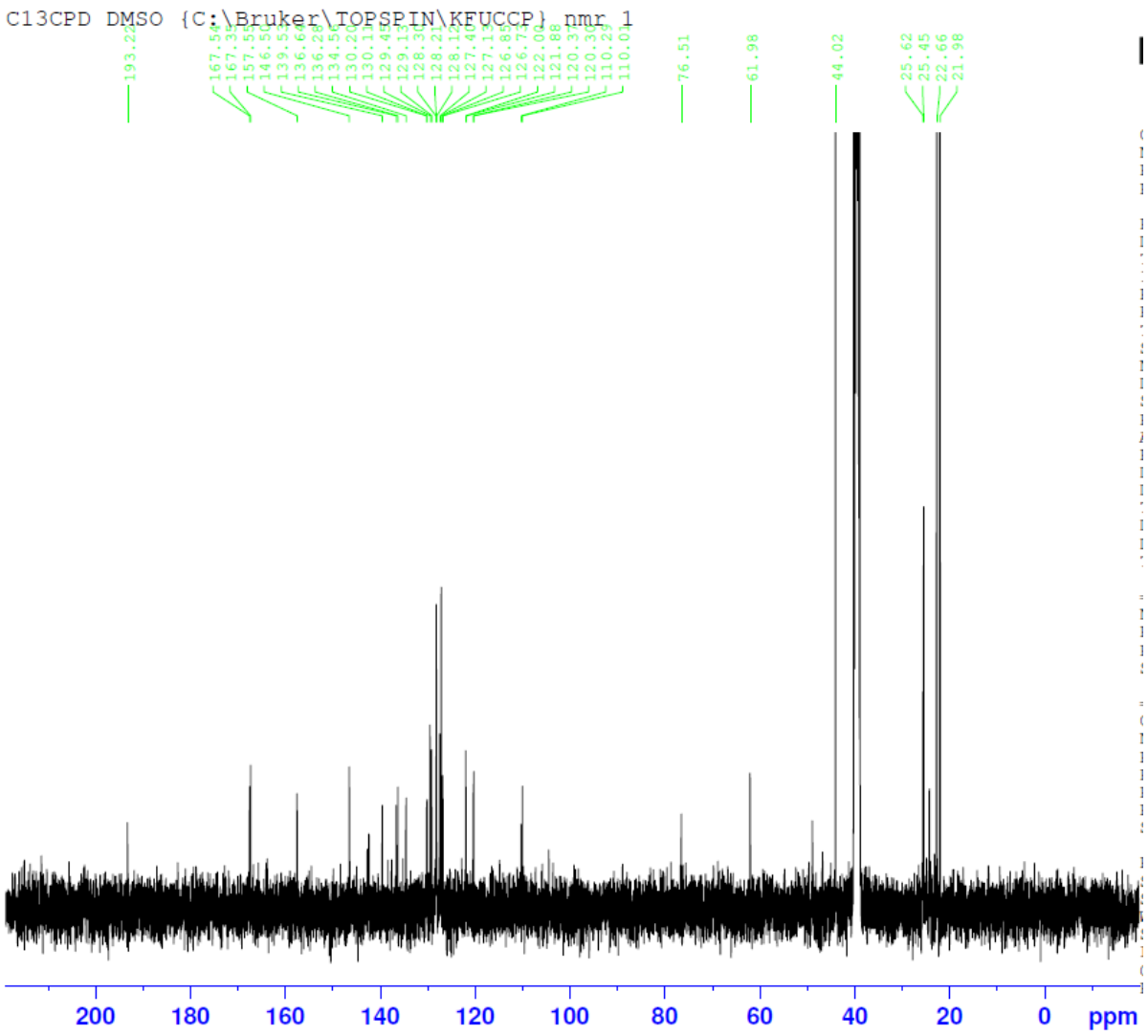

Figure S12: ^{13}C-NMR of (*E*)-3-(2-(benzylidene amino) thiazol-4-yl)-6,8-dichloro-2*H*-chromen-2-one (SVM 1)

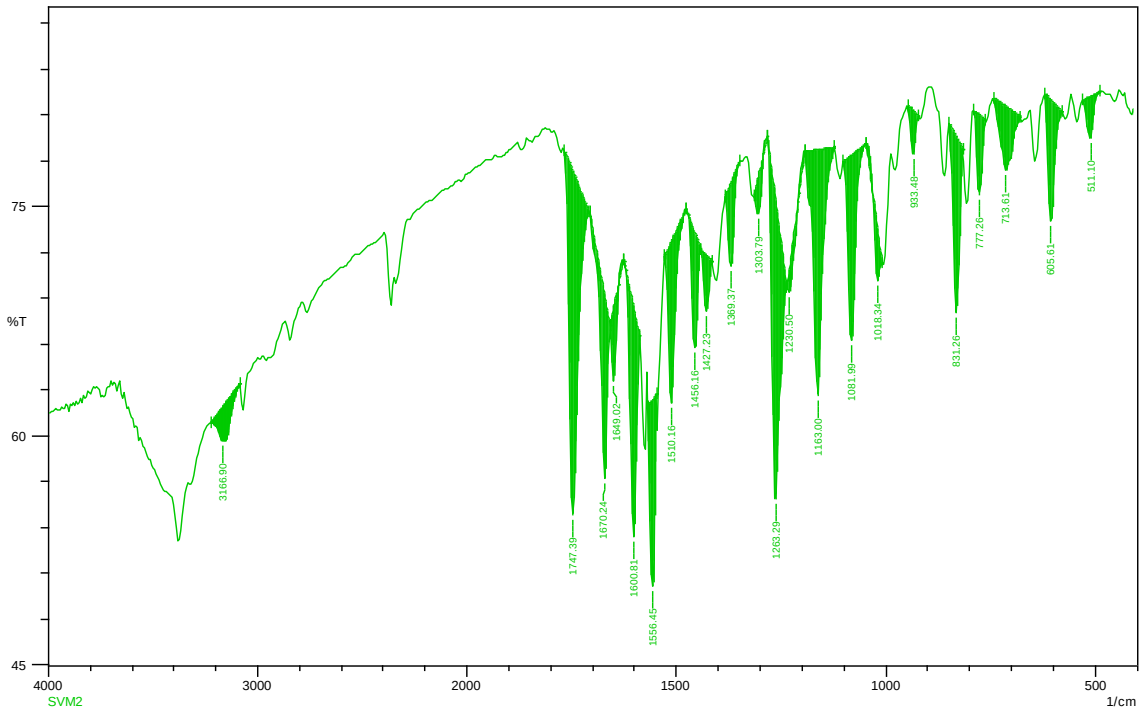

Figure S13: FT-IR of (*E*)-6,8-dichloro-3-(2-((4-methoxybenzylidene) amino) thiazol-4-yl)-2*H*-chromen-2-one (SVM 2)

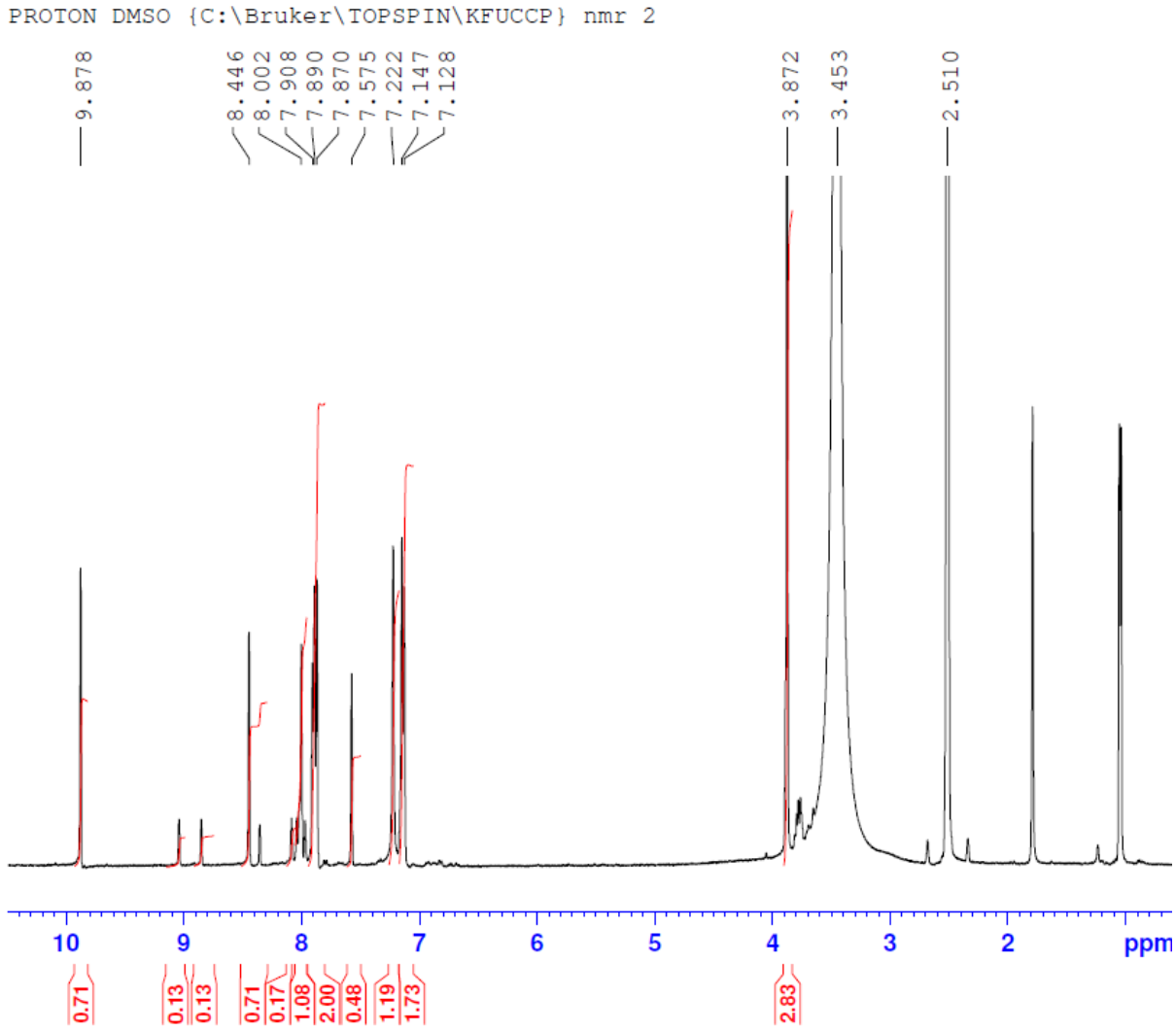

Figure S14: ^{1}H-NMR of (*E*)-6,8-dichloro-3-(2-((4-methoxybenzylidene) amino) thiazol-4-yl)-2*H*-chromen-2-one (SVM 2)

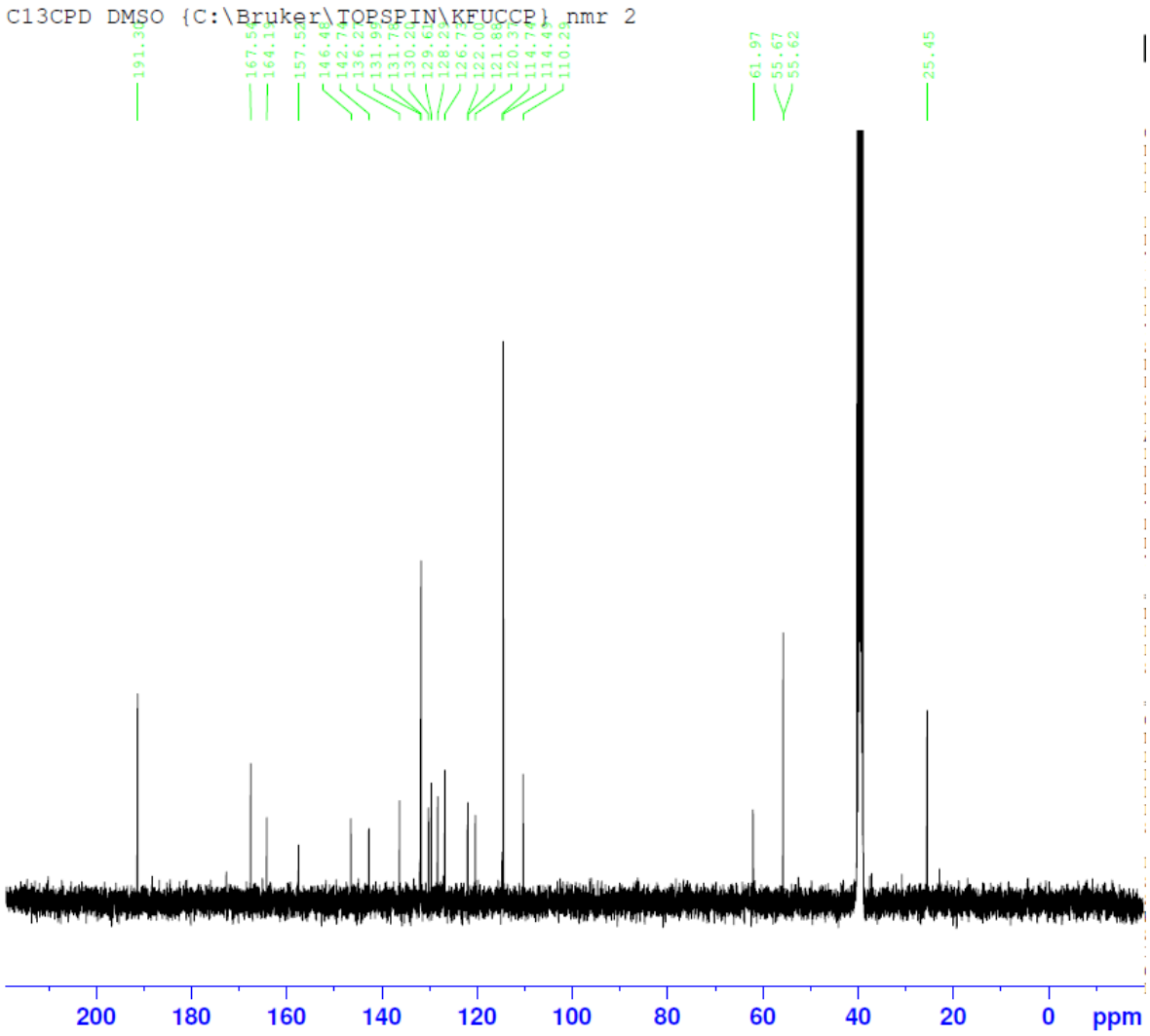

Figure S15: ^{13}C-NMR of (*E*)-6,8-dichloro-3-(2-((4-methoxybenzylidene) amino) thiazol-4-yl)-2*H*-chromen-2-one (SVM 2)

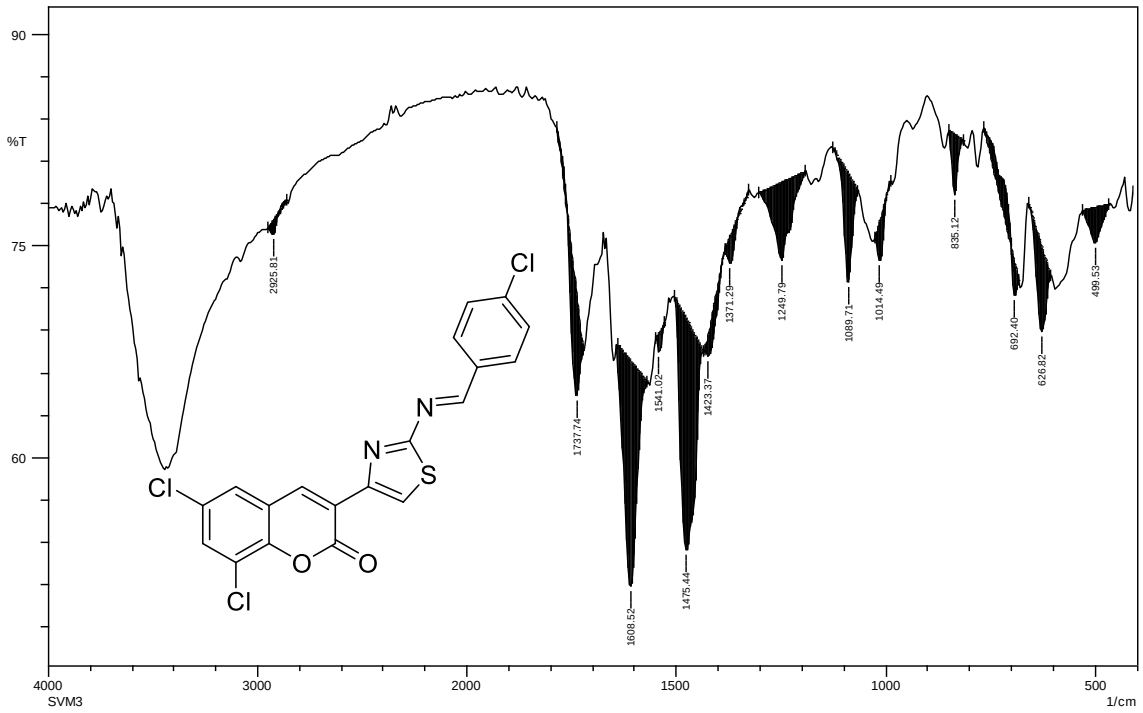

Figure S16: FT-IR of (*E*)-6,8-Dichloro-3-(2-((4-chlorobenzylidene) amino) thiazol-4-yl)-2*H*-chromen-2-one (SVM 3)

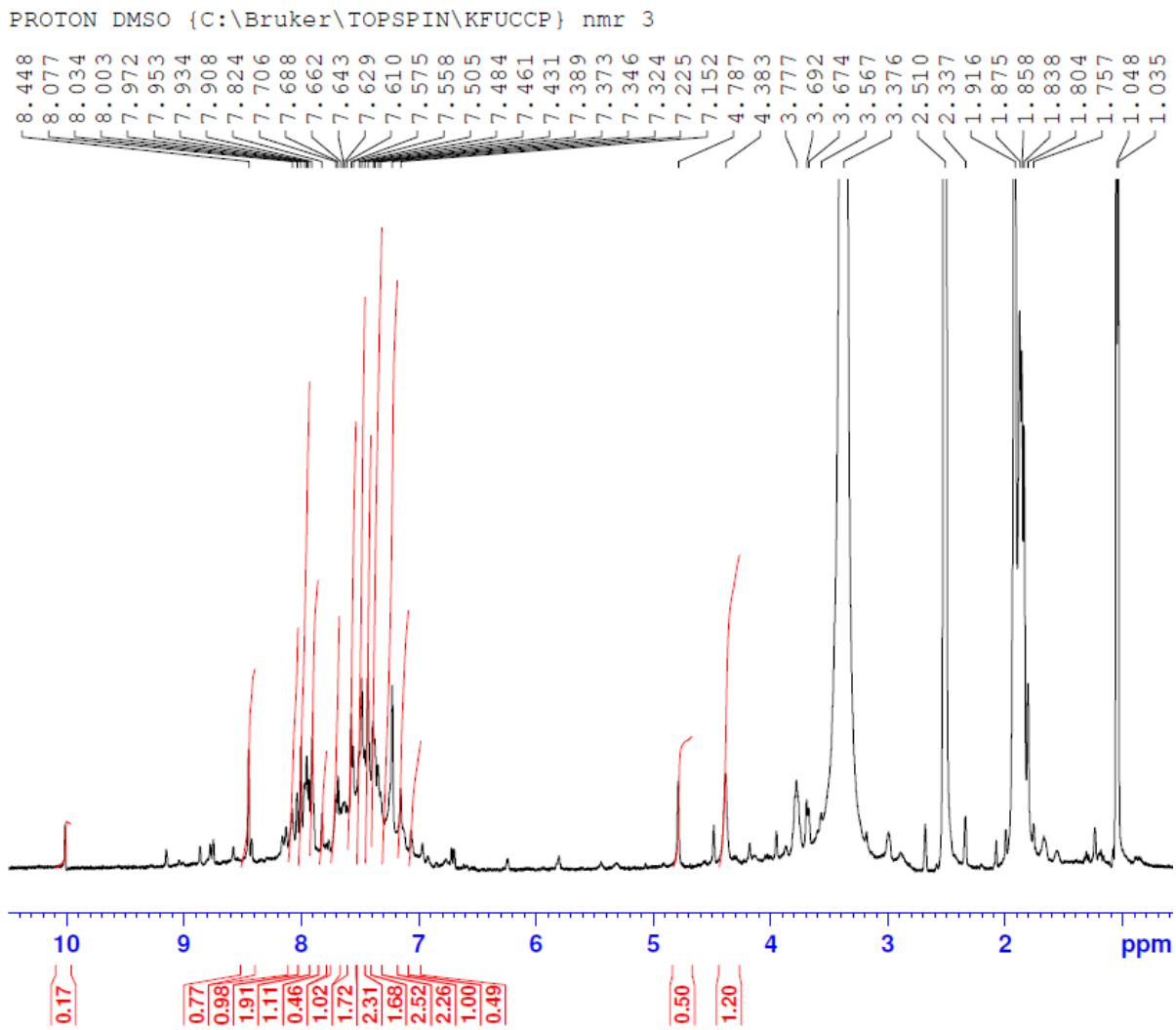

Figure S17: ^{1}H-NMR of (*E*)-6,8-Dichloro-3-(2-((4-chlorobenzylidene) amino) thiazol-4-yl)-2*H*-chromen-2-one (SVM 3)

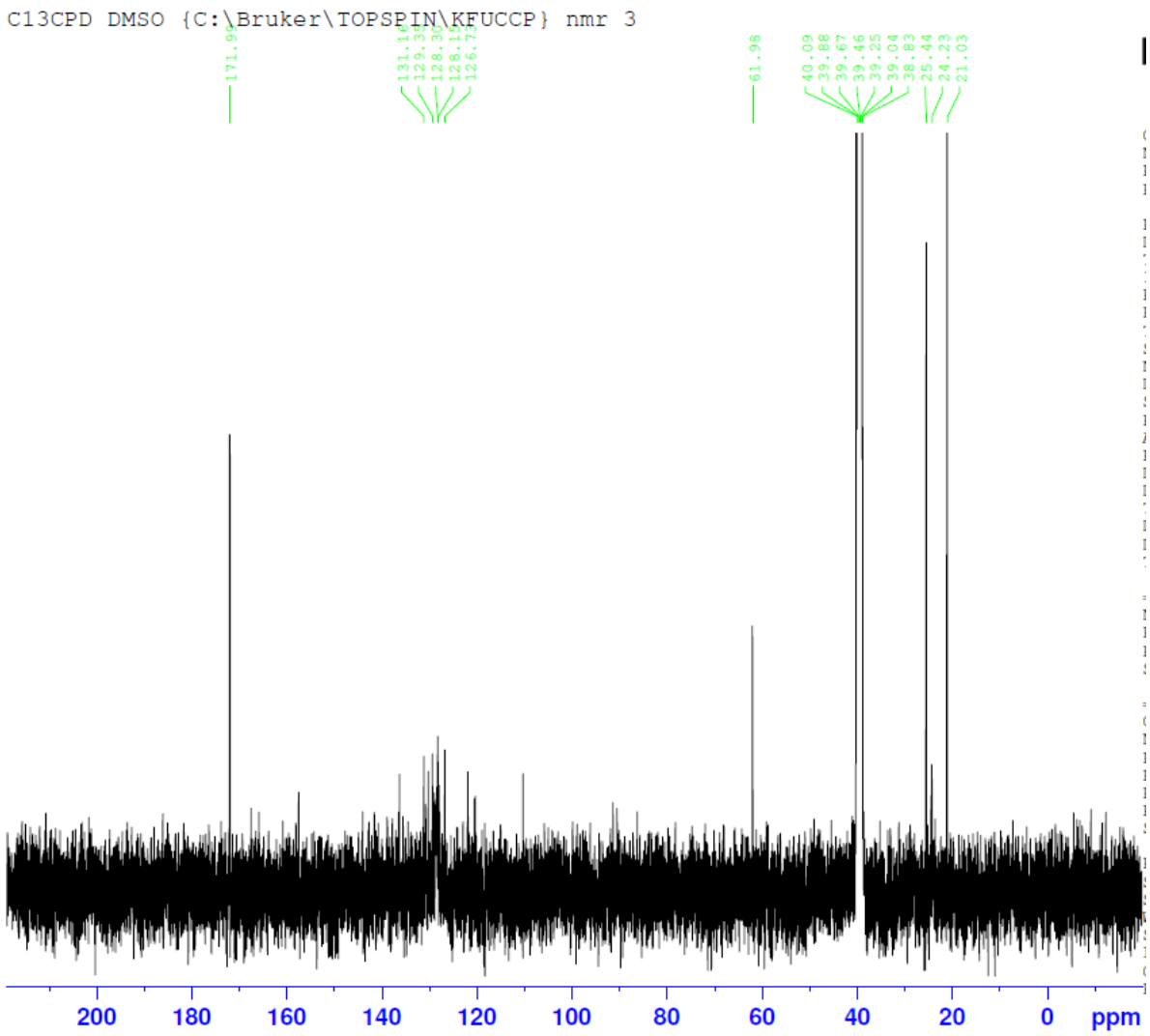

Figure S18: ^{13}C-NMR of (*E*)-6,8-Dichloro-3-(2-((4-chlorobenzylidene) amino) thiazol-4-yl)-2*H*-chromen-2-one (SVM 3)

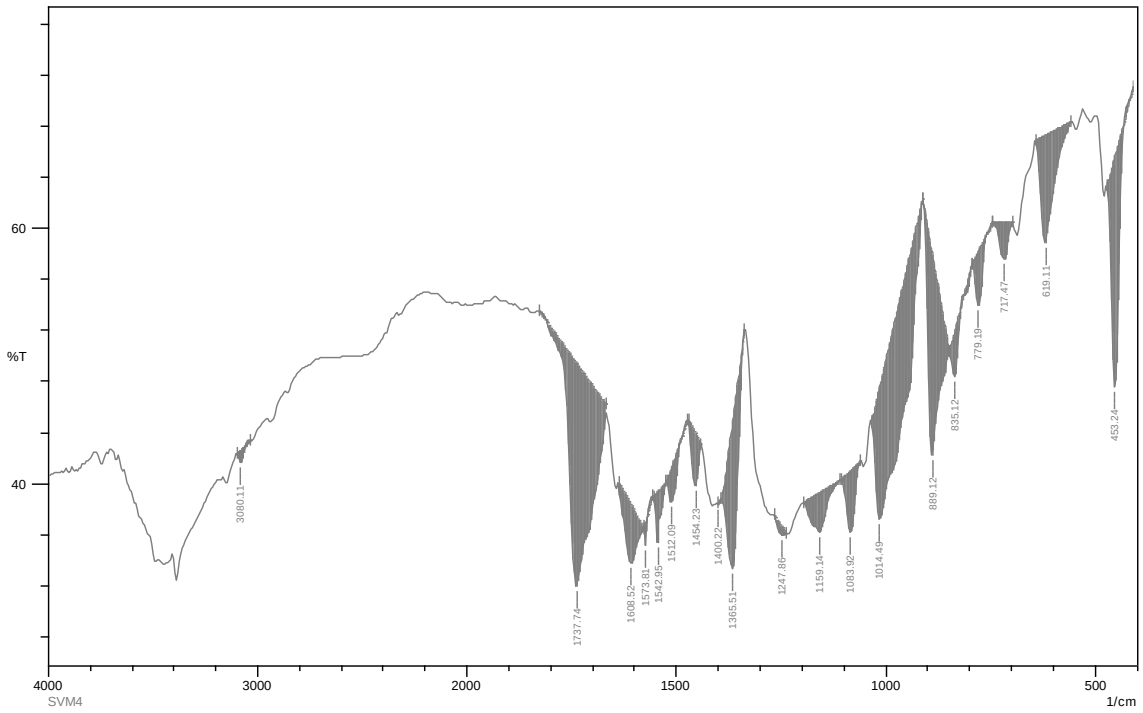

Figure S19: FT-IR of (*E*)-6,8-dichloro-3-(2-((4-fluorobenzylidene) amino) thiazol-4-yl)-2*H*-chromen-2-one (SVM 4)

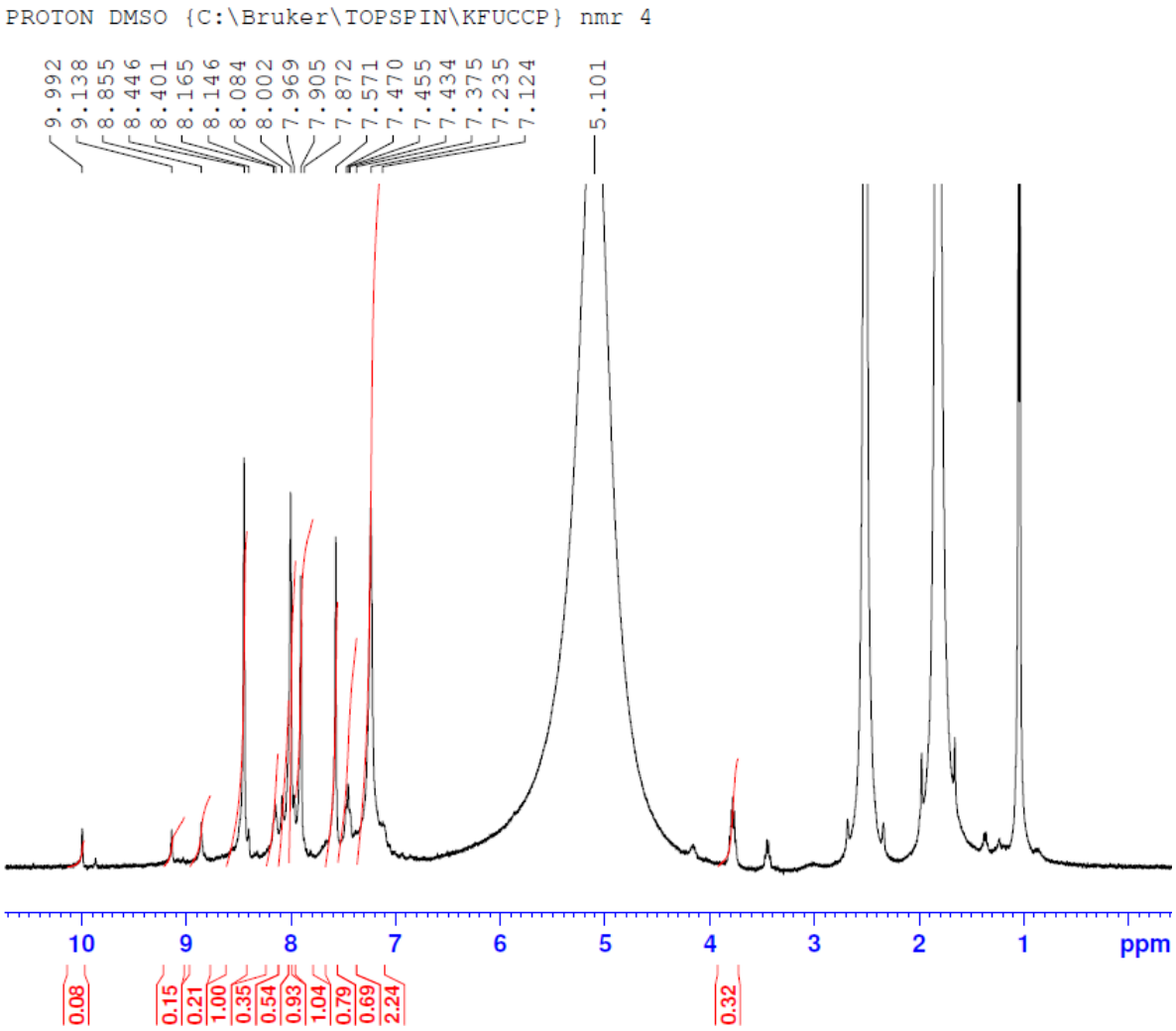

Figure S20: ^{1}H-NMR of (*E*)-6,8-dichloro-3-(2-((4-fluorobenzylidene) amino) thiazol-4-yl)-2*H*-chromen-2-one (SVM 4)

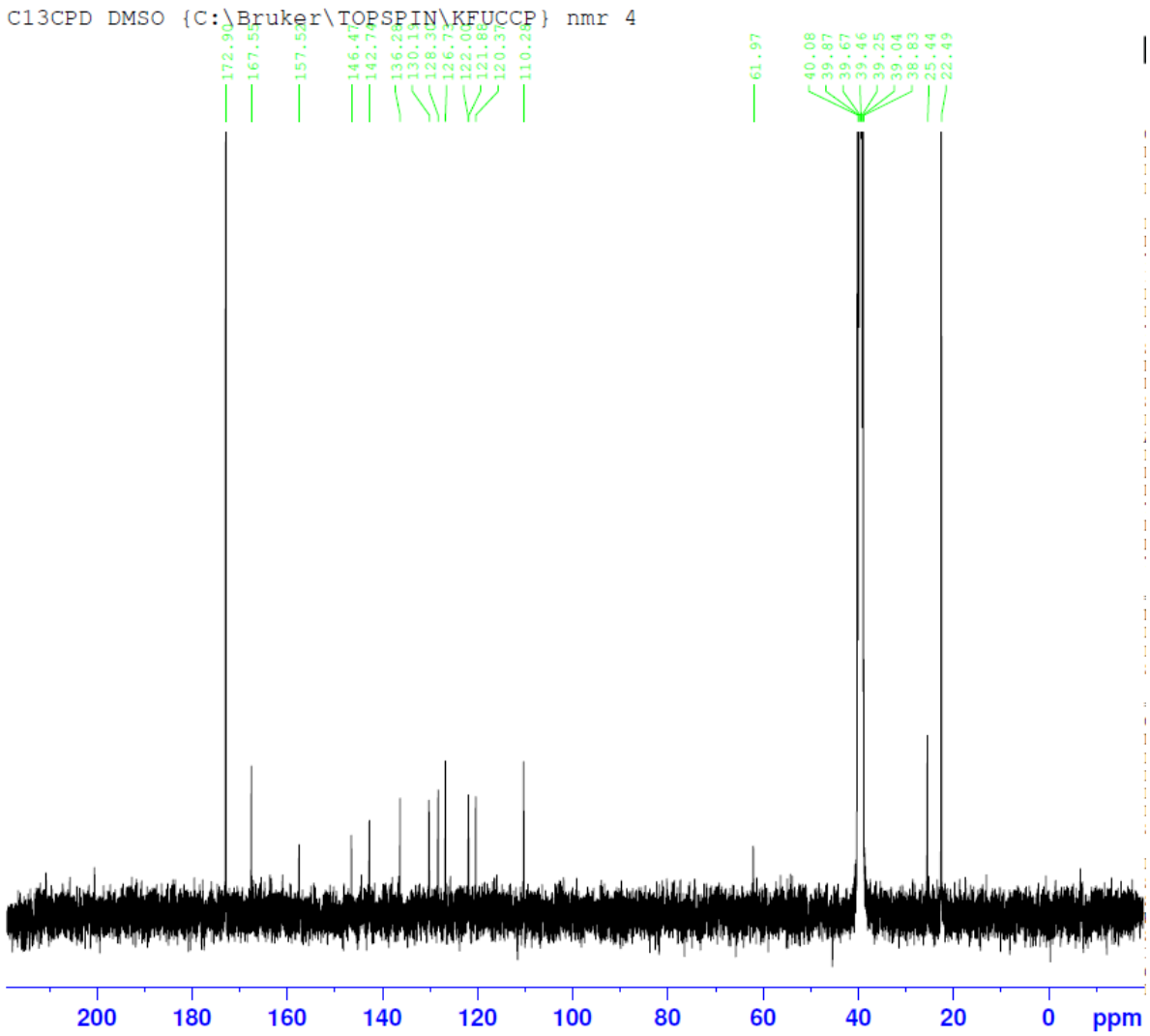

Figure S21: ^{13}C-NMR of (*E*)-6,8-dichloro-3-(2-((4-fluorobenzylidene) amino) thiazol-4-yl)-2*H*-chromen-2-one (SVM 4)

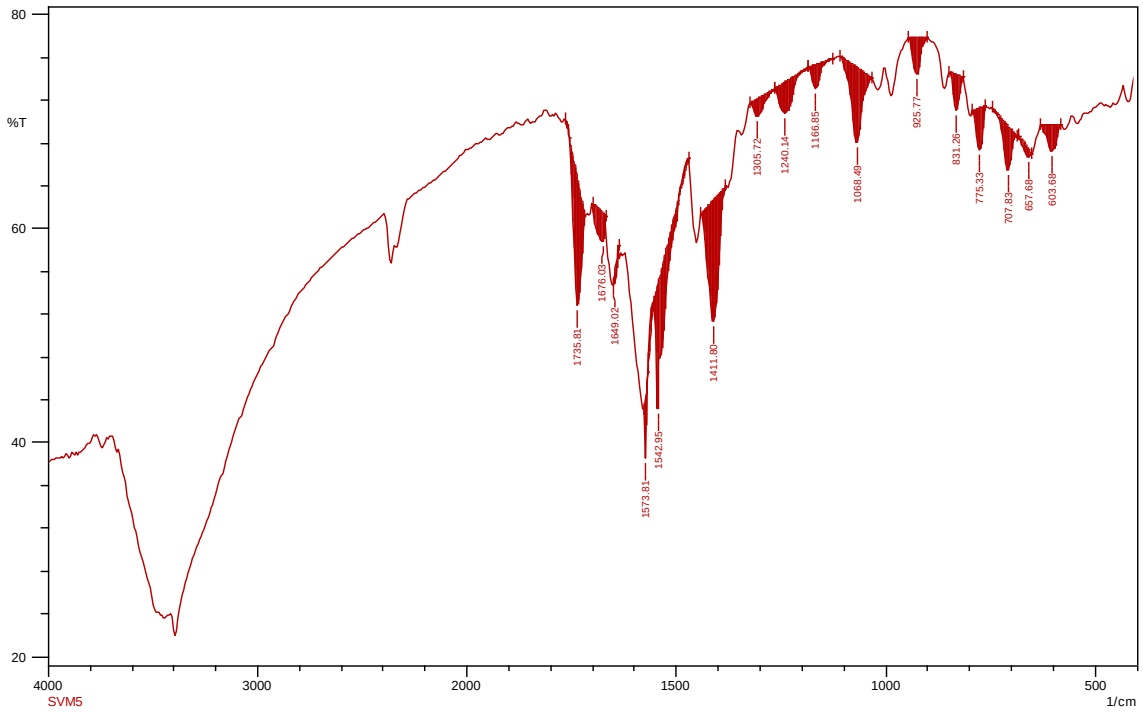

Figure S22: FT-IR of (*E*)-6,8-dichloro-3-(2-((thiophen-2-ylmethylene) amino) thiazol-4-yl)-2*H*-chromen-2-one (SVM 5)

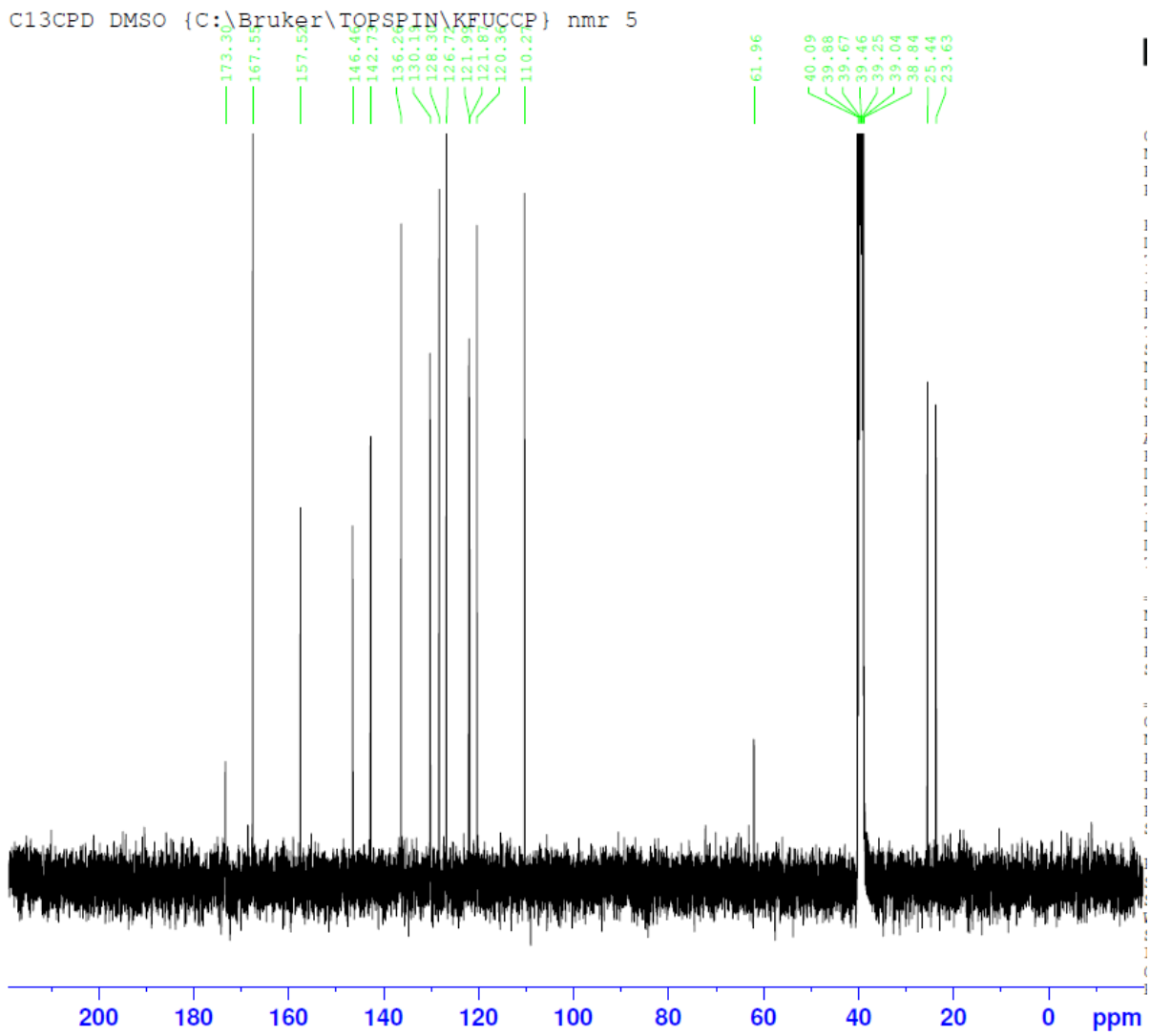

Figure S23: ^{1}H-NMR of (*E*)-6,8-dichloro-3-(2-((thiophen-2-ylmethylene) amino) thiazol-4-yl)-2*H*-chromen-2-one (SVM 5)

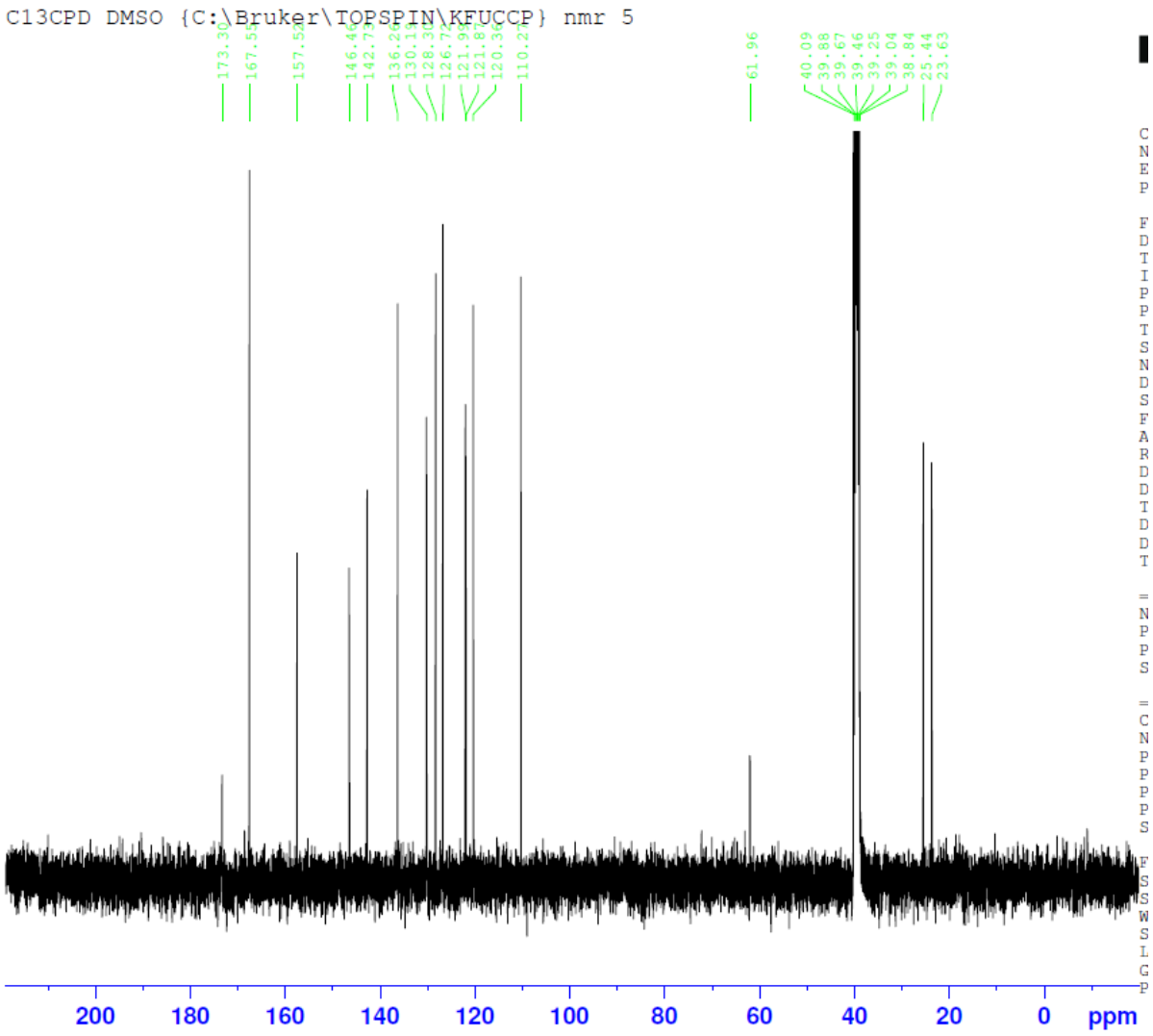

Figure S24: ^{13}C-NMR of (*E*)-6,8-dichloro-3-(2-((thiophen-2-ylmethylene) amino) thiazol-4-yl)-2*H*-chromen-2-one (SVM 5)

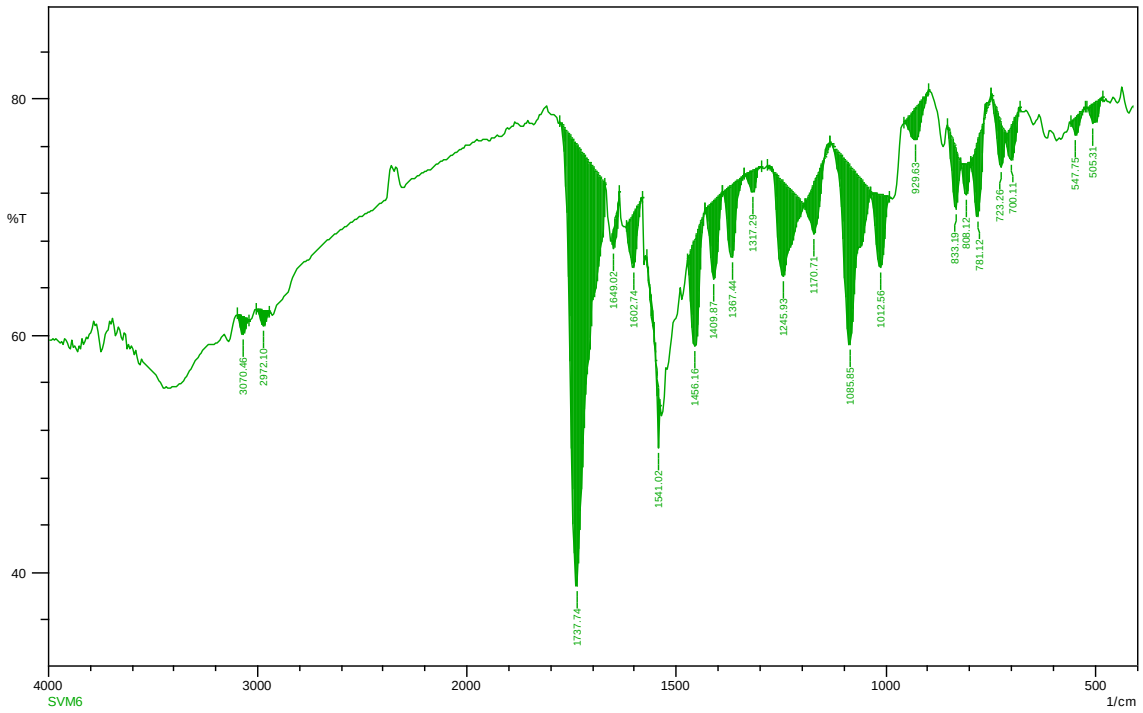

Figure S25: FT-IR of (*E*)-6,8-dichloro-3-(2-((pyridin-4-ylmethylene) amino) thiazol-4-yl)-2*H*-chromen-2-one (SVM 6)

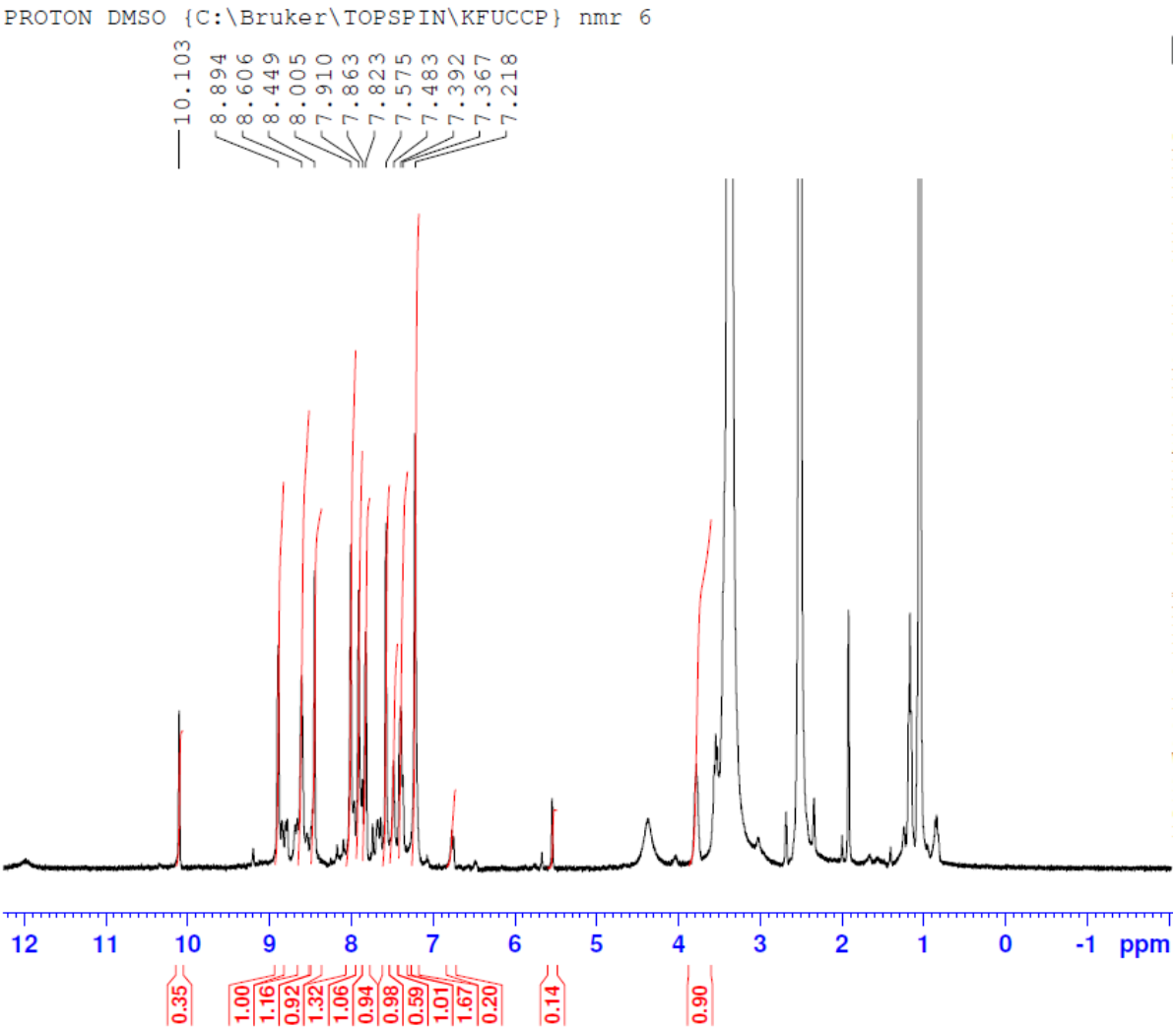

Figure S26: ^{1}H-NMR of (*E*)-6,8-dichloro-3-(2-((pyridin-4-ylmethylene) amino) thiazol-4-yl)-2*H*-chromen-2-one (SVM 6)

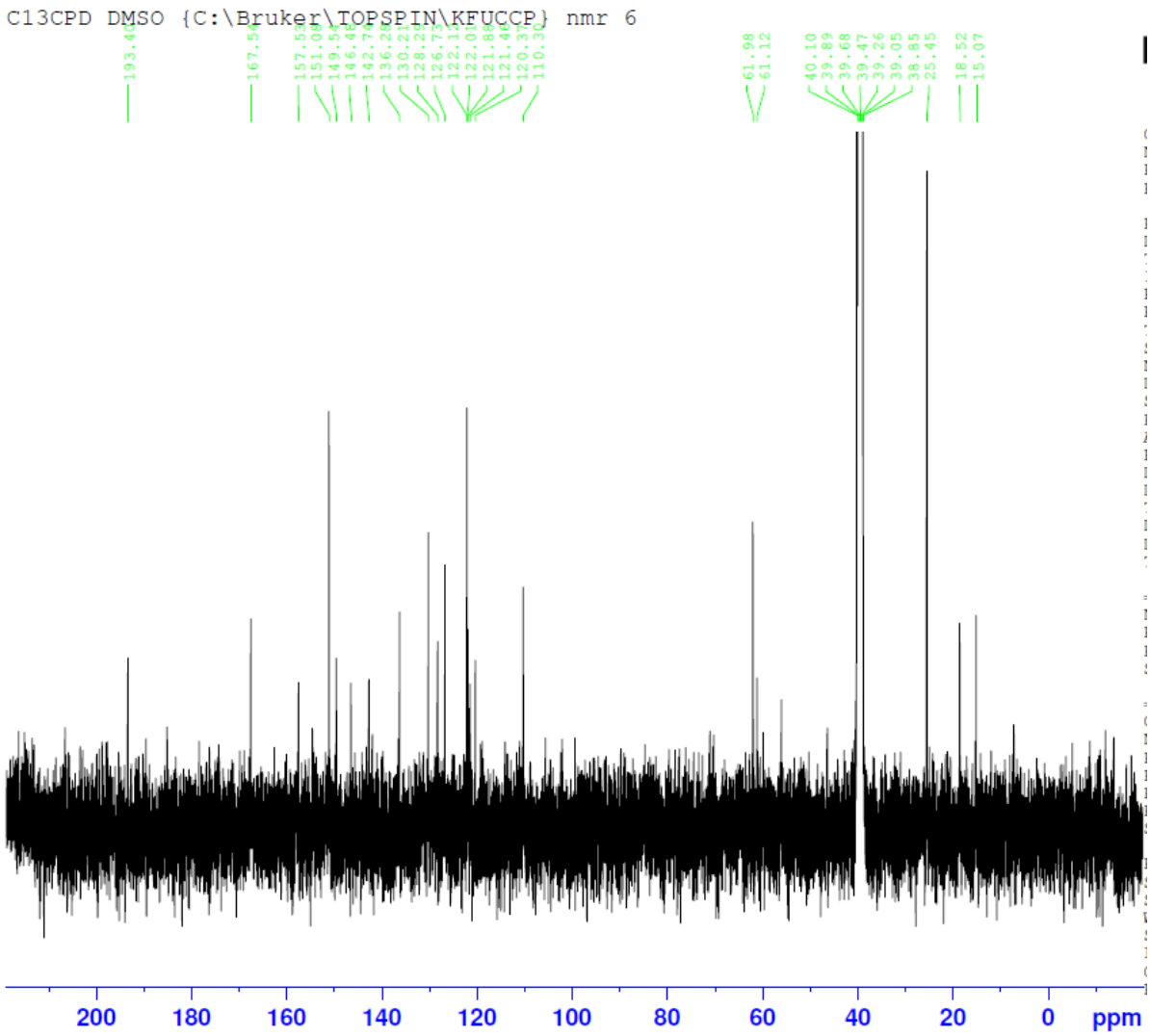

Figure S27: ^{13}C-NMR of (*E*)-6,8-dichloro-3-(2-((pyridin-4-ylmethylene) amino) thiazol-4-yl)-2*H*-chromen-2-one (SVM 6)

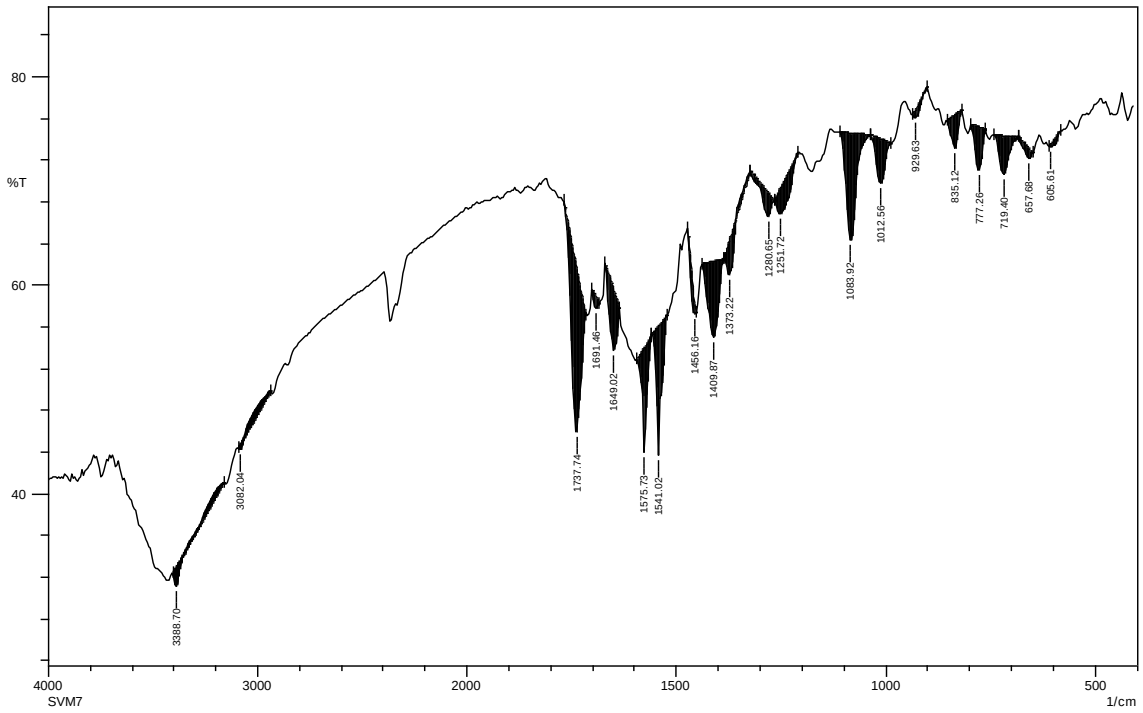

Figure S28: FT-IR of (*E*)-6,8-dichloro-3-(2-((2-hydroxybenzylidene) amino) thiazol-4-yl)-2*H*-chromen-2-one (SVM 7)

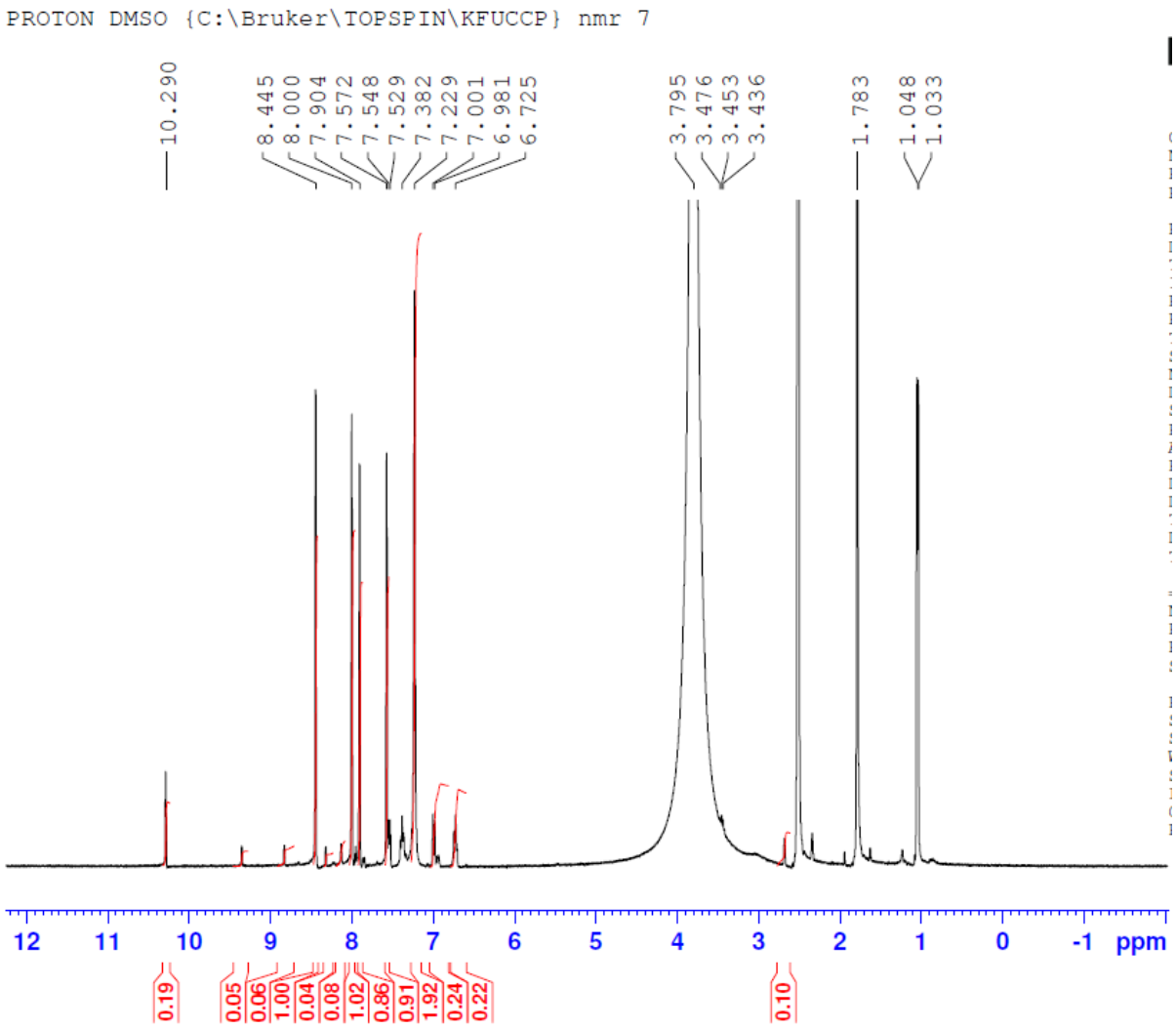

Figure S29: ^{1}H-NMR of (*E*)-6,8-dichloro-3-(2-((2-hydroxybenzylidene) amino) thiazol-4-yl)-2*H*-chromen-2-one (SVM 7)

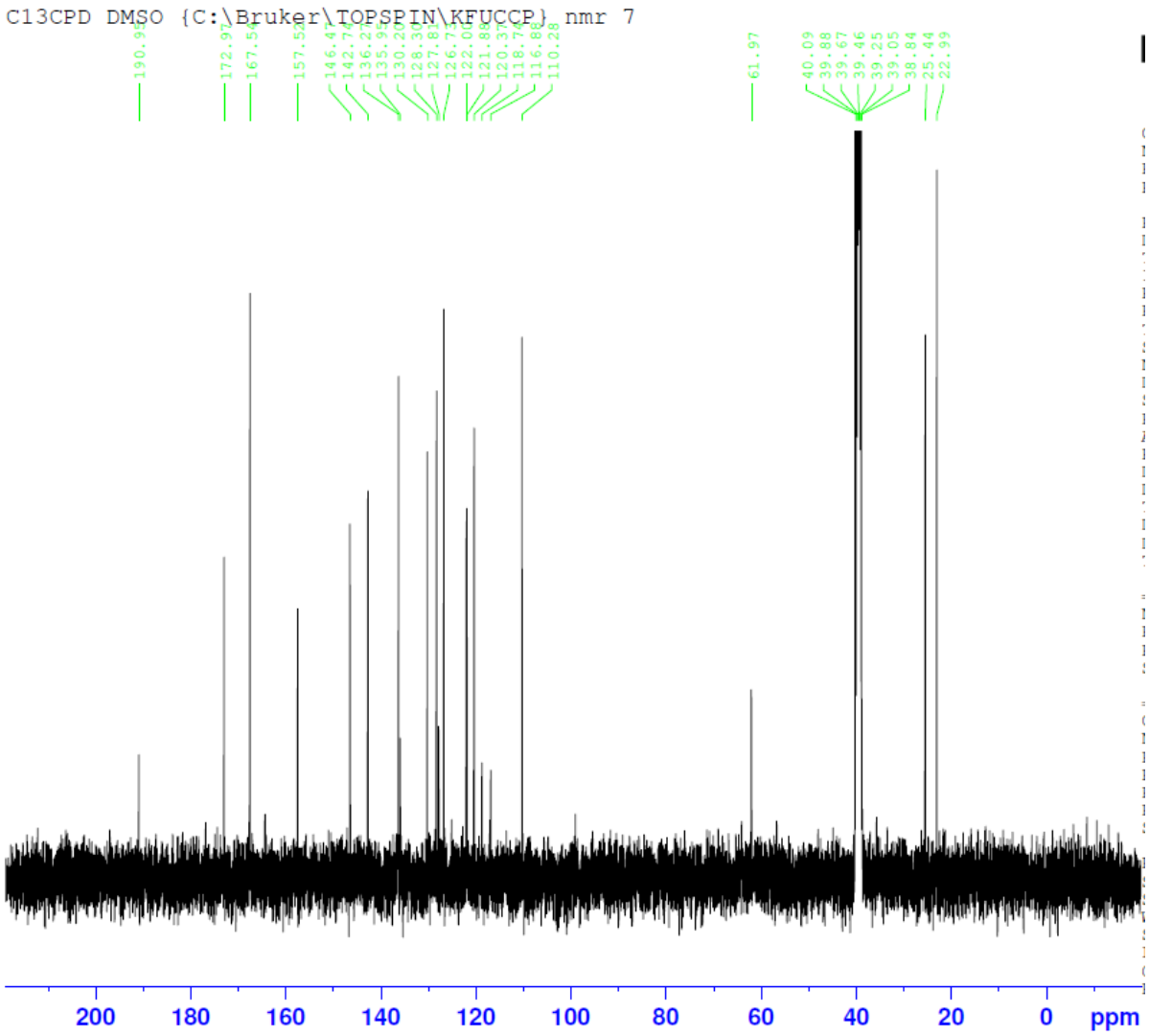

Figure S30: ^{13}C-NMR of (*E*)-6,8-dichloro-3-(2-((2-hydroxybenzylidene) amino) thiazol-4-yl)-2*H*-chromen-2-one (SVM 7)

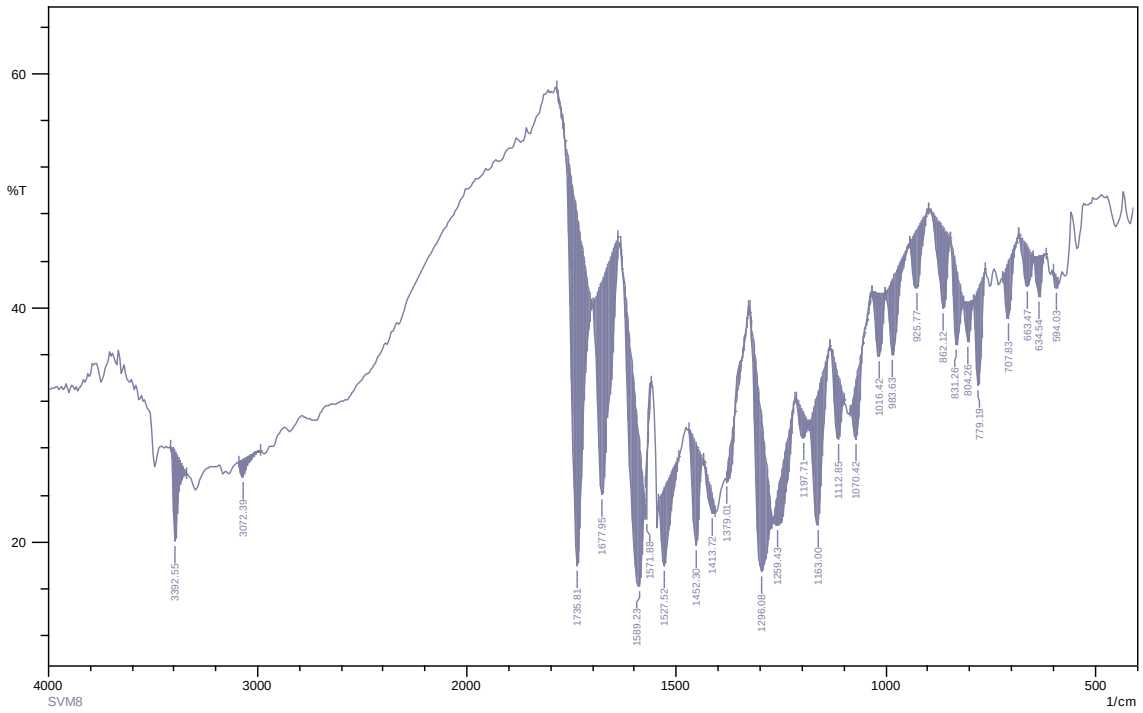

Figure S31: FT-IR of (*E*)-6,8-dichloro-3-(2-((3,4-dihydroxybenzylidene) amino) thiazol-4-yl)-2*H*-chromen-2-one (SVM 8)

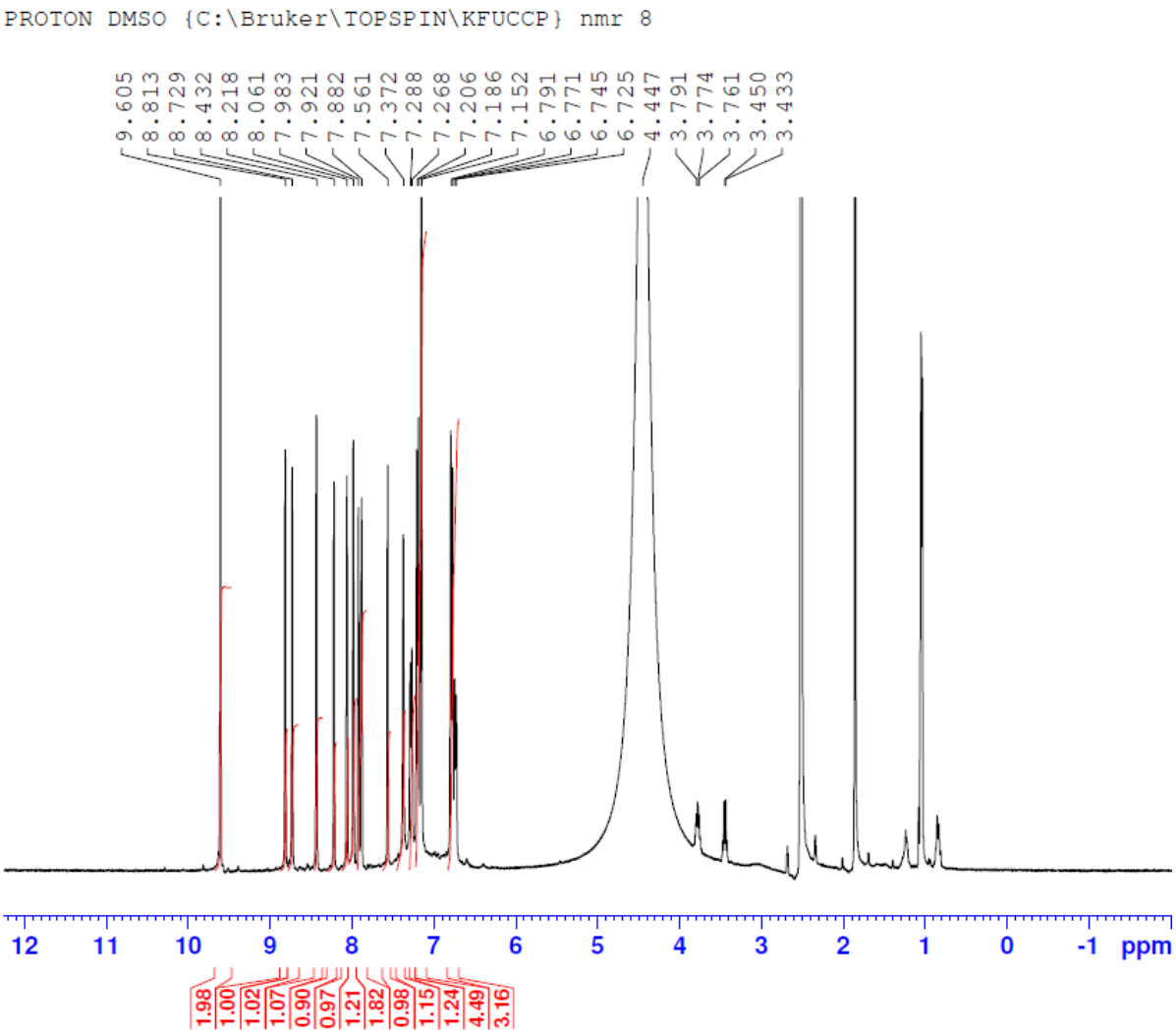

Figure S32: ^{1}H-NMR of (*E*)-6,8-dichloro-3-(2-((3,4-dihydroxybenzylidene) amino) thiazol-4-yl)-2*H*-chromen-2-one (SVM 8)

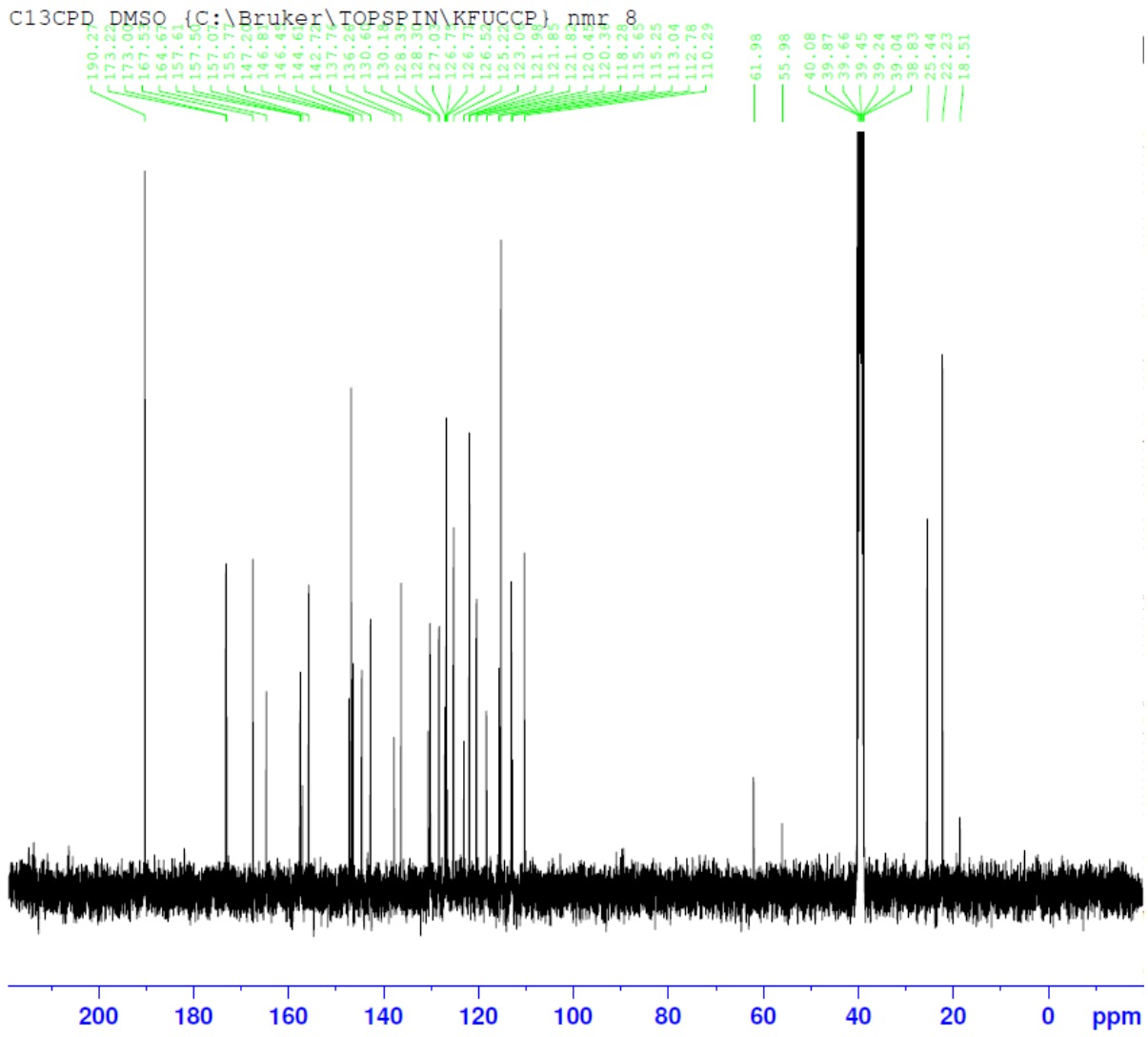

Figure S33: ^{13}C-NMR of (*E*)-6,8-dichloro-3-(2-((3,4-dihydroxybenzylidene) amino) thiazol-4-yl)-2*H*-chromen-2-one (SVM 8)

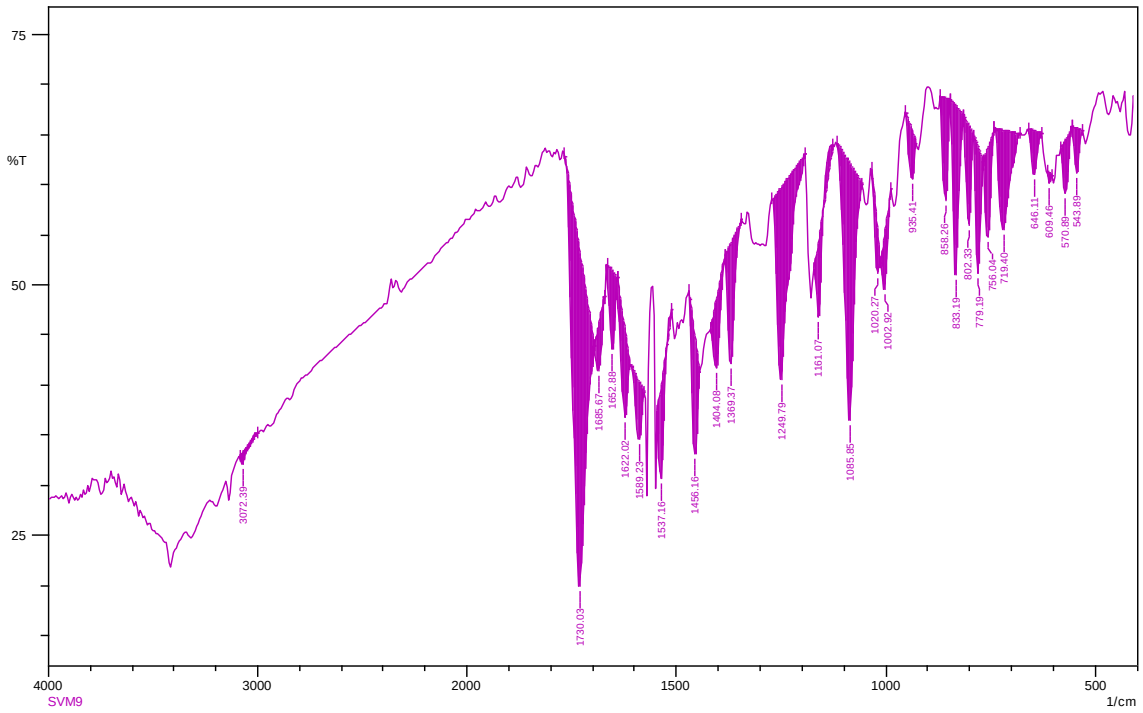

Figure S34: FT-IR of (*E*)-6,8-dichloro-3-(2-((2-methoxybenzylidene) amino) thiazol-4-yl)-2*H*-chromen-2-one (SVM 9)

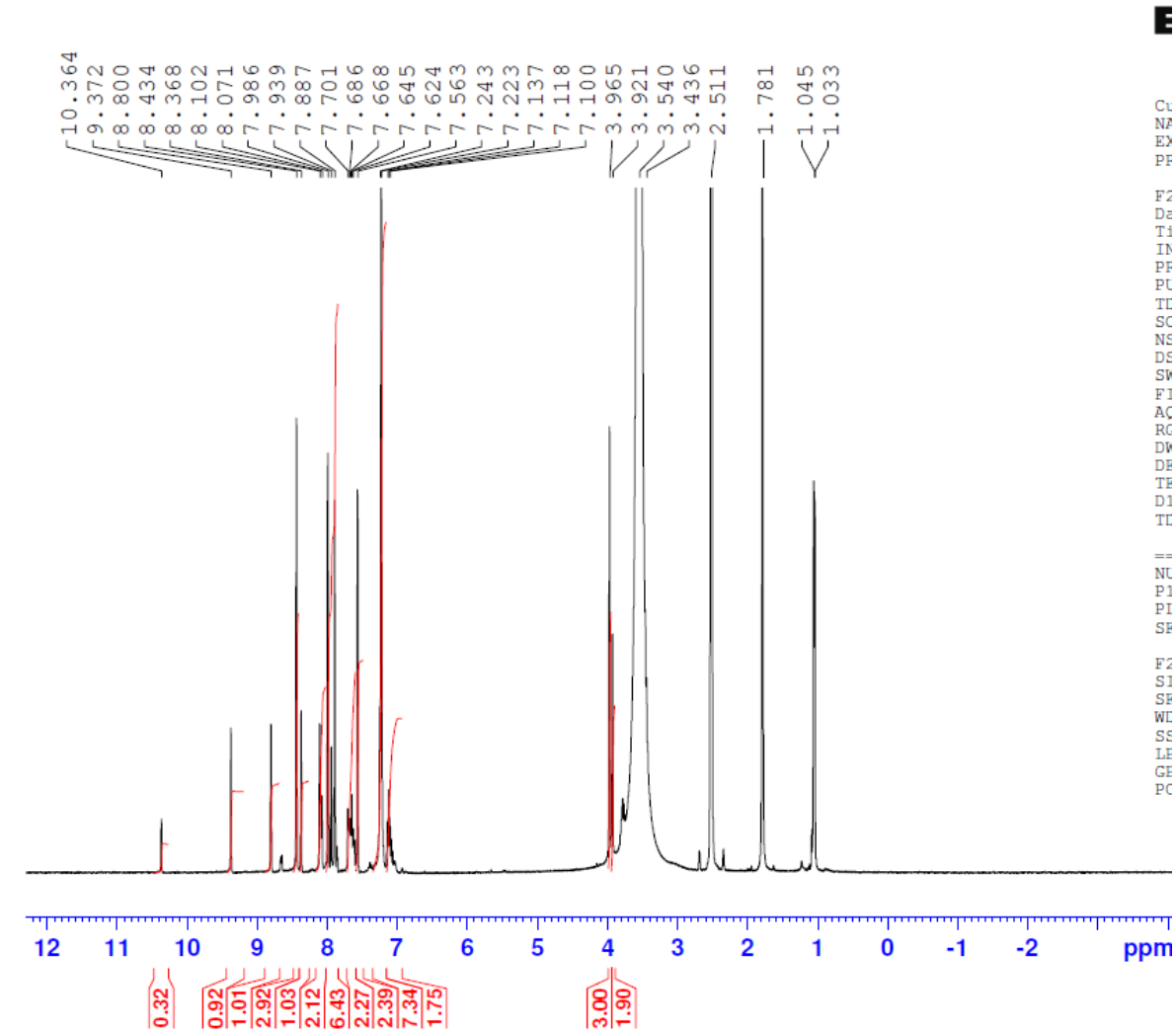

Figure S35: ^{1}H-NMR of (*E*)-6,8-dichloro-3-(2-((2-methoxybenzylidene) amino) thiazol-4-yl)-2*H*-chromen-2-one (SVM 9)

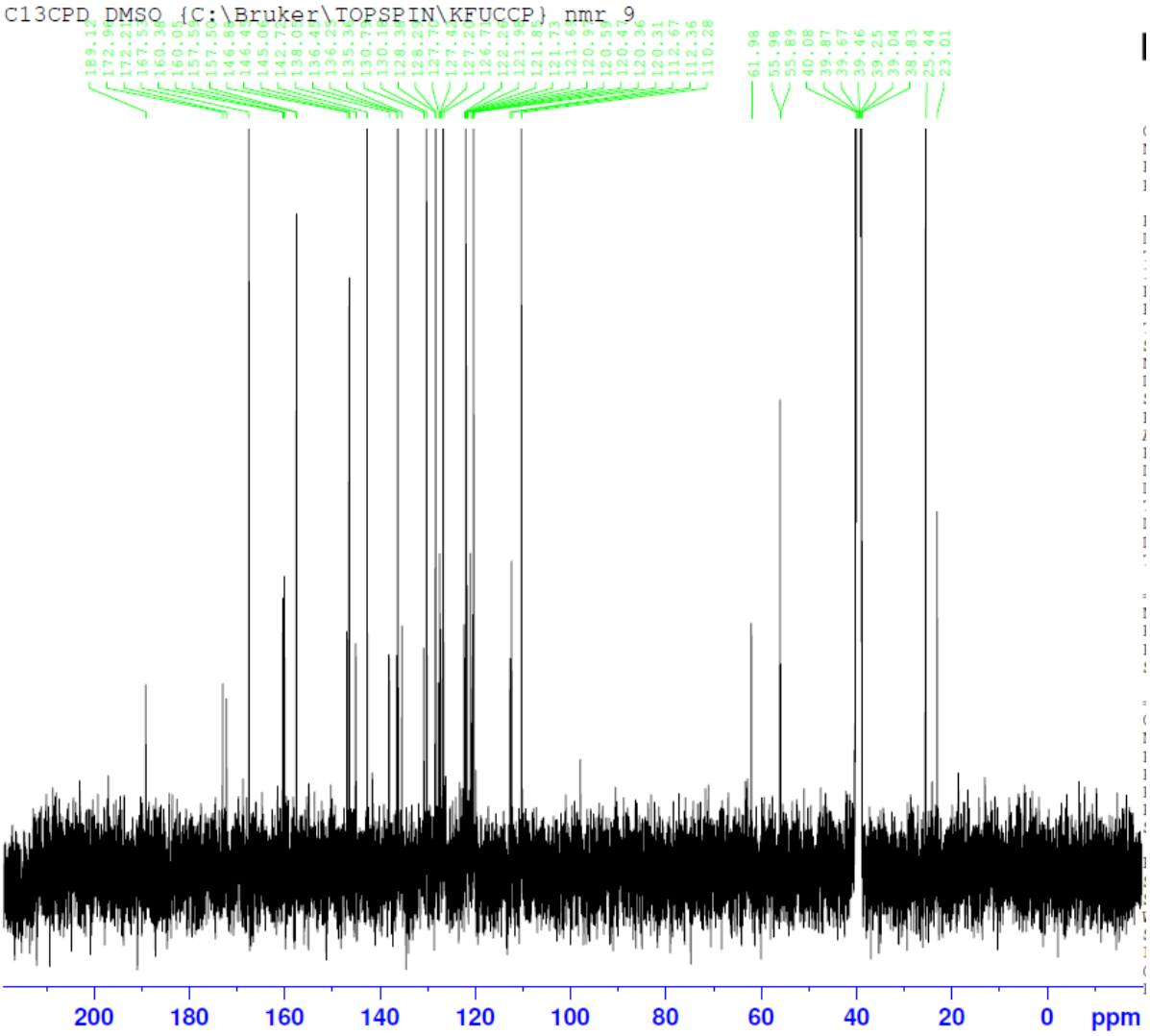

Figure S36: ^{13}C-NMR of (*E*)-6,8-dichloro-3-(2-((2-methoxybenzylidene) amino) thiazol-4-yl)-2*H*-chromen-2-one (SVM 9)

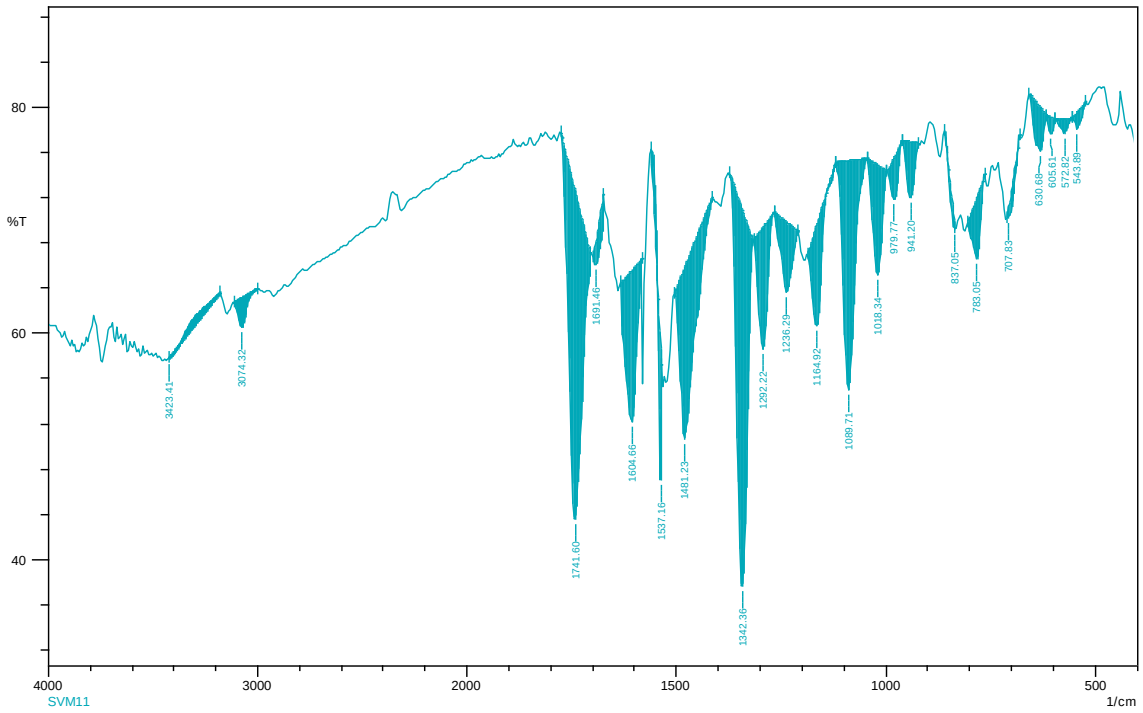

Figure S37: FT-IR of (*E*)-6,8-dichloro-3-(2-((2-hydroxy-5 nitro benzylidene) amino) thiazol-4-yl)-2*H*-chromen-2-one (SVM 10)

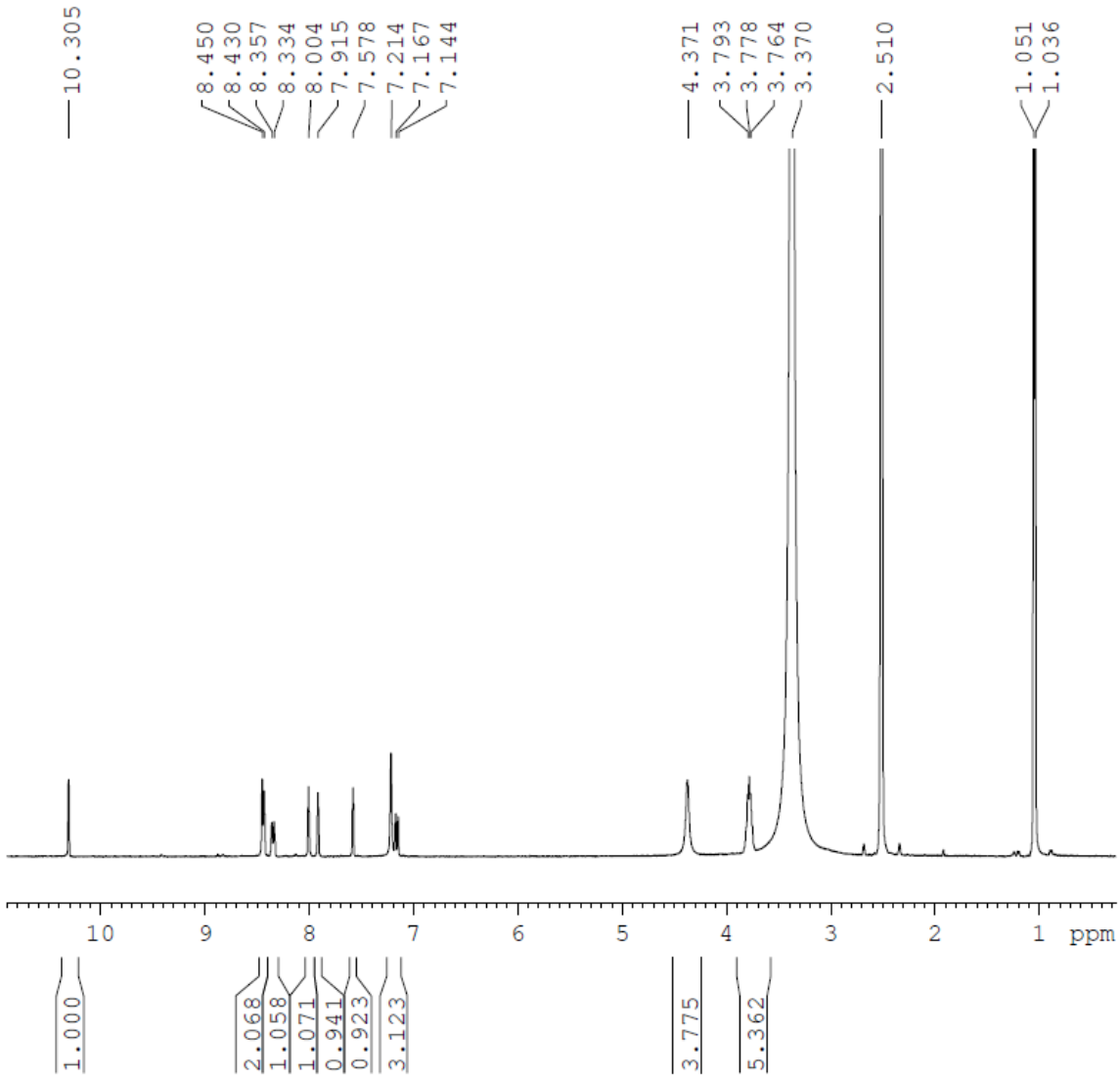

Figure S38: ^{1}H-NMR of (*E*)-6,8-dichloro-3-(2-((2-hydroxy-5 nitro benzylidene) amino) thiazol-4-yl)-2*H*-chromen-2-one (SVM 10)

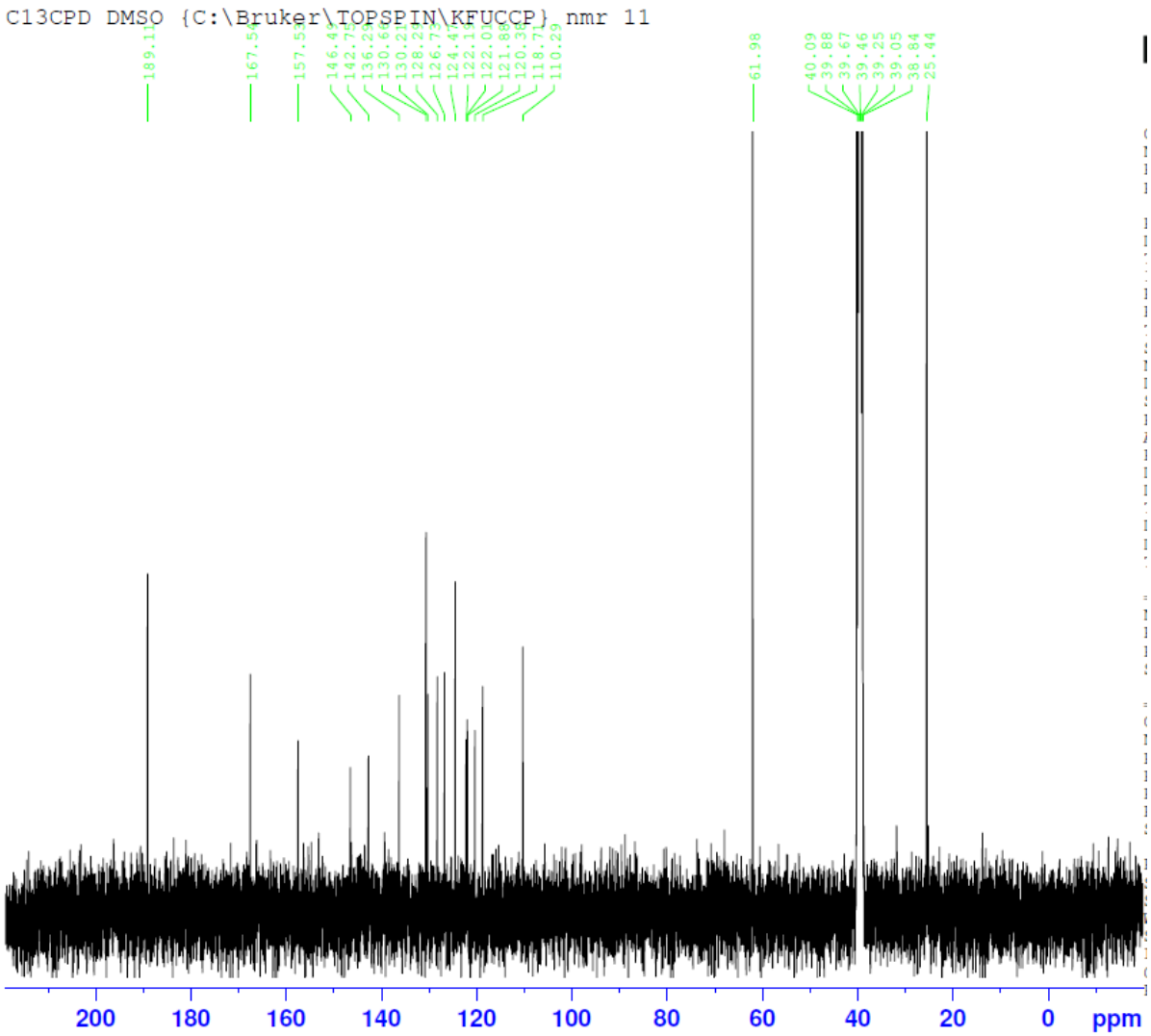

Figure S39: ^{13}C-NMR of (*E*)-6,8-dichloro-3-(2-((2-hydroxy-5 nitro benzylidene) amino) thiazol-4-yl)-2*H*-chromen-2-one (SVM 10)

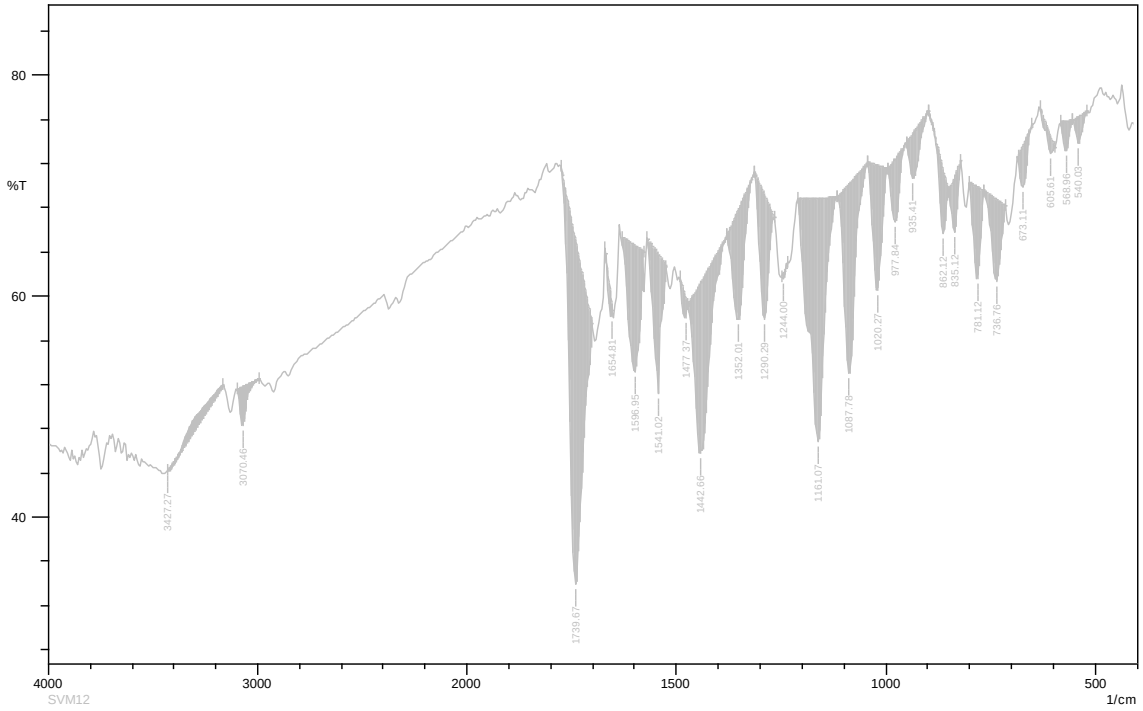

Figure S40: FT-IR of (*E*)-6,8-dichloro-3-(2-((3,5-dichloro 2-hydroxybenzylidene) amino) thiazol-4-yl)-2*H*-chromen-2-one (SVM 11)

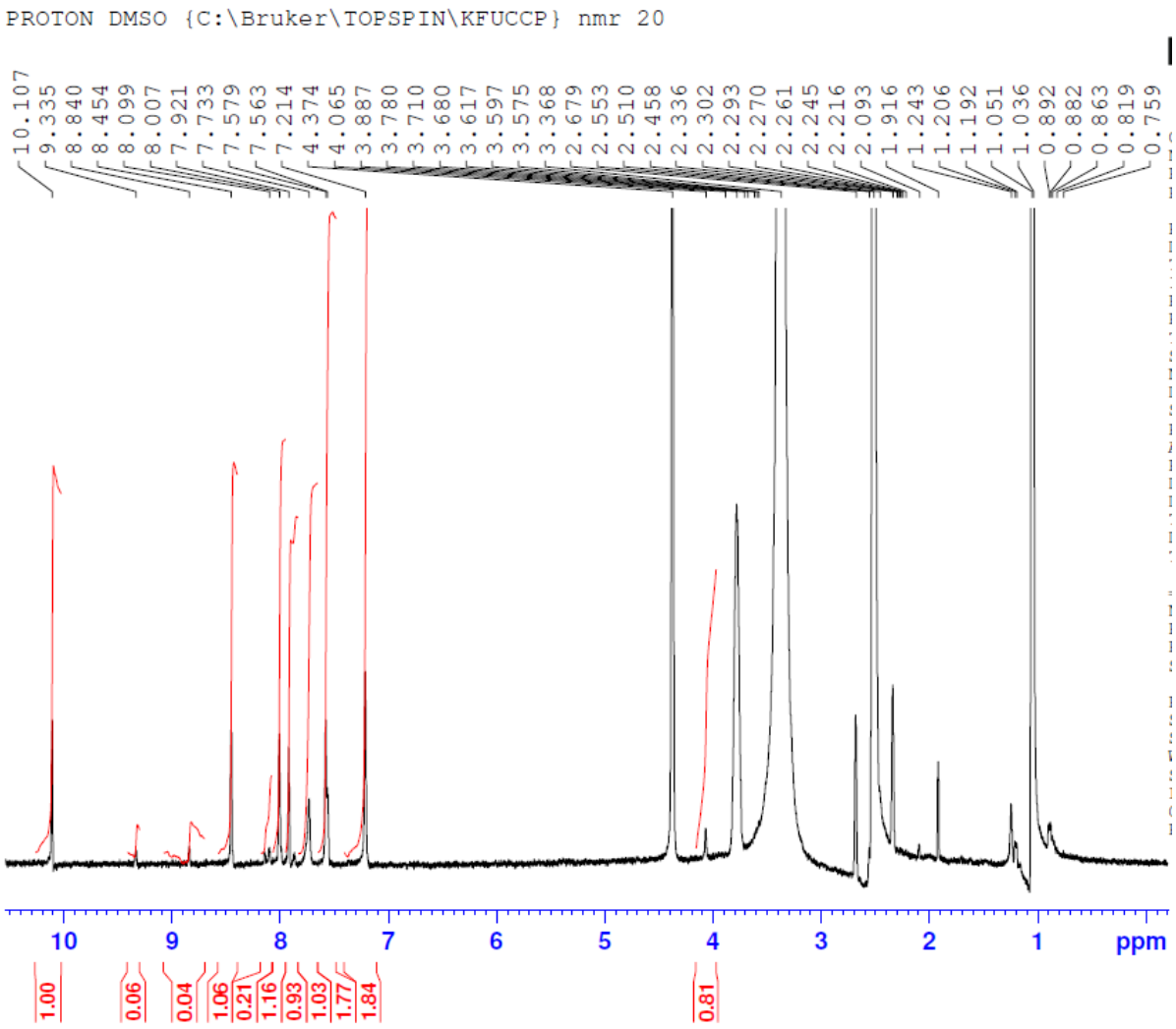

Figure S41: ^{1}H-NMR of (*E*)-6,8-dichloro-3-(2-((3,5-dichloro 2-hydroxybenzylidene) amino) thiazol-4-yl)-2*H*-chromen-2-one (SVM 11)

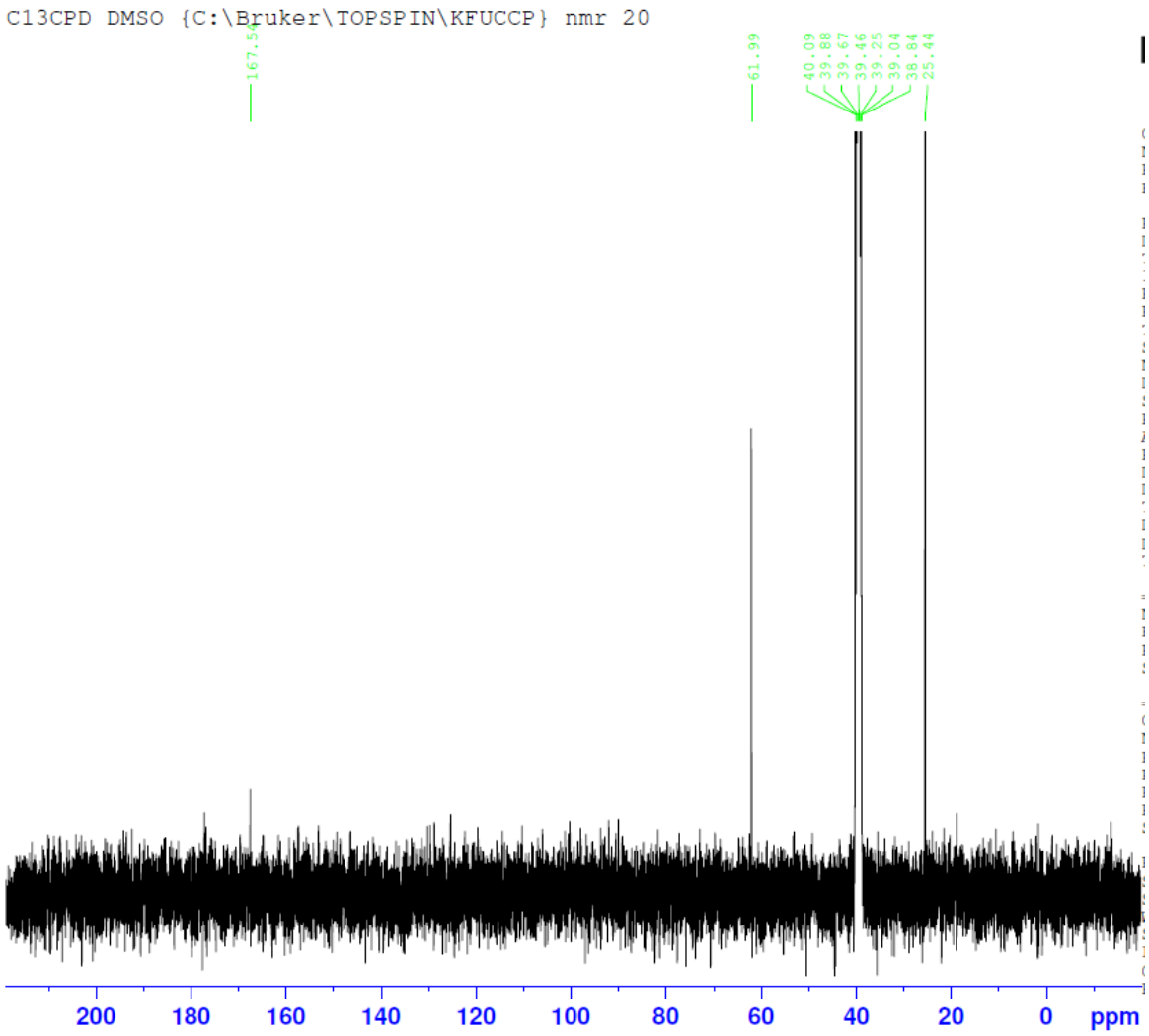

Figure S42: ^{13}C-NMR of (*E*)-6,8-dichloro-3-(2-((3,5-dichloro 2-hydroxybenzylidene) amino) thiazol-4-yl)-2*H*-chromen-2-one (SVM 11)

APPENDIX 3

Sl. No.	IUPAC name	
43.	Figure S1: FT-IR of 3-acetyl-6-nitro-2*H*-chromen-2-one (SVN i1)	
44.	Figure S2: ^{1}H-NMR of 3-acetyl-6-nitro-2*H*-chromen-2-one (SVN i1)	
45.	Figure S3: ^{13}C-NMR of 3-acetyl-6-nitro-2*H*-chromen-2-one (SVN i1)	
46.	Figure S4: FT-IR of 3-(2-bromoacetyl)-6-nitro-2*H*-chromen-2-one (SVN i2)	
47.	Figure S5: ^{1}H-NMR of 3-(2-bromoacetyl)-6-nitro-2*H*-chromen-2-one (SVN i2)	
48.	Figure S6: ^{13}C-NMR of 3-(2-bromoacetyl)-6-nitro-2*H*-chromen-2-one (SVN i2)	
49.	Figure S7: FT-IR of 3-(2-aminothiazol-4-yl)-6-nitro-2*H*-chromen-2-one (SVN i3)	
50.	Figure S8: ^{1}H-NMR of 3-(2-aminothiazol-4-yl)-6-nitro-2*H*-chromen-2-one (SVN i3)	
51.	Figure S9: ^{13}C-NMR of 3-(2-aminothiazol-4-yl)-6-nitro-2*H*-chromen-2-one (SVN i3)	
52.	Figure S10: FT-IR of (*E*)-3-(2-(benzylidene amino) thiazol-4-yl)-6-nitro-2*H*-chromen-2-one (SVN 1)	
53.	Figure S11: ^{1}H-NMR of (*E*)-3-(2-(benzylidene amino) thiazol-4-yl)-6-nitro-2*H*-chromen-2-one (SVN 1)	
54.	Figure S12: ^{13}C-NMR of (*E*)-3-(2-(benzylidene amino) thiazol-4-yl)-6-nitro-2*H*-chromen-2-one (SVN 1)	
55.	Figure S13: FT-IR of (*E*)-3-(2-((4-methoxybenzylidene) amino) thiazol-4-yl)-6-nitro-2*H*-chromen-2-one (SVN 2)	
56.	Figure S14: ^{1}H-NMR of (*E*)-3-(2-((4-methoxybenzylidene) amino) thiazol-4-yl)-6-nitro-2*H*-chromen-2-one (SVN 2)	
57.	Figure S15: ^{13}C-NMR of (*E*)-3-(2-((4-methoxybenzylidene) amino) thiazol-4-yl)-6-nitro-2*H*-chromen-2-one (SVN 2)	
58.	Figure S16: FT-IR of (*E*)-3-(2-((4-chlorobenzylidene) amino) thiazol-4-yl)-6-nitro-2*H*-chromen-2-one (SVN 3)	
59.	Figure S17: ^{1}H-NMR of (*E*)-3-(2-((4-chlorobenzylidene) amino) thiazol-4-yl)-6-nitro-2*H*-chromen-2-one (SVN 3)	
60.	Figure S18: ^{13}C-NMR of (*E*)-3-(2-((4-chlorobenzylidene) amino) thiazol-4-yl)-6-nitro-2*H*-chromen-2-one (SVN 3)	
61.	Figure S19: FT-IR of (*E*)-3-(2-((4-Fluorobenzylidene) amino) thiazol-4-yl)-6-nitro-2*H*-chromen-2-one (SVN 4)	
62.	Figure S20: ^{1}H-NMR of (*E*)-3-(2-((4-Fluorobenzylidene) amino) thiazol-4-yl)-6-nitro-2*H*-chromen-2-one (SVN 4)	
63.	Figure S21: ^{13}C-NMR of (*E*)-3-(2-((4-Fluorobenzylidene) amino) thiazol-4-yl)-6-nitro-2*H*-chromen-2-one (SVN 4)	

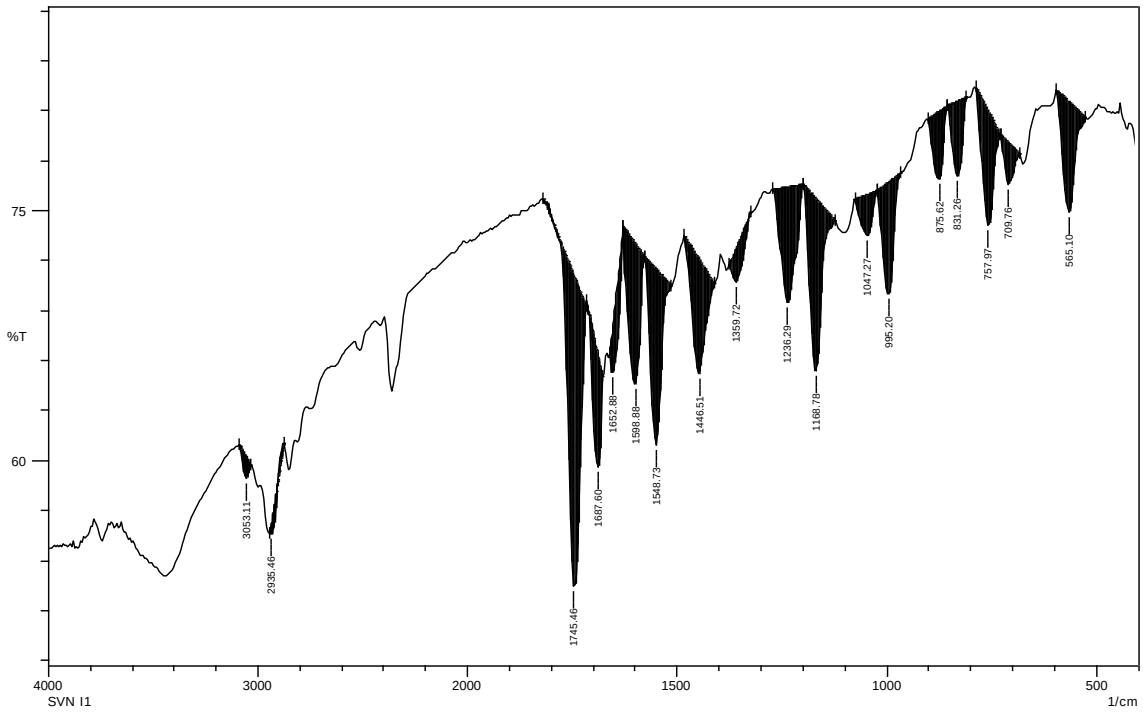

Figure S1: FT-IR of 3-acetyl-6-nitro-2*H*-chromen-2-one (SVN i1)

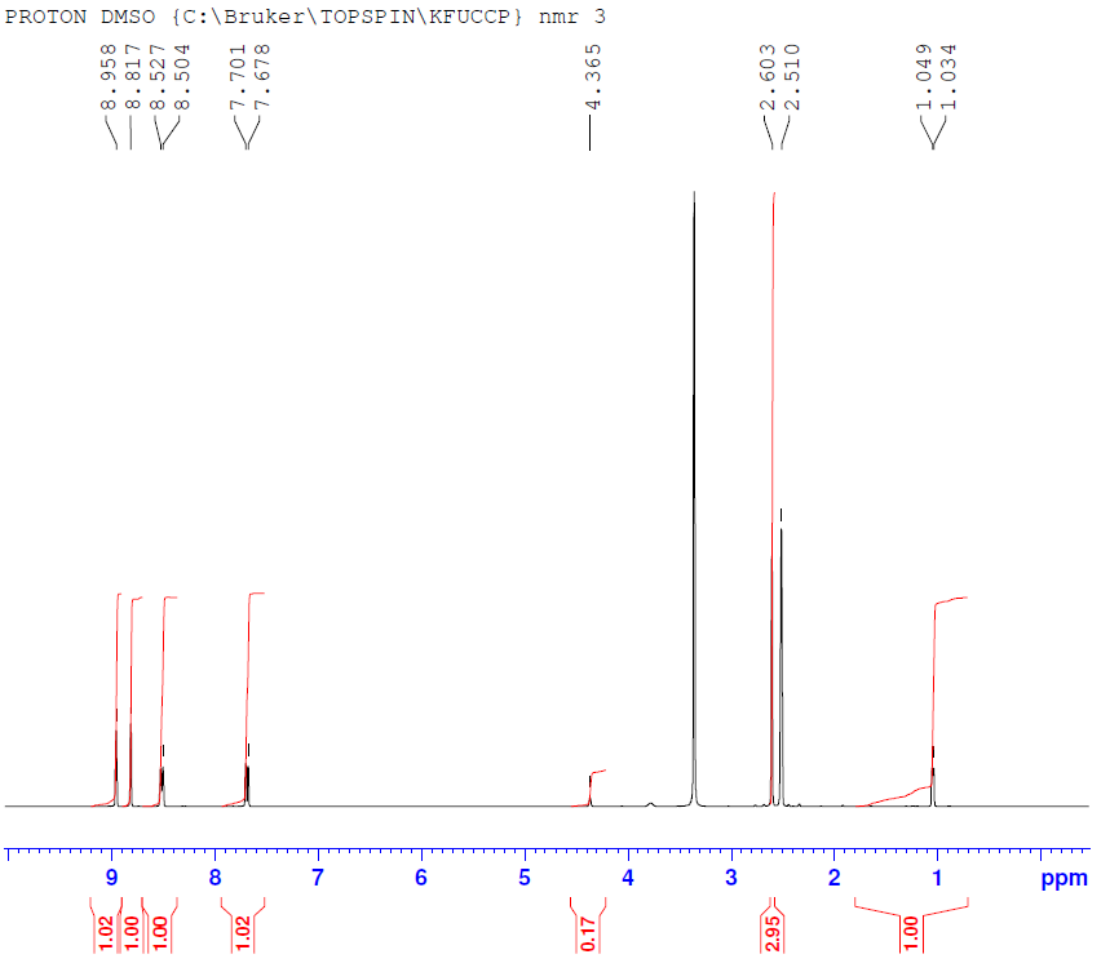

Figure S2: ^{1}H-NMR of 3-acetyl-6-nitro-2*H*-chromen-2-one (SVN i1)

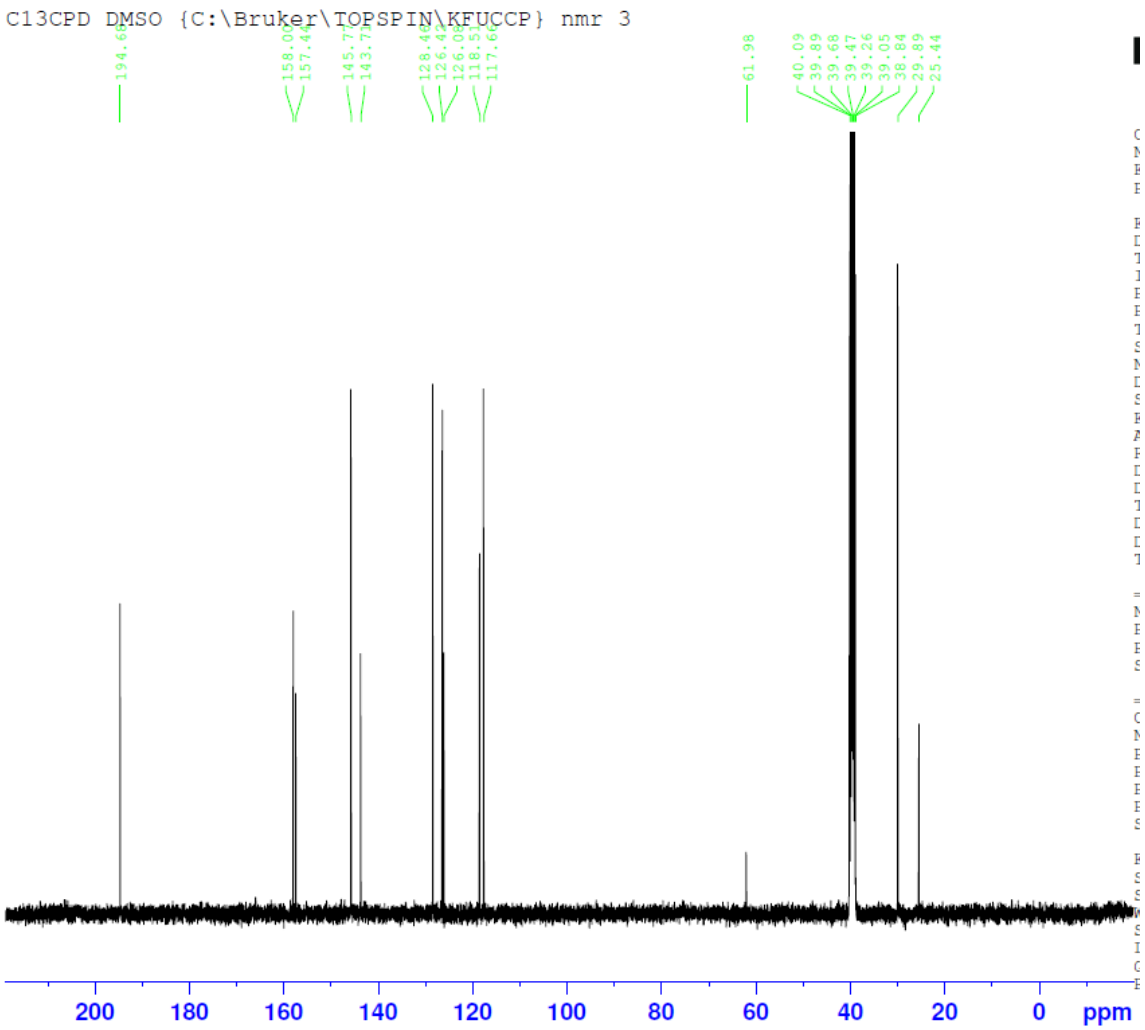

Figure S3: ^{13}C-NMR of 3-acetyl-6-nitro-2*H*-chromen-2-one (SVN i1)

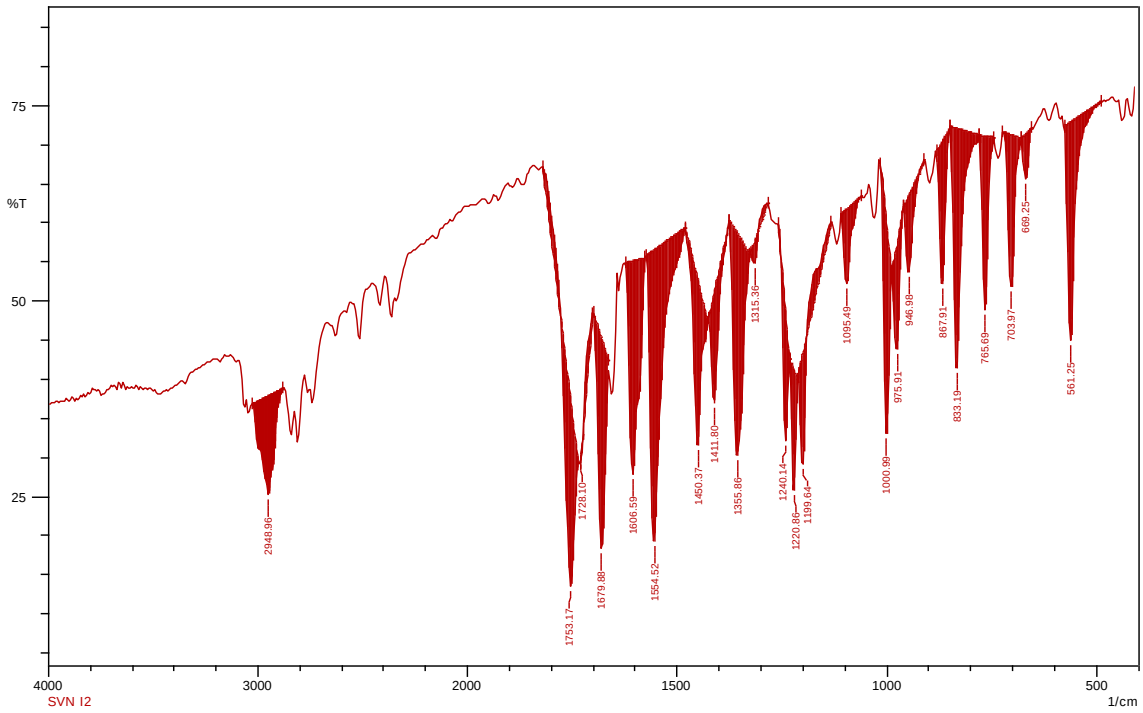

Figure S4: FT-IR of 3-(2-bromoacetyl)-6-nitro-2*H*-chromen-2-one (SVN i2)

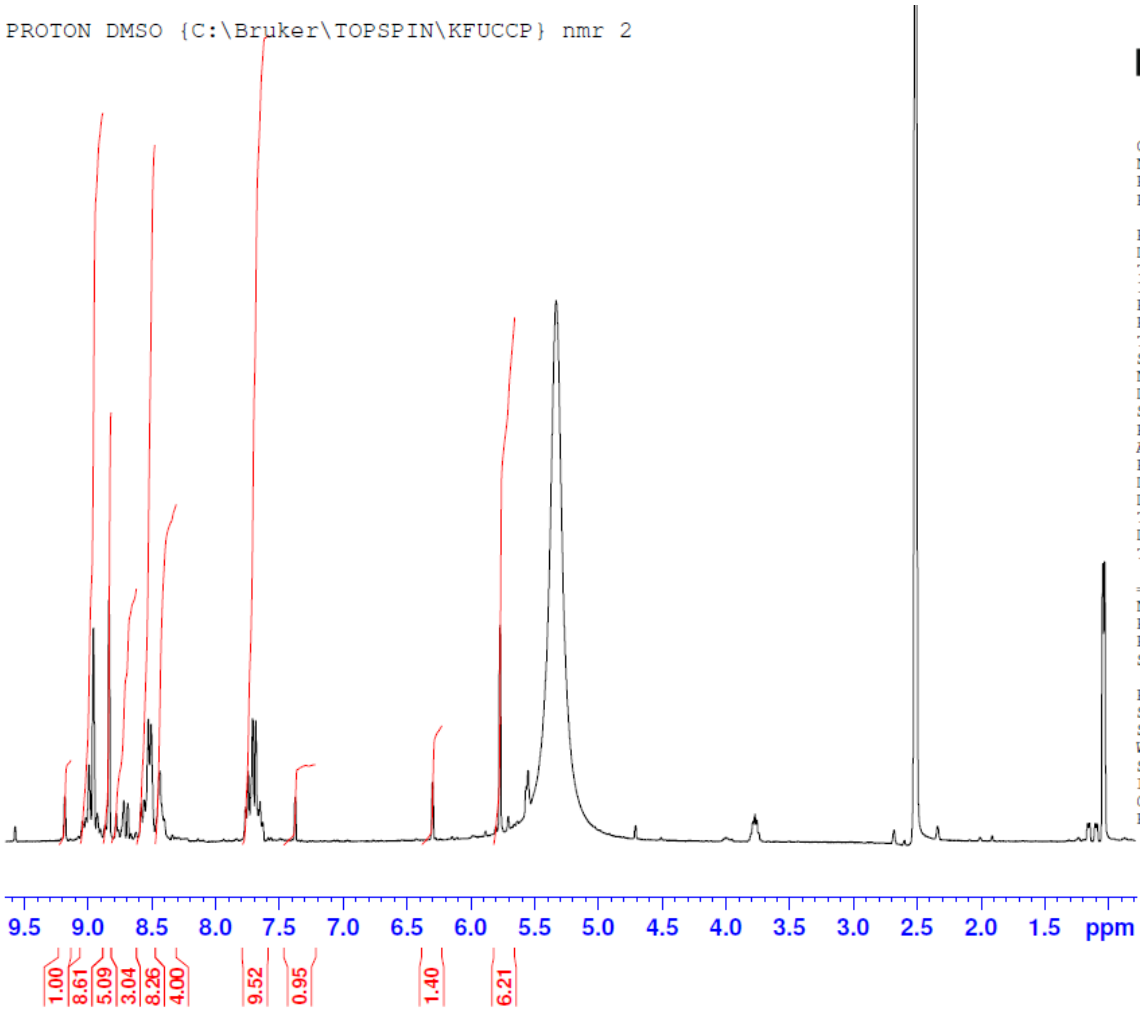

Figure S5: ^{1}H-NMR of 3-(2-bromoacetyl)-6-nitro-2*H*-chromen-2-one (SVN i2)

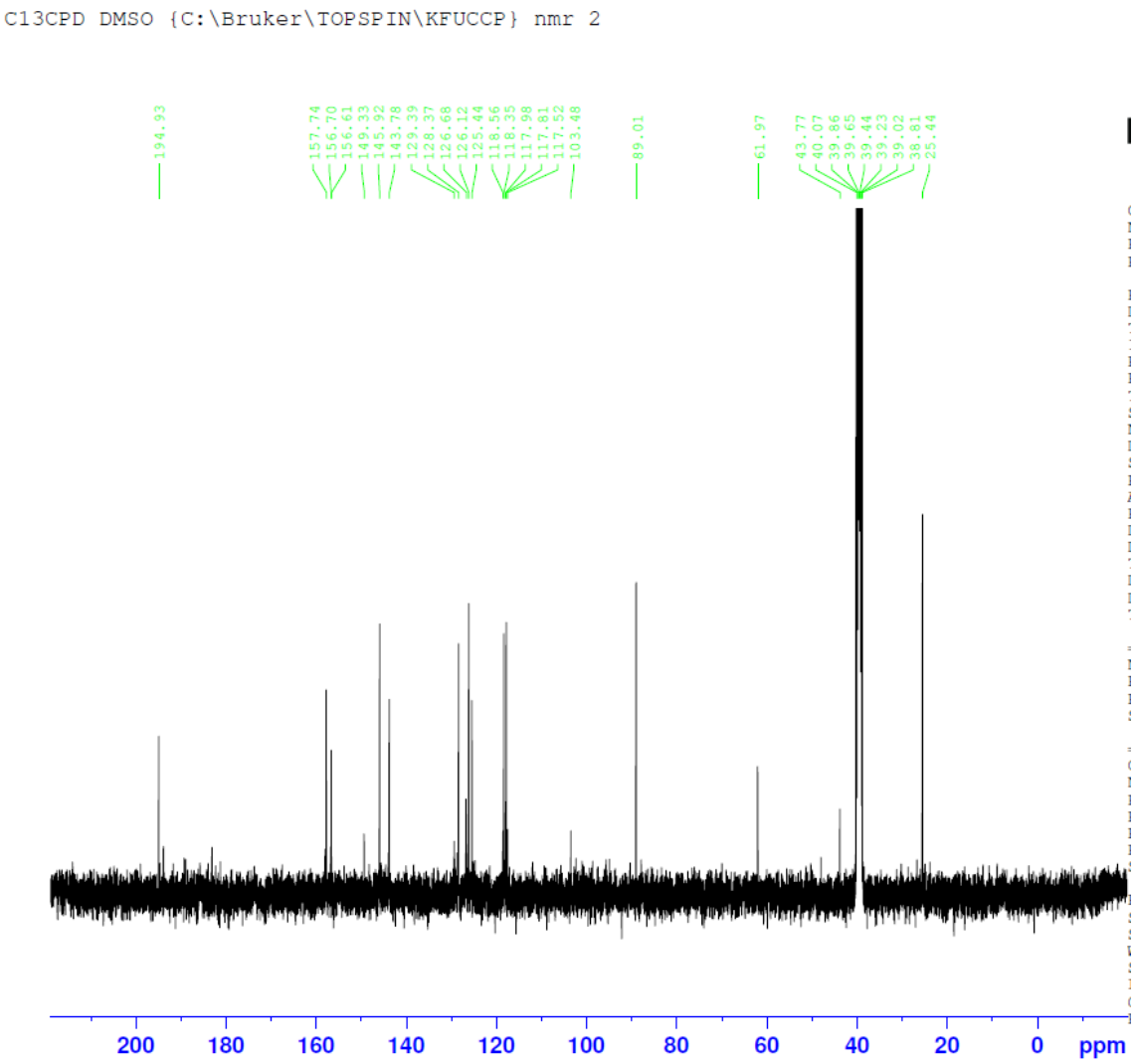

Figure S6: ^{13}C-NMR of 3-(2-bromoacetyl)-6-nitro-2*H*-chromen-2-one (SVN i2)

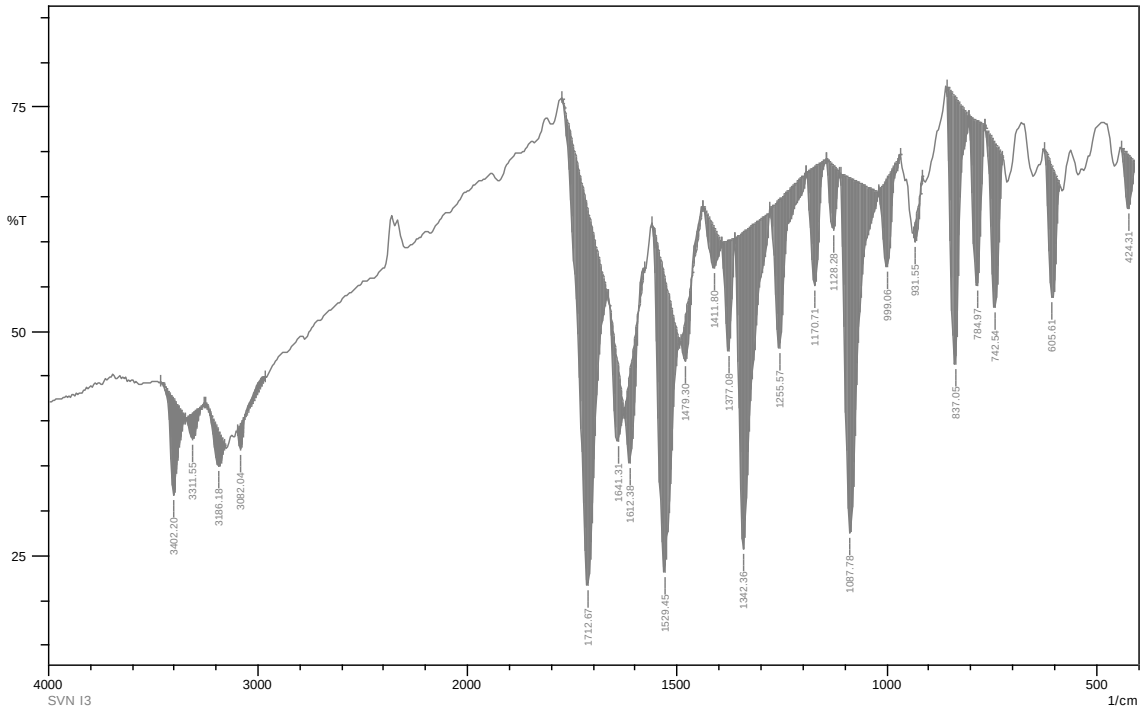

Figure S7: FT-IR of 3-(2-aminothiazol-4-yl)-6-nitro-2*H*-chromen-2-one (SVN i3)

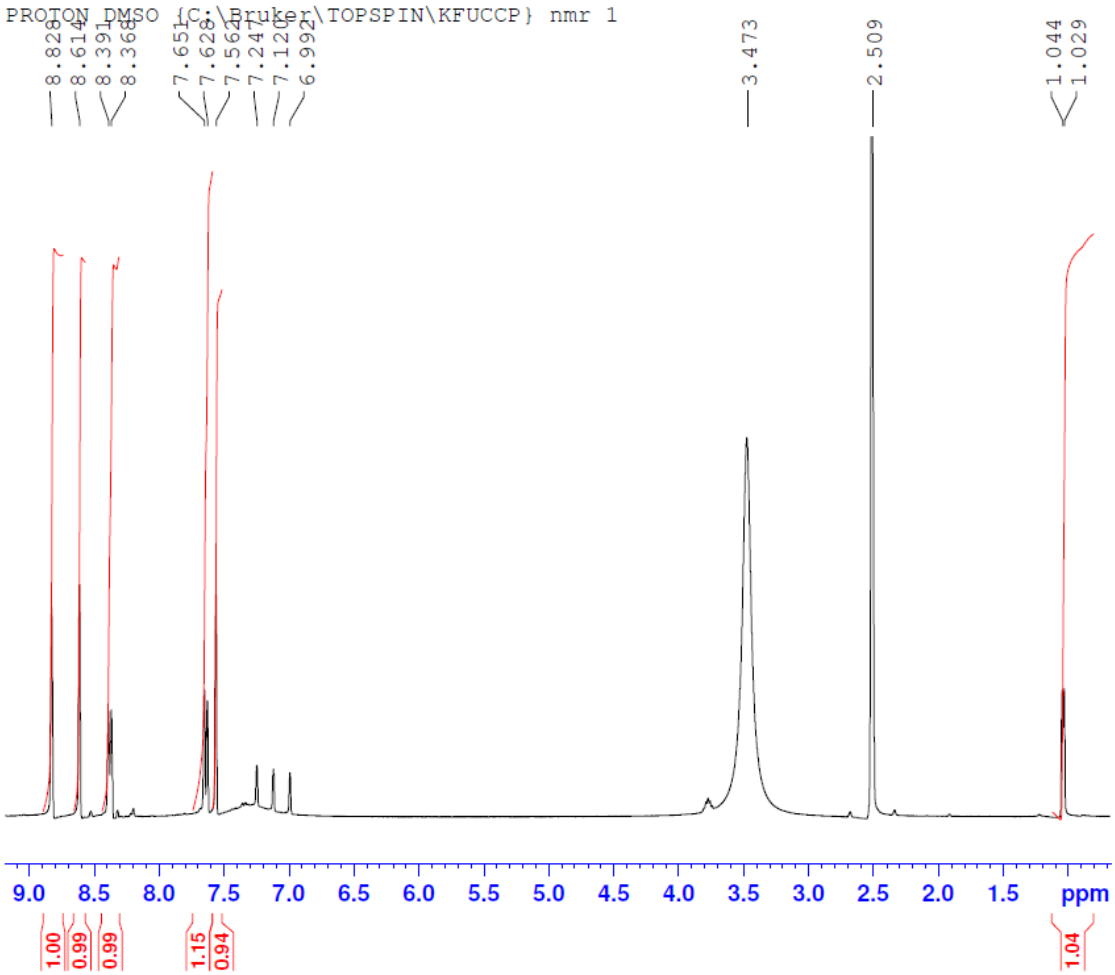

Figure S8: ^{1}H-NMR of 3-(2-aminothiazol-4-yl)-6-nitro-2*H*-chromen-2-one (SVN i3)

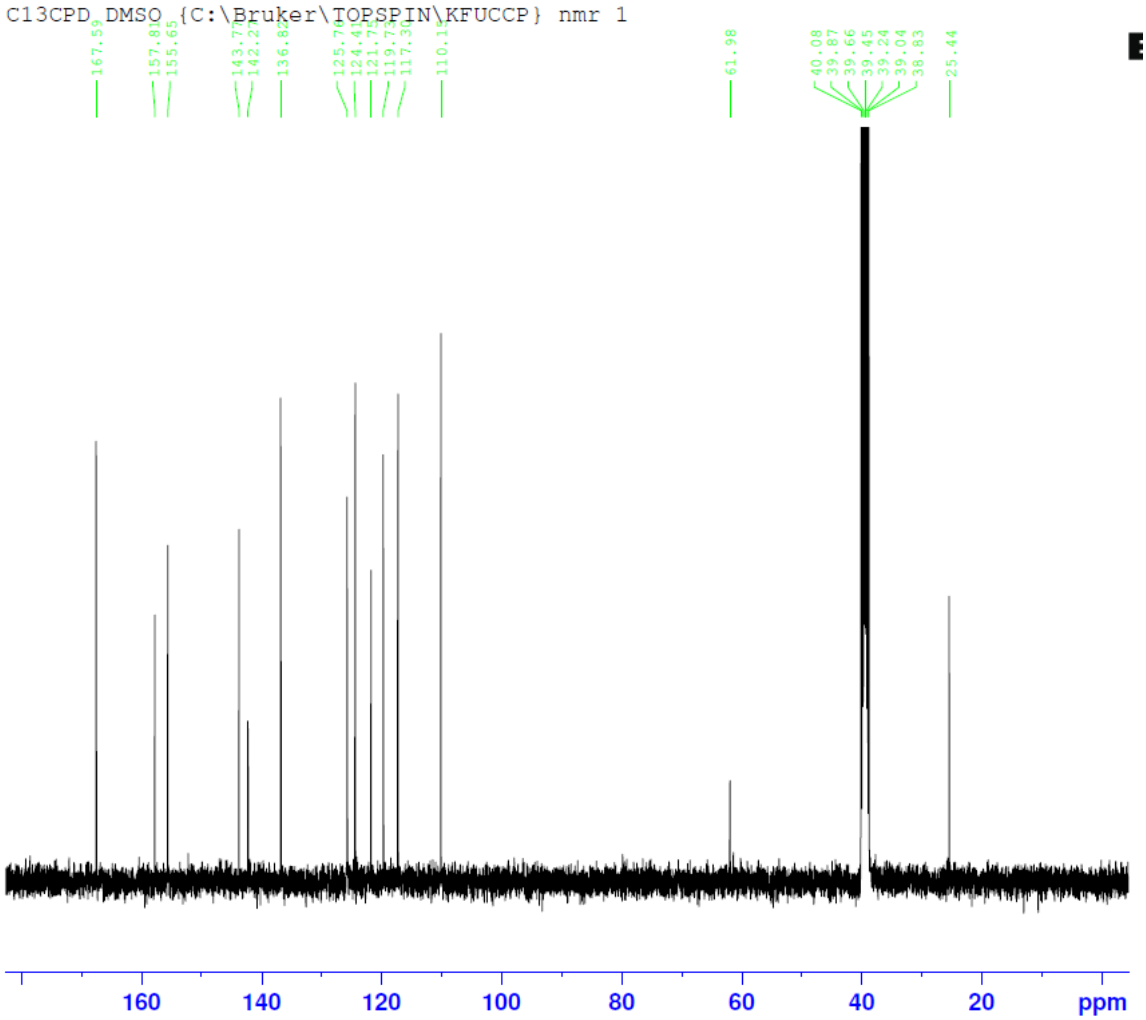

Figure S9: ^{13}C-NMR of 3-(2-aminothiazol-4-yl)-6-nitro-2*H*-chromen-2-one (SVN i3)

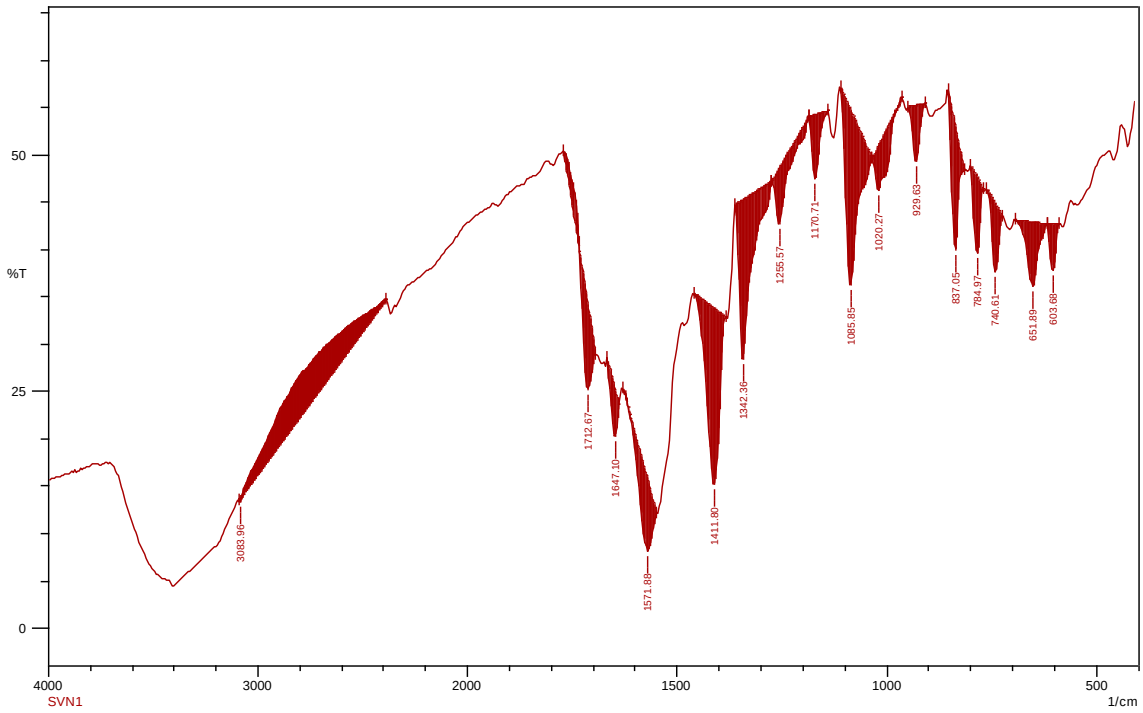

Figure S10: FT-IR of (*E*)-3-(2-(benzylidene amino) thiazol-4-yl)-6-nitro-2*H*-chromen-2-one (SVN 1)

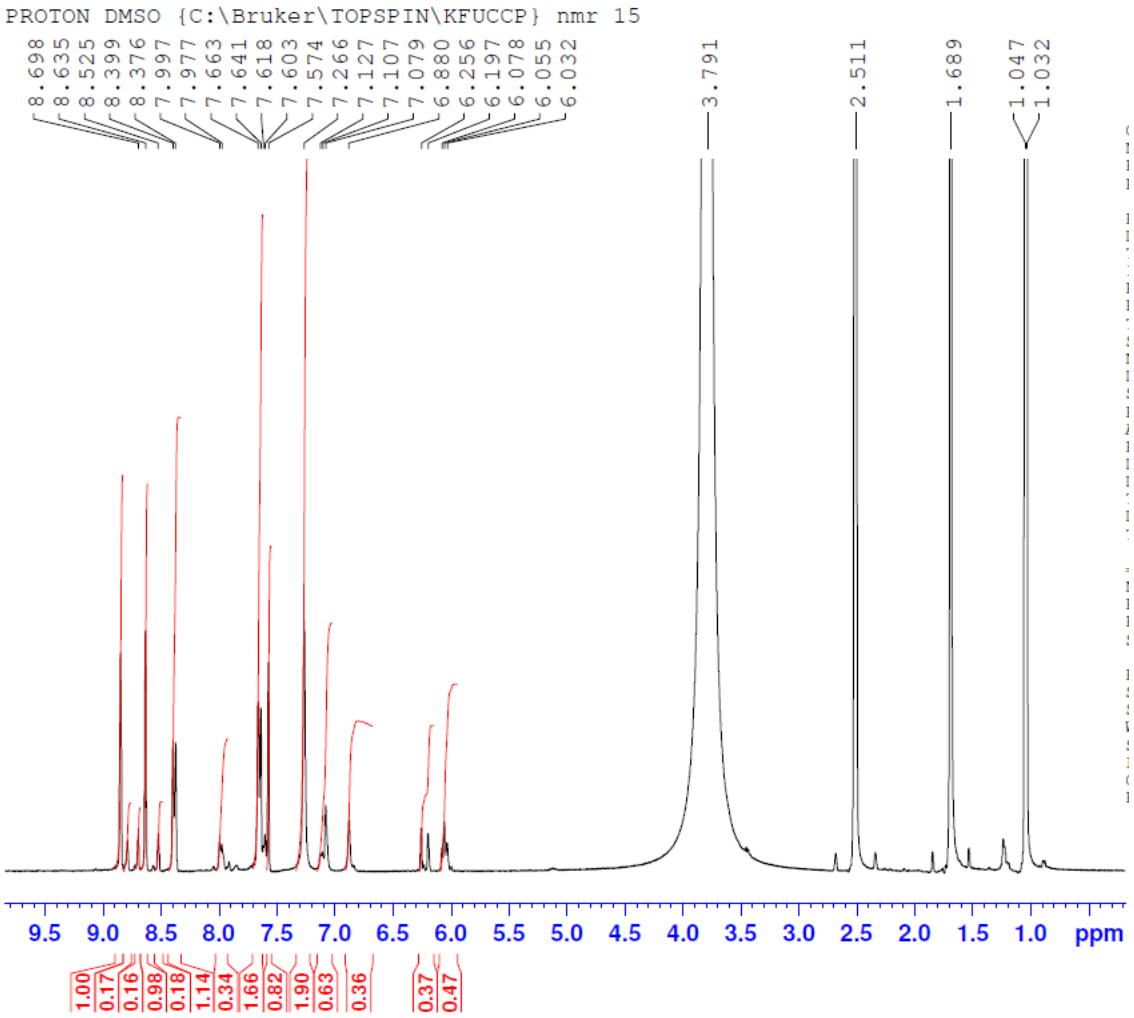

Figure S11: ^{1}H-NMR of (*E*)-3-(2-(benzylidene amino) thiazol-4-yl)-6-nitro-2*H*-chromen-2-one (SVN 1)

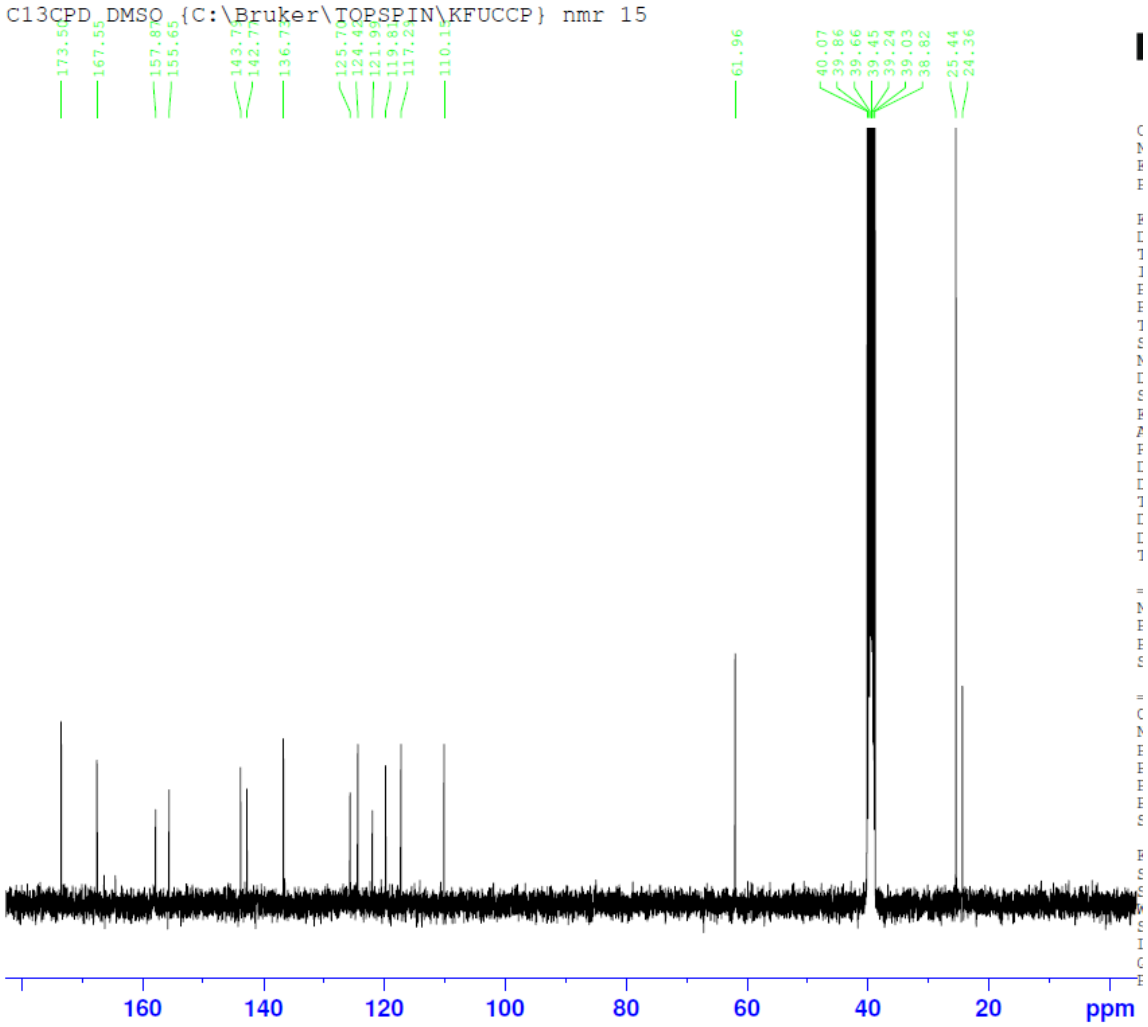

Figure S12: ^{13}C-NMR of (*E*)-3-(2-(benzylidene amino) thiazol-4-yl)-6-nitro-2*H*-chromen-2-one (SVN 1)

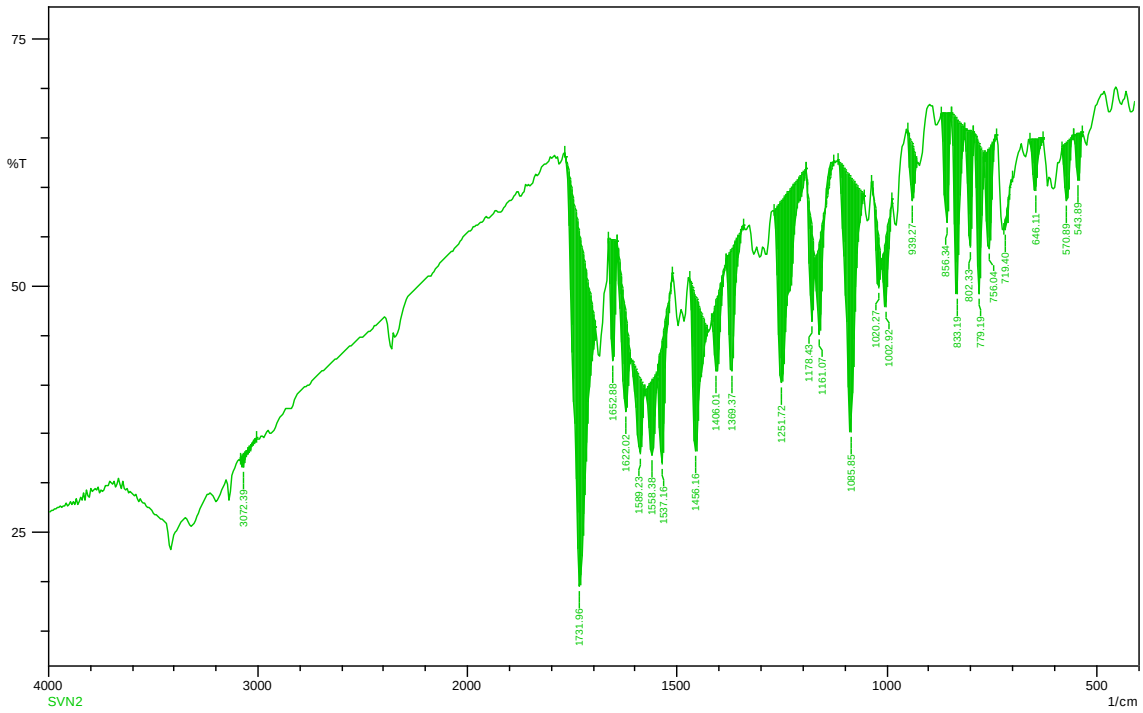

Figure S13: FT-IR of (*E*)-3-(2-((4-methoxybenzylidene) amino) thiazol-4-yl)-6-nitro-2*H*-chromen-2-one (SVN 2)

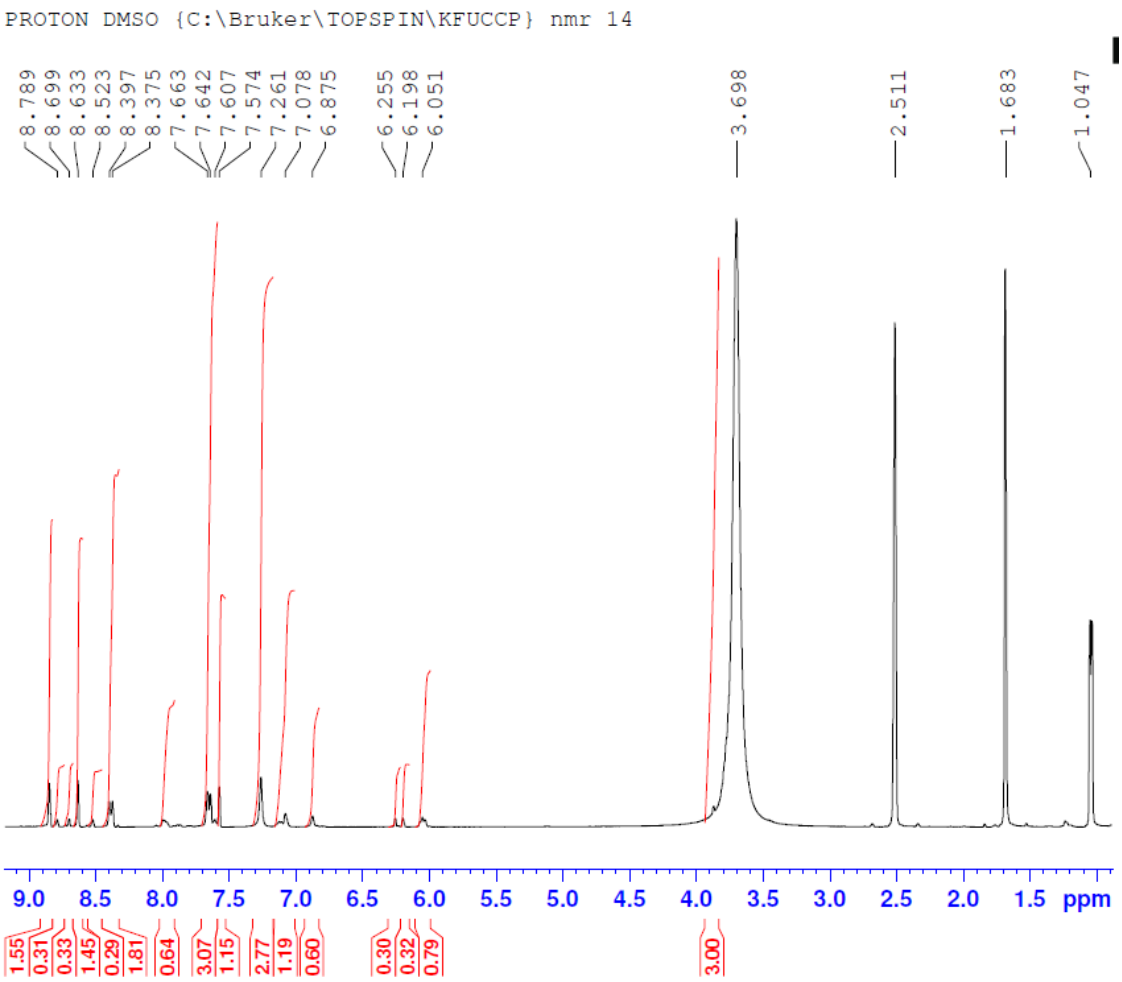

Figure S14: ^{1}H-NMR of (*E*)-3-(2-((4-methoxybenzylidene) amino) thiazol-4-yl)-6-nitro-2*H*-chromen-2-one (SVN 2)

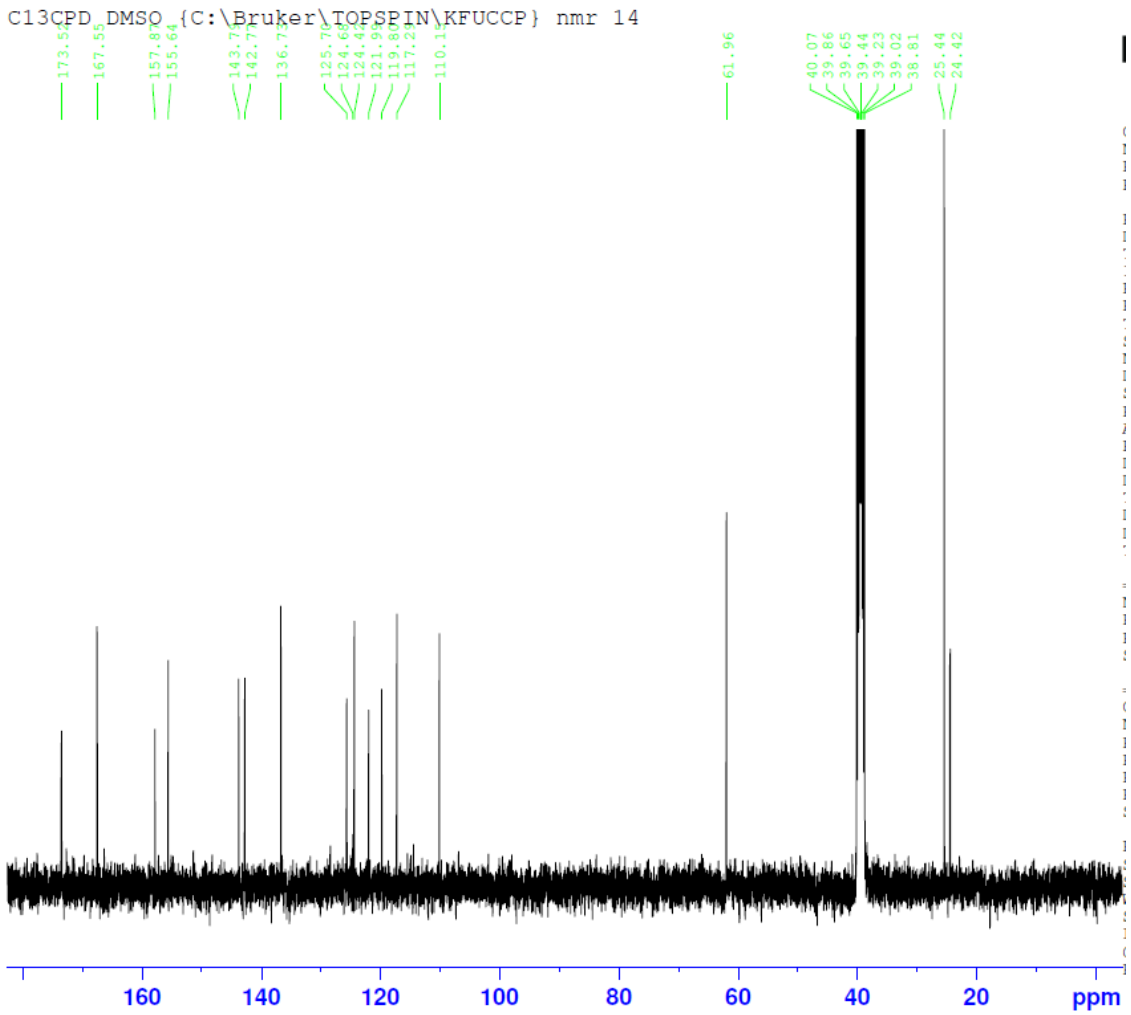

Figure S15: ^{13}C-NMR of (*E*)-3-(2-((4-methoxybenzylidene) amino) thiazol-4-yl)-6-nitro-2*H*-chromen-2-one (SVN 2)

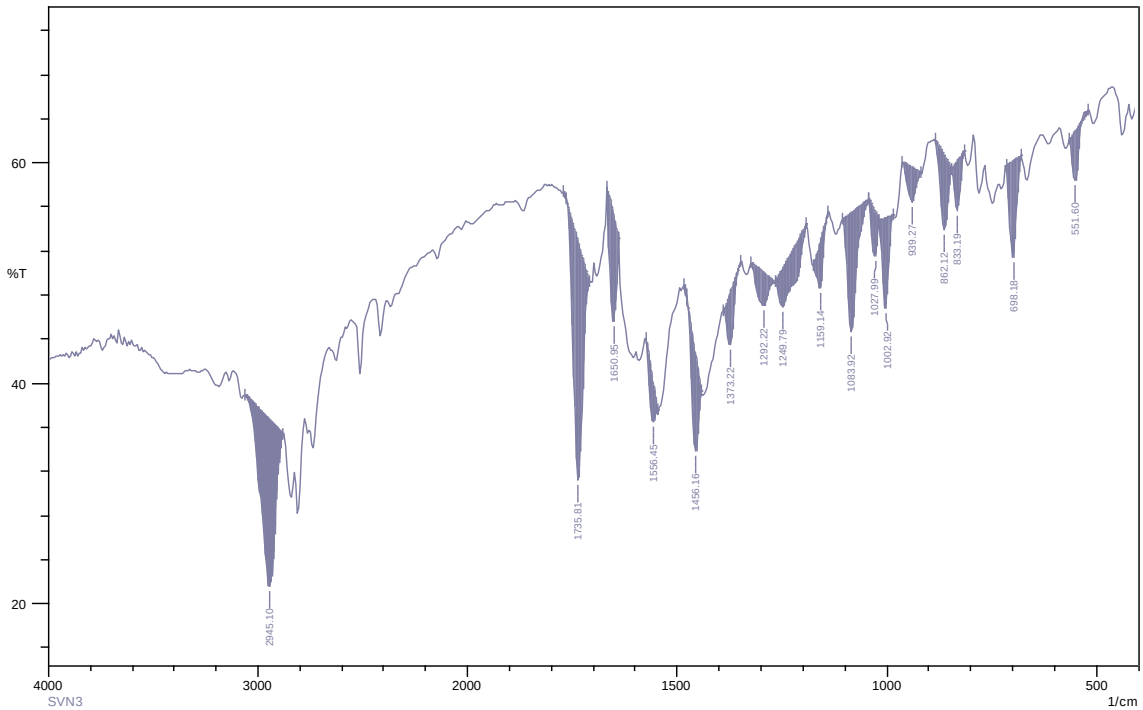

Figure S16: FT-IR of (*E*)-3-(2-((4-chlorobenzylidene) amino) thiazol-4-yl)-6-nitro-2*H*-chromen-2-one (SVN 3)

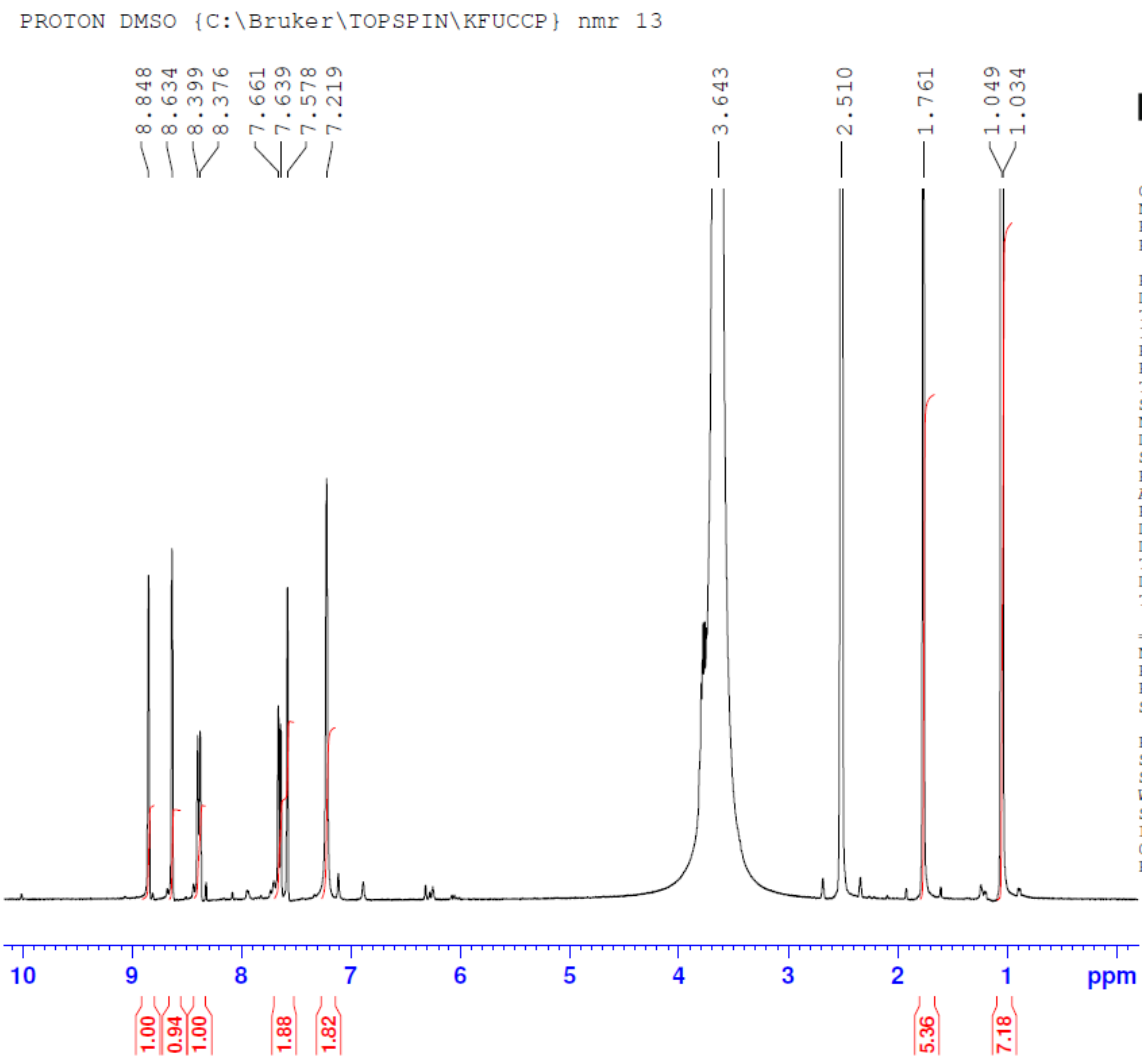

Figure S17: ^{1}H-NMR of (*E*)-3-(2-((4-chlorobenzylidene) amino) thiazol-4-yl)-6-nitro-2*H*-chromen-2-one (SVN 3)

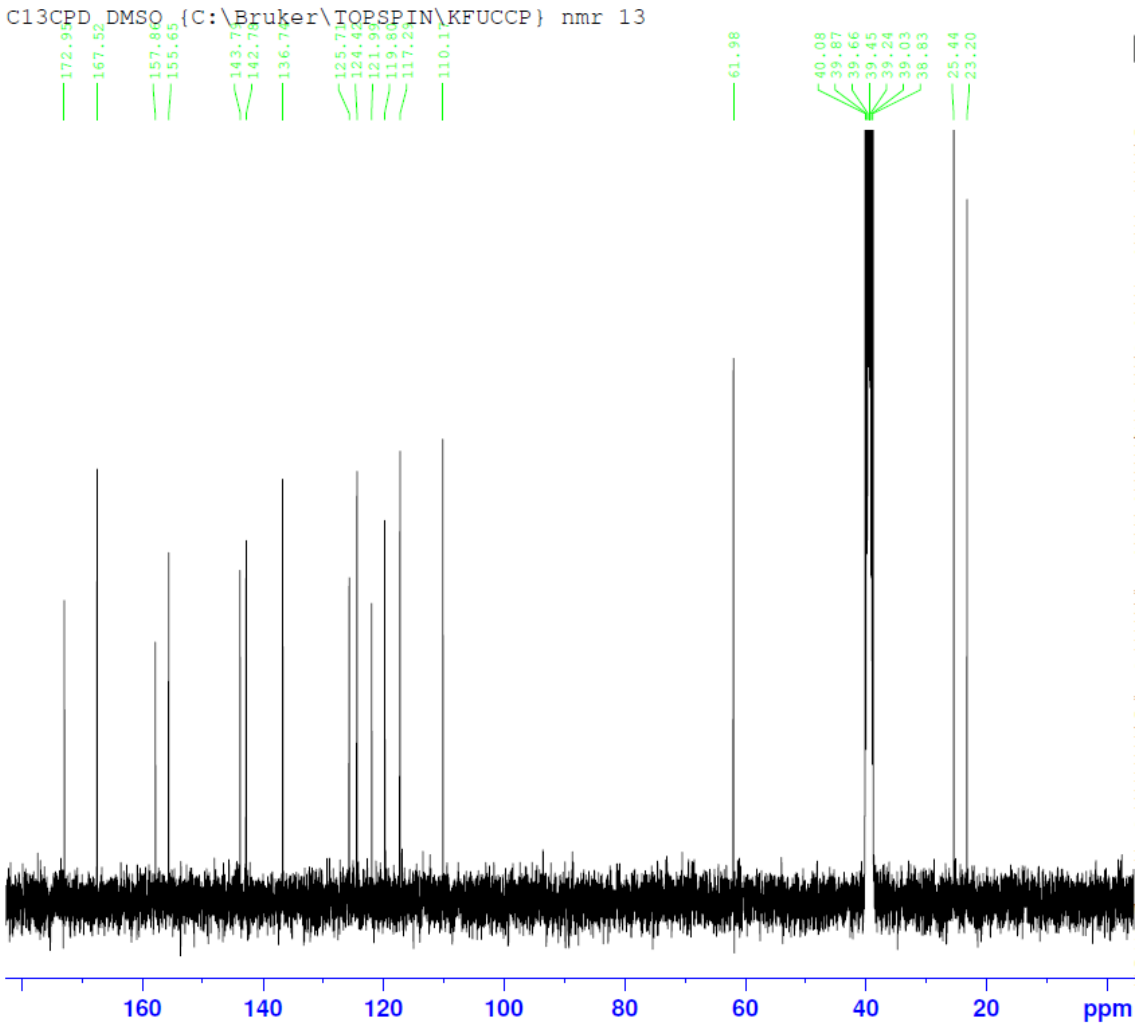

Figure S18: ^{13}C-NMR of (*E*)-3-(2-((4-chlorobenzylidene) amino) thiazol-4-yl)-6-nitro-2*H*-chromen-2-one (SVN 3)

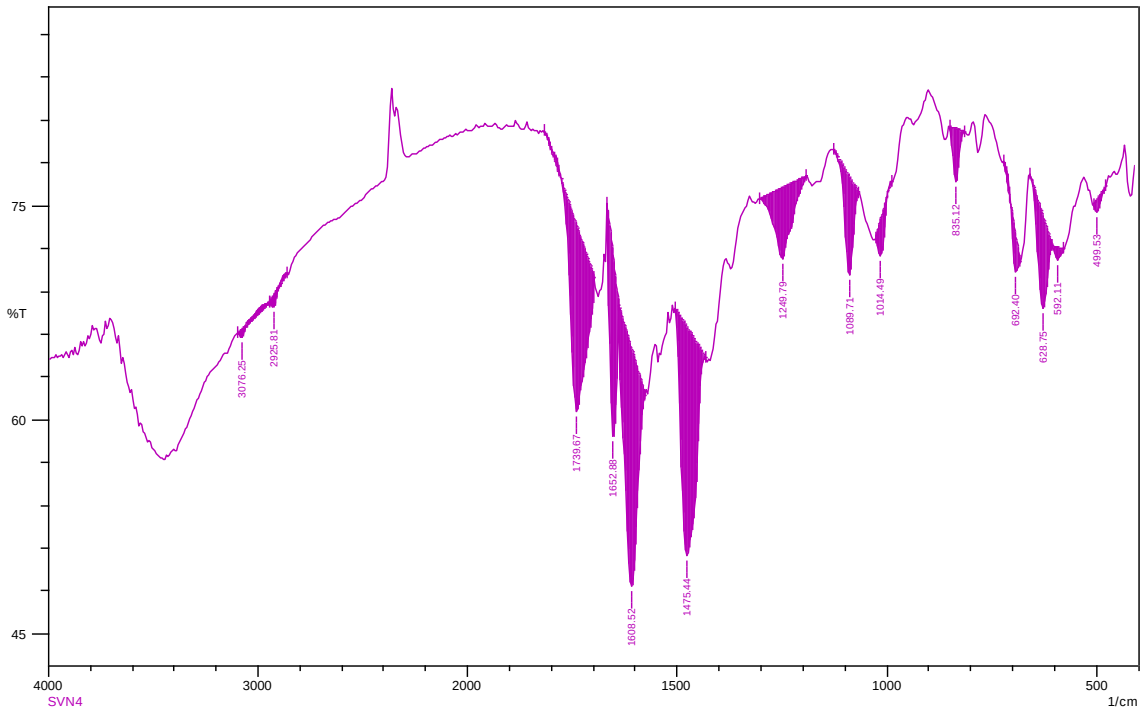

Figure S19: FT-IR of (*E*)-3-(2-((4-Fluorobenzylidene) amino) thiazol-4-yl)-6-nitro-2*H*-chromen-2-one (SVN 4)

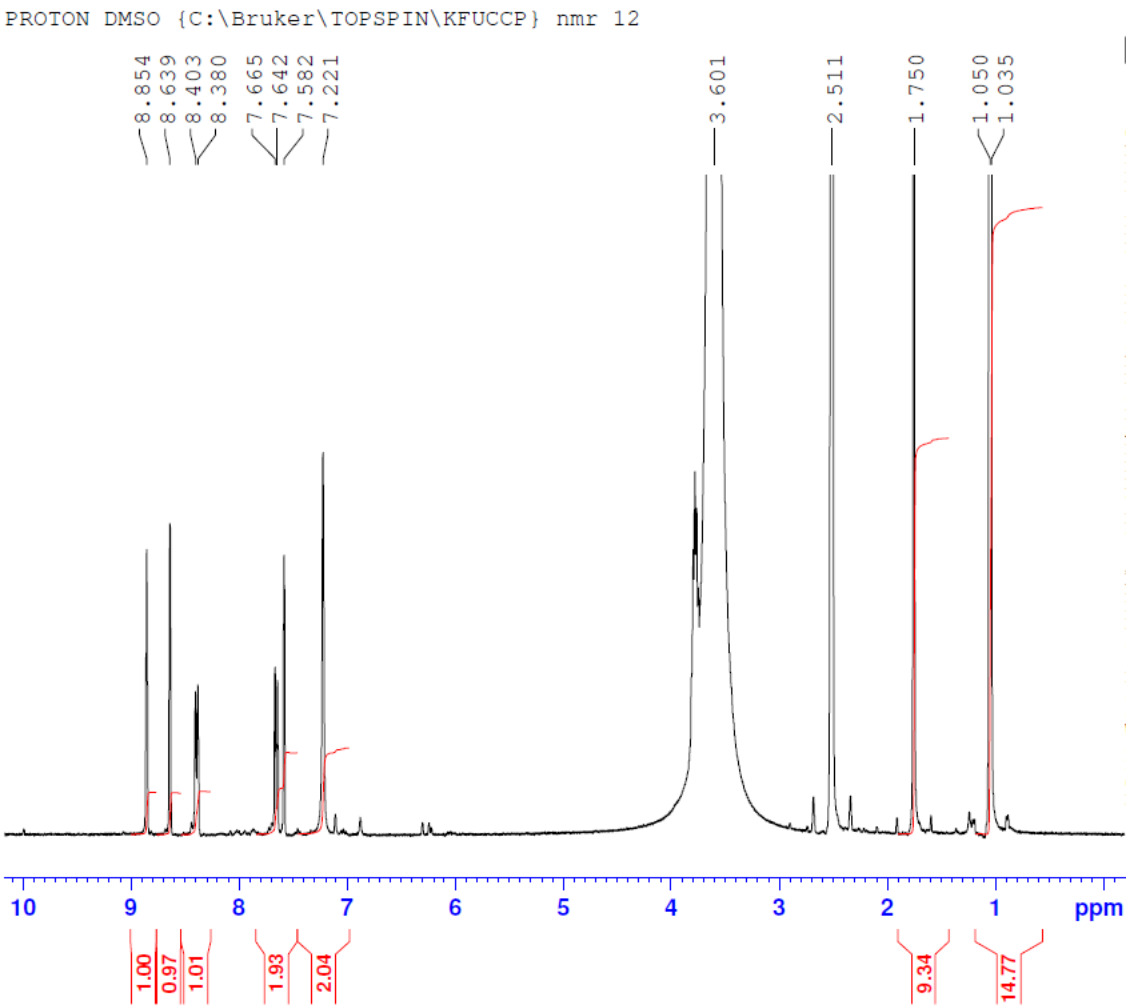

Figure S20: ^{1}H-NMR of (*E*)-3-(2-((4-Fluorobenzylidene) amino) thiazol-4-yl)-6-nitro-2*H*-chromen-2-one (SVN 4)

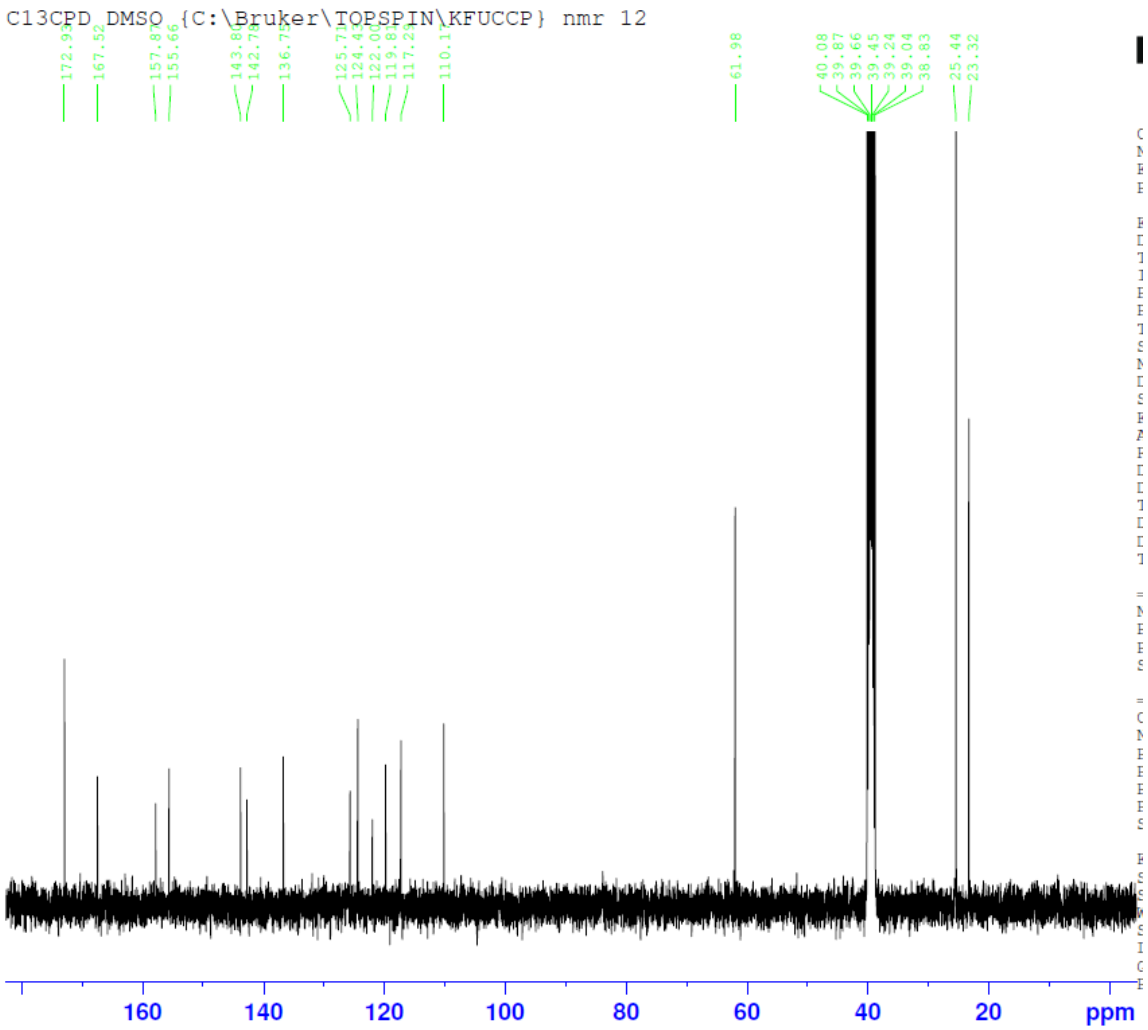

Figure S21: ^{13}C-NMR of (*E*)-3-(2-((4-Fluorobenzylidene) amino) thiazol-4-yl)-6-nitro-2*H*-chromen-2-one (SVN 4)

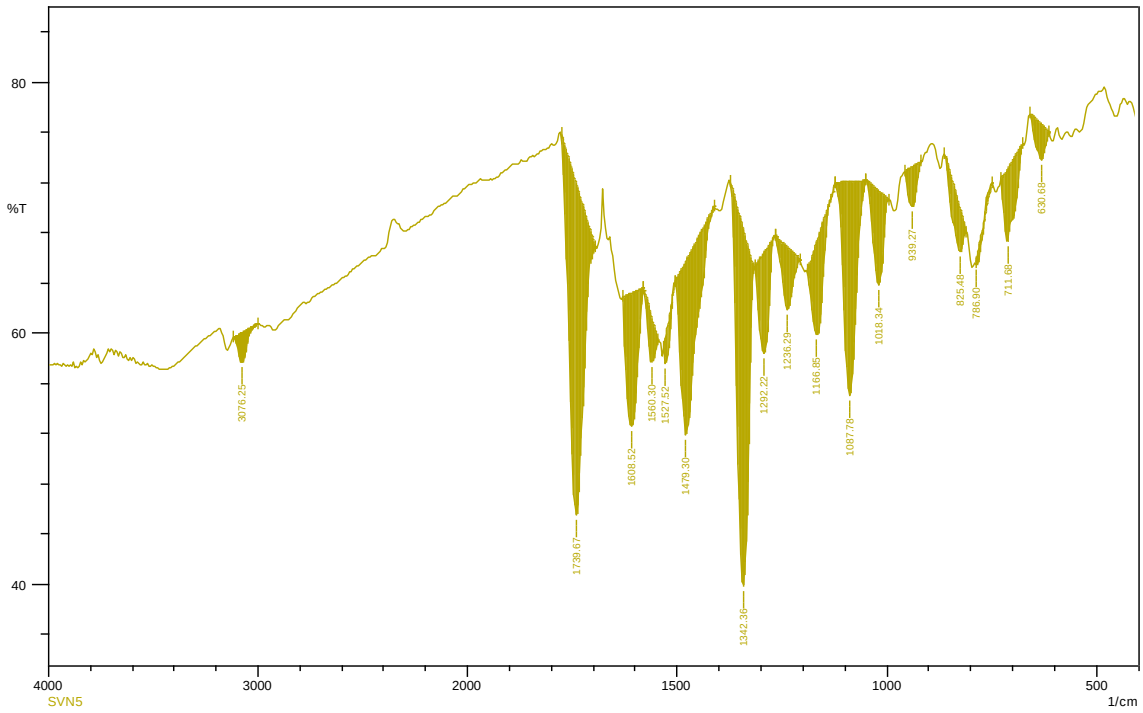

Figure S22: FT-IR of (*E*)-6-nitro-3-(2-((thiophen-2-ylmethylene) amino) thiazol-4-yl)-2*H*-chromen-2-one (SVN 5)

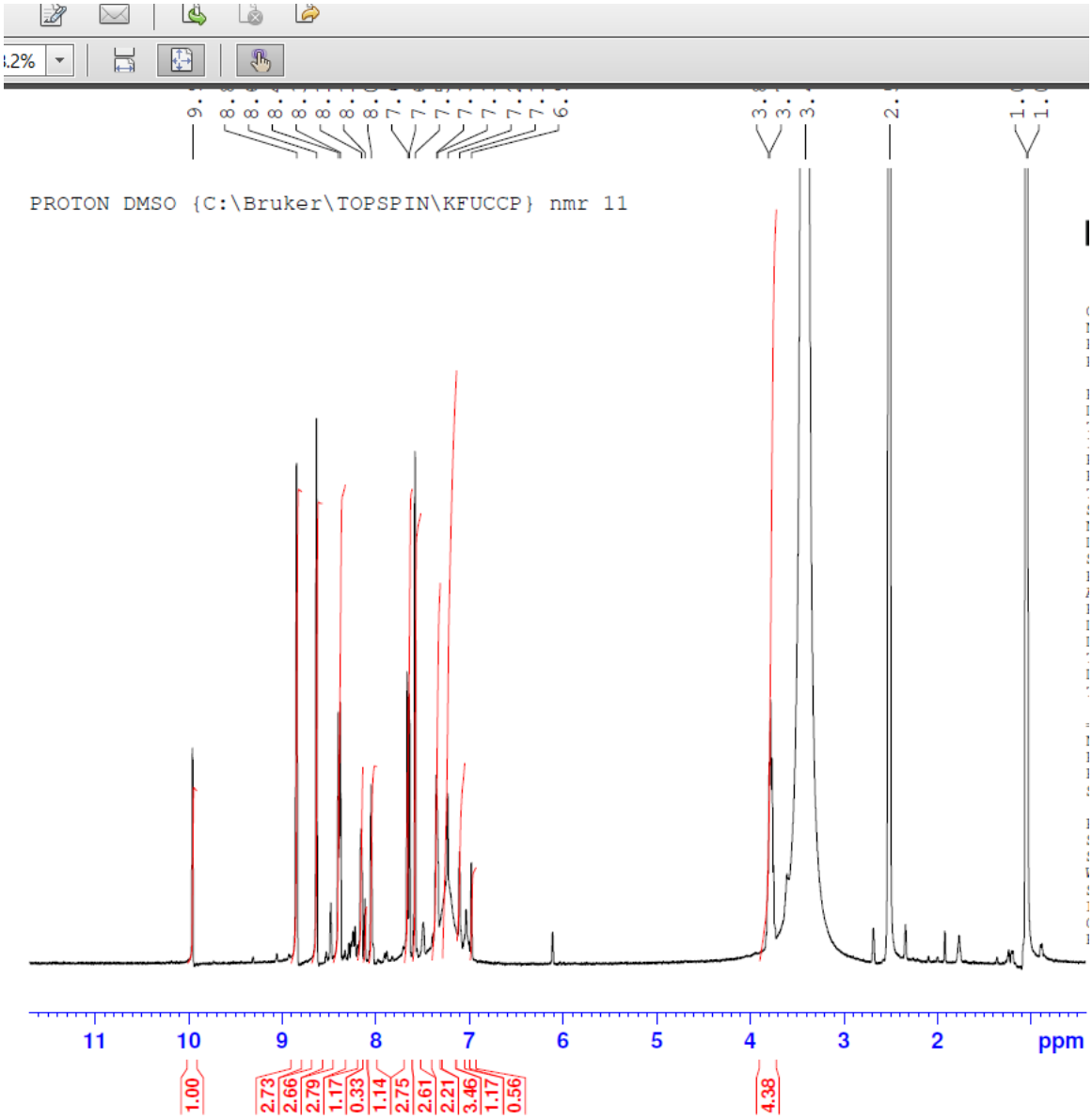

Figure S23: ^{1}H-NMR of (*E*)-6-nitro-3-(2-((thiophen-2-ylmethylene) amino) thiazol-4-yl)-2*H*-chromen-2-one (SVN 5)

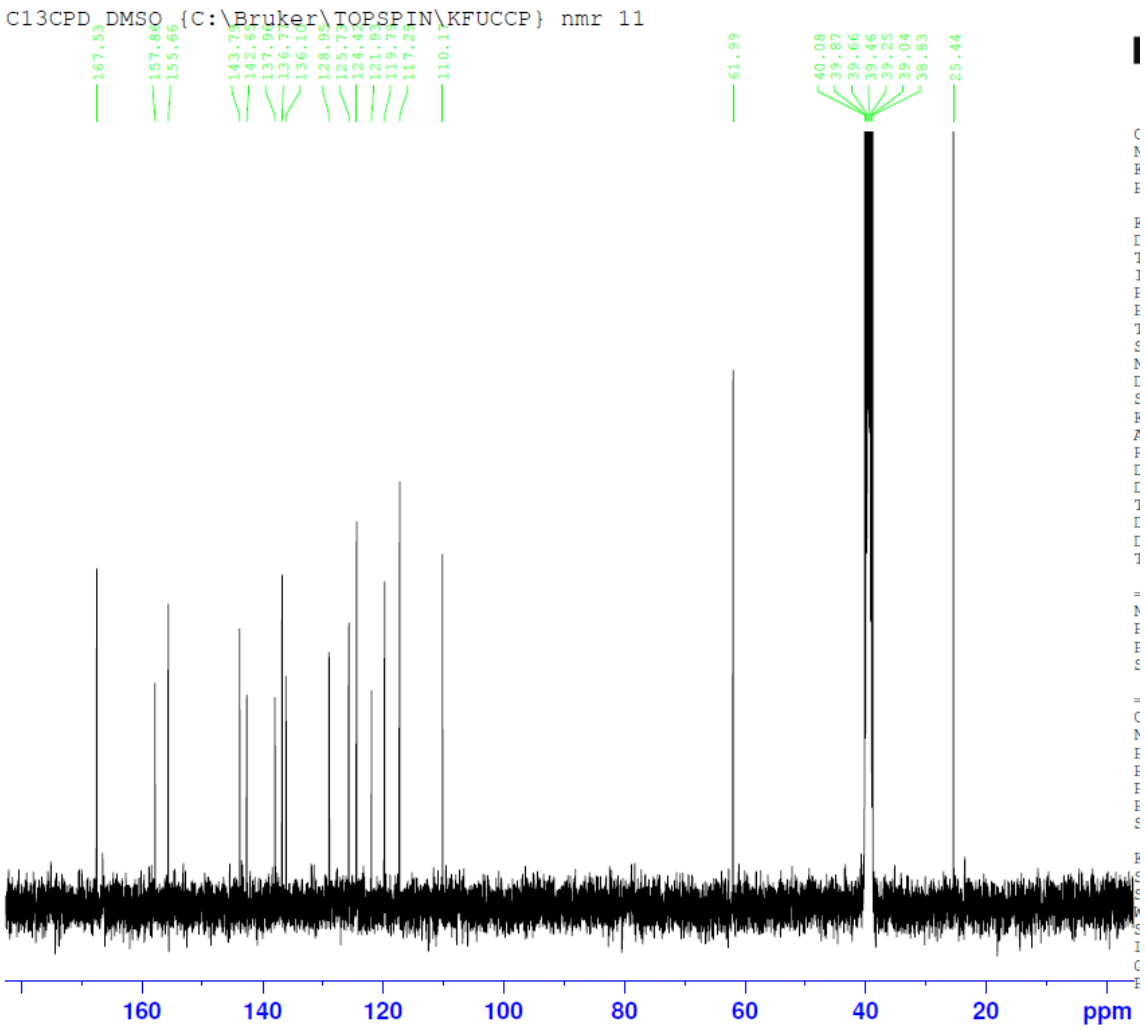

Figure S24: ^{13}C-NMR of (*E*)-6-nitro-3-(2-((thiophen-2-ylmethylene) amino) thiazol-4-yl)-2*H*-chromen-2-one (SVN 5)

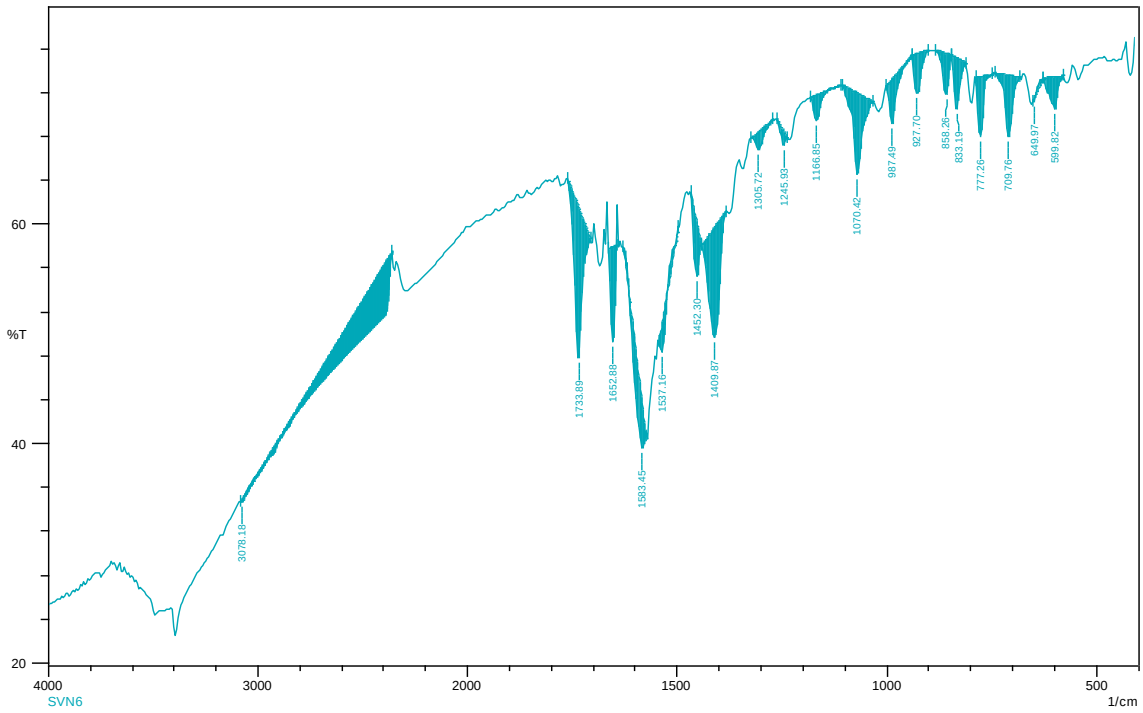

Figure S25: FT-IR of (*E*)-6-nitro-3-(2-((pyridin-4-ylmethylene) amino) thiazol-4-yl)-2*H*-chromen-2-one (SVN 6)

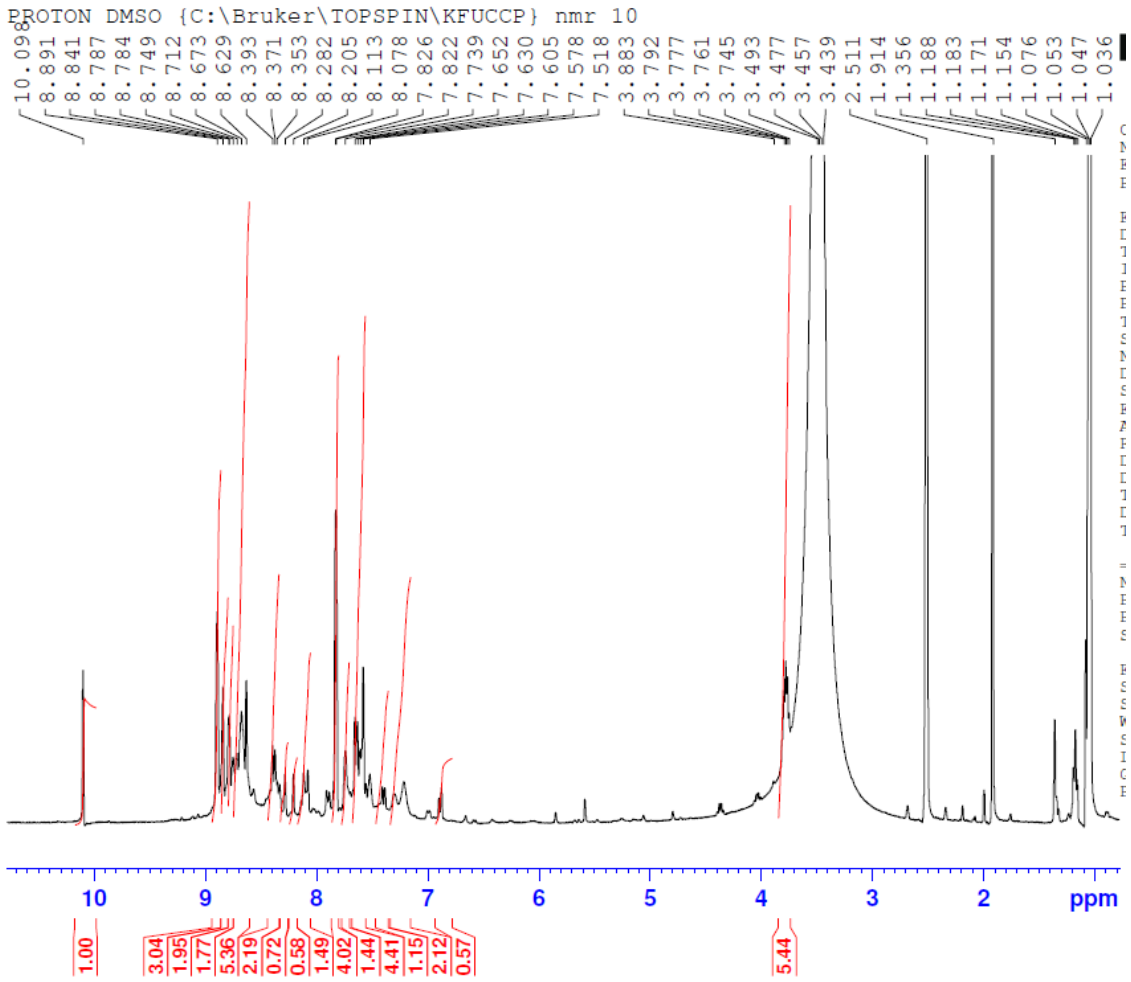

Figure S26: ^{1}H-NMR of (*E*)-6-nitro-3-(2-((pyridin-4-ylmethylene) amino) thiazol-4-yl)-2*H*-chromen-2-one (SVN 6)

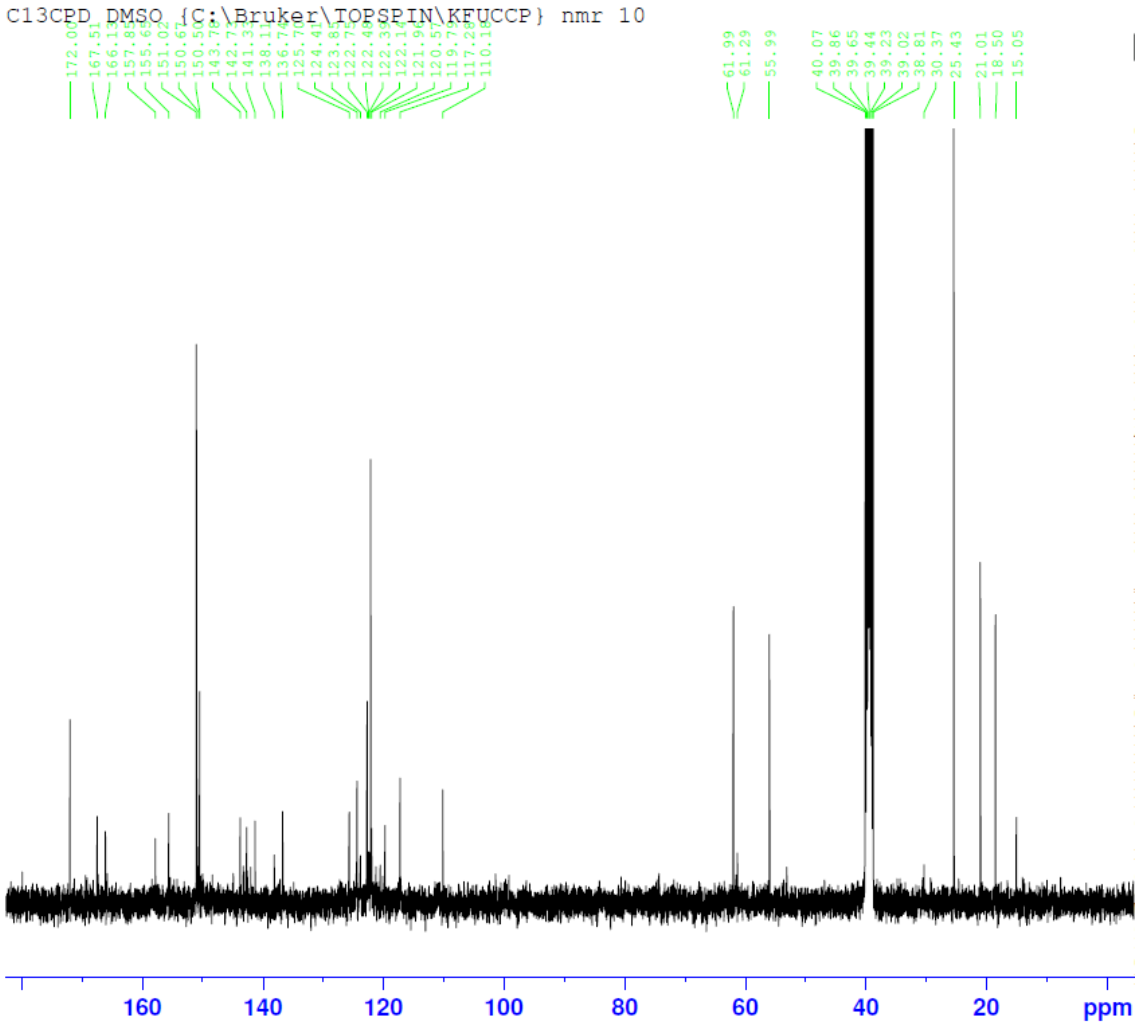

Figure S27: ^{13}C-NMR of (*E*)-6-nitro-3-(2-((pyridin-4-ylmethylene) amino) thiazol-4-yl)-2*H*-chromen-2-one (SVN 6)

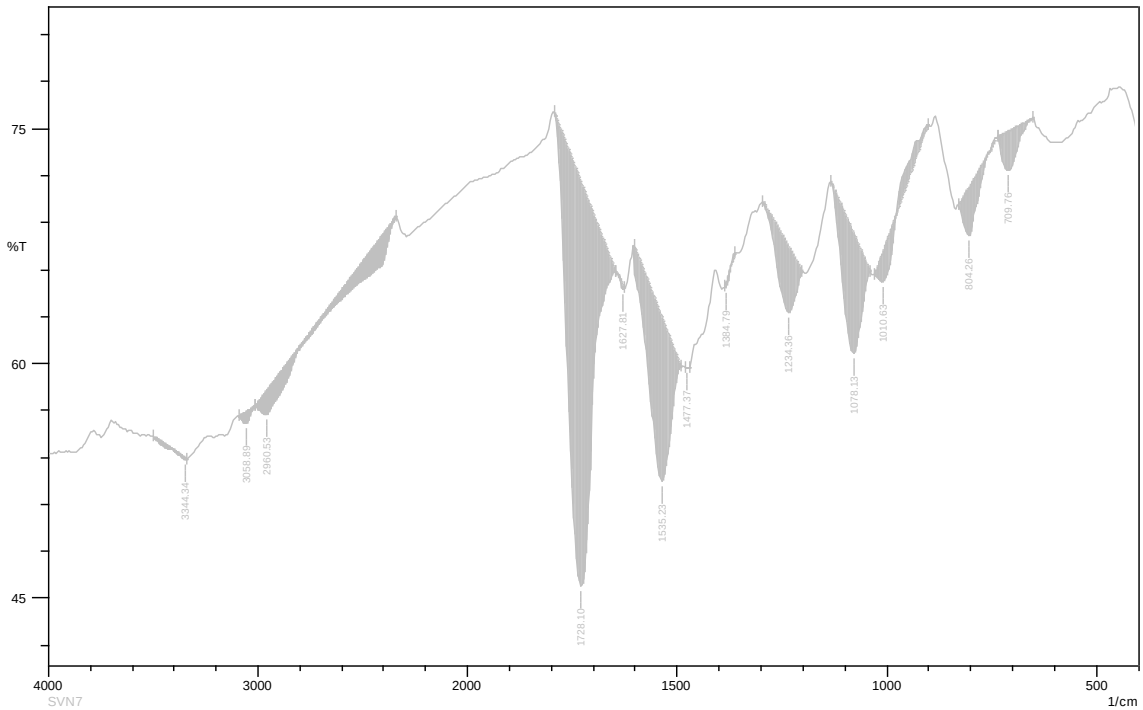

Figure S28: FT-IR of (*E*)-3-(2-((2-hydroxybenzylidene) amino) thiazol-4-yl)-6-nitro-2*H*-chromen-2-one (SVN 7)

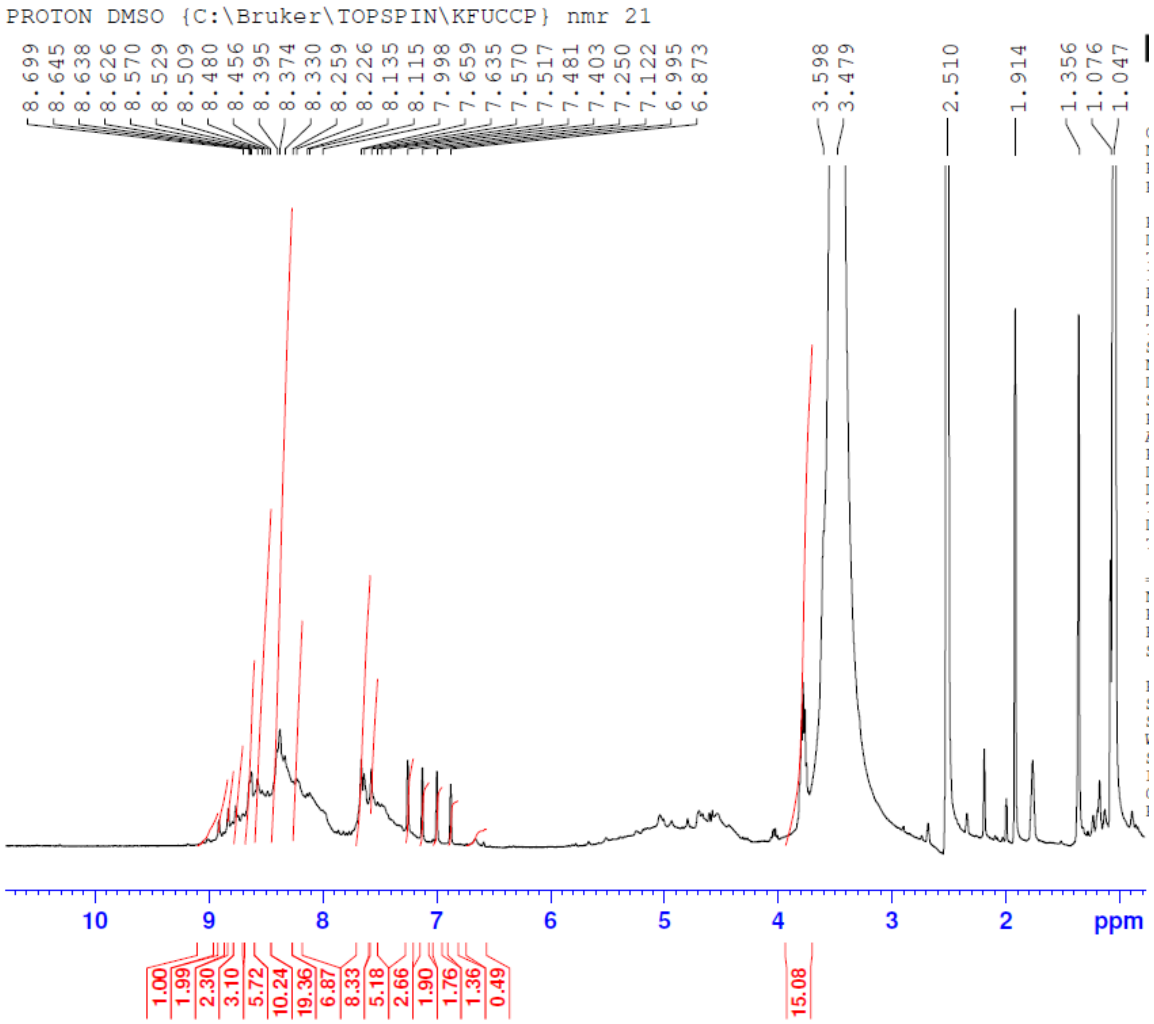

Figure S29: ^{1}H-NMR of (*E*)-3-(2-((2-hydroxybenzylidene) amino) thiazol-4-yl)-6-nitro-2*H*-chromen-2-one (SVN 7)

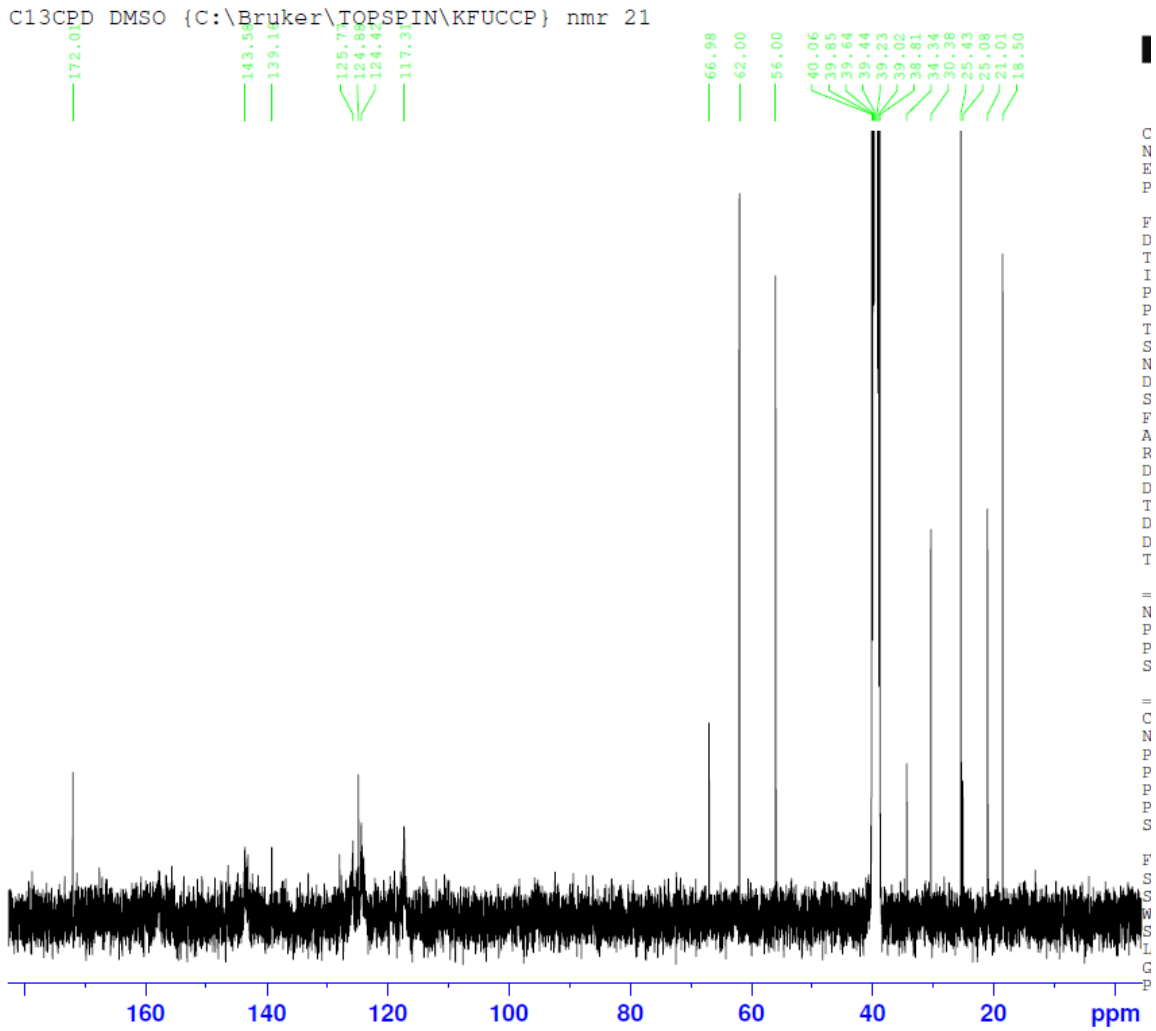

Figure S30: ^{13}C-NMR of (*E*)-3-(2-((2-hydroxybenzylidene) amino) thiazol-4-yl)-6-nitro-2*H*-chromen-2-one (SVN 7)

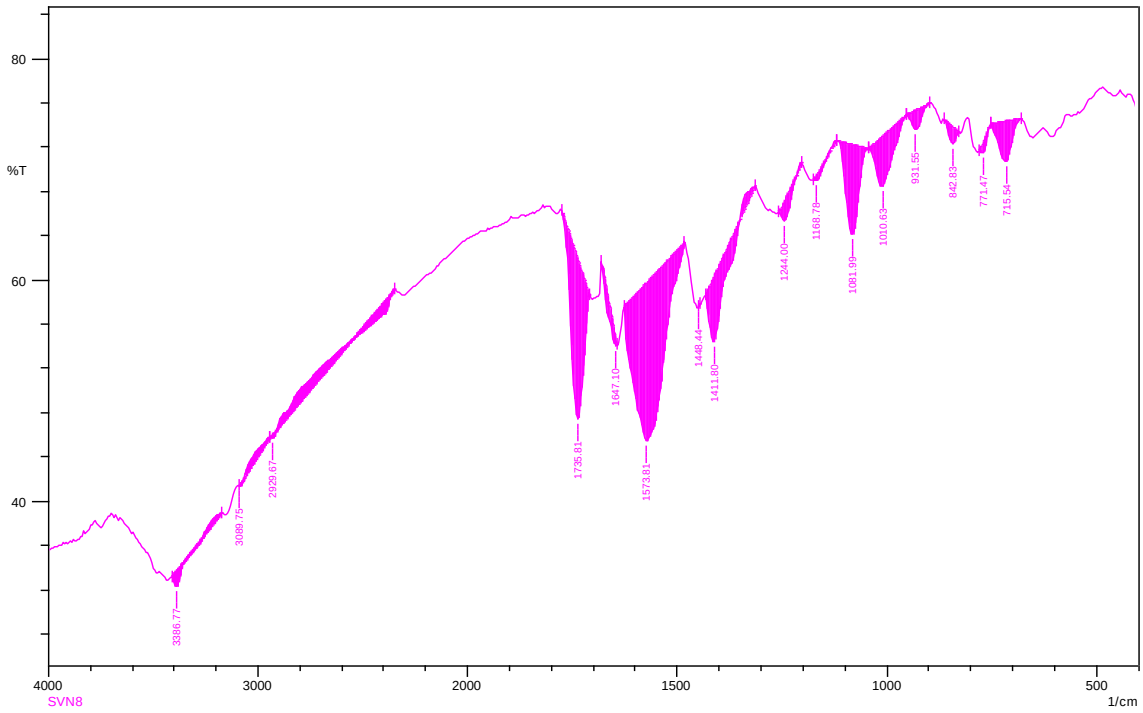

Figure S31: FT-IR of (*E*)-3-(2-((3,4-dihydroxybenzylidene) amino) thiazol-4-yl)-6-nitro-2*H*-chromen-2-one (SVN 8)

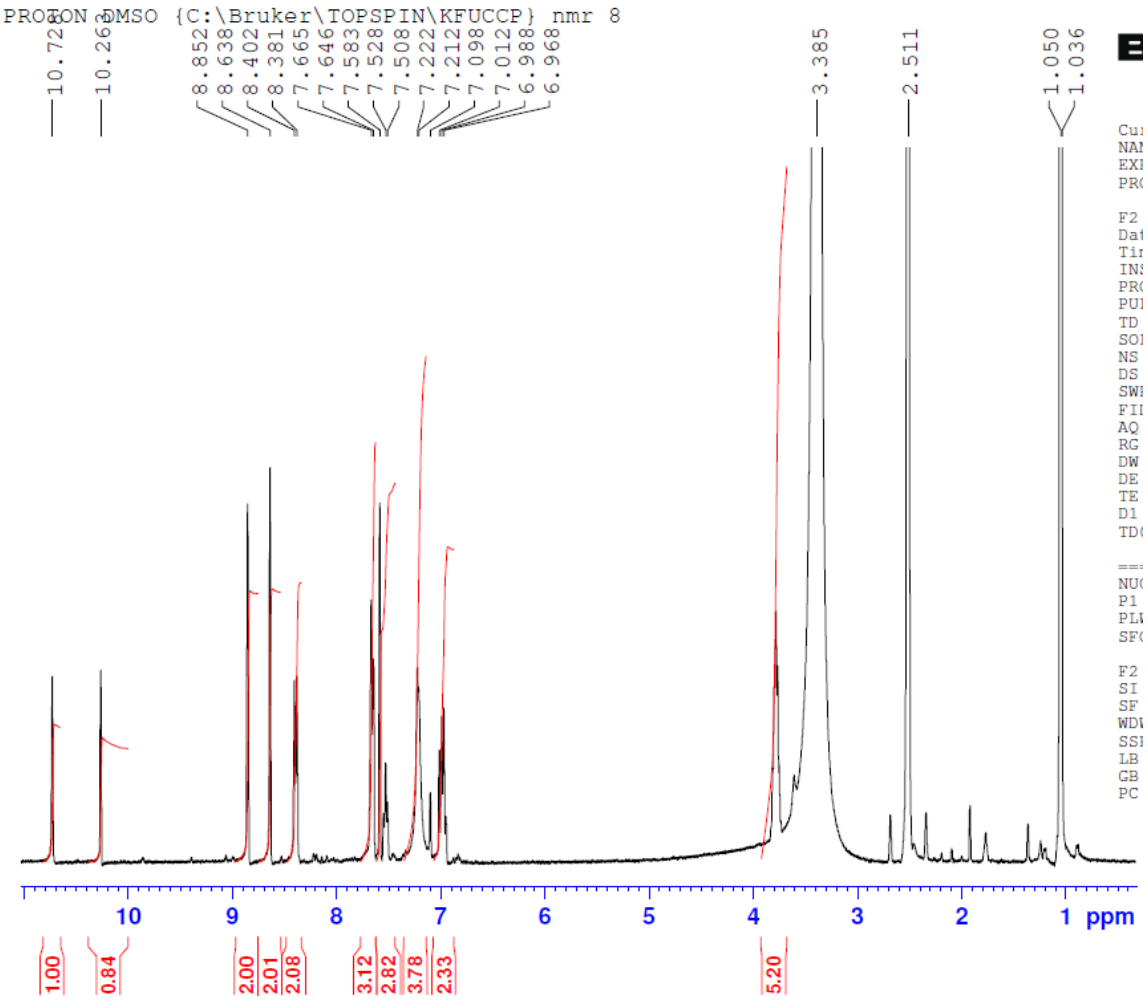

Figure S32: ^{1}H-NMR of (*E*)-3-(2-((3,4-dihydroxybenzylidene) amino) thiazol-4-yl)-6-nitro-2*H*-chromen-2-one (SVN 8)

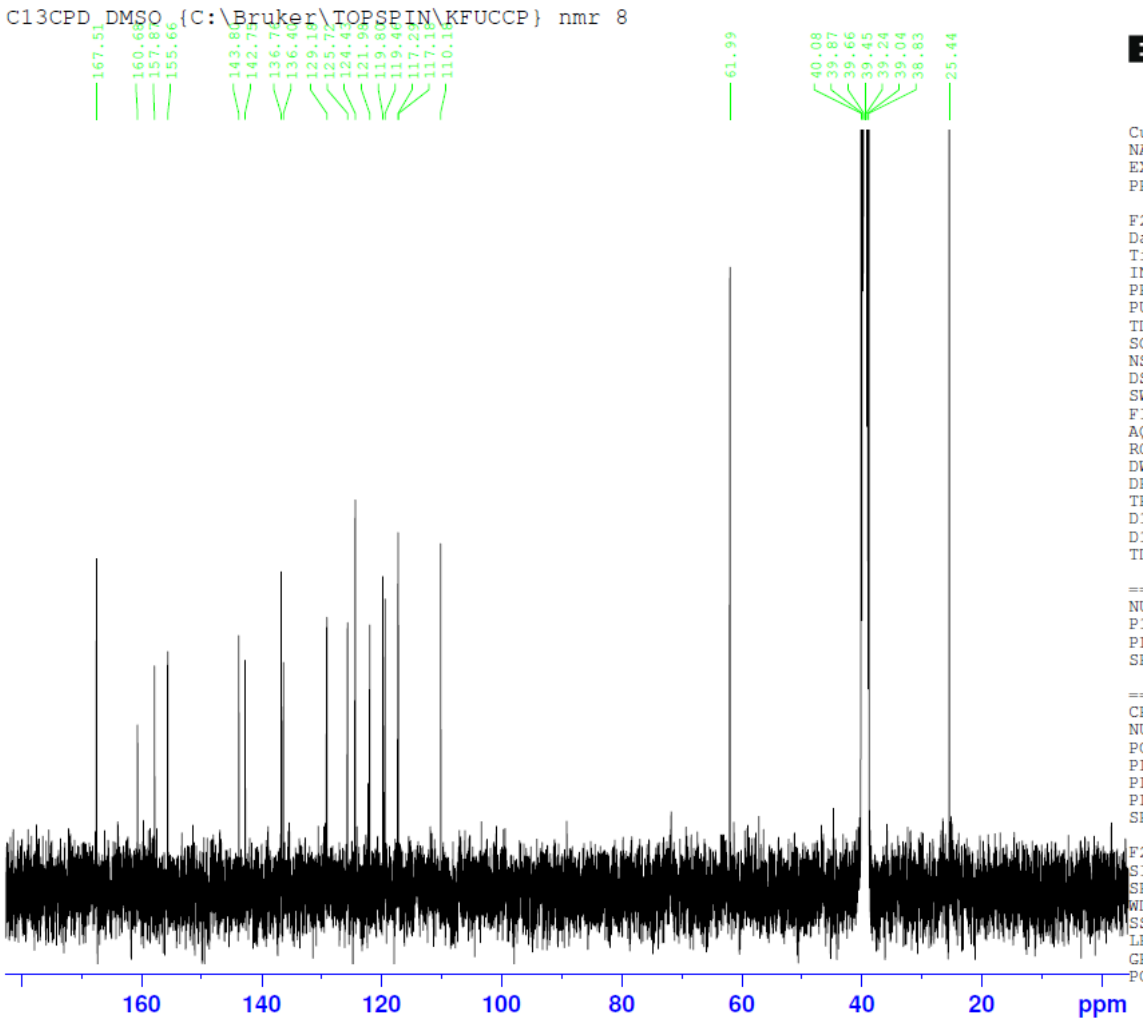

Figure S33: ^{13}C-NMR of (*E*)-3-(2-((3,4-dihydroxybenzylidene) amino) thiazol-4-yl)-6-nitro-2*H*-chromen-2-one (SVN 8)

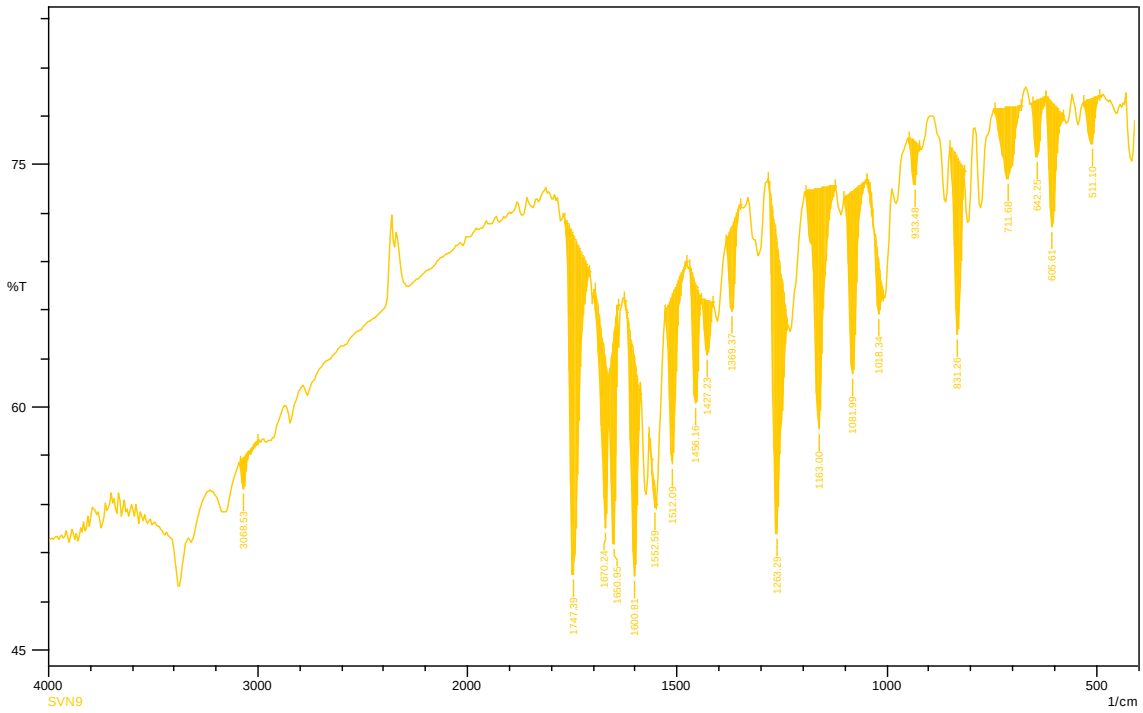

Figure S34: FT-IR of (*E*)-3-(2-((2-methoxybenzylidene) amino) thiazol-4-yl)-6-nitro-2*H*-chromen-2-one (SVN 9)

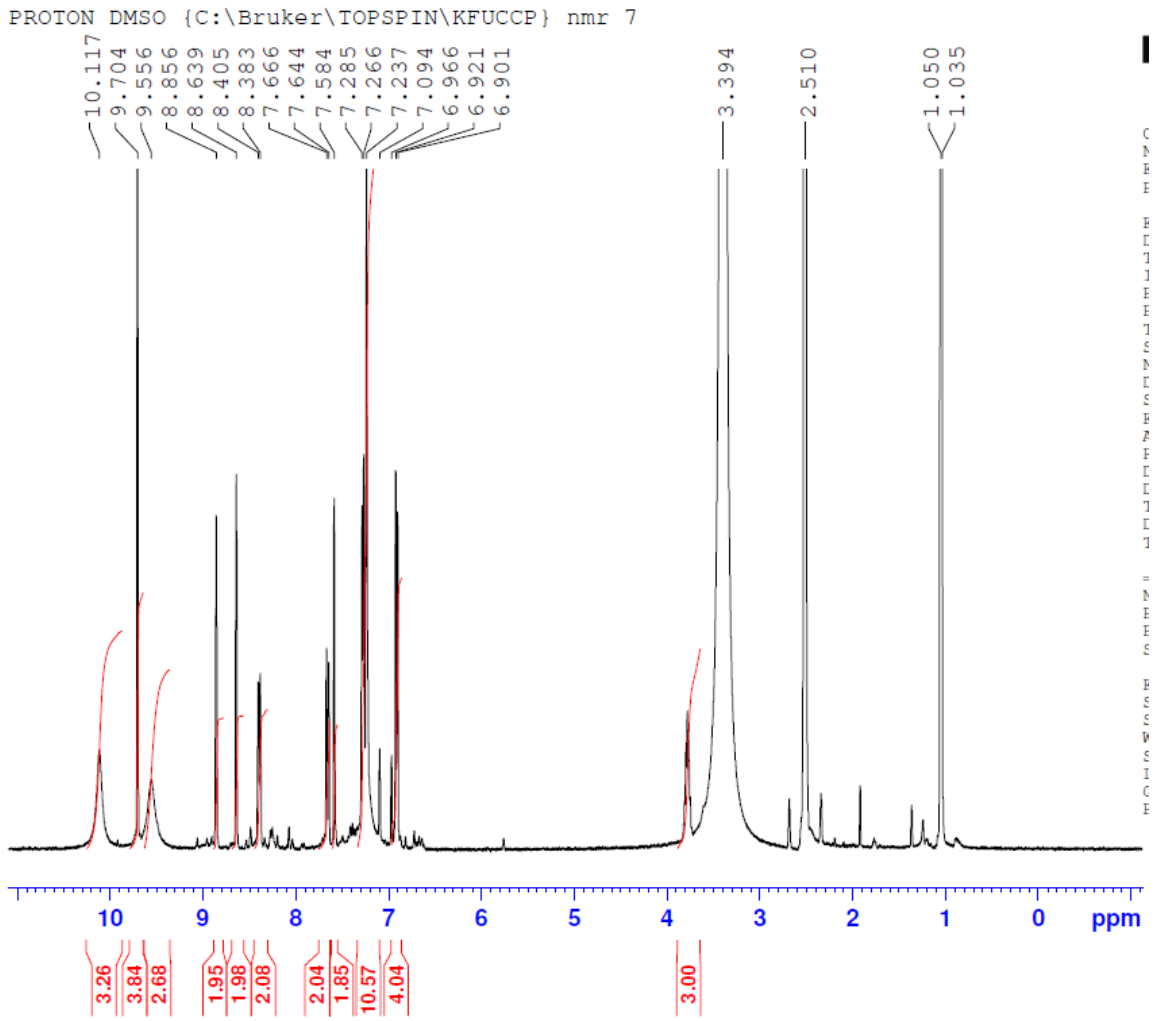

Figure S35: ^{1}H-NMR of (*E*)-3-(2-((2-methoxybenzylidene) amino) thiazol-4-yl)-6-nitro-2*H*-chromen-2-one (SVN 9)

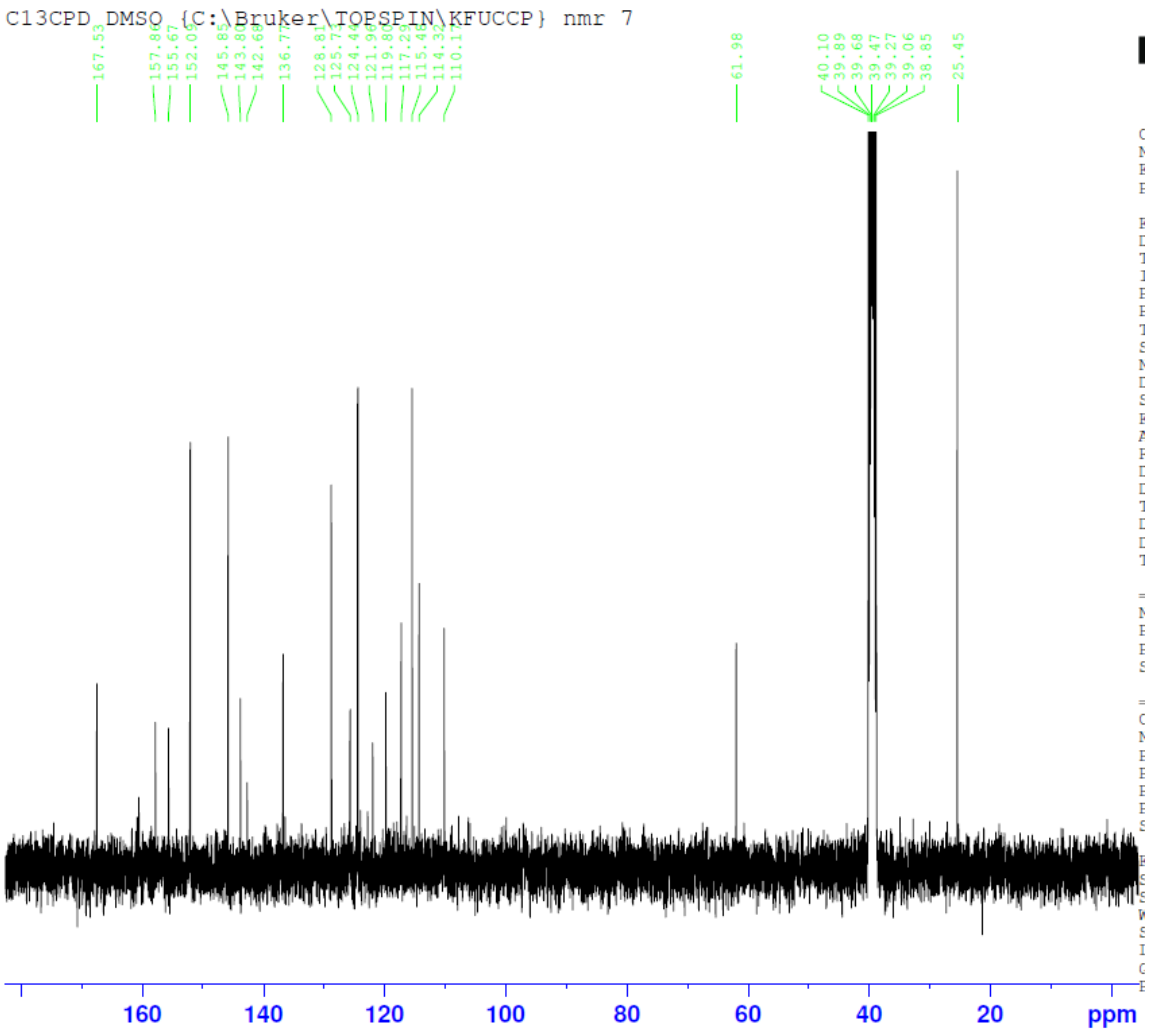

Figure S36: ^{13}C-NMR of (*E*)-3-(2-((2-methoxybenzylidene) amino) thiazol-4-yl)-6-nitro-2*H*-chromen-2-one (SVN 9)

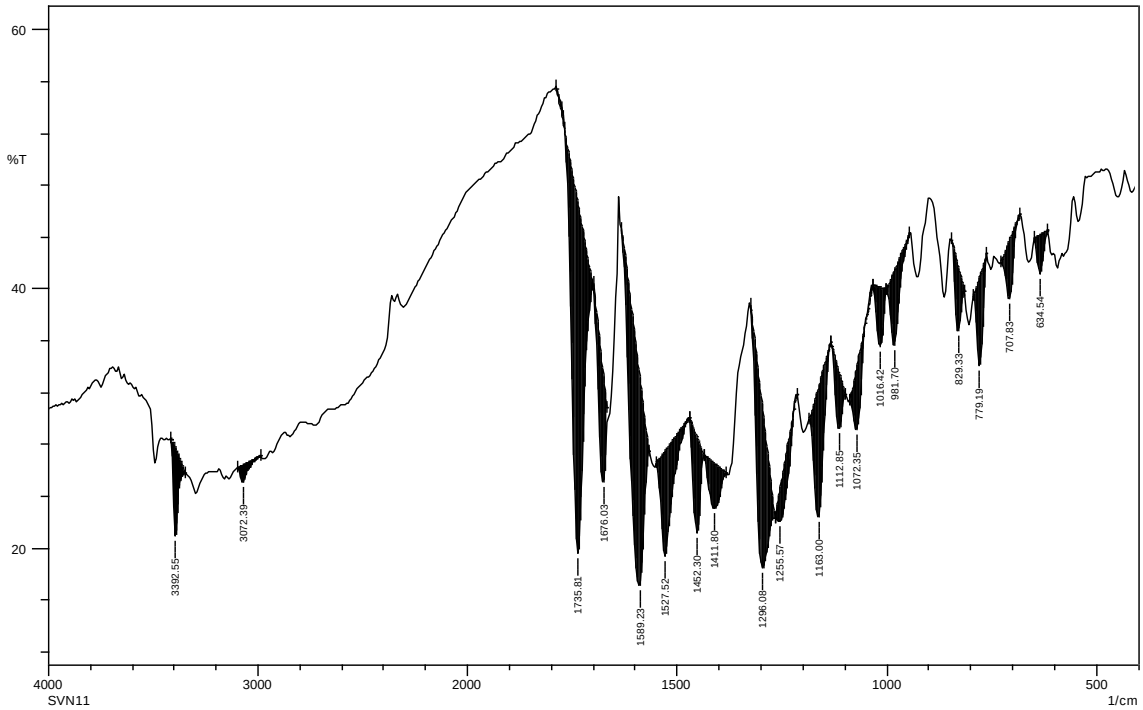

Figure S37: FT-IR of (*E*)-3-(2-((2-hydroxy-5-nitrobenzylidene) amino) thiazol-4-yl)-6-nitro-2*H*-chromen-2-one (SVN 10)

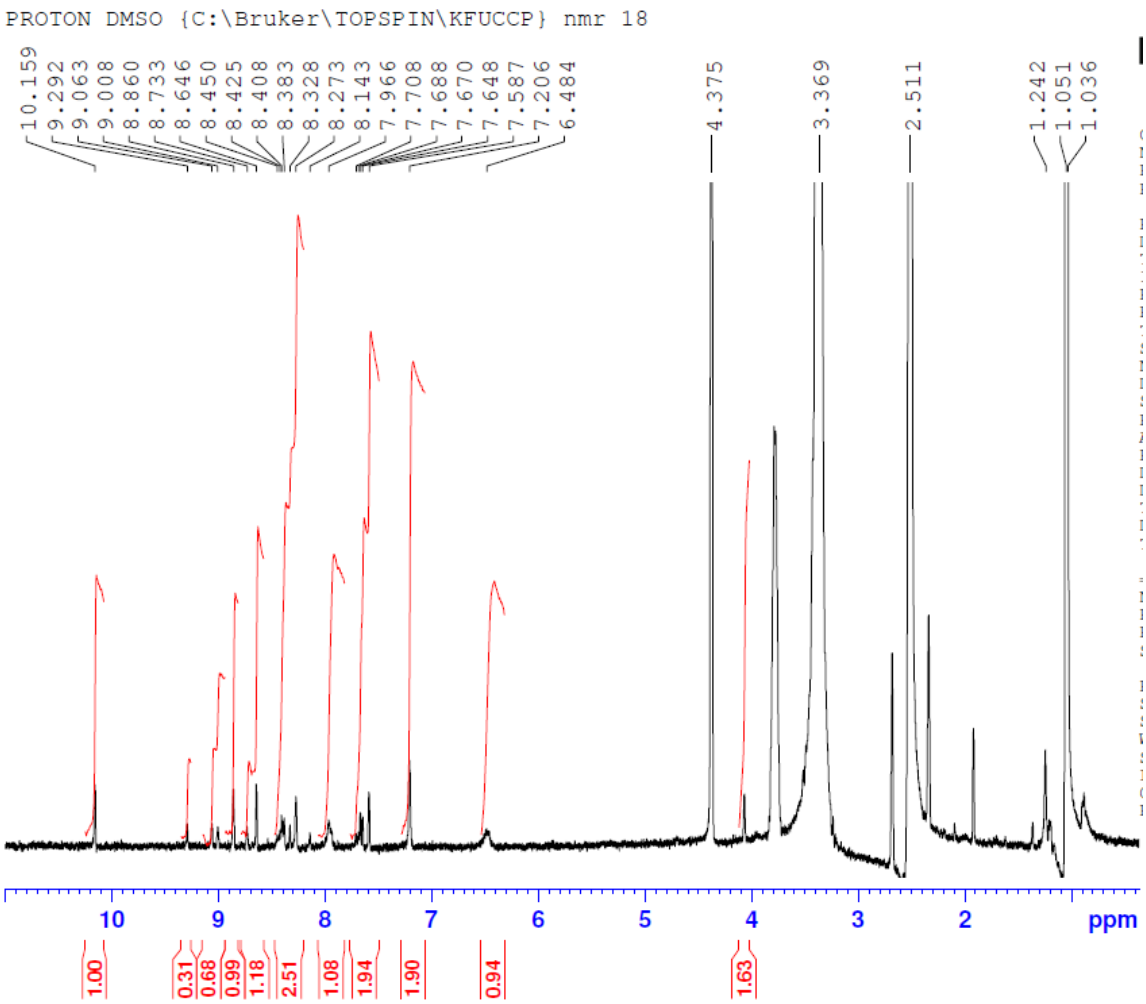

Figure S38: ^{1}H-NMR of (*E*)-3-(2-((2-hydroxy-5-nitrobenzylidene) amino) thiazol-4-yl)-6-nitro-2*H*-chromen-2-one (SVN 10)

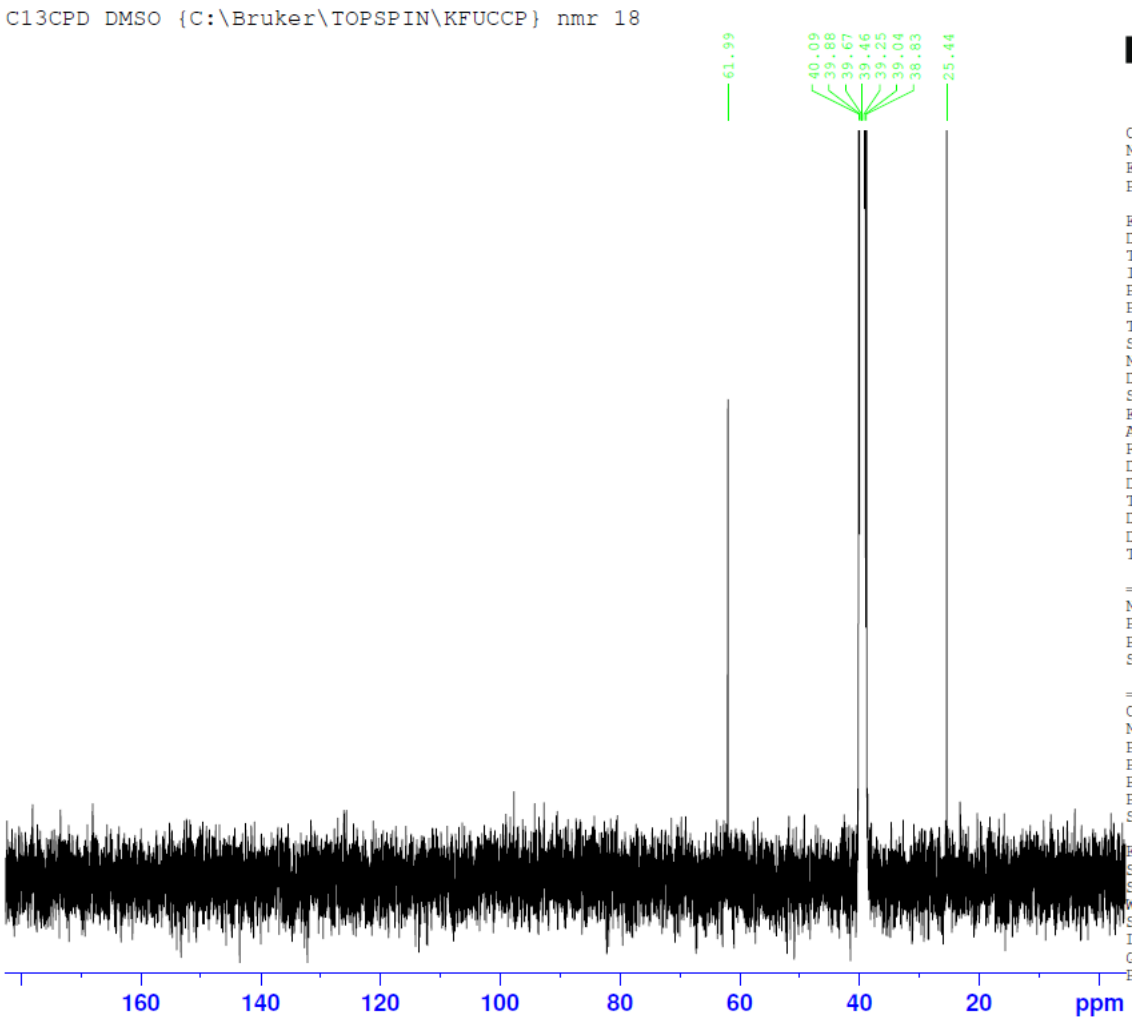

Figure S39: ^{13}C-NMR of (*E*)-3-(2-((2-hydroxy-5-nitrobenzylidene) amino) thiazol-4-yl)-6-nitro-2*H*-chromen-2-one (SVN 10)

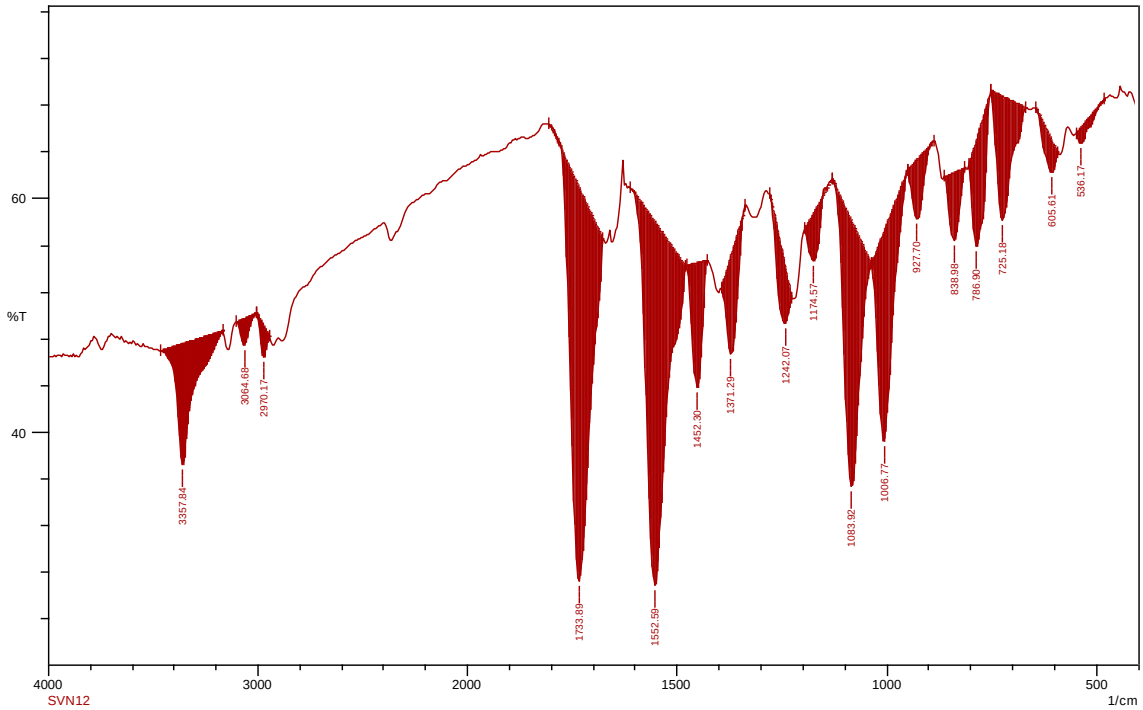

Figure S40: FT-IR of (*E*)-3-(2-((3,5-dichloro-2-hydroxybenzylidene) amino) thiazol-4-yl)-6-nitro-2*H*-chromen-2-one (SVN 11)

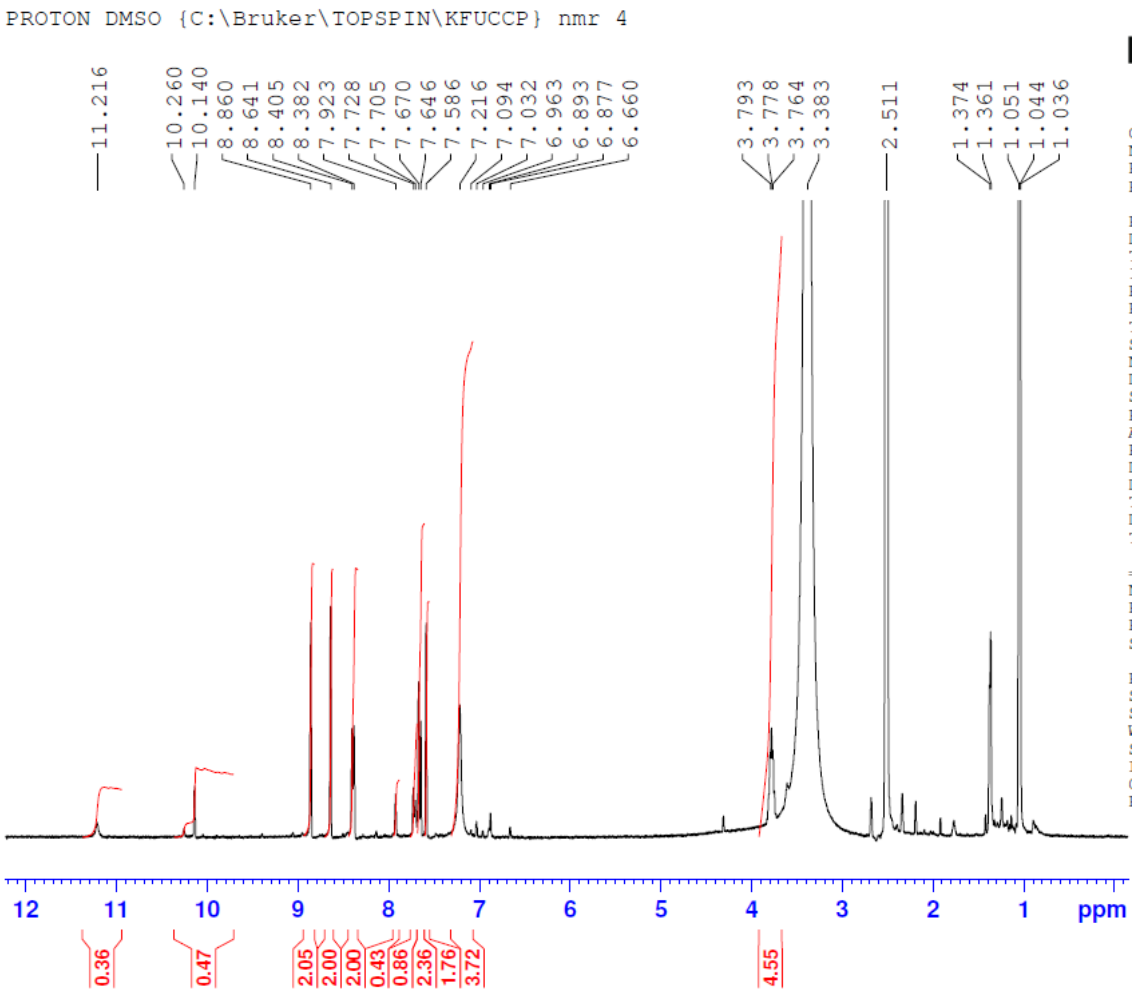

Figure S41: ^{1}H-NMR of (*E*)-3-(2-((3,5-dichloro-2-hydroxybenzylidene) amino) thiazol-4-yl)-6-nitro-2*H*-chromen-2-one (SVN 11)

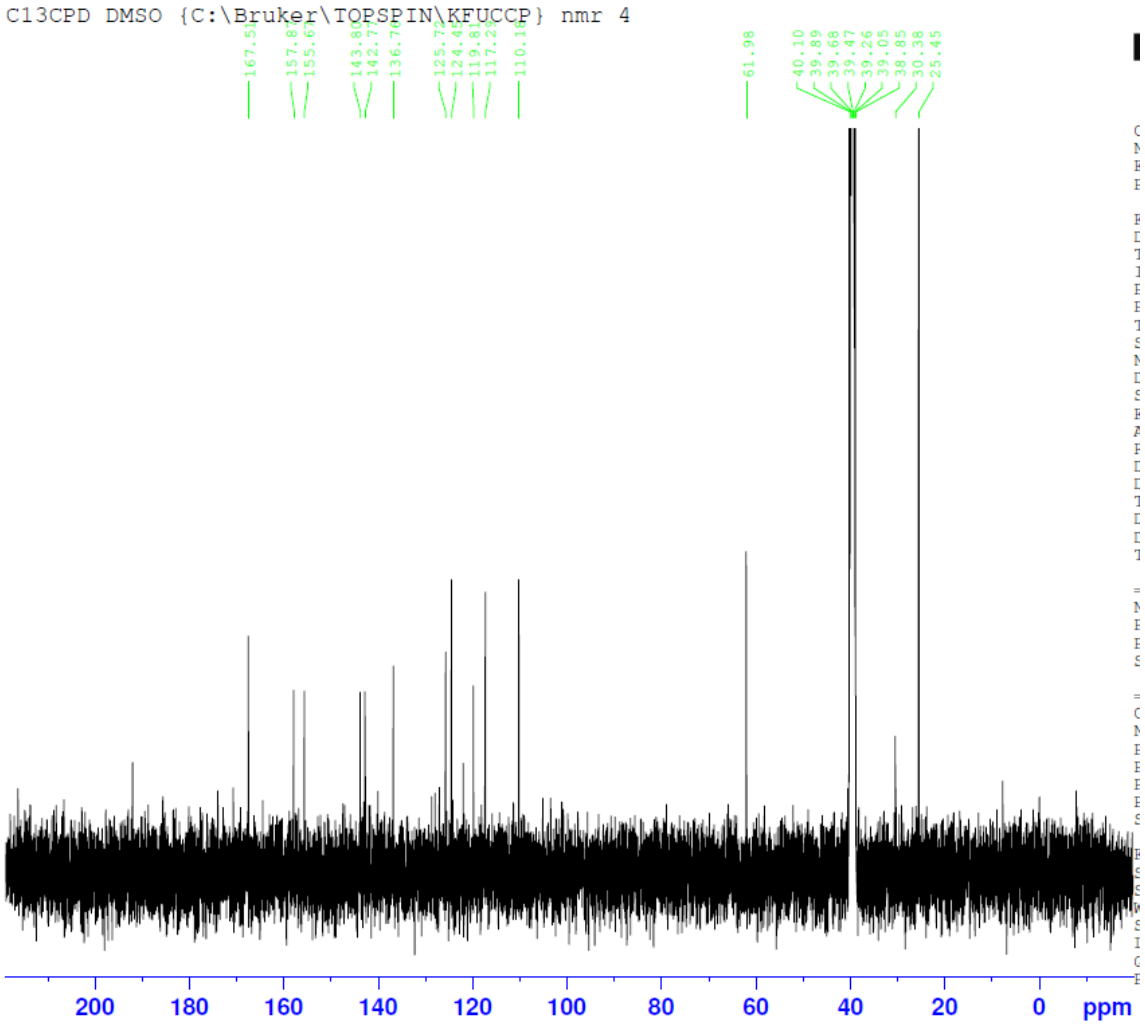

Figure S42: ^{13}C-NMR of (*E*)-3-(2-((3,5-dichloro-2-hydroxybenzylidene) amino) thiazol-4-yl)-6-nitro-2*H*-chromen-2-one (SVN 11)

APPENDIX 4

PhytoChem &BioSub Journal Vol. 15(3) 2021
ISSN 2170-1768, EISSN 2602-5132
CAS-CODEN:PBJHB3

PCBS Journal
ISSN 2170-1768

PhytoChem &BioSub Journal

2021
Vol. 15 No. 3

Coumarin containing hybrids and their pharmacological activities

Kabange Kasumbwe[1]*, Sabiu Saheed[1], Talent R. Makhanya[2], Katharigatta N. Venugopala[1] & Viresh Mohanlall[1]

1. *Department of Biotechnology and Food Technology, Durban University of Technology, P.O Box 1334, Steve Biko Campus, Durban 4001, South Africa*
2. *Department of Chemistry, Durban University of Technology, P.O Box 1334, Steve Biko Campus, Durban 4001, South Africa*

Received: June 24, 2021; Accepted: August 09, 2021
Corresponding author Email: laurel.kasumbwe@gmail.com

DOI:10.163.pcbsj/2021.15.-3-292

Abstract. *Coumarin moiety is of great interest to both chemists and biologists as it is present in a wide variety of naturally occurring bioactive compounds. Studies have lent scientific credence to the biological activities of several coumarin derivatives. The broad spectrum of biological activities linked with coumarin includes antibacterial, antimycobacterial, antioxidant, anticancer, antifungal, anti-inflammatory, anticoagulant and antiviral properties. The electron releasing and withdrawing substituent of coumarin affects the pharmacological properties of its resulting derivatives. Thus, identifying key structural features within the coumarin family is vital to the design and development of new analogues with enhanced pharmacological activity due to the variability in the structural complexity of coumarin. This article presents an up-to-date synopsis on the synthesis of coumarin derivatives and their pharmacological properties.*

Key Words: *Coumarin, anticancer, antimicrobial, antioxidant, analgesic, antidiabetic, antiinflammatory*

1. INTRODUCTION

Coumarin (2*H*-chromen-2-one) is a system of heterocyclic rings fused with benzene and 2-pyran. It belongs to the neo-flavonoid family of secondary plant metabolites [1]. Like coumarin, its derivatives are also essential in heterocyclic compounds because of their physical and pharmacological properties[2]. Coumarin derivatives possess many important electro-optical and pharmacological properties such as antioxidant, antiviral, anticancer, antibacterial, antifungal and antitubercular activities[3-5]. Coumarin derivatives may also be used to mark or label lipid droplets in cancer cells and non-cancer cells to demonstrate their biochemical differences [6].

The synthesis of coumarins and their derivatives has attracted the attention of organic and medicinal chemists because several natural products comprise the heterocyclic nucleus [7, 8]. Numerous heterocyclic compounds, especially coumarins, possess vast biological